frontiers | Research Topics

Immune dysregulation as a critical driver of chronic inflammatory diseases

Edited by
Rizgar A. Mageed, Voon Ong, David John Abraham and Richard Williams

Published in
Frontiers in Immunology

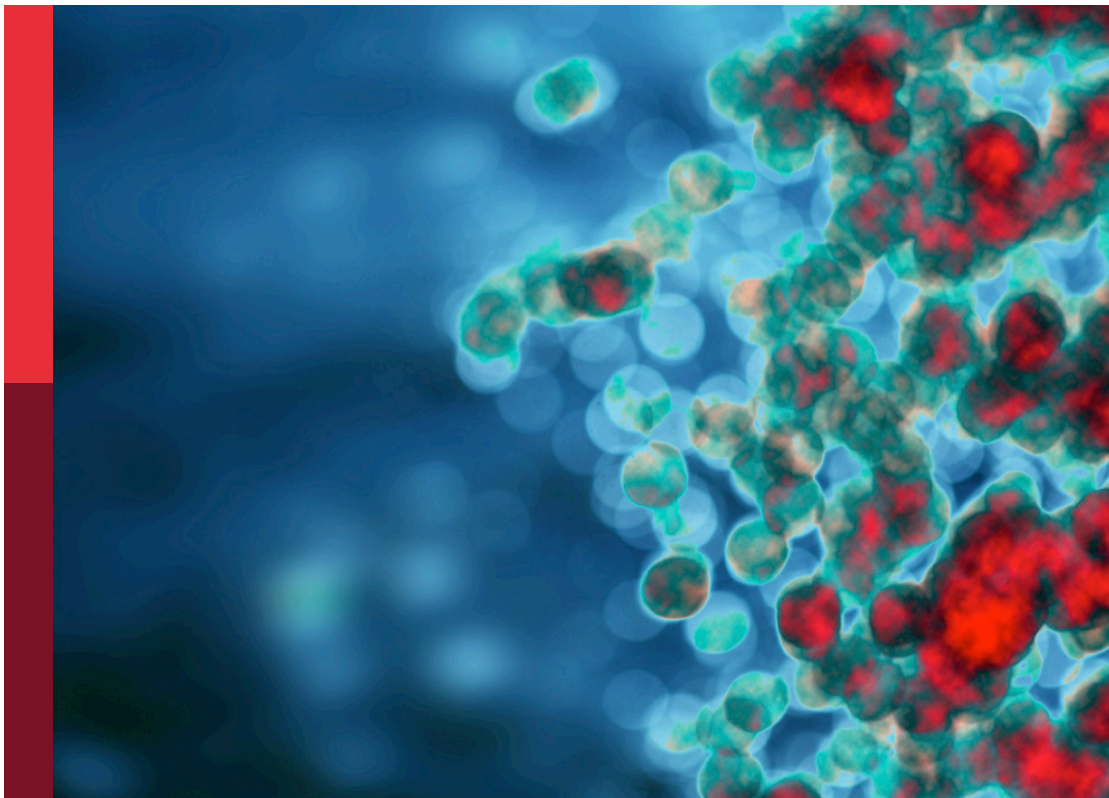

ISSN 1664-8714
ISBN 978-2-8325-2384-1
DOI 10.3389/978-2-8325-2384-1

About Frontiers

Frontiers is more than just an open access publisher of scholarly articles: it is a pioneering approach to the world of academia, radically improving the way scholarly research is managed. The grand vision of Frontiers is a world where all people have an equal opportunity to seek, share and generate knowledge. Frontiers provides immediate and permanent online open access to all its publications, but this alone is not enough to realize our grand goals.

Frontiers journal series

The Frontiers journal series is a multi-tier and interdisciplinary set of open-access, online journals, promising a paradigm shift from the current review, selection and dissemination processes in academic publishing. All Frontiers journals are driven by researchers for researchers; therefore, they constitute a service to the scholarly community. At the same time, the *Frontiers journal series* operates on a revolutionary invention, the tiered publishing system, initially addressing specific communities of scholars, and gradually climbing up to broader public understanding, thus serving the interests of the lay society, too.

Dedication to quality

Each Frontiers article is a landmark of the highest quality, thanks to genuinely collaborative interactions between authors and review editors, who include some of the world's best academicians. Research must be certified by peers before entering a stream of knowledge that may eventually reach the public - and shape society; therefore, Frontiers only applies the most rigorous and unbiased reviews. Frontiers revolutionizes research publishing by freely delivering the most outstanding research, evaluated with no bias from both the academic and social point of view. By applying the most advanced information technologies, Frontiers is catapulting scholarly publishing into a new generation.

What are Frontiers Research Topics?

Frontiers Research Topics are very popular trademarks of the *Frontiers journals series*: they are collections of at least ten articles, all centered on a particular subject. With their unique mix of varied contributions from Original Research to Review Articles, Frontiers Research Topics unify the most influential researchers, the latest key findings and historical advances in a hot research area.

Find out more on how to host your own Frontiers Research Topic or contribute to one as an author by contacting the Frontiers editorial office: frontiersin.org/about/contact

Immune dysregulation as a critical driver of chronic inflammatory diseases

Topic editors

Rizgar A. Mageed — Queen Mary University of London, United Kingdom
Voon Ong — University College London, United Kingdom
David John Abraham — University College London, United Kingdom
Richard Williams — University of Oxford, United Kingdom

Citation

Mageed, R. A., Ong, V., Abraham, D. J., Williams, R., eds. (2023). *Immune dysregulation as a critical driver of chronic inflammatory diseases*. Lausanne: Frontiers Media SA. doi: 10.3389/978-2-8325-2384-1

Table of contents

frontiers in Immunology

ORIGINAL RESEARCH
published: 02 December 2021
doi: 10.3389/fimmu.2021.784975

Proteomics and Organoid Culture Reveal the Underlying Pathogenesis of Hashimoto's Thyroiditis

Hui Xiao[1†], Jianqing Liang[2†], Sunqiang Liu[3†], Qiongyue Zhang[4,5†], Famin Xie[2], Xingyu Kong[2], Shanshan Guo[2], Ruwen Wang[6,7], Rong Fu[8], Zhiqi Ye[2], Yun Li[2], Shuang Zhang[6,9], Li Zhang[5], Keneilwe Kenny Kaudimba[6,7], Ru Wang[6,7], Xingxing Kong[2,4], Bing Zhao[2‡], Xuqin Zheng[3*‡] and Tiemin Liu[1,2,4*‡§]*

[1] Human Phenome Institute, Fudan University, Shanghai, China, [2] State Key Laboratory of Genetic Engineering, School of Life Sciences, Zhongshan Hospital, Fudan University, Shanghai, China, [3] Department of Endocrinology and Metabolism, the First Affiliated Hospital of Nanjing Medical University, Nanjing, China, [4] Shanghai Key Laboratory of Metabolic Remodeling and Health, Institute of Metabolism & Integrative Biology, Fudan University, Shanghai, China, [5] Division of Endocrinology and Metabolism, Department of Internal Medicine, Huashan Hospital, Shanghai Medical College, Fudan University, Shanghai, China, [6] School of Kinesiology, Key Laboratory of Exercise and Health Sciences of Ministry of Education, Shanghai University of Sport, Shanghai, China, [7] Shanghai Frontiers Science Research Base of Exercise and Metabolic Health, Shanghai, China, [8] Department of General Surgery, the First Affiliated Hospital of Nanjing Medical University, Nanjing, China, [9] Department of Kinesiology, Harbin Sport University, Harbin, China

Hashimoto's thyroiditis (HT) is an autoimmune disease, and its incidence continues to rise. Although scientists have studied this disease for many years and discovered the potential effects of various proteins in it, the specific pathogenesis is still not fully comprehended. To understand HT and translate this knowledge to clinical applications, we took the mass spectrometric analysis on thyroid tissue fine-needle puncture from HT patients and healthy people in an attempt to make a further understanding of the pathogenesis of HT. A total of 44 proteins with differential expression were identified in HT patients, and these proteins play vital roles in cell adhesion, cell metabolism, and thyroxine synthesis. Combining patient clinical trial sample information, we further compared the transient changes of gene expression regulation in HT and papillary thyroid carcinoma (PTC) samples. More importantly, we developed patient-derived HT and PTC organoids as a promising new preclinical model to verify these potential markers. Our data revealed a marked characteristic of HT organoid in upregulating chemokines that include C-C motif chemokine ligand (*CCL*) 2 and *CCL3*, which play a key role in the pathogenesis of HT. Overall, our research has enriched everyone's understanding of the pathogenesis of HT and provides a certain reference for the treatment of the disease.

Keywords: Hashimoto's thyroiditis, autoimmune diseases, proteomics, organoid, pathogenesis

OPEN ACCESS

Edited by:
Richard Williams, University of Oxford, United Kingdom

Reviewed by:
Bergithe Eikeland Oftedal, University of Bergen, Norway
Zhanchuan Ma, First Affiliated Hospital of Jilin University, China

***Correspondence:**
Tiemin Liu
tiemin_liu@fudan.edu.cn
Xuqin Zheng
zhengxuqin@njmu.edu.cn
Bing Zhao
bingzhao@fudan.edu.cn

†These authors have contributed equally to this work

‡These authors have contributed equally to this work and share last authorship

§Lead contact

Specialty section:
This article was submitted to Autoimmune and Autoinflammatory Disorders, a section of the journal Frontiers in Immunology

Received: *28 September 2021*
Accepted: *05 November 2021*
Published: *02 December 2021*

Citation:
Xiao H, Liang J, Liu S, Zhang Q, Xie F, Kong X, Guo S, Wang R, Fu R, Ye Z, Li Y, Zhang S, Zhang L, Kaudimba KK, Wang R, Kong X, Zhao B, Zheng X and Liu T (2021) Proteomics and Organoid Culture Reveal the Underlying Pathogenesis of Hashimoto's Thyroiditis. Front. Immunol. 12:784975. doi: 10.3389/fimmu.2021.784975

INTRODUCTION

Hashimoto's thyroiditis (HT) is a common type of autoimmune disease, with far more female patients than male patients aged between 45 and 60 years (1). It has been more than a hundred years since it was first reported (2). In patients with HT, the infiltration of immune cells into thyroid tissue results in the dysfunction of thyroid follicular cells and disorder of thyroxine secretion. In addition, highly expressed thyroid peroxidase antibodies (TPOAb) and thyroglobulin antibodies (TGAb) are detected in HT patients' serum. Although the incidence of HT in the population is as high as 5% (3)

and has continued to rise over the past few decades (4), scientists do not fully comprehend the pathogenesis of this disease, and it is generally recognized that a variety of genetic and environmental factors lead to the occurrence of HT (5). After genetic investigations in HT patients' family members, it has been found that the probability of HT in monozygotic twins is much higher than that of dizygotic twins (6). Several susceptibility loci were found and identified in association with autoimmune disease or autoimmune thyroid disease by genome-wide association studies (GWAS) (7, 8). Recent studies have shown that single-nucleotide polymorphisms in multiple genes such as monocyte chemoattractant protein (*MCP*)1, interleukin (*IL*)1, and transforming growth factor beta (*TGFB*)1 are involved in genetic predisposition to autoimmune diseases, particularly HT (9–11). In addition to intrinsic factors, excessive iodine intake also results in autophagy of thyroid follicular cells and induces HT (12). Chemokines are a family of small, secreted, and structurally related cytokines with a crucial role in inflammation and immunity (13). Considering the basic role that chemokines have in orchestrating the movement of lymphocytes and the formation of lymphoid structures, it is not surprising that chemokines play an important role in HT pathogenesis. In previous studies, scientists found that many chemokines were elevated in the serum and thyroid levels of patients with HT (14), such as *CCL2* and *CCL3*.

As an important endocrine organ of the human body, the thyroid gland affects metabolic, cardiovascular, and developmental processes (15). Thyroid hormone secretion in patients with HT is generally disturbed, which also increases the incidence rate of other diseases. Growing medical statistics indicated that HT patients have an increased risk for papillary thyroid carcinoma (PTC) than healthy people (16, 17), and patients with autoimmune thyroiditis are more likely to develop mood disorders like depression and anxiety (18, 19). Therefore, researches on HT will enrich our knowledge about the functions of the human immune system, endocrine system, and cell metabolism. However, multiple previous pieces of research focused on the role of certain proteins in immune regulation because thyroid cells produce a large number of reactive oxygen species (ROS) such as hydrogen peroxide during the synthesis of thyroxine (20, 21). Whether the disturbance of cell metabolism or other biological process affects the occurrence of HT still remains to be solved. In previous studies, most of the research on the mechanism of HT was carried out in mouse models of autoimmune deficiency. Mouse models could indeed explore HT from the perspective of the whole organism. However, the mouse model of HT still has some drawbacks. First of all, the standards for modeling mice with HT have not been consistent. Some mice were given excessive iodine intake (22), while others were injected with different concentrations of thyroid immunoglobulin (23). Secondly, the mouse model was not consistent with the symptoms of HT patients, including lymphocyte infiltration, TPO antibody positivity, and hypothyroidism (14).

In vitro cell culture is an important research tool to simulate human development and diseases. In the past, traditional monolayer cell culture has been widely used, but due to the lack of tissue structure and complexity, it cannot reflect the true biological process. Organoid technology reproduces the cell heterogeneity, structure, and function of original tissues by establishing powerful three-dimensional models, completely changing the *in vitro* culture tools for biomedical research. Patient-derived organoids enable researchers to reconstruct human organs and diseases in petri dishes, which brings great hope for many transformational applications, such as regenerative medicine, drug discovery, and precision medicine. Recently, organoid cultures derived from patients with PTC have been established (24, 25). However, no one has successfully established the organoids of HT. Therefore, to further understand the pathogenesis of HT, we compared differences between HT patients and healthy people with proteomics analysis. We generated an HT organoid model to assess the treatment prediction potential and find new methods of prevention and treatment of HT.

RESULTS

Overview of Sample Preparation and Analysis of Proteomic Profiling of Hashimoto's Thyroiditis and Healthy Control

In the endocrinology department, patients whose serum was found with positive TPO antibody (TPOAb >34.0 IU/ml or TGAb >115.0 IU/ml) were diagnosed with HT, while those with pure thyroid nodules were considered healthy control. There is no significant difference in body mass index (BMI) of these patients compared with healthy people, but the concentrations of antibodies such as TGAb and TPOAb in HT patients increased (**Figure 1A** and **Table 1**). To explore the difference in protein expression of thyroid in patients with HT, we used fine-needle aspiration biopsy to extract tissue fluid from the thyroid site in 24 HT patients and 24 healthy people who had pure thyroid nodules.

We obtained thyroid fluid samples after obtaining patients' consent. Due to the limitation of protein concentration and total amount in subsequent mass spectrometry (MS) experiments, the tissue fluids of eight individuals were mixed as one sample, and the experiment group (HT) and the control group (Con) were performed in triplicate (**Figure 1B**). Here, 910 proteins were obtained after analysis by MS. We analyzed the relative abundance of all proteins and presented them with principal component analysis (PCA) (**Figure 1C**). The two groups were distinguished to form two sections, which indicates that there is a significant difference in protein expression in thyroid tissue sites between HT patients and healthy people with thyroid nodules. Next, we investigated the relationship between different proteins to functionally explain the co-regulatory clusters between proteins or clinical parameters. The global protein correlation map highlights two main clusters of proteins. For instance, the immune regulation terms such as innate immune system and lymphocyte cell migrating were selectively enriched in the largest cluster. And the other cluster was enriched in proteins relating to the pentose phosphate pathway, biosynthesis of amino acids, and hemoglobin complex (**Figure 1D**).

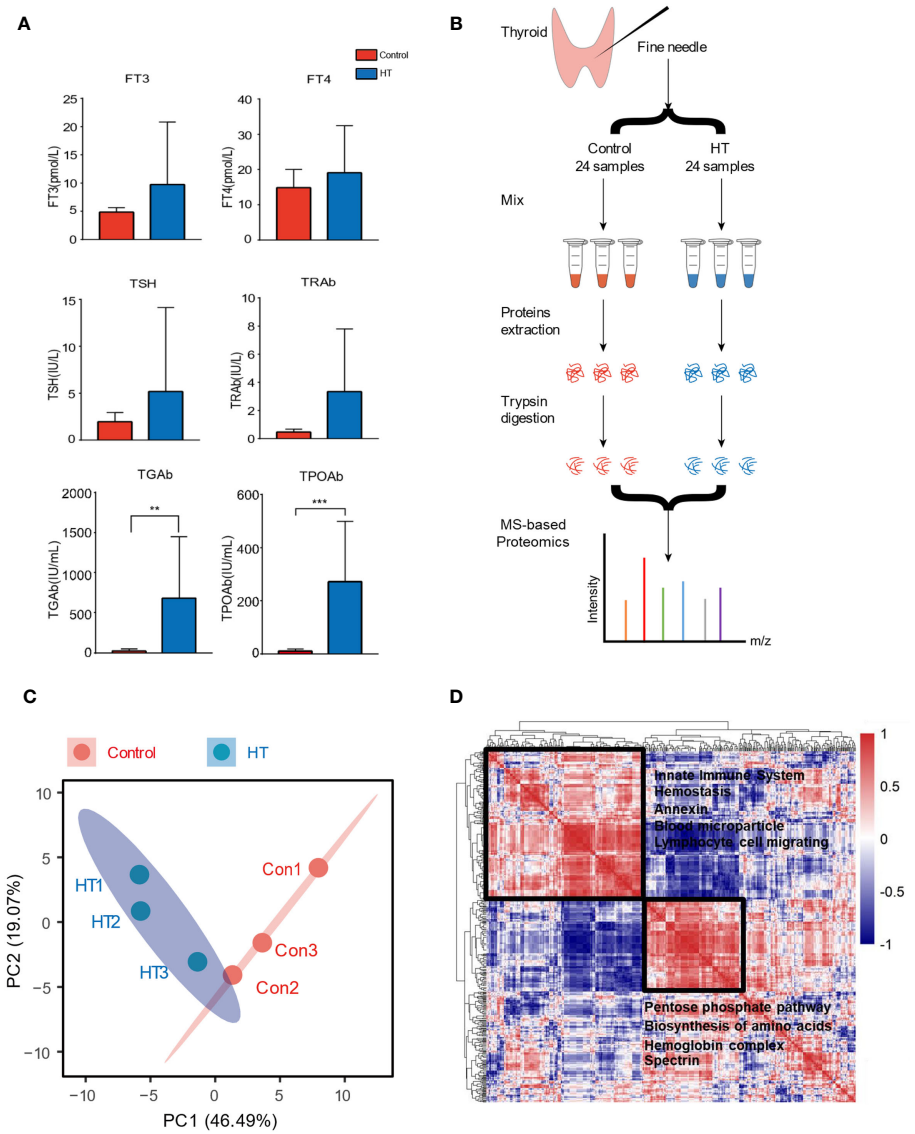

FIGURE 1 | Overview of sample preparation and result analysis presentation of proteomics. **(A)** Comparison of antibody concentration in serum of Hashimoto's thyroiditis (HT) and healthy controls. **(B)** Here, 24 patients and 24 healthy people were divided into two groups, the samples were acquired by fine-needle aspiration, and eight samples were mixed into one tube for subsequent mass spectrometry (MS). **(C)** Principal component analysis (PCA) biplot of protein concentration level; red dots represent the cluster Control, while blue dots represent the cluster HT. The first two axes accounted for 65% of variance. **(D)** Global correlation map of proteins generated by clustering the Pearson correlation coefficients of all possible protein combinations. The abundance of proteins with common regulation correlates across samples, and they therefore form a cluster. Prominent clusters are annotated with functional terms obtained from bioinformatics enrichment analysis. The inset shows the color code for Pearson correlation coefficients. Error bars show the mean ± SEM. Asterisks signify significant differences using one-way ANOVA, $^{**}P < 0.01$; $^{***}P < 0.001$.

Significant Differences in Protein Expression Between Hashimoto's Thyroiditis Patients and Healthy People

To determine the effect of differentially expressed proteins on patients, we further classified the information of the 910 proteins, screened the differentially expressed proteins between the experimental group and the control group, and set the fold change to 1.2 and *P* value less than 0.05 to draw the volcano plot; 125 proteins show a difference in the HT group *vs.* the control group (**Figure 2A**). We set the unique peptides not less than 2 for further screening and eliminated some contaminated protein peptides during the extraction process such as hemoglobin and cytoskeleton-related proteins like actin and tubulin. Ultimately, 44 proteins worthy of attention remained, of which 26 proteins were highly expressed in HT and 18 proteins were relatively low. We displayed the expression information of these differential proteins in a cluster heat map (**Figure 2B**) and performed Gene Ontology (GO) enrichment analysis and Kyoto Encyclopedia of

TABLE 1 | Clinical characteristics of HT samples.

	Control *N = 24*	HT *N = 24*	*P*-value
F	19	23	
M	5	1	
Age (years)	48.54 ± 11.67	41.38 ± 12.98	0.050
BMI (kg/m^2)	22.42 ± 3.40	23.03 ± 2.31	0.554
FT3 (pmol/l)	4.86 ± 0.81	9.76 ± 11.07*	0.041
FT4 (pmol/l)	14.89 ± 5.11	25.83 ± 26.16	0.055
TSH (MIU/l)	1.96 ± 0.98	4.32 ± 8.38	0.183
TPOAb (IU/ml)	10.26 ± 7.06	408.10 ± 238.75***	<0.001
TGAb (IU/ml)	21.43 ± 29.12	982.32 ± 1194.77**	0.001
TRAb (IU/L)	1.82 ± 4.38	3.07 ± 4.32	0.464

HT, Hashimoto's thyroiditis; F, female; M, male; BMI, body mass index; FT3, free triiodothyronine; FT4, free thyroxine; TSH, thyroid-stimulating hormone; TRAb, thyrotropin receptor antibody; TGAb, anti-thyroglobulin antibody; TPOAb, thyroid peroxidase antibody.

Plus–minus values are means ± SD.

**P < 0.05, **P < 0.01, ***P < 0.001.*

Genes and Genomes (KEGG) enrichment analysis on the upregulated and downregulated protein (**Figure 2C**). The results indicated that upregulated proteins are related to cell adhesion, gene expression, and lipid transport by GO enrichment. The pathways of protein expression, cholesterol metabolism, thyroid hormone synthesis, and antigen presentation were enriched through KEGG pathway analysis. The GO analysis in downregulated proteins revealed that enzyme inhibitor activity, redox reactions, and ubiquitination-related protein degradation pathways were significantly enriched in HT patients. By KEGG analysis, these proteins were enriched in cellular metabolism, including the five-carbon phosphate pathway, amino acid biosynthesis, and carbon metabolism pathway. In general, upregulated proteins are related to cell adhesion, protein synthesis, thyroxine synthesis, and cellular immunity, while downregulated proteins are related to cell metabolism and protein degradation.

Based on these results, we then focused on functional proteins from which we selected 44 proteins. Ultimately, we selected 21 proteins relevant to the immune system and metabolism and cancer as summarized in **Figure 2D**. A large proportion of proteins upregulated in the HT group was related to immune response, such as annexin A6 (ANXA6), calreticulin (CALR), cyclase associated actin cytoskeleton regulatory protein 1 (CAP1), major histocompatibility complex, class I, A (HLA-A), heat shock protein family D (Hsp60) member 1 (HSPD1), methyltransferase like 7A (METTL7A), prothymosin alpha (PTMA), ubiquitin conjugating enzyme E2 O (UBE2O), suggesting that the autoimmune system of patients with HT may have been disordered. However, it is not clear whether the changes in expression levels of these proteins occur at the transcriptional level or the translational level. In addition, previous research showed the relationship between HT and PTC (17, 26, 27). So, we next collected 10 cancerous and para-cancerous samples from patients with papillary thyroid cancer (**Table 2**). Seven of these patients had HT disease, and their para-cancerous samples were HT samples. The other three patients had no complications, whose para-cancerous samples were normal samples. We examined the 21 genes' transcriptional level changes using RT-qPCR analyses in three tissues, but due to the large variation of HLA-A and APOA1 expression among individuals in one group, only 19 genes were displayed (**Figure 3**). There were no significant differences between HT and control genes, which indicates that these genes were regulated at the translational level. We further tested the expression levels of these genes in PTC (**Figure 3**). It was found that at the transcriptional level, the expression of these genes did not change between HT and PTC.

In Vitro Self-Renewal and Organoid Formation Derived From Patients With Hashimoto's Thyroiditis and Papillary Thyroid Carcinoma

Due to the difficulty in obtaining clinical samples and constructing mouse models, we established organoids for HT and PTC to facilitate the study of these two diseases. Patients' thyroid tissues were dissociated into single cells and cell clumps using mechanical and enzymatic digestion. Then, single cells were cultured in a thyroid organoid medium that supported the formation and progressive growth of thyroid organoids (**Figure 4A**). To further characterize the HT and PTC organoids, gene expression of specific thyroid markers, HT markers, and PTC markers was assessed in organoids (**Figures 4B, C**). The immune-related gene expression of *IL4*, tumor necrosis factor (*TNF*)-α, and protein tyrosine phosphatase non-receptor type 22 (*PTPN22*) was significantly higher in HT organoids compared with normal, which is consistent with the results of previous studies (28–30). Interestingly, we examined the gene expression levels of four chemokines associated with HT, and the expression levels of these chemokines all showed an upward trend in HT, among which the chemokines *CCL2* and *CCL3* were significantly upregulated. This suggested that the HT organoid from the HT patient well represents the characteristics of the HT tissue. Histological examination using hematoxylin and eosin (H&E) staining also showed that the HT organoids displayed HT-like morphology with nuclear and cellular atypia, a similar morphology to that of the components in their original tissues (**Figure 4D**). More interestingly, the expression of GAL3, a biomarker of PTC disease (31), gradually increased in HT and PTC and significantly

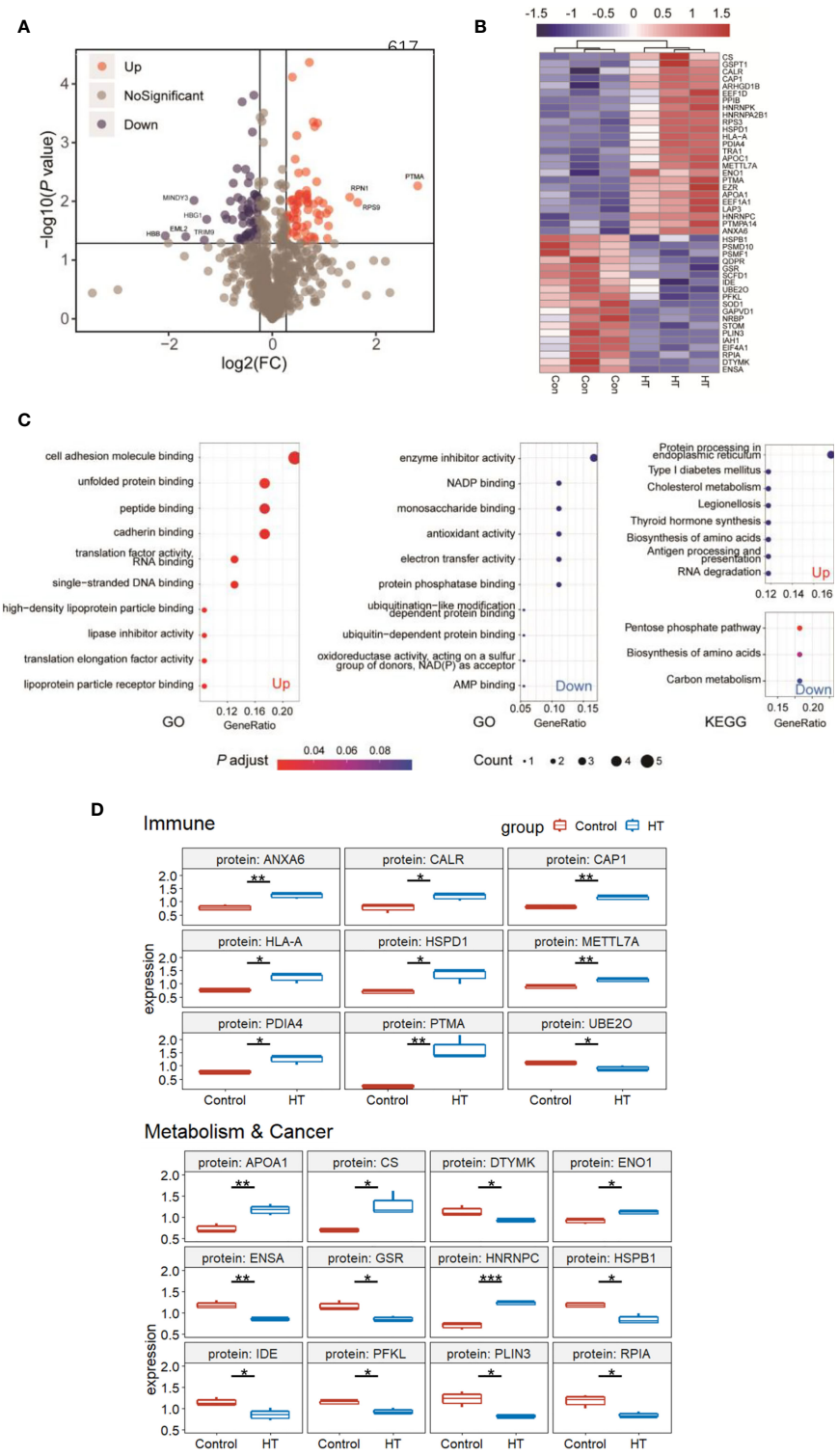

FIGURE 2 | Significant differences in protein expression between Hashimoto's thyroiditis (HT) patients and healthy people. **(A)** Volcano plot of proteomic data. Volcano plots are depicted with the fold change of each protein, and the *P*-value was calculated by performing t-test. Red circles show proteins that have significant increases. Blue circles show proteins that have significant decreases. Gray circles are proteins without any differences. **(B)** Heat map of the 44 differentially expressed protein (DEPs) information. **(C)** GO and KEGG pathway analysis of 26 upregulated and 18 downregulated genes. **(D)** Summary of DEPs in key functional groups that show differences between HT and Control. DEPs related to the immune system and metabolism&cancer are shown in boxplots. Median value was marked. $^{*}P < 0.05$; $^{**}P < 0.01$; $^{***}P < 0.001$.

TABLE 2 | Clinical characteristics of thyroid tumor samples.

Sample	Sex	Age (years)	TI-RADS	TPOAb (IU/ml)	TGAb (IU/ml)	Combined disease
PTC1	F	30	4B	517.4	504.7	HT
PTC2	F	54	4A	68.6	200.9	HT
PTC3	F	42	4B	277.8	120.0	HT
PTC4	F	31	4A	190.5	295.6	HT
PTC5	F	53	5	8.5	16.1	Non
PTC6	M	37	5	5.0	61.6	Non
PTC7	F	28	5	8.2	12.5	Non
PTC8	M	32	4A	104.4	NA	HT
PTC9	F	34	4C	239.7	>4,000	HT
PTC10	F	25	5	92.7	38.1	HT

F, female; M, male; PTC, papillary thyroid carcinoma; TI-RADS, Thyroid Imaging Reporting and Data System; TGAb, anti-thyroglobulin antibody; TPOAb, thyroid peroxidase antibody; NA, not available.

increased in PTC. High positive expression of GAL3 in HT may have a role in the cellular transformation to a cancerous cell with PTC feature when overexpression is continuous (32). These results suggests that HT may have similar characteristics with PTC and may progress to PTC.

In addition, to further characterize the HT organoids, we performed immunofluorescence (IF) analyses of marker expression in thyroid organoids and tissues. The results showed that the marker expression profiles were consistent between thyroid tissues and their derived organoids (**Figure 5**). Combining gene expression data and IF, we showed that our HT organoids are very similar to HT tissue, thus making sense of its use as an *in vitro* model of basic and translational research in HT.

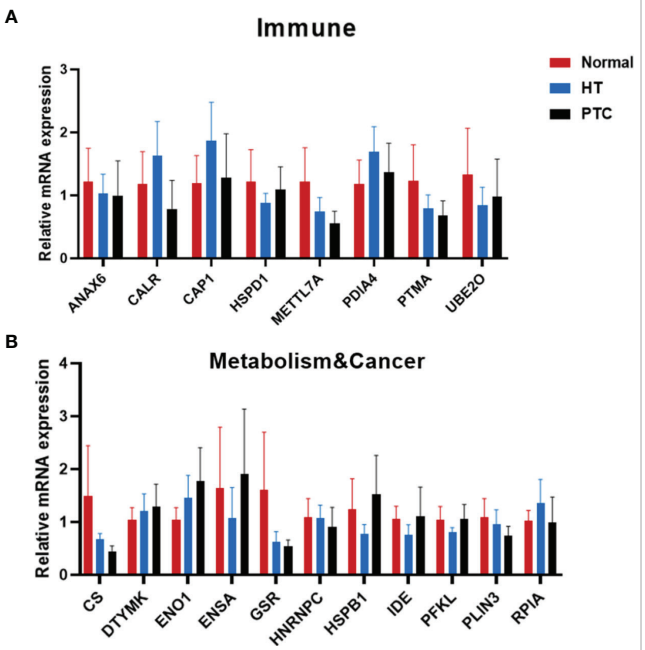

FIGURE 3 | Transcriptional changes with functional groups relevant to the immune system and metabolism&cancer in thyroid tissue. Molecular changes in transcription levels between Hashimoto's thyroiditis (HT) and Control relevant to the immune system **(A)** and metabolism&cancer **(B)** were evaluated by semiquantitative PCR [Normal, n = 3; HT, n = 5; papillary thyroid carcinoma (PTC), n = 6]. Error bars show the mean ± SEM.

Further Confirmation of Hashimoto's Thyroiditis-Associated Gene Alterations in Organoids

Patient-derived organoids have the potential to be used as preclinical models for confirming the proteome results. We performed RT-qPCR assays to examine gene expression levels in thyroid organoids that showed marked differences between the HT and control groups summarized by proteome (**Figures 6A, B**). Interestingly, similar to *CK19*, the expression of deoxythymidylate kinase (DTYMK) in HT and PTC organoids also gradually decreased compared with normal organoids (**Figure 6B**). DTYMK is a nuclear DTYMK, involved in the pathway deoxythymidine triphosphate biosynthesis, which is part of pyrimidine metabolism. In hepatocellular carcinoma, DTYMK expression predicts prognosis and chemotherapeutic response and correlates with the immune infiltration (33). In the PTC organoid, citrate synthase (CS) expression was increased, while phosphofructokinase, liver type (PFKL) and perilipin 3 (PLIN3) expression decreased. PLIN3, which belongs to the perilipin family, is considered to be involved in lipid droplet formation and the storage of lipids in cells (34). PLIN3 serves as a potential diagnostic and prognostic biomarker in renal cell carcinoma, and its expression is upregulated in renal cell carcinoma cells and tissues (35).

DISCUSSION

In this study, we compared the thyroid proteome map between HT and healthy people, and 912 proteins can be quantified and over 120 proteins alter in HT disease condition. Through the bioinformatics analysis, we found that these immune-related genes (ANXA6, CALR, CAP1, HLA-A, HSPD1, METTL7A, PTMA, and UBE2O) were increasing in HT thyroid, which may be candidates of HT pathogenic gene. Among them, the protein level of PTMA is the one that has positive HT at its highest form. Previous research has shown that PTMA was initially isolated from fresh rat thymus (36). Accordingly, inside the cell, PTMA is implicated in crucial intracellular circuits and may serve as a surrogate tumor biomarker, but when found outside the cell, it could be used as a therapeutic agent for treating immune

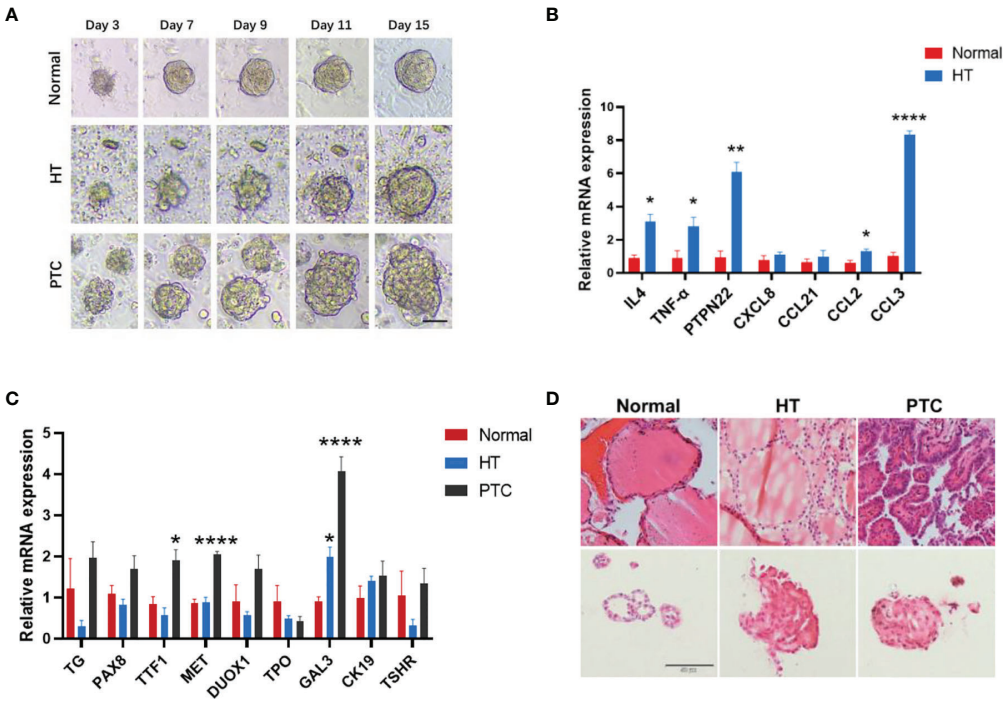

FIGURE 4 | Organoid cultures derived from patients with Hashimoto's thyroiditis (HT) and papillary thyroid carcinoma (PTC). **(A)** Time-lapse imaging sequence of Control, HT, and PTC organoids. Scale bar, 100 μm. **(B)** Quantitative PCR (qPCR) analysis of the HT and chemokine characterization marker mRNA level in thyroid organoids (Normal, n = 4; HT, n = 4). **(C)** qPCR analysis of the HT characterization marker mRNA level in thyroid organoids (Normal, n = 3; HT, n = 5; PTC, n = 6). All data are presented as mean ± SEM. **(D)** H&E staining of the organoids and their corresponding tissues, respectively. Scale bar, 50 μm. Error bars show the mean ± SEM. $^{*}P < 0.05$; $^{**}P < 0.01$; $^{****}P < 0.00001$.

system deficiencies (37). In addition, many studies have reported that HLA-A was a susceptibility gene for autoimmune thyroid diseases (38). HSPD1, which increased in the blood of HT patients compared to controls, could very well mediate thyroid cell damage and destruction, perpetuating inflammation (39). We performed a functional enrichment analysis on proteins identified as downregulated in HT and found that these proteins were mainly related to cell metabolism and protein degradation, including ubiquitination-related protein degradation, amino acid biosynthesis, and carbon metabolism pathway. Thyroid hormone was a key determinant of cell metabolism, regulating the pathways of carbohydrate, lipid, and protein metabolism (40). Hypothyroidism induced a hypometabolic state characterized by reduced energy expenditure, increased cholesterol levels, reduced lipolysis and gluconeogenesis, and weight gain (41). HT was a major cause of hypothyroidism, and many patients with HT eventually developed hypothyroidism (42), which may explain why cell metabolism and protein degradation process were downregulated in HT.

Furthermore, we established a culture system for HT and PTC thyroid organoids in which the thyroid cells maintain similar characteristics with thyroid tissue and a high proliferative capacity. Using thyroid organoids as a tool, we found that the expression of DTWMK gradually decreased in HT organoids and PTC organoids, indicating that DTYMK may be related to the progression of HT to PTC and may be used as a potential therapeutic target for HT. Chemokines fall in a family of small, secreted, and structurally related cytokines with a crucial role in inflammation and immunity (13), which played an important role in HT pathogenesis. In this study, we found that the chemokines *CCL2* and *CCL3* are significantly highly expressed in HT organoids, especially *CCL3* that is upregulated about eight times in HT organoids. These results suggest that the HT organoids we cultivated are consistent with the pathogenesis of the thyroid tissues and that inflammation is caused by lymphocyte infiltration.

Due to the mass spectrometry's requirement for the total protein content of the sample, we mixed the tissue fluids of eight individuals to experiment. Because there is a certain degree of differences between each individual whose protein expression information cannot be obtained, samples from a small number of male individuals were studied with samples from women, and the effects of these individual differences could not be neglected in our experiments. On the other hand, the process of mixing samples from different individuals also has an advantage in the experiment in that it can effectively avoid data deviations caused by a single individual to the entire group. In addition, in the process of screening protein collections, we adopted a method with the number of unique peptides greater than or equal to 2 and neglected some proteins with only one unique peptide being detected. These proteins may also be important markers like small RNA binding exonuclease protection factor La (*SSB*), it is

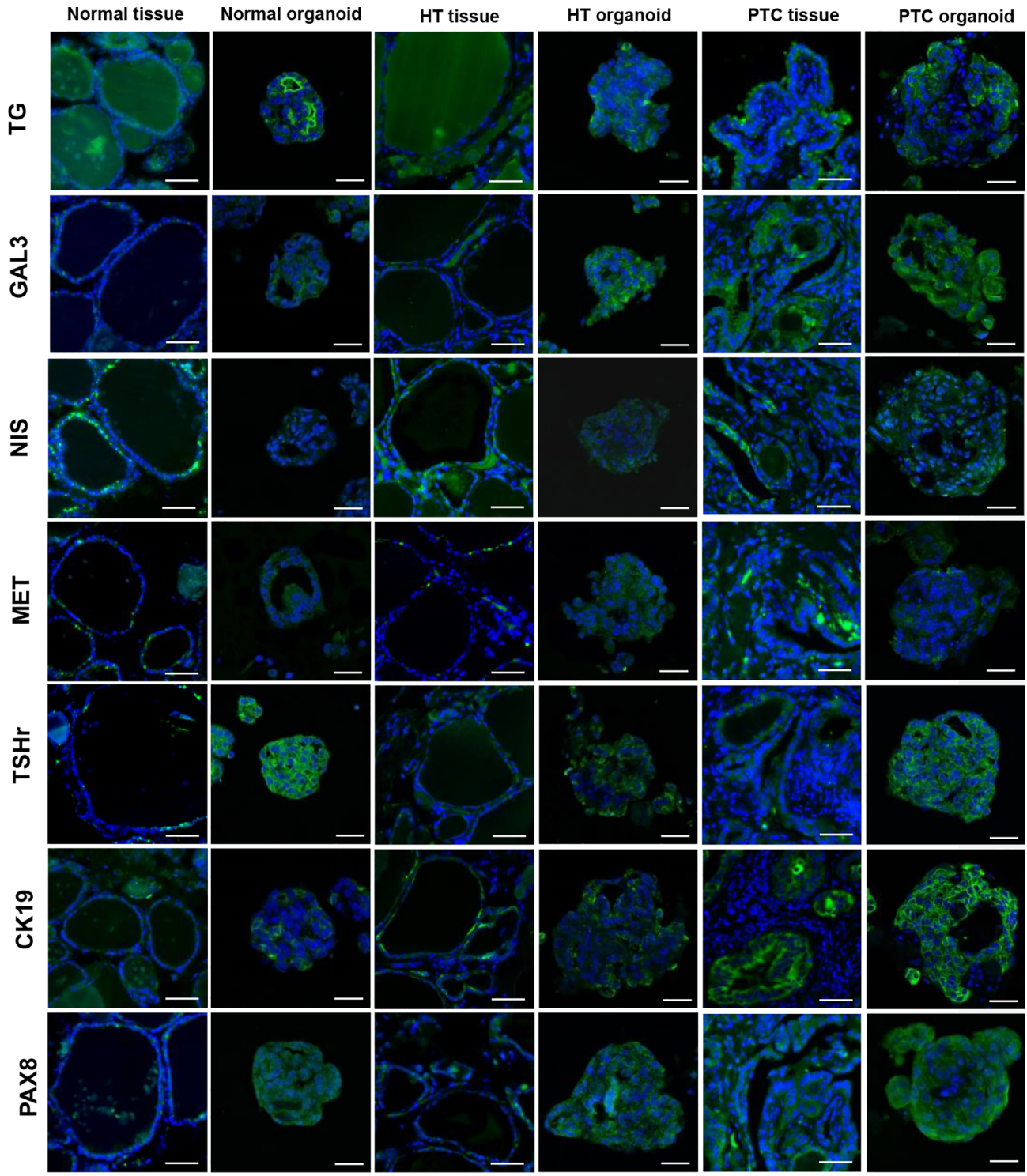

FIGURE 5 | Representative images of thyroids organoids subjected to immunofluorescence analysis for thyroid-specific markers, papillary thyroid carcinoma (PTC) markers. Organoids were cultured for 15 days before fixation and staining with Alexa-488 phalloidin and 4′,6-diamidino-2-phenylindole (DAPI). Scale bars, tissues = 50 μm, organoid = 20 μm. Markers indicated on the left side are shown as a green fluorescent signal. Nuclei are shown as a blue fluorescent signal.

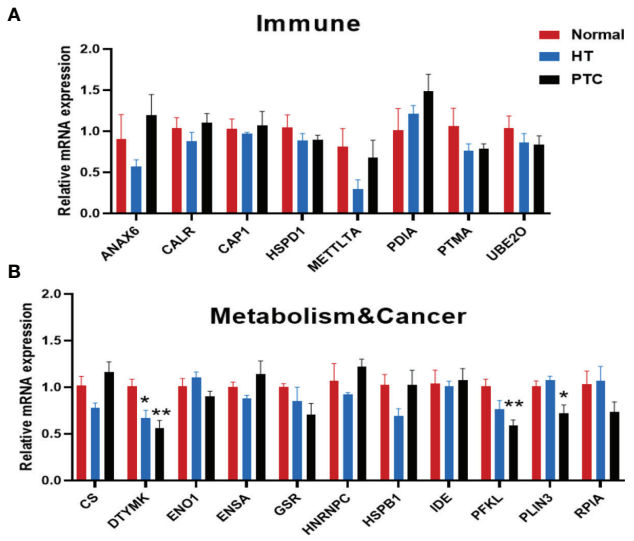

FIGURE 6 | RT-qPCR results of genes relevant to the immune system **(A)** and metabolism & cancer **(B)** in thyroid organoids from Normal, HT and PTC. Thyroid organoids were collected 15 days after plating and RNA prepared for RT-qPCR analysis. (Normal, n = 5; HT, n = 3; PTC, n = 6). Error bars show the mean ± SEM. *$P < 0.05$; **$P < 0.01$.

related to systemic lupus erythematosus, which is another common autoimmune disease. This shows that these autoimmune diseases may have some of the same expression profiles.

In summary, we profiled thyroid aspiration biopsy proteome maps in HT patients and successfully became the first to establish a culture system for HT thyroid organoids in which the thyroid cells maintain a high proliferative capacity. Additional research is needed to further explore and confirm the clinical application of this procedure before providing any basis for clinical decisions.

MATERIALS AND METHODS

Human Specimens

HT fine-needle puncture and PTC tissues were obtained from The First Affiliated Hospital of Nanjing Medical University, with the approval of the Research Ethics Committee (approval no. 2017-SR-346). According to the expressed TPOAb and TGAb detected in HT patients' serum, the patients with TPOAb >34.0 IU/ml or TGAb >115.0 IU/ml were diagnosed with HT (**Table 1**). For PTC patients, the sex, age, tumor size, and Thyroid Imaging Reporting and Data System (TI-RADS) stage were recorded when available (**Table 2**). The diagnosis of each PTC case was confirmed on routine H&E-stained slides by two pathologists. All specimens' identities are renamed with codes instead of the patient's name; written informed consent was provided by all patients.

Protein Extraction

Samples were lysed in a buffer that consisted of 4% sodium dodecyl sulfate (SDS; sodium lauryl sulfonate), 100 mM Tris/HCl pH 7.6, and 0.1 M dithiothreitol (DTT), and the protein concentration was determined by a bicinchoninic acid (BCA) protein assay. An appropriate amount of protein from each sample was collected and lysed with the filter-aided sample preparation (FASP) method (43). The peptides were desalted with C18 Cartridge, lyophilized, redissolved with 40 µl dissolution buffer, and quantified by spectrophotometry method (OD280).

Liquid Chromatography–Tandem Mass Spectrometry Analysis

Here, 100 µg of peptides were taken from each sample and labeled according to the instructions of the AB SCIEX iTRAQ Labeling Kit. Each set of labeled peptides was mixed and graded using AKTA Purifier 100. Buffer solution A: 10 mM KH_2PO_4, 25% ACN, pH 3.0; Buffer solution B: 10 mM KH_2PO_4, 500 mM KCl, 25% ACN, pH 3.0. The column was equilibrated with Buffer solution A, and each sample was loaded from the injector to the column for separation. The flow rate was 1 ml/min. The liquid phase gradient is as follows: 0–25 min, 0%–10% linear gradient Buffer B; 25–32 min, 10%–20% linear gradient Buffer B; 32–42 min, 20%–45% linear gradient Buffer B; 42–47 min, 45%–100% linear gradient Buffer B; 47–60 min, 100% Buffer B; after 60 min, 0% Buffer B. During the elution process, the absorbance at 214 nm was monitored, and the eluted fractions were collected every 1 min. After lyophilization, they were desalted with C18 Cartridge. Each fractionated sample was separated with high-performance liquid chromatography (HPLC) liquid system Easy nLC at a nanoliter flow rate. Buffer solution A: 0.1% formic acid. Buffer solution B: 84% acetonitrile with 0.1% formic acid. The column was equilibrated with 95% Buffer solution A. The sample was loaded by autosampler to the loading column (Thermo Scientific Acclaim PepMap100, 100 µm * 2 cm, nanoViper C18) and separated through the analytical column (Thermo Scientific EASY column, 10 cm, ID 75 µm, 3 µm, C18-A2) with a flow rate of 300 nl/min. The samples were chromatographed for mass spectrometry (MS) using a Q-Exactive mass spectrometer. The detection method was positive ion, the scanning range of the precursor ion was 300–1,800 m/z, the resolution of the primary mass spectrum was 70,000 at 200 m/z, the automatic gain control (AGC) target was 1e6, the maximum IT was 50 ms, and the dynamic exclusion time was 60.0 s. The mass-to-charge ratios of peptides and peptide fragments were collected according to the following method: 10 fragment spectra were acquired after a full scan (MS2 scan) with HCD MS2 Activation Type, isolation window was at 2 m/z, secondary MS resolution was 17,500 at 200 m/z, normalized collision energy was 30 eV, and underfill was 0.1%.

Protein Identification and Quantification

The raw data for MS analysis were RAW files, before the software, and Mascot2.2 and Proteome Discoverer1.4 were used for library identification and quantitative analysis.

Gene Ontology and Pathway Analysis

Differentially expressed proteins were screened according to the criteria that the expression fold change was more than 1.2 times (upregulation more than 1.2-fold or downregulation less than 0.83-fold) and *P*-value <0.05. The list of proteins across

the two sample groups and the differentially expressed sets of proteins from all comparisons were annotated and summarized at various GO categories using the topGO and cluster profile R package.

Organoid Culture

Fresh thyroid specimens were washed by phosphate buffered saline (PBS) and split into several smaller pieces. One piece was frozen and stored at –80°C for RNA isolation, one piece was fixed in paraformaldehyde for histopathological analysis and immunostaining, and the remaining tissues were dissociated and processed for organoid derivation. Human thyroid tissue was cut into smaller pieces (1 to –2 mm) with a surgical blade and digested with Collagenase Type I and Collagenase Type II (final concentration 100 U/ml, Thermo Fisher 17018029, 17101015) in Advanced DMEM/F-12 (Dulbecco's Modified Eagle Medium/Ham's F-12) (Thermo Fisher 12634028) with Rho kinase (ROCK) inhibitor (Y-27632, 10 μM) for 30 min at 37°C. Digested cells were collected by centrifugation at 300g for 3 min, after which the cell suspension was filtered through a 100-μm strainer. Cells were collected by centrifugation and resuspended in ~30 μl ice-cold Matrigel (Corning, No. 356231) and plated into a 12-well plate at 37°C for 15 min. When the Matrigel was solidified, 500 μl human thyroid organoid media were added. The medium includes Advanced DMEM/F-12 (Gibco, 12634-010), fibroblast growth factor (FGF) 10 (100 ng/ml, OrganRegen, Lot 031003), B27 (2%, Thermo Fisher, 17504001), A83-01 (5 μM, PeproTech, No.9094360), N-acetylcysteine (1.25 mM, PeproTech, No. 6169116), Noggin (100 ng/ml, OrganRegen, Lot 040606), epidermal growth factor (EGF; 50 ng/ml, Peprotech, No. AF-100-15), R-spondin-1 (200 ng/ml, OrganRegen, Lot 040407), ROCK inhibitor (Y-27632 10 μM, Abcam, ab143784), and thyroid-stimulating hormone (TSH; 16 mIU/ml, Sigma-Aldrich). Organoid culture medium was added and replaced every 3 days. Organoids were passaged at a 1:2 to 1:4 dilution every 2 weeks and either dissociation using TrypLE (Thermo Fisher 12605036). ROCK inhibitor (Y-27632, 10 μM) was added to the media after passaging to prevent cell death. Organoids were frozen in freezing media (NCM Biotech, C40100) and could be recovered efficiently.

Cell RNA Extraction and qRT-PCR

Total RNA from organoids and patient material was prepared (RNeasy Mini Kit, TIANGEN BIOTECH, DP420) following the manufacturer's instructions. In total, 500 ng total RNA was reverse transcribed by using a Reverse transcription kit (Thermo Fisher, 4366596) with a total of 20 μl for each reaction. A quantitative polymerase chain reaction (qPCR; Accurate Biology, AG11718) was performed using SYBR® Green Premix Pro Taq HS qPCR Kit according to the manufacturer's instructions. A total of 200 ng cDNA was mixed with PCR buffer, SyberGreen, and both forward and reverse primers for genes of interest, with a total volume of 10 μl for each sample. A three-step PCR reaction was applied subsequently (QuantStudio 7, Thermo Fisher). Oligo sequences of primers used were described in the **Supplementary Table**.

Histology and Immunofluorescence

Tissues were fixed in 4% paraformaldehyde for 24 h, embedded in paraffin, and serial sectioned at 5 μm in thickness. In the case of the organoids, Matrigel was dissolved and organoids were washed with PBS centrifuged at 200 rcf for 2 min. The resulting pellet was fixed in 4% paraformaldehyde (2 h, 4°C). Next, the organoids were embedded in 2% agarose gel (Invitrogen, 75510019), and the gel was subjected to dehydration, followed by embedding in paraffin and sectioned at 5 μm in thickness. Sections were deparaffinized in xylene for 10 min. This was followed by washing, blocking in 5% goat serum albumin blocking buffer for 20 min at room temperature, and incubation with primary antibodies at 4°C overnight. Slides were then incubated with secondary antibodies (1:500, Jackson Immune Research, 111-545-003) for 1 h, stained with 4′,6-diamidino-2-phenylindole (DAPI, Beyotime, C1002) for 10 min at room temperature, mounted using an aqueous mounting medium, and imaged using a DM6B microscope (Leica) and a FV1200 confocal microscope (Olympus). For immunofluorescence analysis, the antibodies to MET (1:50, Abclonal, A17366), GAL3 (1:50, Abclonal, A1464), TG (1:50, Proteintech, 60272-1-Ig), *CK19* (1:50, Abclonal, A0247), TSHr (1:50, Abclonal, A6781), NIS (1:50, Proteintech, 24324-1-AP), and PAX8 (1:50, Abclonal, A1009) were used to detect proteins.

Statistical Analysis

Statistical analyses were performed by Prism GraphPad 9.0 (GraphPad Software). Unpaired t-test was used to evaluate differences between two groups, and analysis of variance (ANOVA) was used to evaluate differences among three groups. Significance was set at P-value <0.05.

DATA AVAILABILITY STATEMENT

The mass spectrometry proteomics data have been deposited to the ProteomeXchange Consortium (http://proteomecentral.proteomexchange.org) via the iProX partner repository (44) with the dataset identifier PXD028448.

ETHICS STATEMENT

The studies involving human participants were reviewed and approved by The First Affiliated Hospital of Nanjing Medical University. The patients/participants provided their written informed consent to participate in this study.

AUTHOR CONTRIBUTIONS

TL designed study, interpreted study results, and participated in drafting and editing of manuscript. HX performed the experiments, visualization and statistical analysis, wrote and

edited the manuscript. JL performed organoid experiments. SL and QZ participated in experiments and clinical data analysis. XZ, and BZ assisted in study design, participated in interpretation of results, and edited manuscript. FX, SG, RWW, ZY, YL, SZ and LZ participated in the experiments and visualization. XYK and KKK participated in the data analysis and article modification. RF, SL, and XZ assisted clinical sample collection. RW and XXK supervised the experiments, data analysis and interpretation. All authors contributed to the article and approved the submitted version.

FUNDING

This research was funded by the National Key R&D Program of China (2019YFA0801900, 2018YFA0800300, 2020YFA0803800), the National Natural Science Foundation of China (31971074), Innovation Team and Talents Cultivation Program of National Administration of Traditional Chinese Medicine (ZYYCXTD-D-202001), the Shanghai Municipal Science and Technology Major Project (2017SHZDZX01), Shanghai Frontiers Science Research Base of Exercise and Metabolic Health, the National Natural Science Foundation of China (31971097), the Construction Project of High-Level Local Universities in Shanghai, China, Shanghai Municipal Science and Technology Committee of Shanghai outstanding academic leaders plan (21XD1403200), the 2020 fundamental research Fund of heilongjiang province (2020KYYWF-FC1), China Postdoctoral Science Foundation (2021M690680).

SUPPLEMENTARY MATERIAL

The Supplementary Material for this article can be found online at: https://www.frontiersin.org/articles/10.3389/fimmu.2021.784975/full#supplementary-material

REFERENCES

1. Rose NR, Mackay IR. *The Autoimmune diseases*. Amsterdam: Elsevier (2006).
2. Amino N, Tada H, Hidaka Y, Hashimoto K. Hashimoto's Disease and Dr. Hakaru Hashimoto. *Endocr J* (2002) 49(4):393–7. doi: 10.1507/endocrj.49.393
3. Jacobson DL, Gange SJ, Rose NR, Graham NM. Epidemiology and Estimated Population Burden of Selected Autoimmune Diseases in the United States. *Clin Immunol Immunopathol* (1997) 84(3):223–43. doi: 10.1006/clin.1997.4412
4. Rizzo M, Rossi RT, Bonaffini O, Scisca C, Altavilla G, Calbo L, et al. Increased Annual Frequency of Hashimoto's Thyroiditis Between Years 1988 and 2007 at a Cytological Unit of Sicily. *Ann Endocrinol (Paris)* (2010) 71(6):525–34. doi: 10.1016/j.ando.2010.06.006
5. Pyzik A, Grywalska E, Matyjaszek-Matuszek B, Rolinski J. Immune Disorders in Hashimoto's Thyroiditis: What Do We Know so Far? *J Immunol Res* (2015) 2015:979167. doi: 10.1155/2015/979167
6. Brix TH, Hegedüs L. Twin Studies as a Model for Exploring the Aetiology of Autoimmune Thyroid Disease. *Clin Endocrinol (Oxf)* (2012) 76(4):457–64. doi: 10.1111/j.1365-2265.2011.04318.x
7. Wellcome Trust Case Control C. Genome-Wide Association Study of 14,000 Cases of Seven Common Diseases and 3,000 Shared Controls. *Nature* (2007) 447(7145):661–78. doi: 10.1038/nature05911
8. Simmonds MJ. GWAS in Autoimmune Thyroid Disease: Redefining our Understanding of pathogenesis. *Nat Revs Endocrinol* (2013) 9(5):277–87. doi: 10.1038/nrendo.2013.56
9. Lacka K, Paradowska-Gorycka A, Maciejewski A, Kramer L, Herman WA, Lacki JK. Interleukin 1 Beta (IL1beta) Gene Polymorphisms (SNP-511 and SNP+3953) in Hashimoto's Thyroiditis Among the Polish Population. *Exp Clin Endocrinol Diabetes* (2014) 122(9):544–7. doi: 10.1055/s-0034-1376967
10. Akahane M, Watanabe M, Inoue N, Miyahara Y, Arakawa Y, Inoue Y, et al. Association of the Polymorphisms of Chemokine Genes (IL8, RANTES, MIG, IP10, MCP1 and IL16) With the Pathogenesis of Autoimmune Thyroid Diseases. *Autoimmunity* (2016) 49(5):312–9. doi: 10.3109/08916934.2015.1134507
11. Stanilova SA, Gerenova JB, Miteva LD, Manolova IM. The Role of Transforming Growth Factor-Beta1 Gene Polymorphism and Its Serum Levels in Hashimoto's Thyroiditis. *Curr Pharm Biotechnol* (2018) 19(7):581–9. doi: 10.2174/1389201019666180802142803
12. Xu C, Wu F, Mao C, Wang X, Zheng T, Bu L, et al. Excess Iodine Promotes Apoptosis of Thyroid Follicular Epithelial Cells by Inducing Autophagy Suppression and Is Associated With Hashimoto Thyroiditis Disease. *J Autoimmun* (2016) 75:50–7. doi: 10.1016/j.jaut.2016.07.008
13. Griffith JW, Sokol CL, Luster AD. Chemokines and Chemokine Receptors: Positioning Cells for Host Defense and Immunity. *Annu Rev Immunol* (2014) 32:659–702. doi: 10.1146/annurev-immunol-032713-120145
14. Kimura H, Caturegli P. Chemokine Orchestration of Autoimmune Thyroiditis. *Thyroid* (2007) 17(10):1005–11. doi: 10.1089/thy.2007.0267
15. Hall JE. *Guyton and Hall Textbook of Medical Physiology e-Book*. Amsterdam: Elsevier Health Sciences (2015).
16. Osório J. Thyroid gland: TSH MediatesIincreased Risk of PTC in Hashimoto Thyroiditis. *Nat Rev Endocrinol* (2011) 7(8):436. doi: 10.1038/nrendo.2011.96
17. Lai X, Xia Y, Zhang B, Li J, Jiang Y. A Meta-Analysis of Hashimoto's Thyroiditis and Papillary Thyroid Carcinoma Risk. *Oncotarget* (2017) 8(37):62414–24. doi: 10.18632/oncotarget.18620
18. Cai YJ, Wang F, Chen ZX, Li L, Fan H, Wu ZB, et al. Hashimoto's Thyroiditis Induces Neuroinflammation and Emotional Alterations in Euthyroid Mice. *J Neuroinflamm* (2018) 15(1):299. doi: 10.1186/s12974-018-1341-z
19. Siegmann EM, Müller HHO, Luecke C, Philipsen A, Kornhuber J, Grömer TW. Association of Depression and Anxiety Disorders With Autoimmune Thyroiditis: A Systematic Review and Meta-analysis. *JAMA Psychiatry* (2018) 75(6):577–84. doi: 10.1001/jamapsychiatry.2018.0190
20. Rigutto S, Hoste C, Grasberger H, Milenkovic M, Communi D, Dumont JE, et al. Activation of Dual Oxidases Duox1 and Duox2: Differential Regulation Mediated by Camp-Dependent Protein Kinase and Protein Kinase C-Dependent Phosphorylation. *J Biol Chem* (2009) 284(11):6725–34. doi: 10.1074/jbc.M806893200
21. Leto TL, Morand S, Hurt D, Ueyama T. Targeting and Regulation of Reactive Oxygen Species Generation by Nox family NADPH Oxidases. *Antioxid Redox Signaling* (2009) 11(10):2607–19. doi: 10.1089/ars.2009.2637
22. Vecchiatti SMP, Guzzo ML, Caldini EG, Bisi H, Longatto-Filho A, Lin CJ. Iodine Increases and Predicts Incidence of Thyroiditis in NOD Mice: Histopathological and Ultrastructural Study. *Exp Ther Med* (2013) 5(2):603–7. doi: 10.3892/etm.2012.826
23. Kong Y-cM. Experimental Autoimmune Thyroiditis in the Mouse. *Curr Protoc Immunol* (2007) 78:15.7.1–15.7.21. doi: 10.1002/0471142735.im1507s78
24. Sondorp LHJ, Ogundipe VML, Groen AH, Kelder W, Kemper A, Links TP, et al. Patient-Derived Papillary Thyroid Cancer Organoids for Radioactive Iodine Refractory Screening. *Cancers (Basel)* (2020) 12(11):3212. doi: 10.3390/cancers12113212
25. Chen D, Tan Y, Li Z, Li W, Yu L, Chen W, et al. Organoid Cultures Derived From Patients With Papillary Thyroid Cancer. *J Clin Endocrinol Metab* (2021) 106(5):1410–26. doi: 10.1210/clinem/dgab020
26. Graceffa G, Patrone R, Vieni S, Campanella S, Calamia S, Laise I, et al. Association Between Hashimoto's Thyroiditis and Papillary Thyroid Carcinoma: a Retrospective Analysis of 305 patients. *BMC Endocr Disord* (2019) 19(Suppl 1):26. doi: 10.1186/s12902-019-0351-x
27. Jankovic B, Le KT, Hershman JM. Clinical Review: Hashimoto's Thyroiditis and Papillary Thyroid Carcinoma: Is There a Correlation? *J Clin Endocrinol Metab* (2013) 98(2):474–82. doi: 10.1210/jc.2012-2978

28. Nanba T, Watanabe M, Akamizu T, Iwatani Y. The -590CC Genotype in the IL4 Gene as a Strong Predictive Factor for the Development of Hypothyroidism in Hashimoto Disease. *Clin Chem* (2008) 54(3):621–23. doi: 10.1373/clinchem.2007.099739
29. Inoue N, Watanabe M, Nanba T, Wada M, Akamizu T, Iwatani Y. Involvement of Functional Polymorphisms in the TNFA Gene in the Pathogenesis of Autoimmune Thyroid Diseases and Production of Anti-Thyrotropin Receptor Antibody. *Clin Exp Immunol* (2009) 156(2):199–204. doi: 10.1111/j.1365-2249.2009.03884.x
30. Burn GL, Svensson L, Sanchez-Blanco C, Saini M, Cope AP. Why Is PTPN22 a Good Candidate Susceptibility Gene for Autoimmune Disease? *FEBS Lett* (2011) 585(23):3689–98. doi: 10.1016/j.febslet.2011.04.032
31. Tang W, Huang C, Tang C, Xu J, Wang H. Galectin-3 May Serve as a Potential Marker for Diagnosis and Prognosis in Papillary Thyroid Carcinoma: A Meta-Analysis. *Onco Targets Ther* (2016) 9:455–60. doi: 10.2147/OTT.S94514
32. Mehdi MA, Jasim AM, Al-Ganber MF. The expression of GAL-3 and CK-19 in Hashimoto's Thyroiditis Compared to Papillary Thyroid Carcinoma. *Iraq Med J* (2018) 2(4):86–90.
33. Guo Y, Luo W, Huang S, Zhao W, Chen H, Ma Y, et al. DTYMK Expression Predicts Prognosis and Chemotherapeutic Response and Correlates with Immune Infiltration in Hepatocellular Carcinoma. *J Hepatocell Carcinoma* (2021) 8:871–85.
34. Greenberg AS, Egan JJ, Wek SA, Garty NB, Blanchette-Mackie EJ, Londos C. Perilipin, a Major Hormonally Regulated Adipocyte-Specific Phosphoprotein Associated With the Periphery of Lipid Storage Droplets. *J Biol Chem* (1991) 266(17):11341–6.
35. Wang K, Ruan H, Song Z, Cao Q, Bao L, Liu D, et al. PLIN3 Is Up-Regulated and Correlates With Poor Prognosis in Clear Cell Renal Cell Carcinoma. *Urol Oncol* (2018) 36(7). doi: 10.1016/j.urolonc.2018.04.006
36. Haritos AA, Goodall GJ, Horecker BL. Prothymosin alpha: Isolation and Properties of the Major Immunoreactive Form of Thymosin Alpha 1 in Rat Thymus. *Proc Natl Acad Sci USA* (1984) 81(4):1008–11. doi: 10.1073/pnas.81.4.1008
37. Samara P, Ioannou K, Tsitsilonis OE. Prothymosin Alpha and Immune Responses: Are We Close to Potential Clinical Applications? *Vitam Horm* (2016) 102:179–207. doi: 10.1016/bs.vh.2016.04.008
38. Sasazuki T, Inoko H, Morishima S, Morishima Y. Gene Map of the HLA Region, Graves' Disease and Hashimoto Thyroiditis, and Hematopoietic Stem Cell Transplantation. *Adv Immunol* (2016) 129:175–249. doi: 10.1016/bs.ai.2015.08.003
39. Marino Gammazza A, Rizzo M, Citarrella R, Rappa F, Campanella C, Bucchieri F, et al. Elevated Blood Hsp60, Its structural Similarities and Cross-Reactivity With Thyroid Molecules, and Its Presence on the Plasma Membrane of Oncocytes Point to the Chaperonin as an Immunopathogenic Factor in Hashimoto's Thyroiditis. *Cell Stress Chaperones* (2014) 19(3):343–53. doi: 10.1007/s12192-013-0460-9
40. Mullur R, Liu Y-Y, Brent GA. Thyroid Hormone Regulation of Metabolism. *Physiol Rev* (2014) 94(2):355–82. doi: 10.1152/physrev.00030.2013
41. Cicatiello AG, Di Girolamo D, Dentice M. Metabolic Effects of the Intracellular Regulation of Thyroid Hormone: Old Players, New Concepts. *Front Endocrinol (Lausanne)* (2018) 9:474. doi: 10.3389/fendo.2018.00474
42. Caturegli P, De Remigis A, Rose NR. Hashimoto Thyroiditis: Clinical and Diagnostic Criteria. *Autoimmun Rev* (2014) 13(4-5):391–7. doi: 10.1016/j.autrev.2014.01.007
43. Wiśniewski JR, Zougman A, Nagaraj N, Mann MJNm. Universal Sample Preparation method for Proteome Analysis. *Nucleis Acids Res* (2009) 6 (5):359–62. doi: 10.1038/nmeth.1322
44. Ma J, Chen T, Wu S, Yang C, Bai M, Shu K, et al. Iprox: An Integrated Proteome Resource. *Nucleic Acids Res* (2019) 47(D1):D1211–D7. doi: 10.1093/nar/gky869

Conflict of Interest: The authors declare that the research was conducted in the absence of any commercial or financial relationships that could be construed as a potential conflict of interest.

Publisher's Note: All claims expressed in this article are solely those of the authors and do not necessarily represent those of their affiliated organizations, or those of the publisher, the editors and the reviewers. Any product that may be evaluated in this article, or claim that may be made by its manufacturer, is not guaranteed or endorsed by the publisher.

frontiers in Immunology

ORIGINAL RESEARCH
published: 08 March 2022
doi: 10.3389/fimmu.2022.793855

RA Fibroblast-Like Synoviocytes Derived Extracellular Vesicles Promote Angiogenesis by miRNA-1972 Targeting p53/mTOR Signaling in Vascular Endotheliocyte

Yixiong Chen[1,2†], Junlong Dang[3†], Xiaorong Lin[3†], Manli Wang[4†], Yan Liu[1], Jingrong Chen[1], Ye Chen[1], Xiqing Luo[1], Zuoyu Hu[1], Weizhen Weng[1], Xiaoyi Shi[1], Xuan Bi[1], Yan Lu[3] and Yunfeng Pan[1*]*

[1] Division of Rheumatology, Department of Internal Medicine, The Third Affiliated Hospital of Sun Yat-sen University, Guangzhou, China, [2] Department of Rheumatology, Affiliated Dongguan People's Hospital, Southern Medical University, Dongguan, China, [3] Department of Clinical Immunology, The Third Affiliated Hospital of Sun Yat-Sen University, Guangzhou, China, [4] Medical Research Center, The Eighth Affiliated Hospital, Sun Yat-sen University, Shenzhen, China

Rheumatoid arthritis (RA) is an autoimmune disease characterized by chronic inflammatory in joints. Invasive pannus is a characteristic pathological feature of RA. RA fibroblast-like synoviocytes (FLSs) are showed tumor-like biological characters that facilitate pannus generation. Importantly, it has been documented that extracellular vesicle (EVs) derived microRNAs have a vital role of angiogenesis in various immune inflammatory diseases. However, whether RA FLSs derived EVs can facilitate angiogenesis and the underlying mechanism is undefined. Herein, we aim to investigate the key role of RA FLSs derived EVs on angiogenesis in endothelial cells (ECs). We indicate that RA FLSs derived EVs promote ECs angiogenesis by enhancing migration and tube formation of ECs *in vitro*. Also, we confirm that RA FLSs derived EVs can significantly facilitate ECs angiogenesis with a matrigel angiogenesis mice model. In terms of the mechanisms, both RNAs and proteins in EVs play roles in promoting ECs angiogenesis, but the RNA parts are more fundamental in this process. By combining microRNA sequencing and qPCR results, miR-1972 is identified to facilitate ECs angiogenesis. The blockage of miR-1972 significantly abrogated the angiogenesis stimulative ability of RA FLSs derived EVs in ECs, while the overexpression of miR-1972 reversed the effect in ECs. Specifically, the p53 level is decreased, and the phosphorylated mTOR is upregulated in miR-1972 overexpressed ECs, indicating that miR-1972 expedites angiogenesis through p53/mTOR pathway. Collectively, RA FLSs derived EVs can promote ECs angiogenesis *via* miR-1972 targeted p53/mTOR signaling, targeting on RA FLSs derived EVs or miR-1972 provides a promising strategy for the treatment of patients with RA.

Keywords: rheumatoid arthritis, fibroblast-like synoviocytes, extracellular vesicles, miR-1972, angiogenesis

OPEN ACCESS

Edited by:
Rizgar A. Mageed, Queen Mary University of London, United Kingdom

Reviewed by:
Aline Bozec, University of Erlangen Nuremberg, Germany
Akio Morinobu, Kyoto University, Japan

***Correspondence:**
Yunfeng Pan
panyunf@mail.sysu.edu.cn
Yan Lu
luyan36@mail.sysu.edu.cn

†These authors have contributed equally to this work

Specialty section:
This article was submitted to Autoimmune and Autoinflammatory Disorders, a section of the journal Frontiers in Immunology

Received: *12 October 2021*
Accepted: *10 February 2022*
Published: *08 March 2022*

Citation:
Chen YX, Dang JL, Lin XR, Wang ML, Liu Y, Chen JR, Chen Y, Luo XQ, Hu ZY, Weng WZ, Shi XY, Bi X, Lu Y and Pan YF (2022) RA Fibroblast-Like Synoviocytes Derived Extracellular Vesicles Promote Angiogenesis by miRNA-1972 Targeting p53/mTOR Signaling in Vascular Endotheliocyte. Front. Immunol. 13:793855. doi: 10.3389/fimmu.2022.793855

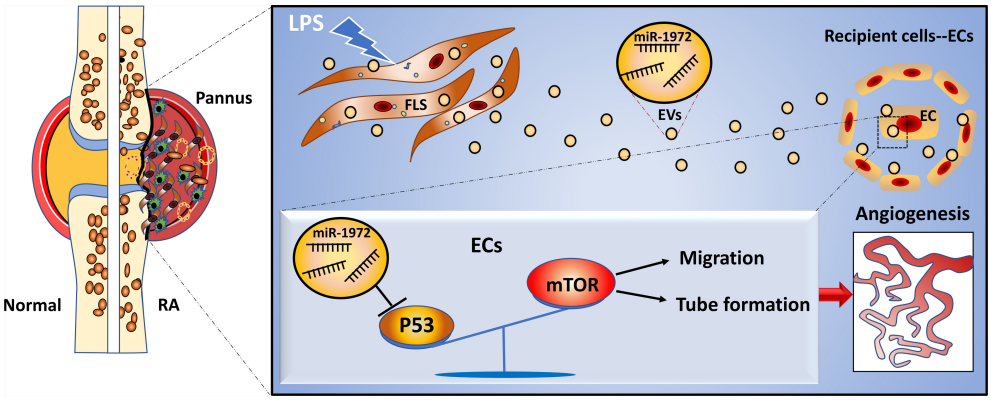

GRAPHICAL ABSTRACT |

INTRODUCTION

Rheumatoid arthritis (RA) is a systemic autoimmune disease principally effecting polyarticular synovitis and bone loss (1). In RA, synovial pannus is a driving pathological process that result in joint erosion (2). RA fibroblast-like synoviocytes (FLSs) are the predominant cell type in synovial intima (3). Furthermore, numerous evidences have indicated that pro-inflammatory cytokines activated RA FLSs possess lots of biological characteristics are similar to tumor cells, which further result in pannus generation and bone erosion *via* interacting with immune cells (4, 5). Therefore, targeting on RA-FLSs or combined with immune suppression can exert a therapeutic effect on RA (6). So far, the main pharmacologic treatments of RA are nonsteroidal anti-inflammatory drugs (NSAIDs), conventional and biologic disease-modifying antirheumatic drugs (DMARDs). However, about 30%-50% of RA patients cannot response to traditional DMARDs adequately (7). Interestingly, pirfenidone (PFD), a vascular targeted candidate, has been verified to suppress endothelial cells (ECs) migration and angiogenesis (8). Moreover, PFD can mitigate the pathological changes of CIA rats, and may serve as a potential drug for the treatment of RA (9).

Extracellular vesicles (EVs) are large parts of membrane-bound microparticles/microvesicles, apoptotic bodies, and exosomes (10). It has been accepted that EVs can mediate cell-to-cell communication by transferring their contents to target cells, alter cell transcription, and cell biological behaviors (11–13). Importantly, EVs exert functions predominantly relay on their contents, such as microRNA (miRNA), mRNA, and protein (14, 15). RA FLSs derived EVs have been documented to aggravate the severity of RA. They are shown to contain membrane-bound TNF-α, which further activate RA FLSs (16). The activated RA FLSs derived EVs can in turn exacerbate inflammatory and facilitate T cells resistant to apoptosis, forming a T cell-to-RA FLSs interaction feedback loop (16). Moreover, the active RA FLSs secrete pro-inflammatory cytokines, such as IL-6 and IL-8, which result in joint inflammation (17). Also, the RA FLSs produce matrix metalloproteinase-1 (MMP-1), MMP-3, MMP-9, and MMP-13, induce extracellular matrix (ECM) destruction and joint tissue breakdown (18). RA FLSs have been reported to activate endothelium and promote angiogenesis (19). Interestingly, CD13 was present in RA biological fluid (plasma, synovial fluid, FLSs culture supernatant), which presented in EVs (20). CD13 has been documented to promote ECs migration, tube formation *in vitro* and angiogenesis *in vivo* (21). Besides, it also has been reported that 80% ID1 in synovial fluid was wrapped in EVs of RA FLSs, the latter can further transmit into ECs to facilitate angiogenesis (19). Thus, it is clear that protein enveloped in RA FLSs derived EVs can promote ECs angiogenesis. However, whether miRNA involved in RA FLSs derived EVs can promote angiogenesis and the underlying mechanism remain unknown.

MicroRNAs (miRNAs) are short endogenous RNAs 19 to 25 nucleotides in size that modulate post-transcriptional silencing of target genes in plants and mammals (22–24). miRNA expression in RA FLSs has been identified to lead to the production of pro-inflammatory cytokines or metalloproteinases, increased proliferation and survival in RA FLSs (25). We have previously reported that RA FLSs derived miR-221-3p facilitate the tumor-like behavior of RA FLSs, down regulation of miR-221-3p can mitigate the tumor-like character (26, 27). Simultaneously, miRNA in RA FLSs derived exosomes have the potential to ignite local inflammation and attenuate osteoclastogenesis (25). Importantly, it has been documented that miRNA in EVs have the capacity to regulate the angiogenesis in cardiovascular and cerebrovascular diseases, immune inflammatory diseases, diabetes and tumors (28–30). However, whether RA FLSs derived miRNAs can regulate the angiogenesis is unclear.

miR-1972 is a rarely investigated miRNA that modulate the process of cancer. miR-1972 has been identified to affect cell viability, invasion and metastasis *via* a ceRNA network in osteosarcoma (31, 32). Additionally, it has been documented that a APCDD1L-AS1-miR-1322/miR-1972/miR-324-3p-SIRT5 axis facilitated icotinib-resistance by suppressing autophagic degradation of EGFR in lung adenocarcinoma. Interestingly, miR-1972 has been verified to decrease the proliferation, and/

or migration as well as tube formation of ECs in preeclampsia (33). However, whether miR-1972 exert the similar role in RA is unknown.

In this study, we investigated the key role of RA FLSs derived EVs on angiogenesis in vascular endotheliocyte. RA FLSs derived EVs expedited angiogenesis by enhancing endothelial cell migration and tube formation. Also, we confirmed that RA FLSs derived EVs can significantly facilitate angiogenesis of ECs with a matrigel angiogenesis mice model. We further observed both RNA and protein of EVs played roles in promoting ECs angiogenesis, but the component of RNA was more fundamental in this process. Using microRNA sequencing, miR-1972 in RA FLSs derived EVs were identified to modulate ECs angiogenesis *in vitro* and *in vivo*. The blockage of miR-1972 significantly abrogated the angiogenesis stimulative ability of RA FLSs derived EVs in ECs, while the overexpression of miR-1972 reversed the effect in ECs. Importantly, we also indicated that the p53 level was decreased, and the phosphorylated mTOR was upregulated in miR-1972 overexpressed ECs. Collectively, RA FLSs derived EVs can promote ECs angiogenesis *via* miR-1972 targeted p53/mTOR signaling, targeting on RA FLSs derived EVs or miR-1972 provides a promising strategy for the treatment of patients with RA.

RESULTS

Identification and Intracellular Localization of RA FLSs Derived EVs

The obtained RA FLSs or Trauma FLSs were identified by morphology imaging and flow cytometry. Both shape imaging and flow cytometry results indicated that RA FLSs and trauma FLSs shared similar morphology and phenotype (**Figure S1**). To obtain a dependable EVs, FLSs were cultured in EVs free FBS to avoid contamination of EVs from serum. Then, FLSs derived EVs were isolated from the supernatant according to the standard procedure. To be faithfully, we identified the obtained EVs from RA patients and trauma patients to confirm their purity. Using transmission electron microscopic image, we confirmed that both RA FLSs and trauma FLSs derived EVs were cup-shaped or spherical in morphology (**Figure 1A**). Moreover, we also measured the particle sizes distribution of the EVs. The results showed that the average particle sizes of the two EVs were at 209 nm (**Figure 1B**), which were consistent with the documented EVs in size (34). Next, we determined the EVs associated markers using western blotting to further confirm the EVs specificity. As expected, were showed CD9, CD63, CD81 and TSG101 were showed in the obtained EVs (**Figure 1C**). It is of vital that whether EVs can internalize into target cell and exert their functions. Therefore, we ought to assess whether EVs from RA FLSs and Trauma FLSs could be internalized by ECs. PKH67 (green) fluorescent labeled EVs were co-cultured with ECs, and the target ECs were labeled with DAPI. The immunofluorescence results indicated that both RA FLSs and Trauma FLSs derived EVs (green) were localized in the cytoplasm of ECs, and gathered around the nucleus of the target cells (blue), indicating that EVs were taken in by ECs (**Figure 1D**). Thus, by combining all those results above, we confirm the isolated EVs are dependable and have the capacity to localized in ECs.

RA FLSs Derived EVs Promote Tube Formation in ECs

Invasive pannus generation is a driving pathological process that result in joint erosion (2). The *in vitro* angiogenesis is often evaluated by the capacity of ECs to sprout, migrate, and form vascular tubules in a matrigel system (35). Therefore, we investigated the capacity of RA FLSs derived EVs to ECs angiogenesis, using transwell chamber system and matrigel system, individually. Trauma patients derived FLSs (Trauma FLSs) were used as negative control since they share similar morphological characteristics but lack pro-inflammatory properties to exclude the non-specific role of RA FLSs in angiogenesis assays. As expected, RA FLSs derived EVs dramatically facilitated tubules generation in matrigel system compared to Trauma FLSs derived EVs (**Figure 2A**, left panel). Both the relative tube length, relative junction count and relative mesh count in RA FLSs derived EVs were significantly higher than the control EVs (**Figure 2A**). Specifically, we also investigated the gradient effects of the angiogenesis of RA FLSs derived EVs at the concentration of 5 μg/mL to 100 μg/mL and the results indicated a dose-dependent effect (**Figure 2B**). Moreover, we further explored the capacity of RA FLSs derived EVs to expediting the migration in ECs. Our data showed that RA FLSs derived EVs can also facilitate the ECs migration compared to the control EVs (**Figure 2C**, left). However, RA FLSs derived EVs did not promote ECs proliferation at 24, 48 and 72 hours compared to the control EVs (**Figure S2**), indicating that RA FLSs derived EVs specifically facilitate ECs angiogenesis without affecting their proliferation at least within 24 hours. Thus, these data indicate that RA FLSs derived EVs promote angiogenesis by facilitating ECs tubule formation and migration.

The stimulative function of RA FLSs derived EVs on ECs *in vitro* does not necessarily reflect their functional capacity *in vivo*. Therefore, we developed a matrigel angiogenesis mice model. Briefly, matrigel mixed with ECs and EVs was injected subcutaneously into NOD SCID mice. Two weeks post the transplantation, blood vessels were analyzed with Masson and CD31 staining (**Figure 2D**, left and middle panel). RA FLSs derived EVs showed a higher ratio of vessels/total tissue than the control EVs. Likewise, the proportion of CD31+ ECs in RA FLSs derived EVs was much higher than the control EVs (**Figure 2E**, left and middle panel). Together, these results demonstrate that RA FLSs derived EVs play a key role in facilitating angiogenesis of ECs *in vitro* and the matrigel angiogenesis mice model.

LPS Stimulated RA FLSs Derived EVs Are More Powerful in Expediting Angiogenesis of ECs

Numerous studies have shown that cell surface expressed Toll-like receptor (TLR) is correlated with RA (34). Moreover, it has been documented that TLR2/4 is highly expressed in synovial

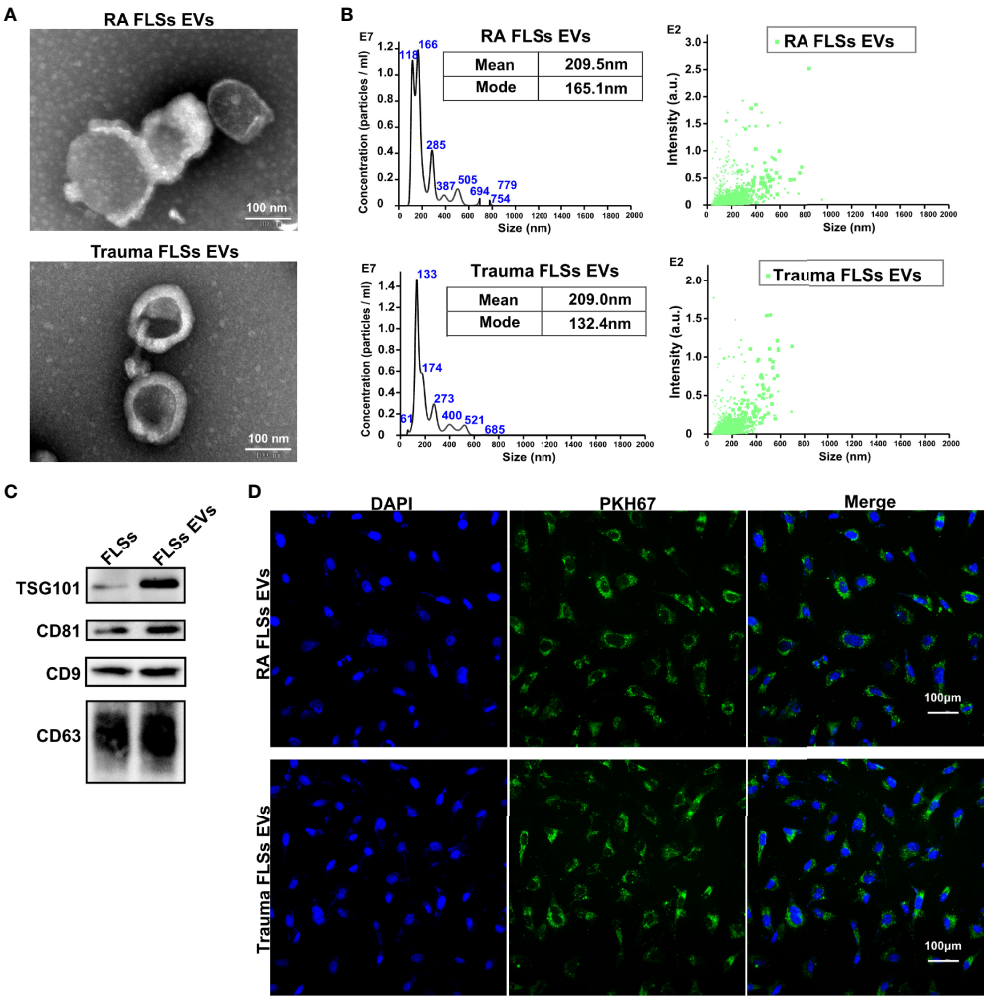

FIGURE 1 | Identification and intracellular localization of RA FLSs derived EVs. RA FLSs were obtained from RA patients. Cells were maintained in DMEM and passages 3-6 were used for the follow-up experiments. EVs were prepared as the established procedure. **(A)** Representative image of EVs photographed using transmission electron microscope (TEM). **(B)** Representative results of nanoparticle tracking analyses of EVs. **(C)** EVs markers of CD9, CD63, CD81 and TSG101 were showed by Western Blot. **(D)** Immunofluorescence image to show the interaction between ECs and EVs (Nucleus: blue, EVs: green). FLSs, fibroblast-like synoviocytes; ECs, endothelial cells; EVs, extracellular vesicles.

tissues and FLSs in RA patients (36, 37). Importantly, LPS from *P. gingivalis* activates TLR2 result in the upregulation of the extracellular matrix protein TSP1 (thrombospondin-1) and IL-33 in monocytes in RA patients (38). Additionally, TLR4 signaling can been induced by LPS in RA FLSs (37). However, whether LPS stimulated RA FLSs derived EVs also aggravate the angiogenesis of ECs and the underlying mechanism is unknown. Hence, we investigated the angiogenesis capacity of LPS stimulated RA FLSs derived EVs using the established systems above. Interestingly, the data showed that LPS stimulated RA FLSs derived EVs significantly promoted tubules generation in matrigel system compared to unstimulated RA FLSs derived EVs (**Figure 2A**, right panel). Both the relative tube length, relative junction count and relative mesh count in LPS stimulated RA FLSs derived EVs were significantly higher than the unstimulated EVs (**Figure 2A**). Furthermore, LPS stimulated RA FLSs derived EVs also facilitated the ECs migration compared to the unstimulated EVs (**Figure 2C**, right panel). Similarly, LPS stimulated RA FLSs derived EVs did not promote ECs proliferation within 24 hours compared to the unstimulated EVs (**Figure S2**). Collectively, our results suggest that the stimulation of RA FLSs with LPS can exacerbate the angiogenesis in ECs.

Additionally, pro-inflammatory cytokines represent a typical inflammatory milieu in RA patients. Therefore, we also compared the angiogenesis effects of pro-inflammatory cytokines IL-1β and TNF-α stimulated EVs respectively. Surprisingly, neither IL-1β nor TNF-α stimulated RA FLSs derived EVs can promote tubules generation in matrigel system compared to Trauma FLSs derived EVs (**Figure S3**). Both the relative tube length, relative junction count and relative mesh count in IL-1β or TNF-α stimulated RA FLSs derived EVs

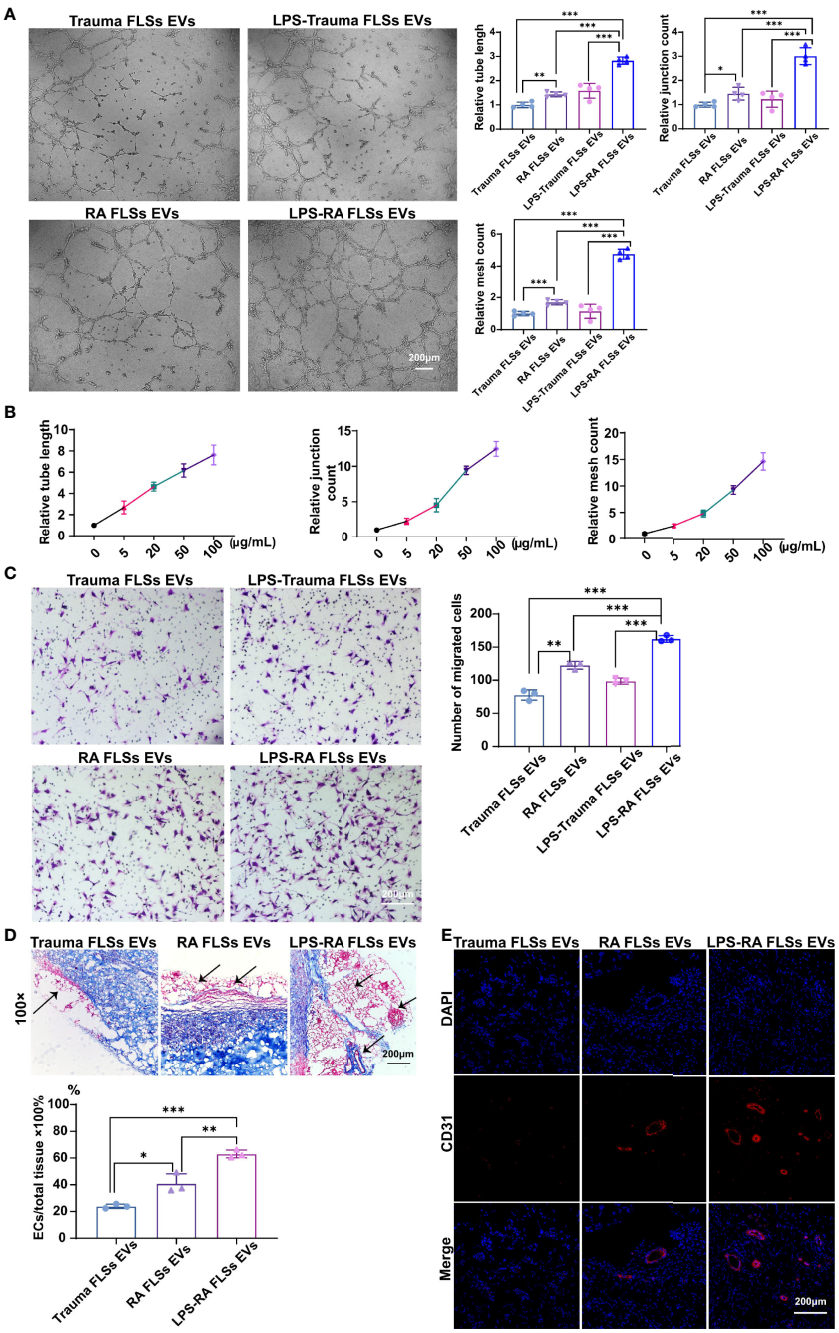

FIGURE 2 | RA FLSs derived EVs promote tube formation in ECs *in vitro* and *in vivo*. **(A–C)** RA FLSs or Trauma FLSs derived EVs were obtained using the established procedure and cultured with ECs in tubule formation system or migration system. For LPS stimulation, RA FLSs were cultured in DMEM with LPS (1 μg/mL) for 3 days. **(A)** The tubule formation capacity of RA FLSs derived EVs was determined. Representative photos (50×) were obtained using microscope imaging (panel upper). The results were summarized by calculating the related parameters (panel lower). **(B)** The dose-dependent effect of RA FLSs derived EVs stimulation of ECs tubule formation *in vitro*. The relative parameters are given. The line graph describes a summary of experiments at relative parameters as indicated (n = 3). **(C)** The migration capacity of RA FLSs derived EVs was determined by transwell chamber system. The final concentration of EVs was 50 μg/mL. Typical photos (100×) (panel left), summary data (panel right) are shown. The data indicate the mean ± S.E.M of three independent experiments. **(D, E)** FLSs derived EVs expedite tubule genesis in matrigel angiogenesis mice model. Matrigel mixed with ECs and EVs was injected subcutaneously into NOD SCID mice. Two weeks post the transplantation, blood vessels were analyzed with Masson and CD31 fluorescence staining. **(D)** Masson staining results. Typical photos (100×) (panel upper), summary data (panel lower) are shown. (Red represented endothelial cells and blood vessels, blue represented matrix gel; n=3). **(E)** CD31 fluorescence staining. Typical photos (100×) are shown. FLSs, fibroblast-like synoviocytes; ECs, endothelial cells; EVs, extracellular vesicles; LPS, lipopolysaccharide. (*P < 0.05, **P < 0.01, ***P < 0.001).

were not significantly increased than Trauma FLSs derived EVs. While LPS stimulated RA FLSs derived EVs can dramatically promote ECs angiogenesis compared to Trauma FLSs derived EVs with enhanced relative tube length, relative junction count and relative mesh count. In short, LPS stimulated EVs but not IL-1β or TNF-α stimulated EVs show enhanced capacities of ECs angiogenesis.

Next, we further investigated the angiogenesis capacity of LPS stimulated RA FLSs derived EVs *in vivo* using the developed matrigel angiogenesis mice model. Consistent with the results *in vitro*, LPS stimulated RA FLSs derived EVs were also efficiency in this model with an elevated ratio of vessels/total tissue than the unstimulated EVs (**Figure 2D**, middle and right panel). Accordingly, the proportion of CD31+ ECs in LPS stimulated RA FLSs derived EVs was dramatically increased than the unstimulated EVs (**Figure 2E**, middle and right panel). Thus, the stimulation of LPS to RA FLSs derived EVs facilitate angiogenesis of ECs in mice model as well.

RNA Parts in RA FLSs EVs Predominately Stimulate Angiogenesis in ECs

EVs exert their functions predominantly depend on the contents, such as microRNA (miRNA), mRNA, and protein (14, 15). RA FLSs derived EVs are capacity in expediting inflammation and bone erosion *via* membrane-bound TNF-α, IL-6 and IL-8, MMPs contained in the EVs (16–18). Importantly, CD13 and ID1 in RA FLSs derived EVs have been confirmed to facilitate angiogenesis in ECs (19, 21), indicating the proteins involved in RA FLSs derived EVs are able to promote angiogenesis. However, the angiogenesis function of RNAs in RA FLSs derived EVs remain unknown. To investigate the individual role of RNAs or proteins of LPS stimulated RA FLSs derived EVs in angiogenesis, we degraded RNAs or proteins in the EVs using RNase A or proteinase K separately. The efficacies of degraded RNAs or proteins were confirmed with RNA electrophoresis and protein silver staining (**Figures S4A, B**). Thereafter, the angiogenesis capacity was assessed with tubule formation system and migration system individually. The results revealed that both degradation of RNAs or proteins can abolish the tubule formation capacity of LPS stimulated RA FLSs derived EVs, but the effects of RNAs degraded EVs were more significant than the proteins degraded EVs (**Figure 3A**, upper panel). Accordingly, both the relative tube length, relative junction count and relative mesh count in RNAs or proteins depleted EVs were significantly lower than the untreated EVs, notably, the RNAs degraded EVs were much more significant than the proteins degraded EVs (**Figure 3A**, lower panel). However, the promotive capacities of proteins or RNA degraded EVs on ECs migration were indistinguishably decayed dramatically compared to the LPS stimulated RA FLSs derived EVs (**Figure 3B**), reflecting that tubule formation promotive capacities of RNAs and proteins in LPS stimulated RA FLSs derived EVs were embodied in different facets. Additionally, depletion of RNAs or proteins in LPS stimulated RA FLSs derived EVs indistinguishably maintained the proliferation promotive capacity of LPS stimulated RA FLSs derived EVs on ECs (**Figure S4C**), indicating that both RNA and protein parts paly roles in promoting ECs proliferation. Collectively, these data indicate that both RNAs and proteins are involved in the ECs angiogenesis stimulative function of LPS stimulated RA FLSs derived EVs, but RNA parts exert a major role in ECs tubule formation while protein parts mainly in ECs migration.

Deservedly, we verified the results in the matrigel angiogenesis mice model. As expected, the capacity of RNAs depleted EVs were maximizing abrogated in this model with a decreased ratio of vessels/total tissue compared to proteins degraded EVs (**Figure 3C**). Accordingly, the proportion of CD31+ ECs was also dramatically decreased than the proteins depleted EVs (**Figure 3D**). Thus, RNA parts in LPS stimulated RA FLSs derived EVs play key role in stimulating angiogenesis of ECs.

miR-1972 Is Upregulated in LPS Stimulated RA FLSs Derived EVs

miRNAs of RA FLSs has been verified to exert a pro-inflammatory role in local joints, modulate the tumor-like behavior of RA FLSs, and result in bone destruction (25–27). However, whether RA FLSs derived miRNAs can regulate the angiogenesis is unclear. Given the conclusion that RNA parts play a key role in facilitating the angiogenesis of ECs, we hypothesis that miRNA in EVs can predominantly regulate angiogenesis of ECs. To accurately identify which miRNAs may function mainly, the miRNA expressions in RA FLSs derived EVs were investigated using miRNA sequencing. In total of 31 miRNAs were significantly changed in the 630 scanned miRNAs in RA FLSs derived EVs, compared to Trauma FLSs derived EVs, with 13 up-regulated miRNAs and 18 down-regulated miRNAs ($P<0.05$; Fold change≥2) (**Figure 4A**). Furthermore, the miRNA expressions in LPS stimulated RA FLSs derived EVs were investigated. In total of 24 miRNAs were significantly changed in the 650 scanned miRNAs in LPS stimulated RA FLSs derived EVs, compared to Trauma FLSs derived EVs, with 13 up-regulated miRNAs and 11 down-regulated miRNAs ($P<0.05$; Fold change≥2) (**Figures 4B, C**). Next, we analyzed the possible biological functions of the expression changed miRNAs using GO analysis. Of note, the results showed that expression altered miRNAs may principally correlate with blood vessel morphogenesis, cardiovascular system development, vasculature development, tube development and some other biologic processes ($P < 0.05$) (**Figure 4D**), which was consistent with the conclusion that RNA parts play key role in stimulating angiogenesis of ECs. Subsequently, we further used KEGG analysis to investigate cellular functions of the expression changed miRNAs in EVs. The results showed that mTOR signaling pathway was the most enriched pathway (**Figure 4E**), which was documented related to angiogenesis in tumor microenvironment (39). It may signify that this pathway also exerts a parallel role in RA. Additionally, we further confirmed the up-regulated miRNAs with qPCR. Notably, miR-1972 and miR-12136 were identified highly expressed in RA FLSs derived EVs compared to Trauma FLSs derived EVs. However, the expression of miR-1972 in LPS stimulated RA FLSs derived EVs was higher than the unstimulated EVs

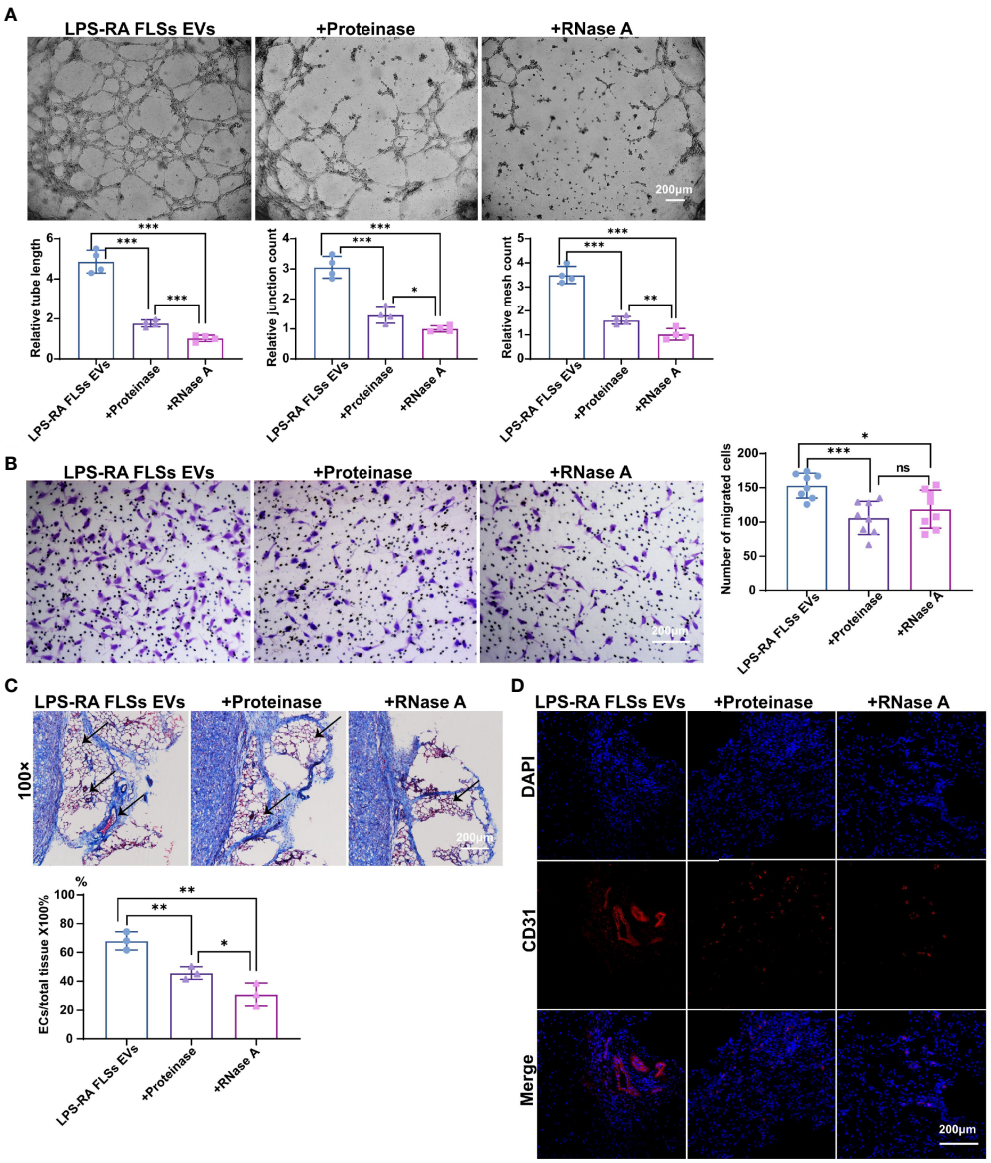

FIGURE 3 | RNAs parts in RA FLSs derived EVs played a pivotal role in promoting ECs angiogenesis. RA FLSs were stimulated with LPS for 3 days. EVs were then obtained using the established procedure. For RNA or protein degradation, EVs were incubated with RNase A or proteinase K. The angiogenesis capacities of EVs were evaluated using the established *in vitro* systems and mice model. **(A)** The tubule formation capacity of RA FLSs derived EVs was determined. Representative photos (50×) were obtained using microscope imaging (panel upper). The results were summarized by calculating the related parameters (panel lower). **(B)** The migration capacity of RA FLSs derived EVs was determined by transwell chamber system. The final concentration of EVs was 50 μg/mL. Typical photos (100×) (panel left), summary data (panel right) are shown. The data indicate the mean ± S.E.M of three independent experiments. **(C, D)** Access of EVs tubule genesis in mice model. **(C)** Masson staining results. Typical photos (100×) (panel upper), summary data (panel lower) are shown. (Red represented endothelial cells and blood vessels, blue represented matrix gel; n=3). **(D)** CD31 fluorescence staining. Typical photos (100×) are shown. (*P < 0.05, **P < 0.01, ***P < 0.001, ns, not significant).

(**Figure 4F**). Thus, by combining with the conclusion that the LPS stimulated RA FLSs can exacerbate the angiogenesis in ECs, miR-1972 is confirmed to mainly stimulate the angiogenesis.

miR-1972 Directly Stimulates Angiogenesis in ECs

To investigate whether miR-1972 can function directly in ECs, we established miR-1972 knock down system and overexpression system individually. The efficiencies of the knock down or overexpression were confirmed using qPCR analysis (**Figure S5**). Thereafter, the tubule generation capacities of ECs under the developed systems were performed. Definitely, tubule formation of ECs in miR-1972 knock down system was dramatically decayed compared to the negative control (**Figure 5A**, left and middle panel). Consequently, both the relative tube length, relative junction count and relative mesh

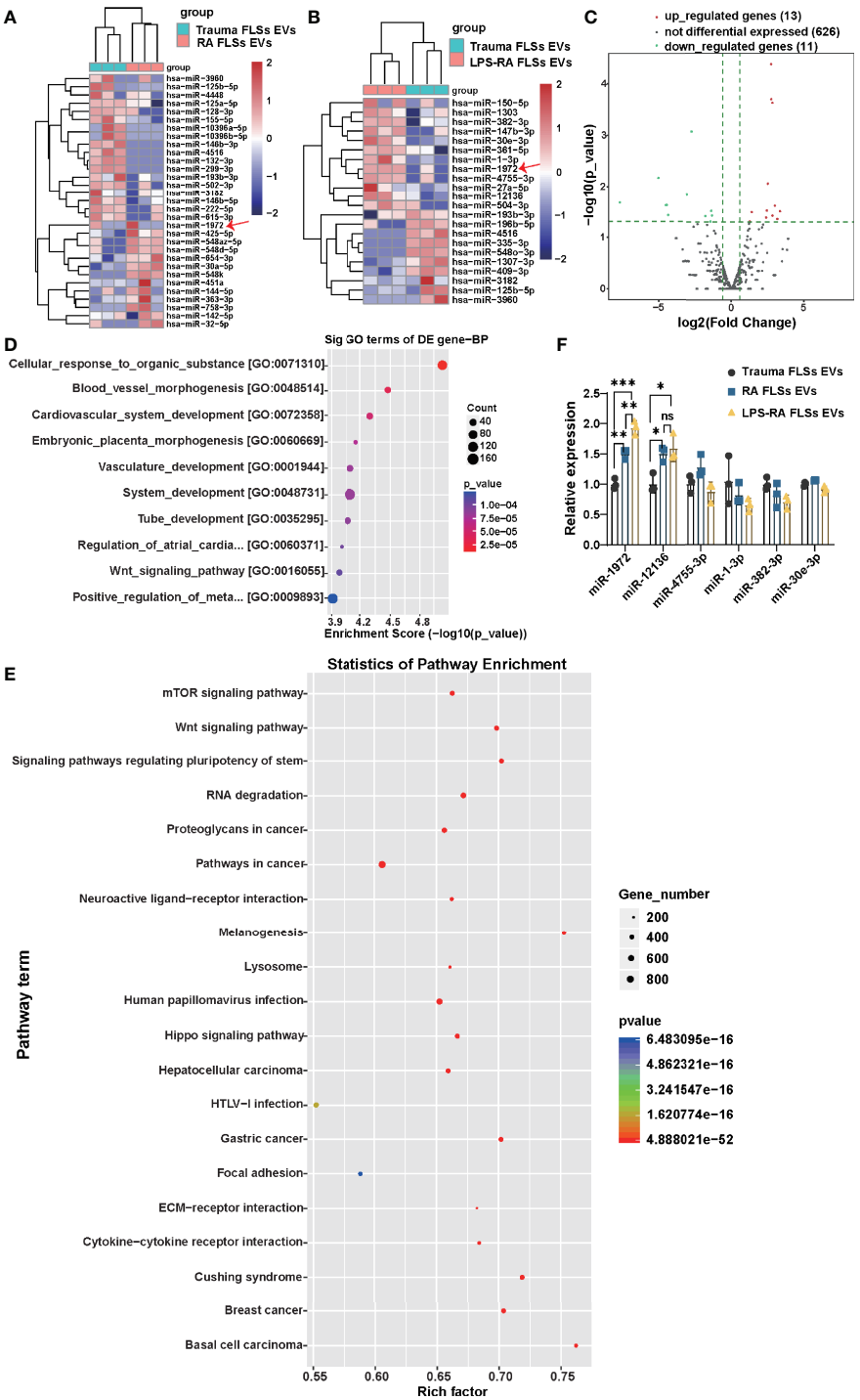

FIGURE 4 | miR-1972 is upregulated in LPS stimulated RA FLSs derived EVs. RNA-seq data of RA FLSs EVs or LPS stimulated RA FLSs EVs versus Trauma FLSs EVs were performed to verify the bioinformatic results. qPCR analysis of RA FLSs versus Trauma FLSs were used to confirm the RNA-seq results. **(A)** The Heat Map was used to show the RNA-seq data of distinguishable miRNA expression profiles in RA FLSs EVs versus Trauma FLSs EVs (fold changes >2 and P <0.05, n=3). **(B)** The Heat Map was used to show the RNA-seq data of distinguishable miRNA expression profiles in LPS stimulated RA FLSs EVs versus Trauma FLSs EVs (fold changes >2 and P <0.05, n=3). **(C)** Expression profile of LPS stimulated RA FLSs EVs versus Trauma FLSs EVs. The results were showed with the volcano plot. **(D, E)** The possible biological functions **(D)** and signaling pathways **(E)** of the differentially expressed miRNAs were analyzed by Gene Set Enrichment Analysis (GSEA) and Gene ontology (GO) analysis. The bubble chart was used to show the partial enrichment results. The color and size of each dot represents the enriched gene number in the GSEA reactome and GO Biological Process. **(F)** The expressions of miRNAs were verified by qPCR in Trauma FLSs EVs and RA FLSs EVs or LPS stimulated RA FLSs EVs. The data indicate the mean ± S.E.M of three independent experiments (n = 3, *P < 0.05, **P < 0.01, ***P < 0.001, ns, not significant).

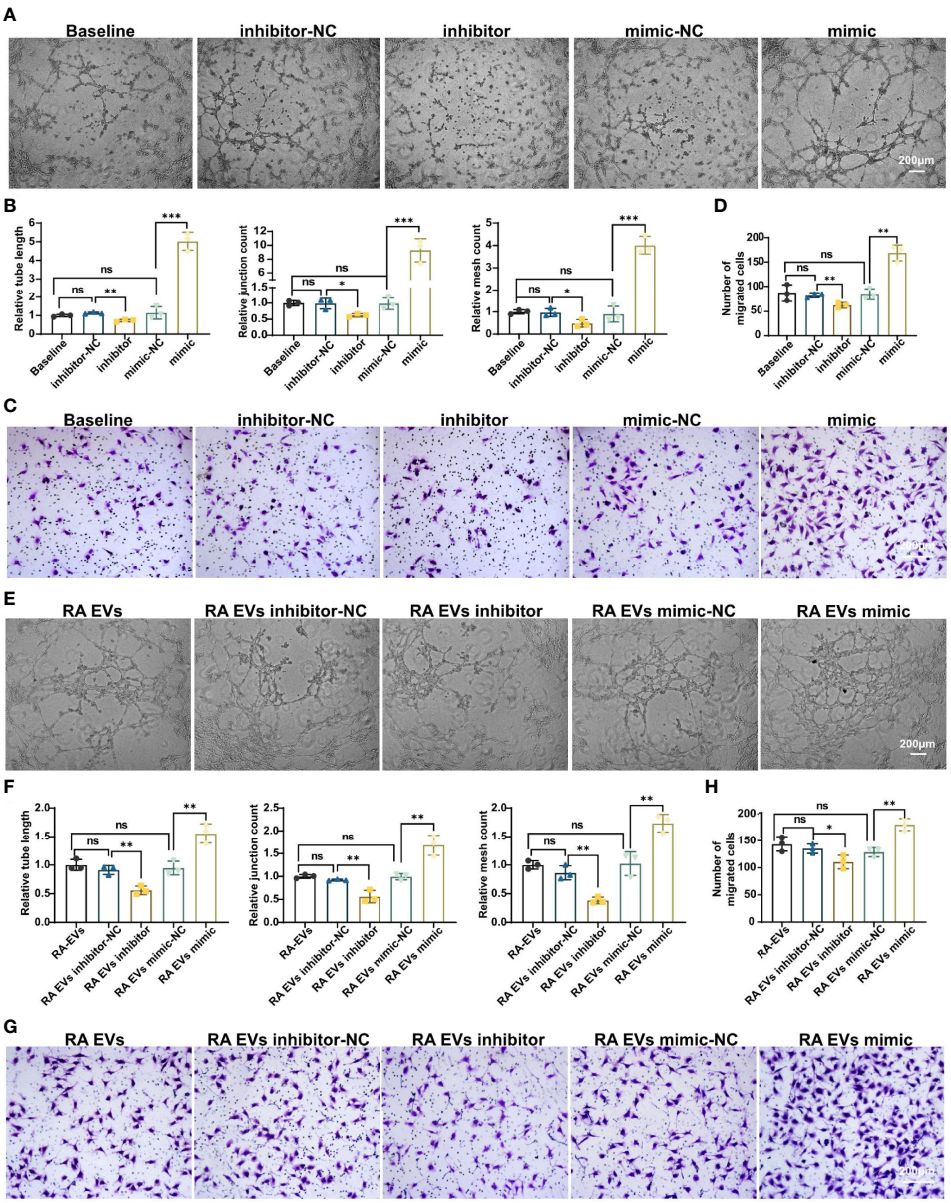

FIGURE 5 | miR-1972 regulates angiogenesis directly in ECs or mediated *via* RA FLSs derived EVs. **(A–D)** ECs in miR-1972 overexpression system or knock down system were prepared for tubule formation or migration detections. The tubule formation capacity of ECs was determined. Representative photos (50×) were obtained using microscope imaging **(A)**. The results were summarized by calculating the related parameters **(B)**. The migration capacity of ECs was determined by transwell chamber system. Typical photos (100×) **(C)**, summary data **(D)** are shown. RA FLSs derived EVs in miR-1972 overexpression system or knock down system were prepared for tubule formation or migration detections. The tubule formation capacity of ECs was determined. Representative photos (50×) were obtained using microscope imaging **(E)**. The results were summarized by calculating the related parameters **(F)**. The migration capacity of ECs was determined by transwell chamber system. Typical photos (100×) **(G)**, summary data **(H)** are shown. The data indicate the mean ± S.E.M of three independent experiments. (n = 3, *P < 0.05, **P < 0.01, ***P < 0.001, ns, not significant).

count in miR-1972 down regulated ECs were significantly decreased than the control ECs (**Figure 5B**). Reversely, both tubule formation and the relevant parameters in miR-1972 overexpression system were elevated (**Figures 5A, B**). Next, we explored the migration capacities of miR-1972 knock down or overexpressed ECs. The results also showed a reversed phenomenon (**Figures 5C, D**), indicating that miR-1972 can directly promote angiogenesis in ECs.

Furthermore, we explored the function of miR-1972 in RA FLSs derived EVs on angiogenesis of ECs using the miR-1972 knock down or overexpression systems. As expected, tubule formation of RA FLSs derived EVs in miR-1972 knock down system was

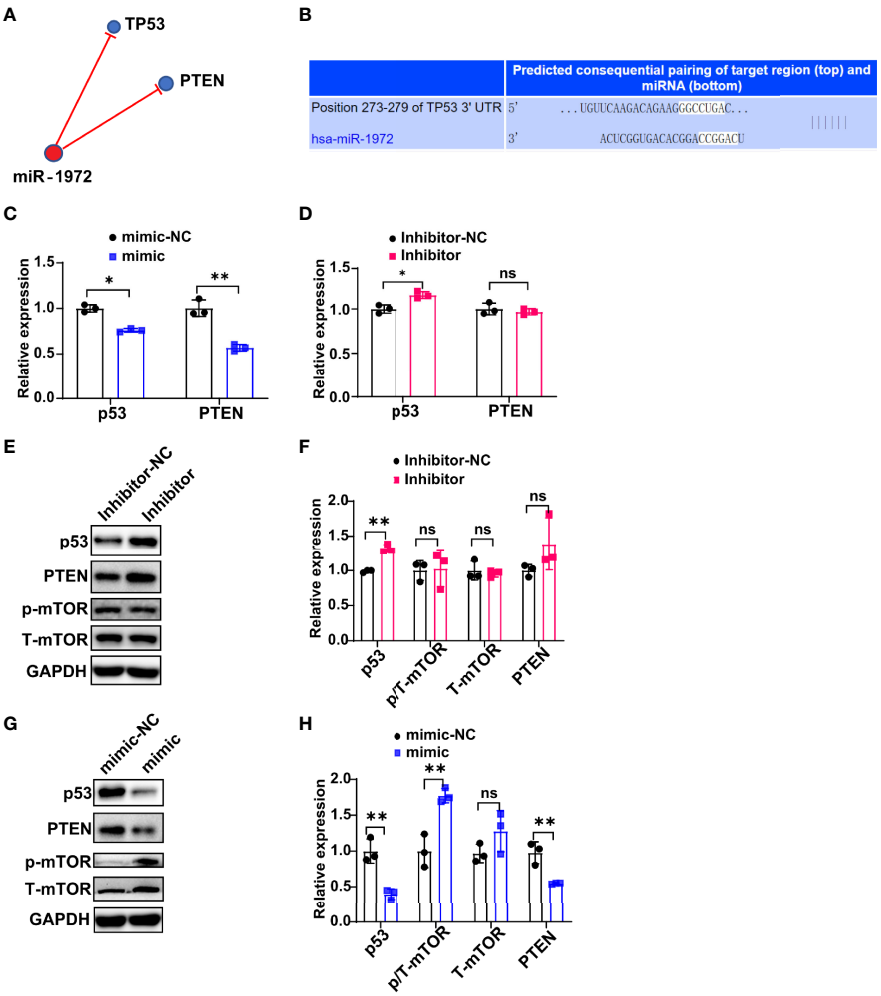

FIGURE 6 | miR-1972 exerts function *via* p53/mTOR signaling in ECs. **(A, B)** Potential related signaling of miR-1972 was predicted using a miRNA targets prediction website (TargetScan, http://www.targetscan.org/) **(A)**. The mRNA that miR-1972 targeted complementally was blasted using TargetScan **(B)**. **(C, D)** The expressions of ECs p53 and PTEN in miR-1972 overexpression system **(C)** or knock down system **(D)** were verified by qPCR. **(E, F)** The expression changes of ECs p53, PTEN and mTOR in miR-1972 knock down system were detected using western blotting. Typical photos **(E)**, summary data **(F)** are shown. **(G, H)** The expression changes of ECs p53, PTEN and mTOR in miR-1972 overexpression system were detected using western blotting. Typical photos **(G)**, summary data **(H)** are shown. The data indicate the mean ± S.E.M of three independent experiments. (n = 3, *P < 0.05, **P < 0.01, ns, not significant).

dramatically decreased compared to the negative control (**Figure 5E**, left and middle panel). Moreover, both the relative tube length, relative junction count and relative mesh count in miR-1972 down regulated EVs were significantly declined than the control ECs (**Figure 5F**). Importantly, the results were reversed when miR-1972 was overexpressed in RA FLSs derived EVs (**Figures 5E, F**). Congruously, expression alterations of miR-1972 in EVs also altered the ECs migration compared to the negative control EVs (**Figures 5G, H**). Together, these data indicated that miR-1972 act as a rheostat in expediting angiogenesis in ECs.

miR-1972 Exerts Function *via* p53/mTOR Signaling in ECs

To investigate the underlying mechanism that how miR-1972 exerts function, we predicted the potential related signaling of miR-1972 using a miRNA targets prediction website (TargetScan, http://www.targetscan.org/). The results showed that miR-1972 may negatively regulate TP53 (also known as p53) signaling and PTEN signaling (**Figure 6A**). Specifically, miR-1972 was predicted bind to TP53 mRNA complementally (**Figure 6B**). Next, we used the overexpression or knock down systems to verify if miR-1972 can modulate p53 signaling and PTEN signaling in ECs. The qPCR results revealed that both the mRNA levels of p53 and PTEN were decreased in the overexpression system (**Figure 6C**), while only p53 mRNA was reversed in the knock down system (**Figure 6D**), indicating that miR-1972 may function mainly *via* p53 signaling. Importantly, it has been reported that both p53 and PTEN pathways are involved in regulating angiogenesis. Therefore, we speculated that miR-1972 might expedite angiogenesis through p53 or

PTEN pathways. To explore the which pathways are more correlated to miR-1972 in ECs, we detected the changes of p53, PTEN, mTOR and phosphorylated mTOR in miR-1972 knock down or overexpression systems. The results showed that p53 but not PTEN level was significantly enhanced in miR-1972 knock down system (**Figures 6E, F**), which confirmed that miR-1972 function *via* p53 pathway. However, both p53 and PTEN levels were significantly decreased in miR-9172 overexpressed ECs ($P<0.01$) (**Figures 6G, H**). Inversely, phosphorylated mTOR was specifically elevated without changing total mTOR level (**Figures 6G, H**), implying that miR-1972 may enhance mTOR phosphorylation by negatively regulating p53 or PTEN levels. Collectively, these data indicate that miR-1972 promote angiogenesis specifically through negatively regulating p53 and then elevating mTOR phosphorylation.

DISCUSSION

Rheumatoid arthritis is a chronic autoimmune disease characterized by inflammation, polyarticular synovitis and bone loss (1). Pannus formation is one of the driving pathologic processes which can lead to the development of joint erosion in RA (2). The possibility of mitigating the generation of pannus by interfering with angiogenesis has been verified efficacy in animal models of arthritis. Thus, it is a potential target by blocking angiogenesis in the treatment of RA (8). Indeed, vascular targeted candidates have been developed in pre-clinic study (9). However, the current candidate development cannot meet the urgent demand of RA patients. Meanwhile, the underlying mechanisms of pannus generation in RA are not completely uncovered. Therefore, it is important to clarify the potential mechanism that contribute to RA pannus formation.

RA FLSs is a crucial determinant of RA pathogenesis that undergo abnormal activation by pro-inflammatory cytokines, interact with neutrophils to accelerate pathogenic adaptive immunity, and contribute to joint damage (40–42). Accumulating evidence showed activated RA FLSs possess lots of biological characteristics, such as hyperproliferation, migration and tissue invasion which are similar to tumor cells (27). The tumor-like biologic characteristics of RA FLSs are further lead to pannus formation, recruiting inflammatory cells infiltrate into local joints and resulting in cartilage destruction and bone erosion. Therefore, it is crucial to elucidate the underlying mechanism that how RA pannus is generated and form network with other cells in joint milieu. Here, consistent with others, we also confirmed that RA FLSs can promote ECs angiogenesis.

Pathologically, RA FLSs have been documented to regulate ECs angiogenesis by producing cytokines, growth factors, chemokines, and adhesion molecules. Also, RA FLSs derived EVs possess multifunction in expediting the pathology of RA by a T cell-to-RA FLSs interaction feedback loop. Here, we showed that RA FLSs derived EVs accelerate ECs angiogenesis by promoting ECs tube formation, migration and proliferation. Importantly, the EVs also function well in matrigel angiogenesis mice model with an increased tubule generation and CD31 expression in ECs. Moreover, LPS can activate RA FLSs result in the their pro-inflammatory phenotype (4, 38). In this study, interestingly, we clarified LPS stimulated RA FLSs also aggravate ECs angiogenesis, underlining the key role of RA FLSs in stimulating pannus formation in RA.

RA FLSs exert function through secreting multiple factors. miRNAs have been verified involved in regulating RA FLSs functions. miR-221-3p expedites tumor-like behavior of RA FLSs *via* uPAR pathway (27). miRNA-146a-5p can suppress pannus formation in CIA mice (2). miR-1972 has been identified to facilitate cell viability, invasion and metastasis *via* a ceRNA network in osteosarcoma (31, 32). Furthermore, a APCDD1L-AS1-miR-1322/miR-1972/miR-324-3p-SIRT5 axis has been investigated to facilitate icotinib-resistance by suppressing autophagic degradation of EGFR in lung adenocarcinoma. Importantly, miR-1972 has been verified to decrease the proliferation, and/or migration as well as tube formation of ECs in preeclampsia (33). Here, consistent with others, we show that miR-1972 promote angiogenesis through negatively regulating p53 and then elevating mTOR phosphorylation. Target on miRNAs may exert a therapeutic role in the treatment of RA. Local injection of liposomes with miR-17-5P mimic in arthritis mice joints can significantly alleviate inflammation and articular damage by directly targeting STAT3 and JAK/STAT pathways (43). Therefore, target on miR-1972 may also have a therapeutic effect in RA patients.

In terms of mechanism, lots of pathways have been documented function the tumor-like behavior of RA FLSs. SHH-JNK signaling has been verified to suppresses the aggressiveness of RA FLSs (44). uPAR-PI3K/Akt pathway promotes tumor-like behavior of RA FLSs (45). Also, numerous studies have revealed that the activation of PI3K/Akt/mTOR pathway is involved in ECs angiogenesis (46, 47), and p53 can suppress this pathway (48). Therefore, p53 is considered to be a key checkpoint of angiogenesis (49). In our study, consistent with others, we revealed that miR-1972 negatively regulates p53 level and enhances mTOR phosphorylation. In ECs angiogenesis, activated PI3K/Akt/mTOR pathway can promote the survival and proliferation of ECs (50). Here, we further confirmed that p53/mTOR signaling also involved in angiogenesis of ECs.

In summary, our data indicate that RA FLSs derived EVs promote ECs angiogenesis by enhancing migration and tube formation of ECs *in vitro* and a matrigel angiogenesis mice model. In terms of the mechanisms, miR-1972 is identified to facilitate ECs angiogenesis. The blockage of miR-1972 significantly abrogated the angiogenesis stimulative ability of RA FLSs derived EVs in ECs, while the overexpression of miR-1972 reversed the effect in ECs. Collectively, RA FLSs derived EVs can promote ECs angiogenesis *via* miR-1972 targeted p53/mTOR signaling (**Graphical Abstract**), targeting on RA FLSs derived EVs or miR-1972 provides a promising strategy for the treatment of patients with RA.

MATERIAL AND METHODS

Patients

Synovial tissues were collected from active RA patients undergoing synovectomy of the knee joint or total knee replacement surgery at the Third Affiliated Hospital of Sun Yat-sen University. RA patients were diagnosed according to the 2010 American College of Rheumatology/European League Against Rheumatism (ACR/EULAR) classification criteria. For negative control, synovial tissues were taken from nine patients who underwent arthroscopic surgery for severe joint trauma without other joint abnormalities or systemic diseases. The protocols were approved by the ethics committee of the Third Affiliated Hospital at Sun Yat-sen University, and all subjects provided written informed consent in accordance with the Declaration of Helsinki. For experiments, FLSs from each donor were employed in one experiment. At least three donors derived FLSs were used in all experiments.

Isolation of FLSs

FLSs were prepared as we previously reported (45). Briefly, synovial tissues were dissected and rinsed 2–3 times with phosphate-buffered solution (PBS), repeatedly shredded into ~ 1 mm^3 pieces, incubated in flasks. The flasks containing an appropriate amount of DMEM (Gibco) culture medium supplemented with 10% fetal bovine serum and were placed in 37°C, 5% CO_2 thermostatic incubator. The cells were considered as type B fibroblast-like synovial cells when the typical spindle-shaped, fibroblast-like appearance was present and surface marker CD90 was positive. FLSs from passages 3 to 6 were used for the following experiments.

Cell Line

Human umbilical vein endothelial cell line (EA. hy926) (51), was purchased from ATCC. Cells were cultured in High Glucose Dulbecco's Modified Eagle's Medium (DMEM; Gibco) containing 10% fetal bovine serum (FBS) and supplemented with 1% Penicillin and Streptomycin under 5% CO_2 at 37°C in a humidified atmosphere.

Identification of FLSs

The obtained FLSs were identified using the surface markers. The following fluorescence conjugated human mABs were used for flow cytometry analysis from BioLegend (San Diego, CA): APC-CD90 (5E10), PerCP/Cy5.5-CD11b (ICRF44), PE-CD29 (TS2116), APC-CD68 (Y1182A), FITC-CD44 (IM7). Cell subsets were stained with human antibodies and isotype control indicated above. Samples were examined using FACS Calibur flow cytometer and analyzed using Cell Quest Software (Becton, Dickinson). Final histogram figures were prepared with FlowJo Software (Tree Star, Ashland, OR).

Isolation of Extracellular Vesicles (EVs)

To obtain a dependable EVs, the any existed EVs in FBS were removed by centrifugation (100,000 g, at 4°C) for 24 hours. The upper serum was carefully collected and filtrated with a 0.22 μm needle filter for the next step. For the preparation of RA or Trauma FLSs derived EVs, the FLSs were incubated with EVs depleted FBS for 72 h. The supernatants were centrifuged at 300 g for 10 min, and another 3000 g for 20 min at 4°C to remove any cells and debris. Next, the supernatants were filtrated with 0.8 μm filter and then a Millipore 100 kD ultrafiltration tube to concentrate the supernatants. The EVs were extracted using QIAGEN's commercialized exoEasy Maxi Kit (Cat.No.76064). The isolated EVs can be directly used for identification, while for the functional experiments, the EVs was eluted twice with PBS in Millipore 100 kD ultrafiltration tube.

Identification of EVs

Morphology of EVs were examined with Transmission Electron Microscope (JEM-1200EX, Japan). Briefly, 10 μL of EVs suspension was loaded onto a carbon-coated copper grid, standing at room temperature. EVs was rinsed with PBS incubated with 3% phosphotungstic acid at room temperature for 5 min. After fixed at least 5 min, the grids were visualized and photographed with transmission electron microscope at 80 kV.

The size range of extracellular vesicles was analyzed with Nanoparticle Tracking Analysis (NTA, NanoSight NS300, Malvern, UK) (52). The particles can be automatically tracked and sized according to Brownian motion and diffusion coefficient. EVs were suspended in 1 mL PBS, while PBS alone was used as blank control. The temperature of NTA was 23 ± 0.5°C, the measurement time was 60 S (25 frames per second). Each sample was counted three times. The protein concentration in EVs was detected with BCA method.

Western Blot

Proteins were prepared as we previously documented (27). Total proteins were extracted from cells with RIPA lysis buffer mixed with phenylmethyl-sulfonyl fluoride (PMSF) and phosphatase inhibitor cocktail I (MedChemExpress, China). An equal amount of protein was separated on 10% or 12% SDS-PAGE gels based upon the molecular weight of the target protein and transferred to polyvinylidene difluoride (PVDF) membranes (Millipore, USA). Membranes were blocked with 5% bovine serum albumin (BSA) at room temperature for 1 h and then incubated overnight at 4°C with primary antibodies (anti-CD9 antibody, abcam, USA, #ab92726; anti-CD63 antibody, abcam, USA, #ab213090; anti-CD81 antibody, abcam, USA, #ab109201; anti-TSG101 antibody, abcam, USA, #ab83; anti-p53 antibody, abcam, USA, #ab179477; anti-PTEN antibody, Cell Signaling Technology, USA, #9559S; anti-mTOR antibody, Cell Signaling Technology, USA, #2983T; anti-phospho mTOR antibody, Cell Signaling Technology, USA, #5536T; anti-GAPDH antibody, SIGMA, USA, #G9545). Subsequently, proteins were detected by an enhanced chemiluminescence (ECL) system reagent (KeyGEN BioTECH, China) after incubated with horseradish peroxidase-conjugated secondary antibodies for 1 h at room temperature. Protein expression was calculated with Image J software and normalized to GAPDH expression.

Localization of EVs in ECs

For fluorescence staining of EVs, 20 μg RA FLSs or Trauma FLSs derived EVs were incubated with a fluorescent dye PKH67 for 5

min at room temperature, according to the instruction of MINI67-1KT(SIGMA). EVs were then washed twice with PBS. In total of 2.5×10^4 ECs were seeded on the cell slides in 24-well plate for adhesion. PKH67 labeled EVs were incubated with ECs for 24 h. Endothelial cell nuclei were stained with DAPI. Then, the images were viewed and captured using fluorescence microscope.

Tubule Formation Assay

To explore the angiogenesis capacity of EVs, tubule formation assay was employed as previously reported (53). Briefly, 60 μl of matrigel matrix (Corning, USA, #354262) was transferred to a prechilled 96-well plate, incubated at 4°C for 5 min, then placed at room temperature for 10 minutes, and finally at 37°C for 30-40 min. ECs were mixed with EVs, and the mixtures were added into the matrix slowly and evenly, the final number ECs were 3×10^4/well. Tubule formation was observed, and images were collected using inverted microscope (ZEISS, Germany) post 8 hours of culture. The number of meshes (NB meshes), junctions (NB Junctions) and total length of tube (Total length) were calculated with the angiogenesis plug-in of Image J software.

Cell Migration Assay

Cell migration experiments were carried out in a 24-well transwell chamber (Corning, Cambridge, with an aperture of 8 μm, MA, USA) system (27). In total of 5×10^3 cells were suspended in 2% fetal bovine serum and inoculated in the upper chamber. Then, 600 μl of medium containing 5% fetal bovine serum was added as a chemical inducer in the lower chamber. After incubation at 37°C in 5% CO_2 for 24 h, non-migratory cells were removed from the upper surface of the filter with cotton swabs. Cells that had migrated through the membrane were fixed in 4% paraformaldehyde (Boster, China) for 20 minutes, stained with crystal violet for another 20 minutes, and counted under a microscope. The number of migrated cells was calculated as the average number of cells passing through the membrane in five randomly selected regions.

CCK-8 Assay

For ECs proliferation experiment, CCK-8 assay was used as previously described with slight modifications (54). Specifically, ECs were inoculated in 96-well plates at different time points with different densities (6×10^3/well for 24 h, 5×10^3/well for 48 h, and 4×10^3/well for 72 h). After the cells adhered, FLSs derived EVs were added into the wells. Cells were incubated with CCK-8 (ESscience, China, #ES7011) at 37°C for 1 h protect from light. The absorbance was detected at 450 nm using BioTek Synergy H1MF(USA). The proliferation rate was expressed as the *OD* values. All the experiments were undertaken three times and showed as mean ± S.E.M.

Matrigel Angiogenesis Mice Model

To determine angiogenic potential of EVs *in vivo*, matrigel mixed with ECs and EVs was injected subcutaneously into NOD SCID mice (55). For the experiment setup, NOD SCID mice were assigned to three groups: Trauma FLSs EVs (500 μl matrigel and 1×10^6 ECs mixture), RA FLSs EVs (500 μl matrigel and 1×10^6 ECs mixture), and LPS stimulated RA FLSs EVs (500 μl matrigel and 1×10^6 ECs mixture). The final concentration of EVs was 150 μg/ml. Matrigel mixtures were subcutaneously injected into the lower dorsal region of SCID mice. Two weeks post the transplantation, the matrigel plugs were removed, fixed in 4% paraformaldehyde for 24 h. Then, the specimens were made to frozen slides for masson staining (Servicebio, China, #G1006) and CD31(Servicebio, China, #GB11063-2) immunofluorescence staining according to the instruction. Images were taken under a positive microscope (Leica, Germany), and the proportions of ECs and blood vessels were analyzed using image J.

Elimination of RNAs or Proteins in EVs

To remove RNAs or proteins of EVs, the EVs were put in liquid nitrogen for 1-2 minutes, and then dissolved in 37°C water bath for 2-3 minutes. EVs were underwent five freeze-thaw cycles as described previously (56). Thereafter, the EVs were treated with RNase A (Takara, 100 μg/mL, 37°C, 30 min) to degrade RNAs in EVs, followed by incubating with RNase A inhibitor (Takara, 2,000 units/mL, 37°C, 30 min) to inactivate RNase A. To degrade proteins, EVs were treated with proteinase K (Sigma, 25 μg/mL, 37°C, 30 min), followed by heating at 95°C for 5min to inactivate proteinase K.

Agarose Gel Electrophoresis of RNAs

Agarose gel (1.0%) was prepared with 1×TAE. RNAs of EVs were extracted and mixed with Loading Buffer. In the horizontal electrophoresis tank, the samples were electrophoresed at 80 V for 10-20 minutes. Images were taken with gel imager (Syngene, UK) to verify whether the RNAs was degraded.

Silver Staining of Proteins

To verify the degradation efficiency of EVs proteins, the proteins were electrophoresed on the 10% SDS-PAGE gel. Then the gel was silver stained with protein silver staining kit (Pierce™ Silver Stain for Mass Spectrometry, Thermo Fisher). Photos were taken to verify whether the EVs proteins were degraded.

EVs microRNA-Sequencing

Total RNA of EVs was extracted with trizol LS (Invitrogen, USA), and quantified with Nanodrop. Agarose electrophoresis was used for quality inspection, and library was constructed after passing the quality inspection. Then, Agilent 2100 Bioanalyzer was used to determine the quality of the library. RNA was denatured with 0.1 M NaOH and sequenced on Illumina NextSeq500. The sequencing results were compared well with the reference genome. The up-regulation or down-regulation of miRNA was defined according to the threshold of $P<0.05$ and fold change>2. The cluster diagram, scatter diagram and volcano diagram were drawn. The differential target genes of microRNAs were enriched by GO and analyzed by KEGG pathway.

GSEA and GO Analysis

Gene Set Enrichment Analysis (GSEA) and Gene Ontology (GO) analysis were used to identify characteristic biological processes in which miRNAs may participate. Gene Set Enrichment Analysis (GSEA) is a computational method that can determine whether a predefined set of genes show a

statistically significant and consistent difference between two biological states. GO analysis covers three domains: Biological Process, Cellular Component and Molecular Function.

Quantitative Real-Time Reverse Transcription PCR

Total RNA from cells was extracted using TRIzol RNA Reagent (Invitrogen, Carlsbad, CA, USA) in accordance with the manufacturer' s instructions, and total RNA from EVs was extracted using TRIzol LS Reagent (Invitrogen, Carlsbad, CA, USA). The main steps were shown in **Supplementary Table 1**. NanoDrop ND-2000 (Thermo Fisher Scientific, Waltham, MA) was used to measure the quantity and quality of RNA samples. To determine the relative expression and transfection efficiency of miR-1972, cDNA was synthesized by equal amounts of RNA from different samples using Mir-X miRNA First-Strand Synthesis Kit (Takara, Mountain View, CA, USA; #638313) and detected using TB GreenTM Premix Ex Taq^{TM}II PCR (Takara Bio-technology; #RR820A). All qPCR reactions were performed on ABI 7500 real-time PCR amplification equipment (Thermo Fisher, QuantStudio 5, USA). The PCR primers were listed in **Supplementary Table 2**. The relative expression of target genes was normalized to the internal reference genes U6 and was calculated using the $2^{-\triangle\triangle Ct}$ method.

Transfection of miR-1972 Mimic and Inhibitor

miR-1972 was down expressed or overexpressed using LIPO3000 and microRNA inhibitor or mimic systems in ECs (in 6-well plate, 2 mL system) and RA FLSs (in 100 mm dish, 6 mL system). Briefly, cells were seeded in 6-well plate (ECs) or 100 mm dish (FLSs) 18 h before transfection, and the cells reached 60% confluence. The specific transfection procedures were as follows (at room temperature): (1) Solution A was prepared: Opti-MEM (125 μL/mL) was mixed with LiPO3000 and incubated for 5 min. (2) Solution B was prepared: Opti-MEM (125 μL/mL) and miR-1972 inhibitor/mimic (and corresponding control) and incubated for 5 min. (3) The above A plus B solution was thoroughly mixed, incubated for 15-20 min, and cultured with DMEM containing 10% fetal bovine serum after 8 h incubation. Subsequent experiments were performed 3 days after infection.

Statistics

The data presented were derived from at least 3 independent experiments. Statistical analysis was performed by SPSS version 25.0 software (SPSS Inc., Chicago, IL, USA). Experimental data are presented as the mean ± Standard Error of Mean (S.E.M). Student's t-test was used for data comparison between two groups, and differences were considered statistically significant when P-values were less than 0.05.

DATA AVAILABILITY STATEMENT

The datasets presented in this study can be found in online repositories. The names of the repository/repositories and accession number(s) can be found below: https://www.ncbi.nlm.nih.gov/geo/query/acc.cgi?acc=GSE185672.

ETHICS STATEMENT

The research was approved by the ethics committee of the Third Affiliated Hospital at the Sun Yat-sen University and all subjects were given the written informed consent in accordance with the Declaration of Helsinki.

AUTHOR CONTRIBUTIONS

YLu, YFP, and YXC designed the experiments. YXC, JLD, XRL, MLW, and YLiu performed the experiments. XQL, WZW, and ZYH collected synovial tissues. YLiu, JRC, YC, XQL, XYS, and XB analyzed these data. YXC wrote the manuscript. YLu and YFP edited the manuscript. All authors contributed to the article and approved the submitted version.

FUNDING

This work was supported by grants provided from the National Natural Science Foundation of China (No.81771750), the National Natural Science Foundation of China (82101899 to YL) and China Postdoctoral Science Foundation Grant (2021M693658 to YL).

ACKNOWLEDGMENTS

We thank Prof. Hongwei Liu from Jinan University for the donation of human umbilical vein endothelial cell line (EA.hy926).

SUPPLEMENTARY MATERIAL

The Supplementary Material for this article can be found online at: https://www.frontiersin.org/articles/10.3389/fimmu.2022.793855/full#supplementary-material

Supplementary Figure S1 | Morphology and surface marker of the obtained FLSs. RA FLSs or Trauma FLSs were isolated according to the previous method. Morphology of the FLSs were imaged using microscope **(A, B)**. The phenotype of FLSs were detected using flow cytometry. Typical histogram figures of RA FLSs and Trauma FLSs are shown **(C)**.

Supplementary Figure S2 | RA FLSs derived EVs do not affect ECs proliferation. RA FLSs or Trauma FLSs derived EVs were obtained using the established procedure and cultured with ECs in proliferation system. For LPS stimulation, RA FLSs were cultured in DMEM with LPS (1 μg/mL) for 3 days. *OD* values were detected at 24, 48 and 72 hours, respectively. The summarized results are shown. The data indicate the mean ± S.E.M of three independent experiments. (*P < 0.05, **P < 0.01, ns, not significant).

Supplementary Figure S3 | Different pro-inflammatory cytokines stimulated EVs effect ECs angiogenesis. RA FLSs or Trauma FLSs derived EVs were obtained using the established procedure and cultured with ECs in tube formation system. For LPS

stimulation, RA FLSs were cultured in DMEM with LPS (1 μg/mL) for 3 days. For pro-inflammatory cytokines stimulation, RA FLSs were cultured in DMEM with IL-1β (1 ng/mL, R&D, 201-LB-010/CF) or TNF-α (10 ng/mL, PeproTech, 300-01A) for 3 days. The summarized results are shown. The data indicate the mean ± S.E.M of three independent experiments. (*P < 0.05, **P < 0.01, ns, not significant).

Supplementary Figure S4 | Efficiencies of RNase A or proteinase K in removing RNA or protein of EVs, and effects on ECs proliferation. RA FLSs were stimulated with LPS for 3 days. EVs were then obtained using the established procedure. For RNA or protein degradation, EVs were incubated with RNase A or proteinase K. For ECs proliferation assay, EVs were cultured with ECs in proliferation system. *OD* values were detected at day1. **(A)** RNA levels of RNase A disposed EVs are shown by agarose gel electrophoresis image. **(B)** Protein levels of proteinase K disposed EVs are shown by silver staining image. **(C)** The summarized ECs proliferation results are shown. The data indicate the mean ± S.E.M of three independent experiments. (*P < 0.05, **P < 0.01, ns, not significant).

Supplementary Figure S5 | The efficiencies of miR-1972 knock down or overexpression in RA FLSs or ECs. RA FLSs or ECs were cultured in 6-well plate. miR-1972 knock down or overexpression of RA FLSs or ECs were performed in the established systems. qPCR analysis of RA FLSs **(A)** or ECs **(B)** versus control were used to confirm the efficiencies of miR-1972 knock down or overexpression. The data indicate the mean ± S.E.M of three independent experiments (n = 3, *P < 0.05, **P < 0.01, ***P < 0.001, ns, not significant).

REFERENCES

1. Smolen JS, Aletaha D, Barton A, Burmester GR, Emery P, Firestein GS, et al. Rheumatoid Arthritis. *Nat Rev Dis Primers* (2018) 4:18001. doi: 10.1038/nrdp.2018.1
2. Sun W, Ma J, Zhao H, Xiao C, Zhong H, Ling H, et al. Resolvin D1 Suppresses Pannus Formation *via* Decreasing Connective Tissue Growth Factor Caused by Upregulation of miRNA-146a-5p in Rheumatoid Arthritis. *Arthritis Res Ther* (2020) 22(1):61. doi: 10.1186/s13075-020-2133-2
3. Bustamante MF, Garcia-Carbonell R, Whisenant KD, Guma M. Fibroblast-Like Synoviocyte Metabolism in the Pathogenesis of Rheumatoid Arthritis. *Arthritis Res Ther* (2017) 19(1):110. doi: 10.1186/s13075-017-1303-3
4. Bartok B, Firestein GS. Fibroblast-Like Synoviocytes: Key Effector Cells in Rheumatoid Arthritis. *Immunol Rev* (2010) 233(1):233–55. doi: 10.1111/j.0105-2896.2009.00859.x
5. Mo BY, Guo XH, Yang MR, Liu F, Bi X, Liu Y, et al. Long Non-Coding RNA GAPLINC Promotes Tumor-Like Biologic Behaviors of Fibroblast-Like Synoviocytes as MicroRNA Sponging in Rheumatoid Arthritis Patients. *Front Immunol* (2018) 9:702. doi: 10.3389/fimmu.2018.00702
6. Nygaard G, Firestein GS. Restoring Synovial Homeostasis in Rheumatoid Arthritis by Targeting Fibroblast-Like Synoviocytes. *Nat Rev Rheumatol* (2020) 16(6):316–33. doi: 10.1038/s41584-020-0413-5
7. Sparks JA. Rheumatoid Arthritis. *Ann Intern Med* (2019) 170(1):ITC1–ITC16. doi: 10.7326/AITC201901010
8. Leblond A, Allanore Y, Avouac J. Targeting Synovial Neoangiogenesis in Rheumatoid Arthritis. *Autoimmun Rev* (2017) 16(6):594–601. doi: 10.1016/j.autrev.2017.04.005
9. Gan D, Cheng W, Ke L, Sun AR, Jia Q, Chen J, et al. Repurposing of Pirfenidone (Anti-Pulmonary Fibrosis Drug) for Treatment of Rheumatoid Arthritis. *Front Pharmacol* (2021) 12:631891. doi: 10.3389/fphar.2021.631891
10. Withrow J, Murphy C, Liu Y, Hunter M, Fulzele S, Hamrick MW. Extracellular Vesicles in the Pathogenesis of Rheumatoid Arthritis and Osteoarthritis. *Arthritis Res Ther* (2016) 18(1):286. doi: 10.1186/s13075-016-1178-8
11. Bruno S, Grange C, Deregibus MC, Calogero RA, Saviozzi S, Collino F, et al. Mesenchymal Stem Cell-Derived Microvesicles Protect Against Acute Tubular Injury. *J Am Soc Nephrol* (2009) 20(5):1053–67. doi: 10.1681/ASN.2008070798
12. Neviani P, Fabbri M. Exosomic microRNAs in the Tumor Microenvironment. *Front Med (Lausanne)* (2015) 2:47. doi: 10.3389/fmed.2015.00047
13. Squadrito ML, Baer C, Burdet F, Maderna C, Gilfillan GD, Lyle R, et al. Endogenous RNAs Modulate microRNA Sorting to Exosomes and Transfer to Acceptor Cells. *Cell Rep* (2014) 8(5):1432–46. doi: 10.1016/j.celrep.2014.07.035
14. Corbeil D, Marzesco AM, Wilsch-Bräuninger M, Huttner WB. The Intriguing Links Between Prominin-1 (CD133), Cholesterol-Based Membrane Microdomains, Remodeling of Apical Plasma Membrane Protrusions, Extracellular Membrane Particles, and (Neuro)Epithelial Cell Differentiation. *FEBS Lett* (2010) 584(9):1659–64. doi: 10.1016/j.febslet.2010.01.050
15. Gibbings DJ, Ciaudo C, Erhardt M, Voinnet O. Multivesicular Bodies Associate With Components of miRNA Effector Complexes and Modulate miRNA Activity. *Nat Cell Biol* (2009) 11(9):1143–9. doi: 10.1038/ncb1929
16. Zhang HG, Liu C, Su K, Yu S, Zhang L, Zhang S, et al. A Membrane Form of TNF-Alpha Presented by Exosomes Delays T Cell Activation-Induced Cell Death. *J Immunol* (2006) 176(12):7385–93. doi: 10.4049/jimmunol.176.12.7385
17. Jüngel A, Distler O, Schulze-Horsel U, Huber LC, Ha HR, Simmen B, et al. Microparticles Stimulate the Synthesis of Prostaglandin E(2) *via* Induction of Cyclooxygenase 2 and Microsomal Prostaglandin E Synthase 1. *Arthritis Rheumatol* (2007) 56(11):3564–74. doi: 10.1002/art.22980
18. van Nieuwenhuijze AE, van de Loo FA, Walgreen B, Bennink M, Helsen M, van den Bersselaar L, et al. Complementary Action of Granulocyte Macrophage Colony-Stimulating Factor and Interleukin-17A Induces Interleukin-23, Receptor Activator of Nuclear Factor-κb Ligand, and Matrix Metalloproteinases and Drives Bone and Cartilage Pathology in Experimental Arthritis: Rationale for Combination Therapy in Rheumatoid Arthritis. *Arthritis Res Ther* (2015) 17(1):163. doi: 10.1186/s13075-015-0683-5
19. Edhayan G, Ohara RA, Stinson WA, Amin MA, Isozaki T, Ha CM, et al. Inflammatory Properties of Inhibitor of DNA Binding 1 Secreted by Synovial Fibroblasts in Rheumatoid Arthritis. *Arthritis Res Ther* (2016) 18:87. doi: 10.1186/s13075-016-0984-3
20. Morgan RL, Behbahani-Nejad N, Endres J, Amin MA, Lepore NJ, Du Y, et al. Localization, Shedding, Regulation and Function of Aminopeptidase N/CD13 on Fibroblast Like Synoviocytes. *PloS One* (2016) 11(9):e0162008. doi: 10.1371/journal.pone.0162008
21. Du Y, Lu C, Morgan RL, Stinson WA, Campbell PL, Cealey E, et al. Angiogenic and Arthritogenic Properties of the Soluble Form of CD13. *J Immunol* (2019) 203(2):360–9. doi: 10.4049/jimmunol.1801276
22. Lu TX, Rothenberg ME. MicroRNA. *J Allergy Clin Immunol* (2018) 141(4):1202–7. doi: 10.1016/j.jaci.2017.08.034
23. Bartel DP. MicroRNAs: Target Recognition and Regulatory Functions. *Cell* (2009) 136(2):215–33. doi: 10.1016/j.cell.2009.01.002
24. Carthew RW, Sontheimer EJ. Origins and Mechanisms of miRNAs and siRNAs. *Cell* (2009) 136(4):642–55. doi: 10.1016/j.cell.2009.01.035
25. Evangelatos G, Fragoulis GE, Koulouri V, Lambrou GI. MicroRNAs in Rheumatoid Arthritis: From Pathogenesis to Clinical Impact. *Autoimmun Rev* (2019) 18(11):102391. doi: 10.1016/j.autrev.2019.102391
26. Yang S, Yang Y. Downregulation of microRNA−221 Decreases Migration and Invasion in Fibroblast−Like Synoviocytes in Rheumatoid Arthritis. *Mol Med Rep* (2015) 12(2):2395–401. doi: 10.3892/mmr.2015.3642
27. Wang M, Chen Y, Bi X, Luo X, Hu Z, Liu Y, et al. LncRNA NEAT1_1 Suppresses Tumor-Like Biologic Behaviors of Fibroblast-Like Synoviocytes by Targeting the miR-221-3p/uPAR Axis in Rheumatoid Arthritis. *J Leukoc Biol* (2021). doi: 10.1002/JLB.3A0121-067RRR
28. Wu X, Liu Y, Wei W, Liu ML. Extracellular Vesicles in Autoimmune Vasculitis - Little Dirts Light the Fire in Blood Vessels. *Autoimmun Rev* (2019) 18(6):593–606. doi: 10.1016/j.autrev.2018.12.007
29. Wang Y, Wang L, Chen C, Chu X. New Insights Into the Regulatory Role of microRNA in Tumor Angiogenesis and Clinical Implications. *Mol Cancer* (2018) 17(1):22. doi: 10.1186/s12943-018-0766-4
30. Todorova D, Simoncini S, Lacroix R, Sabatier F, Dignat-George F. Extracellular Vesicles in Angiogenesis. *Circ Res* (2017) 120(10):1658–73. doi: 10.1161/CIRCRESAHA.117.309681
31. Zhou FC, Zhang YH, Liu HT, Song J, Shao J. LncRNA LINC00588 Suppresses the Progression of Osteosarcoma by Acting as a ceRNA for miRNA-1972. *Front Pharmacol* (2020) 11:255. doi: 10.3389/fphar.2020.00255

32. Wang Y, Zeng X, Wang N, Zhao W, Zhang X, Teng S, et al. Long Noncoding RNA DANCR, Working as a Competitive Endogenous RNA, Promotes ROCK1-Mediated Proliferation and Metastasis *via* Decoying of miR-335-5p and miR-1972 in Osteosarcoma. *Mol Cancer* (2018) 17(1):89. doi: 10.1186/s12943-018-0837-6
33. Lip SV, Boekschoten MV, Hooiveld GJ, van Pampus MG, Scherjon SA, Plösch T, et al. Early-Onset Preeclampsia, Plasma microRNAs, and Endothelial Cell Function. *Am J Obstet Gynecol* (2020) 222(5):497.e1–.e12. doi: 10.1016/j.ajog.2019.11.1286
34. Fu H, Hu D, Zhang L, Tang P. Role of Extracellular Vesicles in Rheumatoid Arthritis. *Mol Immunol* (2018) 93:125–32. doi: 10.1016/j.molimm.2017.11.016
35. Khoo CP, Micklem K, Watt SM. A Comparison of Methods for Quantifying Angiogenesis in the Matrigel Assay *In Vitro*. *Tissue Eng Part C Methods* (2011) 17(9):895–906. doi: 10.1089/ten.tec.2011.0150
36. Radstake TR, Roelofs MF, Jenniskens YM, Oppers-Walgreen B, van Riel PL, Barrera P, et al. Expression of Toll-Like Receptors 2 and 4 in Rheumatoid Synovial Tissue and Regulation by Proinflammatory Cytokines Interleukin-12 and Interleukin-18 *via* Interferon-Gamma. *Arthritis Rheum* (2004) 50 (12):3856–65. doi: 10.1002/art.20678
37. Gutierrez-Canas I, Juarranz Y, Santiago B, Arranz A, Martinez C, Galindo M, et al. VIP Down-Regulates TLR4 Expression and TLR4-Mediated Chemokine Production in Human Rheumatoid Synovial Fibroblasts. *Rheumatology (Oxford)* (2006) 45(5):527–32. doi: 10.1093/rheumatology/kei219
38. Arleevskaya MI, Larionova RV, Brooks WH, Bettacchioli E, Renaudineau Y. Toll-Like Receptors, Infections, and Rheumatoid Arthritis. *Clin Rev Allergy Immunol* (2020) 58(2):172–81. doi: 10.1007/s12016-019-08742-z
39. Conciatori F, Bazzichetto C, Falcone I, Pilotto S, Bria E, Cognetti F, et al. Role of mTOR Signaling in Tumor Microenvironment: An Overview. *Int J Mol Sci* (2018) 19(8):2453. doi: 10.3390/ijms19082453
40. Chen J, Liu M, Luo X, Peng L, Zhao Z, He C, et al. Exosomal miRNA-486-5p Derived From Rheumatoid Arthritis Fibroblast-Like Synoviocytes Induces Osteoblast Differentiation Through the Tob1/BMP/Smad Pathway. *Biomater Sci* (2020) 8(12):3430–42. doi: 10.1039/C9BM01761E
41. Ntougkos E, Chouvardas P, Roumelioti F, Ospelt C, Frank-Bertoncelj M, Filer A, et al. Genomic Responses of Mouse Synovial Fibroblasts During Tumor Necrosis Factor-Driven Arthritogenesis Greatly Mimic Those in Human Rheumatoid Arthritis. *Arthritis Rheumatol* (2017) 69(8):1588–600. doi: 10.1002/art.40128
42. Carmona-Rivera C, Carlucci PM, Moore E, Lingampalli N, Uchtenhagen H, James E, et al. Synovial Fibroblast-Neutrophil Interactions Promote Pathogenic Adaptive Immunity in Rheumatoid Arthritis. *Sci Immunol* (2017) 2(10):eaag3358. doi: 10.1126/sciimmunol.aag3358
43. Najm A, Masson FM, Preuss P, Georges S, Ory B, Quillard T, et al. miR-17-5p Reduces Inflammation and Bone Erosions in Collagen Induced Arthritis Mice and Directly Targets the JAK-STAT Pathway in Rheumatoid Arthritis Fibroblast-Like Synoviocytes. *Arthritis Rheumatol* (2020) 72(12):2030–9.
44. Zhu S, Ye Y, Shi Y, Dang J, Feng X, Chen Y, et al. Sonic Hedgehog Regulates Proliferation, Migration and Invasion of Synoviocytes in Rheumatoid Arthritis *via* JNK Signaling. *Front Immunol* (2020) 11:1300. doi: 10.3389/fimmu.2020.01300
45. Liu Y, Pan YF, Xue YQ, Fang LK, Guo XH, Guo X, et al. uPAR Promotes Tumor-Like Biologic Behaviors of Fibroblast-Like Synoviocytes Through PI3K/Akt Signaling Pathway in Patients With Rheumatoid Arthritis. *Cell Mol Immunol* (2018) 15(2):171–81. doi: 10.1038/cmi.2016.60
46. Wang W, Liu Y, You L, Sun M, Qu C, Dong X, et al. Inhibitory Effects of Paris Saponin I, II, and on HUVEC Cells Through Regulation of VEGFR2, PI3K/AKT/mTOR, Src/eNOS, PLCgamma/ERK/MERK, and JAK2-STAT3 Pathways. *BioMed Pharmacother* (2020) 131:110750. doi: 10.1016/j.biopha.2020.110750
47. Tian D, Xiang Y, Tang Y, Ge Z, Li Q, Zhang Y. Circ-ADAM9 Targeting PTEN and ATG7 Promotes Autophagy and Apoptosis of Diabetic Endothelial Progenitor Cells by Sponging Mir-20a-5p. *Cell Death Dis* (2020) 11(7):526. doi: 10.1038/s41419-020-02745-x
48. Luo YD, Fang L, Yu HQ, Zhang J, Lin XT, Liu XY, et al. P53 Haploinsufficiency and Increased mTOR Signalling Define a Subset of Aggressive Hepatocellular Carcinoma. *J Hepatol* (2021) 74(1):96–108. doi: 10.1016/j.jhep.2020.07.036
49. Wolf ER, Mabry AR, Damania B, Mayo LD. Mdm2-Mediated Neddylation of pVHL Blocks the Induction of Antiangiogenic Factors. *Oncogene* (2020) 39 (29):5228–39. doi: 10.1038/s41388-020-1359-4
50. Tas SW, Maracle CX, Balogh E, Szekanecz Z. Targeting of Proangiogenic Signalling Pathways in Chronic Inflammation. *Nat Rev Rheumatol* (2016) 12 (2):111–22. doi: 10.1038/nrrheum.2015.164
51. Abdollahi Govar A, Toro G, Szaniszlo P, Pavlidou A, Bibli SI, Thanki K, et al. 3-Mercaptopyruvate Sulfurtransferase Supports Endothelial Cell Angiogenesis and Bioenergetics. *Br J Pharmacol* (2019) 177(4):866–83. doi: 10.1111/bph.14574
52. Zheng X, Lu S, He Z, Huang H, Yao Z, Miao Y, et al. MCU-Dependent Negative Sorting of miR-4488 to Extracellular Vesicles Enhances Angiogenesis and Promotes Breast Cancer Metastatic Colonization. *Oncogene* (2020) 39(46):6975–89. doi: 10.1038/s41388-020-01514-6
53. Arnaoutova I, Kleinman HK. *In Vitro* Angiogenesis: Endothelial Cell Tube Formation on Gelled Basement Membrane Extract. *Nat Protoc* (2010) 5 (4):628–35. doi: 10.1038/nprot.2010.6
54. Wang YJ, Zhou SM, Xu G, Gao YQ. Interference of Phenylethanoid Glycosides From Cistanche Tubulosa With the MTT Assay. *Molecules* (2015) 20(5):8060–71. doi: 10.3390/molecules20058060
55. Malinda KM. In Vivo Matrigel Migration and Angiogenesis Assay In: S Martin, C Murray. editor. *Angiogenesis Protocols*. Nottingham, UK: Humana Press (2009). pp. 287–94. doi: 10.1007/978-1-59745-241-0_17
56. Zhang H, Liu J, Qu D, Wang L, Wong CM, Lau CW, et al. Serum Exosomes Mediate Delivery of Arginase 1 as a Novel Mechanism for Endothelial Dysfunction in Diabetes. *Proc Natl Acad Sci U S A* (2018) 115(29):E6927–E36. doi: 10.1073/pnas.1721521115

Conflict of Interest: The authors declare that the research was conducted in the absence of any commercial or financial relationships that could be construed as a potential conflict of interest.

frontiers in Immunology

ORIGINAL RESEARCH
published: 18 March 2022
doi: 10.3389/fimmu.2022.850993

Integrated Bioinformatics and Validation Reveal IL1B and Its Related Molecules as Potential Biomarkers in Chronic Spontaneous Urticaria

*Shixiong Peng[1], Teng Zhang[2], Sisi Zhang[3], Qian Tang[1], Yang Yan[1] and Hao Feng[1]**

[1] Department of Dermatology, The First Affiliated Hospital of Hunan Normal University/Hunan Provincial People's Hospital, Changsha, China, [2] Department of Dermatology, Chinese Traditional Hospital of Changsha, Changsha, China, [3] Nursing Department, Hunan Provincial People's Hospital/The First Affiliated Hospital of Hunan Normal University, Changsha, China

OPEN ACCESS

Edited by:
Richard Williams, University of Oxford, United Kingdom

Reviewed by:
Basavaraj Mallikarjunayya Vastrad, KLE Society's College of Pharmacy, India
Ilaria Puxeddu, University of Pisa, Italy

***Correspondence:**
Hao Feng
doctorfenghao@126.com

Specialty section:
This article was submitted to Autoimmune and Autoinflammatory Disorders, a section of the journal Frontiers in Immunology

Received: *08 January 2022*
Accepted: *22 February 2022*
Published: *18 March 2022*

Citation:
Peng S, Zhang T, Zhang S, Tang Q, Yan Y and Feng H (2022) Integrated Bioinformatics and Validation Reveal IL1B and Its Related Molecules as Potential Biomarkers in Chronic Spontaneous Urticaria. Front. Immunol. 13:850993. doi: 10.3389/fimmu.2022.850993

Background: The etiopathogenesis of chronic spontaneous urticaria (CSU) has not been fully understood, and there has been extensive interest in the interaction between inflammatory dermatosis and pyroptosis. This study intends to investigate the molecular mechanism of pyroptosis-related genes in CSU *via* bioinformatic ways, aiming at identifying the potential key biomarker.

Methods: GSE72540, the RNA expression profile dataset of CSU, was utilized as the training set, and GSE57178 as the validation set. Differently expressed pyroptosis-related genes (DEPRGs), GO, KEGG, and DO analyses were performed. The hub genes were explored by the protein–protein interaction analysis. Moreover, CIBERSORT was employed for estimating immune cell types and proportions. Then, we constructed a DEmRNA–miRNA–DElncRNA ceRNA network and a drug–gene interaction network. Finally, ELISA was used for gene expression analysis.

Results: We recognized 17 DEPRGs, whose enrichment analyses showed that they were mostly enriched in inflammatory response and immunomodulation. Moreover, 5 hub genes (IL1B, TNF, and IRF1 are upregulated, HMGB1 and P2RX7 are downregulated) were identified *via* the PPI network and verified by a validation set. Then immune infiltration analysis displayed that compared with normal tissue, CSU owned a significantly higher proportion of mast cells activated, but a lower proportion of T cells CD4 naive and so on. Furthermore, IL1B was statistically and positively associated with mast cells activated in CSU, and SNHG3, the upstream factor of IL1B in the ceRNA we constructed, also related with mast cells in CSU. Further analysis exhibited that the protein subcellular localization of IL1B was extracellular, according with its intercellular regulation role; IL1B was significantly correlated with key immune checkpoints; and the NOD-like receptor signaling pathway was the mainly involved pathway of IL1B based on the couple databases. What is more, the result of ELISA of CSU patients was the same as the above analyses about IL1B.

In addition, the drug–gene interaction network contained 15 potential therapeutic drugs targeting IL1B, and molecular docking might make this relationship viable.

Conclusion: IL1B and its related molecules might play a key role in the development of CSU and could be potential biomarkers in CSU.

Keywords: chronic spontaneous urticaria (CSU), pyroptosis-related genes, IL1B, bioinformatics, inflammation, immunology

INTRODUCTION

Chronic spontaneous urticaria (CSU) is one of chronic inflammatory dermatosis, which is delineated as, for recognized or unrecognized causes, angioedema, wheal, or both occurring spontaneously for more than 6 weeks (1). The CSU's prevalence is approximately 1% of the population (lifetime prevalence = 1.4%; point prevalence = 0.7%) (2). Moreover, CSU will get the increase of risk for comorbid autoimmune diseases like autoimmune thyroid disease (3). The frequently recurring symptoms, pruritus, urticaria, and angioedema, severely affect patients' performance at school and work and impair their quality of life, which brings much encumbrance to both their households and society (4). Unlike acute urticaria, which is usually caused by an identifiable agent like an allergic reaction to a drug or other, the cause and pathogenesis of CSU are complex and remain largely unclear (5). Consequently, it is of great significance for individualized and effective treatment to reveal the pathogenesis and recognize key biomarkers of CSU.

The CSU's etiopathogenesis has not been totally uncovered, but the existing studies suggest that maladjustment of inflammatory cells (such as mast cells and basophils) is the potentially core contributor (6). It is well known that a series of intracellular signaling cascades result in mast cell activation, after IgE bonds to the high-affinity IgE receptor. The activated mast cell releases proteases, histamines, and cytokines with the generation of platelet-activating mediators and other arachidonic acid metabolites (leukotrienes C4, D4, and E4 and prostaglandin D2). These cytokines give rise to vascular permeability and increased vasodilation, ensuing interstitial edema and sensory nerve stimulation and causing the obvious itchiness, redness, and swelling (7, 8). Besides, some CSU patients could show signs of activation of the coagulation/fibrinolytic system, such as significant elevation of serum factors like D-dimer, sICAM-1, and sVCAM-1 (9, 10). In this setting, some treatment strategies were developed, such as antihistamine, biological agent, and immunosuppressant. The first-line symptomatic treatment for CSU is largely depending on modern 2nd-generation H1 antihistamines, but standard-dosed antihistamines are ineffective in about 40% of the patients (11). Omalizumab, a humanized anti-IgE antibody, is the first licensed biological treatment by the Food and Drug Administration (FDA) for patients with CSU refractory to H1 antihistamines. However, relapse rates following the withdrawal of omalizumab are high (12). Ciclosporin is recommended for combination treatment in patients with severe disease refractory. Nevertheless, it is a problem which cannot be ignored that long-term use of ciclosporin leads to serious side effects (13). It can thus be seen that complete control of symptoms in the majority of patients remains a worldwide challenge. Consequently, further and fuller exploring the inflammatory reaction pathogenesis of CSU is scientifically significant to the clinical therapy.

There has been extensive interest in the interaction between inflammatory reaction and pyroptosis. The pyroptosis is denoted as inflammasome-dependent cell death (14). It was found that it makes a critical difference in the development of numerous inflammatory skin diseases. A research reported that Mdivi-1 significantly suppressed the pyroptotic cell death of keratinocytes and inhibited NLRP3 inflammasome activation to play a protective role in atopic dermatitis (15). Deng et al. indicated that cycloastragenol could inhibit the liberation of inflammatory mediators and macrophage infiltration in psoriasis by inhibiting the pyroptosis which NLRP3 mediated (16). In addition, previous research has established that aberrant NLRP3 inflammasome activation in masts cell contributes to histamine-independent urticaria by production of IL-1β in cryopyrin-associated periodic syndromes (CAPSs) (17). However, our understanding of CSU with pyroptosis is still pretty limited.

Microarray technology has been widely utilized into biological studies in recent years, and the data generated by it like the mRNA dataset could be an advantageous instrument for discovering critical factors of etiopathogenesis of diseases, which offers valuable insulation and foundation for further novel studies (18, 19). In this study, *via* applying the bioinformatic method, we analyzed the data of the Gene Expression Omnibus (GEO) (20), which has its origin in microarray technology, to explore immune cell infiltration and ceRNA network, and further reveal the molecular mechanism of pyroptosis-related genes in CSU and identify key biomarkers.

MATERIAL AND METHOD

Microarray Data Source

The analysis process of this study is shown in **Figure 1**. We downloaded the datasets (GSE72540, GSE57178) from the GEO database (**Table 1**). GSE72540 contained 31 samples' RNA expression profiling, selecting 10 CSU samples and 8 control samples, and GSE57178 contained 18 samples, selecting 6 CSU samples and 7 control samples.

Identifying Differently Expressed Pyroptosis-Related Genes

We normalized and preprocessed data and identified the different expression genes (DEGs) among the CSU sample and

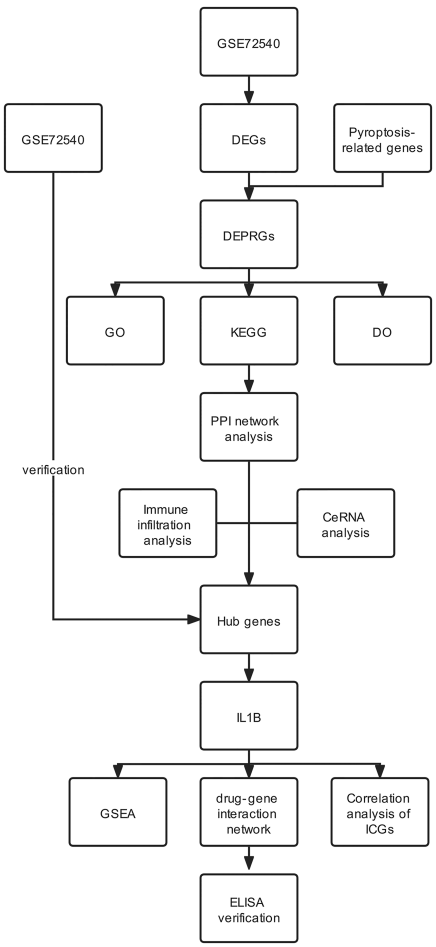

FIGURE 1 | Flowchart of the study.

control *via* the GEO2R tool (21). $|\log_2 FC| > 1$ and $p < 0.05$ as the cutoff. The 161 pyroptosis-related genes (PRGs) were downloaded from the GeneCards database (**Supplementary Table S1**) (22). Altogether consistent genes between DEGs and PRGs were identified as differently expressed pyroptosis-related genes (DEPRGs).

GO, KEGG, and DO Enrichment Analyses of DEPRGs

GO enrichment analysis [included MF (molecular function), BP (biological process), and CC (cellular component)] and KEGG pathway analysis were executed *via* the Metascape database (23). Min Enrichment ≥1.5, Min Overlap ≥3, and $p < 0.01$ were considered as the threshold. The WebGestalt tool (24) was used for DO enrichment analysis, and FDR ≤ 0.05 as the significance level.

Protein–Protein Interaction Network and Module Analyses

To investigate the protein–protein interaction (PPI) network, we used the STRING tool (25) and visualized it and analyzed the interactions of DEPRGs by the Cytoscape software (26).

TABLE 1 | Details of the GEO CSU data.

Dataset	Platform	Number of samples (CSU/control, subjects)
GSE72540	GPL16699	31 (10/8 18)
GSE57178	Agilent-039494 SurePrint G3 Human GE v2 8x60K Microarray 039381 (Feature Number version) GPL6244 [HuGene-1_0-st] Affymetrix Human Gene 1.0 ST Array [transcript (gene) version]	18 (6/7 13)

GEO, Gene Expression Omnibus; CSU, chronic spontaneous urticaria.

The Molecular Complex Detection (MCODE) plug-in was utilized for the module analysis of the PPI network. The cytoHubba tool was used for identifying the hub genes. The hub genes' GO enrichment analysis was performed through the ClueGO plug-in.

Data Verification

The RNA expressed dataset GSE57178, containing 6 CSU lesion samples and 7 healthy control samples, was utilized as the validation set to verify the reliability of hub genes.

Immune Infiltration Analysis

The immune infiltration was calculated by the web tool CIBERSORT (27), which is a deconvolution algorithm that can evaluate the proportion of 22 infiltrating lymphocyte subsets in a large number of tissue samples. The GraphPad Prism 8.0.2 (San Diego, CA, USA) tool (28) was utilized for the correlation analysis between different immune cells, and between immune cells and hub genes, calculating the ratio of every kind of immune cell in CSU tissue and control.

Exploration ceRNA Network of the Hub Genes

To explore the miRNA–mRNA interaction of the ceRNA network, the potential miRNAs targeting the hub gene were identified *via* the TargetScan (29), miRNet (30), and DIANA TOOLS TarBase v.8 databases (31). If this was concurrently recognized in each database, the result was considered as true. Next, the possible lncRNAs targeting the miRNA were predicted through the miRNet database, which was cross-checked with the differently expressed lncRNA (DElncRNA) of CSU. LncRNA subcellular localization was predicted using lncLocator (32). The web-based tools, Wei Sheng Xin (http://www.bioinformatics.com.cn) and Draw Venn Diagram (http://bioinformatics.psb.ugent.be/webtools/Venn/), were used for data visualization.

Gene Set Enrichment Analysis

The Gene Set Enrichment Analysis (GSEA) tool (33) was used for exploring the molecular signaling pathway in which IL1B might be involved in CSU. The pathway enrichment analysis utilized the c2.cp.kegg.v7.3.symbols.gmt gene sets of the official website. False discovery rate q-value <0.01 was regarded as difference.

Analysis of Protein Subcellular Localization and Correlation With Immune Checkpoints

The protein subcellular localization of IL1B was predicted using the Cell-PLoc 2.0 tool (34), which is a package of web servers for predicting subcellular localization of proteins in different organisms. The correlation between IL1B and key immune checkpoints (35) such as HAVCR2(TIM3), LAG3, CTLA4, CD274(PDL1), PDCD1(PD1), and TIGIT were analyzed *via* Pearson's correlation coefficient in GraphPad Prism 8.0.2.

Drug–Gene Interaction and Molecular Docking Analysis

To explore the drug–gene interaction, the DrugBank database (36) was utilized for identifying existing or/and potentially associated drug substances. Moreover, the Cytoscape software was utilized for data visualization. The molecular structure of the ligand and the target protein were obtained from the PubChem database (37) and PDB database (38). Docking simulations were conducted through AutoDock Vina (39) to generate the docking energy. The PyMOL software (40) was performed to visualize docked complexes.

Enzyme-Linked Immunosorbent Assay

To examine the protein levels of IL1B, NLRP3, and mast cell tryptase (MCT), serums from 10 CSU patients and 10 healthy controls were harvested for enzyme-linked immunosorbent assay (ELISA) (the CSU patients without medical treatment within 2 weeks and concomitant autoimmune diseases, whose detailed information is in **Supplementary Table S2**). Specific ELISA kits for IL1B (Neobioscience, Shenzhen, China), NLRP3 (uscnk, Wuhan, China), and MCT (Fufeng, Shanghai, China) were used according to the instructions of the manufacturer. Briefly, the standard samples, which were offered through the kit, of known concentration and the samples from two experimental groups were added to the kit plate and then incubated with the kit reagents (41). The OD450 values were detected using the microplate reader (Huisong, Shenzhen, China).

Statistical Analysis

The unpaired Student's t-test was performed for data analysis of two groups. The potential correlation between the two variables was detected by Pearson's correlation coefficient. $p < 0.05$ was considered as significance level. GraphPad Prism 8.0.2 was performed as the statistical software.

RESULTS

Recognition of DEPRGs of CSU

The CSU RNA expression profile dataset (GSE72540) was normalized as shown in **Figure 2A**. 1,297 DEGs (containing 1,033 DEmRNAs and 173 DElncRNAs) were identified in the GSE72540 dataset (**Supplementary Table S3**), and their volcano plot is shown in **Figure 2B**. As shown in **Figure 2C** and **Table 2**, we identified 17 congruous DEPRGs *via* integrated bioinformatics analysis, including 13 congruously upregulated and 4 congruously downregulated. The heat map of DEPRGs is shown in **Figure 2D**.

Function Enrichment Analyses of the DEPRGs

The GO analysis of DEPRGs was performed to reveal their biology functions. As shown, in the GO BP category, most of DEPRGs were mostly involved into regulation of cytokine production, interleukin-1 beta production, interleukin-1 production, etc. (**Figure 3A**). In the GO CC category, most of

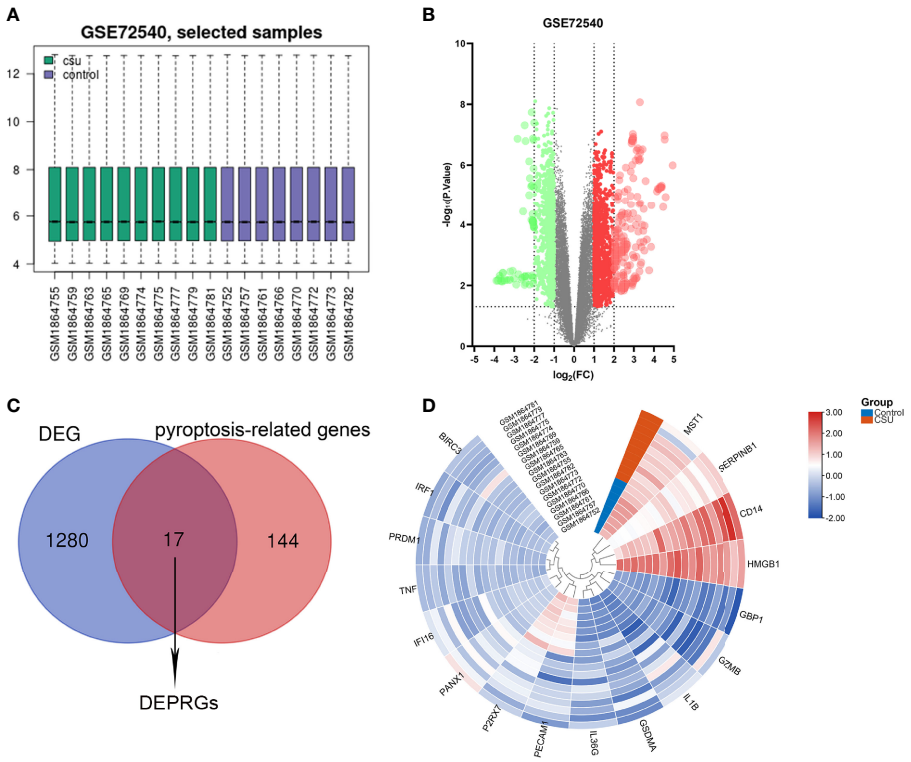

FIGURE 2 | Identification of DEPRGs of CSU. **(A)** Normalization of selected samples of GSE72540. **(B)** The differentially expressed genes of GSE72540. **(C)** The DEPRGs of CSU. **(D)** The heat map of the DEPRGs.

the DEPRGs were enriched into the membrane microdomain and membrane raft (**Figure 3B**). In the GO MF category, the main DEPRGs were enriched in cytokine activities, cytokine receptor binding, and signaling receptor activator activity, etc. (**Figure 3C**). The results of KEGG pathway enrichment exhibited that the mostly involved pathways were the NF-kappa B signaling pathway, TNF signaling pathway, and NOD-like receptor signaling pathway (**Figure 3D**). Utilizing the WebGestalt online database to further explore the function of DEPRGs, the result of DO enrichment showed that dermatomyositis, leishmaniasis, cutaneous, ulcerative colitis, etc., were the major diseases that DEPRGs participated in (**Figure 3E**). These suggested that inflammation and immune response were the major function of DEPRGs.

PPI Network and Hub Gene Analyses

To reveal the interaction of each protein, the PPI network of the DEPRGs was built according to the STRING database, including 15 nodes and 34 edges. In the protein network graph, each node represented a protein, and the edge represented a connection between two proteins. Moreover, among the 15 nodes, 3 nodes were downregulated, and 12 were upregulated (**Figure 4A**). The targets were sorted by target connectivity from small to large in the PPI network, as shown in **Figure 4B**. The most important module was selected, including 10 edges and 8 nodes (**Figure 4C**). Hub genes were detected consistently *via* four algorithms (degree, MNC, stress, and MCC) of cytoHubba (**Figure 4D**). The top five gene scores were considered to be hub genes of CSU: IL1B, TNF, IRF1, HMGB1, and P2RX7 (**Figure 4E** and **Table 3**). Because the more closely knitted gene in the network is more fundamental to regulation, we further investigated the functions of the hub genes through the ClueGO plug-in. As **Figure 4F** shows, they were still primarily enriched in immunomodulation including regulation of adaptive immune response, lymphocyte proliferation, and regulation of phagocytosis. According to GSE57178, the mRNA expression of each hub gene manifested that, compared with the control, IL1B, IRF1, and TNF were significantly overexpressed while P2RX7

TABLE 2 | The DEPRGs of CSU.

Regulation	DEPRGs
Upregulated (n = 13)	SERPINB1 GBP1 IFI16 GSDMA GZMB BIRC3 IL1B IRF1 CD14 PRDM1 IL36G PANX1 TNF
Downregulated (n = 4)	PECAM1 P2RX7 MST1 HMGB1

DEPRGs, differently expressed pyroptosis-related genes; CSU, chronic spontaneous urticaria.

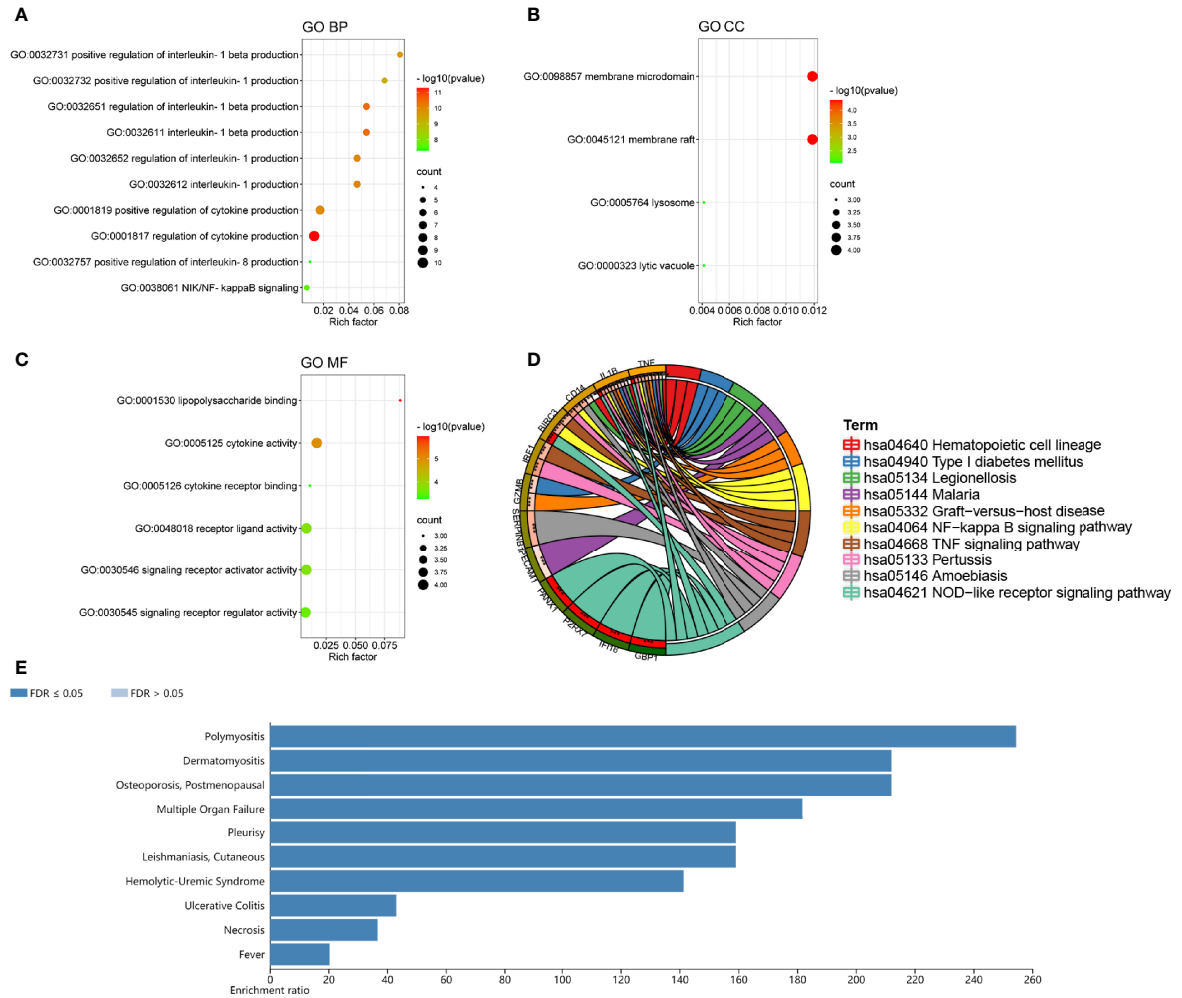

FIGURE 3 | The top ten lists of function enrichment analyses of DEPRGs. **(A)** GO BP; **(B)** GO CC; **(C)** GO MF; **(D)** KEGG signaling pathway; **(E)** DO enrichment. **p < 0.01; ***p < 0.001.

had a significantly lower expression in CSU, which was the same as the above results and indicated that IL1B, IRF1, P2RX7, and TNF were the key genes of CSU (**Figure 4G**).

Immune Infiltration Analysis

We investigated the difference among CSU tissues and control to explore the panorama of immune infiltration of CSU *via* the CIBERSORT algorithm. The ratio of 22 immune cells of samples is shown in **Figure 5A**. The correlation between each of immune cells is shown in **Figure 5B**, among which T cells CD4 memory activated were significantly correlated with macrophages M1 and macrophages M2, and eosinophils were statistically correlated with dendritic cells resting. At the side of control tissue, CSU owned a higher ratio of mast cells activated, and T cells CD4 naive, plasma cells, and B cells memory were significantly lower (**Figure 5C**). Next, we revealed the relation among the abundance of the immune cells and hub gene expression through the Pearson's correlation coefficient. The results displayed that mast cells activated were statistically positively related to the levels of IL1B and TNF, but negatively to HMGB1's; B cells memory and plasma cells were positively correlated with HMGB1 and P2RX7, but negatively with IL1B, IRF1, and TNF; T cells CD4 naive were positively correlated with HMGB1 and P2RX7, but negatively with IL1B (**Figure 6**).

The mRNA–miRNA–lncRNA ceRNA Network of CSU

The non-coding RNA (ncRNA) never participates in encoding proteins but was discovered to be involved in many biological functions, and perturbation of mRNA–miRNA–lncRNA ceRNA networks may affect diseases. The miRNA-targeting hub gene was concurrently recognized by all object databases as true, and their Venn diagrams are shown in **Figure 7A**. In addition, the possible lncRNA targeting the miRNA was predicted *via* miRNet online databases and got the intersection with 173 DElncRNAs. The lncRNA and mRNA of ceRNA must have a consistent

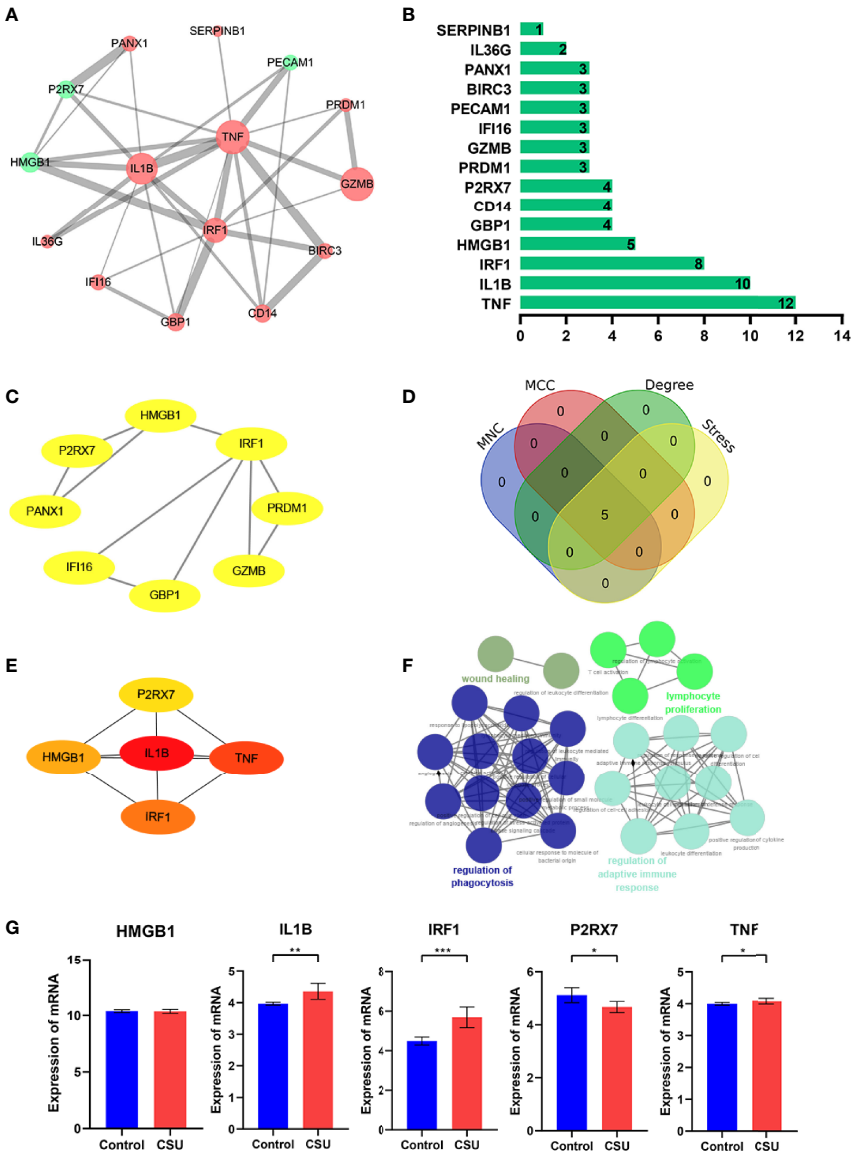

FIGURE 4 | The PPI network and hub gene analyses. **(A)** The PPI network of the DEPRGs, the bigger sizes of the edge and node mean the higher degree. The red means upregulated, and green means downregulated. **(B)** The connectivity rank of genes. **(C)** The first module of the PPI network. **(D)** Four algorithms were utilized to identified hub genes. **(E)** 5 hub genes of CSU. **(F)** The biological process of hub genes *via* the ClueGO tool. **(G)** Data validation of hub genes by GSE57178. *P < 0.05; **P < 0.01; ***P < 0.001.

TABLE 3 | The top 5 hub genes.

Genes	Description	Degree	MCC	MNC	Sterss	Log_2FC	Expression change
IL1B	Interleukin 1 beta	10	38	10	78	3.43222906	Upregulated
TNF	Tumor necrosis factor	12	37	11	130	1.26641463	Upregulated
IRF1	Interferon regulatory factor 1	8	26	8	48	1.17112479	Upregulated
HMGB1	High mobility group box 1	5	18	5	20	-1.01820995	Downregulated
P2RX7	Purinergic receptor P2X 7	4	12	4	10	-1.25950113	Downregulated

MCC, maximal clique centrality; MNC, maximum neighborhood component.

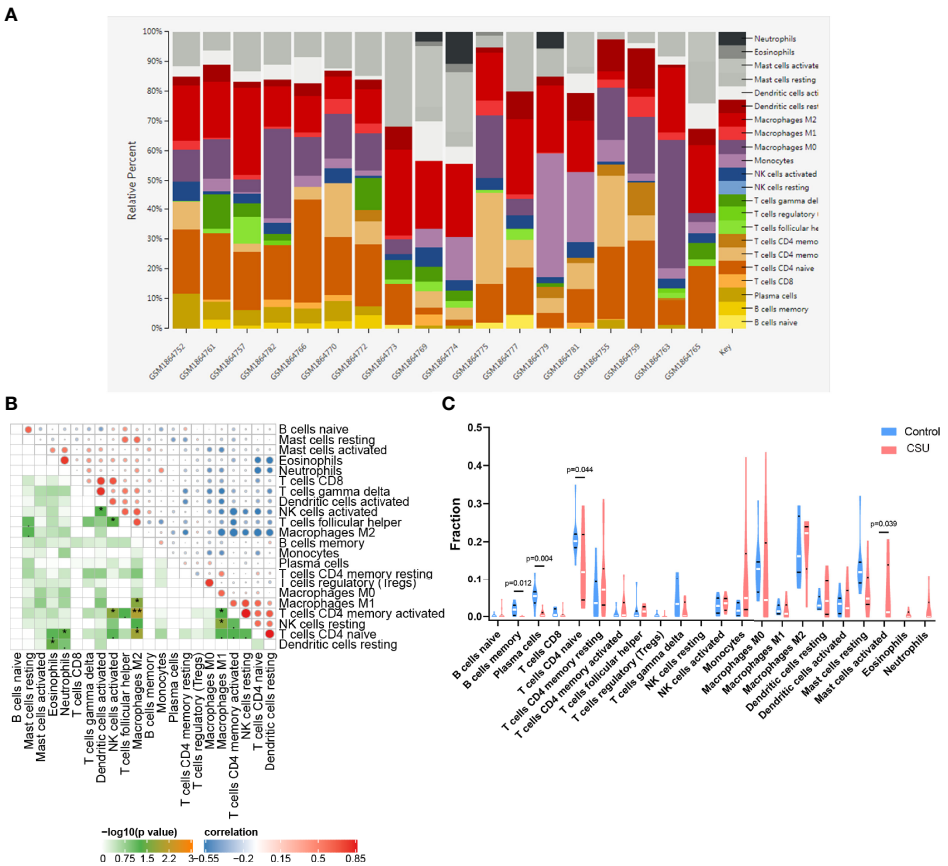

FIGURE 5 | Immune infiltration analysis of CSU. **(A)** The ratio of 22 immune cells of each sample of CSU. **(B)** The correlation between each of immune cells. **(C)** The proportion of immune cells in CSU and control.

expression trend according to the ceRNA mechanism. Then, we got 9 unique DElncRNAs based on the above. The lncRNAs, which compete with miRNAs by acting as ceRNAs to regulate the expression of mRNA targets, should be in the cytoplasm. As a result, only 4 DElncRNAs (HOTAIR, SCARNA9, SNHG3, and TUG1) were predicted in the cytoplasm by lncLocator (**Figure 7B**). Finally, an 18-axis ceRNA network (containing HMGB1/hsa-mir-17-5p/HOTAIR, IL1B/hsa-mir-21-5p/SNHG3, P2RX7/hsa-mir-20a-5p/HOTAIR and so on) was identified (**Figure 7C**). In addition, HOTAIR, SCARNA9, SNHG3, and TUG1 were significantly related to the major infiltration cell of CSU (**Figure 8**).

GSEA of IL1B

Due to the fact that IL1B had been verified and that it played a role in immune infiltration and the ceRNA network of CSU, and simultaneously $\log_2$FC of IL1B was maximal in the hub genes, we chose IL1B for further analysis. The result of GSEA further verified the above results. As **Figure 9** shows, besides ubiquitin-mediated proteolysis, arachidonic acid metabolism, cytosolic DNA sensing pathway, galactose metabolism, and apoptosis, IL1B was still mainly enriched in the NOD-like receptor signaling pathway.

Protein Subcellular Localization and Correlation With Immune Checkpoint Analyses of IL1B

Different subcellular localizations of protein decide different biological functions. The protein subcellular localization of IL1B predicted by Cell-PLoc 2.0 was extracellular (**Figure 10A**). As displayed in **Figure 10B**, IL1B was significantly correlated with familiar immune checkpoints such as CD274(PDL1), CTLA4, HAVCR2(TIM3), and TIGIT, which indicated the important effect of IL1B in immune response further.

Drug–Gene Interaction and Molecular Docking Analyses of IL1B

Developing potential therapeutic drugs for targeting IL1B provides a specific treatment strategy. The drug–gene interaction network of IL1B is exhibited in **Figure 10C**, in which there were 15 potential therapeutic drugs identified and 7 of them were approved (**Table 4**). Then, we worked out the molecular binding site of IL1B and minocycline, one of approved small-molecule drugs (**Figure 10D**).

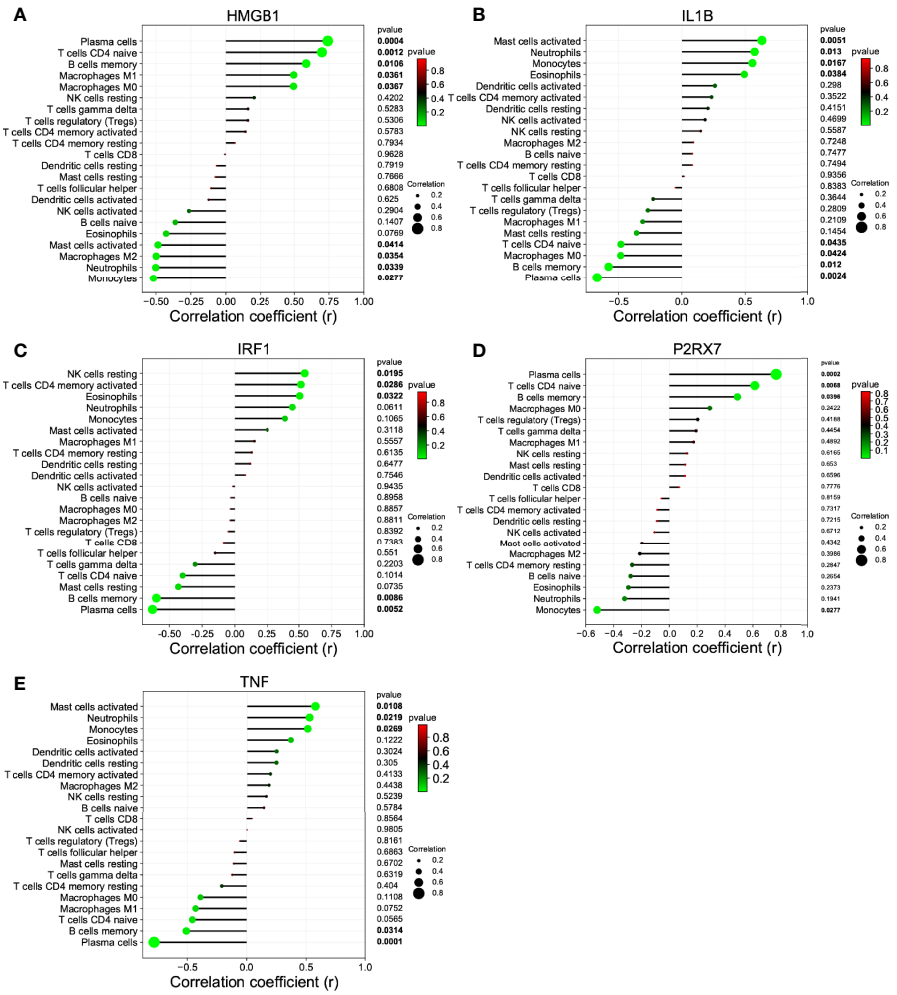

FIGURE 6 | The correlation between the hub gene and the immune cell. **(A)** HMGB1; **(B)** IL1B; **(C)** IRF1; **(D)** P2RX7; and **(E)** TNF.

IL1B Might Participate in Activation of Mast Cells *via* the NLRP3 in CSU

Compared with the healthy control, IL1B showed a significant overexpression in serum of CSU patients *via* ELISA, which is the same as our bioinformatic prediction (**Figure 11A**). The result of the ROC curve analysis showed that the area under the curve was 0.87 (p 0.01), which suggested the role of IL1B in diagnosis of CSU and further that it may be a potential biomarker in CSU (**Figure 11B**). Moreover, the result exhibited that MCT was overexpressed in CSU, and expression of MCT was statistically correlated with IL1B (**Figures 11C, D**). Due to the fact that MCT is the key marker of mast cell activation (42), it indicated that IL1B may participate in mast cell activation. NLRP3 is a subtype of NOD-like receptors and is famous for one of the key pyroptosis cytokines (43). The further ELISA result of CSU patient serum displayed that NLRP3 was significantly overexpressed and correlated with IL1B and MCT (**Figures 11E–G**). It testified the above bioinformatic prediction again which IL1B participated in, in the NOD-like receptor signaling pathway. Moreover, it also advised that it could be *via* the NLRP3 that IL1B participates in activation of mast cells.

DISCUSSION

CSU is a common chronic inflammatory dermatosis, which has significantly negative impacts on the quality of people's life owing to its repeated outbreaks and protracted course (44). Although current treatments of CSU get little effectiveness, how to more effectively mitigate and avert recurrence is still a global challenge as there are still many unknowns in its genesis. In addition, it has reached a consensus in the last guidelines that further research in some areas of CSU is needed, such as identification of mast cell/basophil-activating factors, identification of serum biomarkers of urticarial activity/mast cell activation, and identification of new histological markers (1). Remarkably, pyroptosis was one of deaths associated with

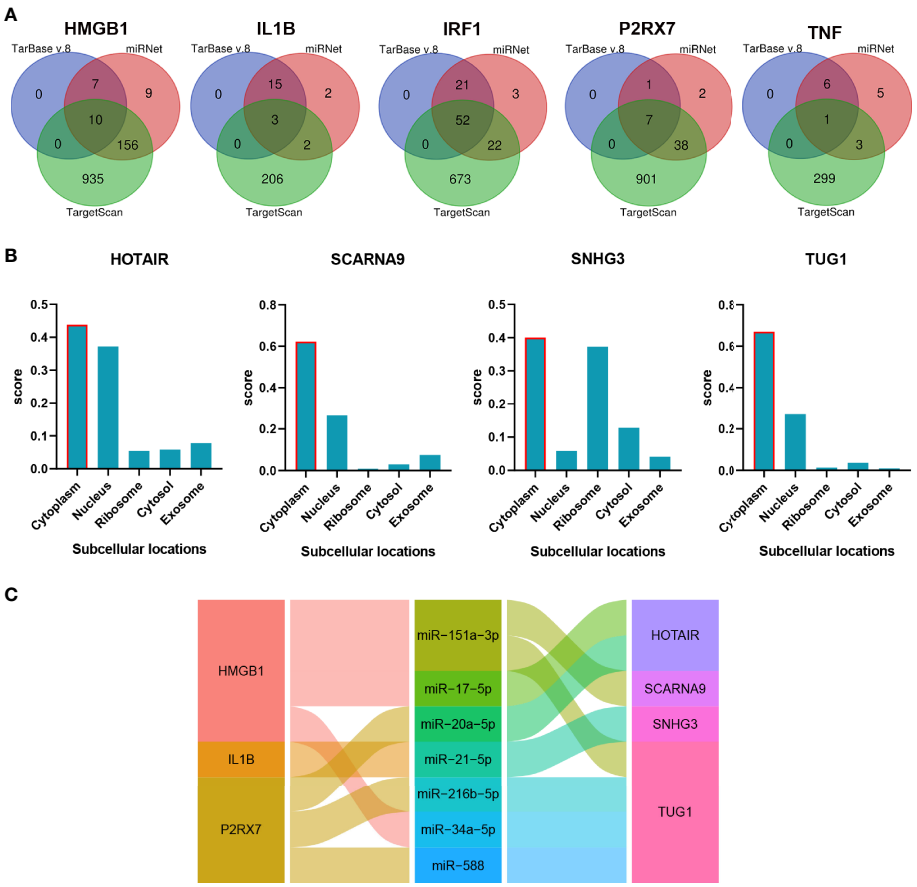

FIGURE 7 | The construction of the lncRNA–miRNA–mRNA ceRNA network of CSU. **(A)** Venn diagram of miRNAs targeting each hub gene. **(B)** The subcellular localization of lncRNA of ceRNA. **(C)** The alluvial diagram of the ceRNA network.

cell membrane rupture. The increased number of cell membranes in mast cells might lead to the liberation of intracellular β-hexosaminidase and histamine (45). Since pyroptosis showed a great research prospect in inflammatory skin diseases, this work tries to identify and verify the potential key biomarkers of CSU from the standpoint of pyroptosis-related genes through bioinformatics ways, especially in inflammatory response, to provide a new perspective for the etiopathogenesis and therapeutic approaches of CSU.

In the present research, we recognized 1,297 DEGs from the CSU RNA expression profile. Then crossing the DEGS with pyroptosis-related genes, 17 DEPRGs (containing 4 downregulated genes and 13 upregulated genes) were recognized and then performed into gene function analysis. As shown, the DEPRGs were mostly involved in inflammatory response, as well as in pro-inflammatory effects (such as positive regulation of interleukin-8 production, positive regulation of interleukin-1 beta production, positive regulation of interleukin-1 production) and biological regulation (including signaling receptor activator activity, receptor ligand activity, cytokine activity), the majority of which are generally accredited to constituent parts of the development of CSU. A research containing 153 CSU patients suggested that the IL1 gene had a significant role in the susceptibility to CSU (46). Kasperska-Zajac et al. indicated that severity of systemic inflammation of CSU was related to elevated il-8 (47). The DEPRGs mainly participated in inflammatory pathways according to KEGG, likely the NF-kappa B signaling pathway, TNF signaling pathway, and NOD-like receptor signaling pathway. In addition, the result of DO further confirms the above. The DEPRGs were majorly enriched in inflammatory diseases like ulcerative colitis and fever. This advises that, to some extent, the DEPRGs could have a function to participate in the systemic inflammation of CSU.

Through the PPI network and module analyses, we identified five hub genes, namely, IL1B, TNF, IRF1 (all upregulated genes) and HMGB1, P2RX72 (both downregulated genes). They are the common inflammatory cytokines, but most of them have not been reported to be implicated in the development of CSU, so this would be a new finding. To fully explore the maladjustment of inflammatory cells of CSU, we executed immune infiltration analysis. It was found that CSU tissue owned a higher proportion of mast cells activated, but relatively lower ones of T cells CD4 naive, plasma cells, and B cells memory. Previous studies

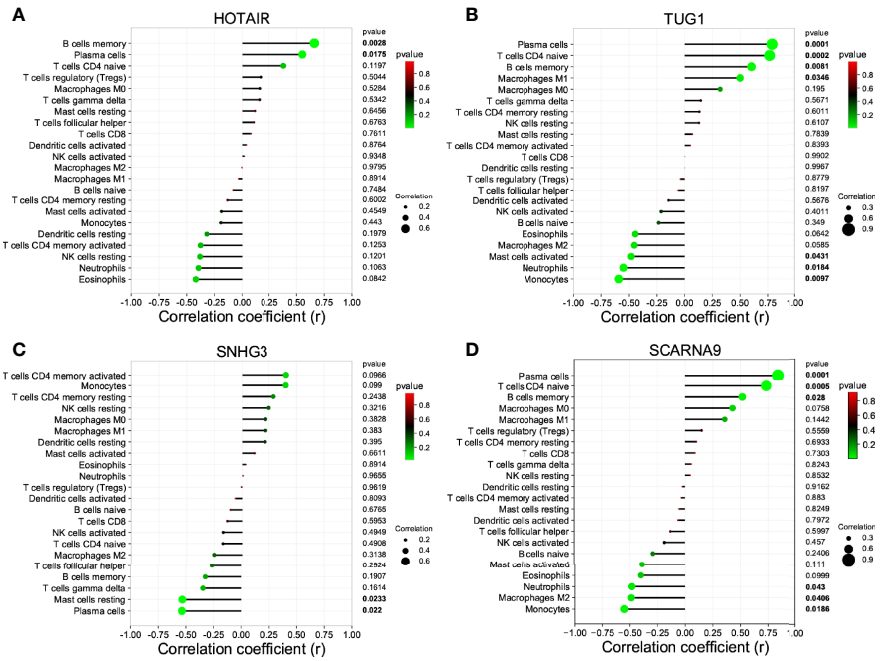

FIGURE 8 | The correlation between the lncRNA of ceRNA and immune cells. **(A)** HOTAIR; **(B)** TUG1; **(C)** SNG3; **(D)** SCARNA9.

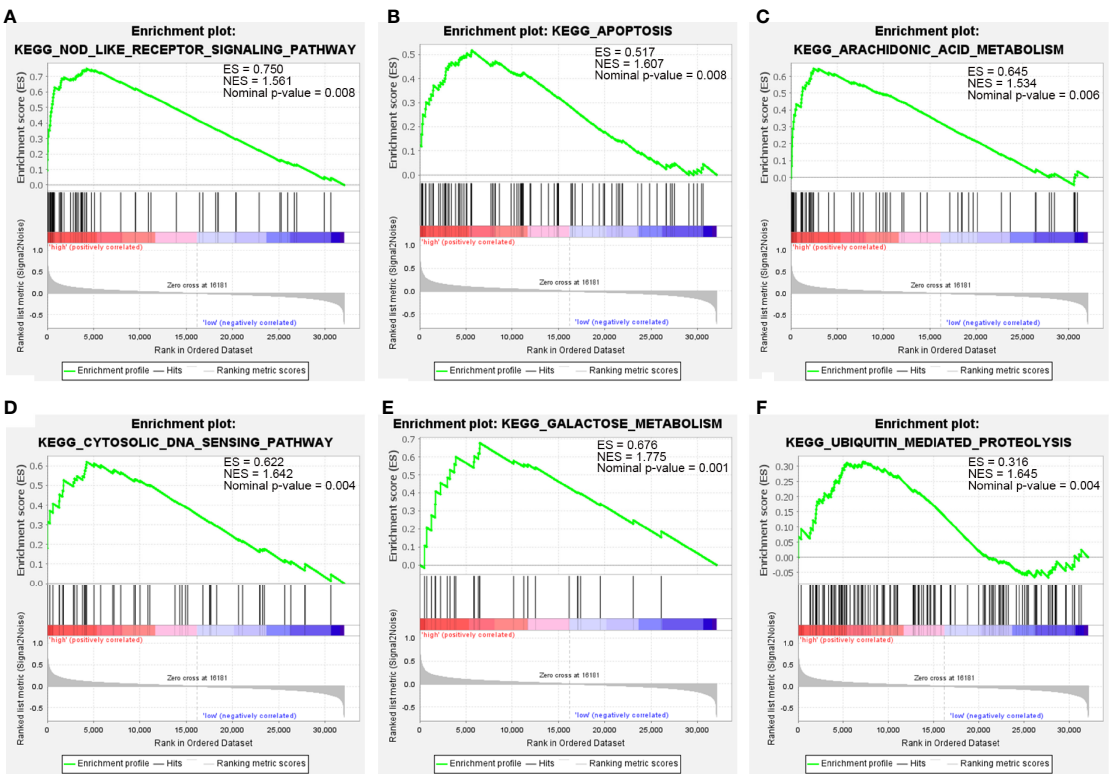

FIGURE 9 | The GSEA of IL1B. **(A)** NOD-like receptor signaling pathway. **(B)** Apoptosis. **(C)** Arachidonic acid metabolism. **(D)** Cytosolic DNA sensing pathway. **(E)** Galactose metabolism. **(F)** Ubiquitin-mediated proteolysis.

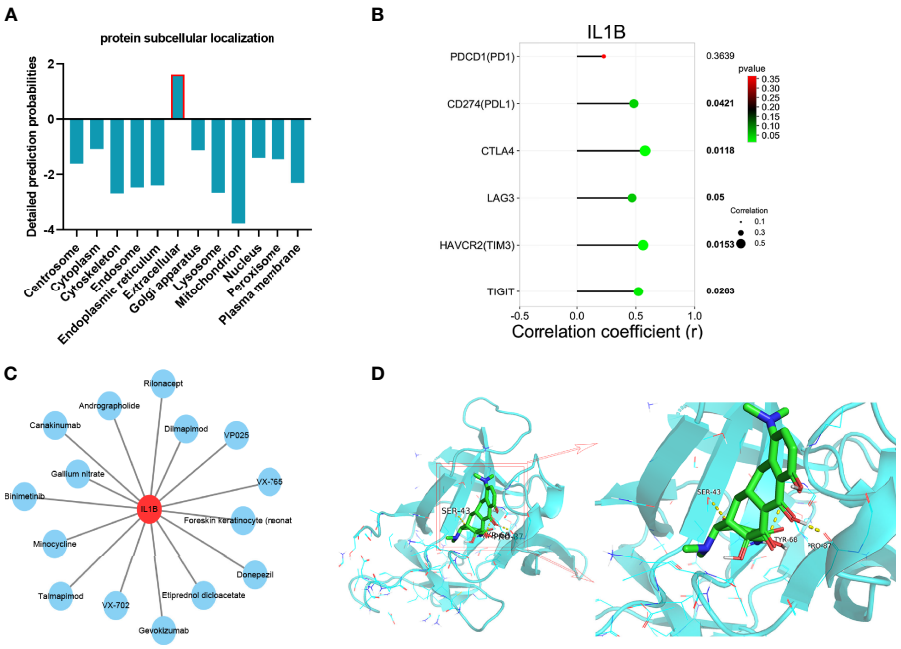

FIGURE 10 | Integrated analyses of IL1B. **(A)** protein subcellular localization of IL1B. **(B)** The correlation between immune checkpoints and IL1B. **(C)** Drug–gene interaction network of IL1B. **(D)** Molecular docking between IL1B and minocycline.

indicated that CSU was considered to be principally a mast cell-driven disease (48). Moreover, it has also been reported that the etiopathogenesis of CSU was closely associated with the dynamical unbalance of Th1/Th2 cells of CD4+T cells (49). However, since there have been few research reports, the relationship between CSU and plasma cells or/and B cells memory might be an interesting finding. Moreover, our research further showed that each of the hub genes (IL1B, TNF, IRF1, HMGB1, and P2RX7) was statistically related to major infiltration cells. Especially, IL1B and TNF were statistically and positively associated with mast cells activated, which suggests that they are related to maladjustment of inflammatory cells of CSU and might be its possible immunomodulation pivots. In addition, to reveal a systemically interactive modulation in CSU, we constructed a ceRNA network, in which there were 8 axes, such as IL1B/miR-21-5p/SNHG3, HMGB1/miR-34a-5p/TUG1, and P2RX7/miR-588/TUG1. It is worth noting that we also found that SNHG3 was significantly and negatively correlated with mast cells resting and plasma cells, and TUG1 was negatively related to mast cells activated, which further verified that the DEmRNA–miRNA–DElncRNA ceRNA network did have a critical role in maladjustment of inflammatory cells of CSU.

We chose IL1B to do further analysis for three reasons. First, it had the biggest fold change in hub genes. Second, it was verified by the validation set GSE57178. Third, both it and its upstream factor SNHG3 were related to the activation of mast cells. These indicated that IL1B could be in a more critical position in the development of CSU. IL1B (IL-1β) is a potent pro-inflammatory cytokine and plays a role in the innate and adaptive immunity of humans (50). Under the stimulation of immune response, inflammation, and infection, IL1B is released from monocytes, macrophages, and dendritic cells, affects local cells by paracrine, and targets distant cells *via* endocrine, ultimately leading to a series of inflammatory cascade responses like activation of immune cells and pyroptosis (51). Abnormal IL1B-related signaling pathways have been shown to be connected with some immune inflammatory diseases like SLE and UC (52, 53).

TABLE 4 | The drugs approved to interact IL1B.

DrugBank ID	Name	Pharmacological action	Actions
DB01017	Minocycline	Unknown	Modulator
DB00843	Donepezil	Unknown	Inhibitor inducer
DB10772	Foreskin keratinocyte (neonatal)	Yes	Agonist
DB06168	Canakinumab	Yes	Binder
DB06372	Rilonacept	Unknown	Binder
DB05260	Gallium nitrate	Yes	Antagonist
DB11967	Binimetinib	Unknown	/

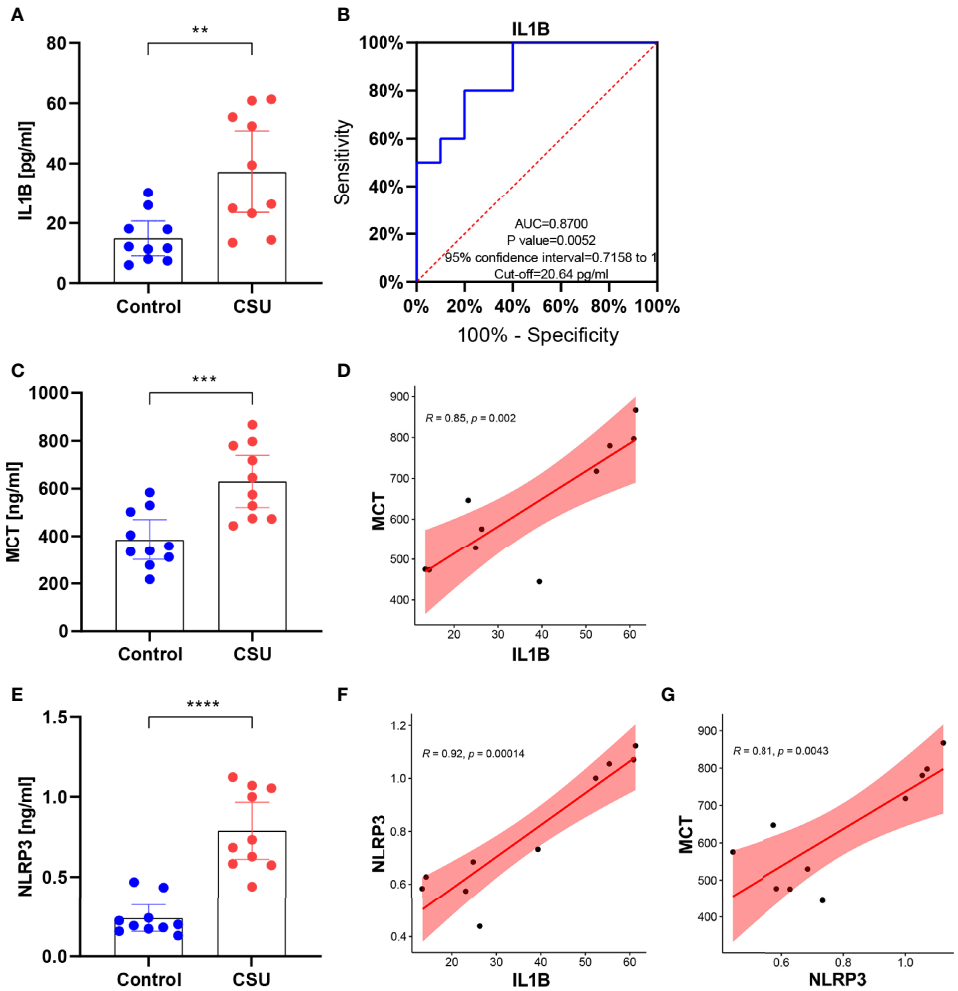

FIGURE 11 | IL1B might participate in activation of mast cells *via* the NLRP3 in CSU. **(A)** The expression of IL1B in CSU and control. **(B)** The ROC curve of IL1B. **(C)** The expression of MCT in CSU and control. **(D)** The correlation between IL1B and MCT in CSU. **(E)** The expression of NLRP3 in CSU and control. **(F)** The correlation between IL1B and NLRP3 in CSU. **(G)** The correlation between NLRP3 and MCT in CSU. **p < 0.01, ***p < 0.001, ****p < 0.0001.

These were in agreement with the result of our research. We predicted that the protein subcellular localization of IL1B was extracellular, which is in accord with its intercellular regulation role. Moreover, it was found that IL1B was significantly correlated with familiar immune checkpoints in CSU, such as PDL1, CTLA4, TIM3, and TIGIT, which someway showed its role of immune regulation in CSU. Furthermore, IL1B was an overexpression examined in clinical CSU patients by ELISA, and the ROC curve analysis confirmed the dependability of its diagnostic value; the point was that mast cells were significantly activated in CSU and IL1B did correlate with it, which verified our bioinformatic analyses and suggests that IL1B could be a potential prognostic and diagnostic biomarker in CSU.

The NOD-like receptor signaling pathway was the major involved pathway according to the enrichment analysis of IL1B in a couple of databases. Moreover, NLRP3 is a subtype of NOD-like receptors and is famous for one of key pyroptosis cytokines; moreover, it is a well-known activator of IL1B (54). The study of Guo et al. showed that the increased expression of NLRP3 in mast cells leads to the activation of caspase-1 and ultimately to production and secretion of IL-1β in endometriosis (55). These are further supported in our work. In clinical CSU patients, NLRP3 was statistically overexpressed and related to the activation of mast cells. NLRP3 was also significantly correlated with IL1B, which might advise that the pyroptosis-related signaling pathway is activated in CSU and it might be related to the activation of mast cells. What is more, it might be *via* the NOD-like receptor signaling pathway, NLRP3, that IL1B participates in activation of mast cells. Moreover, we further identified 15 potential therapeutic drugs targeting IL1B, which provides a possible therapeutic strategy for CSU. Molecular docking revealed that the exact molecular binding makes this relationship more reliable.

Our study also had some limitations. We measured gene expression levels using sera from clinical CSU patients rather than tissues, which is not good enough but still clinically

representative. Besides, we will perform the experiments *in vivo* and *in vitro* to further confirm our results in the future.

In sum, we identified 5 hub genes, IL1B, TNF, IRF1, HMGB1, and P2RX7, from pyroptosis-related genes, which are mainly involved in the inflammatory response and maladjustment of inflammatory cells of CSU. Particularly, ILB and its ceRNA axis might play a role in the activation of mast cells of CUS, and this might be achieved *via* the NOD-like receptor signaling pathway (NLRP3). Therefore, ILB and its related molecules might be potential key biomarkers in the development of CSU, and our study would provide a new perspective for the etiopathogenesis and therapeutic programs of CSU.

DATA AVAILABILITY STATEMENT

The datasets presented in this study can be found in online repositories. The names of the repository/repositories and accession number(s) can be found in the article/**Supplementary Material**.

ETHICS STATEMENT

Written informed consent was obtained from the individual(s)' and minor(s)' legal guardian/next of kin, for the publication of any potentially identifiable images or data included in this article.

AUTHOR CONTRIBUTIONS

SP and HF conceptualized the study design. SP and TZ drafted the manuscript. HF revised the manuscript. SP, SZ, QT, and YY collected data and performed the analysis. All authors contributed to the article and approved the submitted version.

FUNDING

This work was financed by the Hunan Provincial Health Commission scientific research projects (B2016229; B2019055; 202114051780) and Hunan Provincial Innovation Foundation for Postgraduate (CX20200547).

SUPPLEMENTARY MATERIAL

The Supplementary Material for this article can be found online at: https://www.frontiersin.org/articles/10.3389/fimmu.2022.850993/full#supplementary-material

Supplementary Table S1 | 161 pyroptosis-related genes.

Supplementary Table S2 | Population characteristics.

Supplementary Table S3 | 1033 DEmRNAs and 173 DElncRNAs of CSU.

Supplementary Table S4 | The DEGs of GSE72540.

Supplementary Table S5 | The GO and KEGG enrichment of DEPRGs.

Supplementary Table S6 | PPI topology table.

Supplementary Table S7 | Hub genes-mirRNAs.

Supplementary Table S8 | MiRNAs-lncRNAs.

REFERENCES

1. Zuberbier T, Abdul Latiff AH, Abuzakouk M, Aquilina S, Asero R, Baker D, et al. The International EAACI/GA²LEN/EuroGuiDerm/APAAACI Guideline for the Definition, Classification, Diagnosis, and Management of Urticaria. *Allergy* (2022) 77:734–66. doi: 10.1111/all.15090
2. Saini SS. Chronic Spontaneous Urticaria: Etiology and Pathogenesis. *Immunol Allergy Clinics North America* (2014) 34(1):33–52. doi: 10.1016/j.iac.2013.09.012
3. Kolkhir P, Altrichter S, Asero R, Daschner A, Ferrer M, Giménez-Arnau A, et al. Autoimmune Diseases Are Linked to Type IIb Autoimmune Chronic Spontaneous Urticaria. *Allergy Asthma Immunol Res* (2021) 13(4):545–59. doi: 10.4168/aair.2021.13.4.545
4. Gonçalo M, Gimenéz-Arnau A, Al-Ahmad M, Ben-Shoshan M, Bernstein JA, Ensina LF, et al. The Global Burden of Chronic Urticaria for the Patient and Society. *Br J Dermatol* (2021) 184(2):226–36. doi: 10.1111/bjd.19561
5. Zuberbier T, Aberer W, Asero R, Abdul Latiff AH, Baker D, Ballmer-Weber B, et al. The EAACI/GA²LEN/EDF/WAO Guideline for the Definition, Classification, Diagnosis and Management of Urticaria. *Allergy* (2018) 73 (7):1393–414. doi: 10.1111/all.13397
6. Giménez-Arnau AM, DeMontojoye L, Asero R, Cugno M, Kulthanan K, Yanase Y, et al. The Pathogenesis of Chronic Spontaneous Urticaria: The Role of Infiltrating Cells. *J Allergy Clin Immunol Pract* (2021) 9(6):2195–208. doi: 10.1016/j.jaip.2021.03.033
7. Maurer M, Eyerich K, Eyerich S, Ferrer M, Gutermuth J, Hartmann K, et al. Urticaria: Collegium Internationale Allergologicum (CIA) Update 2020. *Int Arch Allergy Immunol* (2020) 181(5):321–33. doi: 10.1159/000507218
8. He L, Yi W, Huang X, Long H, Lu Q. Chronic Urticaria: Advances in Understanding of the Disease and Clinical Management. *Clin Rev Allergy Immunol* (2021) 61(3):424–48. doi: 10.1007/s12016-021-08886-x
9. Asero R. Severe CSU and Activation of the Coagulation/Fibrinolysis System: Clinical Aspects. *Eur Ann Allergy Clin Immunol* (2019) 52:15–7. doi: 10.23822/EurAnnACI.1764-1489.109
10. Puxeddu L, Panza F, Pratesi F, Bartaloni D, Casigliani R, Rocchi V, et al. CCL5/RANTES, sVCAM-1, and sICAM-1 in Chronic Spontaneous Urticaria. *Int Arch Allergy Immunol* (2013) 162(4):330–4. doi: 10.1159/000354922
11. Altrichter S, Staubach P, Pasha M, Singh B, Chang AT, Bernstein JA, et al. An Open-Label, Proof-Of-Concept Study of Lirentelimab for Antihistamine-Resistant Chronic Spontaneous and Inducible Urticaria. *J Allergy Clin Immunol* (2018) 98(7):641–7. doi: 10.2340/00015555-2941
12. Zhao Z, Cai T, Chen H, Chen L, Chen Y, Gao X, et al. Expert Consensus on the Use of Omalizumab in Chronic Urticaria in China. *World Allergy Organ J* (2021) 14(11):100610. doi: 10.1016/j.waojou.2021.100610
13. Hon KL, Leung AKC, Ng WGG, Loo SK. Chronic Urticaria: An Overview of Treatment and Recent Patents. *Recent Patents Inflamm Allergy Drug Discovery* (2019) 13(1):27–37. doi: 10.2174/1872213X13666190328164931
14. McKenzie BA, Dixit VM, Power C. Fiery Cell Death: Pyroptosis in the Central Nervous System. *Trends Neurosci* (2020) 43(1):55–73. doi: 10.1016/j.tins.2019.11.005
15. Li L, Mu Z, Liu P, Wang Y, Yang F, Han X. Mdivi-1 Alleviates Atopic Dermatitis Through the Inhibition of NLRP3 Inflammasome. *Exp Dermatol* (2021) 30(12):1734–44. doi: 10.1111/exd.14412
16. Deng G, Chen W, Wang P, Zhan T, Zheng W, Gu Z, et al. Inhibition of NLRP3 Inflammasome-Mediated Pyroptosis in Macrophage by

Cycloastragenol Contributes to Amelioration of Imiquimod-Induced Psoriasis-Like Skin Inflammation in Mice. *Int Immunopharmacol* (2019) 74:105682. doi: 10.1016/j.intimp.2019.105682
17. Kambe N, Nakamura Y, Saito M, Nishikomori R. The Inflammasome, an Innate Immunity Guardian, Participates in Skin Urticarial Reactions and Contact Hypersensitivity. *Allergol Int: Off J Jpn Soc Allergol* (2010) 59(2):105–13. doi: 10.2332/allergolint.09-RAI-0160
18. Cortés-Ciriano I, Gulhan DC, Lee JJ, Melloni GEM, Park PJ. Computational Analysis of Cancer Genome Sequencing Data. *Nat Rev Genet* (2022) 6(2): e2100785. doi: 10.1002/smtd.202100785
19. Abbott TR, Dhamdhere G, Liu Y, Lin X, Goudy L, Zeng L, et al. Development of CRISPR as an Antiviral Strategy to Combat SARS-CoV-2 and Influenza. *Cell* (2020) 181(4):865–76.e12. doi: 10.1016/j.cell.2020.04.020
20. Clough E, Barrett T. The Gene Expression Omnibus Database. *Methods Mol Biol (Clifton NJ)* (2016) 1418:93–110. doi: 10.1007/978-1-4939-3578-9_5
21. Barrett T, Wilhite SE, Ledoux P, Evangelista C, Kim IF, Tomashevsky M, et al. NCBI GEO: Archive for Functional Genomics Data Sets–Update. *Nucleic Acids Res* (2013) 41(Database issue):D991–5. doi: 10.1093/nar/gks1193
22. Shao Y, Jia H, Huang L, Li S, Wang C, Aikemu B, et al. An Original Ferroptosis-Related Gene Signature Effectively Predicts the Prognosis and Clinical Status for Colorectal Cancer Patients. *Front Oncol* (2021) 11:711776. doi: 10.3389/fonc.2021.711776
23. Zhou Y, Zhou B, Pache L, Chang M, Khodabakhshi AH, Tanaseichuk O, et al. Metascape Provides a Biologist-Oriented Resource for the Analysis of Systems-Level Datasets. *Nat Commun* (2019) 10(1):1523. doi: 10.1038/s41467-019-09234-6
24. Liao Y, Wang J, Jaehnig EJ, Shi Z, Zhang B. WebGestalt 2019: Gene Set Analysis Toolkit With Revamped UIs and APIs. *Nucleic Acids Res* (2019) 47 (W1):W199–w205. doi: 10.1093/nar/gkz401
25. Szklarczyk D, Gable AL, Nastou KC, Lyon D, Kirsch R, Pyysalo S, et al. The STRING Database in 2021: Customizable Protein-Protein Networks, and Functional Characterization of User-Uploaded Gene/Measurement Sets. *Nucleic Acids Res* (2021) 49(D1):D605–d12. doi: 10.1093/nar/gkaa1074
26. Doncheva NT, Morris JH, Gorodkin J, Jensen LJ. Cytoscape StringApp: Network Analysis and Visualization of Proteomics Data. *J Proteome Res* (2019) 18(2):623–32. doi: 10.1021/acs.jproteome.8b00702
27. Chen B, Khodadoust MS, Liu CL, Newman AM, Alizadeh AA. Profiling Tumor Infiltrating Immune Cells With CIBERSORT. *Methods Mol Biol (Clifton NJ)* (2018) 1711:243–59. doi: 10.1007/978-1-4939-7493-1_12
28. Mitteer DR, Greer BD, Randall KR, Briggs AM. Further Evaluation of Teaching Behavior Technicians to Input Data and Graph Using GraphPad Prism. *Behav Anal (Washington DC)* (2020) 20(2):81–93. doi: 10.1037/bar0000172
29. Shi Y, Yang F, Wei S, Xu G. Identification of Key Genes Affecting Results of Hyperthermia in Osteosarcoma Based on Integrative ChIP-Seq/TargetScan Analysis. *Med Sci Monit: Int Med J Exp Clin Res* (2017) 23:2042–8. doi: 10.12659/MSM.901191
30. Chang L, Zhou G, Soufan O, Xia J. Mirnet 2.0: Network-Based Visual Analytics for miRNA Functional Analysis and Systems Biology. *Nucleic Acids Res* (2020) 48(W1):W244–51. doi: 10.1093/nar/gkaa467
31. Bozgeyik I. Therapeutic Potential of miRNAs Targeting SARS-CoV-2 Host Cell Receptor ACE2. *Meta Gene* (2021) 27:100831. doi: 10.1016/j.mgene.2020.100831
32. Lin Y, Pan X, Shen HB. Lnclocator 2.0: A Cell-Line-Specific Subcellular Localization Predictor for Long non-Coding RNAs With Interpretable Deep Learning. *Bioinf (Oxford England)* (2021) 1–9. doi: 10.1093/bioinformatics/btab127
33. Subramanian A, Tamayo P, Mootha VK, Mukherjee S, Ebert BL, Gillette MA, et al. Gene Set Enrichment Analysis: A Knowledge-Based Approach for Interpreting Genome-Wide Expression Profiles. *Proc Natl Acad Sci United States America* (2005) 102(43):15545–50. doi: 10.1073/pnas.0506580102
34. Chou KC, Shen HB. Cell-PLoc: A Package of Web Servers for Predicting Subcellular Localization of Proteins in Various Organisms. *Nat Protoc* (2008) 3(2):153–62. doi: 10.1038/nprot.2007.494
35. Liu D. Cancer Biomarkers for Targeted Therapy. *biomark Res* (2019) 7:25. doi: 10.1186/s40364-019-0178-7
36. Wishart DS, Feunang YD, Guo AC, Lo EJ, Marcu A, Grant JR, et al. DrugBank 5.0: A Major Update to the DrugBank Database for 2018. *Nucleic Acids Res* (2018) 46(D1):D1074–d82. doi: 10.1093/nar/gkx1037
37. Kim S, Chen J, Cheng T, Gindulyte A, He J, He S, et al. PubChem in 2021: New Data Content and Improved Web Interfaces. *Nucleic Acids Res* (2021) 49(D1): D1388–d95. doi: 10.1093/nar/gkaa971
38. Karuppasamy MP, Venkateswaran S, Subbiah P. PDB-2-PBv3.0: An Updated Protein Block Database. *J Bioinf Comput Biol* (2020) 18(2):2050009. doi: 10.1142/S0219720020500092
39. Nguyen NT, Nguyen TH, Pham TNH, Huy NT, Bay MV, Pham MQ, et al. Autodock Vina Adopts More Accurate Binding Poses But Autodock4 Forms Better Binding Affinity. *J Chem Inf Modeling* (2020) 60(1):204–11. doi: 10.1021/acs.jcim.9b00778
40. Lam WW, Siu SW. PyMOL Mcontrol: Manipulating Molecular Visualization With Mobile Devices. *Biochem Mol Biol Educ: Bimonthly Publ Int Union Biochem Mol Biol* (2017) 45(1):76–83. doi: 10.1002/bmb.20987
41. Aydin S. A Short History, Principles, and Types of ELISA, and Our Laboratory Experience With Peptide/Protein Analyses Using ELISA. *Peptides* (2015) 72:4–15. doi: 10.1016/j.peptides.2015.04.012
42. Payne V, Kam PC. Mast Cell Tryptase: A Review of its Physiology and Clinical Significance. *Anaesthesia* (2004) 59(7):695–703. doi: 10.1111/j.1365-2044.2004.03757.x
43. Swanson KV, Deng M, Ting JP. The NLRP3 Inflammasome: Molecular Activation and Regulation to Therapeutics. *Nat Rev Immunol* (2019) 19 (8):477–89. doi: 10.1038/s41577-019-0165-0
44. Hoskin B, Ortiz B, Paknis B, Kavati A. Humanistic Burden of Refractory and Nonrefractory Chronic Idiopathic Urticaria: A Real-world Studyin the United States. *Clin Ther* (2019) 41(2) 205–20. doi: 10.1016/j.clinthera.2018.12.004
45. Liu M, Lu J, Chen Y, Shi X, Li Y, Yang S, et al. Sodium Sulfite-Induced Mast Cell Pyroptosis and Degranulation. *J Agric Food Chem* (2021) 69(27):7755–64. doi: 10.1021/acs.jafc.1c02436
46. Brzoza Z, Rymarczyk B, Grzeszczak W, Trautsolt W, Pluta-Kubicz M, Moczulski D. Interleukin 1 Gene Polymorphisms Presumably Participate in the Pathogenesis of Chronic Spontaneous Autoreactive Urticaria. *J Interferon Cytokine Res: Off J Int Soc Interferon Cytokine Res* (2020) 40(10):497–500. doi: 10.1089/jir.2020.0103
47. Kasperska-Zając A, Damasiewicz-Bodzek A, Grzanka R, Skrzypulec-Frankel A, Bieniek K, Sikora-Żydek A, et al. Circulating Soluble LIGHT/TNFSF14 is Increased and Associated With IL-8 Concentration in Chronic Spontaneous Urticaria. *Int J Immunopathol Pharmacol* (2018) 32:2058738418784431. doi: 10.1177/2058738418784431
48. Ulambayar B, Chen YH, Ban GY, Lee JH, Jung CG, Yang EM, et al. Detection of Circulating IgG Autoantibody to FcεRIα in Sera from Chronic Spontaneous Urticaria Patients. *J Microbiol Immunol Infect* (2020) 53 (1):141–7. doi: 10.1016/j.jmii.2017.10.003
49. Chen Q, Zhong H, Chen WC, Zhai Z, Zhou Z, Song Z, et al. Different Expression Patterns of Plasma Th1-, Th2-, Th17- and Th22-Related Cytokines Correlate With Serum Autoreactivity and Allergen Sensitivity in Chronic Spontaneous Urticaria. *J Eur Acad Dermatol Venereol: JEADV* (2018) 32(3):441–8. doi: 10.1111/jdv.14541
50. Dinarello CA. A Clinical Perspective of IL-1β as the Gatekeeper of Inflammation. *Eur J Immunol* (2011) 41(5):1203–17. doi: 10.1002/eji.201141550
51. Wang Y, Che M, Xin J, Zheng Z, Li J, Zhang S. The Role of IL-1β and TNF-α in Intervertebral Disc Degeneration. *Biomed Pharmacother = Biomed Pharmacother* (2020) 131:110660. doi: 10.1016/j.biopha.2020.110660
52. Mohammadoo-Khorasani M, Salimi S, Tabatabai E, Sandoughi M, Zakeri Z, Farajian-Mashhadi F. Interleukin-1β (IL-1β) & IL-4 Gene Polymorphisms in Patients With Systemic Lupus Erythematosus (SLE) & Their Association With Susceptibility to SLE. *Indian J Med Res* (2016) 143(5):591–6. doi: 10.4103/0971-5916.187107
53. Dinallo V, Marafini I, Di Fusco D, Laudisi F, Franzè E, Di Grazia A, et al. Neutrophil Extracellular Traps Sustain Inflammatory Signals in Ulcerative Colitis. *J Crohn's Colitis* (2019) 13(6):772–84. doi: 10.1093/ecco-jcc/jjy215
54. Mao L, Kitani A, Hiejima E, Montgomery-Recht K, Zhou W, Fuss I, et al. Bruton Tyrosine Kinase Deficiency Augments NLRP3 Inflammasome Activation and Causes IL-1β-Mediated Colitis. *J Clin Invest* (2020) 130 (4):1793–807. doi: 10.1172/JCI128322

55. Guo X, Xu X, Li T, Yu Q, Wang J, Chen Y, et al. NLRP3 Inflammasome Activation of Mast Cells by Estrogen *via* the Nuclear-Initiated Signaling Pathway Contributes to the Development of Endometriosis. *Front Immunol* (2021) 12:749979. doi: 10.3389/fimmu.2021.749979

Conflict of Interest: The authors declare that the research was conducted in the absence of any commercial or financial relationships that could be construed as a potential conflict of interest.

Publisher's Note: All claims expressed in this article are solely those of the authors and do not necessarily represent those of their affiliated organizations, or those of the publisher, the editors and the reviewers. Any product that may be evaluated in this article, or claim that may be made by its manufacturer, is not guaranteed or endorsed by the publisher.

frontiers | Frontiers in Immunology

REVIEW
published: 04 May 2022
doi: 10.3389/fimmu.2022.885609

The Yin and Yang of IL-17 in Systemic Sclerosis

Lanxuan Wei, David Abraham and Voon Ong*

Center for Rheumatology and Connective Tissue Disease, Department of Inflammation, Division of Medicine, University College London, London, United Kingdom

IL-17 (IL-17A) is a pro-inflammatory cytokine produced by a sub-set of T helper cells termed Th17 cells primarily in response to cytokines like TGF-β and IL-23 and play an important role in host defense. IL-17 signals *via* the IL-17RA/RC heterodimer and the adaptor protein Act1 to activate both canonical and non-canonical pathways inducing transcriptional activation and stabilization of mRNAs. IL-17 appears to act not directly on immune cells but stimulates stromal cells such as endothelial and epithelial cells and fibroblasts to secrete other immunomodulatory factors. Fibroblast activated by IL-17 can support the growth and differentiation of immune cells. Studies have begun to uncover a dual role for IL-17; on one hand enhancing immune reactions and promoting inflammatory diseases and on the other decreasing responses and immune activity in established disease settings. The balance of double-edged sword effect of IL-17 and autoimmunity is illustrated in a variety of human diseases and experimental models of diseases. Specifically, the emerging interest in autoimmunity in systemic sclerosis (Scleroderma, SSc) has led to potential role of IL-17A as a target therapy in this disease.

Keywords: IL-17, IL-17A, systemic sclerosis, fibrosis, inflammation

OPEN ACCESS

Edited by:
Kutty Selva Nandakumar, Karolinska Institutet (KI), Sweden

Reviewed by:
Carlo Chizzolini, Université de Genève, Switzerland
Steven O'Reilly, STipe Therapeutics, Denmark

***Correspondence:**
David Abraham
david.abraham@ucl.ac.uk

Specialty section:
This article was submitted to Autoimmune and Autoinflammatory Disorders, a section of the journal Frontiers in Immunology

Received: *28 February 2022*
Accepted: *28 March 2022*
Published: *04 May 2022*

Citation:
Wei L, Abraham D and Ong V (2022) The Yin and Yang of IL-17 in Systemic Sclerosis. Front. Immunol. 13:885609. doi: 10.3389/fimmu.2022.885609

INTRODUCTION: IL-17 AND TH17 CELLS

IL-17 family of cytokines comprises of different members which include IL-17B, IL-17C, IL-17D (also known as IL-27), IL-17E (also known as IL-25) and IL-17F (1), with IL-17A being the most studied one. IL-17 has pleiotropic functional impact on various cell types in human body, contributing to host defense against opportunistic pathogens infection (2) such as Candida and occurrence of chronic inflammatory disorders (2).

Most IL-17-secreting cells belong to the lymphoid lineage including natural killer (NK) cells, NK T cells (NKT), type 3 innate lymphoid cells (ILC3), gamma/delta T cells, and CD4+ T cells (1). Th17 cells are a group of $CD4^+$ helper T cells primarily located in barrier organs in steady state (2) providing a defensive role upon the entry of pathogens. Their principal products are IL-17A, IL-17F, IL-21, and IL-22 (1). It was found that TGF-β, IL-21, IL-6, IL-1β are all critical mediators of the process of Th17 cell differentiation (3). TGF-β and IL-6 (4) can promote the recruitment and phosphorylation of STAT3 (5), leading to induction of the transcription factor retinoic acid receptor-related orphan nuclear receptor gamma t (RORγt) (2) which is the essential and specific

regulator in Th17 cells (5). Regulatory T cells (Tregs) are a group of T cells that function to monitor and contain abnormal activation of immune system. Interleukin-1β and IL-6 downregulate while TGF-β induces transcription factor of Tregs (1). This indicates the delicate conversion between these two separate cell lines and the equilibrium between which (6) play a significant and positive part in the maintenance of immune homeostasis (2). Inhibition of Tregs and Th1 signals/ enhancement of Th17 and Th2 signals (6) has been indicated to contribute to the pathogenesis of SSc. PGI_2 analogues are also suggested to induce Th17 while inhibit Th1 cell responses in SSc (7). IL-23, a heterodimer consisting of an IL-12/IL-23 common p40 subunit and an IL-23 specific p19 subunit (3), stimulates various pathways to promote generation and stabilization of final mature Th17 cells (8). Blimp-1 has been suggested to be an essential transcription factor downstream of IL-23 signaling pathway that acts together with RORγt during the process of differentiation of Th17 cells (8).

IL-17 receptor is found to express ubiquitously in multiple cell lines (8), resulting to the release of an extensive range of cytokines in epithelial cells, endothelial cells and fibroblasts (6) (as shown in **Figure 1**). The IL-17 receptor family is composed of five members (IL-17RA, IL-17RB, IL-17RC, IL-17RD, and IL-17RE) (9). All IL-17 receptor family contain a similar intracellular conserved cytoplasmic SEF/IL-17R (SEFIR) motif (2). IL-17A is secreted either as homodimer of IL-17A/IL-17A or as IL-17A/IL-17F heterodimer (6), and they signal through the same receptor subunits comprised of an IL-17RA chain and an IL-17RC chain (1, 6). IL-17F among other IL-17 family members, is the most analogous one to IL-17A, sharing more than half of similarities structurally with IL-17A. Nevertheless IL-17F signaling strength is much weaker (6) than that of IL-17A possibly due to its weaker affinity upon binding with receptors (10). IL-17A binds with the IL- 17RA/RC receptor complex in order to exert its function. Act1, a ubiquitin ligase in its downstream pathway is recruited to further recruit tumor necrosis factor (TNF) receptor-associated factor 6 (TRAF6). TRAF6 is ubiquitylated by Act1 then activates the nuclear factor kappa B (NF-kB) and mitogen-activated protein (MAP) kinase pathways (2), including extracellular signal-regulated kinase (ERK), p38 and JUN N-terminal kinase (JNK) (11).

ROLE OF IL-17 IN INFLAMMATION

IL-17 exerts a protective role against many infectious diseases, while promoting inflammatory pathology in autoimmune diseases at the same time (8). The delicate control over the balance between protective and pathogenic sides of IL-17 is worthy of further investigation to achieve optimal regulation (12). IL-17 exerts its protective role in barrier immunity through promoting the production of antimicrobial factors and contributing to the recruitment of neutrophils (13). Defective IL-17 secretion could lead to chronic mucocutaneous candidiasis (14) thus confirming its protective function in mucosal immunity. IL-17 exerts its pro-inflammatory roles by inducing various pro-inflammatory genes in its downstream signaling pathways. For instance, IL-17A could induce in target cells the expression of neutrophil chemoattractants such as CXCL1, CXCL2, CXCL5, and CXCL8; CCL20 is expressed stronger under IL-17A stimulation which promotes the recruitment of lymphocytes; growth factors such as G-CSF and GM-CSF are upregulated as well (2, 6, 11). In the meantime CCL20 also facilitates the recruitment of Th17 cells to the site where inflammation occurs thus creating an auto-enhancing loop of Th-17 related pathways (2). IL-17 is significant in its capacity to synergize with other cytokines such as TNF-α, IL-1β, IL-22, IFN-γ, and GM-CSF to enhance production of inflammatory

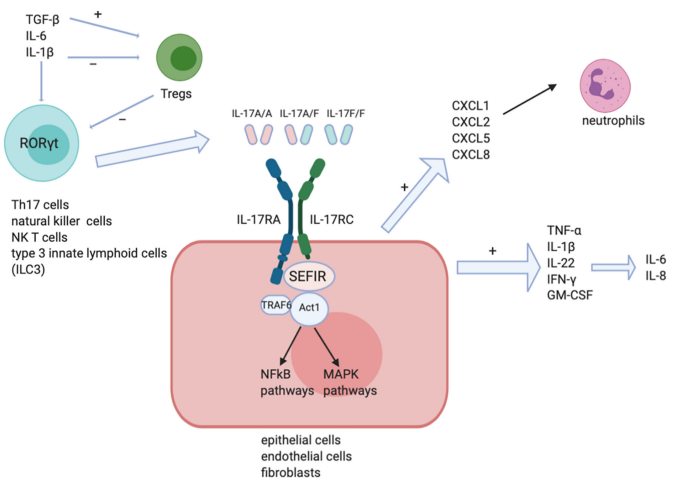

FIGURE 1 | IL-17 signaling pathways. IL-17A/A homodimer, IL-17F/F homodimer and IL-17A/F heterodimer can each stimulate IL-17RA and IL-17RC receptor complexes on the surface of target cells like epithelial cells, endothelial cells and fibroblasts. The SEFIR motif recruits Act1 leading to the induction of downstream NF-kB and MAPK pathways. Pro-inflammatory cytokines like IL-1, IFN-γ, and IL-8 are then induced.

mediators like IL-6 and IL-8 (2). Katz et al. reported in 2000 the regulatory effect of IL-17 in the process of complement protein synthesis. IL-17 alone could stimulate C3 synthesis while IL-17 and TNF-α synergize together to induce factor B production. Pro-inflammatory role of IL-17 is further proved considering the participation of C3 and factor B in immunobiological activities (15). C9 proteins are involved in local inflammatory responses in alveolar epithelial cells. Cipolla et al. first suggested in their studies that IL-17A actively induce C9 cascade in lung fibrosis. This participation in epithelial injury and fibrosis is achieved *via* p38MAPK signaling pathway activation. Antagonizing IL-17A to ameliorate C9 cascade could provide new strategies to abrogate lung fibrosis (16). In all, IL-17 is a key mediator in inflammatory reactions happening in the context of an environment under the influence of mutual actions of various different kinds of cytokines (12).

IL-17 and other Th17 cytokines can contribute to the pathogenesis of a diverse range of multiple autoimmune and inflammatory diseases (8), including psoriasis, inflammatory bowel disease (IBD), rheumatoid arthritis (RA), and multiple sclerosis (MS) (4). In rheumatoid arthritis, for example, IL-17-induced cytokines has a pro-inflammatory impact on flare-ups of this disease (8). IL-6 induced by IL-17 maintains the Th17-cell population, creating a self-reinforcing loop thus promoting and maintaining this chronic inflammatory state of RA (8). IL-17 family cytokines are also known to play a role in cancer immunity. IL-17A/F could manipulate immune cells such as macrophages leading to progression of lung cancer cell growth (17). IL-17-induced EMT contributes to the evolvement of lung cancer, actively stimulating cell migration and invasion *via* its downstream mediator NF-κB (18). The "IL-23-IL-17 axis" is also suggested to be a key driver and IL-23 and IL-17A are critical mediators of autoimmune diseases like psoriasis (19, 20).

IL-17 AND SYSTEMIC SCLEROSIS

Systemic Sclerosis (SSc) is a disease characterized by ECM deposition and diffuse fibrosis of the skin and internal organs (21). Its etiology remains a mystery yet to be discovered. Its etiology in particular autoimmunity has drawn significant interests recently and the emerging positive results from recent clinical trials targeting key immune pathways are testaments to the key role of autoimmunity in SSc pathogenesis (22). The interactions between various altered cell types such as epithelial cells, endothelial cells and immune cells and the pathogenic molecules they secreted resulted in typical changes in fibroblasts properties (21). T cells in particular are said to act an active part in this process (23), and play a prominent role in the pathogenesis of SSc. Being at the site of fibrosis, the soluble profibrotic mediators (IL-4, IL-6, IL-13) released by Th2 cells and their interactions with fibroblasts promoted the deposition of excess ECM and induced fibrosis in SSc (24).

Fibroblasts are a group of cells that can be originated from various different cell types. Once activated during the abnormal pathogenic process, they can transdifferentiate into myofibroblasts (25), which express α-smooth muscle cell actin (α-SMA), rendering its contractile capacity (26). Stimulated by mediators like IL-6, TGF-β, they can promote expression levels of type one collagen and fibronectin (26), contributing to the reprogramming of extracellular matrix and formation of pathological fibrosis of multiple organs. Key factors that are thought to play a critical role in the pathogenesis and progression of SSc are suggested as immunological disorder, environmental factors (silica exposure, chlorinated solvents, trichloroethylene, aromatic solvents), genetic factors and oxidative stress (21).

Abnormal T cell activation is a crucial part in the initiation and progression of systemic sclerosis (23). The subtle regulation between interplay of Th1/Th2 cells have long been the focus of stage. Either by releasing soluble mediators like IFN-γ (Th1 cells), IL-4 and IL-13(Th2 cells), or by contacting directly with fibroblasts, Th1 cells are thought to be anti-fibrotic by inhibiting ECM deposition and promoting MMP secretion (27), while Th2 cells are the opposite. Fibroblasts respond to the refined control over stimulation by Th1/Th2 cells and followed by secretion of mediators. These mediators are anti-angiogenic and anti-fibrotic in the context of Th1 cells induction, while others are pro-fibrotic and pro-angiogenic properties under Th2 cells stimulation (27). Fibroblasts act as 'immune sentinels' through a paracrine manner by releasing cytokines and having direct and indirect cell-cell interactions with immune cells. The ongoing bi-directional communication between immune cells and fibroblasts was considered the major driver of SSc. T cells contribute to endothelial dysfunction and the activation of macrophages and fibroblasts/myofibroblasts through cytokine while fibroblasts secrete ECM, collagens, glycosaminoglycans (GAGs) and fibronectin leading to fibrosis formation in SSc (28). Tregs exert anti-inflammatory role by releasing cytokines like IL-10 thus providing a protective role against aberrant immune activation. TGF-β is a critical inducer involved in the differentiation of Tregs but this induction is inhibited by IL-6 (29). Balance between Th17 cells and Tregs is regulated delicately in the development of SSc. Abnormal inflammatory changes occurred early in fibrosis, involving infiltration of mononuclear immune cells. Chizzolini et al. suggested that activated T cells are the dominant lymphocyte population in lesional skin and notably T cell infiltrates correlates with skin involvement suggesting an association between autoimmunity and fibrosis. Macrophages and mast cells have been suggested to participate in this course as well (27). The role of macrophages in progression of SSc is also worthy of inspection. Macrophages activated by Th1 cytokines produce pro-inflammatory cytokines, reducing ECM deposition, while macrophages activated by Th2 cytokines have an anti-inflammatory, profibrotic phenotype (27). These profibrotic macrophages are considered as activators in the fibrotic process. Though mostly related to vasculopathy, the function of complement in SSc pathogenesis is not fully known. C5a could induce CD4+ cells into a Th17 profile. Recent work highlighted that activated CD4+ T cells from early dcSSc expresses increased IL-17A and this is dependent on activation of intracellular inhibitory receptor, C5a receptor2. Biological coupling of perturbed intracellular complement

(complosome) activation may be operational in an array of autoimmune rheumatic disease states and supports a unique role of Th1-driven pathology and complement activation. Notably, antagonizing C3a and C5a receptors leads to inhibition of EndoMT and abrogation of lung fibrosis in murine model (30, 31).

Previous studies have shown IL-17A plays a key role in the fibrotic process of various organs like lung, kidney, heart and skin. Both the levels of TGF-β and fibroblast TGF-β receptors are reported to be upregulated in the lungs of idiopathic pulmonary fibrosis patients (32). Except for TGF-β other cytokines involved in Th17 differentiation are indicated to induce lung fibrosis as well (32), suggesting potential role of IL-17A in pulmonary remodeling (33). By inhibiting Smad-independent pathways, IL-17A is thought to inhibit TGF-β-induced renal fibroblast activation (34). In animal models of skin fibrosis IL-17A is suggested to be a profibrotic mediator *via* TGF-β-dependent pathways to induce collagen deposition in skin (35). Systemic Sclerosis, characterized by fibrosis of multiple organs, is suggested to be related to a polarization to Th17 pathway-induced activation of immune responses (36) (more detailed proposed mechanisms shown in **Figure 2**).

Studies have shown that Th17 cell–derived IL-17 was significantly higher in the serum of SSc patients (36). Majority studies indicate that the levels of IL-17A in SSc serum is increased while contradictory studies indicating no differences or lower levels of IL-17A in SSc exist (1). Th17 response is regulated towards IL-17A pathway instead IL-17F (10). IL-17A+ cells are increased in the dermis of SSc skin (1) while IL-17F + cells were relatively low in Ssc skin (10). Circulating IL-17A in serum of SSc patients are high while IL-17F levels were not. Also IL-17A mRNA from Ssc lesional skin was higher while the trace of IL-17F mRNA was tiny (10). The numbers of IL-17+ cells are inversely proportional to the extent of severity in SSc (37). It has been demonstrated that IL-17 promoted the proliferation of SSc fibroblasts, but the effect on collagen and ECM protein synthesis is trivial (36). High IL-17E and low IL-17C has been reported in morphea as well (38). IL-21/IL-21R could be potential biomarkers presented in early SSc skin lesions indicating SSc is possibly a Th17-/Th22-driven disorder (39).

IL-17A is indicated to have profibrotic role in mouse models of lung fibrosis (35). As NF-κB signaling pathway is downstream of IL-17A and Act1 being the regulator of it, interference of Act1 leads to inhibition of pulmonary fibroblasts proliferation (13). Previous murine *in vivo* experiments show that IL-17A induces mouse skin fibroblasts to release TGF-β, CTGF and collagen; IL-17 can also promote ECM deposition and epithelial-to-mesenchymal transition in mouse alveolar epithelial cells *via* TGF-β-dependent pathways (23). We can see that IL-17A does have a pro-fibrotic activity in animal models. Karatas et al. reported that secukinumab and metformin ameliorated dermal fibrosis in bleomycin-induced mouse models by decreasing dermal thickness and tissue IL-17A levels, suggesting the association of IL-17A with dermal fibrosis in animals (40). However the pro-fibrotic mechanisms of IL-17A in animal models cannot be applied to humans (1). No definitive evidence can prove the role of IL-17A in lung fibrosis progression involved in SSc patients (1).The dichotomous nature of IL-17 lies in that it is pro-fibrotic in animal models while having a dual pro-inflammatory and anti-fibrotic role in humans (36). This dual role of IL-17A in SSc patients may make it capable of inducing the inflammatory responses while protecting against fibrosis at the same time (41). Zhou et al. have found that IL-17RA is expressed mainly in epidermis in SSc, while keratinocyte-derived mediators are capable of crossing the epidermal–dermal basement membrane. Fibroblasts, endothelial

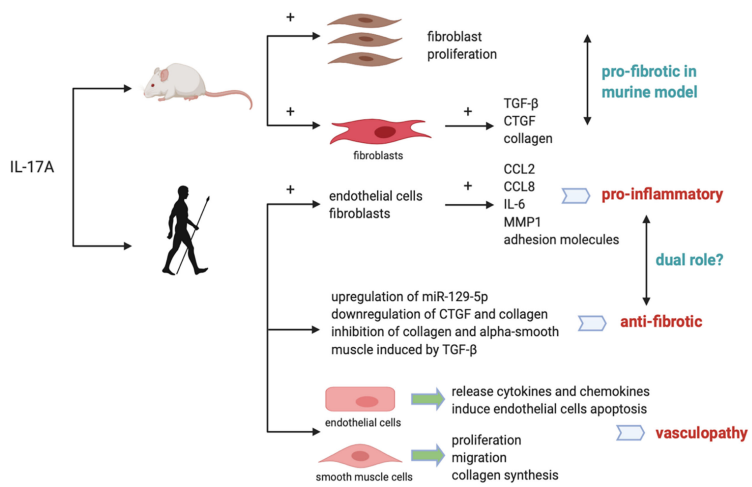

FIGURE 2 | Proposed mechanisms for the role of IL-17A in SSc in mice and humans. In murine models, IL-17A is pro-fibrotic by promoting fibroblast proliferation and inducing synthesis of collagen and CTGF. In humans, IL-17A was reported to induce pro-inflammatory cytokines while inhibit collagen and CTGF synthesis, exerting a dual pro-inflammatory and anti-fibrotic role. IL-17A is also related with vasculopathy by promoting endothelial inflammation and smooth muscle cells proliferation, migration and collagen synthesis.

cells, and leukocytes located in dermis are thus stimulated (41). Dufour et al. observe an anti-fibrotic activity of IL-17A (42) in organotypic full-skin cultures in the context of simulated physiological condition under the synergistic influence of many cell types and cytokines together (1), further confirming the role of IL-17A in promoting pro-inflammatory and anti-fibrotic responses (43). Vettori et al. found that IL-17A regulates T cell-mediated antifibrotic and proapoptotic role in skin fibroblasts (44). The pro-inflammatory property of IL-17A is that it promotes production of CCL2, CCL8, IL-6, MMP1, and the expression of adhesion molecules in dermal fibroblasts and endothelial cells (1). Park et al. reported in two different murine models of SSc, IL-1β and IL-17A showed synergistic effects on inducing pro-inflammatory mediators like IL-6, MMP-9 and TGF-β (45). Thus, targeting IL-1 and IL-17A activity could provide insights into novel treatment strategy in SSc (45). The anti-fibrogenic property of IL-17A is that it inhibits collagen production or alpha-smooth muscle actin expression induced by TGF-β in dermal fibroblasts (1). Dufour et al. reported first the dual role of IL-17A under the influence of TGF-β. IL-17A could exert pro-fibrotic function by synergizing with TGF-β to induce more robust IL-6 production, and in the meantime exert anti-fibrotic function by inhibiting TGF-β-induced collagen synthesis. P38 MAPK signaling pathway is suggested to be the unique joint downstream pathway of this IL-17A and TGF-β synergy (46). IL-17A can also exerts anti-fibrogenic effect *via* the upregulation of miR-129-5p and the downregulation of connective tissue growth factor (CTGF) and collagen. It has been suggested that intrinsic activation of TGF-β in SSc fibroblasts could in turn inhibit expression of IL-17 receptor in fibroblasts, leading to an amplification of collagen levels and fibrosis in SSc (47). One possible reason this anti-fibrogenic effect of IL-17A is not capable of containing the fibrosis in SSc could be that intrinsic differences between normal and SSc fibroblasts show that SSc fibroblasts are more resistant than their normal counterparts in response to collagen inhibition under the influence of IL-17. This property of SSc fibroblasts may help them escape or limit the anti-fibrotic effects of IL-17 (40).

As the earliest stage of the course of SSc, vasculopathy occurred before fibrosis in SSc skin (31). Release of proinflammatory mediator and vasoactive regulators mark the beginning of endothelial aberrant activation (48). Newly expressed adhesion molecules on the surface of endothelial cells facilitate inflammatory cells infiltration and interaction. Xing et al. discovered that IL-17A derived from sera of SSc patients mediates endothelial cell inflammation *via* ERK1/2 phosphorylation (48). IL-17A induces endothelial cells to release cytokines and chemokines that attract neutrophils infiltration. Also, IL-17 is said to induce endothelial cells apoptosis which further promote endothelial cell dysfunction in the context of abnormal inflammation (35).

IL-17A has pleiotropic effect on vascular smooth muscle cells from SSc patients. IL-17A promotes proliferation and migration of these cells, resemblance to the formation of atherosclerosis plug (10). Liu et al. discovered that IL-17A from SSc patients could induce the proliferation, migration and collagen synthesis of DVSMCs *via* ERK1/2 signaling pathway (49), IL-17A exerts its pro-fibrotic role in endothelial inflammation in a dose- and time-dependent pattern (49). IL-17A enhances release of adhesion molecules such as CCL-20, ICAM-1, CXCR-4 and VCAM-1 (10), attracting neutrophils migrating to the inflammation site. Xing et al. also found that T cell adherence to HUVECs is enhance by IL-17A (48).Whether targeting ERK1/2 might be a potential strategy for the treatment of SSc vasculopathy could be an interesting topic. Apart from IL-17A, Fukayama et al. found elevated levels of IL-17F and IL-17E is correlated with vasculopathy in SSc patients as well by interacting with receptors on vascular endothelial cells to induce endothelial cell proliferation (50).

IL-17 TARGETING THERAPY

There are many types of antibodies that block a diverse range of area in IL-17 pathway in clinical use (as shown in **Table 1**). The first clinically used drug that antagonize IL-17A is Secukinumab approved in 2015 (51). Secukinumab and Ixekizumab inhibit IL-17A and IL-17A/F and can be used in the treatment of autoimmune diseases like psoriasis. Bimekizumab is developed to target both IL-17A and IL-17F at the site of the common motif they shared. Brodalumab antagonizes with the ubiquitously expressed common IL-17RA receptor subunit thus have the potential to inhibit different IL-17 family members at the same time, such as IL-17A, IL-17F, IL-17C and IL-17E (2, 19). It has been suggested that blocking IL-17A can also inhibit Calcium cascade which help to attenuate lung fibrosis (52). IL-23 is known to be the key mediator in the maturation of IL-17 and it is consisted of the IL-23-specific p19 subunit and the common p40 subunit (2). Antibodies against IL-23-specific p19 subunit include Tildrakizumab and Risankizumab (2, 51). Antibodies against common p40 subunit shared with IL-12 include Ustekinumab (51). As IL-17A synergizes with TNF-α, antibodies like ABT-122 could potentially target TNF-α at one site and IL-17A at the other (2). IL-17A inhibitors demonstrate a favorable safety, efficacy, and tolerability profile, bringing the success of treating of moderate-to-severe plaque psoriasis (53). Targeting STAT3, the upstream regulator of IL-17 differentiation has the potential to modulate fibrosis since many other signaling pathways in fibrotic events converge on STAT3 (49). However it is exactly because its central role in many immune processes that its off-target effect when targeting STAT3 needs further consideration (30). Since IL-17A signaling pathway involves activation of NF-κB, and Act1 is the upstream regulator of this pathway, silencing Act may provide new insights into next generation of therapies (13). Dual role of IL-17A and the subtle balance over its control raises concerns over the use of antibodies against IL-17——whether it will abrogate fibrosis or antagonize the protective role of IL-17 remains an issue and requires further investigations into it. It is worthy of consideration the protective role of IL-17A in host defense against infection when blocking IL-17 pathway, as it could bring detrimental harm (54).

TABLE 1 | Summary of antibodies that target IL-17 pathways.

IL-17A and IL-17A/F inhibitors	Secukinumab Ixekizumab
IL-17A and IL-17F inhibitors	Bimekizumab
IL-17RA inhibitors	Brodalumab
IL-23 inhibitors	Tildrakizumab Risankizumab Ustekinumab
IL-17A and TNF-α inhibitors	ABT-122

CONCLUDING REMARKS AND FUTURE

IL-17 (IL-17A) is a pro-inflammatory cytokine produced by a subset of T helper cells termed Th17 cells primarily in response to cytokines like TGF-β and IL-23. IL-17 plays an important role in host defense and is linked to various autoimmune diseases pathogenesis. IL-17 signals *via* the IL-17RA/RC heterodimer and the adaptor protein Act1 to activate NF-kB and MAPK pathways. IL-17 stimulates stromal cells such as endothelial, epithelial cells and fibroblasts to secrete other immunomodulatory factors. The pathogenic role of IL-17A in SSc is quite intriguing: on one hand IL-17A promotes secretion of pro-inflammatory cytokines and enhances immune reactions and on the other it decreases fibrotic responses and abrogates fibrosis. The potential target therapy against IL-17A pathways could provide new insights into treatment strategies of SSc and is worthy of further deeper investigation.

AUTHOR CONTRIBUTIONS

DA and VO contributed to helping draft the framework and giving suggestions of modifications for this review. LW as the first author of this review completed most of the writing. All authors contributed to the article and approved the submitted version.

ACKNOWLEDGMENTS

I would like to express my sincere gratitude towards my primary supervisor, DA, and my secondary supervisor, VO, for their contribution and professional help to this review.

REFERENCES

1. Chizzolini C, Dufour AM, Brembilla NC. Is There a Role for IL-17 in the Pathogenesis of Systemic Sclerosis? *Immunol Lett* (2018) 195:61–7. doi: 10.1016/j.imlet.2017.09.007
2. Brigitta S, Omenetti S. The Dichotomous Nature of T Helper 17 Cells. *Nat Rev Immunol* (2017) 17(9):p535–44. doi: 10.1038/nri.2017.50
3. Yao Y, Thomsen SF. The Role of Interleukin-17 in the Pathogenesis of Hidradenitis Suppurativa. *Dermatol Online J* (2017) 23(7). doi: 10.5070/D3237035729
4. Lee GR. The Balance of Th17 Versus Treg Cells in Autoimmunity. *Int J Mol Sci* (2018) 19(3): 730. doi: 10.3390/ijms19030730
5. Abusleme L, Moutsopoulos N. IL-17: Overview and Role in Oral Immunity and Microbiome. *Oral Dis* (2017) 23(7):854–65. doi: 10.1111/odi.12598
6. Speeckaert R, Lambert J, Grine L, Van Gele M, De Schepper S, van Geel N. The Many Faces of Interleukin-17 in Inflammatory Skin Diseases. *Br J Dermatol* (2016) 175(5):892–901. doi: 10.1111/bjd.14703
7. Truchetet M-E, Allanore Y, Montanari E, Chizzolini C, Brembilla NC. Prostaglandin I 2 Analogues Enhance Already Exuberant Th17 Cell Responses in Systemic Sclerosis. *Ann Rheumatic Dis* (2012) 71(12):2044–50. doi: 10.1136/annrheumdis-2012-201400
8. Chen Y, Kanno Y, Joyce-Shaikh B, Vahedi G, Hirahara K, Blumenschein WM., et al. Interleukin-23-Induced Transcription Factor Blimp-1 Promotes Pathogenicity of T Helper 17 Cells. *Immunity* (2016) 44(1):131–42. doi: 10.1016/j.immuni.2015.11.009
9. Kuwabara T, Ishikawa F, Kondo M, Kakiuchi T. The Role of IL-17 and Related Cytokines in Inflammatory Autoimmune Diseases. *Mediators Inflamm* (2017) 11. doi: 10.1155/2017/3908061
10. Bălănescu P, Bălănescu E, Anca B. IL-17 and Th17 Cells in Systemic Sclerosis: A Comprehensive Review. *Romanian J Intern* (2017) 55(4):198–204. doi: 10.1515/rjim-2017-0027
11. Gaffen SL, Jain R, Garg AV, Cua DJ. The IL-23–IL-17 Immune Axis: From Mechanisms to Therapeutic Testing. *Nat Rev Immunol* (2014) 14(9):585–600. doi: 10.1038/nri3707
12. Amatya N, Garg AV, Gaffen SL. IL-17 Signaling: The Yin and the Yang. *Trends Immunol* (2017) 38(5):310–22. doi: 10.1016/j.it.2017.01.006
13. Yang Y, Zhang T, Li Y, Kang Q, Lei W, Cao Y., et al. siRNA-Act1 Inhibits the Function of IL-17 on Lung Fibroblasts *via* the NF-κb Pathway. *Respiration* (2013) 86(4):332–340. doi: 10.1159/000348403
14. Eyerich K, Dimartino V, Cavani A. IL-17 and IL-22 in Immunity: Driving Protection and Pathology. *Eur J Immunol* (2017) 47(4):607–14. doi: 10.1002/eji.201646723
15. Katz Y, Nadiv O, Rapoport MJ, Loos M. IL-17 Regulates Gene Expression and Protein Synthesis of the Complement System, C3 and Factor B, in Skin Fibroblasts. *Clin Exp Immunol* (2000) 120(1):22–9. doi: 10.1046/j.1365-2249.2000.01199.x
16. Fisher AJ, Gu H, Mickler EA, Agarwal M, Wilke CA, Kim KK., et al. IL-17A Deficiency Mitigates Bleomycin-Induced Complement Activation During Lung Fibrosis. *FASEB J* (2017) 31(12):5543–56. doi: 10.1096/fj.201700289R
17. Silvestre R, Granja S. IL-17A and IL-17F Orchestrate Macrophages to Promote Lung Cancer. *Cell Oncol* (2020) 43(4):643–54. doi: 10.1007/s13402-020-00510-y
18. Li MM, Shen J, Liu F, Cao JY, Jin S, Yu Y., et al. Interleukin-17-Induced EMT Promotes Lung Cancer Cell Migration and Invasion *via* NF-Kappa B/ZEB1 Signal Pathway. *Am J Of Cancer Res* (2015) 5(3):pp.1169–1179.
19. Mcgeachy MJ, Cua DJ, Gaffen SL. The IL-17 Family of Cytokines in Health and Disease. *Immunity* (2019) 50(4):892–906. doi: 10.1016/j.immuni.2019.03.021
20. Blauvelt A, Chiricozzi A. The Immunologic Role of IL-17 in Psoriasis and Psoriatic Arthritis Pathogenesis. *Clin Rev Allergy Immunol* (2018) 55(3):379–90. doi: 10.1007/s12016-018-8702-3
21. Chizzolini C, Brembilla NC, Montanari E, Truchetet ME. Fibrosis and Immune Dysregulation in Systemic Sclerosis. *Autoimmun Rev* (2011) 10 (5):276–81. doi: 10.1016/j.autrev.2010.09.016
22. Katsumoto TR, Whitfield ML, Connolly MK. The Pathogenesis of Systemic Sclerosis. *Annu Rev Pathol* (2011) 6:509–37. doi: 10.1146/annurev-pathol-011110-130312
23. Wu W, Sun X, Yang J, Xu J, Fu W, Li M., et al. New Insights Into CD4 T Cell Abnormalities in Systemic Sclerosis. *Cytokine Growth Factor Rev* (2016) 28:31–6. doi: 10.1016/j.cytogfr.2015.12.002
24. O'Reilly S, Hügle T, van Laar JM. T Cells in Systemic Sclerosis: A Reappraisal. *Rheumatol (Ox Eng)* (2012) 51(9):1540–9. doi: 10.1093/rheumatology/kes090
25. Korman B. Evolving Insights Into the Cellular and Molecular Pathogenesis of Fibrosis in Systemic Sclerosis. *Trans Res* (2019) 209:77–89. doi: 10.1016/j.trsl.2019.02.010
26. Wick G, Backovic A, Rabensteiner E, Plank N, Schwentner C, Sgonc R. The Immunology of Fibrosis: Innate and Adaptive Responses. *Trends Immunol* (2010) 31(3): 110–9. doi: 10.1016/j.it.2009.12.001

27. Chizzolini C, Brembilla NC, Montanari E, Truchetet ME. Fibrosis and Immune Dysregulation in Systemic Sclerosis. *Autoimmun Rev* (2011) 10 (5):276–81. doi: 10.1016/j.autrev.2010.09.016
28. Worrell JC, O'Reilly S. Bi-Directional Communication: Conversations Between Fibroblasts and Immune Cells in Systemic Sclerosis. *J Autoimmun* (2020) 113:102526. doi: 10.1016/j.jaut.2020.102526
29. Hammerich L, Heymann F, Tacke F. Role of IL-17 and Th17 Cells in Liver Diseases. *Clin Dev Immunol* (2011), 345803. doi: 10.1155/2011/345803
30. Ahmed S, Misra, Durga P, Agarwal V. Interleukin-17 Pathways in Systemic Sclerosis-Associated Fibrosis. *Rheumatol Int* (2019) 39(7):1135–43. doi: 10.1007/s00296-019-04317-5
31. Ong VH, Costantini B, Denton CP, Abraham D, Placais L, Blighe K., et al. Deep Phenotyping Detects a Pathological CD4 T-Cell Complosome Signature in Systemic Sclerosis. *Cell Mol Immunol* (2020) 17(9):1010–3. doi: 10.1038/s41423-019-0360-8
32. Fusaro E, Nicola S, Bucca C, Peroni C, Parisi S, Cassinis MC., et al. Th-17 Cytokines and Interstitial Lung Involvement in Systemic Sclerosis. *J Breath Res* (2016) 10(4):7. doi: 10.1088/1752-7155/10/4/046013
33. Teodoro WR, Santos Filho A, Andrade PC, Eher E, Fernezlian S, Capelozzi VL., et al . IL-17 IMMUNOEXPRESSION IS CORRELATED WITH INCREASED COLLAGEN V IN SYSTEMIC SCLEROSIS PULMONARY FIBROSIS. *Rev Bras Reumatol* (2017) 57:S95–6. doi: 10.1016/j.rbr.2017.07.046
34. Wang H, Zhang L, Yang X, Zhang M, Zhu X, Ji X., et al. Role of Interleukin 17 in TGF-β Signaling-Mediated Renal Interstitial Fibrosis. *Cytokine* (2018) 106:80–8. doi: 10.1016/j.cyto.2017.10.015
35. Ramani K, Biswas PS. Interleukin-17: Friend or Foe in Organ Fibrosis. *Cytokine* (2019) 120:282–8. doi: 10.1016/j.cyto.2018.11.003
36. Pereira MC, Dantas AT, Almeida AR, Marques CDL, Rego MJBM, Pitta IR, et al. IL-17 and Related Cytokines Involved in Systemic Sclerosis: Perspectives. *Autoimmunity* (2018) 51(1):1–9. doi: 10.1080/08916934.2017.1416467
37. Brembilla NC, Montanari E, Lonati P, Raschi E, Zeni S, Fontao L., et al. Interleukin-17a Cell Counts Are Increased in Systemic Sclerosis Skin and Their Number Is Inversely Correlated With the Extent of Skin Involvement. *Arthritis Rheumatism* (2013) 65(5):1347–56. doi: 10.1002/art.37860
38. Brembilla NC, Montanari E, Fontao L, Gabrielli A, Vettori S, Valentini G., et al. High IL-17E and Low IL-17C Dermal Expression Identifies a Fibrosis-Specific Motif Common to Morphea and Systemic Sclerosis. *PloS One* (2014) 9 (8):.e105008. doi: 10.1371/journal.pone.0105008
39. Hou W, Xu K, Han D, Jiang C, Mou K, Li Y, et al. The Elevated Expression of Th17-Related Cytokines and Receptors is Associated With Skin Lesion Severity in Early Systemic Sclerosis. *Hum Immunol* (2015) 76(1):22–9. doi: 10.1016/j.humimm.2014.12.008
40. Karatas A, Celik C, Oz B, Akar ZA, Etem EO, Dagli AF, et al. Secukinumab and Metformin Ameliorate Dermal Fibrosis by Decreasing Tissue Interleukin-17 Levels in Bleomycin-Induced Dermal Fibrosis. *Int J Rheum Dis* (2021) 24 (6):795–802. doi: 10.1111/1756-185X.14114
41. Brembilla NC, Montanari E, Truchetet ME, Raschi E, Meroni P, Chizzolini C. Th17 Cells Favor Inflammatory Responses While Inhibiting Type I Collagen Deposition by Dermal Fibroblasts: Differential Effects in Healthy and Systemic Sclerosis Fibroblasts. *Arthritis Res Ther* (2013) 15(5):R151. doi: 10.1186/ar4334
42. Borowczyk-Michalowska] J, Alvarez M, Truchetet ME, Modarressi A, Brembilla NC, Chizzolini C., et al. IL-17a Dissociates Inflammation From Fibrogenesis in Systemic Sclerosis. *J Invest Dermatol* (2020) 140(1):103–112.e8. doi: 10.1016/j.jid.2019.05.026
43. Dufour A, Alvarez M, Lemeille S, Truchetet ME, Brembilla NC, Chizzolini C. FRI0411 Dual Pro-Inflammatory and Anti-Fibrotic Role of Il-17a in Systemic Sclerosis Skin. *Ann Rheum Dis* (2018) 77(s2):737–7. doi: 10.1136/annrheumdis-2018-eular.6784
44. Barra G, Russo B, Borgia A, Pasquale G, Pellecchia L, Vicedomini L., et al. T-Cell Proapoptotic and Antifibrotic Activity Against Autologous Skin Fibroblasts *In Vitro* Is Associated With IL-17a Axis Upregulation in Systemic Sclerosis. *Front Immunol* (2020) 11:220. doi: 10.3389/fimmu.2020.00220
45. Moon SJ, Lee EJ, Jung KA, Kim EK, Kim DS, Lee JH, et al. IL-1-IL-17 Signaling Axis Contributes to Fibrosis and Inflammation in Two Different Murine Models of Systemic Sclerosis. *Front Immunol* (2018) 9:1611. doi: 10.3389/fimmu.2018.01611
46. Dufour AM, Alvarez M, Russo B, Chizzolini C. Interleukin-6 and Type-I Collagen Production by Systemic Sclerosis Fibroblasts Are Differentially Regulated by Interleukin-17A in the Presence of Transforming Growth Factor-Beta 1. *Front Immunol* (2018) 9:1865. doi: 10.3389/fimmu.2018.01865
47. Jinnin M, Yamane K, Honda N, Kajihara I, Makino T, Masuguchi S, et al. Impaired IL-17 Signaling Pathway Contributes to the Increased Collagen Expression in Scleroderma Fibroblasts. *J Immunol (Baltimore Md. 1950)* (2012) 188(8):3573–83. doi: 10.4049/jimmunol.1100591
48. Yang J, Yang X, Wei Y, Zhu L, Gao D, Li M., et al. IL-17A Induces Endothelial Inflammation in Systemic Sclerosis *via* the ERK Signaling Pathway. *PloS One* (2013) 8(12):e85032. doi: 10.1371/journal.pone.0085032
49. Liu M, Yang J, Xing X, Cui X, Li M. Interleukin-17A Promotes Functional Activation of Systemic Sclerosis Patient-Derived Dermal Vascular Smooth Muscle Cells by Extracellular-Regulated Protein Kinases Signalling Pathway. *Arthritis Res Ther* (2014) 16(6):4223. doi: 10.1186/s13075-014-0512-2
50. Yoshizaki A, Fukasawa T, Ebata S, Kuzumi A, Yoshizaki-Ogawa A, Asano Y., et al. Interleukin (IL)-17F and IL-17E Are Related to Fibrosis and Vasculopathy in Systemic Sclerosis. *J Dermatol* (2020) 47(11):1287–92. doi: 10.1111/1346-8138.15508
51. Kurschus FC, Moos S. IL-17 for Therapy. *J Dermatol Sci* (2017) 87(3):221–7. doi: 10.1016/j.jdermsci.2017.06.010
52. Derynck R, Zhang YE. Smad-Dependent and Smad-Independent Pathways in TGF-[Beta] Family Signalling. *Nature* (2003) 425(6958):577. doi: 10.1038/nature02006
53. Ly K, Smith MP, Thibodeaux Q, Reddy V, Liao W, Bhutani T. Anti-IL-17 in Psoriasis. *Expert Rev Clin Immunol* (2019) 15(11):1185–94. doi: 10.1080/1744666X.2020.1679625
54. van den Berg WB, McInnes IB. FRCP, 2013. Th17 Cells and IL-17 A—Focus on Immunopathogenesis and Immunotherapeutics. *Semin Arthritis Rheum* (2013) 43(2):158–70. doi: 10.1016/j.semarthrit.2013.04.006

Conflict of Interest: The authors declare that the research was conducted in the absence of any commercial or financial relationships that could be construed as a potential conflict of interest.

frontiers | Frontiers in Immunology

REVIEW
published: 16 June 2022
doi: 10.3389/fimmu.2022.883733

Co-Inhibitory Molecules – Their Role in Health and Autoimmunity; Highlighted by Immune Related Adverse Events

Stinne R. Greisen[1,2]*, *Maithri Aspari*[1] and *Bent Deleuran*[1,2]

[1] Department of Biomedicine, Aarhus University, Aarhus, Denmark, [2] Department of Rheumatology, Aarhus University Hospital, Aarhus, Denmark

Immune checkpoint receptors are key players in regulating the immune response. They are responsible for both generating an immune response sufficient to kill invading pathogens, balancing the same response, and protecting against tissue destruction or the development of autoimmune events. The central role of the co-inhibitory receptors also referred to as inhibitory immune checkpoints, including PD-1 and CTLA-4 has become especially evident with the cancer treatments targeting these receptors. Blocking these pathways enhances the immune activity, resulting in both an increased chance of cancer clearance, at the same time induction of immune-related adverse events (irAE). Some of these irAE progress into actual autoimmune diseases with autoantibodies and symptoms, undistinguished from the naturally occurring diseases. This review will take advantage of the lessons learned from immune checkpoint blockade and relate this knowledge to our understanding of the same pathways in naturally occurring autoimmune diseases, mainly focusing on rheumatic diseases.

Keywords: PD-1, checkpoint inhibition therapy, autoimmunity, co-inhibitory receptors, immune related adverse events, rheumatic diseases

OPEN ACCESS

Edited by:
Rizgar A. Mageed, Queen Mary University of London, United Kingdom

Reviewed by:
Dawn Elaine Smilek, UCSF, United States
Giulia Di Dalmazi, G. d'Annunzio University of Chieti and Pescara, Italy

***Correspondence:**
Stinne R. Greisen
srg@biomed.au.dk

Specialty section:
This article was submitted to Autoimmune and Autoinflammatory Disorders, a section of the journal Frontiers in Immunology

Received: *25 February 2022*
Accepted: *10 May 2022*
Published: *16 June 2022*

Citation:
Greisen SR, Aspari M and Deleuran B (2022) Co-Inhibitory Molecules – Their Role in Health and Autoimmunity; Highlighted by Immune Related Adverse Events. Front. Immunol. 13:883733. doi: 10.3389/fimmu.2022.883733

INTRODUCTION: BALANCING HEALTH AND DISEASE

The immune system is unique when it comes to its ability to protect our body and maintain homeostasis. It can both defend us against foreign pathogens and at the same time recognize and accept self-antigens. This equilibrium is also essential in avoiding cancer and controlling aging. Owing to the complexity of this system, we seem to be only scratching the surface in our understanding of the plethora of factors involved in this balanced regulation.

For T cells, the evolvement of a healthy immune system starts in the thymus where CD4 and CD8 T cells undergo positive and negative selection, to ensure an optimal reactivity to foreign antigens, and high tolerance towards self (1). Once out of the thymus, these cells will use an array of mechanisms when encountering a foreign antigen. The innate immune system is the first line of defense, subsequently resulting in the activation and recruitment of T cells and finally initiating an adaptive immune response. For antigen presenting cells to successfully activate a T cell, the T cell will need a second signal through an immune checkpoint, or co-receptor, which will be upregulated upon T cell receptor signaling or by cytokines (2, 3). The activation of co-receptors can either lead to

increased activation of the T cell or inhibit the activation resulting in a dampened response or even anergy. The outcome from the balanced signaling between the multiple co-receptors thus determines the fate of an antigen-activated T cell. Often, the presentation of a high-affinity antigen that is significantly different from self, will result in an upregulation of the co-stimulatory receptors (CSR), like CD28 or 4-1BB, leading to full activation of the T cell (4). If the presented antigen resembles self or is of low affinity, upregulation of co-inhibitory receptors (CIR), including programmed death-1 (PD-1) and cytotoxic T-lymphocyte-associated protein 4 (CTLA-4) will be more pronounced (5, 6). These pathways will cause downregulation of the T cell activation, including diminished cytokine production, less proliferation, and reduced motility (7). Failure in balancing this second signal may cause chronic infections, cancers, or autoimmune diseases. The innate immune system can also initiate a chronic inflammatory condition, often referred to as autoinflammation. This topic is, however, beyond the scope of this review (8). In the following, we will focus on the CIR, their ligands, and their role in the development of autoimmune diseases. We consider this with the lessons learned from cancer treatment using immune checkpoint inhibitors (ICI), resulting in various inflammatory conditions, referred to as immune-related adverse events (irAE).

RESULTS: THE FIRST 10 YEARS OF IMMUNE CHECKPOINT INHIBITOR THERAPY

One of the central features in cancer development is the escape of immune surveillance. One mechanism exploited by cancer cells is the upregulation of ligands for the CIR, causing infiltrating immune cells to be shut down, thus avoiding immune mediated killing (9). Immune checkpoint inhibitors block CIR or their ligands. The first drug on the market targeted CTLA-4 (10, 11) and has in conjunction with ICI towards the PD-1 pathway, revolutionized cancer treatment. As a result of the increased immune activation, irAE and reduced cancer burden often goes hand-in-hand. However, these drugs provide valuable insight into the understanding of the role of CIR in the development of autoimmunity. In some cases, irAE become chronic conditions, closely resembling an autoimmune disease. Presentation with a full-blown debut of an autoimmune disease, even with autoantibodies is described (12, 13). IrAE are seen with a large variation in intensity, but are very common and affect 50%-70% of patients in monotherapy and more than 90% in combination therapy (12). Often, combination therapy targets both CTLA-4 and PD-1, which makes it difficult to pinpoint a specific clinical manifestation of one or the other. Despite several years in use, it remains difficult to predict which patients will respond to the treatment, and the search for prognostic biomarkers is ongoing (14). The development and treatment of irAE are often the governing steps for patients in ICI treatment. In patients with known systemic immunological disorders, ICI treatment is still limited to very few trials. Worsening, or flare in their disease seems to closely follow tumor regression (15). Considering the occurrence of irAE, it is appealing that the CIR pathways play a prominent role in the development of autoimmune diseases (**Figure 1**).

Many irAE tend to fade or disappear when the ICI treatment is ceased. These irAE thus deviate from what we normally see when examining an autoimmune disease. This supports a role for CIR serving to decrease immune activation, and their absence, or reduced function, leading to temporary symptoms or disease. Contrarily, upon considering the cases where the irAE progress into chronic diseases, these indicate that the dysfunction of CIR can induce a break in tolerance leading to autoimmunity (16). The factors determining these two different outcomes remain to be understood. More than 40% of the irAE develop into chronic conditions, often less responsive to steroids (17). The inflammatory conditions often present within the first 2-6 weeks of therapy, but may also arise already after the first treatment, or not until after several years of treatment (17, 18). Although autoimmune diseases are closely associated with HLA genotypes only a few studies have investigated the association between irAE and HLA type, and with no clear conclusion (19, 20).

It does occur that irAE are much more common than their "counter" autoimmune disease. One case is hypophysitis, an autoimmune reaction in the pituitary gland, very rare in its idiopathic form, but with an overall incidence after ICI treatment reported in a recent meta-analysis as 14%. This is a relatively common irAE, and also of significant severity, subsequently demanding life-long treatment as multiple hormonal axes are involved, and the damage is irreversible (21). Primary hypophysitis is not associated with systemic inflammation, and CIR have to our knowledge, not been investigated in the development of primary hypophysitis, where the mechanisms responsible for development are still largely unknown (22).

From a clinical viewpoint, it remains a challenge to treat patients with irAE especially if the symptoms become chronic, or hinder continued treatment of the oncologic disease. The first line of treatment is often corticosteroids, especially if these can be used locally (23, 24). However, systemic corticosteroid treatment results in both reduced antigen recognition and ability for cellular toxicity, especially ADCC. The use of systemic corticosteroid treatment thus raises a concern about the continued efficacy of the ICI to induce tumor eradication (25). This has resulted in a general consent to reducing corticosteroids to a minimum as quickly as possible, and a tendency to use disease-modifying anti-rheumatic drugs (DMARD) to reach control of the irAE. Anti-TNF antibodies and anti-IL-6R antibodies are the mainly used therapies, but large-scale and long-term studies are still not carried out (26, 27). Therefore, a better understanding of this area is needed, to improve treatment for both the cancer and the irAE.

THE CD28/B7 FAMILY

The CD28/B7 family of CSR and CIR is probably the best described among all co-receptors. CD28 was the first identified

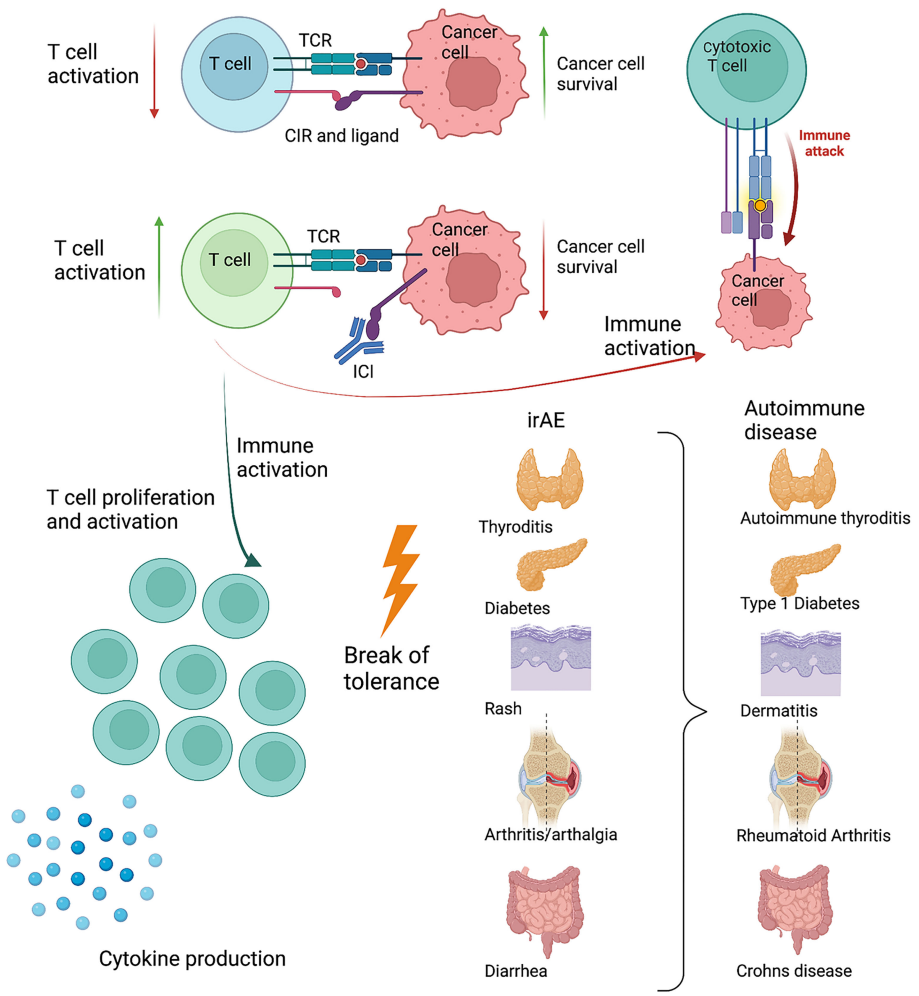

FIGURE 1 | Schematic drawing of the interaction between an activated T cell and a cancer cell. The cancer cell exploits the PD-1 pathway, reducing T cell activity. When blocking the PD-1 pathway with antibodies, the T cell becomes sufficiently activated to kill the cancer cell. As a response to increased T cell activation and inflammation, immune related adverse events (irAE) develop. These target different organs and resembles known autoimmune diseases present in the same organ. Created with BioRender.com.

CSR and is crucial for optimal T cell activation (28). Signaling through the CD28 pathway induces complete T cell activation with increased motility, proliferation, and cytokine production including IL-2 and IFN-y. CD28 signals downstream through PI3K and PKC0, finally resulting in phosphorylation of AKT and NFkB. Mice lacking CD28 have a reduced immunoglobulin concentration and class switch, as well as decreased levels of IL-2. However, cytotoxic T cells do develop in these mice, and they do not succumb to infections (29). CD28 is necessary for the development of Tregs, but also favors the development of immune reactive T cells. Despite promising evidence (30), targeting CD28 in autoimmunity has not reached common clinical use, and especially for rheumatoid arthritis (RA), the focus has been on targeting CTLA-4, which also binds CD80, and competes with CD28 (31). This review will primarily focus on CIR, and the role of CD28 will not be discussed further. The two other two important members in the CD28/B7 family are CTLA-4 and PD-1, these being CIR (**Figure 2**).

THE PD-1 PATHWAY

PD-1 is a trans-membranous receptor mainly expressed by activated lymphocytes, however PD-1 expression has been described on several other cell types and in multiple tissues (32, 33). PD-1 has two ligands, PD-L1 and PD-L2 (34, 35). Engaging the PD-1 receptor causes phosphorylation of the ITSM motif and recruitment of SHP2, subsequently resulting in dephosphorylation of PI3K and AKT, eventually causing reduced activity in NFkB and thereof, a decreased T cell activation (3, 36, 37). Cancer cells utilize the expression of PD-L1 to silence inhibitory signals from cytotoxic T cells and

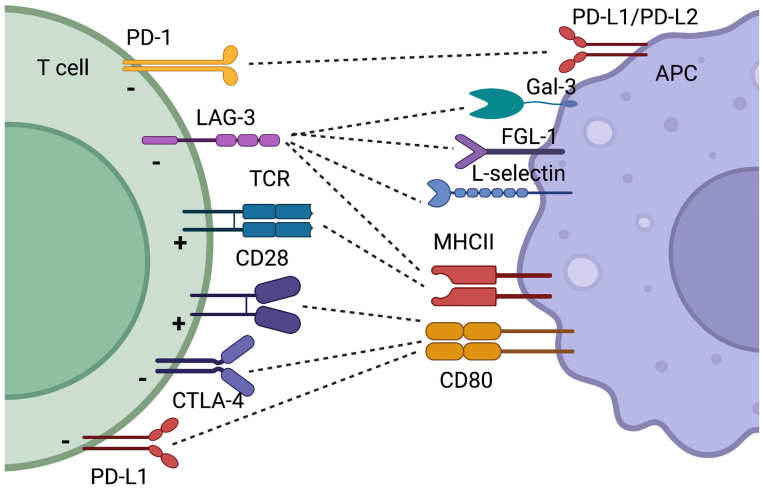

FIGURE 2 | Simplified schematic illustration of CIR and CSR discussed in this review. Some receptors have binding partners which is illustrated by dotted lines. The function on the T cell by the receptor is indicated with a "+" for T cell activation and a "-" when T cell activity is decreased. Created with BioRender.com.

other host immune cells. PD-1 or PD-L1 expression is often used as a marker (though poor) to identify tumors where treatment with ICI seems feasible (38). The PD-1 pathway not only signals through the PD-1 receptor; reverse signaling through PD-L1 is described, increasing cell survival and decreasing type 1 IFN responsiveness (39). This can be exploited by cancer cells, further supporting tumor growth and immune avoidance. PD-L1 reverse signaling is also crucial for chemokine-mediated dendritic cell migration from the skin to the lymph node (40). The role of reverse signaling in autoimmunity remains to be clarified.

Both PD-1 and its ligands are present in soluble (s) forms. These have been investigated as biomarkers of inflammatory diseases and multiple cancers. Most evidence suggests that levels of the soluble receptors increase as a response to inflammation. The functional role, if any, still remains up for debate. The soluble forms have been suggested to both increase immune activity by blocking the PD-1 pathway and decrease immune activity by positively engaging the PD-1 pathway. The role of the soluble forms is further complicated when recombinant proteins are used as surrogates for the soluble forms in both *in vivo* and *in vitro* studies (41–44).

The PD-1 pathway is central in maintaining immunological balance (33) and knockout mice of the PD-1 receptor causes lupus-like disease at a late stage in life (45).

PD-1 inhibitors are better tolerated than CTLA-4 inhibitors, but irAE affecting the joints, lungs and thyroid are more common (12). Hypothyroidism is the most common endocrinopathy seen in 6-10% (46)whereas newly onset T1DM is seen in about 1% of patients. In the development of childhood T1DM, polymorphisms in the PD-1 receptor are associated with an increased risk of T1DM. Patients with newly onset T1DM have decreased numbers of circulating CD4+PD-1+ T cells, and PD-1 fails to upregulate on peripheral T cells (47). The PD-1 axis is only scarcely investigated thyroid autoimmunity, but polymorphism in the PD-1 gene is associated with an increased incidence of autoimmune thyroiditis (48). Increased numbers of PD-1 infiltrating T cells are also seen in autoimmune thyroiditis (49). With hypothyroidism being one of the most prominent irAE after PD-1 blockade, this pathway might be more important than previously considered in the development of thyroid autoimmunity.

Many patients also experience rheumatological toxicities and close to 40% of the patients develop signs of inflammatory joint pain (16). The rheumatological toxicities can develop into diseases with autoantibodies, and both RA, scleroderma-like disease (50, 51), polymyositis and Sjögrens are seen.

Especially blocking the PD-1 pathway can cause pneumonitis which is a severe irAE, with high mortality. Especially, does pre-existing pulmonary fibrosis increase the risk of anti-PD-1-related pneumonitis (52, 53).

In accordance with the development of rheumatological irAE the PD-1 pathway plays a significant role in several rheumatological diseases including; RA, lupus (SLE), polymyalgia, polymyositis, and SSc (54). In RA; we have reported PD-1 expression to be increased both in the synovium and in the peripheral circulation (55–57). The increased expression correlates with disease activity, probably representing an immune activation. Looking further into the cellular and peripheral populations, PD-1 expression is associated with a pathological T cell phenotype involved in B cell activation and plasma cell maturation, resulting in increased antibody production and disease severity (58, 59). However, PD-1 expression also characterize regulatory T cells (Treg) and Tex which both are associated with less immune activation, and a better prognosis in autoimmune diseases (32, 57).

Looking into SLE the picture remains complicated. Genetic variances in the PD-1 gene are considered related to the development of the disease (60), and PD-1 expression is upregulated and associated with disease severity (61, 62). Recent bioinformatic and multi-omics approaches have made it evident that PD-1 is expressed on multiple different cell types, which are not solemnly associated with immune down regulation

(58). The distinction between the different cell types expressing PD-1 is especially important in the understanding of how the PD-1 pathway is associated with disease activity and severity in SLE, where it is demonstrated that the increased PD-1 expression is especially seen in T helper cell populations with more pro-inflammatory properties (63). This has become evident that especially T peripheral helper cells (Tph) cells are upregulated in SLE -supporting the close association with autoantibodies in this disease (64). Turning to Treg, the expression of PD-1 is not reported different in SLE patients, however, the expression of PD-L1 is suggested decreased in SLE Treg, and in accordance is negatively correlated to disease activity (65). Despite lupus-like disease being one of the clinical manifestations in PD-1 KO mice, SLE as an irAE is relatively rare (66). It could be hypothesized that diseases largely driven by auto antibodies will take a long time to develop. When more patients will initiate early treatment with ICI, potentially increasing both survival and treatment duration, SLE-like disease could become a more common irAE.

Systemic scleroderma (SSc) is also a rheumatic disease, where autoantibodies play a significant role. Again, few cases have been reported after ICI treatment (12, 67). In SSc, a dysfunctional PD-1 pathway has been correlated with disease outcomes and clinical parameters (68). Raised levels of sPD-1 and sPD-L2 has been associated with increased skin thickness. In SSc patients, the numbers of PD-1–expressing cells within the Treg cell subset and within γδT cells (69) were significantly increased compared to those of healthy subjects. Increased frequency of T lymphocytes co-expressing PD-1 and T cell immunoreceptor with Ig and ITIM domains (TIGIT) was also observed in SSc patients. This accumulated expression of multiple CIR is in accordance with the hallmarks of exhausted T cells (Tex).

In *in vivo* models of mice with Topoisomerase I(Top-I)–induced SSc, production of IL-10 by Top-I specific B cells in cultures with T cells and Top-I protein was significantly higher than that by conventional B cells, this effect could be overcome by injection with recombinant chimeric PD-1-Fc and PD-L2-Fc (68), thereby supporting activation of the PD-1 pathway. Thus, substantiating the regulatory effect of PD-1 in maintaining homeostasis. Suggesting that interaction of PD-1 and PD-L2 is required for the production of IL-10 by B cells during T cell–B cell autoantigen-specific cognate interactions in SSc.

Taken together, it is clear that signaling through the PD-1 receptor decreases immune activation, and supports immunological tolerance. However, PD-1 is expressed both by exhausted T cells, but also as a result of activation. Therefore, PD-1 can be expressed by T cell driving immune activation, but also by T cells participating in lowering the immune reaction. This adds to the complexity of the understanding of when and how PD-1 expressing T cells are associated with disease activity in inflammatory conditions.

CTLA-4

CTLA-4 is a transmembranous receptor expressed by activated T cells. Expression is upregulated upon T cell antigen encounter, and as for PD-1, low affinity antigens will induce a higher upregulation of CTLA-4. CTLA-4 binds to CD80/CD86 and competes with CD28 upon this binding, but with a higher avidity and affinity than CD28. A signal through CTLA-4 decreases T cell activation by the SHP2 and PP2A pathways, with many similarities to the PD-1 signaling pathway (70).

CTLA-4 is expressed by T cells, B cells, NK cells and regulatory T cells (Treg) (71, 72). T cells only express low levels of CTLA-4 on their surface, even when activated. CTLA-4 is mainly localized intracellular, where CTLA-4 is found in the golgi network, as well as in endosomes, secretory granules, and lysosomal vesicles from where it is circulated to the surface. This process is reviewed by Schneider et al (73).

CTLA-4 is also present in a soluble form, however, the importance of this is still not fully elucidated. Studies do support that sCTLA-4 plays an important role in keeping optimal immune surveillance (74).

In CTLA-4 knock-out mice, severe lymphoid proliferation and death appear, when the animals are 3-4 weeks old (75). Although no disease equivalent is known in humans, the importance of CTLA-4 in keeping tolerance is supported by fact that polymorphisms in the gene are associated with an increased risk of autoimmune disease. Importantly, these are not allocated to one disease but include T1DM, thyroiditis, Mb Addison, Crohn's disease, RA, and multiple sclerosis, among many others (76). Engaging this pathway with CTLA-4:Ig it has been shown to be an effective treatment, highlighting that this pathway plays a role in maintaining immune reaction during autoimmune disease.

Antibodies targeting CTLA-4 are approved in multiple cancers including; metastatic melanoma, hepatocellular, renal carcinoma, mesothelioma, colon cancer, and non-small cell lung cancer, and more will be included in the near future. Monotherapy targeting CTLA-4 is associated with more severe irAE compared with monotherapy targeting the PD-1 pathway (12). This aligns with CTLA-4 KO mice having a much more severe phenotype than PD-1 KO mice (45, 75). The most common irAE from anti-CTLA-4 treatment are related to the gut and skin. This suggests CTLA-4 has a functional implication in preserving gut tolerance and supporting barrier functions (13, 77). Considering the evolving evidence of the major significance of the microbiota in the development of autoimmune diseases, including both rheumatic and gastrointestinal diseases, the role of CTLA-4, in combination with PD-1 is further highlighted by both their abilities to influence IgA synthesis and the microbiome (78, 79). Controversially, the CTLA-4:Ig fusion protein, Abatacept, was shown not to be clinically relevant in controlling Crohn's Disease or ulcerative colitis in a clinical trial (80) . This does not exclude that CTLA-4 play an important role in keeping optimal conditions in the non-inflamed gut. This notion is supported by the observation that genetic changes in CTLA-4 is associated with an early onset of Crohn's disease (81).

CTLA-4 functions in humans are elucidated by the *in vivo* use of CTLA-4-Ig fusion protein, used for the treatment of various immunological diseases. Abatacept was the first CTLA-4-Ig molecule to be approved for humans and has since been

followed by Belatacept, with a higher affinity for CD86, making it 10-fold more potent *in vitro*, than Abatacept (82). These two CTLA-4-Ig molecules have been investigated in multiple autoimmune disorders, including RA, T1DM, diffuse cutaneous systemic sclerosis (dcSSc), psoriasis, and SLE. Both have also been tested, as inducers of tolerance to specific antigens upon organ transplantations. Especially Belatacept has shown to be efficacious in renal transplantation (83).

RA is by far the disease with the highest number of reports, as Abatacept has been approved for the treatment of moderate to severe disease for several of years (84). Its efficacy is in line with anti-TNF-antibodies (85). Since anti-CTLA-4 antibodies are used to treat cancer, it is tempting to suspect that treatment of RA with Abatacept would increase the risk of developing malignancy. However, no clear picture emerges. Some studies have reported a small increased risk, others none (86–88).

This naturally led to the question of why treatment with CTLA-4:Ig in RA, does not result in a greater increase in their cancer risk when blocking CTLA-4 in cancer results in autoimmunity. RA is dominated by a high number of both Tex cells and senescent T cells (89, 90), similar to chronic infections diseases. In patients with chronic hepatitis C, antiviral treatment lead to a decreased number of Tex cells (91). Assuming that Abatacept will do the same in RA the risk of developing cancer will also decrease as Tex favors cancer development. Therefore, it is a balanced outcome of disease activity, disease length, and treatment, thus explaining the low or absent risk of developing cancer in the Abatacept studies. The understanding of CTLA-4's role in RA mainly comes from studying the effects of Abatacept. One major point of action shown for Abatacept is the downregulation of cytokine production in co-cultures, resulting in significantly lower concentration of IL-2, TNF-a and IL-1b (92). Additionally, data suggest that macrophages shift from an M1 to an M2 phenotype, when cultured in the presence of Abatacept (93), favoring a less inflammatory environment.

Fully in line with CTLA-4 function, Abatacept treatment slightly decreases but does not completely inhibit a vaccination response (94, 95).

In SLE and other inflammatory connective tissue diseases, Abatacept has shown efficacy in animal models, but generally failed in clinical studies (96, 97). Since the first casuistic report of Abatacepts efficacy in SSc, a phase II study has supported CTLA-4s possible role in the treatment of this disease (98, 99). Evidence on CTLA-4's role in initiating connective tissue diseases remains to be fully elucidated, and most evidence is only on the genetic polymorphisms of CTLA-4 being associated with an increased risk of connective tissue diseases (100).

LAG-3

Lymphocyte activation gene 3 (LAG-3) is still one of the less described CIR. LAG-3 is expressed upon T cell activation and has high homology with CD4. LAG-3 only binds to stabilized MHC class II molecules, suggesting that this inhibitory pathway exerts its functions when the T cells encounter antigens with a high specificity (101–103). Several other ligands for LAG-3 have been described. Among these, are Fibrinogen-like Protein 1 (FGL-1), L-selectin, and Galectin-3 (Gal-3) (104–106). As LAG-3 is also present in a soluble form, these multiple ligands and potential large multimeric formations suggest that the functionality of LAG-3 is complex. LAG-3 regulates T cell proliferation and homeostasis of both effector T cells and Tregs (107, 108).

Single LAG-3– and PD-1–deficient mice display minimal immunopathologic sequelae, double LAG-3/PD-1 knockout mice develop lethal systemic autoimmunity. Though mice lacking LAG-3 do not develop spontaneous autoimmune disease in non-autoimmune prone mouse strains, LAG-3 induced lethal myocarditis in BALB/c mice deficient for the gene encoding for PD-1. In addition, LAG-3 deficiency alone accelerated T1DM in nonobese diabetic(NOD) mice (10). Moreover, a cytotoxic LAG-3 Ab has been evaluated in a nonhuman primate model of delayed-type hypersensitivity (109). Contrarily, in a phase I clinical trial investigating psoriasis the depletion of LAG-3–positive T cells was linked to a reduced Th1-driven skin inflammation, lasting even in the absence of the depleting antibody (110).

The LAG-3 pathway is shown to be involved in the development of irAE such as colitis, RA, and diabetes (111, 112). Evidence from mouse studies suggests efficacy in cancer treatment, especially in combination with either anti-PD-1 or anti-CTLA-4 therapy. This has led to a recent study evaluating the effects of anti-LAG-3 antibodies in combination with anti-PD-1 antibodies, versus anti-PD-1 as monotherapy in patients with advanced melanoma (113). Here, addition of anti-LAG3 increased to the progression-free survival, but also increased the rate of irAE. With special relation to rheumatology, arthralgia was the most commonly increased irAE induced after targeting LAG-3. This supports LAG-3's role in joint diseases. Currently, drugs that either augment LAG-3's effects or deplete activated T cells that express LAG-3 are under development for chronic inflammatory diseases (114).

Despite emerging clinical trials with both agonistic and antagonistic antibodies targeting LAG-3, it is important to recognize that the knowledge of LAG-3 in relation to autoimmune disease is still rather limited. We have reported that LAG-3 could play a role in juvenile rheumatoid arthritis, supporting that LAG-3 could be important for immunoreactions and immune maturation during infancy (115).

Apart from the immune checkpoint molecules described here, many more are known, but few of these have reached the level of clinical studies. Among these are 4-1BB, TIGIT, TIM-3, B7-H3, B7-H4, ICOS to mention a few. The next decade will lead to new and interesting descriptions of effects and irAE that will help us to a better understanding of the immune system.

CONCLUSION

Integrating our knowledge of irAE provides a better understanding of the role of CIR in both the initiation and progression of inflammatory diseases. It is suggestive that CIR may participate in the break of tolerance, but also in keeping the

diseases in a chronic state. Which additional factors are needed for a break of tolerance when CIR are blocked, remains to be understood. It has also become evident that not all autoimmune diseases are represented equally in the irAE spectrum. Apart from myositis and myocarditis, inflammatory connective tissue diseases like SLE and SSc are still not as common as arthritis and polymyalgia. Among endocrinopathies, the thyroid gland is much more commonly affected than the pancreas. The reasons for this could be plenty. One is the time perspective as ICI treatment has only been around for less than a decade, and both diabetes and connective tissue diseases may develop over a longer period of time. For connective tissue diseases, especially considering that autoantibodies are present years before the development of clinical symptoms (116–118), which suggests a prolonged period to induce the disease. Also, the presence of these autoantibodies may be crucial for initiating the disease, and targeting two CIR may not be enough for autoantibodies to develop. Future observational studies with long term follow-up could change this picture.

With ICI drugs coming to the market targeting different CIR, we might see a more specific organ preference, depending on the targeted CIR and thereby reflecting the pathology of the "natural" autoimmune disease. A blurred picture is starting to emerge, where we see a tendency for CTLA-4 blockade to induce gut affection more often than blockade of the PD-1 pathway. By contrast, PD-1 and LAG-3 blockade more often result in pneumonitis and joint affection (119).

Our knowledge of CIR role is mainly associated with adults. Our major expositor to different antigens is highest during the first part of life, supporting that CIR play distinct functions dependent on age. We do, however, still know very little of their function in the early stages of life.

Taken together, it is clear that we have only scratched the surface, when it comes to understanding the complexity immune checkpoint molecules have on development of diseases related to immunosurveillance.

AUTHOR CONTRIBUTIONS

All authors contributed equally to searching and implementing relevant literature and editing the manuscript. SG prepared the initial draft and BD served as the senior and last author. All authors contributed to the article and approved the submitted version.

FUNDING

Funding was received from Aarhus University, Lundbeck Foundation (R-287-2018-1094) and Danish Rheumatism Association (A6443).

REFERENCES

1. Thapa P, Farber DL. The Role of the Thymus in the Immune Response. *Thorac Surg Clinics* (2019) 29(2):123–31. doi: 10.1016/j.thorsurg.2018.12.001
2. Dubey C, Croft M, Swain SL. Costimulatory Requirements of Naive CD4+ T Cells. ICAM-1 or B7-1 can Costimulate Naive CD4 T Cell Activation But Both Are Required for Optimum Response. *J Immunol* (1995) 155(1):45–57.
3. Croft M, Dubey C. Accessory Molecule and Costimulation Requirements for CD4 T Cell Response. *Crit Rev Immunol* (2017) 37(2-6):261–90. doi: 10.1615/CritRevImmunol.v37.i2-6.60
4. Laderach D, Movassagh M, Johnson A, Mittler RS, Galy A. 4-1bb Co-Stimulation Enhances Human CD8+ T Cell Priming by Augmenting the Proliferation and Survival of Effector CD8+ T Cells. *Int Immunol* (2002) 14 (10):1155–67. doi: 10.1093/intimm/dxf080
5. Sharpe AH. Mechanisms of Costimulation. *Immunol Rev* (2009) 229(1):5–11. doi: 10.1111/j.1600-065X.2009.00784.x
6. Riella LV, Paterson AM, Sharpe AH, Chandraker A. Role of the PD-1 Pathway in the Immune Response. *Am J Transplant* (2012) 12(10):2575–87. doi: 10.1111/j.1600-6143.2012.04224.x
7. Murakami N, Riella LV. Co-Inhibitory Pathways and Their Importance in Immune Regulation. *Transplantation* (2014) 98(1):3–14. doi: 10.1097/TP.0000000000000169
8. Place DE, Kanneganti TD. The Innate Immune System and Cell Death in Autoinflammatory and Autoimmune Disease. *Curr Opin Immunol* (2020) 67:95–105. doi: 10.1016/j.coi.2020.10.013
9. Cha JH, Chan LC, Li CW, Hsu JL, Hung MC. Mechanisms Controlling PD-L1 Expression in Cancer. *Mol Cell* (2019) 76(3):359–70. doi: 10.1016/j.molcel.2019.09.030
10. Savoia P, Astrua C, Fava P. Ipilimumab (Anti-Ctla-4 Mab) in the Treatment of Metastatic Melanoma: Effectiveness and Toxicity Management. *Hum Vaccines Immunother* (2016) 12(5):1092–101. doi: 10.1080/21645515.2015.1129478
11. Leach DR, Krummel MF, Allison JP. Enhancement of Antitumor Immunity by CTLA-4 Blockade. *Science* (1996) 271(5256):1734–6. doi: 10.1126/science.271.5256.1734
12. Ramos-Casals M, Brahmer JR, Callahan MK, Flores-Chavez A, Keegan N, Khamashta MA, et al. Immune-Related Adverse Events of Checkpoint Inhibitors. *Nat Rev Dis Primers* (2020) 6(1):38. doi: 10.1038/s41572-020-0179-8
13. Ghosh N, Chan KK, Jivanelli B, Bass AR. Autoantibodies in Patients With Immune-Related Adverse Events From Checkpoint Inhibitors. *JCR* (2021) 28(2):1–8. doi: 10.1097/RHU.0000000000001777
14. Nakamura Y. Biomarkers for Immune Checkpoint Inhibitor-Mediated Tumor Response and Adverse Events. *Front Med (Lausanne)* (2019) 6:119. doi: 10.3389/fmed.2019.00119
15. Abdel-Wahab N, Shah M, Lopez-Olivo MA, Suarez-Almazor ME. Use of Immune Checkpoint Inhibitors in the Treatment of Patients With Cancer and Preexisting Autoimmune Disease: A Systematic Review. *Ann Intern Med* (2018) 168(2):121–30. doi: 10.7326/M17-2073
16. Johnson DB, Nebhan CA, Moslehi JJ, Balko JM. Immune-Checkpoint Inhibitors: Long-Term Implications of Toxicity. *Nat Rev Clin Oncol* (2022) 19(4):254–67. doi: 10.1038/s41571-022-00600-w
17. Patrinely JRJr., Johnson R, Lawless AR, Bhave P, Sawyers A, Dimitrova M, et al. Chronic Immune-Related Adverse Events Following Adjuvant Anti-PD-1 Therapy for High-Risk Resected Melanoma. *JAMA Oncol* (2021) 7 (5):744–8. doi: 10.1001/jamaoncol.2021.0051
18. Ghisoni E, Wicky A, Bouchaab H, Imbimbo M, Delyon J, Gautron Moura B, et al. Late-Onset and Long-Lasting Immune-Related Adverse Events From Immune Checkpoint-Inhibitors: An Overlooked Aspect in Immunotherapy. *Eur J Cancer* (2021) 149:153–64. doi: 10.1016/j.ejca.2021.03.010
19. Hasan Ali O, Berner F, Bomze D, Fassler M, Diem S, Cozzio A, et al. Human Leukocyte Antigen Variation is Associated With Adverse Events of Checkpoint Inhibitors. *Eur J Cancer* (2019) 107:8–14. doi: 10.1016/j.ejca.2018.11.009
20. Iafolla MAJ, Yang C, Chandran V, Pintilie M, Li Q, Bedard PL, et al. Predicting Toxicity and Response to Pembrolizumab Through Germline Genomic HLA Class 1 Analysis. *JNCI Cancer Spectr* (2021) 5(1):1–9. doi: 10.1093/jncics/pkaa115
21. Jessel S, Weiss SA, Austin M, Mahajan A, Etts K, Zhang L, et al. Immune Checkpoint Inhibitor-Induced Hypophysitis and Patterns of Loss of Pituitary Function. *Front Oncol* (2022) 12:836859. doi: 10.3389/fonc.2022.836859

22. Langlois F, Varlamov EV, Fleseriu M. Hypophysitis, the Growing Spectrum of a Rare Pituitary Disease. *J Clin Endocrinol Metab* (2022) 107(1):10–28. doi: 10.1210/clinem/dgab672
23. Naing A, Hajjar J, Gulley JL, Atkins MB, Ciliberto G, Meric-Bernstam F, et al. Strategies for Improving the Management of Immune-Related Adverse Events. *J ImmunoTher Cancer* (2020) 8(2):1–9. doi: 10.1136/jitc-2020-001754
24. Kumar V, Chaudhary N, Garg M, Floudas CS, Soni P, Chandra AB. Current Diagnosis and Management of Immune Related Adverse Events (irAEs) Induced by Immune Checkpoint Inhibitor Therapy. *Front Pharmacol* (2017) 8. doi: 10.3389/fphar.2017.00311
25. Petrelli F, Signorelli D, Ghidini M, Ghidini A, Pizzutilo EG, Ruggieri L, et al. Association of Steroids Use With Survival in Patients Treated With Immune Checkpoint Inhibitors. *Cancers (Basel)* (2020) 4:1–11.doi: 10.3390/cancers12030546
26. Chen AY, Wolchok JD, Bass AR. TNF in the Era of Immune Checkpoint Inhibitors: Friend or Foe? *Nat Rev Rheumatol* (2021) 17(4):213–23. doi: 10.1038/s41584-021-00584-4
27. Dimitriou F, Hogan S, Menzies AM, Dummer R, Long GV. IL-6 Blockade for Prophylaxis and Management of Immune-Related Adverse Events (irAEs) With Anti-PD-1 Based Immunotherapy. *J Clin Oncol* (2021) 39 (15_suppl):214–24. doi: 10.1200/JCO.2021.39.15_suppl.9553
28. Linsley PS, Ledbetter JA. The Role of the CD28 Receptor During T Cell Responses to Antigen. *Annu Rev Immunol* (1993) 11:191–212. doi: 10.1146/annurev.iy.11.040193.001203
29. Shahinian A, Pfeffer K, Lee KP, Kundig TM, Kishihara K, Wakeham A, et al. Differential T Cell Costimulatory Requirements in CD28-Deficient Mice. *Science* (1993) 261(5121):609–12. doi: 10.1126/science.7688139
30. Vierboom MP, Breedveld E, Kap YS, Mary C, Poirier N, t Hart BA, et al. Clinical Efficacy of a New CD28-Targeting Antagonist of T Cell Co-Stimulation in a non-Human Primate Model of Collagen-Induced Arthritis. *Clin Exp Immunol* (2016) 183(3):405–18. doi: 10.1111/cei.12739
31. Porciello N, Kunkl M, Tuosto L. CD28 Between Tolerance and Autoimmunity: The Side Effects of Animal Models. *F1000Res* (2018) 7. doi: 10.12688/f1000research.14046.1
32. Sharpe AH, Pauken KE. The Diverse Functions of the PD1 Inhibitory Pathway. *Nat Rev Immunol* (2018) 18(3):153–67. doi: 10.1038/nri.2017.108
33. Keir ME, Freeman GJ, Sharpe AH. PD-1 Regulates Self-Reactive CD8 +T Cell Responses to Antigen in Lymph Nodes and Tissues. *J Immunol* (2007) 179(8):5064–70. doi: 10.4049/jimmunol.179.8.5064
34. Butte MJ, Keir ME, Phamduy TB, Sharpe AH, Freeman GJ. Programmed Death-1 Ligand 1 Interacts Specifically With the B7-1 Costimulatory Molecule to Inhibit T Cell Responses. *Immunity* (2007) 27(1):111–22. doi: 10.1016/j.immuni.2007.05.016
35. Liang SC, Latchman YE, Buhlmann JE, Tomczak MF, Horwitz BH, Freeman GJ, et al. Regulation of PD-1, PD-L1, and PD-L2 Expression During Normal and Autoimmune Responses. *Eur J Immunol* (2003) 33(10):2706–16. doi: 10.1002/eji.200324228
36. Marasco M, Berteotti A, Weyershaeuser J, Thorausch N, Sikorska J, Krausze J, et al. Molecular Mechanism of SHP2 Activation by PD-1 Stimulation. *Sci Adv* (2020) 6(5):eaay4458. doi: 10.1126/sciadv.aay4458
37. Patsoukis N, Duke-Cohan JS, Chaudhri A, Aksoylar HI, Wang Q, Council A, et al. Interaction of SHP-2 SH2 Domains With PD-1 ITSM Induces PD-1 Dimerization and SHP-2 Activation. *Commun Biol* (2020) 3(1):1–13. doi: 10.1038/s42003-020-0845-0
38. Doroshow DB, Bhalla S, Beasley MB, Sholl LM, Kerr KM, Gnjatic S, et al. PD-L1 as a Biomarker of Response to Immune-Checkpoint Inhibitors. *Nat Rev Clin Oncol*. (2021) 18(6):345–62. . doi: 10.1038/s41571-021-00473-5
39. Gato-Canas M, Zuazo M, Arasanz H, Ibanez-Vea M, Lorenzo L, Fernandez-Hinojal G, et al. PDL1 Signals Through Conserved Sequence Motifs to Overcome Interferon-Mediated Cytotoxicity. *Cell Rep* (2017) 20(8):1818–29. doi: 10.1016/j.celrep.2017.07.075
40. Lucas ED, Schafer JB, Matsuda J, Kraus M, Burchill MA, Tamburini BAJ. PD-L1 Reverse Signaling in Dermal Dendritic Cells Promotes Dendritic Cell Migration Required for Skin Immunity. *Cell Rep* (2020) 33(2):108258. doi: 10.1016/j.celrep.2020.108258
41. Incorvaia L, Fanale D, Badalamenti G, Porta C, Olive D, De Luca I, et al. Baseline Plasma Levels of Soluble PD-1, PD-L1, and BTN3A1 Predict Response to Nivolumab Treatment in Patients With Metastatic Renal Cell Carcinoma: A Step Toward a Biomarker for Therapeutic Decisions. *OncoImmunology* (2020) 9(1):1832348. doi: 10.1080/2162402X.2020.1832348
42. Mildner F, Sopper S, Amann A, Pircher A, Pall G, Kock S, et al. Systematic Review: Soluble Immunological Biomarkers in Advanced non-Small-Cell Lung Cancer (NSCLC). *Crit Rev Oncol/Hematol* (2020) 153:102948–8. doi: 10.1016/j.critrevonc.2020.102948
43. Shi B, Du X, Wang Q, Chen Y, Zhang X. Increased PD-1 on CD4(+)CD28(-) T Cell and Soluble PD-1 Ligand-1 in Patients With T2DM: Association With Atherosclerotic Macrovascular Diseases. *Metabolism* (2013) 62(6):778–85. doi: 10.1016/j.metabol.2012.12.005
44. Bommarito D, Hall C, Taams LS, Corrigall VM. Inflammatory Cytokines Compromise Programmed Cell Death-1 (PD-1)-Mediated T Cell Suppression in Inflammatory Arthritis Through Up-Regulation of Soluble PD-1. *Clin Exp Immunol* (2017) 188(3):455–66. doi: 10.1111/cei.12949
45. Nishimura H, Nose M, Hiai H, Minato N, Honjo T. Development of Lupus-Like Autoimmune Diseases by Disruption of the PD-1 Gene Encoding an ITIM Motif-Carrying Immunoreceptor. *Immunity* (1999) 11(2):141–51. doi: 10.1016/S1074-7613(00)80089-8
46. Barroso-Sousa R, Barry WT, Garrido-Castro AC, Hodi FS, Min L, Krop IE, et al. Incidence of Endocrine Dysfunction Following the Use of Different Immune Checkpoint Inhibitor Regimens: A Systematic Review and Meta-Analysis. *JAMA Oncol* (2018) 4(2):173–82. doi: 10.1001/jamaoncol.2017.3064
47. Falcone M, Fousteri G. Role of the PD-1/PD-L1 Dyad in the Maintenance of Pancreatic Immune Tolerance for Prevention of Type 1 Diabetes. *Front Endocrinol* (2020) 11:1–11. doi: 10.3389/fendo.2020.00569
48. Hayashi M, Kouki T, Takasu N, Sunagawa S, Komiya I. Association of an a/C Single Nucleotide Polymorphism in Programmed Cell Death-Ligand 1 Gene With Graves' Disease in Japanese Patients. *Eur J Endocrinol* (2008) 158 (6):817–22. doi: 10.1530/EJE-07-0649
49. Alvarez-Sierra D, Marin-Sanchez A, Ruiz-Blazquez P, de Jesus Gil C, Iglesias-Felip C, Gonzalez O, et al. Analysis of the PD-1/PD-L1 Axis in Human Autoimmune Thyroid Disease: Insights Into Pathogenesis and Clues to Immunotherapy Associated Thyroid Autoimmunity. *J Autoimmun* (2019) 103:102285. doi: 10.1016/j.jaut.2019.05.013
50. Barbosa NS, Wetter DA, Wieland CN, Shenoy NK, Markovic SN, Thanarajasingam U. Scleroderma Induced by Pembrolizumab: A Case Series. *Mayo Clinic Proc* (2017) 92(7):1158-63. doi: 10.1016/j.mayocp.2017.03.016
51. Terrier B, Humbert S, Preta LH, Delage L, Razanamahery J, Laurent-Roussel S, et al. Risk of Scleroderma According to the Type of Immune Checkpoint Inhibitors. *Autoimmun Rev* (2020) 19(8):102596–6. doi: 10.1016/j.autrev.2020.102596
52. Yamaguchi T, Shimizu J, Hasegawa T, Horio Y, Inaba Y, Yatabe Y, et al. Pre-Existing Pulmonary Fibrosis is a Risk Factor for Anti-PD-1-Related Pneumonitis in Patients With non-Small Cell Lung Cancer: A Retrospective Analysis. *Lung Cancer* (2018) 125:212-7. doi: 10.1016/j.lungcan.2018.10.001
53. Dobre IA, Frank AJ, D'Silva KM, Christiani DC, Okin D, Sharma A, et al. Outcomes of Patients With Interstitial Lung Disease Receiving Programmed Cell Death 1 Inhibitors: A Retrospective Case Series. *Clin Lung Cancer* (2021) 22(5):e738-e44. doi: 10.1016/j.cllc.2021.01.014
54. Zhang S, Wang L, Li M, Zhang F, Zeng X. The PD-1/PD-L Pathway in Rheumatic Diseases. *J Formosan Med Assoc = Taiwan yi zhi* (2021) 120(1 Pt 1):48–59. doi: 10.1016/j.jfma.2020.04.004
55. Greisen SR, Rasmussen TK, Stengaard-Pedersen K, Hetland ML, Horslev-Petersen K, Hvid M, et al. Increased Soluble Programmed Death-1 (sPD-1) is Associated With Disease Activity and Radiographic Progression in Early Rheumatoid Arthritis. *Scandinavian J Rheumatol* (2013) 43(2):101–8. doi: 10.3109/03009742.2013.823517
56. Greisen SR, Kragstrup TW, Thomsen JS, Horslev-Pedersen K, Hetland ML, Stengaard-Pedersen K, et al. The Programmed Death-1 Pathway Counter-Regulates Inflammation-Induced Osteoclast Activity in Clinical and Experimental Settings. *Front Immunol* (2022) 13:1–12. doi: 10.3389/fimmu.2022.773946
57. Greisen SR, Yan Y, Hansen AS, Veno MT, Nyengaard JR, Moestrup SK, et al. Extracellular Vesicles Transfer the Receptor Programmed Death-1 in

Rheumatoid Arthritis. *Front Immunol* (2017) 8:e1694–14. doi: 10.3389/fimmu.2017.00851
58. Rao DA, Gurish MF, Marshall JL, Slowikowski K, Fonseka CY, Liu Y, et al. Pathologically Expanded Peripheral T Helper Cell Subset Drives B Cells in Rheumatoid Arthritis. *Nature* (2017) 542(7639):110–4. doi: 10.1038/nature20810
59. Marks KE, Rao DA. T Peripheral Helper Cells in Autoimmune Diseases. *Immunol Rev* (2022) 307:1–12. doi: 10.1111/imr.13069
60. Curran CS, Gupta S, Sanz I, Sharon E. PD-1 Immunobiology in Systemic Lupus Erythematosus. *J Autoimmun* (2019) 97(3):1–9. doi: 10.1016/j.jaut.2018.10.025
61. Du Y, Nie L, Xu L, Wu X, Zhang S, Xue J. Serum Levels of Soluble Programmed Death-1 (sPD-1) and Soluble Programmed Death Ligand 1 (sPD-L1) in Systemic Lupus Erythematosus: Association With Activity and Severity. *Scandinavian J Immunol* (2020) 92(1):1–11. doi: 10.1111/sji.12884
62. Jiao Q, Liu C, Yang Z, Ding Q, Wang M, Li M, et al. Upregulated PD-1 Expression is Associated With the Development of Systemic Lupus Erythematosus, But Not the PD-1.1 Allele of the PDCD1 Gene. *Int J Genomics 2014* (2014) p:10–2. doi: 10.1155/2014/950903
63. Han L, Yang X, Yu Y, Wan W, Lv L, Zou H. Associations of Circulating CXCR3–PD-1+Cd4+T Cells With Disease Activity of Systemic Lupus Erythematosus. *Modern Rheumatol* (2019) 29(3):461–9. doi: 10.1080/14397595.2018.1469581
64. Lin J, Yu Y, Ma J, Ren C, Chen W. PD-1+CXCR5-Cd4+T Cells are Correlated With the Severity of Systemic Lupus Erythematosus. *Rheumatol (United Kingdom)* (2019) 58(12):2188–92. doi: 10.1093/rheumatology/kez228
65. Zhao L, Zhou X, Zhou X, Wang H, Gu L, Ke Y, et al. Low Expressions of PD-L1 and CTLA-4 by Induced CD4+CD25+ Foxp3+ Tregs in Patients With SLE and Their Correlation With the Disease Activity. *Cytokine* (2020) 133:155119–9. doi: 10.1016/j.cyto.2020.155119
66. Antonazzo IC, Poluzzi E, De Ponti F. Drug-Induced Systemic Lupus Erythematosus: Should Immune Checkpoint Inhibitors be Added to the Evolving List? *Ann Rheum Dis* (2021) 80(7):e120. doi: 10.1136/annrheumdis-2019-215819
67. Allenbach Y, Anquetil C, Manouchehri A, Benveniste O, Lambotte O, Lebrun-Vignes B, et al. Immune Checkpoint Inhibitor-Induced Myositis, the Earliest and Most Lethal Complication Among Rheumatic and Musculoskeletal Toxicities. *Autoimmun Rev* (2020) 19(8):102586. doi: 10.1016/j.autrev.2020.102586
68. Fukasawa T, Yoshizaki A, Ebata S, Nakamura K, Saigusa R, Miura S, et al. Contribution of Soluble Forms of Programmed Death 1 and Programmed Death Ligand 2 to Disease Severity and Progression in Systemic Sclerosis. *Arthritis {\&} Rheumatol* (2017) 69(9):1879–90. doi: 10.1002/art.40164
69. Fleury M, Belkina AC, Proctor EA, Zammitti C, Simms RW, Lauffenburger DA, et al. Increased Expression and Modulated Regulatory Activity of Coinhibitory Receptors PD-1, TIGIT, and TIM-3 in Lymphocytes From Patients With Systemic Sclerosis. *Arthritis Rheumatol* (2018) 70(4):566–77. doi: 10.1002/art.40399
70. Chuang E, Fisher TS, Morgan RW, Robbins MD, Duerr JM, Vander Heiden MG, et al. The CD28 and CTLA-4 Receptors Associate With the Serine/Threonine Phosphatase PP2A. *Immunity* (2000) 13(3):313–22. doi: 10.1016/S1074-7613(00)00031-5
71. Lindsten T, Lee KP, Harris ES, Petryniak B, Craighead N, Reynolds PJ, et al. Characterization of CTLA-4 Structure and Expression on Human T Cells. *J Immunol* (1993) 151(7):3489–99.
72. Annunziato F, Cosmi L, Liotta F, Lazzeri E, Manetti R, Vanini V, et al. Phenotype, Localization, and Mechanism of Suppression of CD4+CD25+ Human Thymocytes. *J Exp Med* (2002) 196(3):379–87. doi: 10.1084/jem.20020110
73. Schneider H, Rudd CE. Diverse Mechanisms Regulate the Surface Expression of Immunotherapeutic Target CTLA-4. *Front Immunol* (2014) 5:1–10. doi: 10.3389/fimmu.2014.00619
74. Chen Z, Zhou F, Huang S, Jiang T, Chen L, Ge L, et al. Association of Cytotoxic T Lymphocyte Associated Antigen-4 Gene (Rs60872763) Polymorphism With Crohn's Disease and High Levels of Serum sCTLA-4 in Crohn's Disease. *J Gastroenterol Hepatol* (2011) 26(5):924–30. doi: 10.1111/j.1440-1746.2011.06662.x
75. Khattri R, Auger JA, Griffin MD, Sharpe AH, Bluestone JA. Lymphoproliferative Disorder in CTLA-4 Knockout Mice is Characterized by CD28-Regulated Activation of Th2 Responses. *J Immunol* (1999) 162(10):5784–91.
76. Gough SCL, Walker LSK, Sansom DM. CTLA4 Gene Polymorphism and Autoimmunity. *Immunol Rev* (2005) 204:102–15. doi: 10.1111/j.0105-2896.2005.00249.x
77. Dougan M. Checkpoint Blockade Toxicity and Immune Homeostasis in the Gastrointestinal Tract. *Front Immunol* (2017) 8:1547. doi: 10.3389/fimmu.2017.01547
78. Mager LF, Burkhard R, Pett N, Cooke NCA, Brown K, Ramay H, et al. Microbiome-Derived Inosine Modulates Response to Checkpoint Inhibitor Immunotherapy. *Science* (2020) 369(6509):1481–9. doi: 10.1126/science.abc3421
79. Kawamoto S, Tran TH, Maruya M, Suzuki K, Doi Y, Tsutsui Y, et al. The Inhibitory Receptor PD-1 Regulates IgA Selection and Bacterial Composition in the Gut. *Science* (2012) 336(6080):485–9. doi: 10.1126/science.1217718
80. Sandborn WJ, Colombel JF, Sands BE, Rutgeerts P, Targan SR, Panaccione R, et al. Abatacept for Crohn's Disease and Ulcerative Colitis. *Gastroenterology* (2012) 143(1):62–9 e4. doi: 10.1053/j.gastro.2012.04.010
81. Zeissig S, Petersen BS, Tomczak M, Melum E, Huc-Claustre E, Dougan SK, et al. Early-Onset Crohn's Disease and Autoimmunity Associated With a Variant in CTLA-4. *Gut* (2015) 64(12):1889–97. doi: 10.1136/gutjnl-2014-308541
82. Larsen CP, Pearson TC, Adams AB, Tso P, Shirasugi N, Strobert E, et al. Rational Development of LEA29Y (Belatacept), a High-Affinity Variant of CTLA4-Ig With Potent Immunosuppressive Properties. *Am J Transplant* (2005) 5(3):443–53. doi: 10.1111/j.1600-6143.2005.00749.x
83. Badell IR, Parsons RF, Karadkhele G, Cristea O, Mead S, Thomas S, et al. Every 2-Month Belatacept Maintenance Therapy in Kidney Transplant Recipients Greater Than 1-Year Posttransplant: A Randomized, Noninferiority Trial. *Am J Transplant* (2021) 21(9):3066–76. doi: 10.1111/ajt.16538
84. Kremer JM, Westhovens R, Leon M, Di Giorgio E, Alten R, Steinfeld S, et al. Treatment of Rheumatoid Arthritis by Selective Inhibition of T-Cell Activation With Fusion Protein CTLA4Ig. *New Engl J Med* (2003) 349(20):1907–15. doi: 10.1056/NEJMoa035075
85. Fleischmann R, Weinblatt ME, Schiff M, Khanna D, Maldonado MA, Nadkarni A, et al. Patient-Reported Outcomes From a Two-Year Head-To-Head Comparison of Subcutaneous Abatacept and Adalimumab for Rheumatoid Arthritis. *Arthritis Care Res* (2016) 68(7):907–13. doi: 10.1002/acr.22763
86. Simon TA, Boers M, Hochberg M, Baker N, Skovron ML, Ray N, et al. 87 (2019).
87. de Germay S, Bagheri H, Despas F, Rousseau V, Montastruc F. Abatacept in Rheumatoid Arthritis and the Risk of Cancer: A World Observational Post-Marketing Study. *Rheumatology* (2020) 59(9):228. doi: 10.1093/rheumatology/kez604
88. Huss V, Bower H, Wadstrom H, Frisell T, Askling J. Short- and Longer-Term Cancer Risks With Biologic and Targeted Synthetic Disease-Modifying Antirheumatic Drugs as Used Against Rheumatoid Arthritis in Clinical Practice. *Rheumatology* (2021) 61(5):1810–8. doi: 10.1093/rheumatology/keab570
89. Weyand CM, Yang Z, Goronzy JJ. T-Cell Aging in Rheumatoid Arthritis. *Curr Opin Rheumatol* (2014) 26(1):93–100. doi: 10.1097/BOR.0000000000000011
90. Miggelbrink AM, Jackson JD, Lorrey SJ, Srinivasan ES, Waibl-Polania J, Wilkinson DS, et al. CD4 T-Cell Exhaustion: Does it Exist and What are its Roles in Cancer? *Clin Cancer Res* (2021) 27(21):5742–52. doi: 10.1158/1078-0432.CCR-21-0206
91. Osuch S, Laskus T, Berak H, Perlejewski K, Metzner KJ, Paciorek M, et al. Decrease of T-Cells Exhaustion Markers Programmed Cell Death-1 and T-Cell Immunoglobulin and Mucin Domain-Containing Protein 3 and Plasma IL-10 Levels After Successful Treatment of Chronic Hepatitis C. *Sci Rep* (2020) 10(1):16060. doi: 10.1038/s41598-020-73137-6
92. Cutolo M, Soldano S, Montagna P, Sulli A, Seriolo B, Villaggio B, et al. CTLA4-Ig Interacts With Cultured Synovial Macrophages From Rheumatoid Arthritis Patients and Downregulates Cytokine Production. *Arthritis Res Ther* (2009) 11(6):R176. doi: 10.1186/ar2865

93. Cutolo M, Soldano S, Gotelli E, Montagna P, Campitiello R, Paolino S, et al. CTLA4-Ig Treatment Induces M1-M2 Shift in Cultured Monocyte-Derived Macrophages From Healthy Subjects and Rheumatoid Arthritis Patients. *Arthritis Res Ther* (2021) 23(1):306. doi: 10.1186/s13075-021-02691-9
94. Crnkic Kapetanovic M, Saxne T, Jonsson G, Truedsson L, Geborek P. Rituximab and Abatacept But Not Tocilizumab Impair Antibody Response to Pneumococcal Conjugate Vaccine in Patients With Rheumatoid Arthritis. *Arthritis Res Ther* (2013) 15(5):R171. doi: 10.1186/ar4358
95. Alten R, Bingham CO3rd, Cohen SB, Curtis JR, Kelly S, Wong D, et al. Antibody Response to Pneumococcal and Influenza Vaccination in Patients With Rheumatoid Arthritis Receiving Abatacept. *BMC Musculoskel Disord* (2016) 17(1):231. doi: 10.1186/s12891-016-1082-z
96. Furie R, Nicholls K, Cheng TT, Houssiau F, Burgos-Vargas R, Chen SL, et al. Efficacy and Safety of Abatacept in Lupus Nephritis: A Twelve-Month, Randomized, Double-Blind Study. *Arthritis Rheumatol* (2014) 66(2):379–89. doi: 10.1002/art.38260
97. Merrill JT, Burgos-Vargas R, Westhovens R, Chalmers A, D'Cruz D, Wallace DJ, et al. The Efficacy and Safety of Abatacept in Patients With non-Life-Threatening Manifestations of Systemic Lupus Erythematosus: Results of a Twelve-Month, Multicenter, Exploratory, Phase IIb, Randomized, Double-Blind, Placebo-Controlled Trial. *Arthritis Rheumatism* (2010) 62(10):3077–87. doi: 10.1002/art.27601
98. Khanna D, Spino C, Johnson S, Chung L, Whitfield ML, Denton CP, et al. Abatacept in Early Diffuse Cutaneous Systemic Sclerosis: Results of a Phase II Investigator-Initiated, Multicenter, Double-Blind, Randomized, Placebo-Controlled Trial. *Arthritis Rheumatol* (2020) 72(1):125–36. doi: 10.1002/art.41055
99. Chung L, Spino C, McLain R, Johnson SR, Denton CP, Molitor JA, et al. Safety and Efficacy of Abatacept in Early Diffuse Cutaneous Systemic Sclerosis (ASSET): Open-Label Extension of a Phase 2, Double-Blind Randomised Trial. *Lancet Rheumatol* (2020) 2(12):e743–e53. doi: 10.1016/S2665-9913(20)30237-X
100. Kailashiya V, Sharma HB, Kailashiya J. Role of CTLA4 A49G Polymorphism in Systemic Lupus Erythematosus and its Geographical Distribution. *J Clin Pathol* (2019) 72(10):659–62. doi: 10.1136/jclinpath-2019-206013
101. Baixeras E, Huard B, Miossec C, Jitsukawa S, Martin M, Hercend T, et al. Characterization of the Lymphocyte Activation Gene 3-Encoded Protein. A New Ligand for Human Leukocy Antigen Class H Antigens. *J Exp Med* (1992) 176(2):327–37. doi: 10.1084/jem.176.2.327
102. Huard B, Mastrangeli R, Prigent P, Bruniquel D, Donini S, El-Tayar N, et al. Characterization of the Major Histocompatibility Complex Class II Binding Site on LAG-3 Protein. *Proc Natl Acad Sci United States America* (1997) 94(11):5744–9. doi: 10.1073/pnas.94.11.5744
103. Maruhashi T, Okazaki IM, Sugiura D, Takahashi S, Maeda TK, Shimizu K, et al. LAG-3 Inhibits the Activation of CD4 + T Cells That Recognize Stable pMHCII Through its Conformation-Dependent Recognition of pMHCII. *Nat Immunol* (2018) 19(12):1415–26. doi: 10.1038/s41590-018-0217-9
104. Wang J, Sanmamed MF, Datar I, Su TT, Ji L, Sun J, et al. Fibrinogen-Like Protein 1 Is a Major Immune Inhibitory Ligand of LAG-3. *Cell* (2019) 176(1-2):334–347.e12. doi: 10.1016/j.cell.2018.11.010
105. Xu F, Liu J, Liu D, Liu B, Wang M, Hu Z, et al. LSECtin Expressed on Melanoma Cells Promotes Tumor Progression by Inhibiting Antitumor T-Cell Responses. *Cancer Res* (2014) 74(13):3418–28. doi: 10.1158/0008-5472.CAN-13-2690
106. Kouo T, Huang L, Pucsek AB, Cao M, Solt S, Armstrong T, et al. Galectin-3 Shapes Antitumor Immune Responses by Suppressing CD8 T Cells *via* LAG-3 and Inhibiting Expansion of Plasmacytoid Dendritic Cells. *Cancer Immunol Res* (2015) 3(4):412–23. doi: 10.1158/2326-6066.CIR-14-0150
107. Andrews LP, Marciscano AE, Drake CG, Vignali DA. LAG3 (CD223) as a Cancer Immunotherapy Target. *Immunol Rev* (2017) 276(1):80–96. doi: 10.1111/imr.12519
108. Anderson AC, Joller N, Kuchroo VK. Lag-3, Tim-3, and TIGIT: Co-Inhibitory Receptors With Specialized Functions in Immune Regulation. *Immunity* (2016) 44(5):989–1004. doi: 10.1016/j.immuni.2016.05.001
109. Poirier N, Haudebourg T, Brignone C, Dilek N, Hervouet J, Minault D, et al. Antibody-Mediated Depletion of Lymphocyte-Activation Gene-3 (LAG-3 (+))-Activated T Lymphocytes Prevents Delayed-Type Hypersensitivity in non-Human Primates. *Clin Exp Immunol* (2011) 164(2):265–74. doi: 10.1111/j.1365-2249.2011.04329.x
110. Ellis J, JBM D, Srinivasan N, Barrett C, Hopkins TG, Richards A, et al. Depletion of LAG-3(+) T Cells Translated to Pharmacology and Improvement in Psoriasis Disease Activity: A Phase I Randomized Study of mAb Gsk2831781. *Clin Pharmacol Ther* (2021) 109(5):1293–303. doi: 10.1002/cpt.2091
111. Bauche D, Joyce-Shaikh B, Jain R, Grein J, Ku KS, Blumenschein WM, et al. LAG3(+) Regulatory T Cells Restrain Interleukin-23-Producing CX3CR1(+) Gut-Resident Macrophages During Group 3 Innate Lymphoid Cell-Driven Colitis. *Immunity* (2018) 49(2):342–352 e5. doi: 10.1016/j.immuni.2018.07.007
112. Bettini M, Szymczak-Workman AL, Forbes K, Castellaw AH, Selby M, Pan X, et al. Cutting Edge: Accelerated Autoimmune Diabetes in the Absence of LAG-3. *J Immunol* (2011) 187(7):3493–8. doi: 10.4049/jimmunol.1100714
113. Tawbi HA, Schadendorf D, Lipson EJ, Ascierto PA, Matamala L, Castillo Gutierrez E, et al. Relatlimab and Nivolumab Versus Nivolumab in Untreated Advanced Melanoma. *New Engl J Med* (2022) 386(1):24–34. doi: 10.1056/NEJMoa2109970
114. Angin M, Brignone C, Triebel F. A LAG-3-Specific Agonist Antibody for the Treatment of T Cell-Induced Autoimmune Diseases. *J Immunol* (2020) 204(4):810–8. doi: 10.4049/jimmunol.1900823
115. Sag E, Demir S, Aspari M, Nielsen MA, Skejo C, Hvid M, et al. Juvenile Idiopathic Arthritis: Lymphocyte Activation Gene-3 is a Central Immune Receptor in Children With Oligoarticular Subtypes. *Pediatr Res* (2021) 90(4):744–51. doi: 10.1038/s41390-021-01588-2
116. Eriksson C, Kokkonen H, Johansson M, Hallmans G, Wadell G, Rantapaa-Dahlqvist S. Autoantibodies Predate the Onset of Systemic Lupus Erythematosus in Northern Sweden. *Arthritis Res Ther* (2011) 13(1):1–8. doi: 10.1186/ar3258
117. Arbuckle MR, McClain MT, Rubertone MV, Scofield RH, Dennis GJ, James JA, et al. Development of Autoantibodies Before the Clinical Onset of Systemic Lupus Erythematosus. *New Engl J Med* (2003) 349(16):1526–33. doi: 10.1056/NEJMoa021933
118. Jonsson R, Theander E, Sjostrom B, Brokstad K, Henriksson G. Autoantibodies Present Before Symptom Onset in Primary Sjögren Syndrome. *JAMA* (2013) 310(17):1854–5. doi: 10.1001/jama.2013.278448
119. Verspohl SH, Holderried T, Behning C, Brossart P, Schafer VS. Prevalence, Therapy and Tumour Response in Patients With Rheumatic Immune-Related Adverse Events Following Immune Checkpoint Inhibitor Therapy: A Single-Centre Analysis. *Ther Adv Musculoskelet Dis* (2021) 13:1759720X211006963. doi: 10.1177/1759720X211006963

Conflict of Interest: The authors declare that the research was conducted in the absence of any commercial or financial relationships that could be construed as a potential conflict of interest.

Publisher's Note: All claims expressed in this article are solely those of the authors and do not necessarily represent those of their affiliated organizations, or those of the publisher, the editors and the reviewers. Any product that may be evaluated in this article, or claim that may be made by its manufacturer, is not guaranteed or endorsed by the publisher.

frontiers | Frontiers in Immunology

TYPE Original Research
PUBLISHED 25 August 2022
DOI 10.3389/fimmu.2022.975963

OPEN ACCESS

EDITED BY
Rizgar A. Mageed,
Queen Mary University of London,
United Kingdom

REVIEWED BY
Stinne Ravn Greisen,
Aarhus University Hospital, Denmark
Anastas Dimitrov Pashov,
Bulgarian Academy of Sciences (BAS),
Bulgaria

*CORRESPONDENCE
Anne Bordron
anne.bordron@univ-brest.fr

†These authors have contributed equally to this work

SPECIALTY SECTION
This article was submitted to Autoimmune and Autoinflammatory Disorders, a section of the journal Frontiers in Immunology

RECEIVED 22 June 2022
ACCEPTED 03 August 2022
PUBLISHED 25 August 2022

CITATION
Morel M, Pochard P, Echchih W, Dueymes M, Bagacean C, Jousse-Joulin S, Devauchelle-Pensec V, Cornec D, Jamin C, Pers J-O and Bordron A (2022) Abnormal B cell glycosylation in autoimmunity: A new potential treatment strategy.
Front. Immunol. 13:975963.
doi: 10.3389/fimmu.2022.975963

Abnormal B cell glycosylation in autoimmunity: A new potential treatment strategy

Marie Morel[1†], Pierre Pochard[1,2†], Wiam Echchih[1], Maryvonne Dueymes[1,2], Cristina Bagacean[1,2], Sandrine Jousse-Joulin[1,2], Valérie Devauchelle-Pensec[1,2], Divi Cornec[1,2], Christophe Jamin[1,2], Jacques-Olivier Pers[1,2] and Anne Bordron[1*]

[1]LBAI, UMR1227, Univ Brest, Inserm, Brest, France, [2]Laboratoire d'Immunologie et d'Immunothérapie, CHU de Brest, Brest, France

Systemic lupus erythematosus (SLE) and primary Sjögren's syndrome (pSS) are two autoimmune diseases characterised by the production of pathogenic autoreactive antibodies. Their aetiology is poorly understood. Nevertheless, they have been shown to involve several factors, such as infections and epigenetic mechanisms. They also likely involve a physiological process known as glycosylation. Both SLE T cell markers and pSS-associated autoantibodies exhibit abnormal glycosylation. Such dysregulation suggests that defective glycosylation may also occur in B cells, thereby modifying their behaviour and reactivity. This study aimed to investigate B cell subset glycosylation in SLE, pSS and healthy donors and to extend the glycan profile to serum proteins and immunoglobulins. We used optimised lectin-based tests to demonstrate specific glycosylation profiles on B cell subsets that were specifically altered in both diseases. Compared to the healthy donor B cells, the SLE B cells exhibited hypofucosylation, whereas only the pSS B cells exhibited hyposialylation. Additionally, the SLE B lymphocytes had more galactose linked to N-acetylglucosamine or N-acetylgalactosamine (Gal-GlcNAc/Gal-GalNAc) residues on their cell surface markers. Interestingly, some similar alterations were observed in serum proteins, including immunoglobulins. These findings indicate that any perturbation of the natural glycosylation process in B cells could result in the development of pathogenic autoantibodies. The B cell glycoprofile can be established as a preferred biomarker for characterising pathologies and adapted therapeutics can be used for patients if there is a correlation between the extent of these alterations and the severity of the autoimmune diseases.

KEYWORDS

glycosylation, fucosylation, sialylation, N-glycosylation, O-glycosylation, autoimmune diseases, primary Sjogren's syndrome, systemic lupus erythematosus

1 Introduction

Glycobiology is the study of the structure, biosynthesis and biology of glycans. Glycosylation is involved in numerous physiological processes, including cell proliferation, differentiation and apoptosis. It also participates in the intracellular trafficking of several glycoproteins and directs them to their intended destination (1). Glycoconjugates are formed when sugars are added to proteins and lipids, and this phenomenon consists of a succession of enzymatic reactions that mainly occur in the endoplasmic reticulum (ER) and Golgi apparatus. These reactions are specifically performed by glycosyltransferases, which catalyse the transfer of substrates to well-defined sites, and glycosidases, which hydrolyse glycosidic bonds (2).

Saccharides bind to proteins through a wide variety of ligations mediated by N-glycan and O-glycan bonds. The N-glycan bond is initiated in the ER and occurs between the N-acetylglucosamine (GlcNAc) and the NH2 residue of asparagine (Asn). This bound defines the binding site for various complex oligosaccharides on proteins (3, 4). The heterogeneity of N-glycan synthesis in eukaryotes depends on the cell developmental state and the availability of glycosyltransferases, glycosidases and glycans. O-glycan bonds consist of hydroxyl groups of various amino acids (including serine, threonine and tyrosine) and some monosaccharides such as N-acetylgalactosamine (GalNAc), GlcNAc or galactose (Gal). They mainly occur in the Golgi apparatus and use glycosyl nucleotides (e.g. cytidine 5'- monophosphate [CMP-SIA]) as a donor substrate (5). N and O-glycosylation can occur on the same glycoprotein.

Many proteins are modified by N-glycosylation on Asn, which can bind various supplementary monosaccharides, as well as galactosylation, GlcNAclyation, sialylation and fucosylation, all of which determine whether the final structure would be a high-mannose N-glycan, a hybrid N-glycan or a complex N-glycan. However, the glycopeptide O-glycan chains are modified by distinct glycosyltransferases that can elongate the existing structure with Gal and GlcNAc to form different core molecules as well as expand cores with sialic acid and fucose (6) (Figure 1).

Changes in glycosylation have been stated to cause the development of cancers. The modulation of the sialylation of different cell surface receptors promotes survival, proliferation, metastasis development and resistance to drugs and chemotherapy (7–10). In addition to sialylation, aberrant fucosylation and a decrease in GlcNAcylation appear to play a role in solid cancer evolution (11, 12). This aberrant glycosylation has been proposed as a biomarker to predict malignant emergence and cancer progression (13, 14).

Based on these findings, we hypothesised that changes in protein glycosylation could be involved in the development of autoimmune diseases (AIDs), such as primary Sjögren's syndrome (pSS) and systemic lupus erythematosus (SLE). These two chronic systemic diseases, which mainly affect women, are characterised by the production of pathogenic autoantibodies (15, 16). Their aetiology is quite complex, multi-factorial and still unknown. It involves genetic mutations, epigenetic modifications and viral infections (17).

The chronic AID known as pSS is characterised by the development of clinical symptoms on mucosal surfaces, such as the mouth and eyes. It is also called 'sicca syndrome' because of the progressive destruction of exocrine glands and the

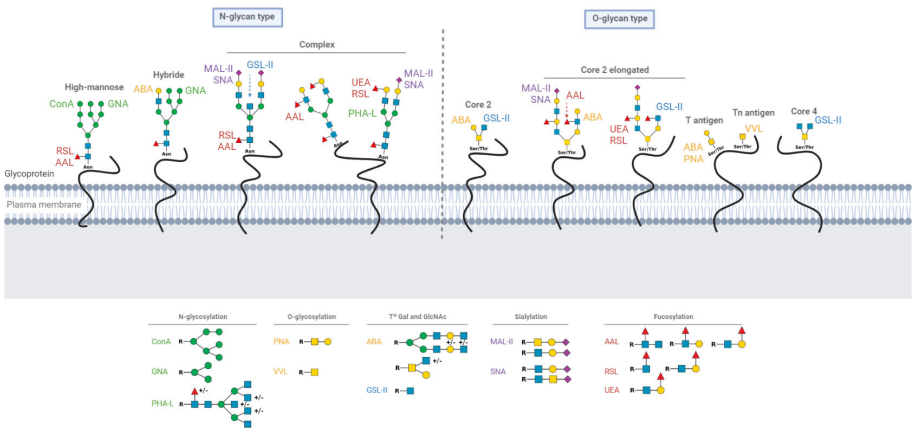

FIGURE 1
Schematic representation of N and O-glycoproteins on cell surface and glycan motives recognized by lectins.The different known forms of N and O-glycoproteins on cell surface are presented as well as glycan motives recognized by lectins. Green circle: Mannose; yellow circle: Galactose; yellow square: N-acetylgalactosamine; blue square: N-acetylglucosamine; purple diamond; Sialic acid and red triangle; Fucose. Asn, Asparagine; Thr, Threonine; Ser, Serine.

emergence of excessive dryness (18). The severity of the disease influences the composition of the salivary gland infiltrates. B and T cells are mainly present in mild lesions, whereas antigen-presenting cells and natural killer cells are present in severe lesions (19). The abnormal abundance of follicular helper T cells, follicular regulatory T cells and plasma cells has also been described (20). B cells play a key role in pSS pathogenesis because they secrete anti-Ro/SSA and La/SSB autoantibodies (15). Glycosylation contributes to the selection of autoreactive B cells since somatic mutations result in the appearance of new N-glycosylation sites and antibodies that can bind autoantigens. The secretion of the N-glycosylation-mutated fragment antigen-binding region of IgG is associated with B cell activation in salivary glands, confirming the importance of the glycoprofile in the development of pSS (21).

SLE is another chronic AID characterised by the production of autoantibodies with various clinical manifestations. The main pathological features in SLE patients are inflammation, immune complex deposits and organs damages, which can lead to nephropathy (22). The severity of SLE has been linked to abnormal T cell subset distribution, such as defects in regulatory T cells, and altered functions (23, 24). B lymphocytes are also actively involved in the development of SLE through different aspects, including the production of pathogenic autoantibodies (25). SLE B cells are also believed to cause disrupted regulation functions. Compared to healthy donors (HDs), SLE patients have B cells that are less efficient in regulating the proliferation of T cells and reducing the production of T helper 1 (Th1) cytokines such as tumour necrosis factor (TNF) alpha and interferon (IFN) gamma when they are co-cultured with autologous T cells (26–28). Moreover, antibodies from SLE patients show glycoprofile abnormalities. Asialylation of IgA results in poor clearance and excessive immune complex accumulation in the kidney, causing chronic inflammation and organ lesions, including nephritis (29, 30).

Based on these findings, we designed a method to evaluate the N-glycosylation and O-glycosylation status of B cells, their subsets and the produced IgA1, IgA2 and IgG immunoglobulins from pSS and SLE patients in comparison to HDs using flow cytometry and ELISA-derived approaches that combine lectins.

2 Material and methods

2.1 Design of control and patient groups

Tonsillar mononuclear cells (TMCs) were isolated from 20 HDs who underwent a routine tonsillectomy at either CHU Morvan or Clinique Pasteur (Brest, France). Peripheral blood mononuclear cells (PBMCs) were isolated from the blood samples of 30 HDs obtained at the Etablissement Français du Sang (Brest, France), 10 pSS patients fulfilling the American College of Rheumatology (ACR)/European Alliance of Association for Rheumatology (EULAR) 2016 criteria and 17 SLE patients fulfilling the ACR/EULAR 2019 criteria. The blood samples from the pSS and SLE patients were collected from the 'CRB Santé de Brest' (BB-0033-00037) and 'Centre de référence des maladies auto-immunes rares' in Brest, France. All patients agreed to participate in the research protocol by signing a consent form.

A cross-matched selection of 13 HDs (12 females and 1 randomly selected male) was performed to make a reliable comparison with autoimmune patients.

For the serum analysis, 10 HD, 10 pSS and 10 SLE sera were obtained from the European PRECISESADS study (Innovative Medicine Initiative Joint Undertaking under the grant agreement number 115565).

All characteristics are described in Table 1.

2.2 Isolation of mononuclear cells

A 5 mL syringe plunger was used to mince and mash tonsils into a 40 µm nylon mesh in phosphate buffer saline (PBS) solution (Eurobio scientific, Les Ulis, France). The cell suspension was layered on density gradient Pancoll (PAN-Biotech GmbH, Aidenbach, Germany) and uninterruptedly

TABLE 1 Demographics and disease activity parameters.

Items		Tonsil HD (n=20)	Blood HD (n=30)	Blood pSS (n=10)	Blood SLE (n=17)	Serum HD (n=10)	Serum pSS (n=10)	Serum SLE (n=10)
Female	MD	12	9	16	9	10	9
Male	MD	18	1	1	1	0	1
Age (mean)	<10	39,6	52,3	44,8	36	67,2	42,8
Disease activity score	N/A	N/A	ESSDAI score [4;6] n=6 [7;8] n=4	SLEDAI score [11;16] n=9 [17;34] n=8	N/A	ESSDAI score MD n= 3 [0;4] n=4 [5;10] n=3	SLEDAI score MD n= 2 [0;4] n=6 [5;10] n=2

HD, Healthy Donors; pSS, primary Sjögren's syndrome; SLE, Systemic lupus erythematosus; ESSDAI, Eular Sjögren Syndrome Disease Activity Index; SLEDAI, Systemic Lupus Erythematosus Disease Activity Index; N/A, not applicable; MD, missing data.

centrifuged at 750 g and room temperature (RT) for 20 min. The isolated cells were washed twice with PBS and counted using a Malassez haemocytometer.

Platelets were removed from the blood samples by low-speed centrifugation (300 g, RT and 15 min). After discarding the supernatant, the blood samples were diluted in half and layered on density gradient Pancoll. After centrifugation at 750 g (RT, 20 min), the isolated cells were washed twice in PBS and counted using the Malassez haemocytometer.

2.3 Cell culture

Burkitt lymphoma Ramos B cell lines were grown in an RPMI-1640 solution (Eurobio scientific, Les Ulis, France) containing 10% fetal bovine serum (Eurobio scientific, Les Ulis, France), 50 U/mL penicillin (Panpharma, La Selle-en-Luitré, France), 50 mg/mL streptomycin (Sigma-Aldrich, St. Louis, MI, USA) and 2 mM L-glutamine (Gibco, Thermo Scientific, Waltham, MA, USA) at 37°C in a humidified 5% CO_2 atmosphere.

2.4 Lectin inhibitory binding tests

Several vegetal lectins were described and used to recognise specific saccharides and their complexity. Agaricus bisporus agglutinin (ABA), Ralstonia solanacearum lectin (RSL) and Sambucus nigra agglutinin (SNA) were purchased from GLYcoDiag (Orléans, France). Aleuria aurantia lectin (AAL), Canavalia ensiformis agglutinin (ConA), Galanthus nivalis agglutinin (GNA), Griffonia (Bandeiraea) simplicifolia lectin-II (GSL-II), Maackia amurensis lectin-II (MAL-II), Phaseolus vulgaris leucoagglutinin (PHA-L), Arachis (peanut) hypogaea agglutinin (PNA), Ulex europaeus agglutinin (UEA) and Vicia villosa lectin (VVL) were obtained from Vector Laboratories, Inc. (Burlingame, CA, USA; Table 2). All lectins were biotinylated. Monosaccharides were used to validate the specificity of the lectin binding. Lectins were pre-incubated with a PBS solution containing monosaccharides at 4°C for 15 min (Table 2) before being used to stain the Ramos cell line for 15 min at 4°C. The cells were washed twice with PBS and subsequently incubated at 4°C for 15 min using 5 µg/mL streptavidine-fluorescein isothiocyanate (FITC) (Biolegend, San Diego, CA, USA). The cells were washed with PBS and analysed using a Beckman Coulter Cytoflex S flow cytometer (Beckman Coulter, Brea, CA, USA).

The competition was evaluated by a decrease in the mean fluorescence intensity (MFI) signal using the following formula where 'MFI monosaccharide' represents staining with pre-incubated lectin binding, 'cell autofluorescence' represents the fluorescence without any lectins and 'MFI' represents staining with only lectin binding.

$$100 - \left(100x \ \frac{MFI \ \ monosaccharide - cell \ \ autofluorescence}{MFI - cell \ \ autofluorescence}\right)$$

The inhibitory test for the sialic acid-binding lectins (MAL-II and SNA) was based on the treatment of the cells with neuraminidase from *Clostridium perfringens* (0.05 U/mL; Sigma-Aldrich, St. Louis, MI, USA) at 37°C for 30 min. After extensive washes with PBS, the treatment efficiency was evaluated using the same formula.

2.5 Analysis of membrane glycosylation by flow cytometry

Next, 1×10^6 isolated TMCs or PBMCs were stained with 10 µg/mL of either biotinylated lectins at 4°C for 15 min (Table 2). The cells were washed twice and incubated with antibodies defined to identify the different B cell subsets (Table 3) and 5 µg/mL streptavidin-FITC (Biolegend, San Diego, CA, USA) at 4°C for 15 min. Thereafter, the cells were washed with PBS at 4°C and analysed using a Cytoflex S flow cytometer (Beckman Coulter, Brea, CA, USA).

The flow cytometer was standardised using Flow-Set Pro Fluorosphere beads (Beckman Coulter, Brea, CA, USA) to ensure an inter-experimental comparison of the fluorescent intensity over time. Data were analysed using Kaluza 2.1 software (Beckman Coulter, Brea, CA, USA). The B cells were defined as CD19+ after doublet exclusion.

The B cell subsets for the tonsillar samples were determined based on CD38 and IgD staining (44). Bm1 cells were identified as IgD+CD38−, Bm2 cells as IgD+CD38+, Bm2' cells as IgD+CD38++, Bm3–4 cells as CD19+CD38+IgD−, eBm5 cells as IgD−CD38+, Bm5 cells as IgD−CD38− and plasmablasts (PBs) as CD38+++IgD−.

Peripheral B cell subsets were determined based on CD24, CD38, CD27 and IgD staining. Transitional (TR) B cells were identified as CD24+++CD38+++, naïve (NA) B cells as CD27−IgD+, unswitched memory (UM) B cells as CD27+IgD+, switched memory (SM) B cells as 7CD27+IgD−, PB as CD27+CD38+++ and double negative (DN) B cells as CD27−IgD−.

2.6 Analysis of serum glycosylation

2.6.1 Determination of protein concentration in serum

To ensure that any differences in serum glycosylation could not be attributed to variations in the protein amount, the protein concentration in all samples was determined using the bicinchoninic acid assay test (Micro BCA Protein Assay kit, Thermo Scientific, Waltham, MA, USA) in accordance with the manufacturer's instructions. The serum volume used in the glycosylation tests was then adjusted to contain 7 µg of proteins.

10.3389/fimmu.2022.975963

TABLE 2 Lectin specificities.

Complete name	Abbreviation	Motif binding	Reference	Concentration of monosaccharide and neuraminidase used for inhibitory tests
Aleuria aurantia lectin	AAL	GlcNAc(β1-4)[Fuc(α1-6])GlcNAc Fuc(α1-3)Gal(β1-4)GlcNAc Gal(β1-4)[Fuc(α1-3)]GlcNAc Gal(β1-3)[Fuc(α1-4)]GlcNAc	(31–33)	200mM of L-Fucose‡
Agaricus bisporus agglutinin	ABA	GlcNAc(β)Gal(β1-3)GalNAc-Ser/Thr Gal(β1-4)GlcNAc Gal(β1-3)[GlcNAc(β1-6)]GalNAc-Ser/Thr	(33–35)	83mM of N-Acetylgalactosamine*
Canavalia ensiformis agglutinin	ConA	Man(α)	(33, 36)	360mM of α-Methyl-Mannoside*
Galanthus nivalis agglutinin	GNA	Man(α1-3)Man(α1-6)	(33, 36)	360mM of α-Methyl-Mannoside*
Griffonia (Bandeiraea) simplicifolia lectin-II	GSL-II	GlcNAc(α/β)	(33, 37)	200mM of N-Acetylglucosamine*
Maackia amurensis lectin-II	MAL-II	Neu5Ac(α2-3)Gal(β1-4)GlcNAc Neu5Ac(α2-3)Gal(β1-3)GalNAc	(33, 38, 39)	0.05U/mL of Neuraminidase‡
Phaseolus vulgaris leucoagglutinin	PHA-L	GlcNAc(β1-6)Man(α1-6)	(33, 40)	720mM of D-Galactose‡
Arachis (Peanut) hypogaea agglutinin	PNA	Gal(β1-3)GalNAc-Ser/Thr (*Thomsen-Friedenreich (T) antigen*)	(33, 41)	200mM of D-Galactose‡
Ralstonia solanacearum lectin	RSL	Fuc(α1-2)GalFuc(α1-6)GlcNAc	(42)	200mM of L-Fucose‡
Sambucus nigra agglutinin	SNA	Neu5Ac(α2-6)Gal(β1-4)GlcNAc Neu5Ac(α2-6)GalNAc(β1-4)GlcNAc	(33, 38, 39)	0.05U/mL of Neuraminidase‡
Ulex europaeus agglutinin	UEA	[Fuc(α1-2)]Gal(β1-4)GlcNAc	(33, 41)	200mM of L-Fucose‡
Vicia villosa lectin	VVL	GalNAc(α/β) (*Tn antigen*)	(33, 43)	83mM of N-Acetylgalactosamine*

* Provided by Vector Laboratories, Inc (Burlingame, CA, USA).
† Provided by GLYcoDiag (Orléans, France).
‡ Provided by Sigma-Aldrich (St. Louis, MI, USA).
Ser, Serine; Thr, Threonine; Fuc, Fucose; GlcNAc, N-acetylglucosamine; GalNAc, N-acetylgalactosamine; Gal, Galactose; Neu5Ac, N-acetylneuraminic Acid; Man, Mannose; Glc, Glucose. mM, millomolar.

TABLE 3 Antibodies used in the flow cytometry analysis.

Antibodies	Clone	Fluorochrome	Manufacturer
Anti-CD5	BL1a	ECD	Beckman Coulter, Brea, CA, USA
Anti-CD19	J3-119	APC Alexa Fluor 700	
Anti-CD24	ALB9	APC Alexa Fluor 750	
Anti-CD24	1A4CD27	PC7	
Anti-CD38	LS198-4-3	PC5.5	
Anti-IgM	SA-DA4	Pacific Blue 450	
Anti-IgD	IA6-2	APC	Biolegend, San Diego, CA, USA

CD, Cluster of differentiation; IgM, immunoglobulin M; IgD, immunoglobulin D; ECD, electron coupled dye; APC, allophycocyanin; PC, phycoerythrin cyanin.

2.6.2 Determination of the glycoprofile of serum proteins using: An ELISA-derived approach

The adjusted serum volume was diluted in PBS and coated in MaxiSorp 96-well Nunc plates under stirring at RT for 2 h. Wells were washed five times in PBS containing 0.05% of Tween 20 (Sigma-Aldrich, St. Louis, MI, USA). Subsequently, 100 µL of biotinylated lectins at an optimised concentration (Table 4) were added inside wells under stirring at RT for 1 h. After washing five times, 0.16 µg/mL of horseradish peroxidase (HRP)-conjugated streptavidin (Biolegend, San Diego, CA, USA) was added for 30 min at RT under stirring. After five washes, a coloured reaction was created using tetramethylbenzidine (TMB; Biolegend, San Diego, CA, USA) and stopped with an 11% sulfuric acid solution. The optical density (OD) was determined at 450 nm with a Multiskan GO microplate spectrophotometer and SkanIt software (Thermo Scientific, Waltham, MA, USA).

2.6.3 Determination of IgA1, IgA2 and IgG glycosylation by ELISA-derived technique

Further, 0.5 µg/mL of mouse anti-human IgA1 (RM124 clone), mouse anti-human IgA2 (RM125 clone) or mouse anti-human IgG (4A10 clone; Thermo Scientific, Waltham, MA, USA) was coated on MaxiSorp 96-well Nunc plates at 4°C overnight. The plates were washed with a PBS solution containing 0.05% Tween 20 and saturated with either a 2% BSA solution (Sigma-Aldrich, St. Louis, MI, USA) or a carbohydrate-free blocking solution (CFBS; Vector Laboratories, Inc, Burlingame, CA, USA) at 37°C for 1 h depending on the lectin (Table 4). An oxidation step was then performed with 0.05 M sodium periodate in 0.05 M pH4 citrate buffer (Sigma-Aldrich, St. Louis, MI, USA) to cleave terminal glycans present on the anti-Ig and saturating buffer. Next, 100 µL of 1:100 diluted sera was added and incubated at 37°C for 1 h. After five washes, biotinylated lectins (Table 4) were added to the plate under stirring at RT for 1 h. After five washes, 0.16 µg/mL of HRP-conjugated streptavidin was added under stirring at RT for 30 min. After five additional washes, a TMB solution was added, and the coloured reaction was stopped with 11% sulfuric acid. The OD was determined at 450 nm using a Multiskan GO microplate spectrophotometer and SkanIt software (Thermo Scientific, Waltham, MA, USA).

2.7 Statistical analysis

GraphPad Prism 9 software was used to plot graphs and conduct a statistical analysis. The normal distribution was verified, and then two groups were compared using the Mann–Whitney U test, while more than two groups were compared using a one-way ANOVA test and Dunn's multiple comparison test without adjustment. The correlation between age and glycosylation was determined by linear regression with p-value< 0.05 and $R2 > 0.50$.

3 Results

We evaluated the lectin specificity to validate the use of flow cytometry to stain with lectins. Several monosaccharide agonists were incubated with lectins before performing the staining (Table 2). As shown in Figure 2, the fluorescent intensity of the signal obtained with the mannose-binding ConA and GNA decreased by 98.90% and 50.56%, respectively, when lectins were pre-incubated with α-methyl-mannoside (aMeMan; 360 mM). When Gal was used at 200 mM, PHA-L and PNA binding decreased by 64.66% and 91.05%. For lectins that recognise

TABLE 4 Lectins, concentrations and saturating conditions used for ELISA.

Lectins	Concentration (µg/mL)	IgA1 saturating solution	IgA2 saturating solution	IgG saturating solution
AAL	2	oxidized CFBS	oxidized CFBS	oxidized CFBS
ABA	10	oxidized CFBS	oxidized CFBS	oxidized CFBS
ConA	0.2	oxidized CFBS	oxidized CFBS	oxidized 2%BSA
GNA	20	2%BSA	2%BSA	CFBS
GSL-II	10	2%BSA	2%BSA	CFBS
MAL-II	0.5	2%BSA	2%BSA	oxidized CFBS
PHA-L	5	2%BSA	2%BSA	CFBS
PNA	20	2%BSA	2%BSA	oxidized CFBS
RSL	0.5	oxidized CFBS	oxidized 2%BSA	oxidized CFBS
SNA	1	oxidized 2%BSA	2%BSA	oxidized CFBS
UEA	40	2%BSA	2%BSA	CFBS
VVL	40	2%BSA	2%BSA	oxidized CFBS

AAL, Aleuria aurantia lectin; ABA, Agaricus bisporus agglutinin; ConA, Canavalia ensiformis agglutinin; GNA, Galanthus nivalis agglutinin; GSL-II, Griffonia (Bandeiraea) simplicifolia lectin II; MAL-II, Maackia amurensis lectin II; PHA-L, Phaseolus vulgaris leucoagglutinin; PNA, Arachis (Peanut) hypogaea agglutinin; RSL, Ralstonia solanacearum lectin; SNA, Sambucs nigra agglutinin; UEA, Ulex europaeus agglutinin and VVL, Vicia villosa lectin. PBS, Phosphate buffer saline; CFBS, Carbohydrate Free Blocking Solution; BSA, Bovine serum albumin; IgA, Immunoglobulin A; IgG, Immunoglobulin G.

10.3389/fimmu.2022.975963

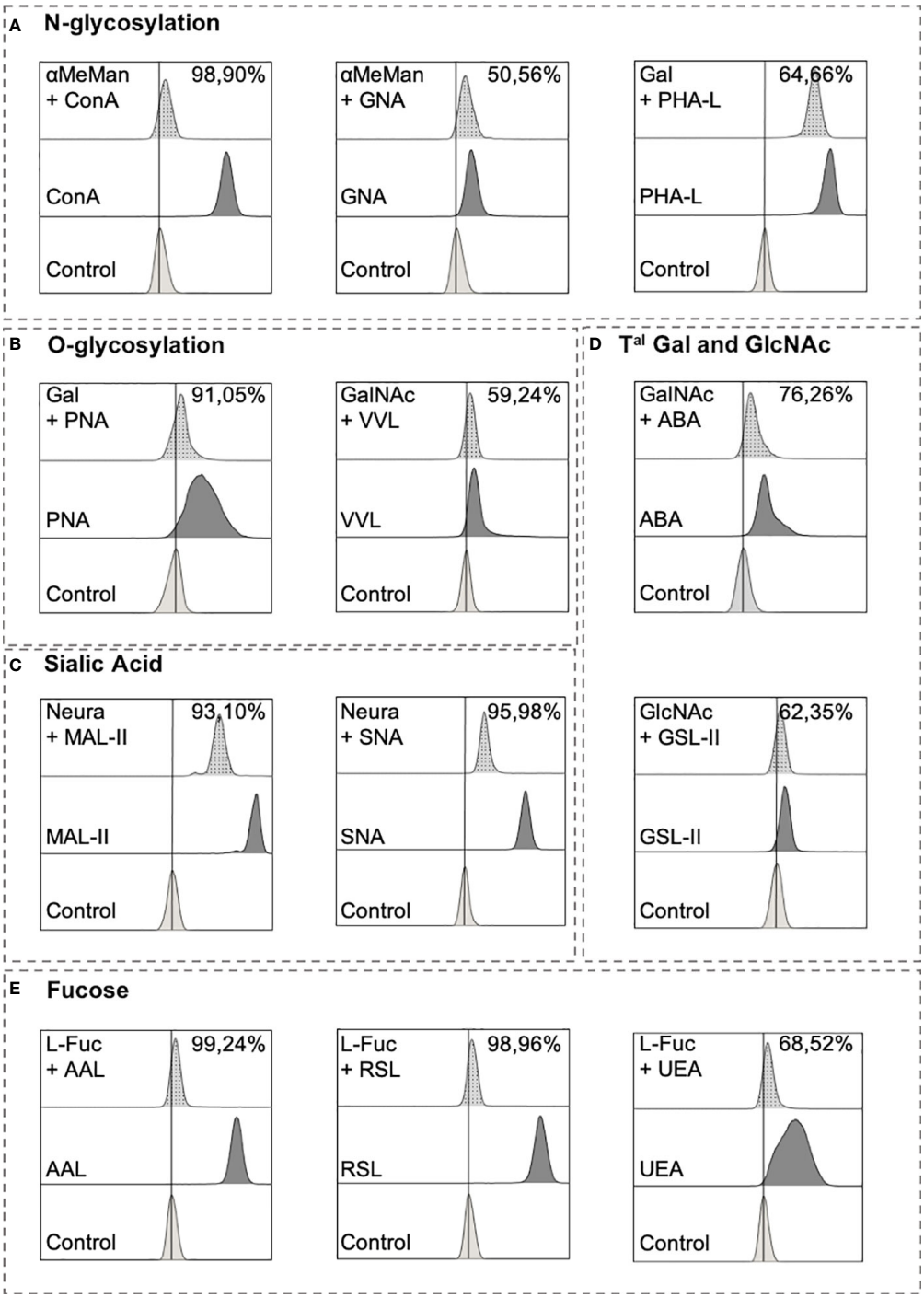

FIGURE 2
Lectin inhibitory tests.Lectins (except MAL-II and SNA) (Table 2) were pre-incubated with a PBS solution containing monosaccharides for 15 min at 4°C with PBS before being used to stain Ramos cell line for 15 min at 4°C. After 2 washes in PBS, cells were incubated for 15 min at 4°C with 5 µg/mL streptavidin-FITC. After wash with PBS, cells were analyzed using Beckman Coulter Cytoflex S. For ConA and GNA, inhibition test consists in pre-incubating lectins with α-methyl-mannoside (360mM). PHA-L and PNA were pre-incubated with 200 mM of galactose (Gal). N-acetylgalactosamine (GalNAc) was pre-incubated at 83mM with VVL and ABA. GSL-II was pre-incubated with 200 mM of N-acetylglucosamine (GlcNAc) and 200mM of L-fucose (L-Fuc) was used for AAL, RSL and UEA lectins. For MAL-II and SNA, cells were treated with neuraminidase (0.05 U/mL) and washed twice followed with a regular staining procedure. Results are presented as followed: N-glycosylation in **(A)**, O-glycosylation in **(B)**, Sialylation in **(C)**, Terminal (T^{al}) Gal and GlcNAc on N and O-glycosylation in **(D)**, and Fucosylation in **(E)**.

GalNAc, 83mM of GalNAc was sufficient to decrease the ABA and VVL bindings by 76.26% and 59.24%, respectively. For the fucose-binding lectins, 200 mM of L-fucose (L-Fuc) was sufficient to decrease AAL, RSL and UEA bindings by 99.24%, 98.96% and 68.52%, respectively. Thereafter, the cells were pre-treated with neuraminidase (0.05 U/mL) for 30 min at 37°C for lectins that recognise sialic acid (MAL-II and SNA), and the fluorescent signal obtained with SNA and MAL-II decreased by 95.27% and by 93.10%, respectively. These results were expected for the lectins that had low inhibition percentages (GNA, PHA-L, VVL, ABA, GSL-II and UEA) because they recognise motifs included in a series of glycans and because we used free monosaccharides. Although these conditions do not exactly reflect the reality of complex glycans, they allowed us to validate the specificity of these tools for further study.

3.1 Association of tonsillar B cell maturation process with important N-glycan and O-glycan remodelling

A panel of antibodies was designed to identify any change in the glycosylation status of the different B cell subsets (Table 3). Antibodies can modify the cell glycoprofile because they carry glycans. Thus, biotinylated lectins were added first, followed by B cell markers. We used this established experimental protocol to perform the lectin staining procedure on the tonsillar cells. Functional B cell subsets can be distinguished using several membrane proteins. In particular, variations in the expression levels of IgD and CD38 have been used to develop a model for mature B cell homeostasis through germinal centre (GC) cells (44). This model suggests that naive Bm1 cells (IgD+CD38−) become Bm2 cells (IgD+CD38+) once they are activated and then develop into GC founder Bm2′ cells (IgD+CD38++). These cells can differentiate into centroblast Bm3 cells, centrocyte Bm4 cells (IgD−CD38++) and eventually early memory Bm5 cells (IgD−CD38+) and memory Bm5 cells (IgD−CD38−) or plasma cells (PB). Figure S1A depicts the gating strategy for assessing these different tonsillar CD19+ B cell subsets.

We were able to identify a differential presence of sugar patterns for most of the lectins, depending on the maturation status of the B cells (Figure 3). Although no statistical difference was obtained with ConA, a significant decrease in the presence of terminal mannose on N-glycans was mainly observed in the Bm3–4 B cells using GNA, and the transition towards eBm5, Bm5 and PB was accompanied by a restoration of an expression

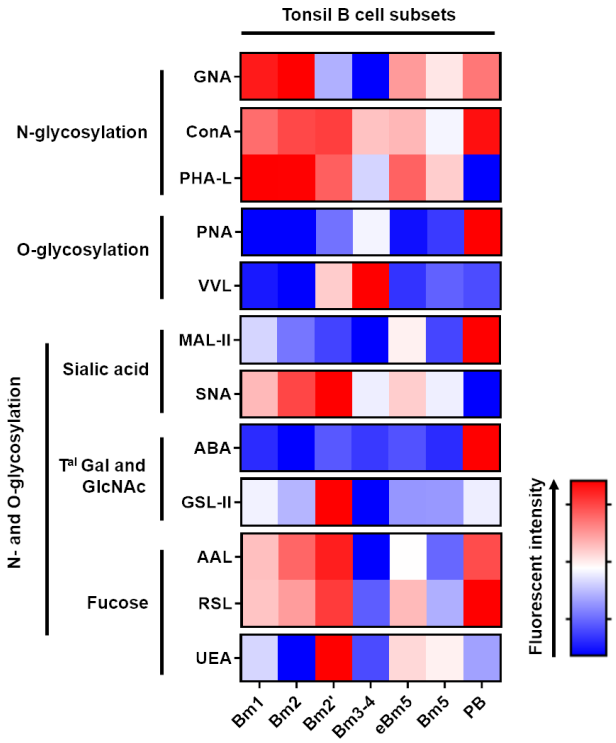

FIGURE 3
Tonsillar B cell maturation process is associated with an important N- and O-glycan remodeling. Freshly isolated tonsillar mononuclear cells were stained with lectins and the specific B cell antibody panel before analysis using Beckman Coulter Cytoflex S. Fluorescence intensity is expressed as geomean. Freshly isolated tonsillar mononuclear cells were stained with lectins (Table 2).

level nearly similar to those of Bm1 and Bm2. In terms of β1-6 branched N-glycans, Bm3–4 and PB were characterised by a reduction in the staining obtained with PHA-L when compared to other states (Figure S2A). In the case of T and Tn antigens, which were identified using PNA and VVL lectins, respectively, a marked expression in the GC B cells (Bm2' and Bm3–4) was observed as expected. Significantly high staining with PNA was identified on PB, indicating the presence of additional T antigens (Figure S2B). When MAL II was used, a progressive decrease in α2-3 sialylation was observed from the Bm1 to Bm3–4 cells. The transition towards eBm5 and Bm5 was accompanied by a complete restoration. Interestingly, the final maturation in PB was associated with an important increase in α2-3 sialic acids. SNA did not reveal any difference in the presence of α2-6 sialic acids on the different B cell subsets (Figure S2C). The same was observed with ABA and GSL II (Gal-GlcNAc/Gal-GalNAc and terminal GlcNAc, respectively; Figure S2D). In terms of fucosylation, AAL staining (α1-3/4/6 fucose linked to GlcNAc residues) mainly decreased on the Bm3–4 cells, while RSL and UEA staining, which targeted α1-6 fucose linked to GlcNAc and α1-2 fucose linked to Gal residues, respectively, did not exhibit any statistical difference in the different B cell subsets (Figure S2E).

Altogether, our flow cytometry analysis using lectins revealed that tonsillar B cell maturation is associated with profound changes in glycans at the cell surface.

3.2 Association of peripheral B cell differentiation with a profound remodelling of N- and O- glycans at the cell surface similar to that in tonsils

A cohort of 30 HDs was selected to analyse the blood glycome of B cells and their subsets (Table 2). The most immature peripheral B cell population in humans has been characterised in detail by the concomitantly high expression of CD24 and CD38 (45). B cells have been divided into four distinct populations using the surface expression of IgD and CD27 as a surrogate marker for human memory B cells. IgD +CD27− B cells represent the NA B cell pool, whereas the expression of CD27 and loss of surface IgD expression on B cells are features of classical SM B cells. B cells that express CD27 and IgD have been characterised as UM B cells. The delineation of human memory B cells by CD27 expression has been challenged by the characterisation of CD27-negative B cells (IgD−CD27−), also called DN, indicating molecular imprints of memory B cells (somatic hypermutation and immunoglobulin class-switch) (46). The gating strategy is shown in Figure S1B. First, the effects of gender and age on the glycoprofile of each B cell subset were evaluated. As presented in Figure S3A, no statistical difference was observed between the male and female HDs. We also assessed if age could affect the glycoprofiles. As shown in Figures S3B (age of men) and S3C (age of women), no direct correlation between age and the glycan signature could be established. We were able to identify a differential presence of sugar patterns for most of the lectins, depending on the diffetentiation state of the B cells (Figure 4).

Although no statistical difference was obtained with ConA, the presence of terminal mannose on N-glycans (GNA) was remarkably decreased on PB (Figure S4A). Considering the results obtained with PHA-L, an important loss in β1-6 branched N glycans was assessed in UM and PB (Figure S4A). The DN B cells and PB were characterised by an increase in the amount of T and Tn antigens (targeted with PNA and VVL lectins, respectively; Figure S4B). Compared to the SM, PB and DN B cells, the NA B cells exhibited a decreased level of α2-3 sialic acids, which were targeted by MAL-II (Figure S4C). A discrete decrease in PB was the only difference that was observed for α2-6, which was recognised by SNA. When stained with ABA, NA exhibited a significant decrease in staining when compared to the SM and PB subsets, and the detection of terminal GlcNAc motive by GSL-II was similar across the subsets with a discrete increase in SM. (Figure S4D). Regarding the fucosylation of B cell surface markers, there was no major difference between each subset with the three lectins used (AAL, RSL and UEA), except for a slight decrease in NA B cells, an increase in SM and DN compared to NA and a discrete increase in PB (Figure S4E).

Analysis of the glycosylation of B cell subsets from peripheral blood demonstrated significant remodelling of membrane glycans similar to that of tonsils in accordance with the different steps of the differentiation process.

3.3 B cells and their subsets from pSS and SLE patients are carrying altered glycoprofiles

As presented in Figure 5, the B cell glycoprofiles of pSS and SLE patients were compared to those of HDs. Regarding N-glycosylation, the SLE B cells demonstrated a decrease in Con A staining when compared to the HD B cells (Figure 5A). Compared to the HDs, the pSS and SLE patients showed a significant reduction in terminal or high-mannose (GNA) in their B cells. O-glycosylation (PNA and VVL) exhibited no difference (Figure 5B). Regarding the sialic acids, although staining with MAL-II exhibited no difference, the staining with SNA revealed desialylated B cells in the pSS patients. A similar observation was made with SLE B cells without reaching any statistical significance (Figure 5C). When ABA was used, the SLE B cells exhibited a stronger signal than the HD and pSS B cells (Figure 5D). Regarding fucosylation, RSL and UEA exhibited no differences, while AAL revealed that the SLE B cells presented a loss in α1-3/4/6 fucose linked to GlcNAc residues (Figure 5E).

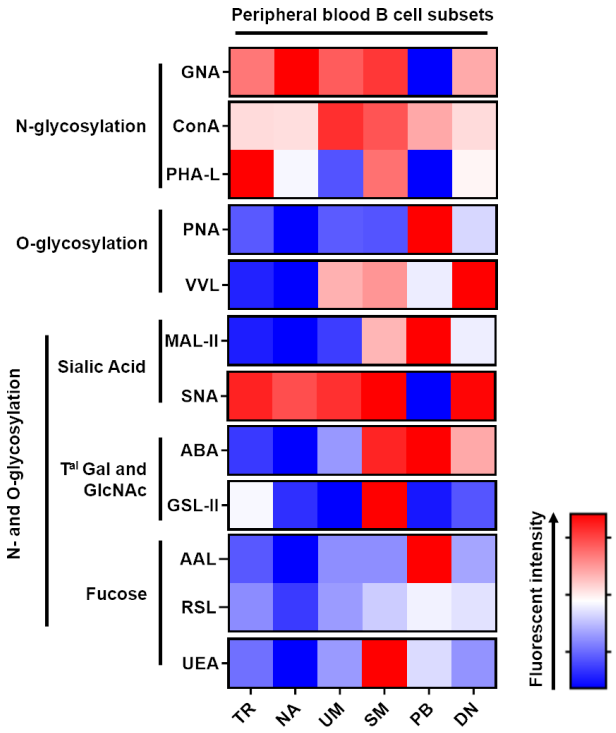

FIGURE 4
Peripheral blood B cell differentiation is associated with a rearrangement of N and O-glycan surface and an increase of Galactose α2-3 N-acetylneuraminic acid residues. Freshly isolated peripheral blood mononuclear cells (PBMC) were stained with lectins the specific B cell antibody panel before analysis using Beckman Coulter Cytoflex S. Fluorescence intensity is expressed as geomean. All the listed annotation stands for; TR: Transitional B cells; NA: Naive B cells; UM: Unswitched-memory B cells; SM: Switched-memory B cells; PB: Plasmablasts and DN: Double negative ($CD27^-IgD^-$) B cells; Gal: Galactose; Tal: terminal; GlcNAc: N-acetylglucosamine. Freshly isolated tonsillar mononuclear cells were stained with lectins (Table 2) and the specific B cell antibody panel.

The glycoprofile of the different B cell subsets (TR, NA, UM, SM, DN and PB) of these two AIDs was assessed, and the results are presented in Supplementary Figure 5. A summary of the differences is presented in Table 5.

The NA and UM cells in the pSS patients presented less high-mannose structures (GNA, ConA) than those in the HDs. The SM B cells carried few β1-6 branched N-glycan structures and T antigen on their surface markers. These discrepancies were associated with an increased level of α2-3 sialic acids (recognised by MAL II) and a decrease in α2-6 (SNA). There were no changes in the glycoprofiles of TR, PB and DN.

Compared to those in the HDs, all the B cell subsets in the SLE patients carried reduced levels of high-mannose structures (Con A and GNA), except for PB, which is consistent with our previous observation on total B cells. The SM B cells presented few β1-6 N-glycan motifs. A significant afucosylation (staining with AAL) was observed on the NA, UM, SM and DN B cells. The SLE DN B cells also displayed few high-mannose motives and significant afucosylation. The most remarkable result was obtained with ABA, which indicated that all the SLE B cell subsets carried more terminal Gal-GlcNAc/Gal-GalNAc elements when compared to the B cells from the HDs and pSS patients. We also noticed that SLE PB had more Tn antigens than pSS PB.

Compared to the HD B cells, the pSS and SLE B cells and their subsets presented important changes in their glycoprofiles. All these modifications could be responsible for the physiological activity and reactivity in those patients.

3.4 Serum proteins from SLE patients are carrying more Gal-GlcNAc/Gal-GalNAc motives

An ELISA-derived approach was developed using biotinylated lectins as a revealing agent to study the glycosylation of serum proteins. Sera from the pSS and SLE patients were compared to those from the HDs (Table 1). Only ABA demonstrated a significant difference, indicating that the serum proteins from the SLE patients carried more Gal-GlcNAc/Gal-GalNAc motives

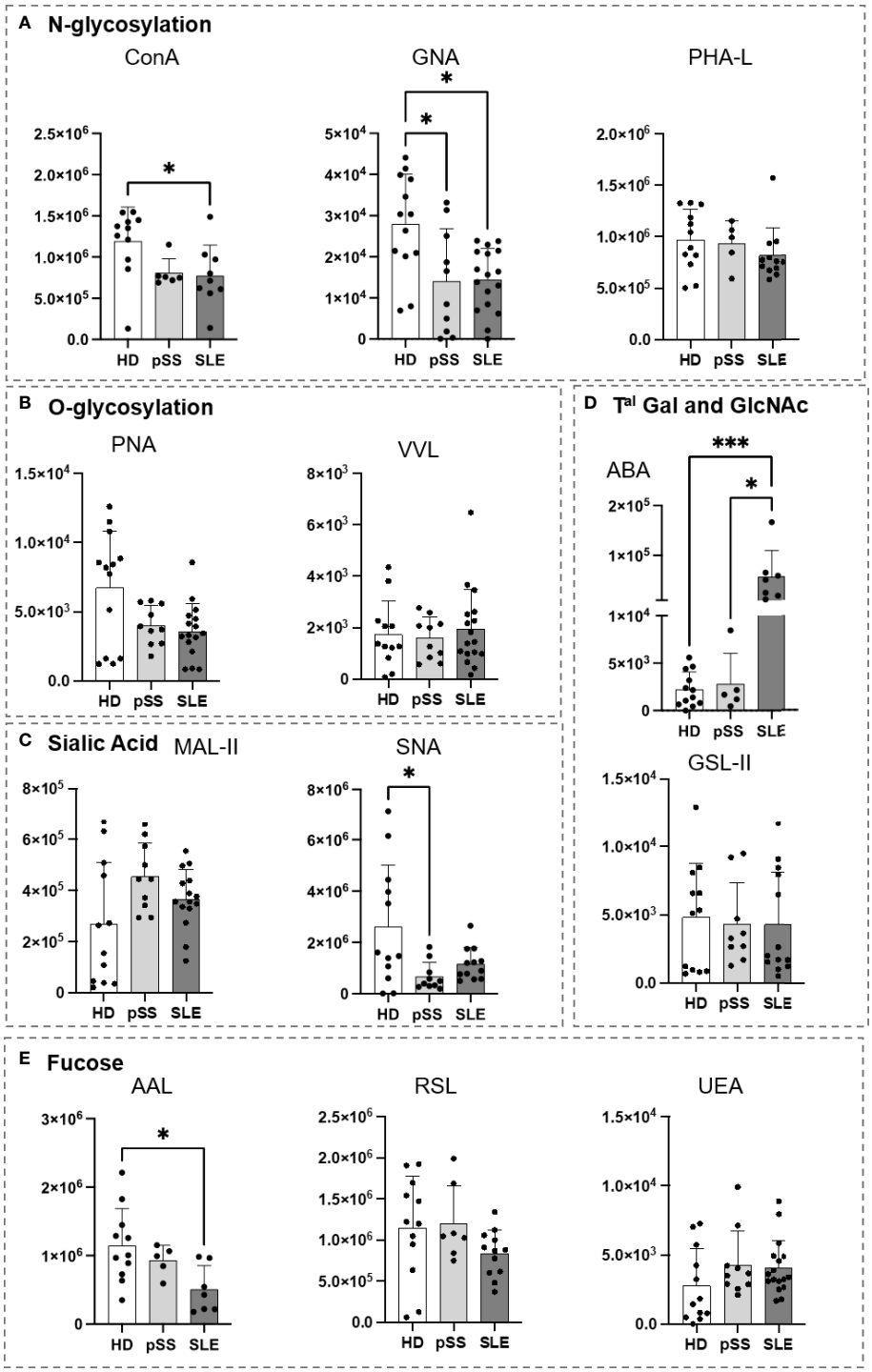

FIGURE 5
Analysis of B cell glycosylation reveals deep alterations in primary Sjögren's syndrome (pSS) and systemic lupus erythematosus (SLE). Freshly isolated peripheral blood mononuclear cells (PBMC) (10^6) from 13 healthy donors (HD), 10 pSS, and 17 SLE patients were stained with lectins at 10 µg/mL for 15 min at 4°C (Table 2). After two wash steps, cells were incubated with streptavidin-FITC (5 µg/mL) and an antibody panel (Table 3) for 15 min at 4°C. After staining and washing in PBS at 4°C, cells were analyzed using Beckman Coulter Cytoflex S. Fluorescence intensity from CD19+ B cells is expressed as geomean. Results are presented as followed: N-glycosylation in **(A)**, O-glycosylation in **(B)**, Sialylation in **(C)**, Terminal (T^{al}) Gal and GlcNAc on N and O-glycosylation in **(D)**, Fucosylation in **(E)**. One-way anova test followed by Dunn's multiple comparison test were performed. ns: not significant p > 0,05, stars are indicated when p< 0,05 (*); < 0,001 (***).

10.3389/fimmu.2022.975963

TABLE 5 Schematic representation of the glycoprofile obtained for each B cell subsets presented in the Supplementary Figure 4.

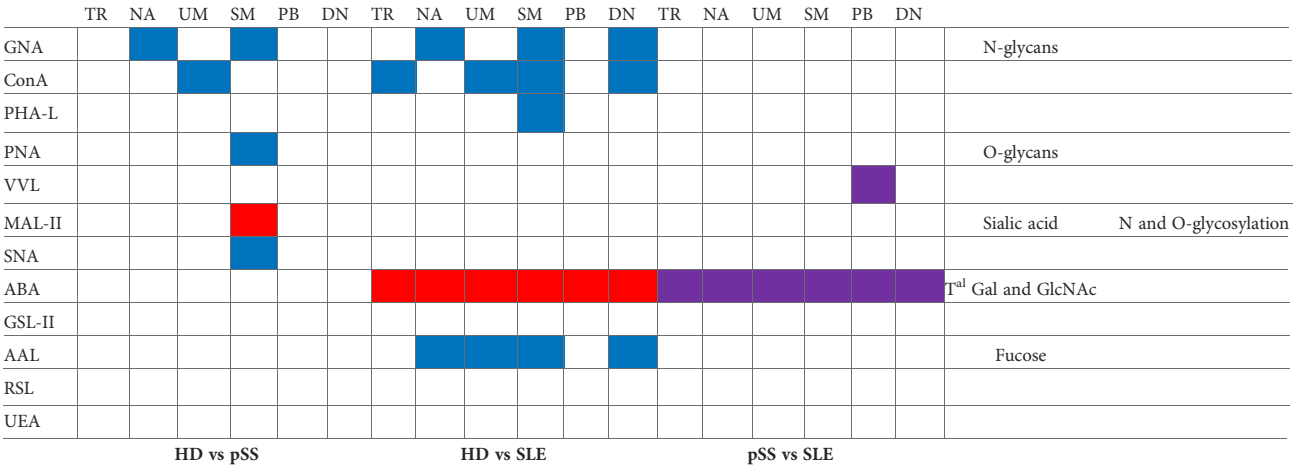

TR, Transitional B cells; NA, Naïve B cells; UM, Unswitched memory B cells; SM, Switched memory B cells; PB, Plasmablasts; DN, Double negative memory B cells.
The white square represents no statistical difference between the two compared groups.
The blue square represents a significant decrease in AID vs HD.
The red square represents a significant increase in AID vs HD.
The purple square represents a significant increase in SLE vs pSS.

(Figure 6). This result supports the results obtained for the SLE B cells and their subsets. This suggests that there were some impairments in this same glycosylation pathway.

3.5 IgA1 and IgA2 from the pSS and SLE patients carried less high-mannose structures and more GlcNAc residues, whereas IgG had less α2-6 sialic acid and hypofucosylation

Another ELISA-derived assay was optimised to focus on IgA1, IgA2 and IgG in order to further our investigations. Compared to that from the HDs, IgA1 from the pSS and SLE patients carried fewer terminal mannose residues on N-glycans revealed by GNA. IgA1 from the SLE patients also presented less VVL staining (Tn antigen) and more terminal GlcNAc (GSL-II lectin) motives than that from the HDs, indicating a decrease in terminal galactosylation. No other difference was observed (Figure 7).

IgA2 from the SLE patients presented less terminal mannose on N-glycans (GNA) than that from the HDs and pSS patients (Figure 8). No other significant difference was observed. The ELISA for PNA and VVL was not conducted because IgA2 had no O-glycosylation site.

The analysis of the IgG glycoprofiles from the AID patients revealed that the N-glycan residues (ConA, GNA and PHA-L) exhibited no difference (Figure 9). A significant decrease in α2-6 sialylation was observed on pSS and SLE IgG (SNA staining) along with a low terminal GlcNAc binding attested by GSL-II. Finally, compared to that from the HDs, IgG from the SLE patients presented a decrease in α1-3/4/6 fucose linked to GlcNAc residues (AAL and RSL) but not in α1-2 fucose linked to Gal (UEA). PNA and VVL were not tested because IgG had no O-glycosylation site.

4 Discussion

Glycosylation plays a key role in physiology and protein secretion. It is also involved in cell proliferation, apoptosis and differentiation (47). Surface glycans change their structure and complexity during the maturation and differentiation of B lymphocytes. We observed this phenomenon in our tonsillar and peripheral blood B cells. In summary, normal B cell differentiation and maturation are accompanied by a decrease in N-glycan complexity, sialic acid and fucose but an increase in T and Tn O-glycans. Specifically, two types of cells are mostly impacted by these modifications: Bm3/4 in tonsils and PB in tonsils and PBMCs. Giovannone et al. (2018) revealed that Bm3/4 in tonsils (GC B cells) express more T and Tn antigens to acquire specific functions such as antigen receptor signalling (48, 49). In the case of PB, the production of antibodies is accompanied by a decrease in complex N-glycans, an increase in T antigens and an increase in α2-3 sialic acid expression (48, 49). In the case of PB, the production of antibodies is accompanied by a decrease in complex N-glycans, an increase in T antigens and an increase in α2-3 sialic acid expression (48). Antigen receptors are essential for B cells, and they are post-translationally modified with N-glycan and O-glycan chains during the maturation process of these cells (50). These modifications change the receptor trafficking, interactions with their cell surface markers, and interactions with the glycoproteins from other cell types. They can also alter the transduced signals from the BCR to the cells directly or indirectly by perturbing the activity of inhibitory proteins such

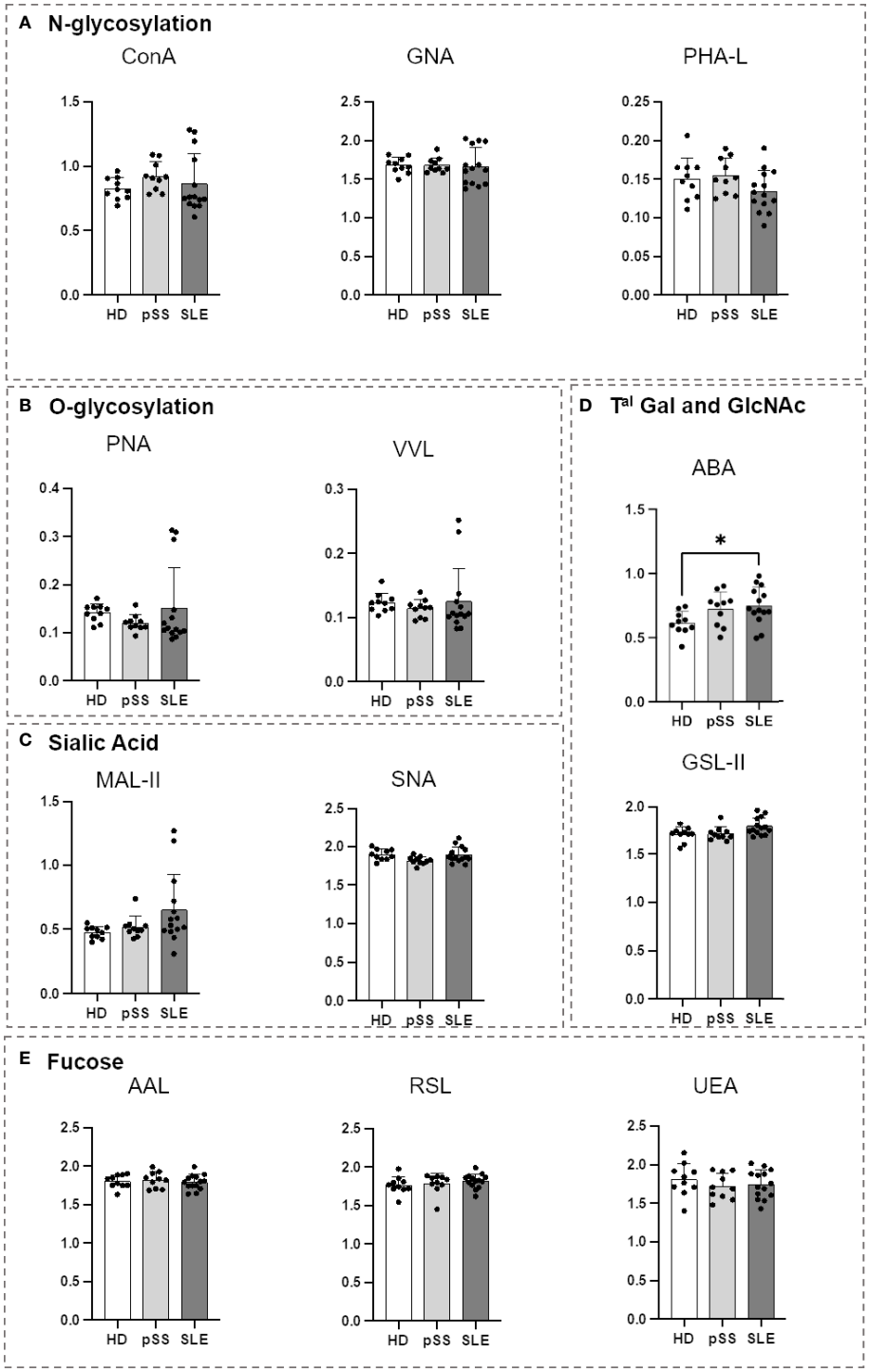

FIGURE 6
Comparison of serum protein N- and O-glycosylation from systemic lupus erythematosus (SLE), primary Sjögren's syndrome (pSS) and healthy donors (HD). First, the serum protein concentration from healthy donors (HD), primary Sjögren's syndrome (pSS) and systemic lupus erythematosus (SLE) patients (10 for each) was quantified using the bicinchoninic acid assay test. The equivalent of 7 µg of serum protein was used from each patient, diluted in PBS and coated in MaxiSorp 96-well Nunc plates for 2 h at room temperature (RT). After 5 washes with PBS supplemented with 0,05% Tween 20, biotinylated lectins (Table 2) were added at optimized concentration for 1 h at RT. After 5 wash steps streptavidin-Horse Radish Peroxydase (HRP) was added for 30 min at RT. After 5 wash steps, Tetramethylbenzidine (TMB) was added was added for 8 min and the reaction was stopped with sulfuric acid. The optical density (OD) at 450 nm was determined for each lectin. Results are presented as followed: N-glycosylation in **(A)**, O-glycosylation in **(B)**, Sialylation in **(C)**, Terminal (T^{al}) Gal and GlcNAc on N and O-glycosylation in **(D)**, Fucosylation in **(E)**. One-way anova test followed by Dunn's multiple comparison test were performed. ns, not significant $p > 0,05$, stars are indicated when $p < 0,05$ (*).

10.3389/fimmu.2022.975963

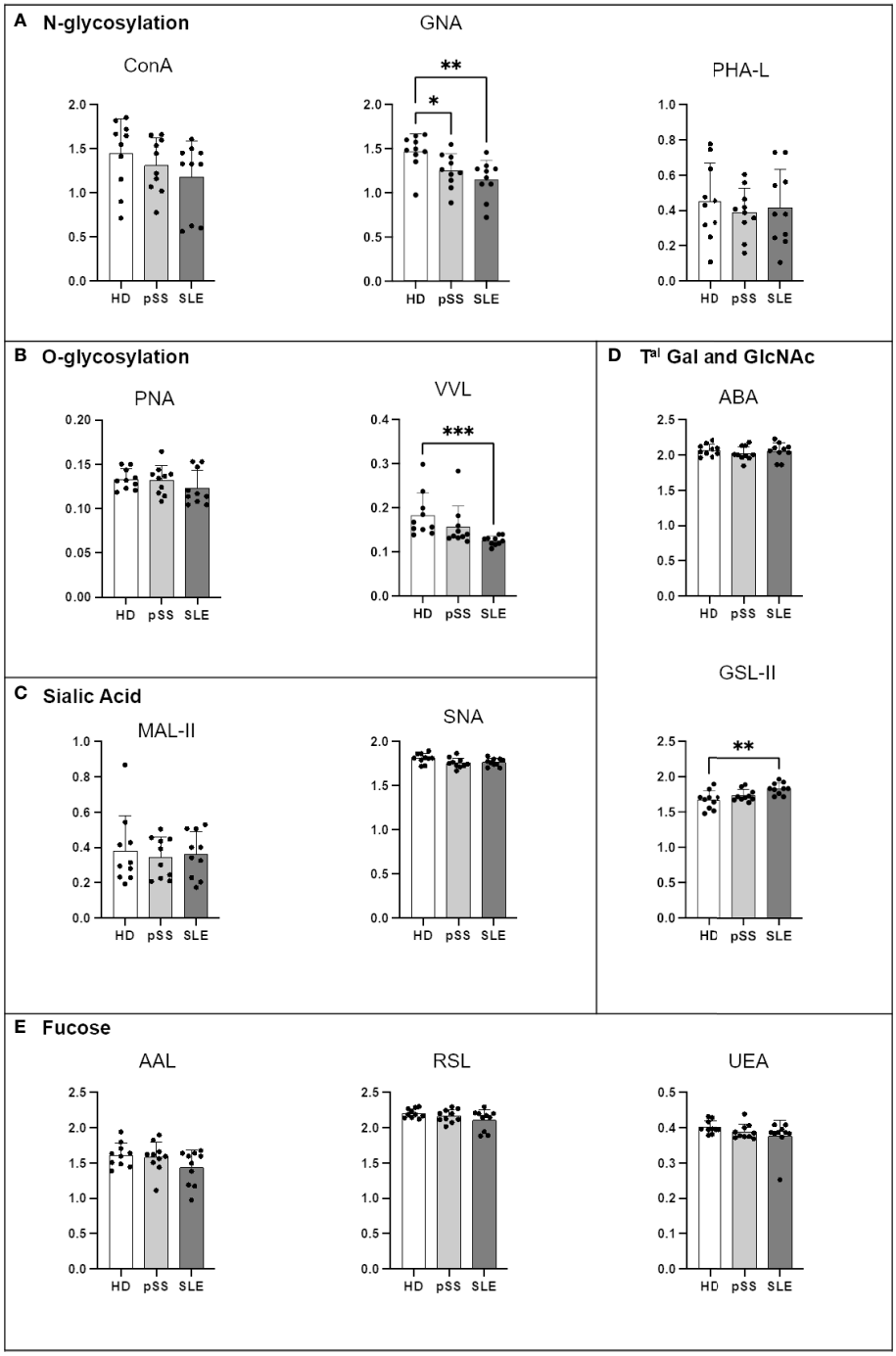

FIGURE 7
Comparison of IgA1 N- and O-glycosylation from systemic lupus erythematosus (SLE), primary Sjögren's syndrome (pSS) and healthy donors (HD). Mouse anti-Human IgA1 (RM124 clone) was coated at 0.5 µg/mL in MaxiSorp 96-well plates overnight at 4°C. A PBS solution containing 2% of Bovine Serum Albumin (BSA) or Carbohydrate-Free Blocking Solution were used for saturation depending on the lectins. This information is described in Table 4. After saturation, an oxidation was performed, to cleave terminal glycans present on anti-Ig and saturating buffer, with a solution of sodium periodate at the final concentration of 0,0 5M in 0,05 M pH=4 citrate buffer. Serum from healthy donors (HD), primary Sjögren's syndrome (pSS) and SLE diluted to 1/100e were added for 1 h at 37°C. After 5 wash steps with PBS 0,05% Tween20, the biotinylated lectins described in Table 2 were added for 1 h. Plate was washed 5 times and streptavidin-Horse Radish Peroxydase (HRP) was added for 30 min at for 2 h at room temperature (RT). After 5 wash steps, a colored reaction using tetramethylbenzidine was performed and stopped with sulfuric acid. The optical density (OD) at 450 nm was determined. Results are presented as followed: N-glycosylation in **(A)**, O-glycosylation in **(B)**, Sialylation in **(C)**, Terminal (T^{al}) Gal and GlcNAc on N and O-glycosylation in **(D)**, Fucosylation in **(E)**. One-way anova test followed by Dunn's multiple comparison test were performed. ns, not significant p > 0,05, stars are indicated when p< 0,05 (*) < 0,01 (**); < 0,001 (***).

10.3389/fimmu.2022.975963

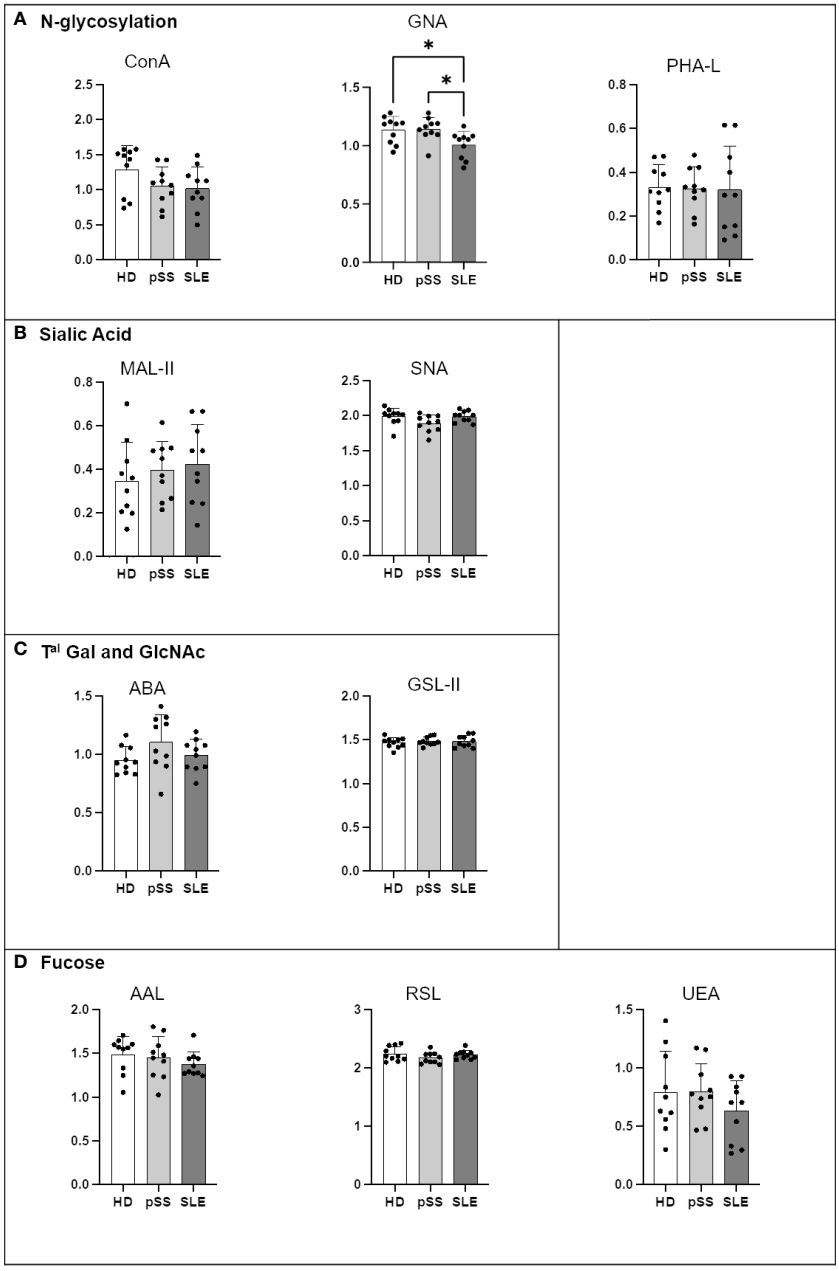

FIGURE 8
Comparison of IgA2 N-glycosylation from systemic lupus erythematosus (SLE), primary Sjögren's syndrome (pSS) and healthy donors (HD). Mouse anti-Human IgA2 (RM125 clone) was coated at 0.5 µg/mL in MaxiSorp 96-well plates overnight at 4°C. A PBS solution containing 2% of BSA or Carbohydrate-Free Blocking Solution were used for saturation depending on the lectins. This information is described in Table 4. After saturation, an oxidation was performed, to cleave terminal glycans present on anti-Ig and saturating buffer, with a solution of sodium periodate at the final concentration of 0,05 M in 0,05 M pH=4 citrate buffer. Serum from healthy donors (HD), pSS and SLE diluted to 1/100e were added for 1 h at 37°C. After 5 wash steps with PBS 0,05% Tween20, the biotinylated lectins described in Table 2 were added for 1 h. Plate was washed 5 times and streptavidin-HRP was added for 30 min at RT. After 5 wash steps, a colored reaction using tetramethylbenzidine was performed and stopped with sulfuric acid. The optical density (OD) at 450 nm was determined. Results are presented as followed: N-glycosylation in **(A)**, Sialylation in **(B)**, Terminal (Tal) Gal and GlcNAc on N and O-glycosylation in **(C)**, and Fucosylation in **(D)**. One-way anova test followed by Dunn's multiple comparison test were performed. ns: not significant p > 0,05, stars are indicated when p< 0,05 (*).

10.3389/fimmu.2022.975963

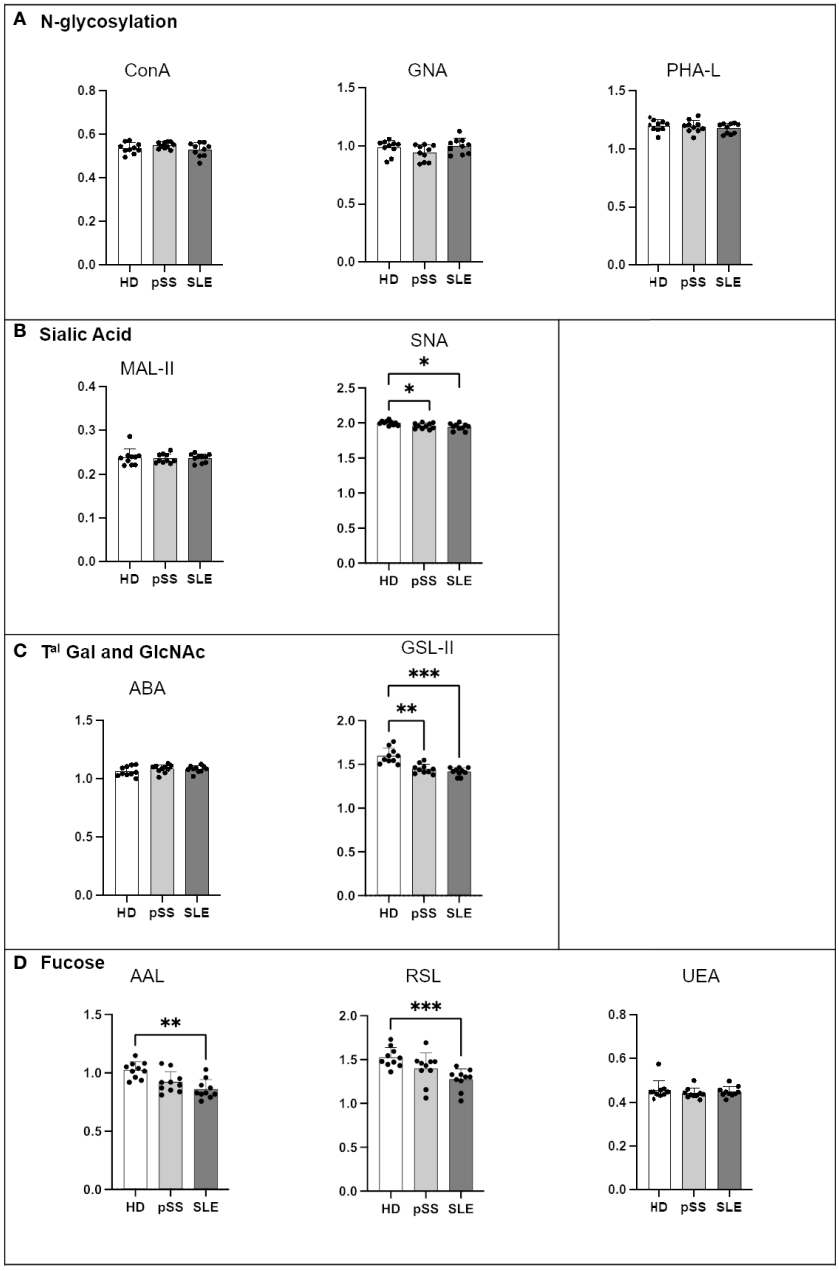

FIGURE 9
Comparison of IgG N-glycosylation from systemic lupus erythematosus (SLE), primary Sjögren's syndrome (pSS) and healthy donors (HD). Mouse anti-Human IgG (4A10 clone) was coated at 0.5 µg/mL in MaxiSorp 96-well plates overnight at 4°C. A PBS solution containing 2% of BSA or Carbohydrate-Free Blocking Solution were used for saturation depending on the lectins. This information is described in Table 4. After saturation, an oxidation was performed, to cleave terminal glycans present on anti-Ig and saturating buffer, with a solution of sodium periodate at the final concentration of 0,05 M in 0,0 5M pH=4 citrate buffer. Serum from healthy donors HD, pSS and SLE diluted to 1/100e were added for 1h at 37°C. After 5 wash steps with PBS 0,0 5% Tween20, the biotinylated lectins described in Table 2 were added for 1h. Plate was washed 5 times and streptavidin-HRP was added for 30 min at RT. After 5 wash steps, a colored reaction using tetramethylbenzidine was performed and stopped with sulfuric acid. The optical density (OD) at 450 nm was determined. Results are presented as followed: N-glycosylation in **(A)**, Sialylation in **(B)**, Terminal (Tal) Gal and GlcNAc on N and O-glycosylation in **(C)**, and Fucosylation in **(D)**. One-way anova test followed by Dunn's multiple comparison test were performed. ns: not significant p > 0,05, stars are indicated when p< 0,05 (*); < 0,01 (**); < 0,001 (***).

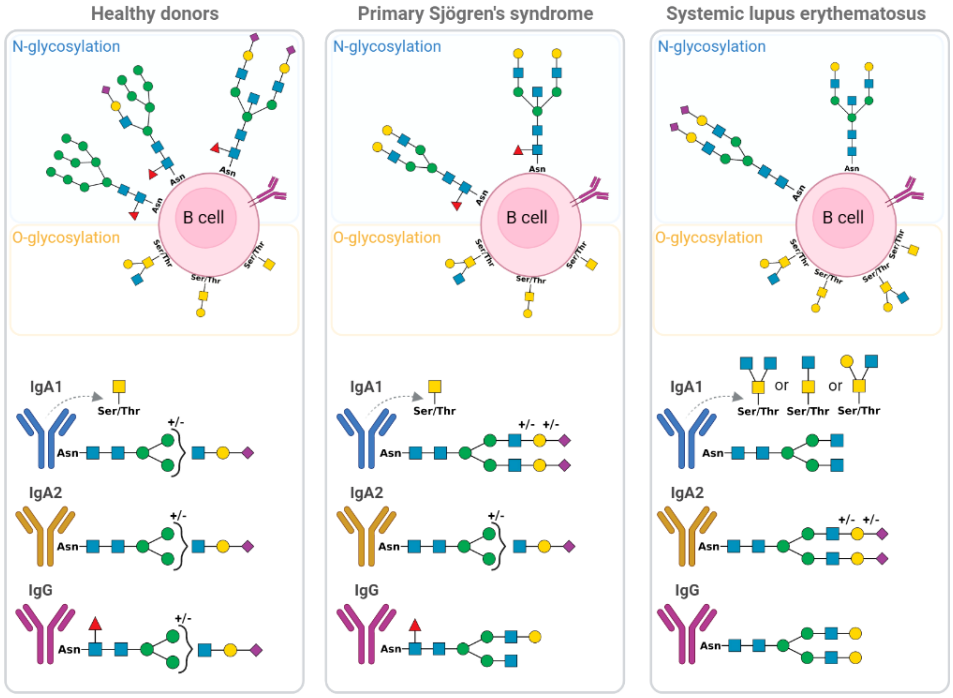

FIGURE 10
Schematic representation of glycosylation alteration of B cell and immunoglobulins IgA1, IgA2 and IgG from primary Sjögren's syndrome (pSS) patients and systemic lupus erythematosus (SLE) patients compared to healthy donors (HD). The different forms of N and O-glycosylation on B cell surface are presented as well as IgA1, IgA2 and IgG glycan. Green circle: Mannose; yellow circle: Galactose; yellow square: N-acetylgalactosamine; blue square: N-acetylglucosamine; purple diamond; Sialic acid and red triangle; Fucose. Asn, Asparagine; Thr, Threonine; Ser, Serine.

as CD22 (51, 52). All these findings demonstrate the importance of glycosylation in controlling B cell behaviour.

Deciphering any changes in the global glycoprofile of B cells and their subsets in SLE and pSS diseases could aid in understanding the loss of self-tolerance and the physiopathology of these two AIDs. As described in Figure 10, B cells from AIDs undergo abnormal glycosylation. Both pSS and SLE exhibit increased N-glycan complexity during the early stages of differentiation. Interestingly, α2-6 sialic acid is absent in pSS B cells and barely present in SLE, whereas α-fucose is reduced only in SLE B cells. In-depth characterisations have revealed that memory B cells are remarkably altered, and these glycosylation changes could explain the positive selection of autoreactive B cells (49, 53), and the increased activation of BCR caused by the absence of CD22 sialic acid ligands (39, 52, 54). In contrast to pSS B cells, SLE B cells exhibit Gal-GlcNAc/Gal-GalNAc terminal patterns, suggesting a lack of terminal glycosylation. All these phenomena could affect BCR signalling and antibody production by B cells in AIDs (21, 55).

Indeed, antibody production is affected by B cells that are altered by glycosylation; immunoglobulins could also be affected. As demonstrated, only IgA1 from SLE had large amounts of core 2 O-glycans, whereas IgA2 had small amounts of Tal mannose. Additionally, both the pSS and SLE patients exhibited hyposialylated IgG with terminal Gal, whereas only the SLE patient exhibited a decrease in core fucose. These alterations could affect the fixation of IgG to the FcγRIIIa receptor and induce the antibody-dependent cell-mediated cytotoxicity (ADCC) phenomenon (56) and C1q recruitment for complement-dependent cytotoxicity (CDC) reactions (57, 58), thereby promoting tissue inflammation. All these results are presented in Figure 10.

It is worth noting that serum proteins, including immunoglobulins, can exhibit aberrant fucosylation and sialylation, which are exclusively found on B cell surface markers. No similar observation was made on T cells from these same patients (data not shown). This finding indicates that there are profound alterations in the biology and functions of B cells in AIDs. These modifications could be due to modified gene expression or mutation, certain epigenetic modifications and transfection factors present at the wrong moment during the B cell differentiation process. As demonstrated by Cao et al., the presence of cytokine in the microenvironment of B cells could regulate intracellular glycosyltransferase and lead to changes in Ig glycans patterns (59). Wang and coworkers observed that plasma cell membrane glycosylation and IgG1 secreted immunoglobulins

glycosylation is affected depending on the activation stimuli of naive B cells (60).

All these modification may be the result of modulated expression of glycosylation-related genes or the modulation of enzymes activity. All these perturbations result in the presence of different immune cells (such as B cells) with a perturbed behaviour. For example, they may carry some receptors with excessive or inefficient affinities for their ligands and/or secrete structurally modified proteins such as antibodies, causing different perturbations in clearance and reactivity to (self)-antigens. All these biological steps can amplify these perturbations mildly or severely, off-setting the immune system homeostasis towards some aggressive inflammation processes. Glycobiology appears to be a more complex science, and significant inquiries at all these levels (glycosylation-enzyme expression and activity for example) are required to understand and manage it. Nevertheless, our simple experimental approaches, such as serum protein glycoprofile analysis, could be used as a biomarker to develop new therapeutic strategies.

Data availability statement

The original contributions presented in the study are included in the article/Supplementary Material. Further inquiries can be directed to the corresponding author.

Ethics statement

The studies involving human participants were reviewed and approved by "CRB Santé de Brest" (BB-0033-00037) and "Centre de référence des maladies auto-immunes rares" Brest, France. Written informed consent to participate in this study was provided by the participants' legal guardian/next of kin.

Author contributions

MM, PP, AB, CB and MD designed the study. MM, PP and AB wrote the first draft of the manuscript and figures. MM, PP and WE performed and analyzed the experiments. VD-P, SJ-J and DC gave access to patient's cohorts. CJ and J-OP participated in the text edition. All authors contributed to the article and approved the submitted version.

Funding

The research leading to these results has received support from the Innovative Medicines Initiative Joint Undertaking under the Grant Agreement Number 115565 (PRECISESADS project), resources of which are composed of financial contribution from the European Union's Seventh Framework Program (FP7/2007–2013) and EFPIA companies' in-kind contribution.

Acknowledgments

The authors would like to acknowledge CRB "Centre de Ressources Biologiques" and CERAINO « Centre de référence des maladies auto-immunes rares », Brest, France, for collection of blood samples from patients, the Hyperion flow core facilities, for their technical help. We thank also Dr Eléonore Betacchioli and Dr Baptiste Chevet for diagnostic cohort's information. We also thank Brest Metropole Oceane for supporting this project.

Conflict of interest

The authors declare that the research was conducted in the absence of any commercial or financial relationships that could be construed as a potential conflict of interest.

Publisher's note

Supplementary material

The Supplementary Material for this article can be found online at: https://www.frontiersin.org/articles/10.3389/fimmu.2022.975963/full#supplementary-material

SUPPLEMENTARY FIGURE 1
Tonsillar mononuclear cells (TMC) and peripheral blood mononuclear cells (PBMC) gating strategies. **(A)** After the doublet removal, within TMC, B cells were identified as expressing CD19: subpopulations were defined as followed based on expression of CD38 and IgD: Bm1 as $CD38^{-}IgD^{+}$, Bm2 as $CD38^{+}IgD^{+}$, Bm2' as $CD38^{++}IgD^{+}$, Bm3-4 cells as $CD19^{+}CD38^{+}IgD^{-}$, eBm5 as $CD38^{+}IgD^{-}$, Bm5 as $CD38^{-}IgD^{-}$ and PB as $CD38^{+++}IgD^{-}$. One representative experiment (out of 20) is shown. **(B)** After the doublet removal, within PBMC, B cells were identified as expressing CD19: subpopulations were defined as followed: Plasmablast (PB) as $CD38^{hi}IgD^{-}$, Transitional (TR) B cells as $CD24^{hi}CD38^{hi}$. After excluding TR B cells, we defined double negative (DN) B cells as $CD27^{-}IgD^{-}$, naïve (NA) B cells as $CD27^{-}IgD^{+}$, unswitched memory (UM) B cells as $CD27^{+}IgD^{+}$ and switched memory (SM) B cells as $CD27^{+}IgD^{-}$. One representative experiment (out of 30) is shown.

SUPPLEMENTARY FIGURE 2
Tonsillar B cell maturation process is associated with an important N- and O-glycan remodeling. Freshly isolated tonsillar mononuclear cells were stained with lectins and the specific B cell antibody panel before analysis

using Beckman Coulter Cytoflex S. Fluorescence intensity is expressed as geomean. Results are presented as followed: N-glycosylation in **(A)**, O-glycosylation in **(B)**, Sialylation in **(C)**, Terminal (T^{al}) Gal and GlcNAc on N and O-glycosylation in **(D)**, and Fucosylation in **(E)**. One-way anova test followed by Dunn's multiple comparison test were performed. ns, not significant p > 0,05, stars are indicated when p< 0,05 (*);< 0,01 (**);< 0,001 (***);<0,0001 (****).

SUPPLEMENTARY FIGURE 3

Sexe and Age parameters do not influence B cell glycosylation. Freshly isolated peripheral blood mononuclear cells (PBMC) (10^6) from 30 healthy donors (HD) including 18 Male (M) and 12 Female (F) were stained with lectins at 10 µg/mL for 15 min at 4°C (). After two wash steps, cells were incubated with streptavidin-FITC (5 µg/mL) and an antibody panel () for 15 min at 4°C. After staining and washing in PBS at 4°C, cells were analyzed using Beckman Coulter Cytoflex S. Fluorescence intensity is expressed as geomean. Results are presented as followed: N-glycosylation in **(A)**, O-glycosylation in **(B)**, Sialylation in **(C)**, Terminal (T^{al}) Gal and GlcNAc on N and O-glycosylation in **(D)**, Fucosylation in **(E)**. **(3A)**. Comparison of B cell glycosylation between Male and Female from healthy donor group. Mann-Whitney T test was performed. ns: not significant p > 0,05, stars are indicated when p< 0,05 (*);< 0,01 (**);< 0,001 (***);<0,0001 (****). **(3B)**. Correlation between Male age and B cell glycosylation. Linear regression was performed. ns, not significant p > 0,05 and R^2 > 0.5. **(3C)**. Correlation between Female age and B cell glycosylation. Linear regression was performed. ns, not significant p > 0,05 and R^2 > 0.5.

SUPPLEMENTARY FIGURE 4

Peripheral blood B cell differentiation is associated with a rearrangement of N and O-glycan surface and an increase of Galactose α2-3 N-acetylneuraminic acid residues. Freshly isolated peripheral blood mononuclear cells (PBMC) were stained with lectins the specific B cell antibody panel before analysis using Beckman Coulter Cytoflex S. Fluorescence intensity is expressed as geomean. Results are presented as followed: N-glycosylation in **(A)**, O-glycosylation in **(B)**, Sialylation in **(C)**, Terminal (T^{al}) Gal and GlcNAc on N and O-glycosylation in **(D)**, and Fucosylation in **(E)**. One-way anova test followed by Dunn's multiple comparison test were performed. ns, not significant p > 0,05, stars are indicated when p< 0,05 (*);< 0,01 (**);< 0,001 (***);<0,0001 (****). All the listed annotation stands for; TR, Transitional B cells; NA, Naive B cells; UM, Unswitched-memory B cells; SM, Switched-memory B cells; PB, Plasmablasts and DN, Double negative ($CD27^-IgD^-$) B cells.

SUPPLEMENTARY FIGURE 5

The analysis of B cell subset glycosylation reveals deep alterations in primary Sjögren's syndrome (pSS) and systemic lupus erythematosus (SLE) compared to healthy donors. Freshly isolated peripheral blood mononuclear cells (PBMC) (10^6) from 13 healthy donors (HD), 10 pSS, and 17 SLE patients were stained with lectins at 10 µg/mL for 15 min at 4°C (). After two wash steps, cells were incubated with streptavidin-FITC (5 µg/mL) and an antibody panel () for 15 min at 4°C. After staining and washing in PBS at 4°C, cells were analyzed using Beckman Coulter Cytoflex S. Fluorescence intensity is expressed as geomean. HD, pSS and SLE glycosylation of transitional B cell **(5A)**, naïve B cells **(5B)**, unswitched-memory B cells **(5C)**, switched-memory B cells **(5D)**, plasmablasts **(5E)** and double negative $CD27^-IgD^-$ B cells **(5F)** was analyzed. Results are presented as followed: N-glycosylation in A, O-glycosylation in B, Sialylation in C, Terminal (T^{al}) Gal and GlcNAc and terminal GlcNAc on N and O-glycosylation in D, Fucosylation in E. One-way anova test followed by Dunn's multiple comparison test were performed. ns, not significant p > 0,05, stars are indicated when p< 0,05 (*);< 0,01 (**);< 0,001 (***);<0,0001 (****).

References

1. Hauri HP, Kappeler F, Andersson H, Appenzeller C. ERGIC-53 and traffic in the secretory pathway. *J Cell Sci* (2000) 113(Pt 4):587–96. doi: 10.1242/jcs.113.4.587

2. Lamari FN, Gioldassi XM, Mitropoulou TN, Karamanos NK. Structure analysis of lipoglycans and lipoglycan-derived carbohydrates by capillary electrophoresis and mass spectrometry. *BioMed Chromatogr* (2002) 16:116–26. doi: 10.1002/bmc.149

3. Spiro RG. Glycoproteins. In: *Advances in protein chemistry*. Edited by Anfisen CB, Edsall JT, Richards FM. Elsevier (1973). p. 349–467. doi: 10.1016/S0065-3233(08)60451-9

4. Marshall RD, Neuberger A. Carbohydrates in protein. VIII. the isolation of 2-Acetamido-1-(L-β-aspartamido)-1,2-dideoxy-β-D- glucose from hen's egg albumin *. *Biochemistry* (1964) 3:1596–600. doi: 10.1021/bi00898a036

5. Brockhausen I, Reck F, Kuhns W, Khan S, Matta KL, Meinjohanns E, et al. Substrate specificity and inhibition of UDP-GlcNAc:GlcNAc?1-2Man?1-6R ?1,6-N-acetylglucosaminyltransferase V using synthetic substrate analogues. *Glycoconj J* (1995) 12:371–9. doi: 10.1007/BF00731340

6. Varki A, Cummings RD, Esko JD, Stanley P, Hart GW, Aebi M, et al. *Essentials of glycobiology* (2015). Cold Spring Harbor (NY: Cold Spring Harbor Laboratory Press. Available at: http://www.ncbi.nlm.nih.gov/books/NBK310274/ (Accessed February 25, 2022).

7. Lu J, Gu J. Significance of β-galactoside α2,6 sialyltranferase 1 in cancers. *Molecules* (2015) 20:7509–27. doi: 10.3390/molecules20057509

8. Schultz MJ, Swindall AF, Bellis SL. Regulation of the metastatic cell phenotype by sialylated glycans. *Cancer Metastasis Rev* (2012) 31:501–18. doi: 10.1007/s10555-012-9359-7

9. Büll C, Stoel MA, den Brok MH, Adema GJ. Sialic acids sweeten a tumor's life. *Cancer Res* (2014) 74:3199–204. doi: 10.1158/0008-5472.CAN-14-0728

10. Gao B, Yang F, Chen W, Li R, Hu X, Liang Y, et al. Multidrug resistance affects the prognosis of primary epithelial ovarian cancer. *Oncol Lett* (2019) 18 (4):4262–9. doi: 10.3892/ol.2019.10745

11. Shan M, Yang D, Dou H, Zhang L. Fucosylation in cancer biology and its clinical applications. In: *Progress in molecular biology and translational science*. Edited by Lijuan Zhang. Elsevier (2019). p. 93–119. doi: 10.1016/bs.pmbts.2019.01.002

12. Okumura M, Yamanoi K, Uehara T, Nakayama J. Decreased alpha-1,4-linked *N* -acetylglucosamine glycosylation in biliary tract cancer progression from biliary intraepithelial neoplasia to invasive adenocarcinoma. *Cancer Sci* (2020) 111:4629–35. doi: 10.1111/cas.14677

13. Yamanoi K, Nakayama J. Reduced αGlcNAc glycosylation on gastric gland mucin is a biomarker of malignant potential for gastric cancer, barrett's adenocarcinoma, and pancreatic cancer. *Histochem Cell Biol* (2018) 149:569–75. doi: 10.1007/s00418-018-1667-8

14. Kim Y-S, Yoo H, Ko J. Implication of aberrant glycosylation in cancer and use of lectin for cancer biomarker discovery. *PPL* (2009) 16:499–507. doi: 10.2174/092986609788167798

15. Fayyaz A, Kurien BT, Scofield H. Autoantibodies in sjögren's syndrome. *Rheum Dis Clin North Am* (2016) 42:419–34. doi: 10.1016/j.rdc.2016.03.002

16. Pisetsky DS. Evolving story of autoantibodies in systemic lupus erythematosus. *J Autoimmun* (2020) 110:102356. doi: 10.1016/j.jaut.2019.102356

17. Hewagama A, Richardson B. The genetics and epigenetics of autoimmune diseases. *J Autoimmun* (2009) 33:3–11. doi: 10.1016/j.jaut.2009.03.007

18. Thorne I, Sutcliffe N. Sjögren's syndrome. *Br J Hosp Med (Lond)* (2017) 78:438–42. doi: 10.12968/hmed.2017.78.8.438

19. Christodoulou MI, Kapsogeorgou EK, Moutsopoulos HM. Characteristics of the minor salivary gland infiltrates in sjögren's syndrome. *J Autoimmun* (2010) 34:400–7. doi: 10.1016/j.jaut.2009.10.004

20. Chen W, Yang F, Xu G, Ma J, Lin J. Follicular helper T cells and follicular regulatory T cells in the immunopathology of primary sjögren's syndrome. *J Leukoc Biol* (2021) 109:437–47. doi: 10.1002/JLB.5MR1020-057RR

21. Koelsch KA, Cavett J, Smith K, Moore JS, Lehoux SD, Jia N, et al. Evidence of alternative modes of b cell activation involving acquired fab regions of n-glycosylation in antibody-secreting cells infiltrating the labial salivary glands of patients with sjögren's syndrome. *Arthritis Rheumatol* (2018) 70:1102–13. doi: 10.1002/art.40458

22. Mok CC, Lau CS. Pathogenesis of systemic lupus erythematosus. *J Clin Pathol* (2003) 56:481–90. doi: 10.1136/jcp.56.7.481

23. Katsuyama T, Tsokos GC, Moulton VR. Aberrant T cell signaling and subsets in systemic lupus erythematosus. *Front Immunol* (2018) 9:1088. doi: 10.3389/fimmu.2018.01088

24. Suárez-Fueyo A, Bradley SJ, Klatzmann D, Tsokos GC. T Cells and autoimmune kidney disease. *Nat Rev Nephrol* (2017) 13:329–43. doi: 10.1038/nrneph.2017.34

25. Taher TE, Muhammad HA, Bariller E, Flores-Borja F, Renaudineau Y, Isenberg DA, et al. B-lymphocyte signalling abnormalities and lupus immunopathology. *Int Rev Immunol* (2013) 32:428–44. doi: 10.3109/08830185.2013.788648

26. Yap DYH, Chan TM. B cell abnormalities in systemic lupus erythematosus and lupus nephritis-role in pathogenesis and effect of immunosuppressive treatments. *Int J Mol Sci* (2019) 20:E6231. doi: 10.3390/ijms20246231

27. Lemoine S, Morva A, Youinou P, Jamin C. Human T cells induce their own regulation through activation of b cells. *J Autoimmun* (2011) 36:228–38. doi: 10.1016/j.jaut.2011.01.005

28. Blair PA, Noreña LY, Flores-Borja F, Rawlings DJ, Isenberg DA, Ehrenstein MR, et al. CD19(+)CD24(hi)CD38(hi) b cells exhibit regulatory capacity in healthy individuals but are functionally impaired in systemic lupus erythematosus patients. *Immunity* (2010) 32:129–40. doi: 10.1016/j.immuni.2009.11.009

29. Basset C, Devauchelle V, Durand V, Jamin C, Pennec YL, Youinou P, et al. Glycosylation of immunoglobulin a influences its receptor binding: Glycosylation of IgA. *Scand J Immunol* (1999) 50:572–9. doi: 10.1046/j.1365-3083.1999.00628.x

30. Bordron A, Morel M, Bagacean C, Dueymes M, Pochard P, Harduin-Lepers A, et al. Hyposialylation must be considered to develop future therapies in autoimmune diseases. *IJMS* (2021) 22:3402. doi: 10.3390/ijms22073402

31. Norton P, Comunale MA, Herrera H, Wang M, Romano PR, Mehta A. Development and application of a novel recombinant aleuria aurantia lectin with enhanced core fucose binding for identification of glycoprotein biomarker of hepatocellular carcinoma. *Proteomics* (2016) 16:3126–36. doi: 10.1002/pmic.201600064

32. Kamerling JP, Gerwig GJ. 2.01 - strategies for the structural analysis of carbohydrates. In: H Kamerling, editor. *Comprehensive glycoscience*. Oxford: Elsevier (2007). p. 1–68. doi: 10.1016/B978-044451967-2/00032-5

33. Bojar D, Meche L, Meng G, Eng W, Smith DF, Cummings RD, et al. A useful guide to lectin binding: Machine-learning directed annotation of 57 unique lectin specificities. *ACS Chem Biol* (2022). doi: 10.1021/acschembio.1c00689

34. Nakamura-Tsuruta S, Kominami J, Kuno A, Hirabayashi J. Evidence that agaricus bisporus agglutinin (ABA) has dual sugar-binding specificity. *Biochem Biophys Res Commun* (2006) 347:215–20. doi: 10.1016/j.bbrc.2006.06.073

35. Presant CA, Kornfeld S. Characterization of the cell surface receptor for the agaricus bisporus hemagglutinin. *J Biol Chem* (1972) 247:6937–45. doi: 10.1016/S0021-9258(19)44676-0

36. Maupin KA, Liden D, Haab BB. The fine specificity of mannose-binding and galactose-binding lectins revealed using outlier motif analysis of glycan array data. *Glycobiology* (2012) 22:160–9. doi: 10.1093/glycob/cwr128

37. Nakamura-Tsuruta S, Kominami J, Kamei M, Koyama Y, Suzuki T, Isemura M, et al. Comparative analysis by frontal affinity chromatography of oligosaccharide specificity of GlcNAc-binding lectins, griffonia simplicifolia lectin-II (GSL-II) and boletopsis leucomelas lectin (BLL). *J Biochem* (2006) 140:285–91. doi: 10.1093/jb/mvj148

38. Knibbs RN, Goldstein IJ, Ratcliffe RM, Shibuya N. Characterization of the carbohydrate binding specificity of the leukoagglutinating lectin from maackia amurensis. comparison with other sialic acid-specific lectins. *J Biol Chem* (1991) 266:83–8. doi: 10.1016/S0021-9258(18)52504-4

39. Schauer R, Kamerling JP. Exploration of the sialic acid world. *Adv Carbohydr Chem Biochem* (2018) 75:1–213. doi: 10.1016/bs.accb.2018.09.001

40. Gerfen CR, Sawchenko PE. An anterograde neuroanatomical tracing method that shows the detailed morphology of neurons, their axons and terminals: Immunohistochemical localization of an axonally transported plant lectin, phaseolus vulgaris- leucoagglutinin (PHA-l). *Brain Res* (1984) 290:219–38. doi: 10.1016/0006-8993(84)90940-5

41. Molin K, Fredman P, Svennerholm L. Binding specificities of the lectins PNA, WGA and UEA I to polyvinylchloride-adsorbed glycosphingolipids. *FEBS Lett* (1986) 205:51–5. doi: 10.1016/0014-5793(86)80864-X

42. Kostlánová N, Mitchell EP, Lortat-Jacob H, Oscarson S, Lahmann M, Gilboa-Garber N, et al. The fucose-binding lectin from ralstonia solanacearum: A NEW TYPE OF β-PROPELLER ARCHITECTURE FORMED BY OLIGOMERIZATION AND INTERACTING WITH FUCOSIDE, FUCOSYLLACTOSE, AND PLANT XYLOGLUCAN *. *J Biol Chem* (2005) 280:27839–49. doi: 10.1074/jbc.M505184200

43. Fouquaert E, Smith DF, Peumans WJ, Proost P, Balzarini J, Savvides SN, et al. Related lectins from snowdrop and maize differ in their carbohydrate-binding specificity. *Biochem Biophys Res Commun* (2009) 380:260–5. doi: 10.1016/j.bbrc.2009.01.048

44. Bohnhorst JØ, Bjørgan MB, Thoen JE, Natvig JB, Thompson KM. Bm1–Bm5 classification of peripheral blood b cells reveals circulating germinal center founder cells in healthy individuals and disturbance in the b cell subpopulations in patients with primary sjögren's syndrome. *J Immunol* (2001) 167:3610–8. doi: 10.4049/jimmunol.167.7.3610

45. Klein U, Rajewsky K, Küppers R. Human immunoglobulin (Ig)M+IgD+ peripheral blood b cells expressing the CD27 cell surface antigen carry somatically mutated variable region genes: CD27 as a general marker for somatically mutated (memory) b cells. *J Exp Med* (1998) 188:1679–89. doi: 10.1084/jem.188.9.1679

46. Ehrhardt GRA, Hsu JT, Gartland L, Leu C-M, Zhang S, Davis RS, et al. Expression of the immunoregulatory molecule FcRH4 defines a distinctive tissue-based population of memory b cells. *J Exp Med* (2005) 202:783–91. doi: 10.1084/jem.20050879

47. Marth JD, Grewal PK. Mammalian glycosylation in immunity. *Nat Rev Immunol* (2008) 8:874–87. doi: 10.1038/nri2417

48. Giovannone N, Antonopoulos A, Liang J, Geddes Sweeney J, Kudelka MR, King SL, et al. Human b cell differentiation is characterized by progressive remodeling of O-linked glycans. *Front Immunol* (2018) 9:2857. doi: 10.3389/fimmu.2018.02857

49. Giovannone N, Liang J, Antonopoulos A, Geddes Sweeney J, King SL, Pochebit SM, et al. Galectin-9 suppresses b cell receptor signaling and is regulated by I-branching of n-glycans. *Nat Commun* (2018) 9:3287. doi: 10.1038/s41467-018-05770-9

50. Ubelhart R, Bach MP, Eschbach C, Wossning T, Reth M, Jumaa H. N-linked glycosylation selectively regulates autonomous precursor BCR function. *Nat Immunol* (2010) 11:759–65. doi: 10.1038/ni.1903

51. Tedder TF, Tuscano J, Sato S, Kehrl JH. CD22, a b lymphocyte-specific adhesion molecule that regulates antigen receptor signaling. *Annu Rev Immunol* (1997) 15:481–504. doi: 10.1146/annurev.immunol.15.1.481

52. Enterina JR, Sarkar S, Streith L, Jung J, Arlian BM, Meyer SJ, et al. Coordinated changes in glycosylation regulate the germinal center through CD22. *Cell Rep* (2022) 38:110512. doi: 10.1016/j.celrep.2022.110512

53. Mortales C-L, Lee S-U, Demetriou M. N-glycan branching is required for development of mature b cells. *J Immunol* (2020) 205:630–6. doi: 10.4049/jimmunol.2000101

54. Özgör L, Meyer SJ, Korn M, Terörde K, Nitschke L. Sialic acid ligand binding of CD22 and siglec-G determines distinct b cell functions but is dispensable for b cell tolerance induction. *J Immunol* (2018) 201:2107–16. doi: 10.4049/jimmunol.1800296

55. Chui D, Sellakumar G, Green R, Sutton-Smith M, McQuistan T, Marek K, et al. Genetic remodeling of protein glycosylation *in vivo* induces autoimmune disease. *Proc Natl Acad Sci USA* (2001) 98:1142–7. doi: 10.1073/pnas.98.3.1142

56. Li T, DiLillo DJ, Bournazos S, Giddens JP, Ravetch JV, Wang L-X. Modulating IgG effector function by fc glycan engineering. *Proc Natl Acad Sci* (2017) 114:3485–90. doi: 10.1073/pnas.1702173114

57. Zhang Z, Shah B, Richardson J. Impact of fc n-glycan sialylation on IgG structure. *mAbs* (2019) 11:1381–90. doi: 10.1080/19420862.2019.1655377

58. Quast I, Keller CW, Maurer MA, Giddens JP, Tackenberg B, Wang L-X, et al. Sialylation of IgG fc domain impairs complement-dependent cytotoxicity. *J Clin Invest* (2015) 125:4160–70. doi: 10.1172/JCI82695

59. Cao Y, Song Z, Guo Z, Zhao X, Gong Y, Zhao K, et al. Cytokines in the immune microenvironment change the glycosylation of IgG by regulating intracellular glycosyltransferases. *Front Immunol* (2021) 12:724379. doi: 10.3389/fimmu.2021.724379

60. Wang J, Balog CIA, Stavenhagen K, Koeleman CAM, Scherer HU, Selman MHJ, et al. Fc-glycosylation of IgG1 is modulated by b-cell stimuli. *Mol Cell Proteomics* (2011) 10(5):M110.004655. doi: 10.1074/mcp.M110.004655

frontiers | Frontiers in Immunology

TYPE Hypothesis and Theory
PUBLISHED 21 September 2022
DOI 10.3389/fimmu.2022.887147

OPEN ACCESS

EDITED BY
Rizgar A Mageed,
Queen Mary University of London,
United Kingdom

REVIEWED BY
Loredana Frasca,
National Institute of Health (ISS), Italy
Diptiman Choudhury,
Thapar Institute of Engineering and Technology, India

*CORRESPONDENCE
Jean-Eric Alard
jeaneric.alard@univ-brest.fr

SPECIALTY SECTION
This article was submitted to Inflammation, a section of the journal Frontiers in Immunology

RECEIVED 02 March 2022
ACCEPTED 01 August 2022
PUBLISHED 21 September 2022

CITATION
Lobognon VD and Alard J-E (2022) Could AMPs and B-cells be the missing link in understanding periodontitis? *Front. Immunol.* 13:887147. doi: 10.3389/fimmu.2022.887147

Could AMPs and B-cells be the missing link in understanding periodontitis?

Vanessa Dominique Lobognon[1] and Jean-Eric Alard[1,2]*

[1]B lymphocytes, Autoimmunity and Immunotherapies (LBAI), Mixed Research Unit (UMR)1227 INSERM, University of Brest, Brest, France, [2]Service d'Odontologie, University Hospital (CHU) de Brest, Brest, France

Periodontal diseases are common inflammatory conditions characterized by bone loss in response to simultaneous bacterial aggression and host defenses. The etiology of such diseases is still not completely understood, however. It has been shown that specific pathogens involved in the build-up of dysbiotic biofilms participate actively in the establishment of periodontitis. This multifactorial pathology also depends on environmental factors and host characteristics, especially defenses. The immune response to the pathogens seems to be critical in preventing the disease from starting but also contributes to tissue damage. It is known that small molecules known as antimicrobial peptides (AMPs) are key actors in the innate immune response. They not only target microbes, but also act as immuno-modulators. They can help to recruit or activate cells such as neutrophils, monocytes, dendritic cells, or lymphocytes. AMPs have already been described in the periodontium, and their expression seems to be connected to disease activity. Alpha and beta defensins and LL37 are the AMPs most frequently linked to periodontitis. Additionally, leukocyte infiltrates, especially B-cells, have also been linked to the severity of periodontitis. Indeed, the particular subpopulations of B-cells in these infiltrates have been linked to inflammation and bone resorption. A link between B-cells and AMP could be relevant to understanding B-cells' action. Some AMP receptors, such as chemokines receptors, toll-like receptors, or purinergic receptors, have been shown to be expressed by B-cells. Consequently, the action of AMPs on B—cell subpopulations could participate to B-cell recruitment, their differentiation, and their implication in both periodontal defense and destruction.

KEYWORDS

B cell, anti-microbial peptides, periodontal diseases, periodontitis, immunomodulation

Introduction

Periodontal diseases are inflammatory conditions with an infectious etiology that can involve various pathogens such as *Aggregatibacter actinomycetemcomitans*, *Fusobacterium nucleatum*, *Porphyromonas gingivalis*, *Prevotella intermedia*, *Treponema denticola*, and *Treponema forsythia* (1). Periodontal diseases are the most common oral

diseases in the world, with the moderate form affecting 45–50% of adults and the severe form 9–11% (2, 3). They can be divided into two main types: gingivitis and periodontitis. Periodontitis are chronic, multifactorial, immuno-inflammatory diseases associated with dysbiotic bacterial biofilms. They are characterized by the progressive destruction of the supporting apparatus of the teeth, often leading to tooth loss and finally to bone resorption (4, 5). The appearance and evolution of these diseases are dependent not only on the pathogenicity of periodonto-pathogenic bacteria, but also on genetics and environmental and behavioral risk factors that affect host susceptibility (1). In addition to being a worldwide public health concern, these diseases provide a strategic model to study inflammatory processes. The oral localization of the periodontium provides access for both clinical assessment and tissue biopsy, facilitating longitudinal studies. Furthermore, the mouth is the first place for most interactions between the self and non-self and is involved in immune system training from birth with probable heritability of microbiota (6). Any advances in the understanding of periodontal disease etiopathogenesis could improve the overall knowledge of chronic inflammation and some systemic conditions such as cardio-metabolic, neurodegenerative, and autoimmune diseases and cancer (1).

In the oral cavity, when facing periodontal pathogens, the innate and adaptive immune systems cooperate to combat this bacterial attack (7). One mechanism of the innate immune system to fight oral infections is the release of antimicrobial peptides (AMPs) (8–10). This appellation gathers small molecules (between 10 and 60 amino acids) expressed in animals with, most of the time, cationic properties (11). Produced by many cells, including neutrophils, macrophages, dendritic cells, and even lymphocytes, AMPs play an important role in innate immunity due to their rapid and broad-spectrum antimicrobial activity (12–15). These molecules are capable of neutralizing a large number of pathogenic microorganisms, including bacteria, fungi, parasites, and viruses (16–18). They have also been shown to perform various biological activities within the innate and adaptive immune systems (18–23). They can induce both chemoattraction and/or cell activation, and they also play a role in inflammation resolution (20). Their known targets are mainly neutrophils, monocytes, dendritic cells, and, to a lesser extent, T cells (24). They can also work in synergy with the cell mediator's cytokine and chemokine, as has been shown for HNP1and RANTES (25) or IL1β (26).

AMPs have also been suggested to potentiate the innate immune response and function as a bridge between innate and adaptive immunity by regulating B and T lymphocytes and natural killer cells (27–29). Indeed, an increasing number of studies have been conducted on the action of AMPs in the regulation of T-cells (30, 31) mainly with TH17 response linked to cathelicidins, but few have explored B-cells, more precisely plasma cells (32). Until recently, the immunomodulatory functions of AMPs have been poorly studied for periodontitis, as most of the approaches were focused on their antimicrobial roles. The first therapeutical approach to these diseases was to target pathogenic bacteria, and AMPs are promising candidates for this purpose (33). However, managing the host reaction seems to be crucial to reach a potential curative strategy, as the appearance of the disease cannot be reduced to only a bacterial presence (34). Furthermore, AMPs are in the frontier between these two strategies, as they can act on both bacteria and leucocytes. Recent research on the immune response during periodontitis has underlined the role of B-cells in both defense mechanisms and bone resorption (35). Few connections, however, have been reported between B-cells and AMPs. This blind spot could be a critical handicap in the understanding of periodontal disease etiology and, more widely, chronic inflammatory diseases. The objective of this review is to answer to the pertinence of studying AMP action of B-cells. In this purpose, it is first needed to sum up which peptides are relevant in periodontal disease, what impact B-cells have on periodontitis, and if they can be a target for AMP. Peptides sharing both a role in periodontitis and a potential receptor on B-cells would be promising candidates for further analysis.

Functions of antimicrobial peptides in periodontal diseases

Oral infections are first managed by the innate immune system, especially with AMPs. Salivary gland epithelial cells, neutrophils, monocytes, and potentially other cells secrete these AMPs in the oral cavity. Their antimicrobial activity against oral pathogenic bacteria and their biofilms plays a central role in oral microbiota homeostasis (33). Three major families of AMP are found in saliva: defensins, cathelicidins, and histatins (34, 36). AMPs are primarily known for their antibacterial activity (elimination or inhibition of the growth of these microorganisms). In addition, they show antifungal and/or antiviral effects against a large number of other microorganisms (37, 38) and even exhibit antitumoral properties (39). Theses lytic activities are linked to AMPs' capacity to create pores in their targets.

Independently of their antimicrobial activities, AMPs may play a role in the inflammatory response and the immune response, even serving as a link between the innate and adaptive immune responses (35). Their antimicrobial effect and their role in the regulation of immune responses are two aspects of particular interest in relation to periodontal disease. Natural AMPs have shown antibacterial effects against periodontal pathogens. Healthy subjects show distinct levels of natural AMPs compared to those with periodontitis (40), with most studies reporting higher levels of LL37, beta defensins, or HNP1, although the result remains heterogeneous between studies. The most studied AMPs in

relation to the periodontal state are LL-37 and alpha and beta defensins (41).

In the literature, several roles have been reported for AMPs in periodontal disease, such as inhibiting the growth of pathogenic bacteria (LL37, HBD-1, HBD-2, HBD-3, histatin-2, HNP1, HNP2, HNP3), promoting periodontal tissue healing (LL37, HBD-1, HBD-2, HBD-3, histatin-2), promoting bone healing (HBD-2, histatin-1), and serving as a potential indicator of the severity of periodontal disease (HBD-2, HNP1, HNP2, HNP3). Additionally, AMPs have been reported to promote osteogenic differentiation and reduce bone loss (42). Histatin-5 has been shown to be an inhibitor of host and bacterial enzymes involved in periodontal destruction (43). Among natural AMPs, HBD are expressed in the buccal bone (44). HBD have been shown to promote the proliferation of human mesenchymal stem cells, osteoblasts, and keratinocytes in cultures (45). In addition, HBD and histatin-1 promote bone regeneration and prevent infection (46–48).

All these findings suggest that the AMPs relevant to the management of periodontal diseases could be LL-37, alpha and beta defensins, and histatins. In contexts other than the oral cavity immunity, these AMPs have all been described as immune modulators. Alpha defensins have been shown to inhibit monocyte/macrophage-produced pro-inflammatory cytokines such as IL6 and IL1β and to increase leucocyte recruitment directly or indirectly. Beta defensins can either be decreased or increased (49). Similar chemoattraction has been reported for beta defensins and LL37 with additional impact on immune cells' signaling pathways (49). LL37 is strongly connected to neutrophil extracellular traps (NETs): DNA strands, released by dying neutrophils, that are covered by multiple proteins and peptides that play critical roles during both inflammation and microbial neutralization (50). These NETs activate BAFF production, which is a major B-cell activator (50). This activation could be critical, as neutrophils are strongly connected to periodontal diseases, and B-cells have been shown to be effectors of a part of periodontitis pathogenesis.

Functions of B-cells in periodontal diseases

The ontogenesis of B-cells takes place in the bone marrow from pluripotent hematopoietic stem cells (51). The latter form lymphocyte progenitors, some of which migrate to the thymus for the formation of T cells, while the rest remain in the bone marrow to form B-cells until the immature B stage. During antigen-independent maturation in the marrow, there are four distinct stages: the early pro-B cell, the late pro-B cell, the pre-B cell (precursor B), and the immature B cell. Immature B-cells then migrate to secondary lymphocyte organs (spleen, lymph nodes, tonsils, and lymphoid tissues associated with mucous membranes) in the form of transitional B-cells (52). These transitional B-cells transform into either marginal zone cells or follicular cells. All of these cells undergo a succession of T-independent or T-dependent differentiation, leading to the formation of memory cells or plasma cells (52).

Few studies have highlighted the roles of B-cells in periodontitis. Certain roles of B-cells in periodontitis have been recently discovered, however. A review of the literature showed the role of B-cells in periodontitis and the potential interest in using B-cells as a target for new treatments for severe periodontitis (53). Additionally, a study carried out by Demoersman highlighted the crucial role of B-cells in periodontal disease with an increase of memory B-cells and a reduction of their regulatory counterpart in severe forms (54). It has also been shown that anti-B lymphocyte therapy could be beneficial in improving periodontitis, suggesting a major role of B-cells in this disease (55). The 2015 study by Abe et al. 2015 suggests that B-cells have a more important role than T cells in bone resorption (56). It has been reported that, in periodontitis, the presence of B-cells specific to periodontal pathogenic bacteria is essential for the establishment of the bone resorption characteristic of periodontitis (57). Some authors have also suggested an involvement of B-cells in bone remodeling (58–60).

Bacterial infection remains important in the etiopathogenesis of periodontal disease. An immuno-inflammatory response is set up by the body against this bacterial infection. This reaction is the origin of the destruction of supporting tissues of the tooth, loss of attachment, and alveolar bone lysis. Inflammation-induced osteoclast genesis in periodontal disease involves several pathways of mechanisms that involve several biological molecules and their products. Cells of the B lymphoid lineage can contribute to the physiopathology of bone disorders by regulating osteoclast genesis in the context of periodontal infection through several pathways of mechanisms. The molecular mechanism pathways by which cells of the B lymphoid lineage regulate osteoclast genesis in periodontal disease have become better understood in recent years. As well as their antibody secretion, B-cells contribute to the destruction of the alveolar bone in RANKL-dependent periodontitis (61). B-cells express RANKL, a protein involved in osteoclast differentiation, activation, and survival. RANKL then binds to its RANK receptor expressed by osteoclast precursor cells and preosteoclasts to stimulate their differentiation into osteoclasts resorbing alveolar bone (59, 62–65). In periodontitis, the main source of RANKL are T-cells and B-cells (66), either of which themselves serve as progenitors of osteoclasts. Normal pro-B-cells may serve as osteoclast progenitor cells (67).

B-cells express SOFAT, an osteoclastogenic cytokine independent of RANKL. By stimulating osteoblasts, SOFAT modulates the production of osteoclastogenic cytokines and contributes to osteoclast formation and bone destruction in periodontitis. Human B-cells, plasma cells, and T-cells express

SOFAT, which is a bone-destroying factor in periodontal disease lesions (68–70).

Pathogens that breach periodontal tissue express molecular patterns associated with pathogenic agents (PAMPs) such as lipopolysaccharides, lipoteichoic acid, peptidoglycan, bacterial DNA, and double-stranded RNA (71, 72). These PAMPs can be recognized by receptors such as Toll-like receptors (TLR) expressed on immune cells: macrophages, Langerhans cells, dendritic cells, and polymorphonuclear neutrophils. They can also be recognized by epithelial cells, gingival fibroblasts, fibroblasts of the periodontal ligament, osteoblasts, osteoclasts endothelial cells, and even lymphocytes (73, 74). The interaction between macrophages, dendritic cells, neutrophils, and PAMPs *via* TLRs leads to the production of pro-inflammatory cytokines and chemokines such as TNF-α, IL-1, IL-6 (CXCL-8: IL-8), IL-12, and IL-18. It should be noted, however, that dendritic cells act as antigen-presenting cells for B and T cells (19, 75–77). Neutrophils are one of the first inflammatory cells to arrive at the site of periodontal inflammation by chemotaxis (78), following chemoattractant such as IL-8 secreted by oral epithelial cells, connective fibroblasts, and immune cells (79) and growth-related gene product-α (80). Neutrophils contain cytoplasmic granules that in turn contain lytic enzymes and molecules with antimicrobial properties such as cathepsins, lactoferrin, lysozyme, and defensins, which destroy microorganisms (81).

Defensins are AMPs known for their antibacterial activity (elimination or total inhibition of the growth of these microorganisms), and several roles have been attributed to them in relation to periodontal diseases, such as inhibiting the growth of pathogenic bacteria, promoting the healing of periodontal tissues, promoting bone healing, and serving as a potential indicator of the severity of periodontal disease (42). TNF-α, IL-1, and IL-6 are osteotropic cytokines that stimulate osteoclast resorption in periodontitis (82) and are found in higher concentrations in patients with periodontal disease than in healthy individuals (83).

Cells of the B lymphoid lineage can participate in osteoclast genesis through two main pathways (Figure 1):

1. The B-cells express RANKL, the main factor involved in the differentiation, activation, and survival of osteoclasts. TNF-α secreted by macrophages and dendritic cells can stimulate osteoblasts, T cells, and B-cells to produce RANKL. In addition, periodontal ligament fibroblasts and gingival fibroblasts can regulate osteoclast activity by secreting RANKL (58, 84).

2. The B-cells express SOFAT, which is a bone-destroying factor in periodontal disease lesions (70), independent of

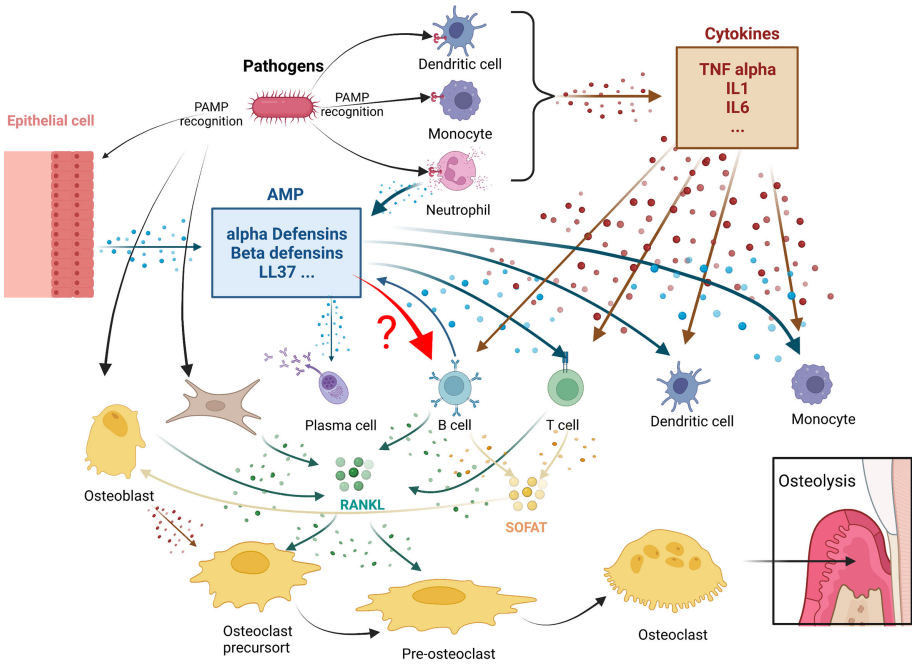

FIGURE 1
Antimicrobial peptides immunomodulation in periodontitis osteolysis: potential connections with leukocytes. In periodontitis, pathogens triggers both cytokines (in brown) or antimicrobial peptides (AMPS) (in blue) production. Both mediator's categories are known to play roles in leukocytes actions. A crucial step in these diseases is the expression of RANKL and SOFAT. B and T cells, which are the main source of RANKL and SOFAT, are central in this orchestration of osteoclast differentiation and activity leading to osteolysis. The effect of AMPs in B in this environment still remain to be determined.

RANKL. By co-opting osteoblasts to increase production of osteoclastogenic cytokines, SOFAT can exacerbate inflammation and promote osteoclast formation and bone destruction (68).

In all these interactions that occur during periodontal disease, however, it is not known whether there is a direct relation between AMPs and B-cells.

Can antimicrobial peptides affect the function of B-cells in periodontal diseases?

Most of the effects of AMPs on host cells are mediated *via* the specific activation of various cell surface receptors, membrane channels, or specific intracellular targets and pathways (85, 86). Relations have been established between the LL-37 peptide and at least nine receptors of different classes, including four G-protein-coupled receptors, three receptor tyrosine kinases, a ligand-gated ion channel, and TLRs (87, 88) (Figure 2). Several receptors and pathways involved in the immune functions of human beta defensins have been studied, such as TLRs, receptors of the purinoceptor family, and chemokine receptors (85) (Figure 2). Some receptors have been described for beta defensin, such as CCR6, CCR4, CCR2, TLR1/2/9, and P2X7 (85). However, specific alpha-defensin (HNP) receptors have not yet been clearly identified, only a G-protein-coupled receptor response has been confirmed so far (85). B-cell expression of some of these receptors conditioned their responsiveness to AMPs. Many chemokine receptors regarded as AMP receptors are expressed on T cells but can also be found on human B-cells, such as CXCR4 (89), CXCR5, CXCR3, CCR7, CCR1 (90, 91), CCR2 (92, 93), and CCR6 (94, 95). CCR6 probably plays an important role in B-cell trafficking in humans and is established as an efficient receptor on human B-cells (92). B-cells express several TLRs. TLR1, TLR2, TLR4, TLR5, TLR6, and TLR10 receptors are expressed on the cell membrane, while TLR3, TLR7, TLR8, and TLR9 are expressed in the endosomes. Some of them can identify AMPs such as TLR1, TLR2, and TLR9 (95–100). Their signaling in B-cells is related to the stage of activation and the tissue situation of the B-cells (101). It has also been reported that certain receptors of the purinoceptor family, such as P2X7 and P2Y11, are expressed on B-cells (102, 103).

Furthermore, the literature also mentions that B-cells themselves express AMPs such as alpha defensins (HNP-1–3), HBD-2, and cathelicidin LL-37 in the presence of pathogens such as *Aggregatibacter actinomycetemcomitans* (104, 105). Thus, B-cells can produce some of the AMPs found in periodontal tissue and potentially react to them. For now, however, the only clear link between B-cell lineage and their response to AMPs is the IgG production induced in plasma cells by LL-37 associated with NETs during systemic lupus erythematosus (32). If this IgG production is useful to predict the installation of the disease and participate in host defense.

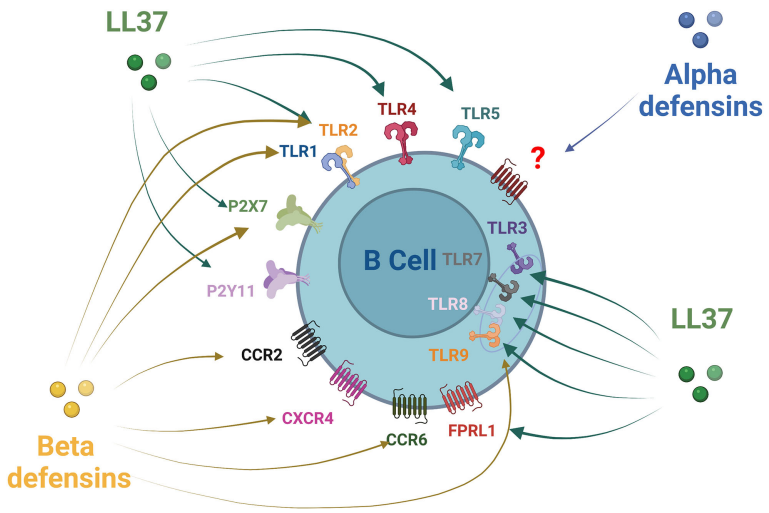

FIGURE 2
Antimicrobial peptides receptors expression on B-cells. Alpha defensin has been shown to recruit B-cells through a non-identified Protein G Coupled Receptor. Beta defensin family receptors are more documented with an action of HBD1 and HBD2 on CCR6 and HBD3 *via* CCR6, CCR2, CXCR4, P2X7, TLR1, TLR2, and TLR9. LL37 act on a larger number of receptors that can be expressed by B-cells: TLRs1-5, TLRs7-9, FPRL1 P2X7, and P2Y11.

initially, no direct connection to osteolysis, the major concern in periodontitis, was described (106). More recently, anti-carbamylated LL37 autoantibodies have been linked to an increase in bone resorption in RA (107). Auto-immunity and periodontitis are connected in many ways. Patients with auto-immune conditions such as Lupus or RA are known to be more prone to developing periodontitis (55, 108). Bone destruction in periodontitis shares similarities with tissue damage observed during RA and presents a TH17 cytokines overexpression that can be also found in RA, Lupus psoriasis, and many other auto-immune conditions (109, 110). In addition, AMPs' participation in autoimmunity has been investigated in the past few years. High concentrations of AMPs have been found in sera of Lupus patients or the joints of RA patients (107, 111, 112). For now, AMPs' immunomodulatory role in autoimmunity is not fully understood, probably due to the difficulty in overcoming AMPs/cytokines/chemokines' roles redundancy combined with dual detrimental and protective effects (113, 114). Regardless, the role of autoantibodies against AMPs can be critical in autoimmunity. LL37/DNA complexes during NETs release can be carbamylated or citrullinated during autoimmune disease, which can be the result of oral cavities pathogens such as PG or AA (115, 116). Modified LL37s can then be recognized by specific autoantibodies leading to the formation of immune complexes that have been described in Lupus, auto-immunes vasculitis, psoriasis, and RA (117–119). The fact that in RA such autoantibodies participate in osteolysis strengthens the idea of the implication of AMP in autoimmunity but also in inflammatory contexts such as periodontitis.

All these elements point to an implication of B-cells by their production of autoantibodies against AMPs in autoimmunity with, in parallel, a potential immunomodulatory action that remains to be investigated. For now, however, no causal relationship has been established between AMPs' immunomodulation and B-cells participation in osteolysis. Presence of autoantibodies against AMPs could be of interest as an actor of osteolysis and potentially as a biomarker in diseases associated with bone self-destruction. As previously mentioned, a large number of AMPs have been identified in the oral cavity, and several exhibit antimicrobial effects against periodontal pathogens. They offer a broad spectrum of roles (antibacterial, antiviral, and/or antifungal or immunomodulation activities) that are critical in periodontal diseases. These characteristics make these natural molecules promising candidates for anti-infection strategies. Moreover, it has been proposed that the differential regulation of AMPs in periodontal disease makes them relevant biomarkers for the disease in saliva and gingival fluid (41). Promising strategies in the treatment of periodontitis can be derived from AMPs in periodontal diseases. They could be considered as a potential alternative to traditional antimicrobial therapy (antibiotics) in periodontal infections (38). Nevertheless, their immunomodulatory action must be better understood to avoid any unwanted effect. In this regard, B-cells' involvement in AMP immunomodulation also needs to be known.

Conclusion

As only sporadic information is available on the effect of AMPs on B-cells, it may be tempting to think that they have no or few connections. However, the B lymphocyte family consists of various subtypes with specific patterns of receptors and functions. Global analysis of lymphocytes tends to be disconnected from functional reality, and the results are unclear due to the heterogeneity and low number of each category of cell. The only way to overcome this limitation is to study each lymphocyte subpopulation. This, however, has not been done for the immunomodulatory action of AMPs on B-cells. Only plasma cells and LL37 have been functionally connected. An in vivo or ex vivo tissue analysis would be convenient to assess this link due to the small B-cell subpopulation. In addition, AMPs have been shown to be critical in both the initiation and the chronicity of inflammation. As AMPs are already known to influence and participate actively in both the initiation and the persistence of inflammation (120), it would be unlikely that they are not involved in periodontitis-related immune system dysregulation. Recent studies on pathogenesis tend to involve more and more B-cells in osteolysis processes. An interaction between B-cells and AMPs could explain the pathogenic action of B-cells. As they can carry some identified AMP receptors, they should react to their presence.

A parallel is frequently made between periodontitis and auto-immune diseases.

In addition, periodontal diseases are chronic inflammatory conditions with changing inflammatory states (1). Longitudinal studies are still rare but may be needed to truly understand the molecular mechanisms. This time-dependent disease activity could explain why studies on AMP presence in periodontitis are frequently contradictory, with AMPs such as LL37 or defensins linked to both protective and pathogenic patterns of the disease. In a similar way, the action of B-cells depends on the result of each subpopulation action found at the same time in tissue. Regulatory B-cells seem decreased or inefficient in situations involving chronic inflammation, which has been confirmed in periodontitis (54). The variability of B-cell subpopulations seems to share some patterns with AMP presence. Elucidation of the relationship between AMPs and B-cells could clarify why the immune system participates in periodontal tissue destruction during its struggle against pathogens, and may clarified whether or not periodontitis can be considered as an autoimmune-like condition. Furthermore, this understanding could open new possibilities for treatments

involving the targeting of B-cells and/or AMPs to optimize the immune response and reduce self-damage.

Data availability statement

The original contributions presented in the study are included in the article/supplementary material. Further inquiries can be directed to the corresponding author.

Author contributions

All authors contributed to the article and approved the submitted version.

Conflict of interest

The authors declare that the research was conducted in the absence of any commercial or financial relationships that could be construed as a potential conflict of interest.

Publisher's note

All claims expressed in this article are solely those of the authors and do not necessarily represent those of their affiliated organizations, or those of the publisher, the editors and the reviewers. Any product that may be evaluated in this article, or claim that may be made by its manufacturer, is not guaranteed or endorsed by the publisher.

References

1. Hajishengallis G, Chavakis T. Local and systemic mechanisms linking periodontal disease and inflammatory comorbidities. *Nat Rev Immunol* (2021) 21(7):426–40. doi: 10.1038/s41577-020-00488-6

2. Nazir MA. Prevalence of periodontal disease, its association with systemic diseases and prevention. *Int J Health Sci* (2017) 11(2):72–80.

3. Chapple IL, Bouchard P, Cagetti MG, Campus G, Carra MC, Cocco F, et al. Interaction of lifestyle, behaviour or systemic diseases with dental caries and periodontal diseases: consensus report of group 2 of the joint EFP/ORCA workshop on the boundaries between caries and periodontal diseases. *J Clin Periodontol* (2017) 44 Suppl 18:S39–51. doi: 10.1111/jcpe.12685

4. Kinane DF, Stathopoulou PG, Papapanou PN. Periodontal diseases. *Nat Rev Dis Primers* (2017) 3(1):1–14. doi: 10.1038/nrdp.2017.38

5. Papapanou PN, Sanz M, Buduneli N, Dietrich T, Feres M, Fine DH, et al. Periodontitis: Consensus report of workgroup 2 of the 2017 world workshop on the classification of periodontal and peri-implant diseases and conditions. *J Periodontology* (2018) 89(S1):S173–S182. doi: 10.1111/jcpe.12946

6. Kaan AMM, Kahharova D, Zaura E. Acquisition and establishment of the oral microbiota. *Periodontol 2000* (2021) 86(1):123–41. doi: 10.1111/prd.12366

7. Wiesner J, Vilcinskas A. Antimicrobial peptides: The ancient arm of the human immune system. *Virulence* (2010) 1(5):440–464. doi: 10.4161/viru.1.5.12983

8. Boman HG. Peptide antibiotics and their role in innate immunity. *Annu Rev Immunol* (1995) 13(1):61–92. doi: 10.1146/annurev.iy.13.040195.000425

9. Pasupuleti M, Schmidtchen A, Malmsten M. Antimicrobial peptides: Key components of the innate immune system. *Crit Rev Biotechnol* (2012) 32(2):143–171. doi: 10.3109/07388551.2011.594423

10. Izadi N, Keikha M, Ghazvini K, Karbalaei M. Oral antimicrobial peptides and new therapeutic strategies for plaque-mediated diseases. *Gene Rep* (2020), 21:100811. doi: 10.1016/j.genrep.2020.100811

11. Lazzaro BP, Zasloff M, Rolff J. Antimicrobial peptides: Application informed by evolution. *Science.* (2020) 368(6490):5480. doi: 10.1126/science.aau5480

12. De la Fuente-Núñez C, Silva ON, Lu TK, Franco OL. Antimicrobial peptides: Role in human disease and potential as immunotherapies. *Pharmacol Ther* (2017) 178:132–140. doi: 10.1016/j.pharmthera.2017.04.002

13. Ganz T. Defensins: Antimicrobial peptides of innate immunity. *Nat Rev Immunol* (2003) 3(9):710–720. doi: 10.1038/nri1180

14. Hoffmann JA, Kafatos FC, Janeway CA, Ezekowitz RAB. Phylogenetic perspectives in innate immunity. *Science* (1999) 284(5418):1313–1318. doi: 10.1126/science.284.5418.1313

15. Wang YJ, Traum D, Schug J, Gao L, Liu CHPAP Consortium, et al. Multiplexed *In situ* imaging mass cytometry analysis of the human endocrine pancreas and immune system in type 1 diabetes. *Cell Metab* (2019) 29:769–783.e4. doi: 10.1016/j.cmet.2019.01.003

16. Mueller SN, Gebhardt T, Carbone FR, Heath WR. Memory T cell subsets, migration patterns, and tissue residence. *Annu Rev Immunol* (2013) 31(1):1377–161. doi: 10.1146/annurev-immunol-032712-095954

17. Rowley DA, Fitch FW. The road to the discovery of dendritic cells, a tribute to Ralph Steinman.*Cell Immunol.* (2012) 273(2): 95–8. doi: 10.1016/j.cellimm.2012.01.002

18. Ohlrich E, Cullinan M, Seymour G. The immunopathogenesis of periodontal disease. *Aust Dental J* (2009) 54:S2–S10. doi: 10.1111/j.1834-7819.2009.01139.x

19. Silva ON, de la Fuente-Núñez C, Haney EF, Fensterseifer ICM, Ribeiro SM, Porto WF, et al. An anti-infective synthetic peptide with dual antimicrobial and immunomodulatory activities. *Sci Rep* (2016) 6(1):17–11. doi: 10.1038/srep35465

20. Choi K-Y, Chow LNY, Mookherjee N. Cationic host defence peptides: Multifaceted role in immune modulation and inflammation. *J Innate Immun* (2012) 4:361–70. doi: 10.1159/000336630

21. Lai Y, Gallo RL. AMPed up immunity: How antimicrobial peptides have multiple roles in immune defense. *Trends Immunol* (2009) 30(3):131–141. doi: 10.1016/j.it.2008.12.003

22. Shin D-M, & Jo E-K. Antimicrobial peptides in innate immunity against mycobacteria. *Immune Network* (2011) 11(5):245. doi: 10.4110/in.2011.11.5.245

23. Steinstraesser L, Kraneburg U, Jacobsen F, & Al-Benna S. Host defense peptides and their antimicrobial-immunomodulatory duality. *Immunobiology* (2011) 216(3):322–333. doi: 10.1016/j.imbio.2010.07.003

24. Zhang QY, Yan ZB, Meng YM, Hong XY, Shao G, Ma JJ, et al. Antimicrobial peptides: mechanism of action, activity and clinical potential. *Mil Med Res* (2021) 8 (1):48. doi: 10.1186/s40779-021-00343-2

25. Alard JE, Ortega-Gomez A, Wichapong K, Bongiovanni D, Horckmans M, Megens RT, et al. Recruitment of classical monocytes can be inhibited by disturbing heteromers of neutrophil HNP1 and platelet CCL5. *Sci Transl Med* (2015) 7 (317):317ra196. doi: 10.1126/scitranslmed.aad5330

26. Yu J, Mookherjee N, Wee K, Bowdish DM, Pistolic J, Li Y, et al. Host defense peptide LL-37, in synergy with inflammatory mediator IL-1beta, augments immune responses by multiple pathways. *J Immunol* (2007) 179(11):7684–91. doi: 10.4049/jimmunol.179.11.7684

27. Allaker RP. Host defence peptides-a bridge between the innate and adaptive immune responses. *Trans R Soc Trop Med Hygiene* (2008) 102(1):3–4. doi: 10.1016/j.trstmh.2007.07.005

28. Kin NW, Chen Y, Stefanov EK, Gallo RL, & Kearney JF. Cathelin-related antimicrobial peptide differentially regulates T-and b-cell function. *Eur J Immunol* (2011) 41(10):3006–3016. doi: 10.1002/eji.201141606

29. Yang D, Chertov O, Bykovskaia SN, Chen Q, Buffo MJ, Shogan J, et al. Beta-defensins: Linking innate and adaptive immunity through dendritic and T cell CCR6. *Science* (1999) 286(5439):525–528. doi: 10.1126/science.286.5439.525

30. Xie GH, Chen QX, Cheng BL, Fang XM. Defensins and sepsis. *BioMed Res Int* (2014) 2014:180109. doi: 10.1155/2014/180109

31. Minns D, Smith KJ, Alessandrini V, Hardisty G, Melrose L, Jackson-Jones L, et al. The neutrophil antimicrobial peptide cathelicidin promotes Th17 differentiation. *Nat Commun* (2021) 12(1):1285. doi: 10.1038/s41467-021-21533-5

32. Gestermann N, Di Domizio J, Lande R, Demaria O, Frasca L, Feldmeyer L, et al. Netting neutrophils activate autoreactive b cells in lupus. *J Immunol* (2018) 200(10):3364–71. doi: 10.4049/jimmunol.1700778

33. da Silva BR, de Freitas VAA, Nascimento-Neto LG, Carneiro VA, Arruda FVS, de Aguiar ASW, et al. Antimicrobial peptide control of pathogenic microorganisms of the oral cavity: A review of the literature. *Peptides* (2012) 36 (2):315–321. doi: 10.1016/j.peptides.2012.05.015

34. De Smet K, Contreras R. Human antimicrobial peptides: Defensins, cathelicidins and histatins. *Biotechnol Lett* (2005) 27(18):1337–1347. doi: 10.1007/s10529-005-0936-5

35. Patrzykat A, Douglas SE. Antimicrobial peptides: Cooperative approaches to protection. *Protein Pept Lett* (2005) 12(1):19–25. doi: 10.2174/0929866053406057

36. Gorr S-U. Antimicrobial peptides of the oral cavity. *Periodontology 2000* (2009) 51(1):152–180. doi: 10.1111/j.1600-0757.2009.00310.x

37. Ageitos JM, Sánchez-Pérez A, Calo-Mata P, Villa TG. Antimicrobial peptides (AMPs): Ancient compounds that represent novel weapons in the fight against bacteria. *Biochem Pharmacol* (2017) 133:117–138. doi: 10.1016/j.bcp.2016.09.018

38. Seo M-D, Won H-S, Kim J-H, Mishig-Ochir T, Lee B-J. Antimicrobial peptides for therapeutic applications: A review. *Molecules* (2012) 17(10):12276–12286. doi: 10.3390/molecules171012276

39. Zhang B, Shi W, Li J, Liao C, Li M, Huang W, et al. Design, synthesis and biological evaluation of novel peptides as potential agents with anti-tumor and multidrug resistance-reversing activities. *Amino Acids* (2017) 49(8):1355–1364. doi: 10.1007/s00726-017-2434-1

40. Gorr S-U. Antimicrobial peptides in periodontal innate defense. *Periodontal Dis* (2012) 15:84–98. doi: 10.1159/000329673

41. Jourdain M-L, Velard F, Pierrard L, Sergheraert J, Gangloff SC, Braux J. Cationic antimicrobial peptides and periodontal physiopathology: A systematic review. *J periodontal Res* (2019) 54(6):589–600. doi: 10.1111/jre.12676

42. Niu JY, Yin IX, Mei ML, Wu WKK, Li Q-L, Chu CH. The multifaceted roles of antimicrobial peptides in oral diseases. *Mol Oral Microbiol* (2021) 36(3):159–71. doi: 10.1111/omi.12333

43. Gusman H, Travis J, Helmerhorst EJ, Potempa J, Troxler RF, Oppenheim FG. Salivary histatin 5 is an inhibitor of both host and bacterial enzymes implicated in periodontal disease. *Infection Immun* (2001) 69(3):1402–1408. doi: 10.1128/IAI.69.3.1402-1408.2001

44. Warnke PH, Springer IN, Russo PAJ, Wiltfang J, Essig H, Kosmahl M, et al. Innate immunity in human bone. *Bone* (2006) 38(3):400–408. doi: 10.1016/j.bone.2005.09.003

45. Warnke PH, Voss E, Russo PAJ, Stephens S, Kleine M, Terheyden H, et al. Antimicrobial peptide coating of dental implants : Biocompatibility assessment of recombinant human beta defensin-2 for human cells. *Int J Oral Maxillofac Implants* (2013) 28(4):982–988. doi: 10.11607/jomi.2594

46. Lee P-H, Chen M-Y, Lai Y-L, Lee S-Y, Chen H-L. Human beta-defensin-2 and-3 mitigate the negative effects of bacterial contamination on bone healing in rat calvarial defect. *Tissue Eng Part A* (2018) 24(7–8):653–661. doi: 10.1089/ten.tea.2017.0219

47. Peng Y, Li L, Yuan Q, Gu P, You Z, Zhuang A, et al. Effect of bifunctional β defensin 2-modified scaffold on bone defect reconstruction. *ACS omega* (2020) 5 (8):4302–4312. doi: 10.1021/acsomega.9b04249

48. Sun P, Shi A, Shen C, Liu Y, Wu G, Feng J. Human salivary histatin-1 (Hst1) promotes bone morphogenetic protein 2 (BMP2)-induced osteogenesis and angiogenesis. *FEBS Open Bio* (2020) 10(8):1503–1515. doi: 10.1002/2211-5463.12906

49. Cai J, Li X, Du H, Jiang C, Xu S, Cao Y. Immunomodulatory significance of natural peptides in mammalians: Promising agents for medical application. *Immunobiology.* (2020) 225(3):151936. doi: 10.1016/j.imbio.2020.151936

50. Dömer D, Walther T, Möller S, Behnen M, Laskay T. Neutrophil extracellular traps activate proinflammatory functions of human neutrophils. *Front Immunol* (2021) 12:636954. doi: 10.3389/fimmu.2021.636954

51. Melchers F. Checkpoints that control B cell development. *J Clin Invest.* (2015) 125(6):2203–10. doi: 10.1172/JCI78083

52. Le Pottier L, Devauchelle V, Pers J-O, Jamin C, Youinou P. The mosaic of b-cell subsets (with special emphasis on primary sjögren's syndrome). *Autoimmun Rev* (2007) 6(3):149–154. doi: 10.1016/j.autrev.2006.09.011

53. Zouali M. The emerging roles of b cells as partners and targets in periodontitis. *Autoimmunity* (2017) 50(1):61–70. doi: 10.1080/08916934.2016.1261841

54. Demoersman J, Pochard P, Framery C, Simon Q, Boisramé S, Soueidan A, et al. B cell subset distribution is altered in patients with severe periodontitis. *PloS One* (2018) 13(2):e0192986. doi: 10.1371/journal.pone.0192986

55. Coat J, Demoersman J, Beuzit S, Cornec D, Devauchelle-Pensec V, Saraux A, et al. Anti-b lymphocyte immunotherapy is associated with improvement of periodontal status in subjects with rheumatoid arthritis. *J Clin Periodontology* (2015) 42(9):817–823. doi: 10.1111/jcpe.12433

56. Abe T, AlSarhan M, Benakanakere MR, Maekawa T, Kinane DF, Cancro MP, et al. The b cell–stimulatory cytokines BLyS and APRIL are elevated in human periodontitis and are required for b cell–dependent bone loss in experimental murine periodontitis. *J Immunol* (2015) 195(4):1427–1435. doi: 10.4049/jimmunol.1500496

57. Harada Y, Han X, Yamashita K, Kawai T, Eastcott JW, Smith DJ, et al. Effect of adoptive transfer of antigen-specific b cells on periodontal bone resorption. *J Periodontal Res* (2006) 41(2):101–107. doi: 10.1111/j.1600-0765.2005.00839.x

58. Algate K, Haynes DR, Bartold PM, Crotti TN, Cantley MD. The effects of tumour necrosis factor-α on bone cells involved in periodontal alveolar bone loss; osteoclasts, osteoblasts and osteocytes. *J periodontal Res* (2016) 51(5):549–566. doi: 10.1111/jre.12339

59. Nagasawa T, Kiji M, Yashiro R, Hormdee D, Lu H, Kunze M, et al. Roles of receptor activator of nuclear factor-κB ligand (RANKL) and osteoprotegerin in periodontal health and disease. *Periodontology 2000* (2007) 43(1):65–84. doi: 10.1159/000232942

60. Taubman MA, Valverde P, Han X, Kawai T. Immune response: The key to bone resorption in periodontal disease. *J Periodontology* (2005) 76(11S):2033–2041. doi: 10.1902/jop.2005.76.11-S.2033

61. Han YK, Jin Y, Miao YB, Shi T, Lin XP. Improved RANKL production by memory b cells: A way for b cells promote alveolar bone destruction during periodontitis. *Int Immunopharmacol* (2018) 64:232–7. doi: 10.1016/j.intimp.2018.08.033

62. Doucet P, Lowenstein M. Activation de l'ostéoclasie par les endotoxines bactériennes au cours des maladies parodontales [Osteoclasts activation by bacterial endotoxins during periodontal diseases]. *Med Sci (Paris)* (2006) 22(6-7):614–20. doi: 10.1051/medsci/20062267614

63. Hofbauer LC, Heufelder AE. Role of receptor activator of nuclear factor-kappaB ligand and osteoprotegerin in bone cell biology. *J Mol Med (Berl)* (2001) 79 (5-6):243–53. doi: 10.1007/s001090100226

64. Walsh MC, Choi Y. Biology of the RANKL-RANK-OPG system in immunity, bone, and beyond. *Front Immunol* (2014) 5:511. doi: 10.3389/fimmu.2014.00511

65. Nagasawa T, Kobayashi H, Kiji M, Aramaki M, Mahanonda R, Kojima T, et al. LPS-stimulated human gingival fibroblasts inhibit the differentiation of monocytes into osteoclasts through the production of osteoprotegerin. *Clin Exp Immunol* (2002) 130(2):338–44. doi: 10.1046/j.1365-2249.2002.01990.x

66. Belibasakis GN, Bostanci N. The RANKL-OPG system in clinical periodontology. *J Clin Periodontol* (2012) 39(3):239–48. doi: 10.1111/j.1600-051X.2011.01810.x

67. Manabe N, Kawaguchi H, Chikuda H, Miyaura C, Inada M, Nagai R, et al. Connection between b lymphocyte and osteoclast differentiation pathways. *J Immunol* (2001) 167(5):2625–31. doi: 10.4049/jimmunol.167.5.2625

68. Napimoga MH, Demasi AP, Jarry CR, Ortega MC, de Araújo VC, Martinez EF. *In vitro* evaluation of the biological effect of SOFAT on osteoblasts. *Int Immunopharmacol* (2015) 26(2):378–83. doi: 10.1016/j.intimp.2015.04.033

69. Jarry CR, Duarte PM, Freitas FF, de Macedo CG, Clemente-Napimoga JT, Saba-Chujfi E, et al. Secreted osteoclastogenic factor of activated T cells (SOFAT), a novel osteoclast activator, in chronic periodontitis. *Hum Immunol* (2013) 74 (7):861–6. doi: 10.1016/j.humimm.2013.04.013

70. Jarry CR, Martinez EF, Peruzzo DC, Carregaro V, Sacramento LA, Araújo VC, et al. Expression of SOFAT by T- and b-lineage cells may contribute to bone loss. *Mol Med Rep* (2016) 13(5):4252–8. doi: 10.3892/mmr.2016.5045

71. Cekici A, Kantarci A, Hasturk H, Van Dyke TE. Inflammatory and immune pathways in the pathogenesis of periodontal disease. *Periodontol 2000* (2014) 64 (1):57–80. doi: 10.1111/prd.12002

72. Han MX, Ding C, Kyung HM. Genetic polymorphisms in pattern recognition receptors and risk of periodontitis: Evidence based on 12,793 subjects. *Hum Immunol* (2015) 76(7):496–504. doi: 10.1016/j.humimm.2015.06.006

73. AlQranei MS, Chellaiah MA. Osteoclastogenesis in periodontal diseases: Possible mediators and mechanisms. *J Oral Biosci* (2020) 62(2):123–30. doi: 10.1016/j.job.2020.02.002

74. Beutler B. Inferences, questions and possibilities in toll-like receptor signalling. *Nature.* (2004) 430(6996):257–63. doi: 10.1038/nature02761

75. Di Benedetto A, Gigante I, Colucci S, Grano M. Periodontal disease: linking the primary inflammation to bone loss. *Clin Dev Immunol* (2013) 2013:503754. doi: 10.1155/2013/503754

76. Tew JG, El Shikh ME, El Sayed RM, Schenkein HA. Dendritic cells, antibodies reactive with oxLDL, and inflammation. *J Dent Res* (2012) 91(1):8–16. doi: 10.1177/0022034511407338

77. Watanabe K, Iizuka T, Adeleke A, Pham L, Shlimon AE, Yasin M, et al. Involvement of toll-like receptor 4 in alveolar bone loss and glucose homeostasis in experimental periodontitis. *J Periodontal Res* (2011) 46(1):21–30. doi: 10.1111/j.1600-0765.2010.01304.x

78. Freire MO, Van Dyke TE. Natural resolution of inflammation. *Periodontol 2000* (2013) 63(1):149–64. doi: 10.1111/prd.12034

79. Han YW, Shi W, Huang GT, Kinder Haake S, Park NH, Kuramitsu H, et al. Interactions between periodontal bacteria and human oral epithelial cells: Fusobacterium nucleatum adheres to and invades epithelial cells. *Infect Immun* (2000) 68(6):3140–6. doi: 10.1128/IAI.68.6.3140-3146.2000

80. Chakravarti A, Allaeys I, Poubelle PE. Neutrophile et immunité: est-ce inné ou acquis? [Neutrophils and immunity: is it innate or acquired?]. *Med Sci (Paris)* (2007) 23(10):862–7. doi: 10.1051/medsci/20072310862

81. Borregaard N. Neutrophils, from marrow to microbes. *Immunity.* (2010) 33 (5):657–70. doi: 10.1016/j.immuni.2010.11.011

82. Hienz SA, Paliwal S, Ivanovski S. Mechanisms of bone resorption in periodontitis. *J Immunol Res* (2015) 2015:615486. doi: 10.1155/2015/615486

83. Laurent F, Romagna C, Laurent Y, Chaux-Bodard AG, Veyre S, Hemar J, et al. Relations entre les pathologies cardiovasculaires et buccodentaires. ce que le cardiologue doit connaître [Relationship between coronary artery disease and periodontal disease. what the cardiologist must know]. *Ann Cardiol Angeiol (Paris)* (2007) 56(6):297–302.

84. Kawai T, Matsuyama T, Hosokawa Y, Makihira S, Seki M, Karimbux NY, et al. B and T lymphocytes are the primary sources of RANKL in the bone resorptive lesion of periodontal disease. *Am J Pathol* (2006) 169(3):987–98. doi: 10.2353/ajpath.2006.060180

85. Fruitwala S, El-Naccache DW, Chang TL. Multifaceted immune functions of human defensins and underlying mechanisms. *Semin Cell Dev Biol* (2019) 88:163–172. doi: 10.1016/j.semcdb.2018.02.023

86. Verjans E-T, Zels S, Luyten W, Landuyt B, Schoofs L. Molecular mechanisms of LL-37-induced receptor activation : An overview. *Peptides* (2016) 85:16–26. doi: 10.1016/j.peptides.2016.09.002

87. Vandamme D, Landuyt B, Luyten W, Schoofs L. A comprehensive summary of LL-37, the factotum human cathelicidin peptide. *Cell Immunol* (2012) 280 (1):22–35. doi: 10.1016/j.cellimm.2012.11.009

88. Xhindoli D, Pacor S, Benincasa M, Scocchi M, Gennaro R, Tossi A. The human cathelicidin LL-37–a pore-forming antibacterial peptide and host-cell modulator. *Biochim Biophys Acta (BBA)-Biomembranes* (2016) 1858(3):546–566. doi: 10.1016/j.bbamem.2015.11.003

89. Burteau C, Willems L, Kettmann R. Les Chémokines et leurs récepteurs : Rôle dans les infections virales et dans les pathologies cancéreuses. biotechnol. *Agron Soc Environ* (2007) 11(2):141–50.

90. Liao F, Shirakawa A-K, Foley JF, Rabin RL, Farber JM. Human b cells become highly responsive to macrophage-inflammatory protein-3α/CC chemokine ligand-20 after cellular activation without changes in CCR6 expression or ligand binding. *J Immunol* (2002) 168(10):4871–4880. doi: 10.4049/jimmunol.168.10.4871

91. Okada T, Ngo VN, Ekland EH, Förster R, Lipp M, Littman DR, et al. Chemokine requirements for b cell entry to lymph nodes and peyer's patches. *J Exp Med* (2002) 196(1):65–75. doi: 10.1084/jem.20020201

92. Liao F, Rabin RL, Smith CS, Sharma G, Nutman TB, Farber JM. CC-chemokine receptor 6 is expressed on diverse memory subsets of T cells and determines responsiveness to macrophage inflammatory protein 3α. *J Immunol* (1999) 162(1):186–194.

93. Frade JM, Mellado M, del Real G, Gutierrez-Ramos JC, Lind P, Martinez-A C. Characterization of the CCR2 chemokine receptor : Functional CCR2 receptor expression in b cells. *J Immunol* (1997) 159(11):5576–5584.

94. Avila EE. Functions of antimicrobial peptides in vertebrates. *Curr Protein Pept Sci* (2017) 18(11):1098–119. doi: 10.2174/1389203717666160813162629

95. Murdoch C, Finn A. Chemokine receptors and their role in inflammation and infectious diseases. *Blood* (2000) 95:3032–3043. doi: 10.1182/blood.v95.10.3032

96. Underhill DM, Gantner B. Integration of toll-like receptor and phagocytic signaling for tailored immunity. *Microbes Infect* (2004) 6(15):1368–73. doi: 10.1016/j.micinf.2004.08.016

97. Dasari P, Nicholson IC, Hodge G, Dandie GW, Zola H. Expression of toll-like receptors on b cells. *Cell Immunol* (2005) 236(1-2):140–5. doi: 10.1016/j.cellimm.2005.08.020

98. Gururajan M, Jacob J, Pulendran B. Toll-like receptor expression and responsiveness of distinct murine splenic and mucosal b-cell subsets. *PloS One* (2007) 2(9):e863. doi: 10.1371/journal.pone.0000863

99. Kang JY, Lee JO. Structural biology of the toll-like receptor family. *Annu Rev Biochem* (2011) 80:917–41. doi: 10.1146/annurev-biochem-052909-141507

100. Ghosh D, Stumhofer JS. Do you see what I see: Recognition of protozoan parasites by toll-like receptors. *Curr Immunol Rev* (2013) 9(3):129–40. doi: 10.2174/15733955096613120322592

101. Singh K, Bayrak B, Riesbeck K. A role for TLRs in moraxella-superantigen induced polyclonal b cell activation. *Front Biosci (Schol Ed)* (2012) 4(3):1031–43. doi: 10.2741/s316

102. Castañeda-Sánchez JI, Duarte ARM, Domínguez-López M, de la Cruz-López JJ, Julieta Luna-Herrera J. B lymphocyte as a target of bacterial infections. In: G Isvoranu, editor. *Lymphocyte updates - cancer, autoimmunity and infection [Internet]*. London: IntechOpen (2017).

103. Conigrave AD, Fernando KC, Gu B, Tasevski V, Zhang W, Luttrell BM, et al. P2Y(11) receptor expression by human lymphocytes: evidence for two cAMP-linked purinoceptors. *Eur J Pharmacol* (2001) 426(3):157–63. doi: 10.1016/S0014-2999(01)01222-5

104. Pippel A, Beßler B, Klapperstück M, Markwardt F. Inhibition of antigen receptor-dependent Ca(2+) signals and NF-AT activation by P2X7 receptors in human b cells. *Cell Calcium* (2015) 57(4):275–89. doi: 10.1016/j.ceca.2015.01.010

105. Agerberth B, Charo J, Werr J, Olsson B, Idali F, Lindbom L, et al. The human antimicrobial and chemotactic peptides LL-37 and alpha-defensins are expressed by specific lymphocyte and monocyte populations. *Blood* (2000) 96 (9):3086–93. doi: 10.1182/blood.V96.9.3086.

106. Han X, Lin X, Seliger AR, Eastcott J, Kawai T, Taubman MA. Expression of receptor activator of nuclear factor-kappaB ligand by b cells in response to oral bacteria. *Oral Microbiol Immunol* (2009) 24(3):190–6. doi: 10.1111/j.1399-302X.2008.00494.x

107. Ebersole JL, Hamzeh R, Nguyen L, Al-Sabbagh M, Dawson D3rd. Variations in IgG antibody subclass responses to oral bacteria: Effects of periodontal disease and modifying factors. *J Periodontal Res* (2021) 56(5):863–76. doi: 10.1111/jre.12882

108. O'Neil LJ, Oliveira CB, Sandoval-Heglund D, Barrera-Vargas A, Merayo-Chalico J, Aguirre-Aguilar E, et al. Anti-carbamylated LL37 antibodies promote pathogenic bone resorption in rheumatoid arthritis. *Front Immunol* (2021) 12:715997. doi: 10.3389/fimmu.2021.715997

109. Bae SC, Lee YH. Causal association between periodontitis and risk of rheumatoid arthritis and systemic lupus erythematosus: a mendelian randomization. kausalzusammenhang zwischen periodontitis und dem risiko für rheumatoide arthritis und systemischen lupus erythematodes: eine Mendel-randomisierung. *Z Rheumatol* (2020) 79(9):929–36. doi: 10.1007/s00393-019-00742-w

110. de Molon RS, Rossa CJr, Thurlings RM, Cirelli JA, Koenders MI. Linkage of periodontitis and rheumatoid arthritis: Current evidence and potential biological interactions. *Int J Mol Sci* (2019) 20(18):4541. doi: 10.3390/ijms20184541

111. Knochelmann HM, Dwyer CJ, Bailey SR, Amaya SM, Elston DM, Mazza-McCrann JM, et al. When worlds collide: Th17 and treg cells in cancer and autoimmunity. *Cell Mol Immunol* (2018) 15(5):458–69. doi: 10.1038/s41423-018-0004-4

112. Vordenbäumen S, Fischer-Betz R, Timm D, Sander O, Chehab G, Richter J, et al. Elevated levels of human beta-defensin 2 and human neutrophil peptides in systemic lupus erythematosus. *Lupus.* (2010) 19(14):1648–53. doi: 10.1177/0961203310377089

113. Bokarewa MI, Jin T, Tarkowski A. Intraarticular release and accumulation of defensins and bactericidal/permeability-increasing protein in patients with rheumatoid arthritis. *J Rheumatol* (2003) 30(8):1719–24.

114. Kienhöfer D, Hahn J, Schubert I, Reinwald C, Ipseiz N, Lang SC, et al. No evidence of pathogenic involvement of cathelicidins in patient cohorts and mouse models of lupus and arthritis. *PloS One* (2014) 9(12):e115474. doi: 10.1371/journal.pone.0115474

115. Liang W, Diana J. The dual role of antimicrobial peptides in autoimmunity. *Front Immunol* (2020) 11:2077. doi: 10.3389/fimmu.2020.02077

116. Konig MF, Abusleme L, Reinholdt J, Palmer RJ, Teles RP, Sampson K, et al. Aggregatibacter actinomycetemcomitans-induced hypercitrullination links periodontal infection to autoimmunity in rheumatoid arthritis. *Sci Transl Med* (2016) 8:369ra176. doi: 10.1126/scitranslmed.aaj1921

117. Moen K, Brun JG, Valen M, Skartveit L, Eribe EK, Olsen I, et al. Synovial inflammation in active rheumatoid arthritis and psoriatic arthritis facilitates trapping of a variety of oral bacterial DNAs. *Clin Exp Rheumatol* (2006) 24:656–63.

118. Lande R, Pietraforte I, Mennella A, Palazzo R, Spinelli FR, Giannakakis K, et al. Complementary effects of carbamylated and citrullinated LL37 in autoimmunity and inflammation in systemic lupus erythematosus. *Int J Mol Sci* (2021) 22(4):1650. doi: 10.3390/ijms22041650

119. Frasca L, Palazzo R, Chimenti MS, Alivernini S, Tolusso B, Bui L, et al. Anti-LL37 antibodies are present in psoriatic arthritis (PsA) patients: New biomarkers in PsA. *Front Immunol* (2018) 9:1936. doi: 10.3389/fimmu.2018.01936

120. Lande R, Palazzo R, Hammel P, Pietraforte I, Surbeck I, Gilliet M, et al. Generation of monoclonal antibodies specific for native LL37 and citrullinated LL37 that discriminate the two LL37 forms in the skin and circulation of Cutaneous/Systemic lupus erythematosus and rheumatoid arthritis patients. *Antibodies (Basel)* (2020) 9(2):14. doi: 10.3390/antib9020014

frontiers | Frontiers in Immunology

TYPE Original Research
PUBLISHED 11 October 2022
DOI 10.3389/fimmu.2022.1004949

OPEN ACCESS

EDITED BY
Francesco Del Galdo,
University of Leeds, United Kingdom

REVIEWED BY
Julie Worrell,
University of Glasgow,
United Kingdom
Steven O'Reilly,
STipe Therapeutics, Denmark

*CORRESPONDENCE
David Abraham
david.abraham@ucl.ac.uk
Jan-Willem Taanman
j.taanman@ucl.ac.uk

†These authors have contributed equally to this work and share first authorship

SPECIALTY SECTION
This article was submitted to Autoimmune and Autoinflammatory Disorders: Autoinflammatory Disorders, a section of the journal Frontiers in Immunology

RECEIVED 27 July 2022
ACCEPTED 26 September 2022
PUBLISHED 11 October 2022

CITATION
Cantanhede IG, Liu H, Liu H, Balbuena Rodriguez V, Shiwen X, Ong VH, Denton CP, Ponticos M, Xiong G, Lima-Filho JL, Abraham D, Abu-Hanna J and Taanman J-W (2022) Exploring metabolism in scleroderma reveals opportunities for pharmacological intervention for therapy in fibrosis. *Front. Immunol.* 13:1004949. doi: 10.3389/fimmu.2022.1004949

Exploring metabolism in scleroderma reveals opportunities for pharmacological intervention for therapy in fibrosis

Isabella Gomes Cantanhede[1,2†], Huan Liu[1,3†], Huan Liu[1], Vestaen Balbuena Rodriguez[1], Xu Shiwen[1], Voo H. Ong[1], Christopher P. Denton[1], Markella Ponticos[1], Guo Xiong[3], José Luiz Lima-Filho[2], David Abraham[1*], Jeries Abu-Hanna[1] and Jan-Willem Taanman[4*]

[1]Centre for Rheumatology and Connective Tissue Diseases, Division of Medicine, University College London, London, United Kingdom, [2]Laboratory of Immunopathology Keizo Asami, Federal University of Pernambuco, Recife, Brazil, [3]Health Science Center, Xi'an Jiaotong University, Xi'an, China, [4]Department of Clinical and Movement Neurosciences, Queen Square Institute of Neurology, University College London, London, United Kingdom

Background: Recent evidence has indicated that alterations in energy metabolism play a critical role in the pathogenesis of fibrotic diseases. Studies have suggested that 'metabolic reprogramming' involving the glycolysis and oxidative phosphorylation (OXPHOS) in cells lead to an enhanced generation of energy and biosynthesis. The aim of this study was to assess the molecular basis of changes in fibrotic metabolism in systemic sclerosis (Scleroderma; SSc) and highlight the most appropriate targets for anti-fibrotic therapies.

Materials and methods: Dermal fibroblasts were isolated from five SSc patients and five healthy donors. Cells were cultured in medium with/without TGF-β1 and with/without ALK5, pan-PIM or ATM kinase inhibitors. Extracellular flux analyses were performed to evaluate glycolytic and mitochondrial respiratory function. The mitochondrial network in TMRM-stained cells was visualized by confocal laser-scanning microscopy, followed by semi-automatic analysis on the ImageJ platform. Protein expression of ECM and fibroblast components, glycolytic enzymes, subunits of the five OXPHOS complexes, and dynamin-related GTPases and receptors involved in mitochondrial fission/fusion were assessed by western blotting.

Results: Enhanced mitochondrial respiration coupled to ATP production was observed in SSc fibroblasts at the expense of spare respiratory capacity. Although no difference was found in glycolysis when comparing SSc with healthy control fibroblasts, levels of phophofructokinase-1 isoform PFKM were significantly lower in SSc fibroblasts ($P<0.05$). Our results suggest that the

10.3389/fimmu.2022.1004949

number of respirasomes is decreased in the SSc mitochondria; however, the organelles formed a hyperfused network, which is thought to increase mitochondrial ATP production through complementation. The increased mitochondrial fusion correlated with a change in expression levels of regulators of mitochondrial morphology, including decreased levels of DRP1, increased levels of MIEF2 and changes in OPA1 isoform ratios. TGF-β1 treatment strongly stimulated glycolysis and mitochondrial respiration and induced the expression of fibrotic markers. The pan-PIM kinase inhibitor had no effect, whereas both ALK5 and ATM kinase inhibition abrogated TGF-β1-mediated fibroblast activation, and upregulation of glycolysis and respiration.

Conclusions: Our data provide evidence for a novel mechanism(s) by which SSc fibroblasts exhibit altered metabolic programs and highlight changes in respiration and dysregulated mitochondrial morphology and function, which can be selectively targeted by small molecule kinase inhibitors.

KEYWORDS

fibrosis, glycolysis, kinase inhibitors, mitochondrial morphology, mitochondrial respiration, myofibroblasts, oxidative phosphorylation, systemic sclerosis

Introduction

Systemic sclerosis (scleroderma, SSc) is a rare immune-mediated inflammatory disease of unknown etiology (1, 2). One of the most characteristic pathological manifestations is the connective tissue fibrosis (3). This is especially marked in the diffuse cutaneous form of the disease, where overproduction of collagen and other extracellular matrix (ECM) proteins by connective tissue fibroblasts results in excessive ECM deposition. The fibroblasts are activated and differentiated into hyperproliferative myofibroblasts by growth factors and cytokines, such as transforming growth factor-β1 (TGF-β1). Progressive replacement of tissue architecture by the collagen-rich ECM results in a functional impairment of the affected organs. The fibrotic process is most prominent in the skin, lungs, gastrointestinal tract, heart, tendons and ligaments, and endocrine glands. Fibrotic damage to these organs accounts for much of the morbidity and mortality. Although clinical outcomes have improved, SSc is still considered incurable and difficult to treat (4).

There are two main biochemical pathways in the cell that generate metabolic energy in the form of ATP: glycolysis in the cytosol and oxidative phosphorylation in the mitochondria. Glycolysis converts glucose to pyruvate with the concomitant production of a small amount of ATP. Under aerobic conditions, pyruvate is imported into the mitochondria and further broken down in the tricarboxylic acid (TCA) cycle. Products of the TCA cycle (NADH, $FADH_2$) are subsequently oxidized, and the free energy of the redox reactions is used to sustain a proton electrochemical gradient across the inner mitochondrial membrane, which is used to drive ATP synthesis (5). This process is called oxidative phosphorylation and is the main source of ATP in aerobic cells. It has been known for a long time that, unlike normal tissues, most cancers use glycolysis as main bioenergetic pathway to produce ATP, even in the presence of oxygen (6). This aerobic glycolysis is known as the Warburg effect and is thought to be important to increase anabolic metabolism (biosynthesis of building blocks) and resistance to apoptosis in hyperproliferative cancer cells (7, 8).

It is increasingly recognized that re-programming of cellular energy metabolism also occurs in fibrotic diseases (9). For instance, keloid "scar" fibroblasts, which share characteristics with fibroblasts from SSc patients, were reported to use glycolysis as their primary energy source (10). A switch to glycolysis was also found in lung tissue and myofibroblasts from patients with idiopathic pulmonary fibrosis (IPF) (11, 12). During early myofibroblast differentiation, the expression of the glycolytic enzymes hexokinase 2 (HK2), phosphofructokinase 1 and 6-phosphofructo-2-kinase/fructose-2,6-biphosphatase 3 (PFKFB3) were found to increase and remained high. Pharmacological inhibition of glycolysis, attenuated the profibrotic phenotype, suggesting that the increased glycolytic flux is essential for development of the fibrosis (12). In addition, alveolar type II cells in IPF patients were found to exhibit marked accumulation of dysfunctional mitochondria (13). Likewise, vascular pulmonary cells in patients with pulmonary arterial hypertension (PAH) showed mitochondrial abnormalities (14) and a shift towards glycolysis, which is likely to play a causal role in the deleterious vascular

remodeling because drug-induced reversal of the metabolic shift prevented remodeling (15). Similarly, differentiation of cultured hepatic stellate cells into myofibroblasts was shown to induce glycolysis (16). Finally, in mouse unilateral ureter obstruction-induced renal fibrosis and TGF-β1-treated renal interstitial fibroblasts, high levels of glucose uptake, glycolytic enzymes and lactate production were observed. Pharmacological inhibition of pyruvate kinase type M2 (PKM2) phosphorylation at Tyr residue 105, which is known to suppress aerobic glycolysis, attenuated renal fibrosis and fibroblast activation (17).

As current treatments of SSc are limited and have substantial side effects, new insights into the pathological processes are needed to develop novel therapeutic approaches. We hypothesize that rewiring of the energy generating pathways contribute to the disease process of SSc to meet the increased demand of energy and anabolic metabolism for fibrogenesis. The aims of the current study were: (a) to investigate possible changes in energy metabolism in cell culture models of SSc, (b) to explore the molecular basis of these changes, and (c) to develop selective therapeutic strategies that target the disrupted metabolism and stop fibrosis.

Material and methods

Cell culturing

Primary dermal fibroblast cultures were established from skin explants of five early diffuse SSc patients (≤2 y from first non-Raynaud's symptom) and five unrelated, healthy, age-matched control subjects (Supplementary Table S1) according to standard procedures (18). From the patients, we took paired skin samples from lesional and uninvolved tissue. Donors provided prior informed written consent. Ethical approval was obtained from the Research Ethics Committee (reference: 6398) of the NHS Health Research Authority (NRES Committee London-Hampstead) in compliance with national legislation and the Declaration of Helsinki.

Cell passages at 3–7 were used for study. Cells were cultured in Dulbecco's modified Eagle medium (DMEM) containing GlutaMAX and 25 mM glucose (Gibco, ThermoFisher Scientific), supplemented with 10% fetal bovine serum (FBS), 1 mM sodium pyruvate, 50 units/ml of penicillin and 50 µg/ml of streptomycin (culture medium) at 37°C in a humidified atmosphere of 5% CO_2 in air. For the experiments with TGF-β1, cells were serum-starved in culture medium containing 0.1% FBS for 24 h before treatment with or without 2 ng/ml of TGF-β1 (R&D Systems) and with or without 10 µM SB431542 (Tocris Bioscience), 20 µM AZD1208 (Tocris Bioscience) or 5 µM KU55933 (Tocris Bioscience) for 24 h in fresh culture medium containing 0.1% FBS. Thousand-fold stock solutions were prepared in water (TGF-β1) or dimethyl sulfoxide (small molecule inhibitors) and stored at -80°C. The concentration of the inhibitors was informed by the literature and verified by viability assays using PrestoBlue Cell Viability Reagent (ThermoFisher Scientific), whereby only doses at which no toxic affects occurred were chosen.

Western blot analysis

For the study of α-smooth muscle actin (α-SMA) and ECM proteins, cell cultures were washed twice with cold phosphate-buffered saline (PBS) followed by extraction in cold RIPA buffer (Merck, Sigma-Aldrich), supplemented with Roche cOmplete Protease Inhibitor Cocktail (Merck, Sigma-Aldrich). Cell monolayers were collected with a cell scraper, centrifuged for 10 min at 16,000 × *g*, 4°C, and supernatants were stored at -20°C for western blot analyses.

For the study of glycolytic pathway and mitochondrial proteins, cell cultures were washed with PBS and, subsequently, dislodged by trypsinization, collected by centrifugation, washed with PBS and extracted with 1% Triton X-100 in PBS, supplemented with protease inhibitors (1 µM phenylmethylsulfonyl fluoride, 1 µg/ml of pepstatin A and 1 µg/ml of leupeptin) and Phosphatase Inhibitor Cocktail 2 and 3 (Merck, Sigma-Aldrich). After 15 min on ice, samples were centrifuged for 10 min at 16,000 × *g*, 4°C, and the supernatants were stored at -80°C for western blot analyses.

Protein concentrations of the samples were determined with the Pierce BCA Protein Assay Kit (ThermoFisher Scientific) as detailed below. To prepare western blots, 10-µg samples in 1× Laemmli Sample Buffer (BioRad) and 1× NuPAGE Sample Reducing Agent (ThermoFisher Scientific) were resolved on 4–20% or 7.5% Criterion TGX Stain-Free Precast Gels (Biorad) alongside SeeBlue Plus2 Pre-stained Protein (ThermoFisher Scientific) or Precision Plus Protein (BioRad) standards and blotted onto Trans-Blot Turbo 0.2-µm PVDF membranes (BioRad) using a BioRad Trans-Blot Transfer System. Protein binding sites on the blots were saturated with 5% bovine serum albumin (BSA; for detection of phospho-proteins) or 10% skimmed milk powder (for detection of all other proteins) in PBS for 1 h, followed by a rinse with PBS, 0.3% Tween-20 and primary antibody incubation in PBS, 0.3% Tween-20, at 4°C, overnight. The primary antibodies are specified in Supplementary Table S2. Excess of primary antibodies was removed with three 10-min washes in PBS, 0.3% Tween-20, followed by a 1-h incubation with the appropriate horse radish peroxidase-conjugated secondary antibodies (Dako; P0160, P0447 and P0448) in PBS, 0.3% Tween-20, and another 3 washes. Blots were developed with Clarity Western ECL Substrate (BioRad). Capturing of the chemiluminescent signals was performed with a BioRad Chemidoc MP Imaging System. Signals were quantified with BioRad Image Lab 5.1 software. Afterwards, all blots were probed with an antibody against β-tubulin to verify loading. Antibody signals were normalized with

the aid of the anti-β-tubulin signal and expressed relative to the mean value of the control samples.

Extracellular flux analyses

Extracellular flux assays were performed on a Seahorse XFp platform (Agilent Technologies). To count the cells for seeding in the XFp cell culture microplates, they were dislodged by trypsinization, collected by centrifugation and resuspended in culture medium, followed by trypan blue exclusion cell counting on C-Chip Neubauer Improved Disposable Hemocytometer slides (NanoEnTek) in duplicate. Fibroblasts were seeded in wells of an XFp cell culture microplate at a density of 8,000 cells/well in 80 µl of culture medium and cultured for 24 h. In the TGF-β1 experiments, cells were serum-starved in the wells of the XFp cell culture microplate for a further 24 h prior to treatment with or without 2 ng/ml of TGF-β1 and with or without 10 µM SB431542, 20 µM AZD1208 or 5 µM KU55933 for 24 h in fresh culture medium containing 0.1% FBS.

To examine glycolytic function in glycolysis stress tests, the culture medium in the wells was replaced with 175 µl XFp Base medium (Agilent Technologies) pH 7.0 (NaOH), containing 2 mM L-glutamine, with or without TGF-β1 and with or without small molecule inhibitors. After 1 h of humidified incubation at 37°C, glycolysis was evaluated on the Seahorse platform. After three measurements under basal conditions, glucose was injected to a final concentration of 10 mM, followed by three measurements. Then, oligomycin A was injected to a final concentration of 1 µM, followed by three measurements. Last of all, 2-deoxy-D-glucose was injected to a final concentration 50 mM, followed by three measurements. Glucose was prepared as a 2.5 M stock solution in water and stored at room temperature, while oligomycin A (Merck, Sigma-Aldrich) was prepared as a 10 mM stock solution in ethanol and 2-deoxy-D-glucose (Merck, Sigma-Aldrich) was prepared as a 500 mM stock solution in XFp Base medium pH 7.0 and both stored at -20°C.

To examine mitochondrial respiratory function in mitostress tests, the culture medium in the wells was replaced with 175 µl XFp Base medium pH 7.0 (NaOH), containing 10 mM D-(+)-glucose, 1 mM sodium pyruvate and 2 mM L-glutamine, with or without TGF-β1 and with or without small molecule inhibitors. After 1 h of humidified incubation at 37°C, respiration was assessed on the Seahorse platform. After three measurements under basal conditions, oligomycin A was injected to a final concentration of 1 µM, followed by three measurements. Then, carbonyl cyanide 4-(trifluoromethoxy) phenylhydrazone (FCCP) was injected to a final concentration of 2 µM, followed by three measurements. To finish, rotenone and antimycin A were injected, both at a final concentration of 1 µM, followed by three measurements. Oligomycin A, FCCP, rotenone and antimycin A were purchased from Merck (Sigma-Aldrich). They were prepared as 10 mM stock solutions in ethanol and stored at -20°C.

On each XFp cell culture plate, two different cultures were compared in triplicate, e.g., fibroblasts from a control subject and fibroblasts from a SSc patient, or fibroblasts from a SSc patient treated with vehicle and fibroblasts from the same SSc patient treated with TGF-β1. All experiments were repeated independently 4 (Figure 8) or 6 (Figure 2) times by conducting two experiments per cell passage of two or three subsequent passages. Data were analyzed with Wave Desktop 2.6.1 software and a Microsoft Excel macro provided by Agilent Technologies. Results are expressed per cell number or amount of protein determined after the extracellular flux assay. Cell numbers in each well of the XFp cell culture plate were determined with the CyQUANT Cell Proliferation Assay Kit (ThermoFisher Scientific) by adding 220 µl of CyQUANT GR dye/lysis solution to the aspirated wells, followed by mixing through pipetting up-and-down. Then, 200 µl of the mixture was transferred to wells of a 96-well black plate with clear bottoms (Greiner). An empty row on the 96-well plate was filled with 200 µl of a serial dilution of 0–25,000 cells in CyQUANT GR dye/lysis solution. The fluorescent signals were recorded at 480 nm excitation and 520 nm emission with a Synergy HT plate reader. In the TGF-β1 experiments, the amount of protein in aspirated wells of the XFp cell culture plates were determined with the Pierce BCA Protein Assay Kit and a serial dilution of BSA. Standard curves for the number of cells *versus* the fluorescent signal or the concentration of BSA *versus* the absorption at 561 nm were constructed in Microsoft Excel. Equations of the standard curves were used to calculate the cell number or amount of protein per well.

Citrate synthase assays

The Triton X-100 extracts of the cell cultures prepared for western blot analyses were also used to determine citrate synthase activity. Assays were carried out in quadruplicate as described (19).

Mitochondrial network analysis

Cells were seeded at low density in 35-mm µ-dishes with a glass bottom (Ibidi). After 3–4 days of culturing, cells were rinsed with Hanks' balanced salt solution (HBSS; ThermoFisher Scientific), followed by incubation in 1 ml of 25 nM tetramethylrhodamine methyl ester (TMRM; Invitrogen, ThermoFisher Scientific) in HBSS. After 15 min of incubation, red fluorescent images (7 z-stacks of 0.15 µm) were captured with a Nikon Eclipse Ti-E inverted confocal laser-scanning microscope, equipped with a ×60 objective. Imaging data were

collected with NIS-Elements software (Nikon). Semi-automated analysis of mitochondrial networks in the cultured cells was performed with the MiNA macro toolset (20) on the FIJI distribution of the ImageJ platform (National Institutes of Health). All 15 different fibroblast cultures were analyzed; five cultures derived from control subjects, five cultures derived from uninvolved skin of SSc patients, and five cultures derived from involved skin of the same SSc patients. Six to 12 randomly chosen microscopic fields were studied of each culture with 1–10 cells per field. In total 17–58 cells of each culture were studied.

Statistical analyses

Graphs and statistical analyses were executed with GraphPad Prism software. Data are presented as mean ± standard deviation. As the sample size was too small to confirm normal distribution, we used non-parametric Kruskal-Wallis tests to examine statistical significance. Mann-Whitney tests were used for pairwise comparisons. Statistical significance levels were set to $P<0.05$ with Bonferroni correction for multiple pairwise comparisons.

Results

Expression levels of fibrotic markers

In this study, we compared paired fibroblasts cultures derived from uninvolved and lesional skin of five SSc patients with dermal fibroblast cultures derived from five control subjects. First, we investigated the expression levels of two markers of fibrosis, α-smooth muscle actin (α-SMA) and collagen type 1 α1 chain (COL-1) on western blots (Figure 1A). Compared to the control samples, α-SMA and COL-1 were clearly overexpressed in the uninvolved SSc samples. In the lesional SSc samples, the expression levels of α-SMA and COL-1 were even higher (Figures 1B, C). These results confirm the fibrotic phenotype of the SSc fibroblasts.

Glycolysis and mitochondrial respiration

To investigate whether energy metabolism in SSc fibroblasts is altered, we evaluated glycolysis and mitochondrial respiration with a Seahorse extracellular flux analyzer. We first determined the extracellular acidification rates (ECAR) as measure of glycolytic flux in glycolysis stress tests (Figure 2A). The experiments were repeated independently six times for each culture. The compiled data of the five pairs of SSc fibroblast cultures and five control cultures showed no differences in basal glycolysis, glycolytic capacity and glycolytic reserve (Figure 2B). Next, we determined the oxygen consumption rates (OCR) as measure of cellular respiration in mitostress tests (Figure 2C). Again, the experiments were repeated independently six times for each culture. The combined data for all 15 cultures revealed no differences in basal respiration and maximal respiration but indicated that the spare respiratory capacity was decreased in SSc fibroblasts, while the respiration coupled to ATP production was increased in SSc fibroblasts compared to the controls. Thus, the extracellular flux assays revealed a shift in mitochondrial respiration towards increased oxidative phosphorylation in SSc fibroblasts, while glycolytic flux did not change.

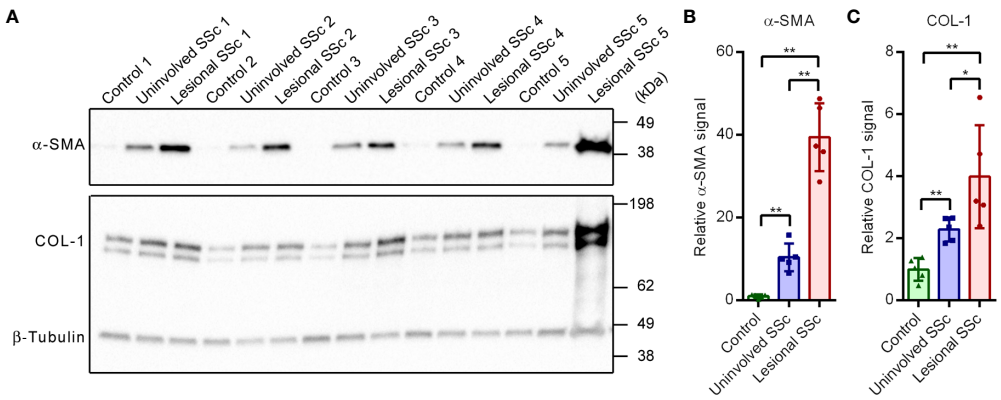

FIGURE 1
The fibrotic markers α-SMA and COL-1 are overexpressed in SSc fibroblasts. **(A)** Western blots with samples from five control, and five paired uninvolved and lesional SSc fibroblast cultures probed with antibodies against α-SMA, COL-1 and β-tubulin. Migration of protein standards is indicated. **(B, C)** Mean α-SMA and COL-1 signals, normalized for the β-tubulin signal and expressed relative to the mean value of the control samples. Data points show relative values of the individual samples. Error bars indicate standard deviations. Asterisks denote statistically significant differences (*$P<0.05$, **$P<0.01$).

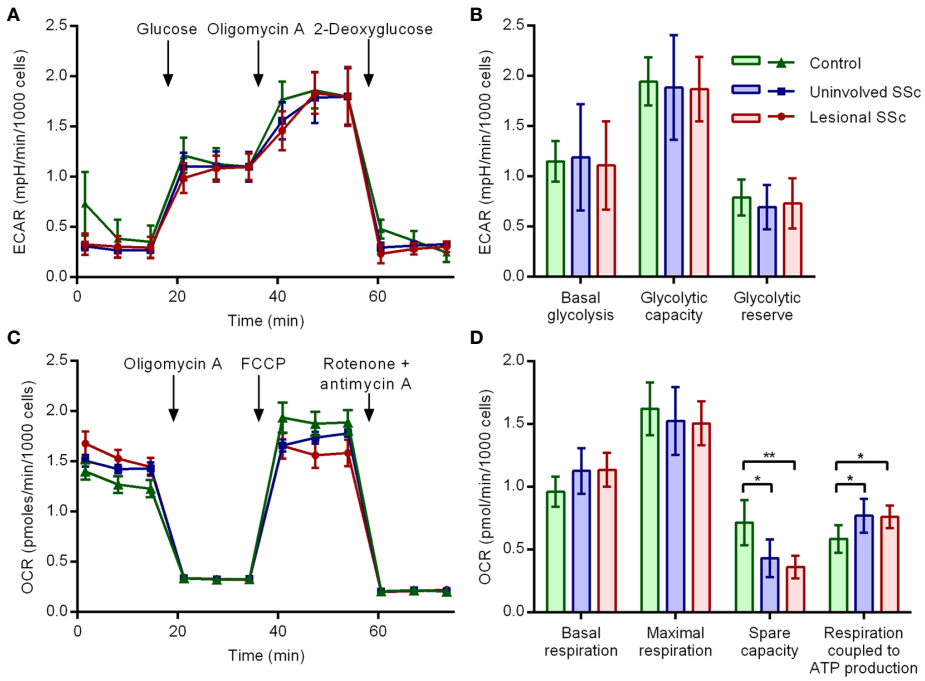

FIGURE 2
Mitochondrial OXPHOS is increased in SSc fibroblasts but glycolysis is unaffected. **(A)** Extracellular acidification rate (ECAR) profiles in representative glycolysis stress tests of a control, an uninvolved SSc and a corresponding lesional SSc fibroblast culture. Glucose, oligomycin A and 2-deoxyglucose were sequentially added to dissect glycolytic function. Error bars indicate standard deviation of technical triplicates. **(B)** Mean basal glycolysis, glycolytic capacity and glycolytic reserve of five control and five paired uninvolved and lesional SSc fibroblast cultures. Error bars indicate standard deviation. **(C)** Oxygen consumption rate (OCR) profiles in representative mitostress tests of a control, an uninvolved SSc and a corresponding lesional SSc fibroblast culture. Oligomycin A, FCCP and rotenone + antimycin A were sequentially added to dissect mitochondrial respiratory function. Error bars indicate standard deviation of technical triplicates. **(D)** Mean basal respiration, maximal respiration, spare respiratory capacity and respiration coupled to ATP production of five control and five paired uninvolved and lesional SSc fibroblast cultures. Error bars indicate standard deviation. Asterisks denote statistically significant differences (*P<0.05, **P<0.01).

Protein expression levels of enzymes of the glycolytic pathway and lactate secretion

Although the glycolytic stress tests did not suggest changes in glycolytic flux in the SSc fibroblasts, we investigated the glycolytic pathway and lactate secretion in more detail by looking at protein expression levels of key enzymes on western blots (Figure 3A). Hexokinase catalyzes the first step of glycolysis, the phosphorylation of glucose to glucose 6-phosphate (Supplementary Figure S1). The two most abundantly expressed isoenzymes HK1 and HK2 are critical for maintaining an elevated rate of glycolysis in cancer cells (21). Western blot analyses revealed no differences in HK1 and HK2 expression levels between control and SSc fibroblasts (Figures 3B, C).

Phosphofructokinase 1 catalyzes the phosphorylation of fructose 6-phosphate to fructose 1,6-bisphosphate in the rate-limiting, third step of glycolysis (Supplementary Figure S1). The active tetrameric enzyme is comprised of different combinations of PFKL, PFKM and PFKP subunit isoforms (22, 23). The western blots showed that levels of PFKL and PFKP were similar in control and SSc fibroblasts, but levels of PFKM were significantly lower in SSc samples compared to controls (Figures 3D–F).

The bifunctional 6-phosphofructo-2-kinase/fructose-2,6-bisphosphatase (PFKFB) catalyzes the synthesis and degradation of fructose 2,6-bisphosphate, thereby regulating its steady-state level (24). Fructose 2,6-bisphosphate is a positive allosteric regulator of phosphofructokinase 1 (Supplementary Figure S1). Four different isoforms of PFKFB have been identified. Isoform PFKFB3, which is highly expressed in most cancers, is inducible by hypoxia and promotes glycolysis under hypoxic conditions (25, 26). Our western blots did not show significant differences of PFKFB3 levels between control and SSc fibroblasts (Figure 3G).

Glyceraldehyde-3-phosphate dehydrogenase (GAPDH) converts glyceraldehyde-3-phosphate to 1,3 bisphosphoglycerate during glycolysis (Supplementary Figure S1). GAPDH is considered to be a constitutively expressed housekeeping protein (27). In agreement with this, we found very similar GAPDH levels in the control and SSc samples on a western blot (Figure 3H).

10.3389/fimmu.2022.1004949

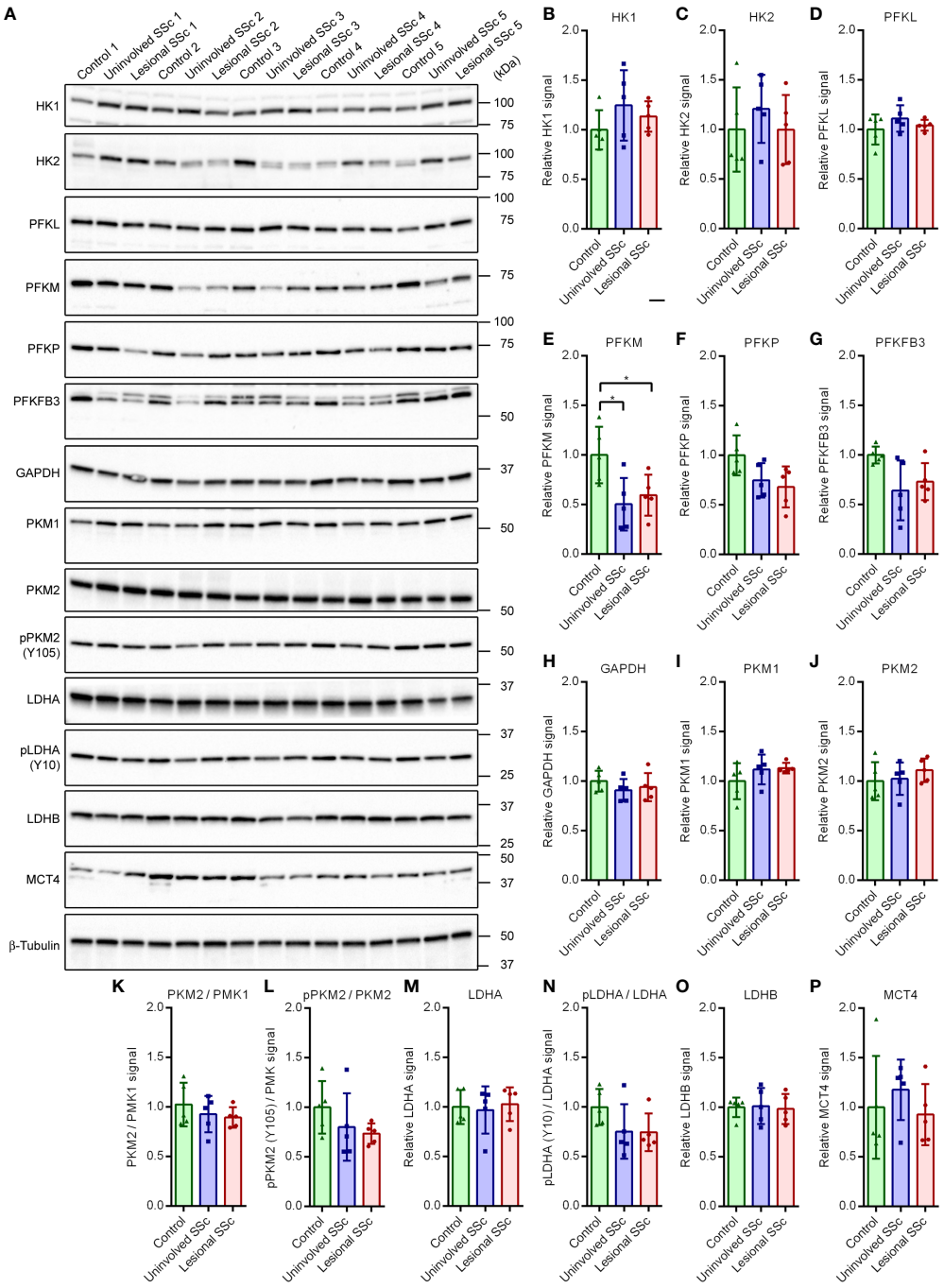

FIGURE 3
Muscle-type phosphofructokinase (PFKM) protein expression is decreased in SSc fibroblasts but the expression of other key enzymes of the glycolytic pathway and lactate secretion are unaffected. **(A)** Western blots with samples from five control, and five paired uninvolved and lesional SSc fibroblast cultures probed with antibodies against enzymes of the glycolytic pathway and lactate secretion as indicated. Blots were reprobed with an antibody against β-tubulin to confirm even loading. Migration of protein standards is shown. **(B–P)** Mean signals of the indicated proteins or protein ratios, normalized for the β-tubulin signal and expressed relative to the mean value of the control samples. Data points show relative values of the individual samples. Error bars indicate standard deviations. Asterisks denote statistically significant differences (*P<0.05).

Pyruvate kinase catalyzes the conversion of phosphoenolpyruvate to pyruvate in the terminal step of glycolysis (Supplementary Figure S1). Isoform PKM1 is expressed in most adult tissues, whereas isoform PKM2 is expressed during embryonic development and is the dominant isoform in tumors (28). PKM2 can switch from a dimeric, inactive to a tetrameric, active form. Formation of tetrameric PKM2 is inhibited by phosphorylation at Tyr residue 105 (pPKM2 (Y105)). Phosphorylation promotes aerobic glycolysis (29). Moreover, in response to glucose restriction, PKM2 translocates to the nucleus and acts as a transcriptional co-activator or protein kinase in cancer stem cells, modulating the metabolic flux (30, 31). Our western blots showed no differences in the expression levels of PKM1 and PKM2, the ratio of PKM2 *versus* PKM1, or the degree of phosphorylation of PKM2 between control and SSc samples (Figures 3I–L).

Lactate dehydrogenase catalyzes the reversible conversion of pyruvate and NADH to lactate and NAD^+. Isoform LDHA possesses a higher affinity for pyruvate and preferentially converts pyruvate and NADH to lactate and NAD^+. In contrast, isoform LDHB has a higher affinity for lactate and preferentially converts lactate and NAD^+ to pyruvate and NADH (Supplementary Figure S1). LDHA phosphorylated at residue Tyr10 (pLDHA (Y10)) is found in a variety of human cancer cells. Phosphorylation enhances LDHA activity to promote aerobic glycolysis (32). On western blots we found similar expression levels of LDHA and LDHB, and the degree of phosphorylation of LDHA (Figures 3M–O).

Monocarboxylate transporters transfer lactate, pyruvate and other monocarboxylates across the plasma membrane. MCT4 facilitates the release of lactate from the cell (Supplementary Figure S1). Its expression is promoted by catabolic transcription factors, such as nuclear factor κ-light-chain-enhancer of activated B cells (NF-κB) (33). Expression levels of MCT4 varied in the different cultures, but we did not detect significant differences between control and SSc fibroblasts on western blots (Figure 3P). Taken together, our western blot analysis of key enzymes of the glycolysis and lactate secretion revealed a decrease of PFKM protein expression levels in SSc fibroblasts compared to controls, but expression levels of other enzymes appeared unaffected.

Expression levels of subunits of the oxidative phosphorylation enzyme complexes

The mitostress tests demonstrated increased oxidative phosphorylation in the SSc fibroblasts. To investigate this further, we determined the expression levels of representative subunits of each of the five oxidative phosphorylation enzyme complexes on western blots (Figure 4A). The blots indicated that expression levels of subunit NDUFB6 of Complex I were significantly decreased in SSc fibroblasts compared to controls (Figure 4B). Conversely, expression levels of the SDHA subunit of complex II were comparable in SSc and control fibroblasts (Figure 4C). Parallel to NDUFB6, however, the expression levels of the UQCRC2 subunit of Complex III and the MTCO1 subunit of Complex IV were decreased in SSc fibroblasts (Figures 4D, E). On the other hand, expression levels of the ATP5A subunit of Complex V showed no significant differences between SSc fibroblasts and controls (Figure 4F). Thus, our results suggest that the oxidative phosphorylation complexes I, III and IV that together form the respirasome supercomplex (34) are decreased in SSc fibroblasts, whereas levels of complexes II and V remain unchanged.

Citrate synthase activity

Citrate synthase is an enzyme of the mitochondrial TCA cycle (Supplementary Figure S1). Citrate synthase is commonly used as biomarker for mitochondrial density in cells (35–37). Although citrate synthase activity showed some variation in the different fibroblast cultures, we did not observe significant differences between SSc and control cells (Figure 4G).

Mitochondrial network morphology

The mitochondrial network in cells is continuously re-modelled through fission and fusion events to adapt to changing physiological conditions (38). Mitochondrial fission generates new organelles and contributes to quality control by facilitating purging of damaged organelles *via* mitophagy. Mitochondrial fusion helps to mitigate stress through complementation of damaged mitochondria and is thought to increase mitochondrial ATP production. We investigated the mitochondrial network morphology in the SSc and control fibroblast cultures through live cell staining with the mitochondrial selective dye TMRM (Figure 5A). Analyses of the images revealed that there was no significant difference between the mitochondrial footprint per cell of SSc and control cultures; however, the mean length of the mitochondrial rods and branches, and the mean number of branches per mitochondrial network were increased in uninvolved SSc fibroblasts compared to controls. In the lesional SSc fibroblasts, these two parameters were still further increased (Figures 5B, C). These findings indicate that SSc fibroblasts have a hyperfused mitochondrial network.

Expression levels of proteins involved in mitochondrial fission and fusion

Mitochondrial network morphology is governed by the balance of mitochondrial fission and fusion events (39). To investigate how this balance is changed in SSc fibroblasts, we determined the

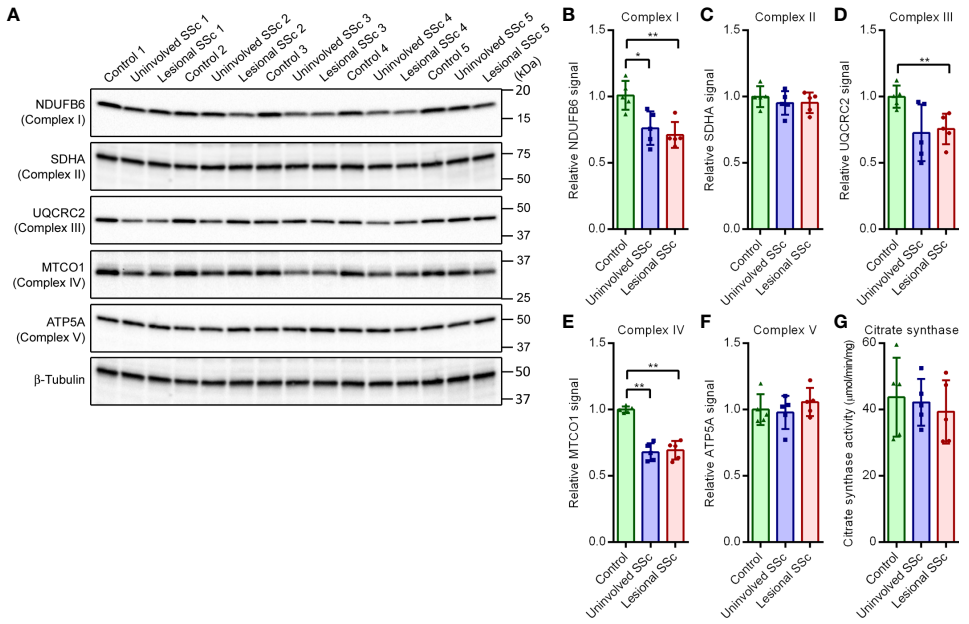

FIGURE 4
Subunits of OXPHOS enzyme complexes I, III and IV show decreased expression in SSc fibroblasts but subunits of OXPHOS enzyme complexes II and V, and citrate synthase activity are unaffected. **(A)** Western blots with samples from five control, and five paired uninvolved and lesional SSc fibroblast cultures probed with antibodies against subunits of the OXPHOS complexes as indicated. Blots were reprobed with an antibody against β-tubulin to confirm even loading. Migration of protein standards is shown. **(B–F)** Mean signals of the indicated proteins, normalized for the β-tubulin signal and expressed relative to the mean value of the control samples. Data points show relative values of the individual samples. **(G)** Mean citrate synthase activity of five control, and five paired uninvolved and lesional SSc fibroblast cultures. Data points show values of the individual samples. Error bars indicate standard deviations. Asterisks denote statistically significant differences (*P <0.05, **P<0.01).

expression levels of dynamin-related GTPases and adaptors/receptors that mediate mitochondrial modelling (Supplementary Figure S1) by western blot analyses (Figure 6A). The GTPase DRP1 is a mainly cytosolic protein that plays a central role in mitochondrial fission. Western blot analysis revealed that the expression levels of DRP1 were slightly, but statistically significant, lower in SSc fibroblasts compared to controls (Figure 6B). Phosphorylation of DRP1 at residue Ser616 (pDRP

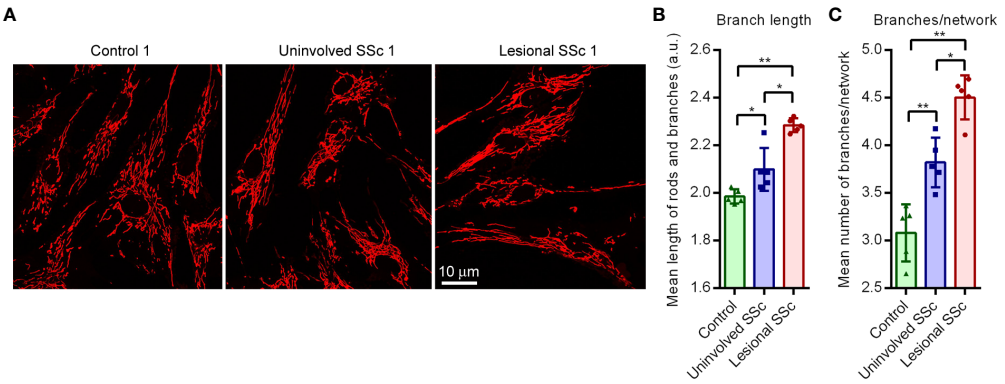

FIGURE 5
Cultured SSc fibroblasts have hyperfused mitochondrial networks. **(A)** Representative fluorescent micrographs of TMRM-stained control, uninvolved SSc and corresponding lesional SSc fibroblasts. **(B)** Mean length of mitochondrial rods and branches in arbitrary units (a.u.), and **(C)** mean number of branches per mitochondrial network in fibroblasts of five control and five paired uninvolved and lesional SSc cultures. Data point represent the mean length or the number of branches per network in 17–58 cells of the 15 individual cultures. Error bars indicate standard deviations. Asterisks denote statistically significant differences (*P <0.05, **P<0.01).

(S616)) promotes mitochondrial fission (40), whereas phosphorylation of DRP1 at residue Ser637 (pDRP (S637)) promotes mitochondrial fusion (41, 42). Our western blots showed that the ratios of pDRP (S616) *versus* total DRP1 were similar in the control and SSc samples (Figure 6C). We did not detect pDRP1 (S637) on western blots, even after prolonged exposure (Supplementary Figure S2). The recruitment of cytosolic DRP1 to mitochondria is a key step in mitochondrial fission. MFF, and the paralogues MIEF1 (also known as MiD51 or SMCR7L) and MIEF2 (also known as MiD49 or SMCR7) are the receptor and adaptor proteins for DRP1 recruitment to the mitochondrial surface (43, 44). We found comparable expression levels of MIEF1 and MFF in control and SSc samples; however, expression levels of MIEF2 were significantly higher in lesional SSc fibroblasts than in control fibroblasts (Figures 6D–F).

Fusion of the inner mitochondrial membrane is mediated by the GTPase OPA1, whereas fusion of the outer mitochondrial membrane is mediated by the GTPase paralogues MFN1 and MFN2 (39). Processing of so-called long OPA1 (L-OPA1) by multiple proteases generates short OPA1 (S-OPA1) forms (45). Fusion of the inner mitochondrial membrane depends on the equilibrium between L-OPA1 and S-OPA1. The western blots showed similar levels of MFN1 and MFN2 in control and SSc fibroblasts (Figures 6G, H). On the other hand, the ratios of L-OPA1 *versus* S-OPA1 were higher in the SSc samples than in the controls (Figure 6I). This may favor mitochondrial fusion.

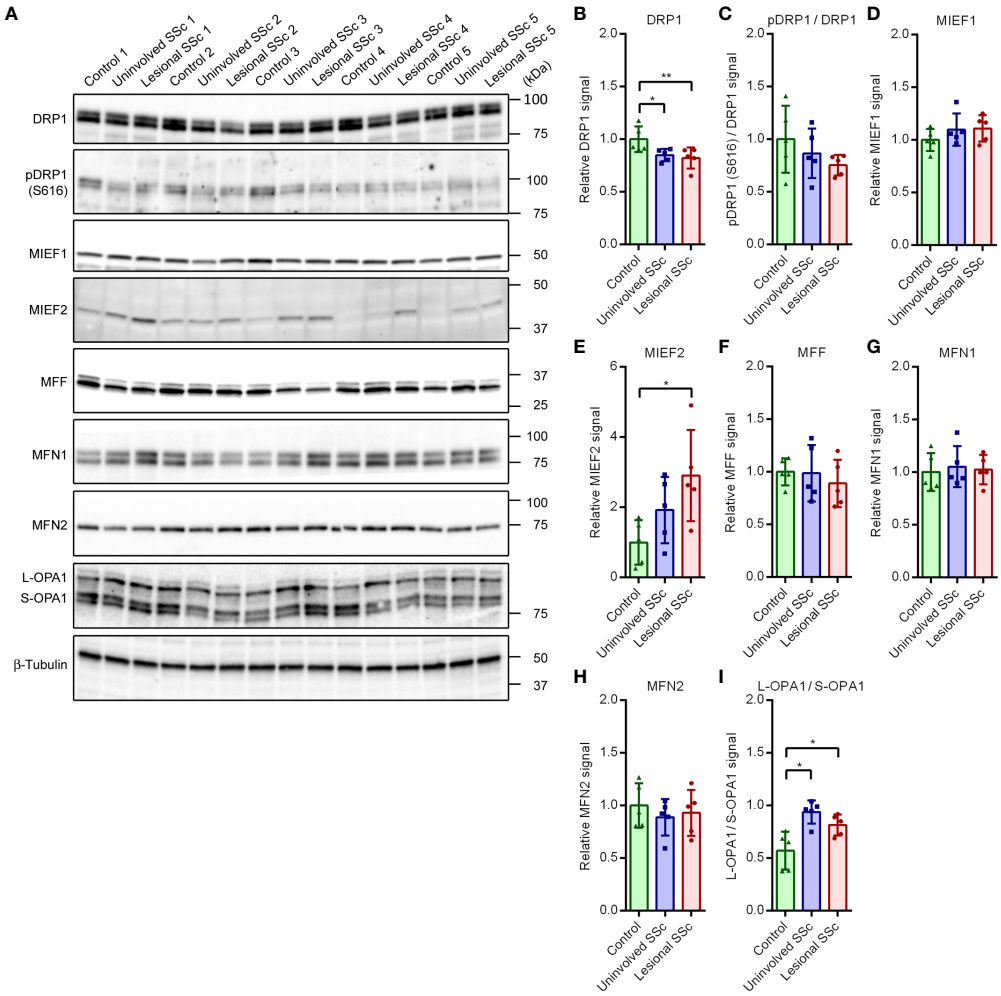

FIGURE 6
Expression of proteins engaged in mitochondrial fission and fusion shift in SSc fibroblasts to promote fusion. **(A)** Western blots with samples from five control, and five paired uninvolved and lesional SSc fibroblast cultures probed with antibodies against proteins involved in mitochondrial fission and fusion as indicated. Blots were reprobed with an antibody against β-tubulin to confirm even loading. Migration of protein standards is shown. **(B–I)** Mean signals of the indicated proteins, normalized for the β-tubulin signal and expressed relative to the mean value of the control samples or given as a ratio. Data points show relative values of the individual samples. Error bars indicate standard deviations. Asterisks denote statistically significant differences (*P<0.05, **P<0.01).

Expression levels of fibrotic markers in TGF-β1-activated fibroblasts treated with kinase inhibitors

When we compared the energy metabolism of SSc and healthy control fibroblasts, we observed no difference in glycolysis but noticed a small increase in respiration coupled to ATP production (Figure 2). To explore whether further induction of the fibrotic phenotype of SSc fibroblasts leads to additional increases in mitochondrial respiration and, possibly, glycolysis, cultures were treated with TGF-β1. This cytokine is a well-known activator of fibrotic genes and has long been implicated in the pathogenesis of SSc (46). In addition, we tested whether three small molecule kinase inhibitors, SB431542, AZD1208 and KU55933, were able to reverse the effects of TGF-β1 treatment. SB431542 is a specific inhibitor of the TGF-β1 activin receptor-like kinase (ALK)-4, -5 and -7 (47). AZD1208 is a specific inhibitor of Proviral Integration site for Moloney murine leukemia virus (PIM) kinase-1, -2 and -3 (48). KU55933 is a selective Ataxia-Telangiectasia Mutated (ATM) kinase inhibitor (49). These inhibitors are known to suppress matrix production, modulate cell proliferation and regulate differentiation programs (50–52).

First, we investigated the effect of TGF-β1 and the three kinase inhibitors on the expression levels of the fibrotic markers fibronectin, Col-1, α-SMA, and Connective Tissue Growth Factor (CTGF) in lesional SSC and control fibroblast cultures. Western blots showed that TGF-β1 treatment markedly induced the expression levels of the four fibrotic markers in both cell types (Figure 7). Treatment with SB431542 completely prevented the increase in expression of the fibrotic markers in TGF-β1-treated cells (Figure 7A; Supplementary Figures S3A–D). AZD1208 treatment, in contrast, had no effect on the expression levels of the fibrotic markers (Figure 7B; Supplementary Figures S3E–H), whereas KU55933 prevented the TGF-β1-induced expression of COL-1, α-SMA and CTGF in control and lesional fibroblasts (Figure 7C; Supplementary Figures S3I–L).

Glycolysis and mitochondrial respiration in TGF-β1-activated lesional SSc fibroblasts treated with kinase inhibitors

Finally, we studied of effects of TGF-β1 activation with or without SB431542, AZD1208 or KU55933 treatment on energy metabolism in lesional SSc fibroblast cultures. We first performed glycolytic stress tests on the Seahorse platform (Figure 8A). The combined results of four different lesional SSc cultures demonstrated that TGF-β1 activation tripled the basal glycolysis as well as the glycolytic capacity (Figure 8B). SB431542 and KU55933 treatment counteracted the glycolytic stimulation of TGF-β1 but AZD1208 treatment had no significant effect. We then carried out mitostress tests to assess mitochondrial respiration (Figure 8C). The compiled data of four different lesional SSc cultures indicated that basal respiration and respiration coupled to ATP production quadrupled after TGF-β1 activation, while maximal respiration more than doubled and spare respiratory capacity increased by about half (Figure 8D). SB431542 treatment prevented the stimulatory effects of TGF-β1 on basal and maximal respiration, and respiration coupled to ATP production. AZD1208 treatment had no significant effect on TGF-β1-

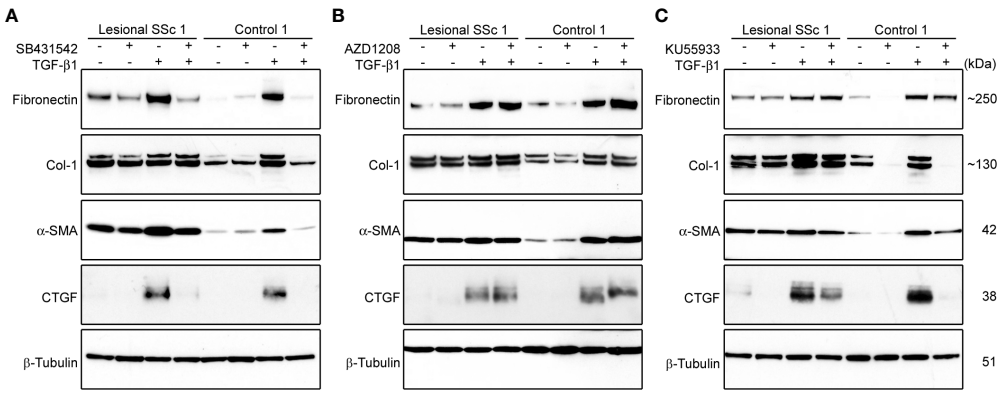

FIGURE 7
The kinase inhibitors SB431542 and KU55933, but not AZD1208, prevent TGF-β1-induced overexpression of α-SMA and ECM proteins in lesional SSc and control fibroblasts. **(A–C)** Western blots with samples from a lesional SSc and a control fibroblast culture treated vehicle or 2 ng/ml of TGF-β1 and/or 10 μM SB431542, 20 μM AZD1208 or 5 μM KU55933, and probed with antibodies against α-SMA or ECM proteins as indicated. Blots were reprobed with an antibody against β-tubulin to verify even loading.

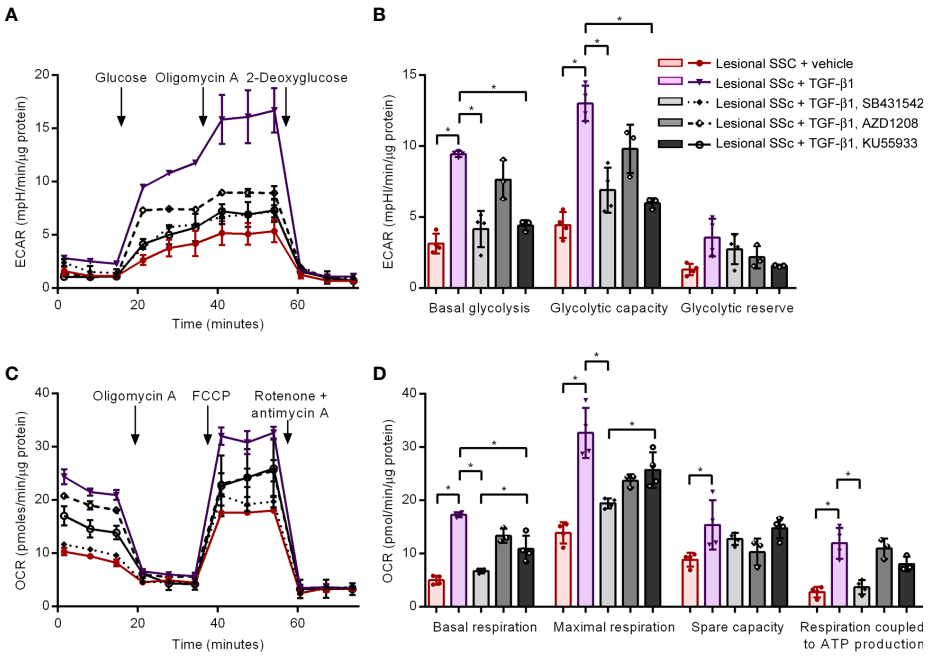

FIGURE 8
The kinase inhibitors SB431542 and KU55933, but not AZD1208, prevent TGF-β1-induced increases in glycolysis and mitochondrial respiration in lesional SSc fibroblasts. **(A)** Extracellular acidification rates (ECAR) in representative glycolysis stress tests of a lesional SSc fibroblast culture treated vehicle or 2 ng/ml of TGF-β1 with or without 10 µM SB431542, 20 µM AZD1208 or 5 µM KU55933. Glucose, oligomycin A and 2-deoxyglucose were sequentially added to delineate glycolytic function. Error bars indicate standard deviation of technical triplicates. **(B)** Mean basal glycolysis, glycolytic capacity and glycolytic reserve of four lesional SSc fibroblast cultures treated vehicle or 2 ng/ml of TGF-β1 with or without 10 µM SB431542, 20 µM AZD1208 or 5 µM KU55933. Error bars indicate standard deviation. **(C)** Oxygen consumption rates (OCR) in representative mitostress tests of a lesional SSc fibroblast culture treated vehicle or 2 ng/ml of TGF-β1 with or without 10 µM SB431542, 20 µM AZD1208 or 5 µM KU55933. Oligomycin A, FCCP and rotenone + antimycin A were sequentially added to delineate mitochondrial respiratory function. Error bars indicate standard deviation of technical triplicates. **(D)** Mean basal respiration, maximal respiration, spare respiratory capacity and respiration coupled to ATP production of four lesional SSc fibroblast cultures treated vehicle or 2 ng/ml of TGF-β1 with or without 10 µM SB431542, 20 µM AZD1208 or 5 µM KU55933. Error bars indicate standard deviation. Asterisks denote statistically significant differences (*P<0.05).

stimulated respiration. KU55933 treatment significantly reduced the TGF-β1-stimulated basal respiration but not as potent as SB431542.

Discussion

The objective of this study was to investigate the remodeling of energy metabolism in cell culture models of SSc in order to develop therapeutic strategies that target the disrupted metabolism and reverse the fibrotic phenotype. Although metabolic remodeling has been documented in other fibrotic diseases, studies of the role of energy metabolism in SSc are limited (53, 54). First, we compared paired fibroblasts cultures derived from uninvolved and lesional skin of five SSc patients with dermal fibroblast cultures from five control subjects. Western blot analyses for the fibrotic markers α-SMA and COL-1 confirmed the fibrotic phenotype of SSc fibroblasts. Glycolytic stress tests did not reveal differences in glycolysis between SSC and control cultures. It is of course possible that our experiments are underpowered and that a larger number of patient and control samples would reveal a difference. The mitostress tests, however, exposed a small but significant increase in mitochondrial respiration coupled to ATP production at the expense of the spare respiratory capacity. These results suggest that SSc fibroblasts boost their oxidative phosphorylation to meet the increased bioenergetic demand of enhanced ECM protein synthesis and proliferation.

Assessment of the expression levels of key, rate-limiting enzymes of the glycolytic pathway and lactate secretion on western blots showed that levels of the phosphofructokinase 1 isoform PFKM were significantly lower in SSc fibroblasts compared to control fibroblasts, while levels of the isoforms PFKL and PFKP were unaffected. Of the three isoforms, PFKM has the highest affinities for fructose 6-phosphate and ATP. In addition, PFKM is the least sensitive to fructose 2,6-bisphosphate allosteric modulation and ATP inhibition (23). In other words, PFKM is the most active enzyme but is less

adaptable than PFKL and PFKP. Therefore, the lower PFKM expression suggests that glycolytic regulation may be of greater importance than activity for SSc fibroblast.

We also determined the expression levels of representative subunits of each of the five oxidative phosphorylation enzyme complexes by western blotting. Our results indicated that subunits of the oxidative phosphorylation complexes I, III and IV are decreased by ~25% in SSc fibroblasts compared to control samples, whereas levels of complexes II and V remain unchanged. The mitochondrial footprint and the activity of the TCA cycle enzyme citrate synthase in SSc fibroblasts corresponded to that of controls, suggesting that the mitochondrial mass in the cells is unaffected. Complexes I, III and IV form a supercomplex called the respirasome (34). When taken together, our results suggest that the number of respirasomes decrease in mitochondria of SSc fibroblasts. This is an unexpected finding because basal respiration and respiratory capacity did not change in SSc fibroblasts. Possibly, post-transcriptional modifications of the respirasome modulate its activity to increase coupling to ATP production. Mitochondrial morphology is controlled by energy metabolism. Live cell staining of the mitochondrial network demonstrated that SSc fibroblasts have a hyperfused network. Mitochondrial fusion is known to be driven by bioenergetic demand and stress (38). Fusion of mitochondria is thought to increase mitochondrial ATP production through complementation. Thus, the mitochondrial hyperfusion in SSc fibroblasts may promote respiration coupled to ATP production, reflecting the increased bioenergetic demand of the cells.

When we investigated the molecular basis of mitochondrial hyperfusion in SSc fibroblasts by western blot analyses of proteins involved in mitochondrial modelling, we found that the fission promoting protein DRP1 was decreased in SSc fibroblasts compared to controls; however, we did not find changes in the level of post-transcriptional phosphorylation of DRP1. As the phosphorylation determines the activity of DRP1 (55), the decreased levels of total DRP1 in SSc fibroblasts do not explain the mitochondrial hyperfusion in these cells. The western blots also revealed that MIEF2 was increased in SSc fibroblasts. MIEF2 acts as an adaptor of DRP1 and its receptor MFF, linking DRP1 with MFF on the mitochondrial surface (44). The higher levels of MIEF2 may recruit inactive DRP1 to the mitochondrial surface resulting in mitochondrial elongation (56). Alternatively, the upregulation of MIEF2 may sequester DRP1 in DRP1-MIEF2-MFF as well as DRP1-MIEF2 complexes, inhibiting direct interaction between DRP1 and MFF and resulting in mitochondrial fusion (57). In addition, western blot analyses indicated that the ratio of L-OPA1 *versus* S-OPA1 were higher in SSc fibroblasts than in the control cells. The inner mitochondrial membrane embedded protein L-OPA1 is processed by multiple proteases to S-OPA proteins that have lost their membrane spanning N-terminus. Fusion of the inner membrane is determined by the balance between L-OPA1 and S-OPA1 (39). The observed shift towards L-OPA in SSc fibroblasts may favor mitochondrial fusion.

In the final experiments, we compared lesional SSc fibroblasts with their TGF-β1-induced myofibroblast derivatives to mimic a more advanced stage of fibrosis. Western blot analyses for the fibrotic markers CTGF, α-SMA, COL-1 and fibronectin demonstrated that TGF-β1 treatment induced the expression of all four fibrotic markers, confirming myofibroblast differentiation. To dissect the key signaling pathways in addition to determining the role of classical TGF-β1 signaling (*via* the kinase ALK5), we also explored the role of two other pathways regulated by PIM kinase (58) and ATM kinase (59) that have been shown to have a role in fibrosis. Co-treatment with the TGF-β1 receptor/ALK5 inhibitor SB431542 completely prevented the TGF-β1-induced expression of the fibrotic markers, whereas co-treatment with the pan-PIM kinase inhibitor AZ1208 was ineffective. Co-treatment with the ATM kinase inhibitor KU55933 prevented the TGF-β1-induced expression of COL-1, α-SMA and CTGF. Glycolytic and mitostress tests demonstrated that TGF-β1 robustly stimulated basal glycolysis and glycolytic capacity, as well as basal and maximal respiration, and respiration coupled to ATP production. TGF-β1-mediated stimulation of glycolysis and glutaminolysis, but not of mitochondrial respiration, was reported in normal human dermal fibroblasts by Henderson et al. (60). However, Bernard et al. (61, 62) and Bates et al. (63) reported a TGF-β1-mediated stimulation of glycolysis and mitochondrial respiration in normal human lung fibroblasts and human primary hepatic stellate cells, respectively. In addition, increased mitochondrial respiration and content has been documented during TGF-β1-mediated differentiation of NIH/3T3 mouse fibroblasts (64) and an upregulation of mitochondrial mass has been reported in TGF-β1-treated normal human lung fibroblasts (65). Thus, our results with SSc dermal fibroblasts are generally supported by findings in other laboratories. Interestingly, co-treatment with SB431542 and KU55933 neutralized the TGF-β1-mediated stimulation of glycolysis and mitochondrial respiration, but AZD1208 treatment had no significant effect. The differential impact of TGF-β1 signaling *via* the canonical Smad pathway, and the PIM and ATM kinase on fibroblast energy generation highlights additional pathways to those previously identified (mTOR/AMPK/p38) as potentially critical to fibroblast metabolism underpinning scarring and fibrosis (61, 66, 67). The interaction(s) between these pathways and the mechanisms involved leading to fibrogenesis are being actively studied and once fully elucidated will allow identification of new markers and crucial candidates for the management and treatment of tissue fibrosis.

Data availability statement

The raw data supporting the conclusions of this article will be made available by the authors, without undue reservation.

Ethics statement

This study was reviewed and approved by Research Ethics Committee (reference: 6398) of the NHS Health Research Authority (NRES Committee London-Hampstead). The patients/participants provided their written informed consent to participate in this study.

Author contributions

Conception and design: DA, JA-H and J-WT. Provision of patients: VO and CD. Collection and preservation of cell cultures: XS. Collection and analysis of results: IC, HL (Xi'an), HL (UCL), VR and JWT. Drafting of manuscript and preparation of figures: J-WT. Editing of manuscript: MP, GX, JL-F, JA-H, DA and J-WT. All authors contributed to the article and approved the submitted version.

Funding

IC was supported by the Conselho Nacional de Desenvolvimento Científico e Tecnológico and Ciência Sem Fronteiras, Brazil. HL (Xi'an) was a recipient of a University Graduate Students Studying Abroad awarded from the Chinese Scholarship Council. HL (UCL) was awarded a Wellcome Trust Biomedical Vacation Scholarship (code: 213295/Z/18/Z). DA obtained funding from Versus Arthritis (formerly Arthritis Research UK; codes: 21810 and 19427), the Royal Free Charity (Fund 97), Scleroderma and Raynaud's UK, and The Rosetrees Trust (code: M96-F1/F2). J-WT obtained funding from the Royal Free Charity (Fund 42).

Acknowledgments

We acknowledge the support from Ms Korsa Khan and Ms Bahja Ahmed Abdi for laboratory management, and Dr Ioannis Papaioannou for technical expertise.

Conflict of interest

The authors declare that the research was conducted in the absence of any commercial or financial relationships that could be construed as a potential conflict of interest.

Publisher's note

Supplementary material

The Supplementary Material for this article can be found online at: https://www.frontiersin.org/articles/10.3389/fimmu.2022.1004949/full#supplementary-material

References

1. Allanore Y, Simms R, Distler O, Trojanowska M, Pope J, Denton CP, et al. Systemic sclerosis. *Nat Rev Dis Primer* (2015) 1:1. doi: 10.1038/nrdp.2015.2

2. Denton CP, Khanna D. Systemic sclerosis. *Lancet* (2017) 390:1685–99. doi: 10.1016/S0140-6736(17)30933-9

3. Varga J, Abraham D. Systemic sclerosis: A prototypic multisystem fibrotic disorder. *J Clin Invest* (2007) 117:557–67. doi: 10.1172/JCI31139

4. Denton CP, Ong VH. Targeted therapies for systemic sclerosis. *Nat Rev Rheumatol* (2013) 9:451–64. doi: 10.1038/nrrheum.2013.46

5. Vercellino I, Sazanov LA. The assembly, regulation and function of the mitochondrial respiratory chain. *Nat Rev Mol Cell Biol* (2022) 23:141–61. doi: 10.1038/s41580-021-00415-0

6. Warburg O, Wind F, Negelein E. The metabolism of tumors in the body. *J Gen Physiol* (1927) 8:519–30. doi: 10.1085/jgp.8.6.519

7. Lunt SY, vander Heiden MG. Aerobic glycolysis: Meeting the metabolic requirements of cell proliferation. *Annu Rev Cell Dev Biol* (2011) 27:441–64. doi: 10.1146/annurev-cellbio-092910-154237

8. Huber HJ, Dussmann H, Kilbride SM, Rehm M, Prehn JHM. Glucose metabolism determines resistance of cancer cells to bioenergetic crisis after cytochrome-c release. *Mol Syst Biol* (2011) 7:470. doi: 10.1038/msb.2011.2

9. Henderson J, O'Reilly S. The emerging role of metabolism in fibrosis. *Trends Endocrinol Metab* (2021) 32:639–53. doi: 10.1016/j.tem.2021.05.003

10. Vincent AS, Phan TT, Mukhopadhyay A, Lim HY, Halliwell B, Wong KP. Human skin keloid fibroblasts display bioenergetics of cancer cells. *J Invest Dermatol* (2008) 128:702–9. doi: 10.1038/sj.jid.5701107

11. Kottmann RM, Kulkarni AA, Smolnycki KA, Lyda E, Dahanayake T, Salibi R, et al. Lactic acid is elevated in idiopathic pulmonary fibrosis and induces myofibroblast differentiation *via* pH-dependent activation of transforming growth factor-β. *Am J Respir Crit Care Med* (2012) 186:740–51. doi: 10.1164/rccm.201201-0084OC

12. Xie N, Tan Z, Banerjee S, Cui H, Ge J, Liu R-M, et al. Glycolytic reprogramming in myofibroblast differentiation and lung fibrosis. *Am J Respir Crit Care Med* (2015) 192:1462–74. doi: 10.1164/rccm.201504-0780OC

13. Bueno M, Lai YC, Romero Y, Brands J, St Croix CM, Kamga C, et al. PINK1 deficiency impairs mitochondrial homeostasis and promotes lung fibrosis. *J Clin Invest* (2015) 125:521–38. doi: 10.1172/JCI74942

14. Ryan J, Dasgupta A, Huston J, Chen KH, Archer SL. Mitochondrial dynamics in pulmonary arterial hypertension. *J Mol Med (Berl)* (2015) 93:229–42. doi: 10.1007/s00109-015-1263-5

15. Sutendra G, Bonnet S, Rochefort G, Haromy A, Folmes KD, Lopaschuk GD, et al. Fatty acid oxidation and malonyl-CoA decarboxylase in the vascular remodeling of pulmonary hypertension. *Sci Transl Med* (2010) 2:44ra58. doi: 10.1126/scitranslmed.3001327

16. Chen Y, Choi SS, Michelotti GA, Chan IS, Swiderska-Syn M, Karaca GF, et al. Hedgehog controls hepatic stellate cell fate by regulating metabolism. *Gastroenterology* (2012) 143:1319–29. doi: 10.1053/j.gastro.2012.07.115

17. Ding H, Jiang L, Xu J, Bai F, Zhou Y, Yuan Q, et al. Inhibiting aerobic glycolysis suppresses renal interstitial fibroblast activation and renal fibrosis. *Am J Physiol Renal Physiol* (2017) 313:F561–75. doi: 10.1152/ajprenal.00036.2017

18. Park IH, Lerou PH, Zhao R, Huo H, Daley GQ. Generation of human-induced pluripotent stem cells. *Nat Protoc* (2008) 3:1180–6. doi: 10.1038/nprot.2008.92

19. Protasoni M, Kroon AM, Taanman JW. Mitochondria as oncotarget: a comparison between the tetracycline analogs doxycycline and COL-3. *Oncotarget* (2018) 9:33818–31. doi: 10.18632/oncotarget.26107

20. Valente JA, Maddalena LA, Robb EL, Moradi F, Stuart JA. A simple ImageJ macro tool for analyzing mitochondrial network morphology in mammalian cell culture. *Acta Histochem* (2017) 119:315–26. doi: 10.1016/j.acthis.2017.03.001

21. Smith TA. Mammalian hexokinases and their abnormal expression in cancer. *Br J BioMed Sci* (2000) 57:170–8.

22. Vora S, Seaman C, Durham S, Piomelli S. Isozymes of human phosphofructokinase: identification and subunit structural characterization of a new system. *Proc Natl Acad Sci USA* (1980) 77:62–6. doi: 10.1073/pnas.77.1.62

23. Fernandes PM, Kinkead J, McNae I, Michels PAM, Walkinshaw MD, Fernandes PM, et al. Biochemical and transcript level differences between the three human phosphofructokinases show optimisation of each isoform for specific metabolic niches. *Biochem J* (2020) 477:4425–41. doi: 10.1042/BCJ20200656

24. Rider MH, Bertrand L, Vertommen D, Michels PA, Rousseau GG, Hue L. 6-phosphofructo-2-kinase/fructose-2,6-bisphosphatase: head-to-head with a bifunctional enzyme that controls glycolysis. *Biochem J* (2004) 381:561–79. doi: 10.1042/BJ20040752

25. Atsumi T, Chesney J, Metz C, Leng L, Donnelly S, Makita Z, et al. High expression of inducible 6-phosphofructo-2-kinase/fructose-2,6-bisphosphatase (iPFK-2; PFKFB3) in human cancers. *Cancer Res* (2002) 62:5881–7.

26. Yi M M, Ban Y, Tan Y, Xiong W, Li G, Xiang B. 6-Phosphofructo-2-kinase/fructose-2,6-biphosphatase 3 and 4: A pair of valves for fine-tuning of glucose metabolism in human cancer. *Mol Metab* (2019) 20:1–13. doi: 10.1016/j.molmet.2018.11.013

27. Barber RD, Harmer DW, Coleman RA, Clark BJ. GAPDH as a housekeeping gene: analysis of GAPDH mRNA expression in a panel of 72 human tissues. *Physiol Genomics* (2005) 21:389–95. doi: 10.1152/physiolgenomics.00025.2005

28. Christofk HR, Vander Heiden MG, Harris MH, Ramanathan A, Gerszten RE, Wei R, et al. The M2 splice isoform of pyruvate kinase is important for cancer metabolism and tumour growth. *Nature* (2008) 452:230–3. doi: 10.1038/nature06734

29. Hitosugi T, Kang S, Vander Heiden MG, Chung T-W, Elf S, Lythgoe K, et al. Tyrosine phosphorylation inhibits PKM2 to promote the warburg effect and tumor growth. *Sci Signal* (2009) 2:ra73. doi: 10.1126/scisignal.2000431

30. Wang H-J, Hsieh Y-J, Cheng W-C, Lin C-P, Lin Y-S, Yang S-F, et al. JMJD5 regulates PKM2 nuclear translocation and reprograms HIF-1α-mediated glucose metabolism. *Proc Natl Acad Sci USA* (2014) 111:279–84. doi: 10.1073/pnas.1311249111

31. Yang Y-C, Chien M-H, Liu H-Y, Chang Y-C, Chen C-K, Lee W-J, et al. Nuclear translocation of PKM2/AMPK complex sustains cancer stem cell populations under glucose restriction stress. *Cancer Lett* (2018) 421:28–40. doi: 10.1016/j.canlet.2018.01.075

32. Fan J, Hitosugi T, Chung T-W, Xie J, Ge Q, Gu T-L, et al. Tyrosine phosphorylation of lactate dehydrogenase a is important for NADH/NAD^+ redox homeostasis in cancer cells. *Mol Cell Biol* (2011) 31:4938–50. doi: 10.1128/MCB.06120-11

33. Wilde L, Roche M, Domingo-Vidal M, Tanson K, Philp N, Curry J, et al. Metabolic coupling and the reverse warburg effect in cancer: Implications for novel biomarker and anticancer agent development. *Semin Oncol* (2017) 44:198–203. doi: 10.1053/j.seminoncol.2017.10.004

34. Gu J, Wu M, Guo R, Yan K, Lei J, Gao N, et al. The architecture of the mammalian respirasome. *Nature* (2016) 537:639–43. doi: 10.1038/nature19359

35. Hood D, Zak R, Pette D. Chronic stimulation of rat skeletal muscle induces coordinate increases in mitochondrial and nuclear mRNAs of cytochrome c oxidase subunits. *Eur J Biochem* (1989) 179:275–80. doi: 10.1111/j.1432-1033.1989.tb14551.x

36. Renner K, Amberger A, Konwalinka G, Kofler R, Gnaiger E. Changes of mitochondrial respiration, mitochondrial content and cell size after induction of apoptosis in leukemia cells. *Biochim Biophys Acta* (2003) 1642:115–23. doi: 10.1016/s0167-4889(03)00105-8

37. Larsen S, Nielsen J, Neigaard Hansen C, Nielsen LB, Wibrand F, Stride N, et al. Biomarkers of mitochondrial content in skeletal muscle of healthy young human subjects. *J Physiol* (2012) 590:3349–60. doi: 10.1113/jphysiol.2012.230185

38. Youle JR, van der Bliek AM. Mitochondrial fission, fusion, and stress. *Science* (2012) 337:1062–5. doi: 10.1126/science.1219855

39. Giacomello M, Pyakurel A, Glytsou C, Scorrano L. The cell biology of mitochondrial membrane dynamics. *Nat Rev Mol Cell Biol* (2020) 21:204–24. doi: 10.1038/s41580-020-0210-7

40. Taguchi N, Ishihara N, Jofuku A, Oka T, Mihara K. Mitotic phosphorylation of dynamin-related GTPase Drp1 participates in mitochondrial fission. *J Biol Chem* (2007) 282:11521–29. doi: 10.1074/jbc.M607279200

41. Chang CR, Blackstone C. Cyclic AMP-dependent protein kinase phosphorylation of Drp1 regulates its GTPase activity and mitochondrial morphology. *J Biol Chem* (2007) 282:21583–7. doi: 10.1074/jbc.C700083200

42. Cribbs JT, Strack S. Reversible phosphorylation of Drp1 by cyclic AMP-dependent protein kinase and calcineurin regulates mitochondrial fission and cell death. *EMBO Rep* (2007) 8:939–44. doi: 10.1038/sj.embor.7401062

43. Losón OC, Song Z, Chen H, Chan DC. Fis1, mff, MiD49, and MiD51 mediate Drp1 recruitment in mitochondrial fission. *Mol Biol Cell* (2013) 24:659–67. doi: 10.1091/mbc.E12-10-0721

44. Yu R, Tong Liu T, Jin S-B, Ning C, Lendahl U, Nistér M, et al. MIEF1/2 function as adaptors to recruit Drp1 to mitochondria and regulate the association of Drp1 with mff. *Sci Rep* (2017) 7:880. doi: 10.1038/s41598-017-00853-x

45. Head B, Griparic L, Amiri M, Gandre-Babbe S, van der Bliek AM. Inducible proteolytic inactivation of OPA1 mediated by the OMA1 protease in mammalian cells. *J Cell Biol* (2009) 187:959–66. doi: 10.1083/jcb.200906083

46. Lafyatis R. Transforming growth factor β–at the centre of systemic sclerosis. *Nat Rev Rheumatol* (2014) 10:706–19. doi: 10.1038/nrrheum.2014.137

47. Inman GJ, Nicolás FJ, Callahan JF, Harling JD, Gaster LM, Reith AD, et al. SB-431542 is a potent and specific inhibitor of transforming growth factor-β superfamily type I activin receptor-like kinase (ALK) receptors ALK4, ALK5, and ALK7. *Mol Pharmacol* (2002) 62:65–74. doi: 10.1124/mol.62.1.65

48. Dakin LA, Block MH, Chen H, Code E, Dowling JE, Feng X, et al. Discovery of novel benzylidene-1,3-thiazolidine-2,4-diones as potent and selective inhibitors of the PIM-1, PIM-2, and PIM-3 protein kinases. *Bioorg Med Chem Lett* (2012) 22:4599–604. doi: 10.1016/j.bmcl.2012.05.098

49. Hickson I, Zhao Y, Richardson CJ, Green SJ, Martin NM, Orr AI, et al. Identification and characterization of a novel and specific inhibitor of the ataxia-telangiectasia mutated kinase ATM. *Cancer Res* (2004) 64:9152–59. doi: 10.1158/0008-5472.CAN-04-2727

50. Laping NJ, Grygielko E, Mathur A, Butter S, Bomberger J, Tweed C, et al. Inhibition of transforming growth factor (TGF)-β1-induced extracellular matrix with a novel inhibitor of the TGF-β type I receptor kinase activity: SB-431542. *Mol Pharmacol* (2002) 62:58–64. doi: 10.1124/mol.62.1.58

51. Li Y, Yang D-Q. The ATM inhibitor KU-55933 suppresses cell proliferation and induces apoptosis by blocking akt in cancer cells with overactivated akt. *Mol Cancer Ther* (2010) 9:113–25. doi: 10.1158/1535-7163.MCT-08-1189

52. Kreuz S, Holmes KB, Tooze RM, Lefevre PF. Loss of PIM2 enhances the anti-proliferative effect of the pan-PIM kinase inhibitor AZD1208 in non-Hodgkin lymphomas. *Mol Cancer* (2015) 14:205. doi: 10.1186/s12943-015-0477-z

53. Zhu H, Chen W, Liu D, Luo H. The role of metabolism in the pathogenesis of systemic sclerosis. *Metabolism* (2019) 93:44–51. doi: 10.1016/j.metabol.2018.12.004

54. O'Reilly S. Metabolic perturbations in systemic sclerosis. *Curr Opin Rheumatol* (2022) 34:91–4. doi: 10.1097/BOR.0000000000000824

55. Chang CR, Blackstone C. Dynamic regulation of mitochondrial fission through modification of the dynamin-related protein Drp1. *Ann N Y Acad Sci* (2010) 1201:34–9. doi: 10.1111/j.1749-6632.2010.05629.x

56. Atkins K, Dasgupta A, Chen K-H, Mewburn J, Archer SL. The role of Drp1 adaptor proteins MiD49 and MiD51 in mitochondrial fission: implications for human disease. *Clin Sci (Lond)* (2016) 130:1861–74. doi: 10.1042/CS20160030

57. Yu R, Lendahl U, Nistér M, Zhao J. Regulation of mammalian mitochondrial dynamics: Opportunities and challenges. *Front Endocrinol* (2020) 11:374. doi: 10.3389/fendo.2020.00374

58. Pham TX, Lee J, Jiazhen Guan J, Caporarello N, Meridew JA, Jones DL, et al. Transcriptional analysis of lung fibroblasts identifies PIM1 signaling as a driver of

aging-associated persistent fibrosis. *JCI Insight* (2022) 7:e153672. doi: 10.1172/jci.insight.153672

59. Daugherity EK, Balmus G, Al Saei A, Moore ES, Abi Abdallah D, Rogers AB, et al. The DNA damage checkpoint protein ATM promotes hepatocellular apoptosis and fibrosis in a mouse model of non-alcoholic fatty liver disease. *Cell Cycle* (2012) 11:1918–28. doi: 10.4161/cc.20259

60. Henderson J, Duffy L, Stratton R, Ford D, O'Reilly S, Henderson J, et al. Metabolic reprogramming of glycolysis and glutamine metabolism are key events in myofibroblast transition in systemic sclerosis pathogenesis. *J Cell Mol Med* (2020) 24:14026–38. doi: 10.1111/jcmm.16013

61. Bernard K, Logsdon NJ, Ravi S, Xie N, Persons BP, Rangarajan S, et al. Metabolic reprogramming is required for myofibroblast contractility and differentiation. *J Biol Chem* (2015) 290:25427–38. doi: 10.1074/jbc.M115.646984

62. Bernard K, Logsdon NJ, Benavides GA, Sanders Y, Jianhua Zhang J, Darley-Usmar VM, et al. Glutaminolysis is required for transforming growth factor-β1-induced myofibroblast differentiation and activation. *J Biol Chem* (2018) 293:1218–28. doi: 10.1074/jbc.RA117.000444

63. Bates J, Vijayakumar A, Ghoshal S, Marchand B, Yi S, Kornyeyev D, et al. Acetyl-CoA carboxylase inhibition disrupts metabolic reprogramming during hepatic stellate cell activation. *J Hepatol* (2020) 73:896–905. doi: 10.1016/j.jhep.2020.04.037

64. Negmadjanov U, Godic Z, Rizvi F, Emelyanova L, Ross G, Richards J, et al. TGF-β1-mediated differentiation of fibroblasts is associated with increased mitochondrial content and cellular respiration. *PloS One* (2015) 10:e0123046. doi: 10.1371/journal.pone.0123046

65. Sun Q, Fang L, Tang X, Lu S, Tamm M, Stolz D, et al. TGF-β upregulated mitochondria mass through the SMAD2/3→C/EBPβ→PRMT1 signal pathway in primary human lung fibroblasts. *J Immunol* (2019) 202:37–47. doi: 10.4049/jimmunol.1800782

66. Selvarajah B, Azuelos I, Anastasiou D, Chambers RC. Fibrometabolism–an emerging therapeutic frontier in pulmonary fibrosis. *Sci Signal* (2021) 14:eaay1027. doi: 10.1126/scisignal.aay1027

67. Higo H, Ohashi K, Tomida S, Okawa S, Yamamoto H, Sugimoto S, et al. Identification of targetable kinases in idiopathic pulmonary fibrosis. *Respir Res* (2022) 23:20. doi: 10.1186/s12931-022-01940-y

frontiers | Frontiers in Immunology

TYPE Review
PUBLISHED 14 October 2022
DOI 10.3389/fimmu.2022.990794

OPEN ACCESS

EDITED BY
Sophie Hillion,
U1227 Lymphocytes B et Autoimmunite (LBAI) (INSERM), France

REVIEWED BY
Joseph Barbi,
University at Buffalo, United States
Anton Gisterå,
Karolinska Institutet (KI), Sweden
Ioannis Mitroulis,
Democritus University of Thrace, Greece
Laura A. Solt,
UF Scripps Biomedical Research, United States

*CORRESPONDENCE
Jonas Bystrom
j.bystrom@qmul.ac.uk
Taher E. Taher
t.e.taher@bham.ac.uk

†These authors have contributed equally to this work and share first authorship

SPECIALTY SECTION
This article was submitted to Autoimmune and Autoinflammatory Disorders: Autoimmune Disorders, a section of the journal Frontiers in Immunology

RECEIVED 10 July 2022
ACCEPTED 06 September 2022
PUBLISHED 14 October 2022

CITATION
Bystrom J, Taher TE, Henson SM, Gould DJ and Mageed RA (2022) Metabolic requirements of Th17 cells and of B cells: Regulation and defects in health and in inflammatory diseases. *Front. Immunol.* 13:990794. doi: 10.3389/fimmu.2022.990794

Metabolic requirements of Th17 cells and of B cells: Regulation and defects in health and in inflammatory diseases

Jonas Bystrom[1*†], Taher E. Taher[2*†], Sian M. Henson[1], David J. Gould[3] and Rizgar A. Mageed[1]

[1]Centre for Translational Medicine and Therapeutics, William Harvey Research Institute, Queen Mary University of London, London, United Kingdom, [2]Institute of Immunology and Immunotherapy, College of Medical and Dental Sciences, University of Birmingham, Birmingham, United Kingdom, [3]Centre for Biochemical Pharmacology, William Harvey Research Institute, Queen Mary University of London, London, United Kingdom

The immune system protects from infections and cancer through complex cellular networks. For this purpose, immune cells require well-developed mechanisms of energy generation. However, the immune system itself can also cause diseases when defective regulation results in the emergence of autoreactive lymphocytes. Recent studies provide insights into how differential patterns of immune cell responses are associated with selective metabolic pathways. This review will examine the changing metabolic requirements of Th17 cells and of B cells at different stages of their development and activation. Both cells provide protection but can also mediate diseases through the production of autoantibodies and the production of proinflammatory mediators. In health, B cells produce antibodies and cytokines and present antigens to T cells to mount specific immunity. Th17 cells, on the other hand, provide protection against extra cellular pathogens at mucosal surfaces but can also drive chronic inflammation. The latter cells can also promote the differentiation of B cells to plasma cells to produce more autoantibodies. Metabolism-regulated checkpoints at different stages of their development ensure the that self-reactive B cells clones and needless production of interleukin (IL-)17 are limited. The metabolic regulation of the two cell types has some similarities, e.g. the utility of hypoxia induced factor (HIF)1α during low oxygen tension, to prevent autoimmunity and regulate inflammation. There are also clear differences, as Th17 cells only are vulnerable to the lack of certain amino acids. B cells, unlike Th17 cells, are also dependent of mechanistic target of rapamycin 2 (mTORC2) to function. Significant knowledge has recently been gained, particularly on Th17 cells, on how metabolism regulates these cells through influencing their epigenome. Metabolic dysregulation of Th17 cells and B cells can lead to chronic inflammation. Disease associated alterations in the genome can, in addition, cause dysregulation to metabolism and, thereby, result in epigenetic alterations in these cells. Recent studies highlight how pathology can result from the cooperation between the two cell types but only few have so far addressed the

10.3389/fimmu.2022.990794

key metabolic alterations in such settings. Knowledge of the impact of metabolic dysfunction on chronic inflammation and pathology can reveal novel therapeutic targets to treat such diseases.

KEYWORDS

metabolism, Th17 cells, B cells, mTORC, OXPHOS, epigenetics, autoimmunity

Introduction

T and B lymphocytes play central and complementary roles in protecting from infections and cancer. Gene rearrangements in these cells generate an extraordinarily diverse array of antigen-specific receptors, the T- and B-cell receptors (TCR and BCR). The two cell lineages originate in the bone marrow, where B cells generate their BCR. T-cell progenitors migrate to the thymus to undergo TCR gene rearrangements and a programmed range of selective processes. Naive T and B cells then migrate from these primary lymphoid organs and circulate through the blood and the lymphatic system to encounter their target antigens, become activated, proliferate, and differentiate to effector cells. Pathways of T- and B-cell activation depends on their target antigens, the microenvironment, and how to most efficiently conferring effective immunity.

In the process of mounting immunity, naive B cells are selected, activated, and differentiate to antibody-producing plasma cells or memory cells dependent on the type of antigen, availability of T-cell help, and also of cytokines produced. Naive helper T cells (Th cells) can differentiate to distinct functional subsets dependent on the type of antigen, antigen-presenting cell type, and cytokines produced. These Th subsets include Th17, Th1, Th2, induced regulatory T (iTreg), and follicular helper T (Tfh) cells. Differentiation of T cells to distinct functional subsets is associated with the upregulation of unique transcription factors. These are T-box expressed in T cells (T-bet) in Th1 cells, GATA-binding protein 3 (GATA-3) in Th2 T cells, and RAR-related orphan receptor γt (RORγt) in Th17 cells. Naive T cells are induced to differentiate to Th17 cells in the presence of interleukin (IL)-1β, IL-6, IL-23, and transforming growth factor-β (TGFβ) leading to upregulation of transcription factors RORγt, basic leucine zipper ATF-like (BATF) and signal transducer and activator of transcription 3 (STAT3) (1). Th1 cells protect from intracellular microorganisms and viruses, while Th2 protects from parasites and helminths. Th17 cells, combat extracellular bacterial and fungal infections primary on mucosal membranes. In addition to these main T-cell subsets, other T-cell subsets exist, and these contribute to the regulation and refinement of immunity. Natural regulatory T cells (nTregs) are generated and educated in the thymus to regulate immunity and limit autoimmune reactions (2, 3). In addition, chronic antigen stimulation in the periphery, in the presence of TGFβ leads to forkhead box P3 (FOXP3) upregulation in T cells to promote the differentiation of T cells to induced Tregs (iTregs) (3). Tfh cells promote B-cell activation and differentiation in germinal centers (GCs). Tfh cells are characterized by the expression of the transcription factor Bcl-6, and differentiation is facilitated by IL-21. Follicular regulatory T (Tfr) cells, in contrast, prevent Tfh-cell activity and suppress autoreactivity (3).

Metabolic requirements of T and B cells

Over the last decade, it has emerged that throughout their life spans, lymphocytes differentiate and function using distinct metabolic pathways, directed by specific functional needs at each stage of their development, the microenvironment, and the availability of nutrients and oxygen (O_2) tension (4). Basic metabolic pathways in these cells involve glycolysis and the pentose-phosphate pathway (PPP) that are key for their effector functions. During glycolysis, glucose is actively transported to the cytoplasm and metabolized by a set of 10 enzymes to generate energy-rich pyruvate and NAD^+. In proliferating T cells that rely on glycolysis for their energy needs, NAD^+ is reduced to NADH with lactate as a by-product. Low O_2 tension in certain niches, such as the bone marrow, the light zone (LZ) of GCs of B-cell follicles, and the mucosa, activates the transcription factor hypoxia-inducible factor 1α (HIF1α) that regulates genes that control glycolysis (5). Mechanistic target of rapamycin (mTOR) is a large protein complex located at the endosome of lymphocytes. The subcomponent Raptor associates with mTOR to form mTORC1, while Rictor associates with mTOR to form mTORC2. mTORC1 senses amino acid availability, regulates cell differentiation to effector cells, and determines the selection, or death of B cells in the LZ of GCs (6–8). mTORC2 is regulated *via* phosphatidylinositol 3-kinase (PI3K) and growth factor signaling and promotes the differentiation of Th cells to Th2 cells. mTORC2 also cooperates with mTORC1 in B-cell activation (9). AMP-

activated protein kinase (AMPK), which is localized to the cytoplasm or the lysosomes, is a crucial energy sensor that reduces cellular activity, augments fatty acid oxidation (FAO), and maintains quiescence of cells (7, 10, 11).

The glycolysis in the cytoplasm generates a limited amount of ATP and substrates for amino acid, nucleotide, and fatty acid biosynthesis as well as pyruvate for the more efficient energy producers, the mitochondria. In the mitochondrial compartment, the tricarboxylic acid (TCA) cycle is replenished by β-fatty acid oxidation, pyruvate and imported amino acids in what is called anaplerotic reactions. Pyruvate, which is transported from the cytoplasm, is converted in the mitochondria to TCA substrate acetyl-coenzyme A (acetyl-CoA) by the pyruvate dehydrogenase (PDH1). The TCA cycle provides substrates for the mitochondrial inner membrane-residing electron transport chain (ETC). The resulting conversion of O_2 to H_2O and NADH to NAD^+ generates ATP in what is known as oxidative phosphorylation (OXPHOS). During this process, the ETC transports protons to the intermembrane space, thereby establishing mitochondrial membrane potential ($\Delta\Psi m$). This potential is essential for the function and metabolism of effector cells and for their early progenitors to develop in the bone marrow (12). During activation, the availability/lack of nutrients and O_2 tension influence $\Delta\Psi m$. The mitochondria also have a role in Ca^{2+} homeostasis, with the ion being transported from the endoplasmic reticulum (ER) and from outside of the cell and, therefore, influencing $\Delta\Psi m$ in the process. TCR and BCR signaling results in increased mitochondrial Ca^{2+} (13). Metabolites generated through anaplerosis contribute to the biomass but also influence epigenetic regulators and gene transcription (see Table 1 for Th17 cells). The TCA cycle and OXPHOS provide basal functional requirements to all cells and are the only pathways that drive naive and non-activated memory T, B, and Tregs. It is now widely recognized that changes to the metabolic properties of different cell subsets are of fundamental importance to the regulation of the cell-specific transcriptional programs and effector functions.

The focus of this review is on the changing metabolic requirements of Th17 cells and of B cells at different stages of their development and activation. These two cell types have been selected because of their role in promoting chronic inflammation that underpins pathology in most chronic diseases. Generally, metabolism-regulated checkpoints at different stages of lymphocyte development are instilled to prevent the emergence of self-reactive B- and T-cell clones (Table 2 for B cells). Metabolic regulation of B cells and Th17 cells have similarities. For example, both cell types utilize HIF1α during low oxygen tension. In addition, both cells express the anti-inflammatory adenosine-sensing CD73 molecule (4, 5, 29). The two cell types, nevertheless, have differences too. As will be discussed later on, Th17 cells are particularly vulnerable to the lack of certain amino acids. This latter issue has not been reported in B cells (15, 30). B cells, unlike Th17 cells, are dependent on mTORC2 for their functions (9). Although lymphocyte activation following TCR and BCR engagements induce metabolic changes required for immunity against pathogens, it is increasingly recognized that metabolic dysregulation of Th17 cells or B cells relates to the development of autoimmune diseases due to defective tolerance (17, 31). Disease-associated genetic variations might be one cause of metabolism and epigenetic dysregulation in these cells (32, 33). Recent reports have highlighted autoimmune pathology-inducing interactions between the two cell types,

TABLE 1 Metabolic alterations resulting in epigenetic changes to Th17 cells.

Metabolic alteration	Effect	Epigenetic / transcription factor change	Th17/ Treg	Reference
Glutamine intake	↑α-ketoglutarate and 2-HG	↑Methylation of the *Foxp3* promoter	Treg ↓	(14)
Lack of glutamine	↑ ROS	↑ H3K27 trimethylation globally	Th17 ↓	(15)
Lack of methionine	↓ SAM	↓ H3K4 methylation, promoter of genes involved in Th17 cell differentiation; *Il17 and Batf* and cell cycle	Th17 ↓	(16)
High (GLS1 and) Acetyl-CoA		↑ Acetylation of H3K9Ac and H3K27Ac in the *Il17* promoter	Th17 ↑	(17)
Lack of MTHFD2	↓ Succinate, fumarate	↓ DNA demethylation in the *Foxp3* promoter	Treg ↑	(18)
Inhibition of polyamine metabolism		FOXP3 ↑	Th17 ↓/ Treg ↑	(19)
HIF1α		1) Associate with RORγt and p300 on the *Il17* promoter 2) Binds FOXP3	Th17↑ / Treg ↓	(20)
Pentanoate from SFB		Histone deacetylase inhibitor	Th17 ↓	(21)

GLS, glutaminase 1; GOT1, glutamate oxaloacetate transaminase 1; 2-HG, 2-hydroxyglutarate; MTHFD2, bifunctional methylenetetrahydrofolate dehydrogenase/cyclohydrolase; SAM, S-adenosylmethionine; SFB, segmented filamentous bacteria. ↑: increased, ↓: decreased.

TABLE 2 Metabolism at B-cell stages where clones with low antigen specificity or self-reactivity are excluded.

	Exclusion selection due to self reactivity / low antigen specificity	Metabolism type	Reference
Bone marrow			
Large pre-B cells	Autoreactivity of the IgH chain	Glycolysis ↑, OXPHOS ↑ Low O_2, HIF1α ↑	(22, 23)
Immature B cells	Autoreactivity of BCR	Glycolysis ↓, OXPHOS ↓ FOXO1↑	(23, 24)
Spleen			
Transitional B cell	Autoreactivity of BCR	Glycolysis ↑, OXPHOS ↑	(7)
Spleen and lymph nodes			
Activated B cell	BCR not recognized via CD40 or TLR	Glycolysis ↑, OXPHOS ↑	(25, 26)
Light Zone B cell	Competition for BCR selection, IgH class switch	GSK3 ↑, Low O_2, HIF1α ↑	(5, 8, 27, 28)

↑: increased, ↓: decreased.

but only a few have so far assessed altered metabolic properties of the two cell types during such scenarios (34–36).

Metabolism in T cells

T-cell progenitors are produced in the bone marrow. They migrate to the thymus where they undergo development, including rearrangement of their TCR genes, positive recognition of the major histocompatibility complex II, and tolerance to prevent self-reactivity. During these developmental phases, the functioning metabolic pathway changes with high glycolysis and OXPHOS during TCR arrangement followed by low metabolic activity during positive and negative selections (37). Thymic outputs are highest during childhood, continue at a slower rate in adolescence, and are then much reduced after the third decade of life, and these changes are reflected by changes in thymocyte metabolism (38).

After exiting the thymus, naive T cells remain quiescent while circulating through blood and the lymphatics (30). The cells express low amino acid transporter levels, have low glucose transport capacity, and rely on OXPHOS and FAO (30). Expression of the T-bet gene, *TBX21*, an immune cell transcription factor in naive T cells, indicates that the cells are primed to become Th1 cells (39). This is reflected by chromosomal markers favoring a Th1 gene signature including activation of the *IFNG* gene locus (40). T-bet also appears to play a role in metabolism in these cells, as *Tbx21*$^{-/-}$ mice have increased visceral adiposity but are more insulin-sensitive, exhibiting reduced immune cell numbers and cytokine secretion specifically in the visceral fat depot, perhaps due to altered T-cell trafficking (14). The effector Th1 program is activated in lymph nodes (LNs) following TCR engagement. This leads to the upregulation of the glucose transporter GLUT1, activation of glycolysis and mTORC1, and differentiation of the cells (15). Th2 cells, in contrast, rely on mTORC2 for their differentiation that also inhibits the Th1 program (16, 41). nTregs and iTregs rely on OXPHOS and FAO during their resting state but require glycolysis and mTORC1 when activated in LNs or in the periphery (10, 42, 43). Perhaps paradoxically, however, this activation was also shown to reduce their suppressive activity (44). Tfh cells use glycolysis and OXPHOS selectively in response to changes in substrate availability in the GC where they reside (45). Being a focus of the review, Th17-cell metabolism will be described in more detail below. Interestingly, metabolism of activated Th17 cells has many similarities with that of Th1 cells. Antigen presentation in mesenteric LNs induces metabolic changes and the establishment of a Th17 differentiation program in naive T cells (46). Following TCR engagement, just as for Th1 cells, transcription of genes involved in glycolysis, including *GLUT1*, is upregulated (Figure 1A). Stromal interaction molecule 1 (STIM1) expressed in the ER undergoes conformational changes that augment Ca^{2+} release from intracellular compartments and its influx through cell membrane channels in Th1 and Th17 cells. These events promote glycolysis and OXPHOS and lead ultimately to IL-17 production, while RORγt level remains unaffected by the change in Ca^{2+} levels (47). Hence, not only is glycolysis, but also OXPHOS is essential for the early molecular events leading to Th17 differentiation. Induction of the transcription factors BATF and STAT3 are such early events (48). TCR engagement activates mTORC1 *via* PI3K/Akt, which also promotes cell differentiation (49). Th17 cells lacking Raptor lose the ability to develop effector functions (6). In addition, activated effector Th17 cells have a high $\Delta\Psi m$ (12). Interestingly, among T lymphocytes, Th17 cells are unique in displaying functional flexibility. For example, Th17 cells can transdifferentiate to both Tregs and pathogenic Th17 cells, the latter often associated with the ability to produce Interferon-γ (IFNγ) (Figure 1C) (1, 46). Th17 cells can transdifferentiate to pathogenic Th17 cells in response to severe bacterial and fungal infections (described in the section on *Changes in Th17-Cell Metabolism Are Related to Its Physiological Functions*) (46, 47).

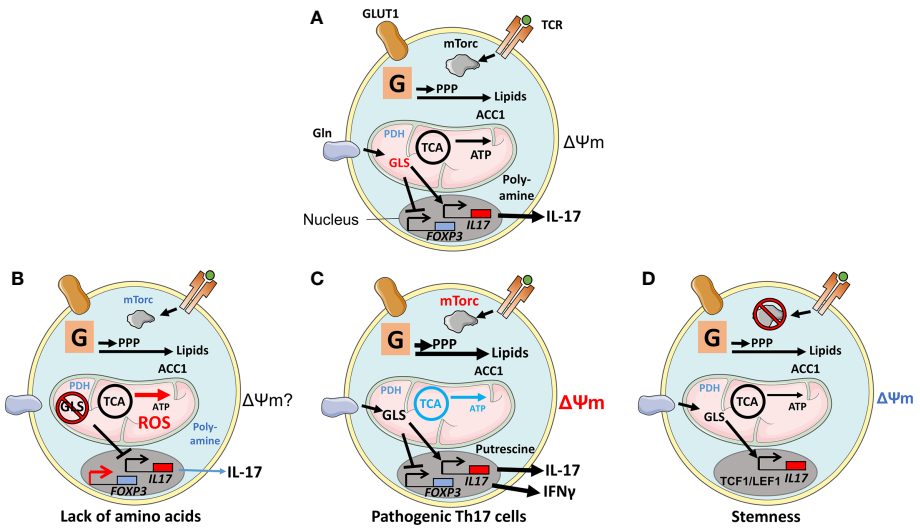

FIGURE 1
Physiological and experimentally induced metabolic states of Th17 cells. **(A)** After T cell receptor (TCR) engagement, Glucose transporter 1(GLUT1) is upregulated in support of glycolysis (denoted as a G within a square). TCR engagement also augments mechanistic target of rapamycin (mTORC1) activity *via* Akt/PI3K, leading to cell differentiation. Products generated by glycolysis are utilized in the pentose-phosphate pathway (PPP) and in lipid biogenesis; the latter was regulated by Acetyl-CoA carboxylase 1 (ACC1) but not by mitochondrial anaplerosis, as the cells have limited expression of Pyruvate dehydrogenase (PDH1). Anaplerosis is driven by amino acids, such as glutamine that is imported through the amino acid transporter SLC1A5 and metabolized by glutaminase 1 (GLS1). The metabolite 2-Hydroxyglutarate (2-HG), generated by Glutamic-oxaloacetic transaminase 1 (GOT1), suppresses the activity of the FOXP3 promoter. Other amino acid metabolites favor an epigenetic configuration that promotes the Th17-cell transcriptional program. **(B)** Deprivation of amino acids glutamine, serine, or methionine or ablation of GLS1 or of an enzyme involved in the one-carbon pathway Bifunctional methylenetetrahydrofolate dehydrogenase/cyclohydrolase (MTHFD2) or inhibition of the poly-amine pathway prevents Th17 cell proliferation. Increased ROS production, perhaps due to the lack of glutathione and substrate (succinate) for mitochondrial electron transport, alters epigenetic configuration to favor FOXP3 expression and Treg-mediated suppressive activities. **(C)** Pathogenic Th17 cells, signified by active mTORC1, lack of OXPHOS, production of IFNγ, and high ΔΨm, rely on the polyamine pathway and putrescin. **(D)** Ablation of mTORC1 and reduced ΔΨm result in Th17 cells expressing stemness markers T-cell factor 1 (TCF1) and Lymphoid enhancer-binding factor 1 (LEF1).

Th17-cell metabolism

Th17 cells, unlike Th1 cells, divert glycolysis-derived pyruvate away from the TCA cycle as PDH1 is downregulated in the cells (50). PDH1 is Ca^{2+} sensitive, but whether the increased levels of Ca^{2+} in Th17 cells in response to TCR stimulation influence PDH1 differently to Th1 cells has not been addressed (13). In Tregs, however, PDH1 is required for their function and, consequently, limiting autoimmunity, inflammation, and chronic disease (18). Since pyruvate is diverted from OXPHOS, Th17 cells will become dependent on amino acids as substrates for anaplerosis (Figure 1A). The importance of certain amino acids for Th17 functions is highlighted by the fact that only these cells among all T-cell subsets cease to proliferate when the glutamate-proline tRNA ligase EPRS1 is inhibited, or cysteine or methionine is depleted, resulting in phosphorylation of the stress sensor general control nonderepressible 2 (GCN2). The importance of glutamine as a substrate for Th17-cell metabolism is highlighted by that the glutamine transporter SLC1A5 and the glutamine-degrading enzyme glutaminase 1 (GLS1) are being expressed at high levels in these cells. Hence, the culture of Th17 cells in media lacking glutamine, or the ablation of GLS1, inhibits the function of the cells (15). Glutamate, the product of glutamine degradation, is a constituent to the reactive oxygen species (ROS)-scavenging glutathione but can also be metabolized to 2-hydroxyglutarate (2-HG) *via* α-ketoglutarate (α-KG) (51). GLS1 deficiency both increases ROS and alters cells' epigenetic status by inducing trimethylation of histone H3K27 at many chromosomal locations (Table 1). Inhibition of ROS alters these epigenetic marks, indicating that glutamine supports Th17 cells by inhibiting ROS and its influence on epigenetic gene control. ROS is also an activator of mTORC1, underpinning the importance of this protein complex in Th17-cell functions. In support of this theme, ablation of the catalytic subunit of glutamate cysteine ligase (Gclc) in T cells results in glutathione depletion and impaired mTORC1 activity (52). Th1 cells, in contrast, adapt to GLS inhibition and increase glucose uptake for anaplerotic reactions to maintain cell phenotypes (15). Methionine restriction, in contrast, reduces the production of S-adenosyl methionine (SAM) that is required for histone H3K4 methylation at the promoter regions of Th17 cells, thus, inhibiting their proliferation and IL-17 production (Figure 1B, Table 1) (53).

Cytoplasmic acetyl-coenzyme carboxylase 1 (ACC1) is upregulated in Th17 cells. ACC1 utilizes pyruvate-derived acetyl-CoA as metabolite for lipid synthesis (54). Lipids generated because of this reaction interact with RORγt and increase its activity in driving Th17-cell differentiation. Acetyl-CoA produced from glutamine also regulates IL-17 production by acetylation of histone H3, thereby exposing the IL-17A promoter for RORγt transcriptional activity (17).

In addition, Th17 cells have a unique response pattern to environmental stresses. Thus, these cells cease to proliferate to deficit in specific amino acids (15, 55). In contrast, low O_2 tension, both high and low levels of glucose, mannitol-induced osmotic stress, and high levels of NaCl promote Th17-cell proliferation (19, 56, 57). Low glucose levels reduce IL-2 production and STAT5 signaling, which is unfavorable for T cells other than Th17 cells (58). Relevant to these observations is that Th17 cells require a lower TCR signaling strength than Th1 cells to be activated. However, this results in reduced IL-2 production (58, 59). High levels of glucose, in contrast, induce Th17 cells. In this setting, neither glycolysis nor OXPHOS is affected, but high glucose levels induce mitochondrial ROS (mtROS) production. mtROS is released extracellularly where it converts TGFβ from its latent form to its active one that, in turn, supports the development of Th17 cells (57). Mannitol-induced osmotic stress promotes Ca^{2+} release from Th17 cells' ER, and this influx augments Th17 cell responses (19). Compared with Th1 cells, Th17 cells are specifically regulated by HIF1α and mTORC1. Of note, in mice, HIF1α did directly associate with RORγt to promote Th17-cell differentiation (20). It is, thus, intriguing to speculate that this reliance of HIF1α reflects the Th17-cell localization to mucosal membranes where the O_2 tension can be low and antigen-presenting cells are scarce (4, 22, 29).

As cited in the previous section, Th17 cells can transdifferentiate to Tregs or to pathogenic Th17 cells, and this process manifest metabolic alterations. Such alterations can be induced experimentally, or by disease. Experimentally induced metabolic dysregulation can induce Th17 transdifferentiation to Tregs. One carbon (1C) metabolism is important for T-cell activation (30). The 1C metabolism consists of a series of interlinking metabolic pathways, including the methionine and folate cycles. The methionine/folate pathways, thus, involve folate/methionine providing 1 methyl group for the synthesis of purine nucleotides for DNA synthesis, polyamines, amino acids, creatine, and phospholipids. One of the enzymes in the mitochondrial branch of the 1C pathway, the bifunctional methylenetetrahydrofolate dehydrogenase/cyclohydrolase 2 (MTHFD2), is important for Th17-cell functions. Inhibition of MTHFD2 results in reduced mTORC1 activity, increased OXPHOS, and reduced abundance of succinate and fumarate (60). MTHFD2 deficiency results in increased DNA demethylation including in the FOXP3 promoter-locus, thereby shifting pathogenic Th17 cells to acquire a Treg phenotype (Table 1) (60). Another study revealed that 2-HG produced by glutamate oxaloacetate transaminase 1 (GOT1) facilitated methylation and silencing of the FOXP3 promoter. Inhibition of GOT1 activity on the other hand converted Th17 cells to iTregs (51). Furthermore, chronic infection, malignancy, and T-cell exhaustion are known to upregulate the receptor PD-1 on T cells. PD-1 augmentation promotes FAO and inhibits glycolysis which could impede on Th17-cell effector function and promote a regulatory phenotype shift (61). Along similar lines, TGFβ and IL-6 upregulate CD73 expression on Th17 cells and this renders the cells anti-inflammatory in a tumor microenvironment (23). CD73 is an ecto-5'-nucleotidase that degrades AMP, derived from ATP or from NAD, generating the anti-inflammatory metabolite adenosine (23, 24). Adenosine, in turn, binds receptors on immune cells to trigger anti-inflammatory activities. Intriguingly, CD73 is also expressed on B cells (24).

Different approaches have been used to probe the heterogeneity of Th17 cells (62). Enrichment of Th17 cells based on their ΔΨm identified high-ΔΨm cells expressing higher levels of IL-17, while cells with low ΔΨm expressed higher levels of the stemness markers TCF1 and LEF1 (12). Furthermore, mice with T cells lacking Raptor produced Th17 cells with low metabolic activity, and expression of TCF1 (Figure 1D) (6). In contrast, Th17 cells with intact mTORC1 showed a capacity to transdifferentiate to pathogenic Th17 cells signified by the ability to produce IFNγ. A study using single-cell RNA sequencing (scRNA-seq) confirmed the Th17 cells' metabolic heterogeneity. The study revealed that protective Th17 cells accumulate arginine while pathogenic Th17 cells synthesize and recycle polyamines, with putrescine being the mediator that best augments the cells' activities. Inhibition of polyamine metabolism also promotes FOXP3 expression (Figure 1C) (62). In another study, putrescine was shown to have no impact on Th17 differentiation when added during *in vitro* cultures (63). These findings highlight the difference between studies of Th17-cell metabolism *in vitro* and *in vivo* and the value identifying of specific differences using scRNA-seq (62, 63).

B-cell metabolism

Early studies have identified two distinct B-cell lineages in mice and, probably in humans. These two B-cell lineages are distinguished phenotypically by the expression of CD5, a primarily T cell-associated membrane protein. The two subsets were designated conventional or $CD5^-$ B cells (also called B2 cells) and $CD5^+$ B cells (B1 cells) that produce natural polyreactive IgM antibodies. The developmental pathway of the B2-cell lineage is shown in Figure 2. Cellular metabolism during clonal B2-cell selection/exclusion influenced by their BCR is shown in Table 2 and Figure 2. B1 cells have been

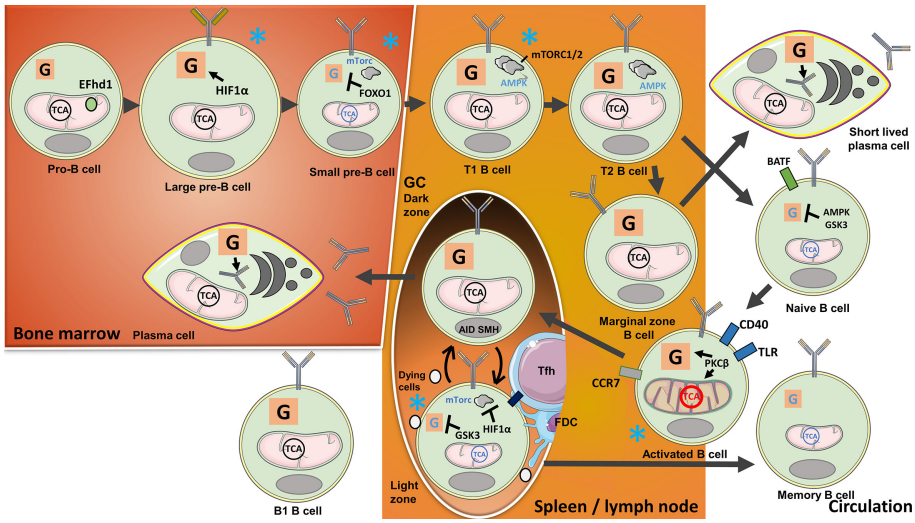

FIGURE 2
B-cell metabolism changes during their development, activation, and purging of clones with no available target antigens or those that are autoreactive. In the bone marrow, metabolism changes during B-cell development with the highest activity at pro-B cell and large B-cell stages: Heavy-chain gene rearrangements during the pro-B cell stage are associated with high $\Delta\Psi m$, while cell expansion during the large B-cell stage is signified by increasing glycolytic activity. The mitochondrial Ca^{2+} binding EF-hand domain family member D1 (hEFd1) protects pro-B cells from heavy-chain synthesis-induced late surge in Ca^{2+}. Large B cells localized to a niche with low O_2 tension upregulate Hypoxia-inducible factor 1α (HIF1α) activating glycolysis during cell expansion. Light-chain gene arrangements and removal of self-reactive clones during the small pre-B-cell and immature B-cell stages are, in contrast, associated with suppressed mechanistic target of rapamycin 1(mTORC1) and low metabolic activity controlled by Forkhead box protein O1(FOXO1). Transitional (T) B cells again have high metabolic activity, OXPHOS, and mTORC1/2. Residual autoreactive clones are removed when the cells locate to the spleen and transition from T1 to T2 stage. Naive and Marginal zone (MZ) B cells develop from T2 B cells. Naive B cells found in the circulation have low metabolic activity regulated by AMP-activated protein kinase (AMPK) and Glycogen synthase kinase-3 (GSK3). Tonic B cell receptor (BCR) signaling and B-cell activating factor (BAFF) receptor engagement provide survival signals. When naive B cells encounter antigens, the cells are activated and undergo metabolic changes with the expansion of mitochondria guided by Protein kinase C β (PKCβ). Activated B cells will migrate to lymph nodes and the spleen, requiring T-cell help or Toll like receptor (TLR) stimulation for survival. T cell-stimulated B cells locate to B-cell follicles to initiate Germinal centre (GC) reactions. Highly metabolically active B cells proliferate in the Dark zone (DZ) and undergo activation-induced cytidine deaminase (AID)-guided somatic hypermutations (SHM). The cells subsequently move to the Light zone (LZ), where HIF1α, induced by low O_2 tension, suppresses mTORC1, while GSK3 suppresses glycolysis. The cells compete for selection by follicular T cells (Tfh) cells and follicular dendritic cells (FDCs) in the LZ. Selected cells utilize lipids from unselected counterparts for anaplerosis. The cells can reenter the DZ for further selection, or leave the GC, in the latter case either differentiating to long-lived plasma cells (LLPC) or memory B cells. LLPCs with high metabolic activity will locate to the bone marrow, there producing antibodies. Glycolysis provides a substrate for glycosylation of antibodies. Circulating memory B cells, on the other hand, are signified by low metabolic activity. MZ B cells, another progeny of transitional B cells, develop into short-lived plasma cells with a metabolic signature similar to LLPCs, independently of GC reactions. B1 cells developing in the embryo are signified by high glycolysis and OXPHOS. Blue stars indicate B-cell stages where clones with low antigen specificity or self-reactivity are excluded.

suggested to have diverged during the embryonic stage in mice and have the ability for self-renewal. These cells are endowed with high glycolysis and OXPHOS activity (64). In addition to these two lineage cells, a subset of B cells that regulates immunity and inflammation and promotes differentiation of naive T cells to iTregs, called Bregs, have been identified. Bregs' functions are contact-dependent and can involve IL-10 production [metabolism reviewed in Iperi et al. (65)].

Conventional B2 cells are produced in the bone marrow from hematopoietic stem cells. B2 precursors undergo gene rearrangements in the bone marrow that ultimately result in the expression of diverse BCR repertoires at the latter stages of pro- and pre-B-cell developments. The progenitor cells localize to different niches in the bone marrow with varying degrees of oxygen tension, thus, influencing the cells' metabolic characteristics. Pro-B cells have the highest $\Delta\psi m$, but this is incrementally diminished during the subsequent stages of their development. OXPHOS activity is similar in pro- and large pre-B-cell stages, but the latter cells have the highest glycolytic activities among the progenitors, accompanied by high levels of ROS. Reflecting a niche with low oxygen tension, HIF1α is active during the pre-B-cell stages, thus, driving glycolysis. When HIF1α is experimentally deleted, B cells switch their metabolism to TCA anaplerosis for their energy needs (66). The Ca^{2+}-binding protein Swiprosin-2/EF-hand domain family member D1 (EFhd1) was found to be located to the inner mitochondrial membrane of pro-B cells. Due to the emergence of the pre-BCR in late pro-B cells, Ca^{2+} is directed from the ER to the mitochondria. This results in an increased mitochondrial pH and a drop in $\Delta\psi m$ and ATP production. Detectable

"mitoflashes," likely due to a drop in mitochondrial pH, occur in regions with EFhd1 and Ca^{2+}. This is likely to be a means to rescue $\Delta\psi m$ and increase ATP production in these cells. Ca^{2+} signaling downstream of SYK is important for pre-BCR signaling in pro-B cells and is related to these noted events (27, 67). EFhd1 is downregulated at the pre-B-cell stage consequent to the localization of the pre-BCR to the membrane and the migration of the cells to a niche with low O_2. Subsequent anaplerotic reactions provide protection from ROS and growth (67, 68). Glycolysis and OXPHOS are reduced in pre-B cells compared with the B-cells at their earlier developmental stages. Downregulation of PI3K/Akt and ROS-mediated induction of FOXO1 together with the expression of the lineage-defining transcription factor paired box 5 (PAX5) induce cell cycle arrest while light-chain genes are rearranged (69). Provided that the BCR does not bind avidly to self-antigens, a program of maturation follows surface expression of the complete BCR (25).

Immature B cells eventually exit the bone marrow as transitional 1 (T1) B cells. T1 B cells express higher levels of genes involved in ribosome biogenesis, aerobic respiration, and mTORC1 than B cells at later stages of their maturational pathway but, in contrast, express low AMPK levels. Interestingly, studies of mice deficient in the mTORC2 component Sin1 showed a reduction in T1 and T2 B cells. mTORC2 was reported to increase Akt signaling, stabilize mTORC1, and suppress glycogen synthase kinase-3 (GSK3) (9). *In vitro* treatment with the AMPK agonist 5-Aminoimidazole-4-carboxamide ribonucleotide (AICAR) supports the evolution of T1 B cells to conventional B2 cells (7).

In vivo, the progression of T1 to T2 B cells takes place mostly in the spleen where tolerance checkpoints are in place to eliminate residual autoreactive T1 B-cell clones and to prevent their transition to mature B cells (26). B cells that survive peripheral tolerance checkpoints develop either to mature naive B cells or to marginal zone B cells (MZB, see below). Naive B cells are metabolically inactive and circulate through the blood and lymphatics (30). Tonic signaling through the BCR and signals mediated by B-cell activating factor (BAFF) preserve homeostatic mitochondrial signals in naive B cells (70). In contrast, AMPK, GSK3, and PAX5 suppress glucose uptake and maintain quiescence in mature non-activated B cells (7, 71, 72).

Mature naive B cells are activated when they encounter and bind their target antigens through their BCRs, mostly, in the presence of T-cell help. This results in Myc- and PI3K-mediated GLUT1 expression, glycolysis, and glutamine-supplemented anaplerosis for OXPHOS (73). The cells initiate a transcriptional program to remodel the mitochondria and increase their glycolytic activities. To prevent abnormal activation and/or the expansion of residual uncensored autoreactive B cells, the cells require a second stimulation within 24 h that can either be T cell mediated (CD40) or through Toll-like receptor (TLR9) (74). Stimulated B cells upregulate chemokine (C-C motif) receptor 7 (CCR7) and move to nearby secondary lymphoid organs to proliferate inside or outside GCs. Ectopic GCs can be initiated in non-lymphoid organs during chronic inflammation and autoimmunity. Without a second activation signal, increasing intracellular Ca^{2+} levels transported through calcium channels and increasing levels of ROS will ultimately lead to the apoptosis of antigen-primed B cells (74).

In lymphoid organs, on the boundaries between T- and B-cell areas, B cells present fragments of the antigen recognized by their BCRs for cognate Th-cell interaction together with costimulatory signals. These B cells can develop independent of GCs into short-lived extrafollicular plasma cells that are important for the initial wave of protective antibodies. Alternatively, these cells can differentiate to unswitched memory B cells. Other B cells will migrate into B-cell follicles to initiate GC reactions and become founders for clones whose antibodies acquire increasing affinity for the antigen in the newly formed GCs. GCs will evolve into two zones, the dark zone (DZ) closest to the T-cell zone in LNs and the LZ that is closest to the capsule in LNs and marginal zones of the spleen and with cells shuttling in-between guided by chemokine signals. B cells actively divide in the DZ and express activation-induced cytidine deaminase (AID) enzyme and mediate somatic hypermutation (SHM). BCR and CD40 are required for Myc-regulated expression of metabolic enzymes and membrane transporters. B cells do not proliferate in the LZ and, instead, compete for selection during interactions with antigens expressed on follicular dendritic cells (FDCs) and obtaining help from Tfh cells. FDCs and Tfh cells regulate positive selection, while Tfr cells suppress the output of activated B cells (28). Strength of the B cell/Tfh cell interaction determines later proliferation efficiency in the DZ (75). As the LZ is farthest from the blood supply and oxygen in GCs, HIF1α is activated. This activation prevents AID activity and, thereby, restricts Ig class switching but, interestingly, not SHM. mTORC1 regulates HIF1α and the Von Hippel–Lindau tumor suppressor while GSK3 protects B cells from deprivation of glucose and nutrients (5, 8, 71). Fatty acids (FAs) from other surrounding B cells, dying due to lack of costimulation, supply OXPHOS (76). PKCβ regulates antigen presentation in B cells and, therefore, the development of Tfh cells to support further B-cell proliferation and differentiation (77). Class-switched B cells subsequently undergo repeated expansion in the DZ or exit the GC. Memory B cells and long-lived plasma cells (LLPCs) have exit cues from the GC that correlate with BCR affinity and time since the response began (75). Memory B cells circulate and when reactivated by their target antigens start producing antibodies or initiate another GC reaction for further affinity maturation. Memory B cells are signified by low-level metabolism relying primarily on OXPHOS. LLPCs migrate to the bone marrow and, guided by the transcription factor Blimp-1, mature to cells

dedicated to antibody production. These cells have high OXPHOS activity and glycolysis, the latter providing the substrate for glycosylation of the antibodies that are produced (78).

Activated B cells residing in the MZ of lymphoid organs express TLRs and are activated through TLR9 for survival (79). These cells act as an early response element and produce, mostly polyreactive, antibodies with low affinity. Stimulation through the TLR together with transmembrane activator and CAML interactor (TACI) activates mTORC1 signaling in MZB cells leading to high expression of the glucose transporter GLUT1 and consumption of glucose. This leads to B-cell proliferation and, subsequently, to immunoglobulin G (IgG) class switching and differentiation to plasmablasts (80). IL-10 production by MZ precursor B cells has been shown to regulate the differentiation of Th17, Tfh, and Tfr cells (81). The MZ precursors could therefore, be considered to have potential Breg-related functions (65).

Changes in Th17-cell metabolism are related to its physiological functions

During homeostasis, IL-22-producing Th17 cells are primarily found in the mucosa of the intestine conferring protection and supporting intestinal barriers. DCs present antigens from the intestinal microflora to naive T cells in mesenteric LNs leading to the expression of RORγt and the gut homing receptor α4β7 by the cells. The cells subsequently proliferate and migrate to Peyer's patches and intestinal mucosa to start protective activities (21, 46, 82). Infection with the commensal segmented filamentous bacteria (SFB) in mice results in effector Th17 cells in the intestine with elongated mitochondria, relying on OXPHOS to produce Nicotinamide adenine dinucleotide phosphate (NADPH) and glutathione. Infection with the pathogen *Citrobacter rodentium*, in contrast, results in pathogenic Th17 cells that coproduce IL-17 and IFNγ. The latter Th17 cells have fragmented mitochondrial morphology and rely on glycolysis for their metabolic needs. The IFNγ-producing Th17 cells cannot transdifferentiate from resident intestinal Th17 cells but are originated in the LNs. The pathogenic Th17 cells, unlike Th17 cells from SFB-infected mice, can also disseminate to spleens of infected mice (46). The bacterial flora produces short-chain fatty acids (SCFAs) such as pentanoate. These SCFAs act in Th17 cells as a histone deacetylase inhibitor, thereby suppressing IL-17 transcription. Pentanoate from SFB can, therefore, reduce Th17 activity in the intestine (83).

Studies in mice have revealed that Th17 cells differentiate to tissue-resident memory T (Trm) cells to provide protection against bacterial and fungal infections in the lungs and skin (84, 85). These cells provide protection mainly through the recruitment of neutrophils (47). Deletion, or mutations described in patients, of *STIM1* that regulates Ca^{2+} uptake in Th17 cells leads to impaired fungal defenses, dissemination in kidneys, and eventual death. *In vitro* analyses of non-pathogenic and pathogenic STIM1-deficient Th17 cells showed that the non-pathogenic subset of cells was most dependent on STIM1. Expression of HIF1α target genes, mTORC1 activation, glycolysis, and OXPHOS are reduced in these cells, while the FOXO1 pathway is upregulated. Thus, specifically for non-pathogenic Th17 cells, extracellular Ca^{2+} is important for effective immunity to fungal infections (47). Hence, non-pathogenic Th17 cells rely on Ca^{2+} imported *via* STIM1, glycolysis, and OXPHOS, while pathogenic Th17 cells, stimulated by severe bacterial and fungal infections, utilize glycolysis only (46, 47). Low oxygen tension (activation of HIF1α) may thus, promote a pathogenic phenotype. Such findings are in line with a recent study comparing pathogenic and non-pathogenic Th17 cells in a model of multiple sclerosis (22). This, apparently, is associated with a lack or reduced supply of amino acids (15, 49).

The contribution of dysregulated Th17-cell metabolism to disease pathogenesis

Th17-cell metabolism in psoriasis

Psoriasis is the consequence of uncontrolled proliferation of dermal keratinocytes. The disease affects 2%–3% of populations worldwide and manifests in scaly plaques that in the disease's severe from cover more than 10% of the body. Th17 cells, present in the dermis of patients as IL-17-producing Trm cells, contribute to psoriasis pathology, evidenced by therapeutic efficacy of treatment with anti-IL-17 antibody in reducing plaques (86). Th17-cell metabolism was studied in an animal model of psoriasis and discovered that the production of the mucosa-associated lymphoid tissue lymphoma translocation protein 1 (MALT1) was dysregulated in Th17 cells. MALT1 stabilizes c-jun that could then bind and activate GLS1 expression, resulting in increased glutaminolysis in Th17 cells. GLS1's overexpression in patients' Th17 cells leads to high levels of acetyl-CoA production. This metabolite, in turn, induces histone H3 acetylation; specifically, H3K9Ac and H3K27Ac marks in the IL-17A gene promoter region resulting in increased IL-17 production leading to pathology (Figure 3A). This investigation revealed that GLS, or MALT1 inhibitors, previously considered as cancer therapy, can be a potential treatment for psoriasis (17).

Th17-cell metabolism in rheumatoid arthritis

Rheumatoid arthritis (RA) is a debilitating disease mainly affecting joints in 0.5%–1% of populations worldwide. The synovial lining of RA joints is targeted by an immune

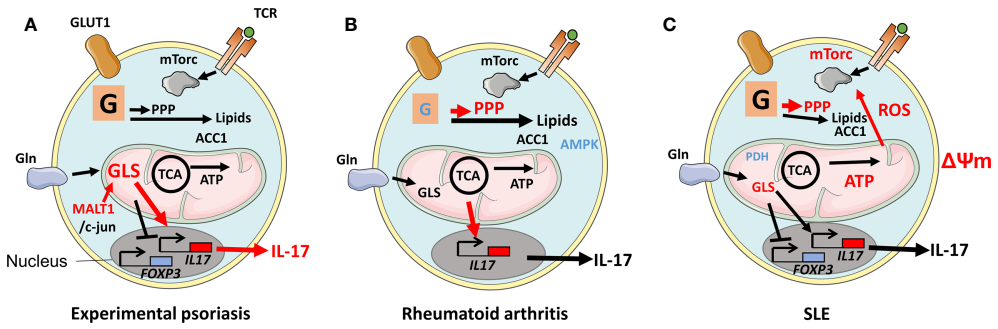

FIGURE 3
Disease-associated changes in metabolic pathways in Th17 cells. **(A)** During experimental psoriasis, dysregulated expression of Mucosa-associated lymphoid tissue lymphoma translocation protein 1 (MALT1) results in overexpression of Glutaminase 1 (GLS1) and generation of acetyl-CoA from metabolized glutamine. Histone H3K9Ac and H3K27Ac acetylation marks were found in the *il17* gene promoter leading to increased IL-17 production and psoriasis. **(B)** Defective glycolysis and TCA cycle in naive T cells in RA patients and a lack of mechanistic target of rapamycin (mTORC1) restraint due to inactive AMP-activated protein kinase (AMPK) result in an inflammatory phenotype with increased migratory properties and the production of IL-17 and IFNγ. The metabolism of glutamine in Th17 cells contributes to a Th17 cell phenotype. **(C)** Th17 cells in patients with SLE are signified by increased glycolysis and OXPHOS, elongated mitochondria, elevated ΔΨm, and mitochondrial reactive oxygen species (mtROS). The elongation of mitochondria is a consequence of oxidative stress-induced reduction of Rab4A-mediated recycling of Dynamin-related protein 1 (Drp1). Rab4A defect also results in increased mTORC1 activity. Reduced expression of Protein phosphatase 2 (PP2A) results in reduced expression of Pyruvate dehyrogenase 1 (PDH1).

response that causes juxta-articular and generalized bone loss. The level of IL-17 is reduced at disease onset compared with before onset (87). Naive CD4+ T cells in patients with established RA are, however, prone to differentiate to Th17 cells (39). Naive T cells from RA patients manifest defective glycolysis resulting in diminished levels of ATP, low ROS, and an overall defective mitochondrial function (88). The GDP-forming β subunit of succinate-CoA ligase (SUCLG2), part of the TCA, was reported suppressed, resulting in reversal of the cycle. This reversal induces IL-17- and IFNγ-mediated inflammation, as shown by the transfer of patient peripheral blood mononucleated cells (PBMCs) to immune compromised NOD Scid gamma mice that harbor patient synovium transplants. Overexpression of SUCLG2 in these PBMCs reduced IL-17 production. As a consequence of the SUCLG2 defect, citrate was transported out of mitochondria and converted to acetyl-CoA, clustering mitochondria perinuclear and increasing T-cell invasiveness (31). Inflammation and migratory properties suggest that mTORC1 activation and efficient OXPHOS are involved. However, the above-cited studies suggest that these pathways are dysregulated in RA. AMPK was found to be displaced and, thereby, could not regulate mTORC1, resulting in high-level production of IL-17 and IFNγ. This AMPK defect could, therefore, explain the inflammation caused by the cells (Figure 3B) (11). Indeed, an appropriately located AMPK is able to drive FAO favoring Tregs instead of Th17 cells (10). In arthritic joints, there is an enrichment of Th17 cells that can promote arthritis by inducing the production of pro-inflammatory cytokines and receptor activator of nuclear factor κB ligand (RANKL) while inhibiting apoptosis in synoviocytes. Hypoxia in the inflamed synovium favors both the development of Th17 cells and T cells with defective OXPHOS. Furthermore, levels of glutamine and glutamate are high in the synovial fluid of RA patients (89). In a study using an animal model of RA, mTORC1 and glutamine metabolism were simultaneously suppressed using rapamycin and 6-diazo-5-oxo-L-norleucine (DON). This combination reduced Th17 proliferation and arthritic scores. Rapamycin, but not DON, also increased Tregs. Although prior usage of DON as therapy for malignancy was hampered by side effects, inhibition of autoreactive immune cells' utility of glutamine might be worth considering (90, 91). The inflammatory environment increases the level of lactate in patients' synovial fluid. One study observed that Th17 cells that took up lactate were unable to migrate, therefore, residing in the synovium (92). It should be pointed out, however, that although Th17 cells are a prominent part of RA pathology, treatment using anti-IL-17 has not shown strong beneficial effects at a level comparable to anti-TNFα (93). A better characterization of these heterogeneous cells and stratification of patients can, potentially, provide better understanding of when anti-IL-17 therapy would be of optimal therapeutic benefit. In that context, a recent study has shown that T cells from RA patients, already as naive, have a dysregulated malate-aspartate cycle, resulting in elevated levels of NAD^+ and the expansion of the ER where TNFα was produced. T cells were noted to be a major producer of TNFα compared with monocytes/macrophages (94, 95). Anti-TNFα is currently used as an efficacious therapy in RA patients, but the targeting of the mitochondria-ER cross talk might be a novel more specific therapeutic option (94). Studies have shown that non-responsiveness to anti-TNFα is, however, associated with a Th17-cell signature, potentially, indicating that T cells from

these individuals suffer from a metabolic disorder that is distinct from anti-TNFα responder patients (96). Better understanding of such disease-associated defective metabolism might prove useful for the development of therapeutics to induce durable tolerance in anti-TNFα non-responders (60, 62).

Th17-cell metabolism in systemic lupus erythematosus

Systemic lupus erythematosus (SLE) is another autoimmune disease that affects 20–70 individuals per 100,000 of the population. Patients suffer a range of symptoms; skin and kidneys are affected, probably, due to a defective removal of apoptotic bodies leading to the accumulation of cell debris of nuclear, cytosolic, and membrane origins. This debris activates autoreactive B cells in GCs and elsewhere to proliferate and activate autoreactive T cells leading to the production of anti-nuclear autoantibodies that form complement- and phagocyte-activating immune complexes. Th17 cells in SLE are signified by increased mTORC1, glycolysis, and OXPHOS. Mitochondria from lymphocytes in SLE patients are elongated, have high $\Delta\Psi m$, and produce mtROS (97). Excessive elongation of mitochondria can be explained by increased degradation of Drp1, which regulates mitochondrial fission. High levels of oxidative stress lead to overexpression of the regulator of endocytic recycling Rab4A. Rab4A, which is genetically associated with SLE, therefore, recycles Drp1 leading to the elongated mitochondria phenotype (32). A long terminal repeat polymorphism in the *RAB4A* promoter has, moreover, been identified and shown to be associated with SLE. This induces mTORC1 activity in T cells in the patients (98). The protein phosphatase 2A (PP2A) is another protein genetically associated with SLE and is shown to be reduced in Th17 cells in the patients. This finding is related to the PP2A ability to induce the expression of the Th17-inhibiting mitochondria protein PDH1 (Figure 3C) (33, 50). Th17 cells directly promote GC reactions, or produce IL-21 that can influence Tfh, and animal studies have indicated that the cells can transdifferentiate to Tfh cells (1, 34, 99). It is currently unknown whether the overactive Th17 cells associated with SLE can influence Tfh and Tfr present in GC and that are involved in the regulation of B-cell proliferation.

Defective B-cell metabolism and role in chronic inflammatory diseases

B cells differentiate to plasma cells that produce antibodies conferring humoral immunity against infectious pathogens and to memory cells. As cited in the B-cell section, metabolism is continuously regulated and changes selectively during B-cell development and activation, so they can develop a highly variable antibody repertoire that does not react with self (Figure 2, Table 2). In addition to phases of B-cell development, factors such as severity and chronicity of an infection and the age of an individual also influence B cells' metabolic properties. Aberrant regulation of cellular metabolism in B cells can lead to chronic inflammation and autoimmunity (100–102).

In RA and SLE, it is widely recognized that a breach in B-cell tolerance is an initiating step for disease development (103). In RA, B cells produce autoantibodies that recognize citrullinated antigens (anti-CCP) or the Fc part of IgG [rheumatoid factors (RFs)], the presence of which is associated with a more severe disease (104). In SLE, autoantibodies are mostly specific for nuclear antigens. Research is ongoing to understand how alteration to the B-cell metabolism in these diseases leads to immune dysregulation and autoimmunity. Assessment of the B-cell subset present in synovial tissues and synovial fluids has identified switched memory and double-negative memory B cells. These cells produce inflammatory cytokines when cultured in hypoxic conditions that mimic the synovial microenvironment. A proportion of these cells express PD1 and have active mTORC1 and a glycolytic gene signature. Assessment of intracellular NAD^+ levels confirmed that the cells are primarily driven by glycolysis (105). As cited earlier, active glycolysis is a feature of activated antibody-producing B cells.

In SLE, B-cell metabolic dysregulation can take place during the GC reaction and in B cells that produce antibodies independent of the GC reaction. One study noted increased mTORC1 activity in B cells from patients with SLE, and the presence of cells with this activity correlated to plasmablast accumulation (106). Unswitched memory B cells develop independently of GC reactions (107). The study showed that *in vitro* stimulation of unswitched memory B cells with CpG/TLR9 and IFNα led to the development of plasmablasts dependent on mTORC1. CpG-only stimulation of the unswitched memory cells on the other hand induced a memory cell phenotype that was promoted by AMPK augmentation (106). Specific stimulation and mTORC1 upregulation can, therefore, promote B-cell pathology independent of GCs. The potential involvement of GC reactions in SLE pathology has, on the other hand, been proposed based on observations that autoantibodies in the disease are generated because of defects in the clearance of apoptotic cells within the LZ of GCs leading to BCR-mediated internalization of nuclear antigens and TLR-mediated activation. B cells that undergo GC reactions express high levels of the anti-inflammatory adenosine generating ecto-5'-nucleotidase CD73. A study noted inefficient functions of B cells from patients due to defective CD73's nucleotidase activity (24). The authors suggested that the CD73 defect may promote autoimmunity due to two factors. First, there is the lack of adenosine that can render Th cells to differentiate to pro-inflammatory cells. This enables the Th cells to promote the survival of autoreactive B cells. Second, the accumulation of undegraded AMP prompts inflammation through augmenting IL-6 production by B cells (24). In GCs, mTORC1 activity is required for the selection of B

cells in the LZ (8). A study using the Roquin lupus mouse model reported that treatment of mice with metformin reduced the number of GC B cells. Furthermore, Tfh and Th17 cells were inhibited, while Tregs were increased by treatment with metformin. Inhibition of immune cells was associated with an increase in AMPK levels (108). The study, therefore, concluded that therapeutic targeting of metabolic pathways might be a strategy to suppress autoimmune GC reactions. Th17 cells may also be involved, as they play an important role in the GC reactions (34). The interaction between B cells and Th17 cells changes the metabolism of Th17 cells and leads to their activation. After TCR engagement, naive B cells prompt IL-17 production by Th17 cells through the inducible T-cell costimulator (ICOS)/inducible T-cell costimulator ligand (ICOSL) interaction (94). Intriguingly, naive B cells appear to be better inducers of T-cell responses than memory B cells. This interaction induces mTORC1 and glycolysis in the Th17 cells and IFNγ production (36, 109). T cells in patients with RA and SLE express ICOS, and the level appears to be associated with RA patients' plasma anti-CCP and RF levels. In line with the dysregulated Th17-cell phenotypes described earlier, naive B cells induce higher levels of IL-17 in RA and SLE patients' Th17 cells than Th17 cells from healthy controls (36).

Conclusions and prospects

Metabolic activity is intertwined with the functional status and stage of development and activation of immune cells and is impacted by disease. Th17 cells differentiate in response to various stresses but they do not utilize pyruvate for anaplerosis. Thus, while protective Th17 cells are reliant on glycolysis and OXPHOS, pathogenic Th17 cells only utilize glycolysis and produce putrescine that may reflect the environment in which they reside. Th17 cells are vulnerable to deficiency of certain amino acids or to deregulation of their processing in mitochondria. Stress increases $\Delta\psi m$, leading to ROS production, that would be sensed by mTORC1, and this will favor pathogenic Th17 transdifferentiation during low oxygen tension. Furthermore, deprivation from amino acids reduces survival but also influences epigenetic regulation to favor Th17 to Treg transdifferentiation. The tumor microenvironment can promote such transdifferentiation. Further studies are required to understand the physiological relevance of such transdifferentiation and whether this has a role in protection from disease or a break of tolerance. Disturbances in the transcription of genes involved in metabolism can render Th17 cells hyperactive in patients with psoriasis, RA, and SLE. Furthermore, inherited genetic changes can contribute to immune hyperreactivity. It remains to be determined, however, whether such hyperactivity directly influences/promotes the expansion of B-cell autoreactivity too, directly or indirectly Th17 cells.

During their maturation, B cells are censored at several checkpoints. At each of these developmental stages, B cells manifest different metabolic signatures. The activity of mTORC1/2 in B cells is associated with effector functions and antibody production, while AMPK promotes B cells to become memory cells. Furthermore, unlike Th17 cells, B cells display a metabolic plasticity and can replenish anaplerosis through glycolysis. Recent studies have revealed that metabolism-associated activation, stress, and exhaustion can promote B cell-mediated pathology through the breach of their tolerance. Such aberrant metabolism seems to influence both B cells involved in GC reactions and the ones that mature extrafollicularly. Furthermore, Bregs affected by aberrant metabolism lack suppressive abilities leading, potentially, to autoimmune pathology. However, knowledge on how altered metabolism influences B-cell tolerance at epigenetic levels is currently lacking.

Although Th17 cells and B cells are part of different lineages, there are similarities with their cellular metabolic responses due to similarities in microenvironments in which they can reside and are activated. In addition, disease-associated polymorphisms are known to alter metabolism in both cell types leading to the breach to immunological tolerance and the transdifferentiation of Th17 to pathogenic cells. Furthermore, Th17 cells contribute to GC reactions and the production of autoantibodies by contribution to B-cell differentiation to plasma cells. However, the metabolic status of B cells and/or Th17 cells during their interactions, leading to disease, has not yet been thoroughly examined (34, 35). Bregs, on the other hand, regulate Th17 cells. Better understanding of metabolic properties of the distinct functional subsets of B cells and T cells and how they influence each other can be of profound importance in understanding the pathogenesis of inflammatory diseases. Such information can potentially lead to the discovery of new therapeutic strategies. As overviewed in this review, such therapeutic strategies could involve inhibition of glutaminolysis, or supplementation with the SCFA pentanoate to alter cell metabolism. Future studies may need to define at what cell stage/type is modulation of metabolism most beneficial for disease amelioration while retaining the immune system intact and functional.

Author contributions

JB, TT and RM wrote the first draft which was critically scrutinized by SH and DG. RM finalized the manuscript which was then approved by all the co-authors.

Conflict of interest

The authors declare that the research was conducted in the absence of any commercial or financial relationships that could be construed as a potential conflict of interest.

Publisher's note

References

1. Stockinger B, Omenetti S. The dichotomous nature of T helper 17 cells. *Nat Rev Immunol* (2017) 17(9):535–44. doi: 10.1038/nri.2017.50

2. Chung Y, Tanaka S, Chu F, Nurieva RI, Martinez GJ, Rawal S, et al. Follicular regulatory T cells expressing Foxp3 and bcl-6 suppress germinal center reactions. *Nat Med* (2011) 17(8):983–8. doi: 10.1038/nm.2426

3. Stadhouders R, Lubberts E, Hendriks RW. A cellular and molecular view of T helper 17 cell plasticity in autoimmunity. *J Autoimmun* (2018) 87:1–15. doi: 10.1016/j.jaut.2017.12.007

4. Konjar S, Pavsic M, Veldhoen M. Regulation of oxygen homeostasis at the intestinal epithelial barrier site. *Int J Mol Sci* (2021) 22(17):9170. doi: 10.3390/ijms22179170

5. Cho SH, Raybuck AL, Stengel K, Wei M, Beck TC, Volanakis E, et al. Germinal centre hypoxia and regulation of antibody qualities by a hypoxia response system. *Nature* (2016) 537(7619):234–8. doi: 10.1038/nature19334

6. Karmaus PWF, Chen X, Lim SA, Herrada AA, Nguyen TM, Xu B, et al. Metabolic heterogeneity underlies reciprocal fates of TH17 cell stemness and plasticity. *Nature* (2019) 565(7737):101–5. doi: 10.1038/s41586-018-0806-7

7. Farmer JR, Allard-Chamard H, Sun N, Ahmad M, Bertocchi A, Mahajan VS, et al. Induction of metabolic quiescence defines the transitional to follicular b cell switch. *Sci Signal* (2019) 12(604):eaaw5573. doi: 10.1126/scisignal.aaw5573

8. Ersching J, Efeyan A, Mesin L, Jacobsen JT, Pasqual G, Grabiner BC, et al. Germinal center selection and affinity maturation require dynamic regulation of mTORC1 kinase. *Immunity* (2017) 46(6):1045–58.e6. doi: 10.1016/j.immuni.2017.06.005

9. Li M, Lazorchak AS, Ouyang X, Zhang H, Liu H, Arojo OA, et al. Sin1/mTORC2 regulate b cell growth and metabolism by activating mTORC1 and myc. *Cell Mol Immunol* (2019) 16(9):757–69. doi: 10.1038/s41423-018-0185-x

10. Gualdoni GA, Mayer KA, Goschl L, Boucheron N, Ellmeier W, Zlabinger GJ. The AMP analog AICAR modulates the Treg/Th17 axis through enhancement of fatty acid oxidation. *FASEB J* (2016) 30(11):3800–9. doi: 10.1096/fj.201600522R

11. Wen Z, Jin K, Shen Y, Yang Z, Li Y, Wu B, et al. N-myristoyltransferase deficiency impairs activation of kinase AMPK and promotes synovial tissue inflammation. *Nat Immunol* (2019) 20(3):313–25. doi: 10.1038/s41590-018-0296-7

12. Sukumar M, Liu J, Mehta GU, Patel SJ, Roychoudhuri R, Crompton JG, et al. Mitochondrial membrane potential identifies cells with enhanced stemness for cellular therapy. *Cell Metab* (2016) 23(1):63–76. doi: 10.1016/j.cmet.2015.11.002

13. Wang Y, Tao A, Vaeth M, Feske S. Calcium regulation of T cell metabolism. *Curr Opin Physiol* (2020) 17:207–23. doi: 10.1016/j.cophys.2020.07.016

14. Stolarczyk E, Vong CT, Perucha E, Jackson I, Cawthorne MA, Wargent ET, et al. Improved insulin sensitivity despite increased visceral adiposity in mice deficient for the immune cell transcription factor T-bet. *Cell Metab* (2013) 17(4):520–33. doi: 10.1016/j.cmet.2013.02.019

15. Johnson MO, Wolf MM, Madden MZ, Andrejeva G, Sugiura A, Contreras DC, et al. Distinct regulation of Th17 and Th1 cell differentiation by glutaminase-dependent metabolism. *Cell* (2018) 175(7):1780–95.e19. doi: 10.1016/j.cell.2018.10.001

16. Castellanos CA, Ren X, Gonzalez SL, Li HK, Schroeder AW, Liang HE, et al. Lymph node-resident dendritic cells drive TH2 cell development involving MARCH1. *Sci Immunol* (2021) 6(64):eabh0707. doi: 10.1126/sciimmunol.abh0707

17. Xia X, Cao G, Sun G, Zhu L, Tian Y, Song Y, et al. GLS1-mediated glutaminolysis unbridled by MALT1 protease promotes psoriasis pathogenesis. *J Clin Invest* (2020) 130(10):5180–96. doi: 10.1172/JCI129269

18. Danileviciute E, Zeng N, Capelle CM, Paczia N, Gillespie MA, Kurniawan H, et al. PARK7/DJ-1 promotes pyruvate dehydrogenase activity and maintains treg homeostasis during ageing. *Nat Metab* (2022) 4(5):589–607. doi: 10.1038/s42255-022-00576-y

19. Brucklacher-Waldert V, Ferreira C, Stebegg M, Fesneau O, Innocentin S, Marie JC, et al. Cellular stress in the context of an inflammatory environment supports TGF-beta-Independent T helper-17 differentiation. *Cell Rep* (2017) 19(11):2357–70. doi: 10.1016/j.celrep.2017.05.052

20. Dang EV, Barbi J, Yang HY, Jinasena D, Yu H, Zheng Y, et al. Control of T (H)17/T(reg) balance by hypoxia-inducible factor 1. *Cell* (2011) 146(5):772–84. doi: 10.1016/j.cell.2011.07.033

21. Kawabe T, Sun SL, Fujita T, Yamaki S, Asao A, Takahashi T, et al. Homeostatic proliferation of naive CD4+ T cells in mesenteric lymph nodes generates gut-tropic Th17 cells. *J Immunol* (2013) 190(11):5788–98. doi: 10.4049/jimmunol.1203111

22. Wu L, Hollinshead KER, Hao Y, Au C, Kroehling L, Ng C, et al. Niche-selective inhibition of pathogenic Th17 cells by targeting metabolic redundancy. *Cell* (2020) 182(3):641–54.e20. doi: 10.1016/j.cell.2020.06.014

23. Chalmin F, Mignot G, Bruchard M, Chevriaux A, Vegran F, Hichami A, et al. Stat3 and gfi-1 transcription factors control Th17 cell immunosuppressive activity *via via* the regulation of ectonucleotidase expression. *Immunity* (2012) 36(3):362–73. doi: 10.1016/j.immuni.2011.12.019

24. Hesse J, Siekierka-Harreis M, Steckel B, Alter C, Schallehn M, Honke N, et al. Profound inhibition of CD73-dependent formation of anti-inflammatory adenosine in b cells of SLE patients. *EBioMedicine* (2021) 73:103616. doi: 10.1016/j.ebiom.2021.103616

25. Nemazee D. Mechanisms of central tolerance for b cells. *Nat Rev Immunol* (2017) 17(5):281–94. doi: 10.1038/nri.2017.19

26. Taher TE, Ong VH, Bystrom J, Hillion S, Simon Q, Denton CP, et al. Association of defective regulation of autoreactive interleukin-6-Producing transitional b lymphocytes with disease in patients with systemic sclerosis. *Arthritis Rheumatol* (2018) 70(3):450–61. doi: 10.1002/art.40390

27. Turner M, Mee PJ, Costello PS, Williams O, Price AA, Duddy LP, et al. Perinatal lethality and blocked b-cell development in mice lacking the tyrosine kinase syk. *Nature* (1995) 378(6554):298–302. doi: 10.1038/378298a0

28. Mesin L, Ersching J, Victora GD. Germinal center b cell dynamics. *Immunity* (2016) 45(3):471–82. doi: 10.1016/j.immuni.2016.09.001

29. Shi LZ, Wang R, Huang G, Vogel P, Neale G, Green DR, et al. HIF1alpha-dependent glycolytic pathway orchestrates a metabolic checkpoint for the differentiation of TH17 and treg cells. *J Exp Med* (2011) 208(7):1367–76. doi: 10.1084/jem.20110278

30. Ron-Harel N, Santos D, Ghergurovich JM, Sage PT, Reddy A, Lovitch SB, et al. Mitochondrial biogenesis and proteome remodeling promote one-carbon metabolism for T cell activation. *Cell Metab* (2016) 24(1):104–17. doi: 10.1016/j.cmet.2016.06.007

31. Wu B, Qiu J, Zhao TV, Wang Y, Maeda T, Goronzy IN, et al. Succinyl-CoA ligase deficiency in pro-inflammatory and tissue-invasive T cells. *Cell Metab* (2020) 32(6):967–80 e5. doi: 10.1016/j.cmet.2020.10.025

32. Caza TN, Fernandez DR, Talaber G, Oaks Z, Haas M, Madaio MP, et al. HRES-1/Rab4-mediated depletion of Drp1 impairs mitochondrial homeostasis and represents a target for treatment in SLE. *Ann Rheum Dis* (2014) 73(10):1888–97. doi: 10.1136/annrheumdis-2013-203794

33. Apostolidis SA, Rauen T, Hedrich CM, Tsokos GC, Crispin JC. Protein phosphatase 2A enables expression of interleukin 17 (IL-17) through chromatin remodeling. *J Biol Chem* (2013) 288(37):26775–84. doi: 10.1074/jbc.M113.483743

34. Hsu HC, Yang P, Wang J, Wu Q, Myers R, Chen J, et al. Interleukin 17-producing T helper cells and interleukin 17 orchestrate autoreactive germinal center development in autoimmune BXD2 mice. *Nat Immunol* (2008) 9(2):166–75. doi: 10.1038/ni1552

35. Pfeifle R, Rothe T, Ipseiz N, Scherer HU, Culemann S, Harre U, et al. Regulation of autoantibody activity by the IL-23-TH17 axis determines the onset of autoimmune disease. *Nat Immunol* (2017) 18(1):104–13. doi: 10.1038/ni.3579

36. Zeng QH, Wei Y, Lao XM, Chen DP, Huang CX, Lin QY, et al. B cells polarize pathogenic inflammatory T helper subsets through ICOSL-dependent glycolysis. *Sci Adv* (2020) 6(37):eabb6296. doi: 10.1126/sciadv.abb6296

37. Sun V, Sharpley M, Kaczor-Urbanowicz KE, Chang P, Montel-Hagen A, Lopez S, et al. The metabolic landscape of thymic T cell development *In VivoIn vivo* and in VitroIn vitro. *Front Immunol* (2021) 12:716661. doi: 10.3389/fimmu.2021.716661

38. Palmer DB. The effect of age on thymic function. *Front Immunol* (2013) 4:316. doi: 10.3389/fimmu.2013.00316

39. Baricza E, Marton N, Kiralyhidi P, Kovacs OT, Kovacsne Szekely I, Lajko E, et al. Distinct *In VitroIn vitro* T-helper 17 differentiation capacity of peripheral naive T cells in rheumatoid and psoriatic arthritis. *Front Immunol* (2018) 9:606. doi: 10.3389/fimmu.2018.00606

40. Mukasa R, Balasubramani A, Lee YK, Whitley SK, Weaver BT, Shibata Y, et al. Epigenetic instability of cytokine and transcription factor gene loci underlies plasticity of the T helper 17 cell lineage. *Immunity* (2010) 32(5):616–27. doi: 10.1016/j.immuni.2010.04.016

41. Heikamp EB, Patel CH, Collins S, Waickman A, Oh MH, Sun IH, et al. The AGC kinase SGK1 regulates TH1 and TH2 differentiation downstream of the mTORC2 complex. *Nat Immunol* (2014) 15(5):457–64. doi: 10.1038/ni.2867

42. Sun IH, Oh MH, Zhao L, Patel CH, Arwood ML, Xu W, et al. mTOR complex 1 signaling regulates the generation and function of central and effector Foxp3(+) regulatory T cells. *J Immunol* (2018) 201(2):481–92. doi: 10.4049/jimmunol.1701477

43. De Rosa V, Galgani M, Porcellini A, Colamatteo A, Santopaolo M, Zuchegna C, et al. Glycolysis controls the induction of human regulatory T cells by modulating the expression of FOXP3 exon 2 splicing variants. *Nat Immunol* (2015) 16(11):1174–84. doi: 10.1038/ni.3269

44. Gerriets VA, Kishton RJ, Johnson MO, Cohen S, Siska PJ, Nichols AG, et al. Foxp3 and toll-like receptor signaling balance treg cell anabolic metabolism for suppression. *Nat Immunol* (2016) 17(12):1459–66. doi: 10.1038/ni.3577

45. Mayberry CL, Logan NA, Wilson JJ, Chang CH. Providing a helping hand: Metabolic regulation of T follicular helper cells and their association with disease. *Front Immunol* (2022) 13:864949. doi: 10.3389/fimmu.2022.864949

46. Omenetti S, Bussi C, Metidji A, Iseppon A, Lee S, Tolaini M, et al. The intestine harbors functionally distinct homeostatic tissue-resident and inflammatory Th17 cells. *Immunity* (2019) 51(1):77–89.e6. doi: 10.1016/j.immuni.2019.05.004

47. Kahlfuss S, Kaufmann U, Concepcion AR, Noyer L, Raphael D, Vaeth M, et al. STIM1-mediated calcium influx controls antifungal immunity and the metabolic function of non-pathogenic Th17 cells. *EMBO Mol Med* (2020) 12(8):e11592. doi: 10.15252/emmm.201911592

48. Shin B, Benavides GA, Geng J, Koralov SB, Hu H, Darley-Usmar VM, et al. Mitochondrial oxidative phosphorylation regulates the fate decision between pathogenic Th17 and regulatory T cells. *Cell Rep* (2020) 30(6):1898–909 e4. doi: 10.1016/j.celrep.2020.01.022

49. Delgoffe GM, Pollizzi KN, Waickman AT, Heikamp E, Meyers DJ, Horton MR, et al. The kinase mTOR regulates the differentiation of helper T cells through the selective activation of signaling by mTORC1 and mTORC2. *Nat Immunol* (2011) 12(4):295–303. doi: 10.1038/ni.2005

50. Gerriets VA, Kishton RJ, Nichols AG, Macintyre AN, Inoue M, Ilkayeva O, et al. Metabolic programming and PDHK1 control CD4+ T cell subsets and inflammation. *J Clin Invest* (2015) 125(1):194–207. doi: 10.1172/JCI76012

51. Xu T, Stewart KM, Wang X, Liu K, Xie M, Ryu JK, et al. Metabolic control of TH17 and induced treg cell balance by an epigenetic mechanism. *Nature* (2017) 548(7666):228–33. doi: 10.1038/nature23475

52. Mak TW, Grusdat M, Duncan GS, Dostert C, Nonnenmacher Y, Cox M, et al. Glutathione primes T cell metabolism for inflammation. *Immunity* (2017) 46(4):675–89. doi: 10.1016/j.immuni.2017.03.019

53. Roy DG, Chen J, Mamane V, Ma EH, Muhire BM, Sheldon RD, et al. Methionine metabolism shapes T helper cell responses through regulation of epigenetic reprogramming. *Cell Metab* (2020) 31(2):250–66 e9. doi: 10.1016/j.cmet.2020.01.006

54. Berod L, Friedrich C, Nandan A, Freitag J, Hagemann S, Harmrolfs K, et al. *De novoDe novo* fatty acid synthesis controls the fate between regulatory T and T helper 17 cells. *Nat Med* (2014) 20(11):1327–33. doi: 10.1038/nm.3704

55. Sundrud MS, Koralov SB, Feuerer M, Calado DP, Kozhaya AE, Rhule-Smith A, et al. Halofuginone inhibits TH17 cell differentiation by activating the amino acid starvation response. *Science* (2009) 324(5932):1334–8. doi: 10.1126/science.1172638

56. Kleinewietfeld M, Manzel A, Titze J, Kvakan H, Yosef N, Linker RA, et al. Sodium chloride drives autoimmune disease by the induction of pathogenic TH17 cells. *Nature* (2013) 496(7446):518–22. doi: 10.1038/nature11868

57. Zhang D, Jin W, Wu R, Li J, Park SA, Tu E, et al. High glucose intake exacerbates autoimmunity through reactive-Oxygen-Species-Mediated TGF-beta cytokine activation. *Immunity* (2019) 51(4):671–81.e5. doi: 10.1016/j.immuni.2019.08.001

58. Laurence A, Tato CM, Davidson TS, Kanno Y, Chen Z, Yao Z, et al. Interleukin-2 signaling *via via* STAT5 constrains T helper 17 cell generation. *Immunity* (2007) 26(3):371–81. doi: 10.1016/j.immuni.2007.02.009

59. Revu S, Wu J, Henkel M, Rittenhouse N, Menk A, Delgoffe GM, et al. IL-23 and IL-1beta drive human Th17 cell differentiation and metabolic reprogramming in absence of CD28 costimulation. *Cell Rep* (2018) 22(10):2642–53. doi: 10.1016/j.celrep.2018.02.044

60. Sugiura A, Andrejeva G, Voss K, Heintzman DR, Xu X, Madden MZ, et al. MTHFD2 is a metabolic checkpoint controlling effector and regulatory T cell fate and function. *Immunity* (2022) 55(1):65–81.e9. doi: 10.1016/j.immuni.2021.10.011

61. Patsoukis N, Bardhan K, Chatterjee P, Sari D, Liu B, Bell LN, et al. PD-1 alters T-cell metabolic reprogramming by inhibiting glycolysis and promoting lipolysis and fatty acid oxidation. *Nat Commun* (2015) 6:6692. doi: 10.1038/ncomms7692

62. Wagner A, Wang C, Fessler J, DeTomaso D, Avila-Pacheco J, Kaminski J, et al. Metabolic modeling of single Th17 cells reveals regulators of autoimmunity. *Cell* (2021) 184(16):4168–85.e21. doi: 10.1016/j.cell.2021.05.045

63. Carriche GM, Almeida L, Stuve P, Velasquez L, Dhillon-LaBrooy A, Roy U, et al. Regulating T-cell differentiation through the polyamine spermidine. *J Allergy Clin Immunol* (2021) 147(1):335–48 e11. doi: 10.1016/j.jaci.2020.04.037

64. Clarke AJ, Riffelmacher T, Braas D, Cornall RJ, Simon AK. B1a b cells require autophagy for metabolic homeostasis and self-renewal. *J Exp Med* (2018) 215(2):399–413. doi: 10.1084/jem.20170771

65. Iperi C, Bordron A, Dueymes M, Pers JO, Jamin C. Metabolic program of regulatory b lymphocytes and influence in the control of malignant and autoimmune situations. *Front Immunol* (2021) 12:735463. doi: 10.3389/fimmu.2021.735463

66. Kojima H, Kobayashi A, Sakurai D, Kanno Y, Hase H, Takahashi R, et al. Differentiation stage-specific requirement in hypoxia-inducible factor-1alpha-regulated glycolytic pathway during murine b cell development in bone marrow. *J Immunol* (2010) 184(1):154–63. doi: 10.4049/jimmunol.0800167

67. Stein M, Dutting S, Mougiakakos D, Bosl M, Fritsch K, Reimer D, et al. A defined metabolic state in pre b cells governs b-cell development and is counterbalanced by swiprosin-2/EFhd1. *Cell Death Differ* (2017) 24(7):1239–52. doi: 10.1038/cdd.2017.52

68. Akkaya M, Pierce SK. From zero to sixty and back to zero again: the metabolic life of b cells. *Curr Opin Immunol* (2019) 57:1–7. doi: 10.1016/j.coi.2018.09.019

69. Herzog S, Hug E, Meixlsperger S, Paik JH, DePinho RA, Reth M, et al. SLP-65 regulates immunoglobulin light chain gene recombination through the PI(3)K-PKB-Foxo pathway. *Nat Immunol* (2008) 9(6):623–31. doi: 10.1038/ni.1616

70. Adams WC, Chen YH, Kratchmarov R, Yen B, Nish SA, Lin WW, et al. Anabolism-associated mitochondrial stasis driving lymphocyte differentiation over self-renewal. *Cell Rep* (2016) 17(12):3142–52. doi: 10.1016/j.celrep.2016.11.065

71. Jellusova J, Cato MH, Apgar JR, Ramezani-Rad P, Leung CR, Chen C, et al. Gsk3 is a metabolic checkpoint regulator in b cells. *Nat Immunol* (2017) 18(3):303–12. doi: 10.1038/ni.3664

72. Chan LN, Chen Z, Braas D, Lee JW, Xiao G, Geng H, et al. Metabolic gatekeeper function of b-lymphoid transcription factors. *Nature* (2017) 542(7642):479–83. doi: 10.1038/nature21076

73. Waters LR, Ahsan FM, Wolf DM, Shirihai O, Teitell MA. Initial b cell activation induces metabolic reprogramming and mitochondrial remodeling. *iScience* (2018) 5:99–109. doi: 10.1016/j.isci.2018.07.005

74. Akkaya M, Traba J, Roesler AS, Miozzo P, Akkaya B, Theall BP, et al. Second signals rescue b cells from activation-induced mitochondrial dysfunction and death. *Nat Immunol* (2018) 19(8):871–84. doi: 10.1038/s41590-018-0156-5

75. Ise W, Fujii K, Shiroguchi K, Ito A, Kometani K, Takeda K, et al. T Follicular helper cell-germinal center b cell interaction strength regulates entry into plasma cell or recycling germinal center cell fate. *Immunity* (2018) 48(4):702–15 e4. doi: 10.1016/j.immuni.2018.03.027

76. Weisel FJ, Mullett SJ, Elsner RA, Menk AV, Trivedi N, Luo W, et al. Germinal center b cells selectively oxidize fatty acids for energy while conducting minimal glycolysis. *Nat Immunol* (2020) 21(3):331–42. doi: 10.1038/s41590-020-0598-4

77. Tsui C, Martinez-Martin N, Gaya M, Maldonado P, Llorian M, Legrave NM, et al. Protein kinase c-beta dictates b cell fate by regulating mitochondrial remodeling, metabolic reprogramming, and heme biosynthesis. *Immunity* (2018) 48(6):1144–59 e5. doi: 10.1016/j.immuni.2018.04.031

78. Lam WY, Becker AM, Kennerly KM, Wong R, Curtis JD, Llufrio EM, et al. Mitochondrial pyruvate import promotes long-term survival of antibody-secreting plasma cells. *Immunity* (2016) 45(1):60–73. doi: 10.1016/j.immuni.2016.06.011

79. Rubtsov AV, Swanson CL, Troy S, Strauch P, Pelanda R, Torres RM. TLR agonists promote marginal zone b cell activation and facilitate T-dependent IgM responses. *J Immunol* (2008) 180(6):3882–8. doi: 10.4049/jimmunol.180.6.3882

80. Sintes J, Gentile M, Zhang S, Garcia-Carmona Y, Magri G, Cassis L, et al. mTOR intersects antibody-inducing signals from TACI in marginal zone b cells. *Nat Commun* (2017) 8(1):1462. doi: 10.1038/s41467-017-01602-4

81. Lal G, Kulkarni N, Nakayama Y, Singh AK, Sethi A, Burrell BE, et al. IL-10 from marginal zone precursor b cells controls the differentiation of Th17, tfh and tfr cells in transplantation tolerance. *Immunol Lett* (2016) 170:52–63. doi: 10.1016/j.imlet.2016.01.002

82. Sano T, Kageyama T, Fang V, Kedmi R, Martinez CS, Talbot J, et al. Redundant cytokine requirement for intestinal microbiota-induced Th17 cell differentiation in draining lymph nodes. *Cell Rep* (2021) 36(8):109608. doi: 10.1016/j.celrep.2021.109608

83. Luu M, Pautz S, Kohl V, Singh R, Romero R, Lucas S, et al. The short-chain fatty acid pentanoate suppresses autoimmunity by modulating the metabolic-epigenetic crosstalk in lymphocytes. *Nat Commun* (2019) 10(1):760. doi: 10.1038/s41467-019-08711-2

84. Amezcua Vesely MC, Pallis P, Bielecki P, Low JS, Zhao J, Harman CCD, et al. Effector TH17 cells give rise to long-lived TRM cells that are essential for an immediate response against bacterial infection. *Cell* (2019) 178(5):1176–88 e15. doi: 10.1016/j.cell.2019.07.032

85. Kirchner FR, LeibundGut-Landmann S. Tissue-resident memory Th17 cells maintain stable fungal commensalism in the oral mucosa. *Mucosal Immunol* (2021) 14(2):455–67. doi: 10.1038/s41385-020-0327-1

86. Langley RG, Elewski BE, Lebwohl M, Reich K, Griffiths CE, Papp K, et al. Secukinumab in plaque psoriasis–results of two phase 3 trials. *N Engl J Med* (2014) 371(4):326–38. doi: 10.1056/NEJMoa1314258

87. Kokkonen H, Soderstrom I, Rocklov J, Hallmans G, Lejon K, Rantapaa Dahlqvist S. Up-regulation of cytokines and chemokines predates the onset of rheumatoid arthritis. *Arthritis Rheumatol* (2010) 62(2):383–91. doi: 10.1002/art.27186

88. Yang Z, Fujii H, Mohan SV, Goronzy JJ, Weyand CM. Phosphofructokinase deficiency impairs ATP generation, autophagy, and redox balance in rheumatoid arthritis T cells. *J Exp Med* (2013) 210(10):2119–34. doi: 10.1084/jem.20130252

89. Qiu J, Wu B, Goodman SB, Berry GJ, Goronzy JJ, Weyand CM. Metabolic control of autoimmunity and tissue inflammation in rheumatoid arthritis. *Front Immunol* (2021) 12:652771. doi: 10.3389/fimmu.2021.652771

90. Ueda Y, Saegusa J, Okano T, Sendo S, Yamada H, Nishimura K, et al. Additive effects of inhibiting both mTOR and glutamine metabolism on the arthritis in SKG mice. *Sci Rep* (2019) 9(1):6374. doi: 10.1038/s41598-019-42932-1

91. Cervantes-Madrid D, Romero Y, Duenas-Gonzalez A. Reviving lonidamine and 6-Diazo-5-oxo-L-norleucine to be used in combination for metabolic cancer therapy. *BioMed Res Int* (2015) 2015:690492. doi: 10.1155/2015/690492

92. Pucino V, Certo M, Bulusu V, Cucchi D, Goldmann K, Pontarini E, et al. Lactate buildup at the site of chronic inflammation promotes disease by inducing CD4(+) T cell metabolic rewiring. *Cell Metab* (2019) 30(6):1055–74 e8. doi: 10.1016/j.cmet.2019.10.004

93. Miossec P. Local and systemic effects of IL-17 in joint inflammation: a historical perspective from discovery to targeting. *Cell Mol Immunol* (2021) 18(4):860–5. doi: 10.1038/s41423-021-00644-5

94. Wu B, Zhao TV, Jin K, Hu Z, Abdel MP, Warrington KJ, et al. Mitochondrial aspartate regulates TNF biogenesis and autoimmune tissue inflammation. *Nat Immunol* (2021) 22(12):1551–62. doi: 10.1038/s41590-021-01065-2

95. Bystrom J, Clanchy FI, Taher TE, Al-Bogami MM, Muhammad HA, Alzabin S, et al. Response to treatment with TNFalpha inhibitors in rheumatoid arthritis is associated with high levels of GM-CSF and GM-CSF(+) T lymphocytes. *Clin Rev Allergy Immunol* (2017) 53(2):265–76. doi: 10.1007/s12016-017-8610-y

96. Alzabin S, Abraham SM, Taher TE, Palfreeman A, Hull D, McNamee K, et al. Incomplete response of inflammatory arthritis to TNFalpha blockade is associated with the Th17 pathway. *Ann Rheum Dis* (2012) 71(10):1741–8. doi: 10.1136/annrheumdis-2011-201024

97. Yin Y, Choi SC, Xu Z, Perry DJ, Seay H, Croker BP, et al. Normalization of CD4+ T cell metabolism reverses lupus. *Sci Transl Med* (2015) 7(274):274ra18. doi: 10.1126/scitranslmed.aaa0835

98. Godavarthy A, Kelly R, Jimah J, Beckford M, Caza T, Fernandez D, et al. Lupus-associated endogenous retroviral LTR polymorphism and epigenetic imprinting promote HRES-1/RAB4 expression and mTOR activation. *JCI Insight* (2020) 5(1):e134010. doi: 10.1172/jci.insight.134010

99. Vogelzang A, McGuire HM, Yu D, Sprent J, Mackay CR, King C. A fundamental role for interleukin-21 in the generation of T follicular helper cells. *Immunity* (2008) 29(1):127–37. doi: 10.1016/j.immuni.2008.06.001

100. Frasca D, Romero M, Garcia D, Diaz A, Blomberg BB. Hyper-metabolic b cells in the spleens of old mice make antibodies with autoimmune specificities. *Immun Ageing* (2021) 18(1):9. doi: 10.1186/s12979-021-00222-3

101. Jing Y, Luo L, Chen Y, Westerberg LS, Zhou P, Xu Z, et al. SARS-CoV-2 infection causes immunodeficiency in recovered patients by downregulating CD19 expression in b cells *via via* enhancing b-cell metabolism. *Signal Transduct Target Ther* (2021) 6(1):345. doi: 10.1038/s41392-021-00749-3

102. Frasca D, Pallikkuth S, Pahwa S. Metabolic phenotype of b cells from young and elderly HIV individuals. *Immun Ageing* (2021) 18(1):35. doi: 10.1186/s12979-021-00245-w

103. Tipton CM, Hom JR, Fucile CF, Rosenberg AF, Sanz I. Understanding b-cell activation and autoantibody repertoire selection in systemic lupus erythematosus: A b-cell immunomics approach. *Immunol Rev* (2018) 284(1):120–31. doi: 10.1111/imr.12660

104. Lee DM, Schur PH. Clinical utility of the anti-CCP assay in patients with rheumatic diseases. *Ann Rheum Dis* (2003) 62(9):870–4. doi: 10.1136/ard.62.9.870

105. Floudas A, Neto N, Marzaioli V, Murray K, Moran B, Monaghan MG, et al. Pathogenic, glycolytic PD-1+ b cells accumulate in the hypoxic RA joint. *JCI Insight* (2020) 5(21):e139032. doi: 10.1172/jci.insight.139032

106. Torigoe M, Iwata S, Nakayamada S, Sakata K, Zhang M, Hajime M, et al. Metabolic reprogramming commits differentiation of human CD27(+)IgD(+) b cells to plasmablasts or CD27(-)IgD(-) cells. *J Immunol* (2017) 199(2):425–34. doi: 10.4049/jimmunol.1601908

107. Taylor JJ, Pape KA, Jenkins MK. A germinal center-independent pathway generates unswitched memory b cells early in the primary response. *J Exp Med* (2012) 209(3):597–606. doi: 10.1084/jem.20111696

108. Lee SY, Moon SJ, Kim EK, Seo HB, Yang EJ, Son HJ, et al. Metformin suppresses systemic autoimmunity in roquin(san/san) mice through inhibiting b cell differentiation into plasma cells *via via* regulation of AMPK/mTOR/STAT3. *J Immunol* (2017) 198(7):2661–70. doi: 10.4049/jimmunol.1403088

109. Paulos CM, Carpenito C, Plesa G, Suhoski MM, Varela-Rohena A, Golovina TN, et al. The inducible costimulator (ICOS) is critical for the development of human T(H)17 cells. *Sci Transl Med* (2010) 2(55):55ra78. doi: 10.1126/scitranslmed.3000448

10.3389/fimmu.2022.990794

Glossary

2-HG	2-hydroxyglutarate
ACC1	acetyl-coenzyme carboxylase 1
acetyl-CoA	acetyl-coenzyme A
AID	activation-induced cytidine deaminase
APC	antigen-presenting cell
anti-CCP	anti-cyclic citrullinated peptide antibody
ATP	adenosine triphosphate
Akt	Ak strain transforming (also known as protein kinase B or PKB)
AICAR	5-Aminoimidazole-4-carboxamide ribonucleotide
AMPK	AMP-activated protein kinase
BAFF	B-cell activating factor
BATF	basic leucine zipper ATF-like transcription factor
Bcl-6	B-cell lymphoma 6
BCR	B-cell receptor
Breg	regulatory B cell
CCR7	chemokine (C-C motif) receptor 7
ΔΨm	mitochondrial membrane potential
DC	dendritic cell
DON	6-diazo-5-oxo-L-norleucine
Drp1	dynamin-related protein 1
EFhd1	EF-hand domain family member D1
ETC	electron transport chain
FAO	fatty acid oxidation
FDC	follicular dendritic cell
FOXO1	forkhead box protein O1
FOXP3	forkhead box P3
GATA-3	GATA-binding protein 3
GCN2	general control nonderepressible 2
GC	germinal center
GLS1	glutaminase 1
GLUT1	glucose transporter 1
GOT1	glutamate oxaloacetate transaminase 1
GSK3	glycogen synthase kinase-3
HIF1α	hypoxia-inducible factor 1α
ICOS	inducible T-cell costimulator
ICOSL	inducible T-cell costimulator ligand
LEF1	lymphoid enhancer-binding factor 1
LLPC	long-lived plasma cell
LN	lymph node

(Continued)

Continued

LZ	light zone
MALT1	mucosa-associated lymphoid tissue lymphoma translocation protein 1
MTHFD2	bifunctional methylenetetrahydrofolate dehydrogenase/ cyclohydrolase
mTORC	mechanistic target of rapamycin
mtROS	mitochondrial reactive oxygen species
MZB	marginal zone B cell
NADH	nicotinamide adenine dinucleotide
NADPH	Nicotinamide adenine dinucleotide phosphate
OXPHOS	oxidative phosphorylation
PAX5	paired box 5
PDH1	pyruvate dehydrogenase 1
PI3K	phosphatidylinositol 3-kinase
PKCβ	protein kinase Cβ
PP2A	protein phosphatase 2A
PPP	pentose-phosphate pathway
Rab4A	Ras-related protein Rab-4A
RANKL	receptor activator of nuclear factor kappa-β ligand
RF	rheumatoid factor
RORγt	RAR-related orphan receptor γt
ROS	reactive oxygen species
SAM	S-adenosylmethionine
SCFAs	short-chain fatty acids
SFB	segmented filamentous bacteria
SHM	somatic hypermutation
SUCLG2	GDP-forming β subunit of succinate-CoA ligase
STAT3	signal transducer and activator of transcription 3
STIM1	stromal interaction molecule 1
SYK	spleen-associated tyrosine kinase
T1/2 B cell	transitional 1/2 B cell
TACI	transmembrane activator and CAML interactor
T-bet	T-box expressed in T cells
TCA	tricarboxylic acid
TCF1	T-cell factor 1
TCR	T-cell receptor
Tfh	follicular helper T cell
Tfr	follicular regulatory T cell
TGFβ	transforming growth factor-β
TLR	Toll-like receptor
Treg	regulatory T cell
Trm	tissue-resident memory T cell

frontiers | Frontiers in Immunology

TYPE Original Research
PUBLISHED 09 December 2022
DOI 10.3389/fimmu.2022.1001911

OPEN ACCESS

EDITED BY
Rizgar A. Mageed,
Queen Mary University of London,
United Kingdom

REVIEWED BY
Juandy Jo,
University of Pelita Harapan, Indonesia
Mahnaz Jamee,
Research Institute for Children's
Health (RICH), Iran

*CORRESPONDENCE
Li Wei
liweihx_hxyy@scu.edu.cn

†These authors have contributed
equally to this work

SPECIALTY SECTION
This article was submitted to
Autoimmune and Autoinflammatory
Disorders: Autoinflammatory
Disorders,
a section of the journal
Frontiers in Immunology

RECEIVED 24 July 2022
ACCEPTED 23 November 2022
PUBLISHED 09 December 2022

CITATION
Zeng-Yun-Ou Z, Zhong-Yu J and
Wei L (2022) Bidirectional associations
between eosinophils, basophils, and
lymphocytes with atopic dermatitis:
A multivariable Mendelian
randomization study.
Front. Immunol. 13:1001911.
doi: 10.3389/fimmu.2022.1001911

Bidirectional associations between eosinophils, basophils, and lymphocytes with atopic dermatitis: A multivariable Mendelian randomization study

Zhang Zeng-Yun-Ou[1†], Jian Zhong-Yu[2†] and Li Wei[3*]

[1]Department of Dermatology, West China Hospital, Sichuan University, Chengdu, China, [2]Department of Urology, Institute of Urology (Laboratory of Reconstructive Urology), West China Hospital, Sichuan University, Chengdu, China, [3]Department of Dermatology and Rare Disease Center, West China Hospital, Sichuan University, Chengdu, Sichuan, China

Background: Despite being prone to reverse causation and having unmeasured confounding factors, many clinical observational studies have highlighted the critical association between basophils, eosinophils, and lymphocytes and atopic dermatitis (AD). Whether these cells play a causal role in AD development remains uncertain.

Methods: Data were obtained from the UK Biobank and the Blood Cell Consortium, from a large publicly available genome-wide association study (GWAS) with more than 500,000 subjects of European ancestry and for AD from three independent cohorts with more than 700,000 subjects of European ancestry. We performed single-variable Mendelian randomization (SVMR), followed by multivariable Mendelian randomization (MVMR) to assess the total and direct effects of immune cell counts on AD risk.

Results: SVMR estimates showed that genetically predicted higher eosinophil [odds ratio (OR): 1.23, 95% confidence interval (CI): 1.17–1.29, p = 5.85E–16] and basophil counts (OR: 1.11, 95% CI: 1.03–1.19, p = 0.004) had an adverse effect on the risk of AD, while a higher lymphocyte count (OR: 0.93, 95% CI: 0.89–0.98, p = 0.006) decreased the risk. Reverse MR analysis showed higher basophil (beta: 0.04, 95% CI: 0.01–0.07, p = 0.014) and lower lymphocyte counts (beta: −0.05, 95% CI: −0.09 to −0.01, p = 0.021) in patients with AD. In MVMR, the effects of eosinophils (OR: 1.19, 95% CI: 1.09–1.29, p = 8.98E–05), basophils (OR: 1.19, 95% CI: 1.14–1.24, p = 3.72E–15), and lymphocytes (OR: 0.93, 95% CI: 0.89–0.98, p = 0.006) were still significant.

Discussion: Mendelian randomization (MR) findings suggest that an increase in the eosinophil and basophil counts and a decrease in the lymphocyte counts are potential causal risk factors for AD. These risk factors are independent of each other.

KEYWORDS

eosinophils, basophils, lymphocytes, atopic dermatitis (AD), Mendelian randomization

Introduction

Atopic dermatitis (AD) is a relapsing chronic inflammatory skin disease characterized by intense itching episodes, elevated eosinophilia, and a dysregulated immune response. The global prevalence of AD is approximately 15%–20% in children and 1%–3% in adults. It has increased two- to threefold, reaching 15%–20% among children and up to 10% among adults, with over 15% overall prevalence in Europe (1, 2). The Global Burden of Disease study showed that AD has the highest disease burden and seriously affects the quality of life and social functioning of patients (3). The complex interplay between immune cells, which leads to immune dysfunction, is an underlying pathogenic mechanisms (4). Many clinical observational studies have revealed that basophils, eosinophils, and lymphocytes are dysregulated in peripheral blood and skin lesions, highlighting their role in the development of AD (5–9).

Basophils are rare circulating granulocytes associated with pruritus that promote AD-like allergic skin inflammation (10). They are activated systemically and promote immune dysregulation in the AD models (10–12). However, the specific mechanism of pathogenesis remains unclear. The activation of eosinophils in peripheral blood and skin lesions is critical for the pathogenesis of AD. Elevated eosinophil levels are risk factors characteristic of AD (13–15) and serve as clinical biomarkers for its assessment. However, the limitations of observational studies result in a lack of evidence highlighting the increased eosinophil count as a definite risk factor. Immune dysregulation in AD is also related to lymphocytes. Typically, the peripheral blood lymphocyte count of patients is normal, and the role of lymphocyte subtypes in immune dysregulation has garnered more interest than the overall lymphocyte count (16, 17). However, the relationship between peripheral blood lymphocyte count and AD is unclear.

Eosinophils, basophils, and lymphocytes play critical roles in augmenting the immune response in AD. Observational epidemiological designs are prone to reverse causation and unmeasured confounding, and the causal role of immune cells in AD development remains uncertain. Mendelian randomization (MR), which is widely used to explore the causality between candidate risk factors and diseases (18, 19), employs single-nucleotide polymorphisms (SNPs) as genetic tools and reliably estimates their effects on the outcomes of interest. The MR approach investigates causal relationships by exploiting genetic variants as instrumental variables (IVs) that influence exposure status, thereby accounting for observational study bias in epidemiological studies, including reverse causation (18). Therefore, we used this method to evaluate the causal relationships between AD and immune cells, specifically the number of eosinophils, basophils, and lymphocytes.

Materials and methods

Study design

Single-variable MR (SVMR) and reverse MR were conducted to explore the bidirectional associations between immune cell counts (eosinophils, basophils, and lymphocytes) and AD. Given the interplay among the three cell types, multivariable MR (MVMR) was performed to assess the influence of these cell types independently on AD risk (Figure 1A). SVMR [inverse variance weighted (IVW), MR–Egger, weighted median, and weighted mode] and MVMR were applied to the estimates. When the genetic variants were independent of each other and no evidence of targeted pleiotropy was observed in the selected IVs (Egger-intercept p-value > 0.05), the IVW method was considered the most efficient.

These methods provide useful sensitivity analyses to explore whether the variants are pleiotropic. MR analysis uses IVW as the primary method when all the genetic variants are valid IVs. MR estimates are reported as odds ratios (ORs), which are interpreted as the risk of AD observed with a per-unit increase in inverse normalized immune cell count. The per unit of immune cell count was defined as the relative count (per unit volume of blood) of all immune cells (eosinophils, basophils, and lymphocytes) that was $\log_{10}$ transformed before regression modeling and then inverse normalized for cohort level association analysis or genome-wide association studies (GWAS) (20).

Data resources

A multiple-sample MR analysis with multiple genetic variants as instrumental variables was performed based on summary statistics. Summary statistics of SNPs were retrieved for immune cells (eosinophils, basophils, and lymphocytes) from a subset of the GWAS, which included 29 blood cell phenotypes, to perform a genome-wide discovery analysis examining 563,946 participants of European ancestry from the UK Biobank cohort and the Blood Cell Consortium (21, 22). For AD, we used the summary GWAS statistics, with FinnGen Preparatory Phase Data Freeze 6 comprising data corresponding to 244,544 Finnish adults (8,383 AD cases; 236,161 controls), the Estonian Biobank cohort data from 136,724 participants (11,187 AD cases; 125,537 controls),

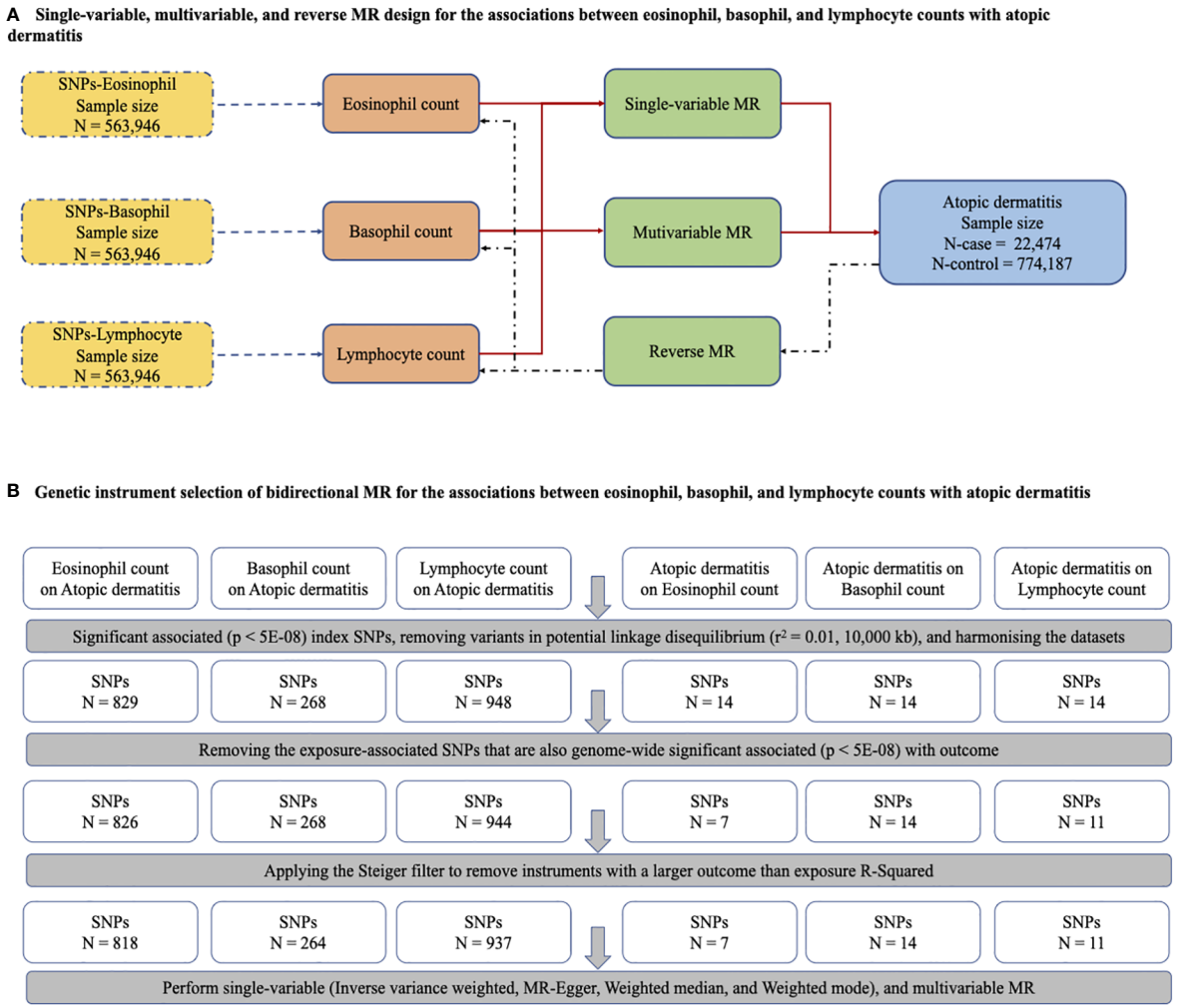

FIGURE 1
The main design of MR, identification of genetic instruments, and data and MR methods used for analyses. **(A)** Single-variable, multivariable, and reverse MR design for the association between eosinophil, basophil and lymphocyte with atopic dermatitis. **(B)** Genetic instrument selection of bidirectional MR for the associations between eosinophil, basophil and lymphocyte with atopic dermatitis. SNPs, single-nucleotide polymorphisms; MR, Mendelian randomization.

and the UK Biobank data from 2,904 AD cases and 412,489 controls. The details are presented in Supplementary Table 1.

Instrument selection

All genetic variants that were characterized as significantly associated index SNPs (p < 5E−08) with immune cell counts (eosinophils, basophils, and lymphocytes) were selected as IVs. Since the SNPs were in a state of corresponding linkage disequilibrium, we harmonized the datasets by removing variants in potential linkage disequilibrium (r^2 = 0.01, 10,000 kb). Next, SNPs that were also significantly associated with outcomes (p < 5E−08) were removed, and the Steiger filter was applied to eliminate instruments with a larger outcome than the exposure R^2. Finally, criteria-compliant SNPs were included in our model of bidirectional MR analysis, including the counts on AD of eosinophils (SNPs, N = 818), basophils (SNPs, N = 264), and lymphocytes (SNPs, N = 937), and AD on the counts of eosinophils (SNPs, N = 7), basophils (SNPs, N = 14), and lymphocytes (SNPs, N = 11) (Figure 1B). The F statistics related to the proportion of variance in the exposure explained by the genetic variants and the strength of all 2,051 SNPs as genetic instruments measured by the F statistics ranged from 70.58 to 171.22, indicating a smaller possibility of weak IV bias

(Supplementary Table 2). The details of all SNPs for immune cells are presented in Supplementary Table 3.

MR assumption

Three key assumptions were made for each of the genetic variants in this MR analysis. First, in the relevance assumption, the genetic variants were associated with the risk factor of interest in a large genome-wide study and the IVs with blood cells with GWAS significance. Next, in the independence assumption, the associations between IVs and outcomes had no unmeasured confounders. Finally, in the exclusion restriction assumption, IVs affected the outcome only through their effect on the risk factor of interest. Genetic variants may affect the outcome through pathways other than the target exposure factor of interest. When genetic variants have pleiotropic effects, IVW, MR–Egger, weighted median, and weighted methods are used to estimate the robust effects. The weighted median method provides reliable evidence when at least half of the valid instrumental variables have no pleiotropic effects, while MR–Egger regression provides consistent estimates when 100% of genetic variants are invalid IVs. In addition, we reduced the weak association between potential confounders and genetic variations by rigorous screening for IVs.

Statistical analysis

Analyses were performed using the packages Two-Sample MR and MVMR in R v.4.0.3 (www.r-project.org), and power calculations were performed using an online tool (http://cnsgenomics.com/shiny/mRnd/).

Results

Univariable MR analysis of the association between eosinophil, basophil, and lymphocyte counts and AD risk

In standard IVW SVMR analysis, after removing pleiotropic SNPs, we found evidence for genetically predicted eosinophil count (OR: 1.23, 95% CI: 1.17–1.29, p = 5.85E−16) with an effect estimate that was consistent with an increased risk for AD (Figure 2). The estimates were consistent between MR–Egger sensitivity analyses and the weighted median methods (Figure 3). SVMR analyses also showed that the basophil count (OR: 1.11, 95% CI: 1.03–1.19, p = 0.004) was associated with an increased risk of AD (Figure 2). The sensitivity analysis results showed a consistent trend (Figure 3). However, genetic variants associated with lymphocyte count (OR: 0.93, 95% CI: 0.89–0.98, p = 0.006) showed a decreased risk for AD (Figure 2). The effect directions of the sensitivity analyses were consistent (Figure 3). The weighted model (OR: 0.85, 95% CI: 0.75–0.96, p = 0.007) showed that a 1-unit increase in lymphocyte count (per nl volume of blood) was causally associated with a 15% relative decrease in AD risk. For all considered outcomes, the intercept test of the Egger-intercept p-value did not demonstrate statistical significance and did not indicate horizontal pleiotropy (Supplementary Table 2).

We also performed reverse causation analyses. When performing an MR analysis with AD as the exposure, reverse causation indicated a significant effect of the immune cell count on AD (Table 1). In our analyses, we observed a strong causal association between AD and

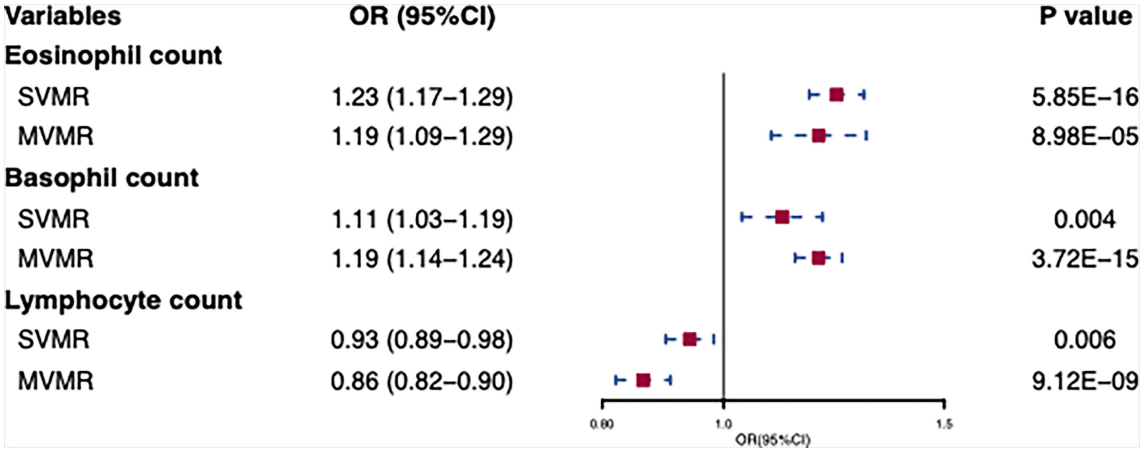

FIGURE 2
Univariable and multivariable MR of the effect of eosinophils, basophils, and lymphocytes on atpic dermatitis. OR, odds ratio; CI, confidence interval; SVMR, Single-variable MR; MVMR, multivariable MR.

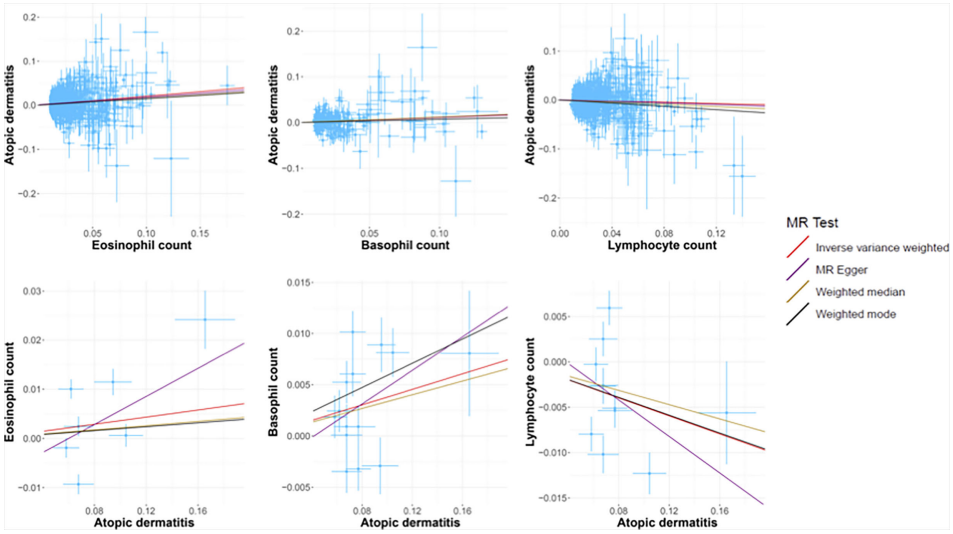

FIGURE 3
The scatter plots of all MR test results. The red, purple, yellow, and black line represents the IVW, MR-Egger, Weighted median, and Weighted mode effect, respectively. The slope of the line represents the MR effect size.

basophil (beta: 0.04, 95% CI: 0.01–0.07, p = 0.014) and lymphocyte counts (beta: −0.05, 95% CI: −0.09 to −0.01, p = 0.021). However, reverse causation analyses between AD and eosinophil (beta: 0.05, 95% CI: −0.04 to −0.11, p = 0.354) count did not offer meaningful insights. The scatter plots of all the MR tests also showed a consistent trend (Figure 3).

Multivariable MR analysis of the association between eosinophil, basophil, and lymphocyte counts and AD risk

In IVW-MVMR, upon assessing the association of genetic liabilities between immune cell count and AD, eosinophil (OR: 1.19, 95% CI: 1.09–1.29, p = 8.98E−05) and basophil counts (OR: 1.19, 95% CI: 1.14–1.24, p = 3.72E−15) retained a positive relationship with AD (Figure 2), while lymphocyte count (OR: 0.93, 95% CI: 0.89–0.98, p = 0.006) had a negative relationship (Figure 2). These results were broadly consistent with those observed in SVMR. In MVMR–Egger sensitivity analyses, horizontal pleiotropy was not indicated, leading to very similar effect estimates (eosinophil count, OR: 1.15, 95% CI: 1.09–1.22, p = 9.77E−07; basophil count, OR: 1.19, 95% CI: 1.09–1.30, p = 1.2E−04; lymphocyte count, OR: 0.86, 95% CI: 0.82–0.90, p = 3.48E−09) to those observed with IVW-MVMR.

Discussion

Using conventional MVMR, potential bidirectional associations between the genetic liability for immune cell count and AD were evaluated, and genetic evidence indicated that an increase in the count of eosinophils and basophils was associated with increased AD risk. Strikingly, a decrease in lymphocyte count increased AD risk in individuals of European descent.

Immune cell count estimates were consistent in magnitude and direction across IVW, weighted median, weighted mode, and MR–Egger analyses. Furthermore, as typically expected in MR genetic association studies, eosinophil and basophil counts indicated a strong positive association with AD, but lymphocyte count had the opposite relationship. The results of MVMR analysis were consistent with those of SVMR analyses. The MR–Egger and Egger-intercept p-value results in the MR analysis indicated the absence of pleiotropy. These findings validated the clinical phenomenon reported in observational literature that indicates an increase in some immune cells in the peripheral blood of patients with AD (14, 23), revealing that increased eosinophil and basophil counts increased AD risk. A decrease in lymphocyte count could increase the risk of AD; however, this hypothesis has garnered little interest in clinical settings.

In atopic diseases, eosinophils are recruited and activated by thymic stromal lymphopoietin and interleukin 33 (IL-33). Activated eosinophils migrate to the target organ and enhance

10.3389/fimmu.2022.1001911

TABLE 1 Associations between eosinophil, basophil, and lymphocyte counts with atopic dermatitis using two-sample Mendelian randomization.

Exposure	Outcome	N-SNPs	MR—method	OR (Beta)	95% LCI	95% UCI	*p*-value	Heterogeneity (I^2)	Egger-intercept *p*-value
Eosinophil count	Atopic dermatitis	818	IVW	1.23	1.17	1.29	5.85E−16	47%	
			MR Egger	1.19	1.08	1.32	6.43E−04		0.466
			Weighted median	1.17	1.09	1.25	3.87E−06		
			Weighted mode	1.16	0.96	1.41	0.121		
Basophil count	Atopic dermatitis	264	IVW	1.11	1.03	1.20	0.004	24%	
			MR Egger	1.12	0.97	1.29	0.125		0.965
			Weighted median	1.13	1.02	1.25	0.025		
			Weighted mode	1.07	0.87	1.32	0.516		
Lymphocyte count	Atopic dermatitis	937	IVW	0.94	0.90	0.98	0.006	28%	
			MR Egger	0.92	0.84	1.01	0.065		0.571
			Weighted median	0.89	0.83	0.96	0.001		
			Weighted mode	0.85	0.75	0.96	0.007		
Atopic dermatitis	Eosinophil count	7	IVW	0.04	−0.04	0.11	0.354	92%	
			MR Egger	0.14	−0.15	0.44	0.388		0.496
			Weighted median	0.02	−0.02	0.06	0.271		
			Weighted mode	0.02	−0.03	0.06	0.420		
Atopic dermatitis	Basophil count	14	IVW	0.04	0.01	0.07	0.014	73%	
			MR Egger	0.08	−0.07	0.24	0.321		0.580698484
			Weighted median	0.03	0.01	0.06	0.014		
			Weighted mode	0.06	−0.01	0.13	0.131		
Atopic dermatitis	Lymphocyte count	11	IVW	−0.05	−0.09	−0.01	0.021	86%	
			MR Egger	−0.10	−0.32	0.12	0.387		0.650469385
			Weighted median	−0.04	−0.07	−0.01	0.009		
			Weighted mode	−0.05	−0.10	0.00	0.076		

Th2 responses by inducing the expression of specific chemokines such as CCL22 and CCL17 (24). Many studies have observed that eosinophils are typically increased in the peripheral blood in atopic diseases (AD, asthma, allergic rhinitis, eosinophilic esophagitis, and food allergy) (13, 23, 25). Although atopic disorders differ in their pathogenesis, they share a similar atopic phenotype, such as an increased eosinophil count in the peripheral blood. Many observational studies have shown that personal or parental history of allergic rhinitis and asthma are risk factors for the development of AD (26–28). Compared to the general population, patients with other atopic diseases have a higher rate of AD (29). This may be related to the activation and increased number of eosinophils in the blood. However, this hypothesis cannot be proven because of the complex pathogenesis of atopic disorders and many confounding factors. Since univariable MR analyses indicate eosinophil count to be a strong causal risk factor for AD but do not support a causal relationship between AD and eosinophil count, our findings provide genetic evidence that eosinophil count is a risk factor for AD.

Although basophils constitute only <1% of peripheral blood leukocytes in humans, they play a critical role in mediating immune mechanisms and are promising novel markers for measuring the severity of AD. Basophils are associated with the development of inflammation and barrier function imbalance in AD (11, 12) and are activated by immunoglobulin (Ig)E. They

may also be activated independently of IgE. Activated basophils are increased in skin lesions and peripheral blood and promote inflammation and itching by secreting histamine, Th2 cytokines (basophil-derived IL-4 promotes Th2 differentiation), proteases, and eicosanoids (30, 31). Two observational studies found a positive association between AD and basophil count in peripheral blood. Although peripheral basophil count was significantly higher in patients with AD than in healthy controls (23, 32), it has not been proven to be a risk factor for AD. In this study, we found genetic evidence that increased basophil count was associated with increased AD risk and *vice versa*. These findings imply that patients with AD may have a higher peripheral blood basophil count that may not be above the normal upper limit compared to that in healthy individuals. Individuals with high basophil levels are at a higher risk of AD than healthy individuals. This may explain why the basophil count in the blood of patients with AD may be normal.

B and T lymphocyte imbalance is an important immune mechanism involved in AD. Recently, the specific subtypes of lymphocytes and their roles, rather than their overall count, have garnered significant interest. The findings of two retrospective studies indicating that the peripheral lymphocyte count of the AD group is higher than that of the healthy controls (33, 34) need to be confirmed by epidemiological data and clinical studies. SVMR analysis proved the negative relationship between lymphocyte count and AD and *vice versa*. A 1-unit increase in lymphocyte count was causally associated with a 15% relative decrease in AD risk. This was the first study to propose a relationship between the lymphocyte count and AD. Although the lymphocyte count is normal in the blood of most patients with AD, lower lymphocyte counts may be detrimental to disease control. Our findings indicate that the normal ranges of lymphocyte count in the blood may not be appropriate for patients with AD.

Redefining the range of these cells in specific disorders may be beneficial for the prevention and surveillance of AD. Disorders characterized by increased eosinophils and basophils or decreased lymphocytes in the peripheral blood should be examined, as they may also induce AD. Overall, our findings fill the gap in the association between the number of eosinophils, basophils, and lymphocytes and AD observed in previous epidemiological observational studies.

Strength and limitations

This study had several strengths. The large sample size in GWAS increased the measurement precision. The MVMR models had major strengths, and rigorous screening of IVs greatly improved the confidence of our results. The consistent trends observed in the MR sensitivity analysis indicated high reliability. The limitations of this study should also be noted. Although the sensitivity analyses failed to find evidence of horizontal pleiotropy, we could not exclude the association, which could be mediated *via* other causal pathways. Next, as our cohorts included mostly European populations, caution is warranted before applying the findings to non-European populations. Finally, the sourcing of our cohorts from different countries in Europe may have resulted in data overlap; however, the inclusion of larger cohorts may reduce this effect.

Conclusion

MR findings suggest that an increase in the eosinophil and basophil counts and a decrease in the lymphocyte counts are potential causal risk factors for AD. These risk factors are independent of each other.

Data availability statement

The datasets presented in this study can be found in online repositories. The names of the repository/repositories and accession number(s) can be found below: https://www.ncbi.nlm.nih.gov/genbank/, The GWAS data of immune cells were from MRC Integrative Epidemiology Unit (IEU) OpenGwas project (ieu-b-33 for eosinophils, ieu-b-29 for basophils and ieu-b-32 for lymphocytes) https://www.ebi.ac.uk/metagenomics/, The GWAS data of AD were from the NHGRI-EBI Catalog (https://www.ebi.ac.uk/gwas/) with ID GCST90027161.

Author contributions

LW and JZ-Y conceived the study, participated in its design and coordination, and critically revised the manuscript. JZ-Y and ZZ-Y-O searched the databases, and reviewed the GWAS datasets and finished the data collection. JZ-Y finished the data analysis. ZZ-Y-O drafted the manuscript. All authors contributed to the article and approved the submitted version.

Funding

This work including the Rapid Service Fee was supported in part by the 1.3.5 project for disciplines of excellence, West China Hospital, Sichuan University (Grant. ZYJC21050) and the Key R&D project of Science and Technology Department of Sichuan Pro- vince (Grant. 2021YFG0306).

Conflict of interest

The authors declare that the research was conducted in the absence of any commercial or financial relationships that could be construed as a potential conflict of interest.

Publisher's note

All claims expressed in this article are solely those of the authors and do not necessarily represent those of their affiliated organizations, or those of the publisher, the editors and the reviewers. Any product that may be evaluated in this article, or claim that may be made by its manufacturer, is not guaranteed or endorsed by the publisher.

Supplementary material

The Supplementary Material for this article can be found online at: https://www.frontiersin.org/articles/10.3389/fimmu.2022.1001911/full#supplementary-material

References

1. Nutten S. Atopic dermatitis: global epidemiology and risk factors. *Ann Nutr Metab* (2015) 66(Suppl 1):8–16. doi: 10.1159/000370220

2. Avena-Woods C. Overview of atopic dermatitis. *Am J Manag Care* (2017) 23 (8 Suppl):S115–23.

3. Stander S. Atopic dermatitis. *N Engl J Med* (2021) 384(12):1136–43. doi: 10.1056/NEJMra2023911

4. Strathie Page S, Weston S, Loh R. Atopic dermatitis in children. *Aust Fam Physician* (2016) 45(5):293–6.

5. Werfel T, Allam JP, Biedermann T, Eyerich K, Gilles S, Guttman-Yassky E, et al. Cellular and molecular immunologic mechanisms in patients with atopic dermatitis. *J Allergy Clin Immunol* (2016) 138(2):336–49. doi: 10.1016/j.jaci.2016.06.010

6. Celakovska J, Bukac J, Ettler K, Vaneckova J, Krcmova I, Ettlerova K, et al. Evaluation of peripheral blood eosinophilia in adolescent and adult patients suffering from atopic dermatitis and the relation to the occurrence of allergy to aeroallergens. *Indian J Dermatol* (2019) 64(1):34–40. doi: 10.4103/ijd.IJD_509_17

7. Wang F, Anna MT, Li F, Kim S, Chen Z, Chai JN, et al. A basophil-neuronal axis promotes itch. *Cell* (2021) 184(2):422–440.e17. doi: 10.1016/j.cell.2020.12.033

8. David Boothe W, Tarbox JA, Tarbox MB. Atopic dermatitis: Pathophysiology. *Adv Exp Med Biol* (2017) 1027:21–37. doi: 10.1007/978-3-319-64804-0_3

9. Kader HA, Azeem M, Jwayed SA, Al-Shehhi A, Tabassum A, Ayoub MA, et al. Current insights into immunology and novel therapeutics of atopic dermatitis. *Cells* (2021) 10(6):1392. doi: 10.3390/cells10061392

10. Hou T, Tsang MSM, Kan LLK, Li P, Chu IMT, Wong CK, et al. IL-37 targets TSLP-primed basophils to alleviate atopic dermatitis. *Int J Mol Sci* (2021) 22 (14):7393. doi: 10.3390/ijms22147393

11. Pellefigues C, Naidoo K, Mehta P, Schmidt AJ, Jagot F, Roussel E, et al. Basophils promote barrier dysfunction and resolution in the atopic skin. *J Allergy Clin Immunol* (2021) 148(3):799–812.e10. doi: 10.1016/j.jaci.2021.02.018

12. Yamanishi Y, Mogi K, Takahashi K, Miyake K, Yoshikawa S, Karasuyama H. Skin-infiltrating basophils promote atopic dermatitis-like inflammation *via* IL-4 production in mice. *Allergy* (2020) 75(10):2613–22. doi: 10.1111/all.14362

13. Byeon JH, Yoon W, Ahn SH, Lee HS, Kim S, Yoo Y. Correlation of serum interleukin-31 with pruritus and blood eosinophil markers in children with atopic dermatitis. *Allergy Asthma Proc* (2020) 41(1):59–65. doi: 10.2500/aap.2020.41.190016

14. Holm JG, Hurault G, Agner T, Clausen ML, Kezic S, Tanaka RJ, et al. Immunoinflammatory biomarkers in serum are associated with disease severity in atopic dermatitis. *Dermatology* (2021) 237(4):513–20. doi: 10.1159/000514503

15. Wu T, Tang L, Feng Y, Jia Y, Li F. Eosinophils and associated parameters in different types of skin diseases related to elevated eosinophil levels. *Ann Transl Med* (2022) 10(2):73. doi: 10.21037/atm-22-99

16. Alkon N, Bauer WM, Krausgruber T, Goh I, Griss J, Nguyen V, et al. Single-cell analysis reveals innate lymphoid cell lineage infidelity in atopic dermatitis. *J Allergy Clin Immunol* (2022) 149(2):624–39. doi: 10.1016/j.jaci.2021.07.025

17. Gu Y, Li K, Sun J, Zhang J. Characterization of CD19(+) CD24(hi) CD38(hi) b cells in Chinese adult patients with atopic dermatitis. *J Eur Acad Dermatol Venereol* (2020) 34(12):2863–70. doi: 10.1111/jdv.16399

18. Davies NM, Holmes MV, Davey Smith G. Reading mendelian randomisation studies: a guide, glossary, and checklist for clinicians. *BMJ* (2018) 362:k601. doi: 10.1136/bmj.k601

19. Skrivankova VW, Richmond RC, Woolf BAR, Yarmolinsky J, Davies NM, Swanson SA, et al. Strengthening the reporting of observational studies in epidemiology using mendelian randomization: The STROBE-MR statement. *JAMA* (2021) 326(16):1614–21. doi: 10.1001/jama.2021.18236

20. Vuckovic D, Bao EL, Akbari P, Lareau CA, Mousas A, Jiang T, et al. The polygenic and monogenic basis of blood traits and diseases. *Cell* (2020) 182 (5):1214–1231.e11. doi: 10.1016/j.cell.2020.08.008

21. Hemani G, Zheng J, Elsworth B, Wade KH, Haberland V, Baird D, et al. The MR-base platform supports systematic causal inference across the human phenome. *Elife* (2018) 7:e34408. doi: 10.7554/eLife.34408

22. Elsworth B, Lyon M, Alexander T, Liu Y, Matthews P, Hallett J, et al. The MRC IEU OpenGWAS data infrastructure. *bioRxiv* (2020). doi: 10.1101/2020.08.10.244293

23. Hu Y, Liu S, Liu P, Mu Z, Zhang J. Clinical relevance of eosinophils, basophils, serum total IgE level, allergen-specific IgE, and clinical features in atopic dermatitis. *J Clin Lab Anal* (2020) 34(6):e23214. doi: 10.1002/jcla.23214

24. Folci M, Ramponi G, Arcari I, Zumbo A, Brunetta E. Eosinophils as major player in type 2 inflammation: Autoimmunity and beyond. *Adv Exp Med Biol* (2021) 1347:197–219. doi: 10.1007/5584_2021_640

25. Inokuchi-Sakata S, Ishiuji Y, Katsuta M, Kharma B, Yasuda K, Tominaga M, et al. Role of eosinophil relative count and neutrophil-to-Lymphocyte ratio in the assessment of severity of atopic dermatitis. *Acta Derm Venereol* (2021) 101(7): adv00491. doi: 10.2340/00015555-3838

26. Amat F, Soria A, Tallon A, Bourgoin-Heck A, Lambert A, Deschildre J, et al. New insights into the phenotypes of atopic dermatitis linked with allergies and asthma in children: An overview. *Clin Exp Allergy* (2018) 48(8):919–34. doi: 10.1111/cea.13156

27. Illi S, von Mutius E, Lau S, Nickel R, Grüber C, Niggemann B, et al. The natural course of atopic dermatitis from birth to age 7 years and the association with asthma. *J Allergy Clin Immunol* (2004) 113(5):925–31. doi: 10.1016/j.jaci.2004.01.778

28. Saunes M, Øien T, Dotterud CK, Romundstad PR, Storrø O, Holmen TL, et al. Early eczema and the risk of childhood asthma: a prospective, population-based study. *BMC Pediatr* (2012) 12:168. doi: 10.1186/1471-2431-12-168

29. Spergel JM. An allergist's perspective to the evaluation of eosinophilic esophagitis. *Best Pract Res Clin Gastroenterol* (2015) 29(5):771–81. doi: 10.1016/j.bpg.2015.06.011

30. Tang H, Cao W, Kasturi SP, Ravindran R, Nakaya HI, Kundu K, et al. The T helper type 2 response to cysteine proteases requires dendritic cell-basophil

cooperation *via* ROS-mediated signaling. *Nat Immunol* (2010) 11(7):608–17. doi: 10.1038/ni.1883

31. Otsuka A, Nakajima S, Kubo M, Egawa G, Honda T, Kitoh A, et al. Basophils are required for the induction of Th2 immunity to haptens and peptide antigens. *Nat Commun* (2013) 4:1739. doi: 10.1038/ncomms2740

32. Mashiko S, Mehta H, Bissonnette R, Sarfati M. Increased frequencies of basophils, type 2 innate lymphoid cells and Th2 cells in skin of patients with atopic dermatitis but not psoriasis. *J Dermatol Sci* (2017) 88(2):167–74. doi: 10.1016/j.jdermsci.2017.07.003

33. Jiang Y, Ma W. Assessment of neutrophil-to-Lymphocyte ratio and platelet-to-Lymphocyte ratio in atopic dermatitis patients. *Med Sci Monit* (2017) 23:1340–6. doi: 10.12659/MSM.900212

34. Silverberg JI. Association between childhood atopic dermatitis, malnutrition, and low bone mineral density: a US population-based study. *Pediatr Allergy Immunol* (2015) 26(1):54–61. doi: 10.1111/pai.12315

frontiers | Frontiers in Immunology

TYPE Review
PUBLISHED 16 January 2023
DOI 10.3389/fimmu.2022.999008

OPEN ACCESS

EDITED BY
Susan A. Boackle,
University of Colorado Denver,
United States

REVIEWED BY
Takashi Matsushita,
Kanazawa University, Japan
David Fox,
University of Michigan, United States

*CORRESPONDENCE
Claire F. Beesley
claire.beesley.20@ucl.ac.uk

SPECIALTY SECTION
This article was submitted to Autoimmune and Autoinflammatory Disorders: Autoimmune Disorders, a section of the journal Frontiers in Immunology

RECEIVED 20 July 2022
ACCEPTED 22 December 2022
PUBLISHED 16 January 2023

CITATION
Beesley CF, Goldman NR, Taher TE, Denton CP, Abraham DJ, Mageed RA and Ong VH (2023) Dysregulated B cell function and disease pathogenesis in systemic sclerosis.
Front. Immunol. 13:999008.
doi: 10.3389/fimmu.2022.999008

Dysregulated B cell function and disease pathogenesis in systemic sclerosis

Claire F. Beesley[1*], Nina R. Goldman[1], Taher E. Taher[2], Christopher P. Denton[1], David J. Abraham[1], Rizgar A. Mageed[3] and Voon H. Ong[1]

[1]Centre for Rheumatology, Division of Medicine, University College London, London, United Kingdom, [2]Institute of Immunology and Immunotherapy, University of Birmingham, Birmingham, United Kingdom, [3]Centre for Translational Medicine and Therapeutics, William Harvey Research Institute, Queen Mary University of London, London, United Kingdom

Systemic sclerosis (SSc) is a complex, immune-mediated rheumatic disease characterised by excessive extracellular matrix deposition in the skin and internal organs. B cell infiltration into lesional sites such as the alveolar interstitium and small blood vessels, alongside the production of defined clinically relevant autoantibodies indicates that B cells play a fundamental role in the pathogenesis and development of SSc. This is supported by B cell and fibroblast coculture experiments revealing that B cells directly enhance collagen and extracellular matrix synthesis in fibroblasts. In addition, B cells from SSc patients produce large amounts of profibrotic cytokines such as IL-6 and TGF-β, which interact with other immune and endothelial cells, promoting the profibrotic loop. Furthermore, total B cell counts are increased in SSc patients compared with healthy donors and specific differences can be found in the content of naïve, memory, transitional and regulatory B cell compartments. B cells from SSc patients also show differential expression of activation markers such as CD19 which may shape interactions with other immune mediators such as T follicular helper cells and dendritic cells. The key role of B cells in SSc is further supported by the therapeutic benefit of B cell depletion with rituximab in some patients. It is notable also that B cell signaling is impaired in SSc patients, and this could underpin the failure to induce tolerance in B cells as has been shown in murine models of scleroderma.

KEYWORDS

autoantibodies, systemic sclerosis (scleroderma), autoimmunity, B cells, fibrosis

10.3389/fimmu.2022.999008

1 Introduction

Systemic sclerosis (SSc) is a rare, immune-mediated rheumatic disease characterised by pathogenic microvascular damage and progressive fibrosis of the skin and internal organs. It has the highest case-specific mortality of any rheumatic disease and carries significant morbidity for the patient. Although the updated American College of Rheumatology (ACR) and European League Against Rheumatism (EULAR) classification criteria have improved sensitivity and specificity of diagnosis, understanding of disease aetiopathogenesis and development remains unclear (1–3). In addition, SSc is highly heterogenous, so it can be difficult to stratify patients and devise optimal treatment strategies (2, 4).

Skin fibrosis is the major diagnostic feature of SSc, and the extent of skin involvement is used to stratify patients into two subsets. These are limited cutaneous systemic sclerosis (lcSSc) and diffuse cutaneous systemic sclerosis (dcSSc) (5). Patients with lcSSc generally exhibit skin fibrosis which is distal to the elbows and knees, whereas diffuse involvement occurs proximally to the elbows and knees (3). Patients with dcSSc are at an increased risk of complications such as scleroderma renal crisis and interstitial lung disease (ILD), although some patients with lcSSc can also develop these complications (4, 6, 7). Importantly, there is no difference in the frequency and timing of development of significant ILD between patients for both skin subsets (8). Therefore, classification based upon skin subset alone does not offer accurate risk stratification of internal organ involvement.

Pathogenesis of systemic sclerosis is mediated by several immune and inflammatory cells. Currently, it is thought that vascular injury drives an infiltration of mast cells, T lymphocytes and macrophages into lesional tissues early on in the disease. Ultimately, this results in an unresolving pro-inflammatory and pro-fibrotic response mediated by myofibroblast differentiation and the production of cytokines such as interleukin-6 (IL-6) and transforming growth factor β (TGF-β). Evidence for B cell involvement comes from multiple studies outlining dysregulated B cell signaling and homeostasis within SSc patients, as well as evidence from mouse models and B cell modulating therapeutics. The key immunological feature of SSc is the presence of high levels of self-reactive antibodies in the blood. Patients present with various autoantibody profiles and, in clinical practice, this is one of the best indications to stratify patients and predict organ involvement (9). In addition, detection of autoantibodies can precede clinical onset of SSc, highlighting their pathological relevance (10). As such it is likely that autoreactive B cells are a driving factor in SSc, but the complete relevance and origin of these cells has not been fully determined.

2 B cell biology

B lymphocytes are pleiotropic cells with multiple functions including antibody and cytokine production, antigen presentation to T cells, modulation of dendritic cell function, and lymphoid organogenesis. As a result, B cells can orchestrate immune responses and influence the local environment at sites of infection and tissue injury/inflammation. With regards to the latter, dysregulated B cell responses have been implicated in a number of autoimmune diseases including systemic lupus erythematosus (SLE), Sjogren's syndrome and rheumatoid arthritis (RA) (11).

B lymphocytes develop within the bone marrow from hematopoietic stem cells where they acquire a functional B cell receptor (BCR) following rearrangement of their immunoglobulin (Ig) heavy (H) and light (L) genes in the presence of selective growth factors. Following Ig gene rearrangements, immature B cells express surface IgM and are then purged of autoreactive cells that recognise self-antigens in the bone marrow with high affinity. Most self-reactive clones are tolerised at this central checkpoint through mechanisms of receptor editing and clonal deletion. Immature B cell clones that do not recognise local self-antigens leave the bone marrow and migrate to the periphery for development as transitional cells to naïve mature B cells in a linear pathway (Figure 1) (12, 13).

3 B cell regulation in scleroderma

Differences in B cell homeostasis in SSc patients compared with healthy individuals have been documented in a number of studies (14–16). Typically, these studies have reported an overall increase in the number of B cells and/or differences in the distribution of B cell subsets in scleroderma patients compared with healthy individuals (14–16). However, it is pertinent to highlight that disease duration and immunosuppressive medications are likely to have impacts on lymphocyte homeostasis and subset distribution. Therefore, inclusive analyses are important to mitigate the effect of these factors on altered B cell homeostasis in SSc.

An early study by Sato et al. analysed B cell subsets in 39 Japanese SSc patients who had not received any immunosuppressive therapy. This study observed an increase in the number of circulating $CD27^-$ naïve B cells compared with healthy individuals with a reduction in $CD27^+$ memory B cells and $CD27^+$ plasmablasts (15). Additionally, memory B cells from SSc patients displayed augmented ability to undergo apoptosis and an overexpression of CD19 – possibly relating to their functional hyperactivity (15). These findings have been

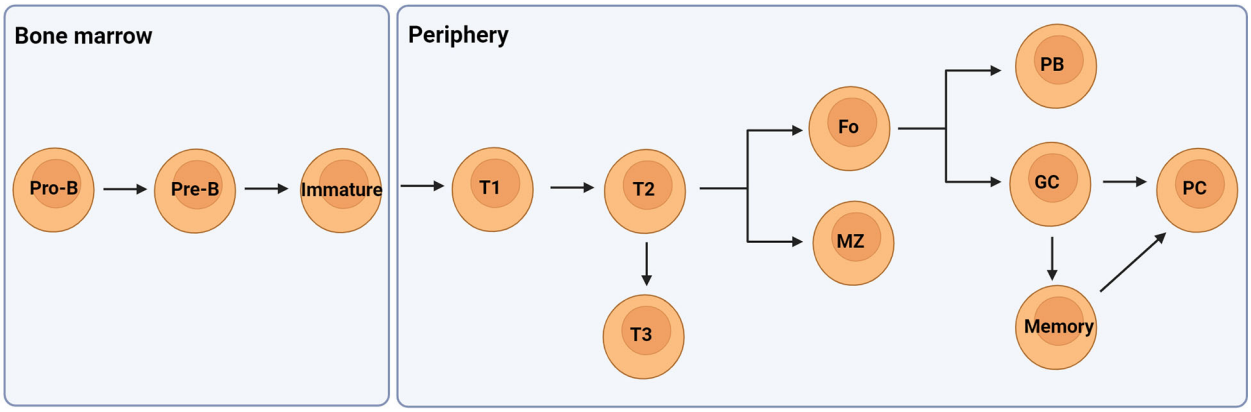

FIGURE 1
A simplified overview of the developmental pathway of B cells. They develop in the bone marrow from hematopoietic stem cells to pro- and pre-B cells once the IgH genes are rearranged. Following successful IgL gene rearrangement the cells develop to immature B cells expressing IgM. These cells then migrate from the bone marrow to the periphery as transitional 1 (T1) B cells which pass through peripheral checkpoints with most autoreactive B cells becoming anergic-like T3 cells. T2 cells can mature to become either follicular (Fo) or marginal zone (MZ) B cells expressing IgM and IgD. Fo B cells can differentiate to low affinity antibody producing plasmablasts (PB) or undergo class switching and affinity maturation in germinal centres (GC) to become high affinity antibody producing plasma cells or memory cells. Figure created with BioRender.com.

confirmed in subsequent studies which have revealed further differences between $CD27^-$ naïve B cells in healthy individuals and patients. Following from these earlier studies, transitional $CD27^-CD24^{hi}CD38^{hi}$ B cells have also been implicated in scleroderma (17–19). Transitional B cells encompass a heterogenous population comprised of at least three distinct subsets (T1 – T3) with differential expression of IgM and IgD and a differential capacity to respond to antigen stimulation. T1 B cells define a population which has recently emigrated from the bone marrow and must acquire survival signals and undergo peripheral tolerance before the cells can proceed through the T2/3 pathway and develop to maturity (20). The T1 and T2 subsets are distinguishable by their differential capacity to survive or undergo apoptosis following BCR engagement, whilst the T3 subset display a functional status which is similar to that of anergic B cells (20). In some studies, a $CD27^+$ subset has also been identified (18, 20). This subset responds rapidly to T cell independent stimulation and is able to produce natural IgM antibodies and secrete high levels of IL-10 (18). Taher et al. studied transitional B cells in SSc patients and reported reduced numbers of T1 cells and expanded T2 cells in SSc patients compared with matched healthy individuals (18). Importantly, T1 cells from SSc patients displayed reduced capacity to undergo apoptosis and contained large numbers of B cells that were specific against the SSc-associated antigen Scl-70. Furthermore, B cell specificity for Scl-70 was demonstrated in patients who were seropositive for Scl-70 autoantibodies, highlighting the significance of this finding (18). This study also analysed the phosphorylation of the STAT-3 signalling pathway when transitional B cells were stimulated through toll-like receptor (TLR)9. STAT-3 has a fundamental role in suppressing pro-inflammatory signal transduction through the TLRs and is crucial for anti-inflammatory IL-10 signalling (21). Taher and colleagues observed a significant reduction in STAT-3 phosphorylation in transitional T1 and $CD27^+$ cells from SSc patients and this is consistent with reduced IL-10 production from these cells (18). Taken together this may implicate a failed tolerance checkpoint at the developmental T1 – T2 stage in SSc patients and similar findings have been reported in a recent study by Glauzy and colleagues who concluded that central and peripheral B cell tolerance checkpoints are likely breached in SSc patients (18, 19). However, STAT-3 is also involved in the regulation of several other cytokines including IL-6, indicating that the observation of reduced IL-10 production in SSc B cells may relate to a signalling molecule upstream of STAT-3 (22, 23).

Differences in the number and function of IL-10 producing regulatory B cells, or Bregs have been noted in multiple studies of SSc (24–26). There is no definitive marker to define Bregs, therefore, current classification is based upon Breg capacity to produce high levels of anti-inflammatory IL-10 and immune-regulatory IL-35 and TGF-β – a key cytokine also involved in fibrotic pathways (27). In SSc patients, IL-10 producing B cells are markedly reduced compared with healthy individuals and B cell capacity to produce IL-10 is reduced (16, 18, 24, 25). Diminished Breg populations have been linked with an increased risk of ILD, whilst IL-10 specific B cell expansion has been shown to correlate positively with patient responses to autologous haematopoietic stem cell transplant (16, 25, 28).

A study to examine $CD27^+$ memory B cell populations in SSc patients highlighted a reduction in the non-switched memory compartment, resulting in an imbalance between tolerogenic and activated memory B cells (29). In addition, elevated numbers of switched and activated memory B cells were associated with dcSSc and are likely to be relevant through

autoantibody and cytokine production. However a significant proportion (52.6%) of the dcSSc patients had received immunosuppressive medications suggesting that these results should be interpreted with caution (29).

4 Autoantibodies in SSc

Whilst the pathological relevance of SSc-specific autoantibodies remains incompletely understood, autoantibodies are strongly associated with the disease and are the strongest predictors of disease course and outcome. This means that autoantibodies are valuable clinical tools which are routinely used to stratify patients and predict patient prognosis (9, 30). Typically, these autoantibodies are of high specificity against nuclear antigens and are present at a high concentration (10).

The three autoantibodies which are most frequently associated with SSc are anti-centromere antibodies (ACA), anti-topisomerase I antibodies (ATA) and anti-RNA polymerase III antibodies (ARA). A patient will typically present with one dominant autoantibody specificity and is unlikely to change this autoantibody subtype. One of these three subsets of autoantibodies (ACA, ATA or ARA) are present in over 50% of those with scleroderma (9).

ACA are the most frequently observed autoantibodies in SSc patients (9). These autoantibodies are highly specific for SSc and are associated with lcSSc (31). Most commonly, ACA are specific for centromere protein B (9). Centromere protein B is a highly conserved nuclear protein which facilitates centromere formation. Patients with ACA are often thought to be at risk of developing pulmonary hypertension (PAH) but these studies are either based on enriched cohorts or have used echocardiogram-diagnosed PAH which is not sufficient for PAH diagnosis (32, 33). However, a number of studies have demonstrated that B cell depletion or B cell deficiency can be protective against vascular remodeling in rodent models of PAH (34–36).

ATA positivity is strongly associated with SSc and is present in up to 40% of individuals with the disease. ATA was initially named as anti-Scl-70 as these autoantibodies react with a 70 kDa protein on immunoblots, but it was later realised that Scl-70 was in fact a breakdown product of the larger 100 kDa topoisomerase I protein (37). ATA-positive patients can be dcSSc or lcSSc, although there is a slight predominance of dcSSc with ATA (9). ATA are a strong predictor of digital ulcer, pulmonary fibrosis and ILD development irrespective of skin involvement and ATA levels positively correlate with disease severity and activity (10). Multiple studies have shown that purified ATA from SSc sera can bind to the cell surface of fibroblasts, providing a potential mechanism by which ATA-positivity could influence disease (38, 39).

Unlike anti-RNA polymerase I and II autoantibodies that can be detected across various autoimmune rheumatic diseases, anti-RNA polymerase III antibodies (ARA) are strongly associated with SSc (9). In a recent meta-analysis, the pooled prevalence of ARA positivity in SSc patients was 11% (40). ARA positivity is a strong predictor of scleroderma renal crisis and up to 59% of those with scleroderma renal crisis are seropositive for ARA (41). ARA levels correlate with skin involvement, but they do not predict organ complications or disease outcome (9). However, patients with ARA have a higher risk of cancer (42).

In terms of disease pathogenesis, autoantibodies can amplify immune responses and initiate inflammation and fibrosis through immune complex formation. Recently, a new class of autoantibodies reactive against various cell surface receptors have been identified in those with SSc. These include antibodies with specificity for platelet-derived growth factor receptor alpha (PDGFRα), angiotensin II type 1 receptor (AT1R) and endothelin-1 type A receptor (ETAR). Antibodies against PDGFRα have been linked with fibrosis in both *in vitro* and *in vivo* studies, whilst antibodies against AT1R and ETAR have been linked with vascular damage (43). These autoantibodies, however, are only detected in a small number of SSc patients and have low disease specificity compared with ACA, ATA and ARA positivity (44).

Additionally, autoantibodies with specificity for CD22 have been detected in a subset of patients. CD22 is an inhibitory B cell receptor that dampens BCR signalling *via* a tyrosine phosphorylation-dependent mechanism. Patients with CD22 autoantibodies exhibit significantly worse skin scores than SSc patients without these antibodies and it is hypothesised that anti-CD22 autoantibodies are likely to interfere with CD22-mediated suppression of B cell activation, resulting in further dysregulation of B cell homeostasis (45). However, these autoantibodies have been found in other autoimmune diseases and are only present in a small subset of SSc patients so are not likely to be a driving factor of disease (17, 45).

5 Abnormalities in B cell signalling and B cell activation

In order to mount an effective immune response, B cells must coordinate signalling through multiple innate and adaptive immune receptors. Alongside the BCR, B cells express a variety of coactivating and coinhibitory receptors that regulate B cell activation status. Remarkably, even a minor change in the expression or function of these receptors can result in a defective B cell response. These abnormalities have been reported in murine models of autoimmunity and in patients with autoimmune diseases including SSc (Figure 2).

There is considerable evidence to show that B cells in SSc patients are in a hyperactivated state induced, at least partly, by increased levels of BAFF (46). This hyperactivation state is marked by increased expression of the BCR coreceptor CD19 (approximately 20% higher) in SSc patients compared with healthy controls (15, 47). As CD19 lowers the threshold for

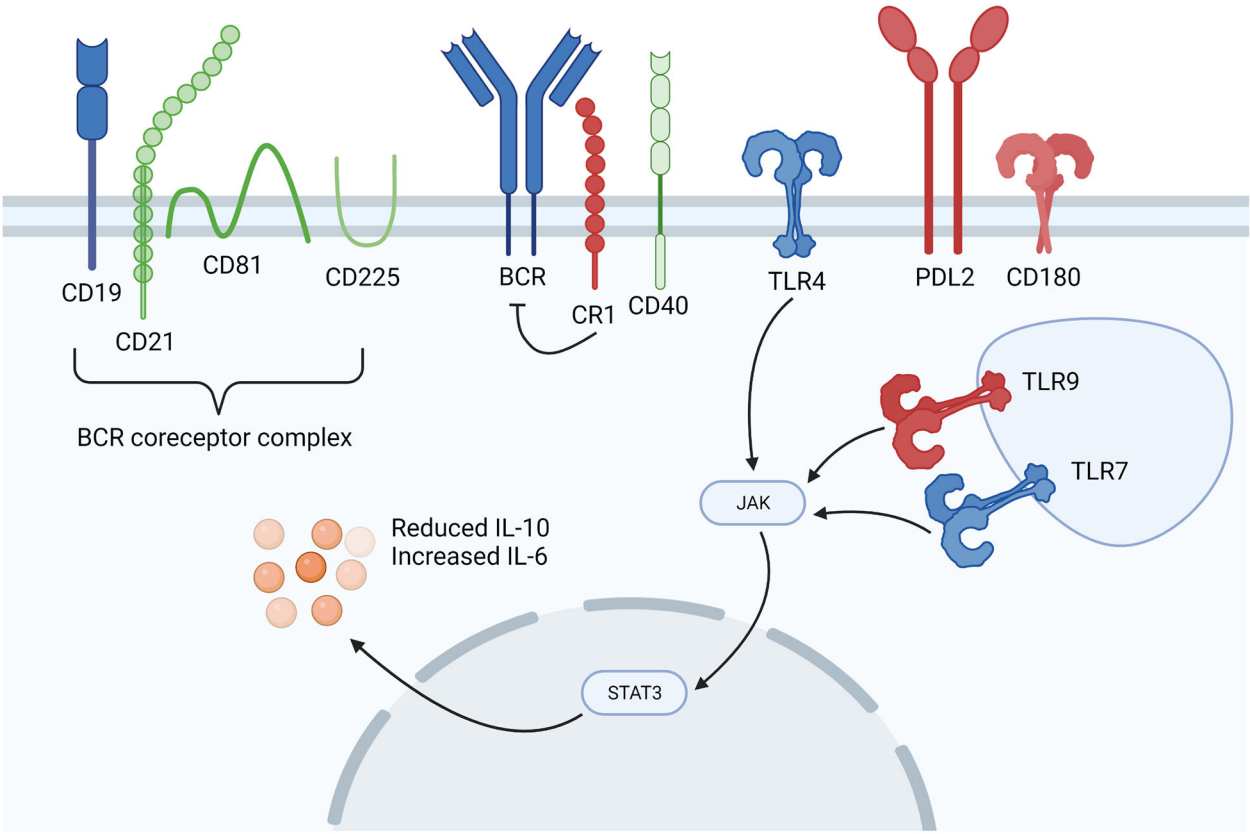

FIGURE 2
Dysregulated B cell signalling in SSc patients. Overexpressed molecules are shown in blue, underexpressed molecules are shown in red and those shown in green are of interest in SSc, but are neither up or downregulated. SSc B cells are in a hyperactive state marked by differential expression of the BCR coreceptors CD19 and inhibitory CR1. TLR signalling is augmented through differential TLR4, TLR7, TLR9 and CD180 expression, whilst increased levels of serum soluble PD-1 and PD-L2 inhibit the PD-1 and PD-L2 interaction between T and B cells. Figure created with BioRender.com.

antigen-dependent stimulation of the BCR, enhanced CD19 expression could augment B cell signalling, resulting in an autoimmune humoral response. Indeed, various autoantibodies, including SSc-specific ATA antibodies were considerably enhanced in transgenic mice that overexpressed CD19 by 20%. This implies that a minor increase in CD19 expression in human SSc may be enough to skew B cell signalling and, thus, trigger autoantibody production (48, 49). CD19 also strengthens antigenic signals generated by the BCR and with CD40 engagement by the CD40 ligand (CD40L) expressed on activated T cells (50). Upregulation of CD19 has been observed in other autoimmune diseases and is considered to be a possible target for future therapy in SSc (17). On B cells, CD19 forms a complex with CD21, also called complement receptor 2 (CR2) which binds to cleavage products of the C3 complement component and transduces signals through CD19, thus lowering the threshold for B cell activation (48). Besides CD21, CD19 also forms a complex with CD225 and CD81, where CD225 could regulate CD19-mediated PI3K signalling (51). On the other hand, CD81 interaction with CD19 is important for CD19 expression and function.

In contrast to CD21, which delivers a costimulatory signal, the complement receptor CD35 (CR1) transduces inhibitory signals by inhibiting the induced increase of cytoplasmic Ca^{2+} levels through BCR and CD40 signalling (17, 52, 53). This suggests that CR1 is a late checkpoint to prevent autoreactive B cell maturation and reduced CR1 expression has been found in memory B cells from SSc patients, potentially augmenting their ability to respond to self-antigen (17).

Programmed cell death protein 1 (PD-1) is a cell surface molecule which is expressed on leukocytes and has been linked to the loss of B cell tolerance and development of autoimmunity. PD-1 regulates immunity by promoting self-tolerance when it is engaged with its ligands PD-L1 and PD-L2 (54, 55). PD-L1 is expressed on many cell types while PD-L2 is expressed on antigen presenting cells. The interaction between PD-1/PD-L2 on B cells and T cells is suggested to suppress tumor necrosis factor alpha (TNF-α) production from antigen-specific B cells

and increase IL-10 production (56, 57). This interaction can be blocked by serum soluble PD-1 (sPD-1) and PD-L2 (sPD-L2), resulting in augmented T and B cell responses. Indeed, sPD-1 and sPD-L2 levels are elevated in SSc patients and this correlates with severity of disease, as well as an increase in TNF-α producing B cells and a reduction in IL-10 producing B cells (56, 58).

Signalling through innate immune receptors, such as TLRs can associate with the development of autoimmunity and the loss of B cell tolerance. TLR signalling enables immune cell responses to various stimuli such as pathogen associated molecular signals (PAMPs) and danger associated molecular signals (DAMPs). Defects in TLR signalling have been implicated in several fibrotic diseases and B cell-specific TLR expression dictates developmental trajectories within these cells (59). For example, TLR4 which recognises lipopolysaccharide is thought to promote B cell survival and maturation during transitional development, whilst TLR2 arrests this process (60). In addition, DAMP induced TLR4 activation is known to be a key mediator of myofibroblast differentiation and is relevant in scleroderma as TLR4 and several associated DAMPs are significantly elevated in lesional tissues of SSc patients (61). Additionally, TLR7 and TLR9 can operate in conjunction with BCR-mediated signals and these receptors have important regulatory functions in B cell development and autoimmunity. TLR7 and TLR9 are intracellular endosomal receptors found in eosinophils, dendritic cells and B cells. They recognise bacterial and viral DNA and induce IRF7 signalling and IFN-α production (62). In SLE patients, high TLR7 expression driven by the *TLR7* polymorphism *rs3853839 C/G* was associated with increased disease activity and an upregulation of IFN-responsive genes. Patients with higher TLR7 expression had greater numbers of B cells than patients with lower TLR7 expression and this was most notable in the transitional B cell subset (63). Analysis of the expression of TLR7, TLR9 and JAK2 in PBMC samples from 50 SSc patients and 13 healthy individuals revealed significant TLR7 upregulation in the SSc patients and decreased levels of TLR9 and JAK2. However, this study was carried out using total PBMC and most of the patient cohort were receiving immunosuppressive therapy (64). An *in vitro* study on B cells isolated from SSc patients and healthy donors reported significantly reduced IL-10 production when the SSc B cells were stimulated *via* TLR9 perhaps indicating defective TLR9 signalling in the B cells from SSc patients (18).

Upon BCR engagement, intracellular protein kinases such as SYK and BTK are activated. These kinases then phosphorylate CD19 and B cell adapter for PI3K (BCAP) which provide docking sites for PI3Ks leading to PI3K activation. PI3K activation leads to further downstream activation of Akt and mTOR serine/threonine kinase signalling, as well as NF-κB pathway activation (65–69). These pathways are critical for B cell survival, proliferation and differentiation with defective class 1A PI3K function preventing B cell development beyond the pre-BCR stage (70). Additionally, ubiquitination is a key mechanism for regulating BCR-driven signalling where inappropriate ubiquitination has been associated with autoimmunity. A20 is a widely expressed deubiquitinating and ubiquitin-editing enzyme which restricts NF-κB signalling and protects against TNF-α induced programmed cell death. A20 has been linked with SSc in multiple genome-wide association studies (GWAS) and single nucleotide polymorphism (SNP) analyses which implicate the *Tnfaip3* gene (71, 72). Tavares and colleagues studied this gene using a floxed allele of *Tnfaip3* to generate mice deficient in A20 in B cells (73). The B cells from these mice were hyper-responsive and displayed enhanced NF-κB signalling through CD40 induced signals. The B cells were also resistant to Fas mediated cell death, likely due to increased expression of anti-apoptotic proteins such as Bcl-x produced *via* the NF-κB pathway, potentially providing a mechanism by which autoreactive B cells in genetically susceptible individuals may survive tolerance checkpoints and develop to maturity in SSc (74).

Similar to other autoimmune diseases, SSc development likely results from a combination of genetic and environmental factors with genome-wide association studies (GWAS) identifying a number of polymorphisms associated with SSc. Some of these polymorphisms relate to B cell signalling, but a 2011 association study of B cell gene polymorphisms in a cohort of 900 SSc patients and 1034 heathy individuals did not find evidence of SSc-associated polymorphisms in CD19, CD20, CD22 and CD24 (68). However, there is evidence for increased SSc susceptibility resulting from genetic polymorphisms in coding domains of other B cell signalling molecules. These include polymorphisms in BANK1, BLK, PTPN22 and CSK (69, 75–77). Some of these polymorphisms are known to be associated with multiple autoimmune diseases and are associated with a patient's ethnicity and autoantibody subset. For example, the *PTPN22* 1858T risk allele is associated with patients who are seropositive for ATA autoantibodies and results in a memory B cell deficit with reduced responsiveness to antigen stimulation *via* the BCR (77). In addition, polymorphisms in the negative regulators of B and T cell activation, suppressors of cytokine signalling 2 (*SOCS2*) and *SOCS3*, were noted to be associated with SSc (78). Further research is needed to understand the functional relevance of these polymorphisms in SSc disease development.

A recent study analysed the expression of PI3K associated molecules in 21 patients with early dcSSc (79). The study identified altered mRNA expression in PI3K associated signalling molecules including TLR homolog CD180, TLR4 and C3 (79). Co-engagement of CD180 and the BCR enhanced NF-κB phosphorylation in dcSSc B cells, but not in healthy controls, whilst activation *via* CD180 increased the percentage of switched memory B cells in dcSSc patients compared with healthy controls (79). Additionally, in 2001, Koarada and colleagues reported that the percentage of SSc patients with CD180-negative B cells was

significantly higher than healthy controls, although not as high as those with Sjogren's syndrome or dermatomyositis (80). This may be significant as ligation of CD180 induces affinity maturation and programs immature (including T1) and mature B cell subsets to become efficient antigen presenting cells to T follicular helper cells (81, 82). Interestingly, another study confirmed these findings and reported reduced CD180 mRNA expression in B cells from dcSSc patients. In lupus CD180-negative B cells have been described as highly activated and CD180 can be internalised after stimulation, indicating that CD180-negative B cells may result from B cell activation *via* CD180. Of note, anti-CD180 stimulation induced natural autoantibody production and significantly increased the concentration of IL-6 in the supernatant of healthy tonsillar B cells providing a mechanism by which CD180 stimulation could increase the number of CD180-negative autoantibody producing B cells in SSc (83).

6 Perturbations in the B cell repertoire in SSc patients

Xiadong Shi and colleagues completed a study to analyse the B cell repertoire in SSc patients compared with healthy controls. These investigators reported differential IGHV-J gene usage in SSc patients compared with healthy controls. In addition, they noted that the average CDR3 region was significantly shorter in SSc patients compared with the healthy controls. This is important as the CDR3 region is the most variable region of the BCR and is the prime determinant of antigen specificity (84). Conversely, using immunoglobulin repertoire analyses in new emigrant/transitional B cells in SSc patients and healthy controls, Glauzy and colleagues observed a significantly higher frequency of long IgH CDR3s which are associated with self-reactivity (19). The discrepancy between these studies may reflect the different B cell populations which were sampled as the CDR3 region varies in length between subsets such as naïve and memory B cells (85). Therefore, more research is needed to determine whether the CDR3 region is involved in autoimmunity in SSc.

7 Profibrotic and proinflammatory B cell cytokines

B cells contribute to fibrosis *via* a number of mechanisms, including direct cell-cell contact and production of stimulating cytokines such as IL-6 (Figure 3). IL-6 is a pleotropic, proinflammatory cytokine which can promote fibrosis (86). Serum levels of IL-6 are increased in SSc patients and this has been linked to worsening disease in human and animal studies (11, 17, 86, 87). IL-6 promotes $CD4^+$ T cell differentiation into pro-inflammatory and pro-fibrotic Th1 and Th17 cells (86, 88). Furthermore, B cell derived IL-6 drives spontaneous germinal centre formation in murine lupus, thus, providing a mechanism by which excessive IL-6 production by B cells can result in autoantibody production and autoimmunity (87). IL-6 also acts as a stimulant for B cell proliferation and it enhances plasma cell generation and antibody production, potentially inducing a pathogenic IgG autoantibody response as has been described in a murine model of lupus (89, 90).

Additionally, activated B cells produce high levels of TGF-β which is a central player in fibrosis (91). When TGF-β binds to its receptor on fibroblasts, it induces collagen synthesis and extracellular matrix deposition through Smad signalling (91). In addition, TGF-β promotes fibrosis *via* the inhibition of matrix degrading proteolytic enzymes such as serine proteinases (92). Elevated levels of TGF-β and enhanced expression of its receptors have been found in the skin of SSc patients (93).

IL-10 is a potent anti-inflammatory cytokine and is, therefore, very important in the context of autoimmune disease (94). IL-10 can suppress $CD4^+$ T cell proliferation through downregulation of CD86 in an autocrine manner. This also reduces IFN-γ and TNF-α production which are functionally important in scleroderma due to their profibrotic and proinflammatory effects (88). In SSc patients, IL-10 producing B cells are markedly reduced compared with healthy controls and B cell capacity to produce IL-10 when stimulated *via* TLR9 is also reduced (18, 95).

IL-13 is another important Th2-type cytokine with several unique effector functions. IL-13 has been demonstrated to mediate tissue fibrosis in asthma, indicating that it is a key regulator of the extracellular matrix (96). In the context of B cells, IL-13 can upregulate MHC class II expression, induce Ig production, promote IgE class switching and induce B cell proliferation and differentiation (96–98). Serum levels of IL-13 are increased in SSc patients and this correlates with levels of C-reactive protein which is a biomarker of inflammation (99). In addition to IL-13, IL-33 is another important Th2 cytokine which is overexpressed in SSc. This cytokine is constitutively expressed at epithelial barrier sites and its overexpression is of interest since IL-33 can drive tissue fibrosis (100). Importantly, chronic exposure to IL-33 can also promote significant BAFF production *via* neutrophils and dendritic cells resulting in germinal centre formation and an IgG autoantibody response (101).

CXCL-13 is a chemokine that regulates B cell migration through secondary lymphoid tissues and is important for neogenesis of ectopic lymphoid structures in the lungs (102). It is overexpressed in SSc patients and CXCL-13 blood concentrations have been linked with worsening prognosis in patients with idiopathic pulmonary fibrosis (95, 103). It is currently thought that CXCL-13 is produced by monocyte-derived macrophages and that its gene expression is controlled by TNF-α and IL-10 (103, 104).

In addition to these key cytokines, high levels of BAFF have long been noted in SSc patients and are associated with disease

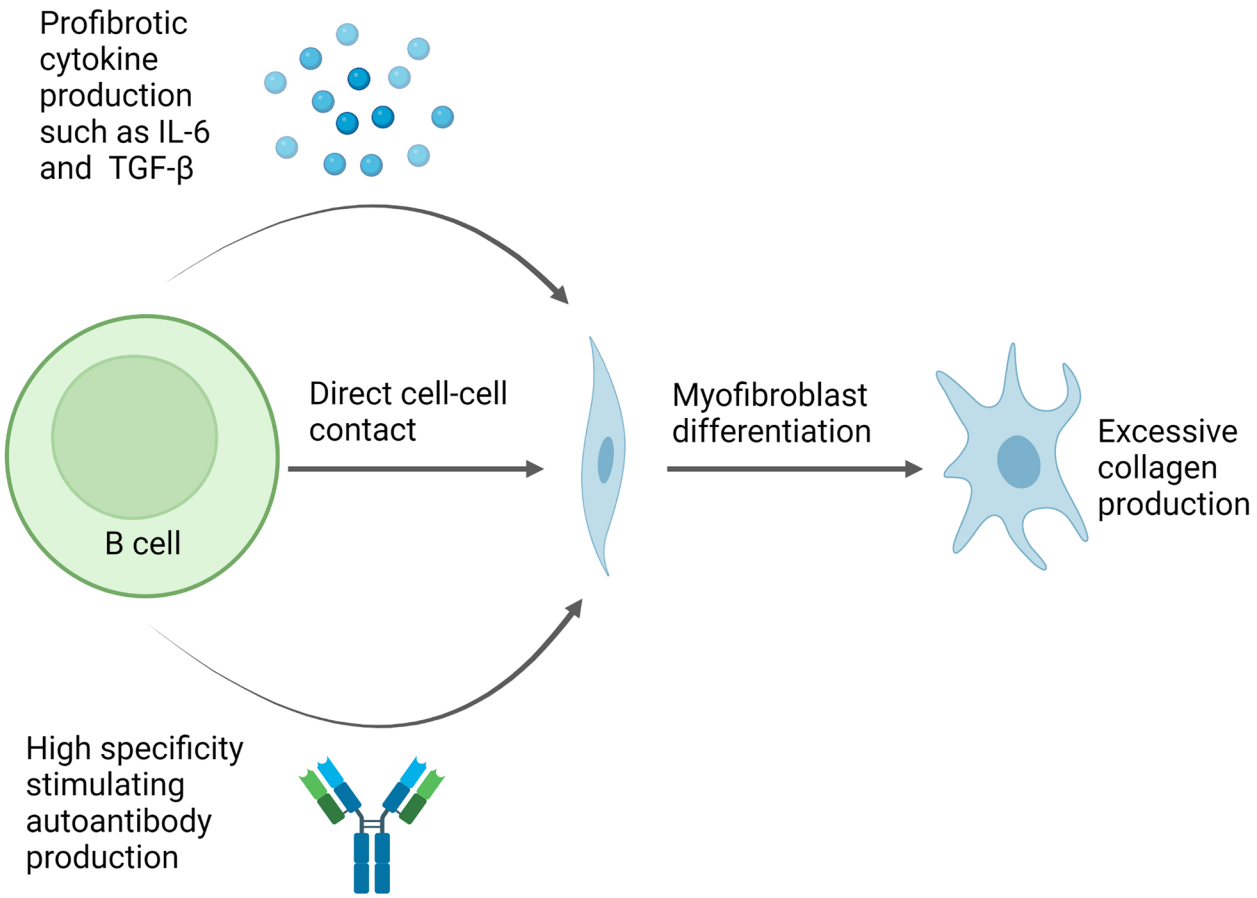

FIGURE 3
Potential pathway for B cell mediated fibrosis in scleroderma. Direct cell-cell contact can induce changes in gene expression in fibroblasts leading to increased collagen production and myofibroblast differentiation. In addition, B cell production of cytokines such as IL-6 and TGF-β also induce myofibroblast differentiation. Meanwhile, autoantibodies can form immune complexes which bind to fibroblasts and trigger pro-fibrotic effects, whilstsome autoantibody specificities, such as PDGF, observed in a subset of SSc patients can bind fibroblasts directly and have stimulating effects. Figure created with BioRender.com.

progression (46). BAFF is a pleiotropic cytokine (also known as BLyS) which promotes B cell proliferation and is a key regulator of peripheral tolerance. BAFF is also a fundamental survival factor and is involved in multiple cell-fate decisions during B cell development (105–107). BAFF overexpression has been linked with autoimmunity in human and animal studies and BAFF inhibition attenuated skin and lung fibrosis in a mouse model of scleroderma (108). As a homologue of BAFF, elevated levels of a proliferation-inducing ligand (APRIL) have also been reported in SSc patients and have been identified as a marker for pulmonary fibrosis, whilst high BAFF levels indicate severe skin sclerosis (109). A recent study by Glauzy and colleagues, however, did not find elevated BAFF levels in SSc patients compared with healthy controls and hence these authors concluded that BAFF is unlikely to be a driving factor in SSc pathogenesis (19).

Finally, T follicular helper (Tfh) cell production of IL-21 drives autoantibody producing plasma cell differentiation from effector B cells and can promote fibrosis through induction of IL-6, TGF-β and CC chemokine ligand 2 (CCL2) and B cell interaction with fibroblasts. In this respect it is notable that SSc fibroblasts have increased IL-21R expression (110).

8 B cell involvement in scleroderma pathogenesis: Evidence from animal models

SSc is a complex disease with high patient-patient heterogeneity. As such, it has been difficult to develop an animal model of SSc which captures all aspects of disease pathogenesis. Generally, these models are murine based and have a fibrotic skin and lung signature induced by either pro-fibrotic agents such as bleomycin, or genetic manipulations leading to pro-fibroblast signalling (111).

The tight-skin mouse (TSK) model of SSc is characterised by skin fibrosis and autoantibody production, as well as an abundance of BAFF and overexpression of CD19 (112–114). Using this model, it was shown that B cell activation is important for fibrosis and autoantibody production as CD19 deficiency decreased skin fibrosis and abrogated autoantibody production in TSK mice (113). Moreover, skin fibrosis and autoantibody production were prevented with the use of a BAFF antagonist (114).

Another mouse model of SSc involves using a subcutaneous injection of bleomycin to induce skin and lung fibrosis as well as autoantibody production. In this setting, bleomycin induces hyaluronan production which activates B cells through TLR4 (115). In the bleomycin model for lung fibrosis, it was demonstrated that CD19 signalling is crucial for B cell infiltration into the lung tissue and is associated with up-regulation of the chemokine CXCR3. Loss of CD19 attenuated inflammation and reduced mortality, while CD19 overexpression increased mortality (115). Moreover, transgenic mice that overexpress CD19 spontaneously produce autoantibodies and lose immunotolerance (16, 116).

Sanges and colleagues developed a new murine model of SSc which was induced through daily intradermal injections of hypochlorous acid (HOCL) (26). The authors found significant B cell infiltration in the skin of HOCL injected mice in the later stages of disease but not in the earlier stages when compared with PBS-treated mice. In addition, splenic B cells in HOCL-treated mice produced significantly more IL-6 and CCL3 while IL-10 production was significantly reduced during the early stages of the disease, but levels of IL-10 production matched those of control mice at the later stage (26). This model showed high concordance with observations of B cell perturbations in human scleroderma patients. This is defined by B cell involvement through an early expansion of transitional B cells and late expansion of the mature naïve subset with an overall decrease in the number of Bregs, plasmablasts and memory B cells (26).

Interestingly, a study using a bleomycin-induced model of scleroderma highlighted how B cell-specific IL-6 deficient mice had attenuated skin and lung fibrosis whilst B cell-specific IL-10-deficient mice had more severe fibrosis. Using this model it was also shown that IL-6 producing B effector cells or Beffs infiltrated inflamed skin and were induced to proliferate through BAFF. However, BAFF suppressed Breg generation. In addition, a BAFF antagonist attenuated skin and lung fibrosis and reduced Beffs but not Bregs. These data provide further evidence for a pathogenic role for BAFF and IL-6 produced by B cells in scleroderma models and a protective role for IL-10 (108).

Recently, a new mouse model of SSc has emerged. This model depends on topoisomerase I injection with complete Freud's adjuvant. The mice then develop skin and lung fibrosis with a defined Th2/Th17 response and increased IL-6 production. Using this model, it was shown that loss of IL-6 expression significantly improved skin and lung fibrosis (117).

9 B cell infiltration in the skin and lungs

Various studies have examined the cellular infiltrates in lesional tissue of SSc patients (118–122). Bosello and colleagues characterised the inflammatory cell infiltrate in scleroderma skin and found $CD20^+$ B cells in 60.7% of SSc patients. There was an increased number of $CD20^+$ B cells in patients with early disease and B cell infiltration appeared to correlate with worsening skin score. Importantly, no $CD20^+$ B cells were found in the skin of healthy individuals (120). Evidence suggests that IL-10 producing B cells migrate from the peritoneum to inflamed skin sites where they play important regulatory and protective functions. Hence, if B cell capacity to produce IL-10 is reduced in SSc patients, then the function of these regulatory skin-homing B cells are likely to be impaired (123).

B cell aggregates have been found in lung tissues of SSc patients with ILD, whilst transcriptomic data has also found evidence of lesional B cell infiltration (118, 121, 122). Furthermore, foci of B cell aggregates have been found in lung alveolar interstitium of SSc patients with ILD (122). Recent data using next-generation RNA sequencing in patients with early dcSSc demonstrated B cell signatures in 67% of patients, higher than published data in established disease (121).

10 Therapeutic strategies targeting B cells in SSc

The benefits of immunosuppressive therapies for scleroderma lung and skin disease provide further evidence for the role of B cell autoimmunity in SSc. However, the mixed effects of these biologic treatments also reveal the complexity of SSc pathogenesis and the strategic challenges faced when treating this disease (124).

The Scleroderma Lung Study (SLS) 1, comparing oral cyclophosphamide for 1 year vs placebo, reported a small improvement in forced vital capacity (FVC) with the treatment alongside improvements in dyspnoea scores and skin thickening (125). Using single cell analysis, an individual's B cell profile has been associated with cyclophosphamide response. Of note, cyclophosphamide responders had increased IL-10 producing regulatory B cells and reduced IL-6 effector B cells post-treatment (126). The SLS 2 study subsequently showed equivalence between 24 months of mycophenolate mofetil (MMF) and 12-months of oral cyclophosphamide followed by placebo with the average improvement in FVC of 7-8% (127). *Post-hoc* analysis of both the SENSCIS trial assessing nintedanib (a tyrosine kinase inhibitor) and the RESOLVE-1 trial assessing lenabasum (a cannabinoid type 2 receptor) in SSc, further demonstrated the efficacy of MMF in SSc. MMF inhibits both B and T cell proliferation and antibody production (128–130). With

cyclophosphamide and MMF both impacting B cells alongside other mechanisms of action, further research is needed to disentangle the relative importance of their effects on B cell mediated pathogenesis.

Autologous stem cell transplant (aSCT) has emerged as a treatment option for autoimmune diseases with the rationale that a subsequent new self-tolerant immune system develops post-transplant (131). Three randomised controlled trials have supported this approach in patients with severe SSc with the ASSIST and ASTIS studies performing non-myeloablative aSCT and SCOT trial using myelo-ablative aSCT (132–134). All three trials reported sustained improvements in both skin and lung disease compared with standard of care with cyclophosphamide. The SCOT trial reported a lower treatment related mortality than previous studies, however, early treatment mortality due to increased rates of infection remains a concern (133). Gernert and colleagues demonstrated that the predominant B cell population post-transplantation was naïve B cells ($CD27^-/IgD^+$) with reduced percentages of memory B cells at 1-year post aSCT. An increased regulatory B cell phenotype with increased B cell IL-10 production was also found post-aSCT (28). A further study on 22 patients pre- and post- aSCT for SSc demonstrated similar changes in B cell populations with increased naïve B cells over prolonged follow-ups and sustained decreases in unswitched, switched and double negative B cells (135).

Rituximab, a chimeric monoclonal antibody against human CD20 on B cells provides compelling and more specific evidence for the role of B cells in SSc. Initial studies including small case series and open label trials demonstrated promising results with improvements of lung and skin fibrosis with rituximab (136–144). Alongside these studies, an initial observational EUSTAR study comparing 63 patients who received rituximab in routine clinical practice to matched controls found improved skin thickening and stabilisation of ILD with rituximab treatment (145). These findings are supported by mechanistic evidence that dermal B cells are completely, or nearly completely, depleted by rituximab therapy and a significant reduction in IL-6 at 6 months post treatment occurred with IL-6 known to be predictive of decline in FVC (136, 139, 146). A downregulation of fibroblast type I collagen gene expression with rituximab has also been demonstrated and early depletion of peripheral B cells at 2 weeks after rituximab therapy was negatively correlated with % forced vital capacity improvement at week 24 (147, 148).

The subsequent larger prospective EUSTAR study including 254 patients treated with rituximab vs 9575 propensity-score matched patients showed a significant improvement in skin fibrosis but failed to show an effect of rituximab on FVC or carbon monoxide diffusion capacity (DLCO) decline (149). A recent meta-analysis of rituximab in SSc-ILD from Goswami and colleagues, included 20 studies, with 575 SSc patients receiving rituximab treatment. Rituximab improved FVC and DLCO by 4.48% and 3.47%, respectively at 6 months and 7.03% and 4.08% at 12 months. Additionally, there were concomitant reductions in the Modified Rodnan skin score (mRSS) which is used to evaluate skin thickness, with a higher score indicating thicker skin (150). It must be noted that only 2 of the 20 studies included were randomised control trials and neither were double-blinded. Another meta-analysis published in 2020 by Tang and colleagues including 14 studies with 597 participants found rituximab resulted in stability but not improvement of FVC (151).

The DESIRES trial, a double-blind placebo-controlled trial published in 2021, randomised both diffuse and limited SSc patients with an mRSS of ≥10 to receive weekly rituximab for 4 weeks, or placebo with absolute change in mRSS at 6 months as the primary endpoint (152). An improvement in skin score with rituximab vs placebo (absolute change in mRSS at 6 months -6.30 rituximab vs 2.14 placebo, difference -8.44 $p<0.0001$) was found and although most patients included in this study had relatively mild associated interstitial lung disease (ILD), rituximab did improve % FVC at 24 weeks (0.09% vs -2.87%, difference 2.96%, 95% CI 0.08 – 5.84, $p=0.044$). This provides more definitive evidence for the role of B cell depletion. We will wait to see if these results are reinforced by the soon to be published randomised controlled RECITAL trial assessing the effect of rituximab vs cyclophosphamide in connective tissue-disease-associated ILD (153).

Changes in autoantibody levels have been inconsistently reported following rituximab therapy (154–156) with the inability of rituximab to deplete autoantibody-producing long lived plasma cells seen in SSc (157). CD19 is expressed on a broader range of B cell subsets than CD20, including earlier B cell precursor cells, plasmablasts and some plasma cells (157). Elevated plasma cell gene signatures have been found in SSc compared with healthy controls and correlated with disease activity (158). A phase-I randomised placebo-controlled trial assessing a humanised monoclonal antibody targeting CD19 (MEDI551, inebilizumab) found it effectively depleted B cells and plasma cells and appeared well tolerated in SSc (159). At baseline patients with a high plasma cell gene signature were more likely to respond to inebilizumab than those with low plasma cell gene signatures, thereby supporting a role for plasma cells in disease pathogenesis (158). Targeting CD38, a type II glycoprotein highly expressed on several B cell subsets including short and long lived plasma cells, may provide another approach to target autoantibody production; however, studies are yet to assess anti-CD38 therapy in SSc (160).

Belimumab, a treatment licensed in SLE, binds soluble BAFF/BLyS. A double blind randomised control trial of belimumab vs placebo with background MMF including 20 SSc patients failed to reach statistical significance but demonstrated greater improvement in mRSS with belimumab compared with MMF alone (161). Responders to belimumab had significant changes in gene expression involved in B cell signalling and fibrotic signalling, consistent with the mechanism of action of the drug (161).

Blocking IL-6 signalling using tocilizumab, a humanized monoclonal antibody against the human IL-6 receptor α chain

has been assessed in the phase II FaSScinate trial and subsequent phase III FocuSSced trial (162, 163). Although both failed to meet their primary endpoint regarding difference in mean change in baseline mRSS at week 24 and 48, both found that tociluzumab slowed lung function decline in early active disease (FVC decline >10%: 17% placebo vs 5% tocilizumab). The interaction of IL-6 and B cells discussed earlier in this review suggests some treatment effects are likely driven by effects of the drug on B cells; however, further research is required to delineate this (89, 90).

Both the SENSCIS trial and the ongoing Scleroderma lung study III are assessing the effect of combination therapy with oral anti-fibrotics and MMF. It is therefore likely that future treatment approaches will include a combination of immune modulatory and anti-fibrotic therapy with B cells appearing to play a crucial role in the interaction of these pathways (164, 165).

11 Future perspectives

B cells are able to shape SSc pathogenesis through a number of mechanisms as described throughout this review. Improved understanding of these mechanisms is needed to demonstrate the overall relevance and description of these pathogenic B cells and outline their involvement in the wider context of SSc such as their interaction with other immune and endothelial cells. A potential pathway for B cell autoreactivity and pathogenic SSc involvement could be triggered by an initial environmental signal such as high levels of IL-6. This could then lead to inappropriate B cell activation and survival marked by inflammatory cytokine and autoantibody production. Autoreactive B cells are likely to interact with other immune cells throughout this process such as fibroblasts, Tfh cells during germinal centre reactions and $CD4^+$ T helper cells in antigen presentation. In the future, increased knowledge of these interactions in the context of SSc will improve overall understanding of disease pathways and could lead to new and more targeted therapeutic strategies with less side effects.

Thus, as studies continue to delineate the relevant pathogenic B cell signalling pathways, disease treatment is likely to significantly improve with better and safer biologic therapies. For example, improved understanding of the biomarkers which predict patient response to B cell modulating drugs through single-cell RNA sequencing is likely to improve patient stratification. Meanwhile, other studies may reveal B cell signalling pathways or protein targets that are responsible for maintaining the pro-fibrotic disease state.

12 Conclusions

SSc is a complex disease with multiple cell types and pathways likely to contribute towards pathogenesis. B cells can interact with many of these pathways directly contributing to the inflammatory and profibrotic phenotype characteristic of SSc. It is currently thought that the initial stages of disease are marked by a proinflammatory response which later leads to a more pronounced fibrotic response. This has implications for when to treat patients and with which biologics. No matter the disease stage, B cells are key immune mediators and are, therefore, likely to be central in scleroderma pathology. As understanding of disease development, B cell involvement and patient heterogeneity continue to improve, this will result in improved patient prognosis in SSc.

Author contributions

CB and NG wrote the draft manuscript with VO, TT, DA, CD, and RM as editors. All authors contributed to the text and approved the final submission. CB was responsible for figure design and legend assembly.

Funding

The authors are grateful for a Versus Arthritis grant (22534) and a Medical Research Council UK/Scleroderma & Raynaud's UK co-funded grant (MR/V030108/1).

Acknowledgments

We would like to thank Dr Fabian Flores Borja and Dr Louisa James for their continued support at Queen Mary University of London. All figures were created with BioRender.com.

Conflict of interest

The authors declare that the research was conducted in the absence of any commercial or financial relationships that could be construed as a potential conflict of interest.

Publisher's note

References

1. Pattanaik D, Brown M, Postlethwaite BC, Postlethwaite AE. Pathogenesis of systemic sclerosis. *Front Immunol* (2015) 6:272. doi: 10.3389/fimmu.2015.00272

2. Sakkas LI, Bogdanos DP. Systemic sclerosis: New evidence re–enforces the role of b cells. *Autoimmun Rev* (2016) 15:155–61. doi: 10.1016/j.autrev.2015.10.005

3. Van Den Hoogen F, Khanna D, Fransen J, Johnson SSR, Baron M, Tyndall A, et al. 2013 classification criteria for systemic sclerosis: an American college of rheumatology/European league against rheumatism collaborative initiative. *Ann Rheum Dis* (2013) 72:1747–55. doi: 10.1136/ANNRHEUMDIS–2013–204424

4. Denton CP, Khanna D. Systemic sclerosis. *Lancet* (2017) 390:1685–99. doi: 10.1016/S0140–6736(17)30933–9

5. Carwile LeRoy E, Black C, Fleischmajer R, Jablonska S, Krieg T, Medsger TA, et al. Scleroderma (systemic sclerosis): Classification, subsets and pathogenesis. *J Rheumatol* (1988) 15:202–5.

6. Gu YS, Kong J, Cheema GS, Keen CL, Wick G, Gershwin ME. The immunobiology of systemic sclerosis. *Semin Arthritis Rheum* (2008) 38:132–60. doi: 10.1016/j.semarthrit.2007.10.010

7. Winstone TA, Assayag D, Wilcox PG, Dunne JV, Hague CJ, Leipsic J, et al. Predictors of mortality and progression in scleroderma–associated interstitial lung disease: A systematic review. *Chest* (2014) 146:422–36. doi: 10.1378/chest.13–2626

8. Nihtyanova SI, Denton CP. Pathogenesis of systemic sclerosis associated interstitial lung disease. *J Scleroderma Relat Disord* (2020) 5:6–16. doi: 10.1177/2397198320903867

9. Nihtyanova SI, Denton CP. Autoantibodies as predictive tools in systemic sclerosis. *Nat Rev Rheumatol* (2010) 6:112–6. doi: 10.1038/nrrheum.2009.238

10. Burbelo PD, Gordon SM, Waldman M, Edison JD, Little DJ, Stitt RS, et al. Autoantibodies are present before the clinical diagnosis of systemic sclerosis. *PloS One* (2019) 14:e0214202. doi: 10.1371/journal.pone.0214202

11. Bosello S, De Luca G, Tolusso B, Lama G, Angelucci C, Sica G, et al. B cells in systemic sclerosis: A possible target for therapy. *Autoimmun Rev* (2011) 10:624–30. doi: 10.1016/j.autrev.2011.04.013

12. Bemark M. Translating transitions – how to decipher peripheral human b cell development. *J BioMed Res* (2015) 29:264. doi: 10.7555/JBR.29.20150035

13. Martin VG, Wu YCB, Townsend CL, Lu GHC, O'Hare JS, Mozeika A, et al. Transitional b cells in early human b cell development – time to revisit the paradigm? *Front Immunol* (2016) 7:546/BIBTEX. doi: 10.3389/FIMMU.2016.00546/BIBTEX

14. Fox DA, Lundy SK, Whitfield ML, Berrocal V, Campbell P, Rasmussen S, et al. Lymphocyte subset abnormalities in early diffuse cutaneous systemic sclerosis. *Arthritis Res Ther 2021 231* (2021) 23:1–12. doi: 10.1186/S13075–020–02383–W

15. Sato S, Fujimoto M, Hasegawa M, Takehara K. Altered blood b lymphocyte homeostasis in systemic sclerosis: Expanded naive b cells and diminished but activated memory b cells. *Arthritis Rheum* (2004) 50:1918–27. doi: 10.1002/art.20274

16. Mavropoulos A, Simopoulou T, Varna A, Liaskos C, Katsiari C, Bogdanos D, et al. Breg cells are numerically decreased and functionally impaired in patients with systemic sclerosis. *Arthritis Rheumatol* (2016) 68:494–504. doi: 10.1002/ART.39437

17. Soto L, Ferrier A, Aravena O, Fonseca E, Berendsen J, Biere A, et al. Systemic sclerosis patients present alterations in the expression of molecules involved in b–cell regulation. *Front Immunol* (2015) 6:496. doi: 10.3389/fimmu.2015.00496

18. Taher TE, Ong VH, Bystrom J, Hillion S, Simon Q, Denton CP, et al. Association of defective regulation of autoreactive interleukin–6–Producing transitional b lymphocytes with disease in patients with systemic sclerosis. *Arthritis Rheumatol* (2018) 70:450–61. doi: 10.1002/art.40390

19. Glauzy S, Olson B, May CK, Parisi D, Massad C, Hansen JE, et al. Defective early b cell tolerance checkpoints in patients with systemic sclerosis allow the production of self–antigen–specific clones. *Arthritis Rheumatol* (2022) 74(2):307–17. doi: 10.1002/ART.41927

20. Simon Q, Pers JO, Cornec D, Le Pottier L, Mageed RA, Hillion S. In–depth characterization of CD24highCD38high transitional human b cells reveals different regulatory profiles. *J Allergy Clin Immunol* (2016) 137:1577–1584.e10. doi: 10.1016/j.jaci.2015.09.014

21. Hillmer EJ, Zhang H, Li HS, Watowich SS. STAT3 signaling in immunity. *Cytokine Growth Factor Rev* (2016) 31:1–15. doi: 10.1016/J.CYTOGFR.2016.05.001

22. Niemand C, Nimmesgern A, Haan S, Fischer P, Schaper F, Rossaint R, et al. Activation of STAT3 by IL–6 and IL–10 in primary human macrophages is differentially modulated by suppressor of cytokine signaling 3. *J Immunol* (2003) 170:3263–72. doi: 10.4049/JIMMUNOL.170.6.3263

23. Kasmi KCEl, Holst J, Coffre M, Mielke L, Pauw A, Lhocine N, et al. General nature of the STAT3–activated anti–inflammatory response. *J Immunol* (2006) 177:7880–8. doi: 10.4049/JIMMUNOL.177.11.7880

24. Aravena O, Ferrier A, Menon M, Mauri C, Aguillón JC, Soto L, et al. TIM–1 defines a human regulatory b cell population that is altered in frequency and function in systemic sclerosis patients. *Arthritis Res Ther* (2017) 19. doi: 10.1186/s13075-016-1213-9

25. Matsushita T, Hamaguchi Y, Hasegawa M, Takehara K, Fujimoto M. Decreased levels of regulatory b cells in patients with systemic sclerosis: association with autoantibody production and disease activity. *Rheumatology* (2016) 55:263–7. doi: 10.1093/rheumatology/kev331

26. Sanges S, Jendoubi M, Kavian N, Hauspie C, Speca S, Crave J, et al. B cell homeostasis and functional properties are altered in an hypochlorous acid–induced murine model of systemic sclerosis. *Front Immunol* (2017) 8:53. doi: 10.3389/FIMMU.2017.00053

27. Rosser EC, Mauri C. Regulatory b cells: Origin, phenotype, and function. *Immunity* (2015) 42:607–12. doi: 10.1016/J.IMMUNI.2015.04.005

28. Gernert M, Tony HP, Schwaneck EC, Gadeholt O, Schmalzing M. Autologous hematopoietic stem cell transplantation in systemic sclerosis induces long–lasting changes in b cell homeostasis toward an anti–inflammatory b cell cytokine pattern. *Arthritis Res Ther* (2019) 21:1–10. doi: 10.1186/S13075–019–1889–8/FIGURES/4

29. Simon D, Balogh P, Bognár A, Kellermayer Z, Engelmann P, Németh P, et al. Reduced non–switched memory b cell subsets cause imbalance in b cell repertoire in systemic sclerosis. *Clin Exp Rheumatol* (2016) 34 Suppl 1:30–6.

30. Steen VD. Autoantibodies in systemic sclerosis. *Semin Arthritis Rheum* (2005) 35:35–42. doi: 10.1016/j.semarthrit.2005.03.005

31. Hesselstrand R, Scheja A, Shen GQ, Wiik A, A°Ckesson A. The association of antinuclear antibodies with organ involvement and survival in systemic sclerosis. *Rheumatology* (2003) 42:534–40. doi: 10.1093/RHEUMATOLOGY/KEG170

32. Bae S, Saggar R, Bolster MB, Chung L, Csuka ME, Derk C, et al. Baseline characteristics and follow–up in patients with normal haemodynamics versus borderline mean pulmonary arterial pressure in systemic sclerosis: results from the PHAROS registry. *Ann Rheum Dis* (2012) 71:1335–42. doi: 10.1136/ANNRHEUMDIS–2011–200546

33. Hudson M, Mahler M, Pope J, You D, Tatibouet S, Steele R, et al. Clinical correlates of CENP–a and CENP–b antibodies in a large cohort of patients with systemic sclerosis. *J Rheumatol* (2012) 39:787–94. doi: 10.3899/RHEUM.111133

34. Tomaszewski M, Bębnowska D, Hrynkiewicz R, Dworzyński J, Niedźwiedzka–rystwej P, Kopeć G, et al. Role of the immune system elements in pulmonary arterial hypertension. *J Clin Med* (2021) 10:3757. doi: 10.3390/JCM10163757

35. Breitling S, Hui Z, Zabini D, Hu Y, Hoffmann J, Goldenberg NM, et al. The mast cell–b cell axis in lung vascular remodeling and pulmonary hypertension. *Am J Physiol – Lung Cell Mol Physiol* (2017) 312:L710–21. doi: 10.1152/AJPLUNG.00311.2016/ASSET/IMAGES/LARGE/ZH50041772100008.JPEG

36. Mizuno S, Farkas L, Al Husseini A, Farkas D, Gomez–Arroyo J, Kraskauskas D, et al. Severe pulmonary arterial hypertension induced by SU5416 and ovalbumin immunization. *Am J Respir Cell Mol Biol* (2013) 47:679–87. doi: 10.1165/RCMB.2012–0077OC

37. Kayser C, Fritzler MJ. Autoantibodies in systemic sclerosis: Unanswered questions. *Front Immunol* (2015) 6:167. doi: 10.3389/fimmu.2015.00167

38. Senécal J–L, Hénault J, Raymond Y. The pathogenic role of autoantibodies to nuclear autoantigens in systemic sclerosis (scleroderma). *J Rheumatol* (2005) 32:1643–9. doi: 10.1177/2397198319870667

39. Hénault J, Tremblay M, Clément I, Raymond Y, Senécal J. Direct binding of anti–DNA topoisomerase I autoantibodies to the cell surface of fibroblasts in patients with systemic sclerosis. *Arthritis Rheum* (2004) 50:3265–74. doi: 10.1002/ART.20515

40. Sobanski V, Dauchet L, Lefèvre G, Lambert M, Morell–Dubois S, Sy T, et al. Prevalence of anti–RNA polymerase III antibodies in systemic sclerosis: New data from a French cohort and a systematic review and meta–analysis. *Arthritis Rheumatol* (2014) 66:407–17. doi: 10.1002/art.38219

41. Rigamonti C, Shand LM, Feudjo M, Bunn CC, Black CM, Denton CP, et al. Clinical features and prognosis of primary biliary cirrhosis associated with systemic sclerosis. *Gut* (2006) 55:388–94. doi: 10.1136/gut.2005.075002

42. Moinzadeh P, Fonseca C, Hellmich M, Shah AA, Chighizola C, Denton CP, et al. Association of anti–RNA polymerase III autoantibodies and cancer in scleroderma. *Arthritis Res Ther* (2014) 16:R53. doi: 10.1186/ar4486

43. Moroncini G, Svegliati Baroni S, Gabrielli A. Agonistic antibodies in systemic sclerosis. *Immunol Lett* (2018) 195:83–7. doi: 10.1016/J.IMLET.2017.10.007

44. Raschi E, Privitera D, Bodio C, Lonati PA, Borghi MO, Ingegnoli F, et al. Scleroderma–specific autoantibodies embedded in immune complexes mediate endothelial damage: an early event in the pathogenesis of systemic sclerosis. *Arthritis Res Ther 2020 221* (2020) 22:1–17. doi: 10.1186/S13075–020–02360–3

45. Odaka M, Hasegawa M, Hamaguchi Y, Ishiura N, Kumada S, Matsushita T, et al. Autoantibody–mediated regulation of b cell responses by functional anti–CD22 autoantibodies in patients with systemic sclerosis. *Clin Exp Immunol* (2010) 159:176–84. doi: 10.1111/j.1365–2249.2009.04059.x

46. Matsushita T, Hasegawa M, Matsushita Y, Echigo T, Wayaku T, Horikawa M, et al. Elevated serum BAFF levels in patients with localized scleroderma in contrast to other organ–specific autoimmune diseases. *Exp Dermatol* (2007) 16:87–93. doi: 10.1111/J.1600–0625.2006.00485.X

47. Sato S, Hasegawa M, Fujimoto M, Tedder TF, Takehara K. Quantitative genetic variation in CD19 expression correlates with autoimmunity. *J Immunol* (2000) 165:6635–43. doi: 10.4049/JIMMUNOL.165.11.6635

48. Mongini PK, Vilensky MA, Highet PF, Inman JK. The affinity threshold for human b cell activation *via* the antigen receptor complex is reduced upon co–ligation of the antigen receptor with CD21 (CR2). *J Immunol* (1997) 159:3782–91.

49. Asano N, Fujimoto M, Yazawa N, Shirasawa S, Hasegawa M, Okochi H, et al. B lymphocyte signaling established by the CD19/CD22 loop regulates autoimmunity in the tight–skin mouse. *Am J Pathol* (2004) 165:641–50. doi: 10.1016/S0002–9440(10)63328–7

50. Elgueta R, Benson MJ, De Vries VC, Wasiuk A, Guo Y, Noelle RJ. Molecular mechanism and function of CD40/CD40L engagement in the immune system. *Immunol Rev* (2009) 229:152–72. doi: 10.1111/J.1600–065X.2009.00782.X

51. Fujimoto M, Poe JC, Hasegawa M, Tedder TF. CD19 regulates intrinsic b lymphocyte signal transduction and activation through a novel mechanism of processive amplification. *Immunol Res* (2000) 22:281–98. doi: 10.1385/IR:22:2–3:281

52. Kremlitzka M, Polgar A, Fulop L, Kiss E, Poor G, Erdei A. Complement receptor type 1 (CR1, CD35) is a potent inhibitor of b–cell functions in rheumatoid arthritis patients. *Int Immunol* (2013) 25:25–33. doi: 10.1093/intimm/dxs090

53. Isaak A, Gergely P, Szekeres Z, Prechl J, Poor G, Erdei A, et al. Physiological up–regulation of inhibitory receptors fc RII and CR1 on memory b cells is lacking in SLE patients. *Int Immunol* (2008) 20:185–92. doi: 10.1093/intimm/dxm132

54. Dai S, Jia R, Zhang X, Fang Q, Huang L. The PD–1/PD–Ls pathway and autoimmune diseases. *Cell Immunol* (2014) 290:72–9. doi: 10.1016/J.CELLIMM.2014.05.006

55. Yamane H, Isozaki H, Takeyama M, Ochi N, Kudo K, Honda Y, et al. Programmed cell death protein 1 and programmed death–ligand 1 are expressed on the surface of some small–cell lung cancer lines. *Am J Cancer Res* (2015) 5:1553.

56. Fukasawa T, Yoshizaki A, Ebata S, Nakamura K, Saigusa R, Miura S, et al. Contribution of soluble forms of programmed death 1 and programmed death ligand 2 to disease severity and progression in systemic sclerosis. *Arthritis Rheumatol* (2017) 69:1879–90. doi: 10.1002/ART.40164

57. Yoshizaki A. Pathogenic roles of b lymphocytes in systemic sclerosis. *Immunol Lett* (2018) 195:76–82. doi: 10.1016/J.IMLET.2018.01.002

58. Yanaba K, Hayashi M, Yoshihara Y, Nakagawa H. Serum levels of soluble programmed death–1 and programmed death ligand–1 in systemic sclerosis: Association with extent of skin sclerosis. *J Dermatol* (2016) 43:954–7. doi: 10.1111/1346–8138.13339

59. Hua Z, Hou B. TLR signaling in b–cell development and activation. *Cell Mol Immunol 2013 102* (2012) 10:103–6. doi: 10.1038/cmi.2012.61

60. Cheng S, Wang H, Zhou H. The role of TLR4 on b cell activation and anti–β2GPI antibody production in the antiphospholipid syndrome. *J Immunol Res* (2016) 2016. doi: 10.1155/2016/1719720

61. Bhattacharyya S, Varga J. Endogenous ligands of TLR4 promote unresolving tissue fibrosis: Implications for systemic sclerosis and its targeted therapy. *Immunol Lett* (2018) 195:9–17. doi: 10.1016/J.IMLET.2017.09.011

62. Suthers AN, Sarantopoulos S. TLR7/TLR9– and b cell receptor–signaling crosstalk: Promotion of potentially dangerous b cells. *Front Immunol* (2017) 8:775/BIBTEX. doi: 10.3389/FIMMU.2017.00775/BIBTEX

63. Wang T, Marken J, Chen J, Tran VB, Li QZ, Li M, et al. High TLR7 expression drives the expansion of CD19+CD24HiCD38hi transitional b cells and autoantibody production in SLE patients. *Front Immunol* (2019) 10:1243/BIBTEX. doi: 10.3389/FIMMU.2019.01243/BIBTEX

64. Vreća M, Zeković A, Damjanov N, Andjelković M, Ugrin M, Pavlović S, et al. Expression of TLR7, TLR9, JAK2, and STAT3 genes in peripheral blood mononuclear cells from patients with systemic sclerosis. *J Appl Genet* (2018) 59:59–66. doi: 10.1007/S13353–017–0415–4

65. Jellusova J, Rickert RC. The PI3K pathway in b cell metabolism. *Crit Rev Biochem Mol Biol* (2016) 51:359. doi: 10.1080/10409238.2016.1215288

66. Limon JJ, Fruman DA. Akt and mTOR in b cell activation and differentiation. *Front Immunol* (2012) 3:228/BIBTEX. doi: 10.3389/FIMMU.2012.00228/BIBTEX

67. Wang LD, Clark MR. B–cell antigen–receptor signalling in lymphocyte development. *Immunology* (2003) 110:411–20. doi: 10.1111/J.1365–2567.2003.01756.X

68. Dawidowicz K, Dieudé P, Avouac J, Wipff J, Hachulla E, Diot E, et al. Association study of b–cell marker gene polymorphisms in European Caucasian patients with systemic sclerosis. *Clin Exp Rheumatol* (2011) 29:839–42.

69. Dieudé P, Wipff J, Guedj M, Ruiz B, Melchers I, Hachulla E, et al. BANK1 is a genetic risk factor for diffuse cutaneous systemic sclerosis and has additive effects with IRF5 and STAT4. *Arthritis Rheum* (2009) 60:3447–54. doi: 10.1002/ART.24885

70. Abdelrasoul H, Werner M, Setz CS, Okkenhaug K, Jumaa H. PI3K induces b–cell development and regulates b cell identity. *Sci Rep* (2018) 8:1–15. doi: 10.1038/s41598–018–19460–5

71. Dieudé P, Guedj M, Wipff J, Ruiz B, Riemekasten G, Matucci–Cerinic M, et al. Association of the TNFAIP3 rs5029939 variant with systemic sclerosis in the European Caucasian population. *Ann Rheum Dis* (2010) 69:1958–64. doi: 10.1136/ARD.2009.127928

72. Koumakis E, Giraud M, Dieudé P, Cohignac V, Cuomo G, Airò P, et al. Brief report: Candidate gene study in systemic sclerosis identifies a rare and functional variant of the TNFAIP3 locus as a risk factor for polyautoimmunity. *Arthritis Rheum* (2012) 64:2746–52. doi: 10.1002/ART.34490

73. Tavares RM, Turer EE, Liu CL, Advincula R, Scapini P, Rhee L, et al. The ubiquitin modifying enayme A20 restricts b cell survival and prevents autoimmunity. *Immunity* (2010) 33:181. doi: 10.1016/J.IMMUNI.2010.07.017

74. Srinivasan L, Sasaki Y, Calado DP, Zhang B, Paik JH, DePinho RA, et al. PI3 kinase signals BCR–dependent mature b cell survival. *Cell* (2009) 139:573–86. doi: 10.1016/J.CELL.2009.08.041

75. Martin JE, Broen JC, David Carmona F, Teruel M, Simeon CP, Vonk MC, et al. Identification of CSK as a systemic sclerosis genetic risk factor through genome wide association study follow–up. *Hum Mol Genet* (2012) 21:2825–35. doi: 10.1093/HMG/DDS099

76. Gourh P, Agarwal SK, Martin E, Divecha D, Rueda B, Bunting H, et al. Association of the C8orf13–BLK region with systemic sclerosis in north–American and European populations. *J Autoimmun* (2010) 34:155–62. doi: 10.1016/J.JAUT.2009.08.014

77. Dieudé P, Guedj M, Wipff J, Avouac J, Hachulla E, Diot E, et al. The PTPN22 620W allele confers susceptibility to systemic sclerosis: findings of a large case–control study of European caucasians and a meta–analysis. *Arthritis Rheum* (2008) 58:2183–8. doi: 10.1002/ART.23601

78. Mahoney JM, Taroni J, Martyanov V, Wood TA, Greene CS, Pioli PA, et al. Systems level analysis of systemic sclerosis shows a network of immune and profibrotic pathways connected with genetic polymorphisms. *PloS Comput Biol* (2015) 11:1004005. doi: 10.1371/JOURNAL.PCBI.1004005

79. Simon D, Erdő–Bonyár S, Rapp J, Balogh P, Minier T, Nagy G, et al. Analysis of PI3K pathway associated molecules reveals dysregulated innate and adaptive functions of b cells in early diffuse cutaneous systemic sclerosis. *Int J Mol Sci* (2021) 22:1–13. doi: 10.3390/IJMS22062877

80. Koarada S, Tada Y, Kikuchi Y, Ushiyama O, Suzuki N, Ohta A, et al. CD180 (RP105) in rheumatic diseases. *Rheumatology* (2001) 40:1315–6. doi: 10.1093/RHEUMATOLOGY/40.11.1315

81. Chaplin JW, Kasahara S, Clark EA, Ledbetter JA. Anti–CD180 (RP105) activates b cells to rapidly produce polyclonal ig *via* a T cell and MyD88–independent pathway. *J Immunol* (2011) 187:4199–209. doi: 10.4049/JIMMUNOL.1100198

82. Roe K, Shu GL, Draves KE, Giordano D, Pepper M, Clark EA. Targeting antigens to CD180 but not CD40 programs immature and mature b cell subsets to become efficient APCs. *J Immunol* (2019) 203:1715–29. doi: 10.4049/JIMMUNOL.1900549/–/DCSUPPLEMENTAL

83. Erdő–Bonyár S, Rapp J, Minier T, Ráth G, Najbauer J, Czirják L, et al. Toll–like receptor mediated activation of natural autoantibody producing b cell subpopulations in an autoimmune disease model. *Int J Mol Sci* (2019) 20. doi: 10.3390/IJMS20246152

84. Shi X, Shao T, Huo F, Zheng C, Li W, Jiang Z. An analysis of abnormalities in the b cell receptor repertoire in patients with systemic sclerosis using high–throughput sequencing. *PeerJ* (2020) 2020:e8370. doi: 10.7717/peerj.8370

85. Galson JD, Clutterbuck EA, Trück J, Ramasamy MN, Münz M, Fowler A, et al. BCR repertoire sequencing: different patterns of b cell activation after two meningococcal vaccines. *Immunol Cell Biol* (2015) 93:885. doi: 10.1038/ICB.2015.57

86. Fielding CA, Jones GW, McLoughlin RM, McLeod L, Hammond VJ, Uceda J, et al. Interleukin–6 signaling drives fibrosis in unresolved inflammation. *Immunity* (2014) 40:40. doi: 10.1016/J.IMMUNI.2013.10.022

87. Arkatkar T, Du SW, Jacobs HM, Dam EM, Hou B, Buckner JH, et al. B cell–derived IL–6 initiates spontaneous germinal center formation during systemic autoimmunity. *J Exp Med* (2017) 214:3207–17. doi: 10.1084/JEM.20170580

88. Zhou Y, Zhang Y, Han J, Yang M, Zhu J, Jin T. Transitional b cells involved in autoimmunity and their impact on neuroimmunological diseases. *J Transl Med* (2020) 18. doi: 10.1186/S12967-020-02289-W

89. Maeda K, Mehta H, Drevets DA, Coggeshall KM. IL–6 increases b–cell IgG production in a feed–forward proinflammatory mechanism to skew hematopoiesis and elevate myeloid production. *Blood* (2010) 115:4699. doi: 10.1182/BLOOD–2009–07–230631

90. Alarcon–Riquelme ME, Moller G, Fernandez C. Macrophage depletion decreases IgG anti–DNA in cultures from (NZB x NZW)F1 spleen cells by eliminating the main source of IL–6. *Clin Exp Immunol* (1993) 91:220–5. doi: 10.1111/j.1365-2249.1993.tb05886.x

91. Zi Z, Chapnick DA, Liu X. Dynamics of TGF–β/Smad signaling. *FEBS Lett* (2012) 586:1921–8. doi: 10.1016/J.FEBSLET.2012.03.063

92. Leivonen SK, Lazaridis K, Decock J, Chantry A, Edwards DR, Kähäri VM. TGF–β–Elicited induction of tissue inhibitor of metalloproteinases (TIMP)–3 expression in fibroblasts involves complex interplay between Smad3, p38α, and ERK1/2. *PloS One* (2013) 8. doi: 10.1371/JOURNAL.PONE.0057474

93. Kubo M, Ihn H, Yamane K, Tamaki K. Upregulated expression of transforming growth factor–beta receptors in dermal fibroblasts of skin sections from patients with systemic sclerosis. *J Rheumatol* (2002) 29(12):2558–64.

94. Fillatreau S, Sweenie CH, McGeachy MJ, Gray D, Anderton SM. B cells regulate autoimmunity by provision of IL–10. *Nat Immunol 2002 310* (2002) 3:944–50. doi: 10.1038/ni833

95. Forestier A, Guerrier T, Jouvray M, Giovannelli J, Lefèvre G, Sobanski V, et al. Altered b lymphocyte homeostasis and functions in systemic sclerosis. *Autoimmun Rev* (2018) 17:244–55. doi: 10.1016/J.AUTREV.2017.10.015

96. Wynn TA. IL–13 effector functions. *Annu Rev Immunol* (2003) 21:425–56. doi: 10.1146/ANNUREV.IMMUNOL.21.120601.141142

97. Punnonen J, de Vries JE. IL–13 induces proliferation, ig isotype switching, and ig synthesis by immature human fetal b cells. *J Immunol* (1994) 152:1094–102.

98. Cocks BG, de Waal Malefyt R, Galizzi J–P, de Vries JE, Aversa G. IL–13 induces proliferation and differentiation of human b cells activated by the CD40 ligand. *Int Immunol* (1993) 5:657–63. doi: 10.1093/INTIMM/5.6.657

99. Hasegawa M, Fujimoto M, Kikuchi K, Takehara K. Elevated serum levels of interleukin 4 (IL–4), IL–10, and IL–13 in patients with systemic sclerosis. *J Rheumatol* (1997) 24:328–32.

100. Rankin AL, Mumm JB, Murphy E, Turner S, Yu N, McClanahan TK, et al. IL–33 induces IL–13–Dependent cutaneous fibrosis. *J Immunol* (2010) 184:1526–35. doi: 10.4049/JIMMUNOL.0903306

101. Rose WA, Okragly AJ, Hu NN, Daniels MR, Martin AP, Koh YT, et al. Interleukin–33 contributes toward loss of tolerance by promoting b–Cell–Activating factor of the tumor–Necrosis–Factor family (BAFF)–dependent autoantibody production. *Front Immunol* (2018) 9:2871/BIBTEX. doi: 10.3389/FIMMU.2018.02871/BIBTEX

102. Ebisuno Y, Tanaka T, Kanemitsu N, Kanda H, Yamaguchi K, Kaisho T, et al. Cutting edge: The b cell chemokine CXC chemokine ligand 13/B lymphocyte chemoattractant is expressed in the high endothelial venules of lymph nodes and peyer's patches and affects b cell trafficking across high endothelial venules. *J Immunol* (2003) 171:1642–6. doi: 10.4049/JIMMUNOL.171.4.1642

103. Bellamri N, Viel R, Morzadec C, Lecureur V, Joannes A, de LB, et al. TNF–α and IL–10 control CXCL13 expression in human macrophages. *J Immunol* (2020) 204:2492–502. doi: 10.4049/JIMMUNOL.1900790

104. Carlsen HS, Baekkevold ES, Morton HC, Haraldsen G, Brandtzaeg P. Monocyte–like and mature macrophages produce CXCL13 (B cell–attracting chemokine 1) in inflammatory lesions with lymphoid neogenesis. *Blood* (2004) 104:3021–7. doi: 10.1182/BLOOD–2004–02–0701

105. Kalled SL. The role of BAFF in immune function and implications for autoimmunity. *Immunol Rev* (2005) 204:43–54. doi: 10.1111/J.0105–2896.2005.00219.X

106. Nemazee D. Mechanisms of central tolerance for b cells. *Nat Rev Immunol* (2017) 17:281–94. doi: 10.1038/nri.2017.19

107. Stadanlick JE, Cancro MP. BAFF and the plasticity of peripheral b cell tolerance. *Curr Opin Immunol* (2008) 20:158. doi: 10.1016/J.COI.2008.03.015

108. Matsushita T, Kobayashi T, Mizumaki K, Kano M, Sawada T, Tennichi M, et al. BAFF inhibition attenuates fibrosis in scleroderma by modulating the regulatory and effector b cell balance. *Sci Adv* (2018) 4:9944–55. doi: 10.1126/SCIADV.AAS9944

109. Matsushita T, Hasegawa M, Yanaba K, Kodera M, Takehara K, Sato S. Elevated serum BAFF levels in patients with systemic sclerosis: Enhanced BAFF signaling in systemic sclerosis b lymphocytes. *Arthritis Rheum* (2006) 54:192–201. doi: 10.1002/art.21526

110. Worrell JC, O'Reilly S. Bi–directional communication: Conversations between fibroblasts and immune cells in systemic sclerosis. *J Autoimmun* (2020) 113. doi: 10.1016/J.JAUT.2020.102526

111. Melissaropoulos K, Daoussis D. B cells in systemic sclerosis: from pathophysiology to treatment. *Clin Rheumatol* (2021) 40:2621–31. doi: 10.1007/S10067–021–05665–Z

112. Green MC, Sweet HO, Bunker LE. Tight–skin, a new mutation of the mouse causing excessive growth of connective tissue and skeleton. *Am J Pathol* (1976) 82:493.

113. Saito E, Fujimoto M, Hasegawa M, Komura K, Hamaguchi Y, Kaburagi Y, et al. CD19–dependent b lymphocyte signaling thresholds influence skin fibrosis and autoimmunity in the tight–skin mouse. *J Clin Invest* (2002) 109:1453. doi: 10.1172/JCI15078

114. Matsushita T, Fujimoto M, Hasegawa M, Matsushita Y, Komura K, Ogawa F, et al. BAFF antagonist attenuates the development of skin fibrosis in tight–skin mice. *J Invest Dermatol* (2007) 127:2772–80. doi: 10.1038/SJ.JID.5700919

115. Komura K, Yanaba K, Horikawa M, Ogawa F, Fujimoto M, Tedder T, et al. CD19 regulates the development of bleomycin–induced pulmonary fibrosis in a mouse model. *Arthritis Rheum* (2008) 58:3574–84. doi: 10.1002/ART.23995

116. Tedder TF, Poe JC, Fujimoto M, Haas KM, Sato S. The CD19–CD21 signal transduction complex of b lymphocytes regulates the balance between health and autoimmune disease: Systemic sclerosis as a model system. *Curr Dir Autoimmun* (2005) 8:55–90. doi: 10.1159/000082087

117. Yoshizaki A, Yanaba K, Ogawa A, Asano Y, Kadono T, Sato S. Immunization with DNA topoisomerase I and freund's complete adjuvant induces skin and lung fibrosis and autoimmunity *via* interleukin–6 signaling. *Arthritis Rheum* (2011) 63:3575–85. doi: 10.1002/ART.30539

118. Whitfield ML, Finlay DR, Murray JI, Troyanskaya OG, Chi JT, Pergamenschikov A, et al. Systemic and cell type–specific gene expression patterns in scleroderma skin. *Proc Natl Acad Sci U.S.A.* (2003) 100:12319–24. doi: 10.1073/pnas.1635114100

119. Roumm AD, Whiteside TL, Medsger TA, Rodnan GP. Lymphocytes in the skin of patients with progressive systemic sclerosis. *Arthritis Rheum* (1984) 27:645–53. doi: 10.1002/art.1780270607

120. Bosello S, Angelucci C, Lama G, Alivernini S, Proietti G, Tolusso B, et al. Characterization of inflammatory cell infiltrate of scleroderma skin: B cells and skin score progression. *Arthritis Res Ther* (2018) 20:1–11. doi: 10.1186/s13075–018–1569–0

121. Skaug B, Khanna D, Swindell WR, Hinchcliff ME, Frech TM, Steen VD, et al. Global skin gene expression analysis of early diffuse cutaneous systemic sclerosis shows a prominent innate and adaptive inflammatory profile. *Ann Rheum Dis* (2020) 79:379–86. doi: 10.1136/ANNRHEUMDIS–2019–215894

122. Lafyatis R, O'Hara C, Feghali–Bostwick CA, Matteson E. B cell infiltration in systemic sclerosis–associated interstitial lung disease. *Arthritis Rheum* (2007) 56:3167–8. doi: 10.1002/art.22847

123. Geherin SA, Gómez D, Glabman RA, Ruthel G, Hamann A, Debes GF. IL–10 + innate–like b cells are part of the skin immune system and require α4β1 integrin to migrate between the peritoneum and inflamed skin. *J Immunol* (2016) 196:2514–25. doi: 10.4049/JIMMUNOL.1403246/–/DCSUPPLEMENTAL

124. Khanna D, Lescoat A, Roofeh D, Bernstein EJ, Kazerooni EA, Roth MD, et al. Systemic sclerosis–associated interstitial lung disease: How to incorporate two food and drug administration–approved therapies in clinical practice. *Arthritis Rheumatol* (2022) 74:13–27. doi: 10.1002/art.41933

125. Tashkin DP, Elashoff R, Clements PJ, Goldin J, Roth MD, Furst DE, et al. Cyclophosphamide versus placebo in scleroderma lung disease. *N Engl J Med* (2006) 354:2655–66. doi: 10.1056/NEJMOA055120/SUPPL_FILE/NEJM_TASHKIN_2655SA1.PDF

126. Ebata S, Yoshizaki A, Fukasawa T, Sato S. Single–cell analysis of autoreactive b cells in patients with systemic sclerosis revealed that responses to therapy are determined by effector and regulatory b cell balance. *J Immunol* (2020) 204:238. doi: 10.4049/jimmunol.204.Supp.238.16

127. Tashkin DP, Roth MD, Clements PJ, Furst DE, Khanna D, Kleerup EC, et al. Mycophenolate mofetil versus oral cyclophosphamide in scleroderma–related interstitial lung disease (SLS II): a randomised controlled, double–blind, parallel group trial. *Lancet Respir Med* (2016) 4:708–19. doi: 10.1016/S2213–2600(16)30152–7

128. Allison AC, Eugui EM. Mycophenolate mofetil and its mechanisms of action. *Immunopharmacology* (2000) 47:85–118. doi: 10.1016/S0162–3109(00)00188–0

129. Highland KB, Distler O, Kuwana M, Allanore Y, Assassi S, Azuma A, et al. Efficacy and safety of nintedanib in patients with systemic sclerosis–associated

interstitial lung disease treated with mycophenolate: a subgroup analysis of the SENSCIS trial. *Lancet Respir Med* (2021) 9:96–106. doi: 10.1016/S2213–2600(20)30330–1

130. Spiera R, Furst DE, Frech TM, Kuwana M, Hummers L, Stevens W, et al. Background mycophenolate (MMF) treatment is associated with improved outcomes in a phase 3 trial of lenabasum in diffuse cutaneous systemic sclerosis (dcSSc). *ACR Meet Abstr* (2021).

131. Gratwohl A, Passweg J, Bocelli–Tyndall C, Fassas A, van Laar JM, Farge D, et al. Autologous hematopoietic stem cell transplantation for autoimmune diseases. *Bone Marrow Transplant 2005 359* (2005) 35:869–79. doi: 10.1038/sj.bmt.1704892

132. Burt RK, Shah SJ, Dill K, Grant T, Gheorghiade M, Schroeder J, et al. Autologous non–myeloablative haemopoietic stem–cell transplantation compared with pulse cyclophosphamide once per month for systemic sclerosis (ASSIST): an open–label, randomised phase 2 trial. *Lancet* (2011) 378:498–506. doi: 10.1016/S0140–6736(11)60982–3

133. Sullivan KM, Goldmuntz EA, Keyes–Elstein L, McSweeney PA, Pinckney A, Welch B, et al. Myeloablative autologous stem–cell transplantation for severe scleroderma. *N Engl J Med* (2018) 378:35–47. doi: 10.1056/NEJMOA1703327

134. Van Laar JM, Farge D, Sont JK, Naraghi K, Marjanovic Z, Larghero J, et al. Autologous hematopoietic stem cell transplantation vs intravenous pulse cyclophosphamide in diffuse cutaneous systemic sclerosis: a randomized clinical trial. *JAMA* (2014) 311:2490–8. doi: 10.1001/JAMA.2014.6368

135. Lima–Júnior JR, Arruda LCM, Gonçalves MS, Dias JBE, Moraes DA, Covas DT, et al. Autologous haematopoietic stem cell transplantation restores the suppressive capacity of regulatory b cells in systemic sclerosis patients. *Rheumatol (Oxford)* (2021) 60:5538–48. doi: 10.1093/RHEUMATOLOGY/KEAB257

136. Bosello S, De Santis M, Lama G, Spanò C, Angelucci C, Tolusso B, et al. B cell depletion in diffuse progressive systemic sclerosis: Safety, skin score modification and IL–6 modulation in an up to thirty–six months follow–up open–label trial. *Arthritis Res Ther* (2010) 12. doi: 10.1186/ar2965

137. Daoussis D, Liossis SNC, Tsamandas AC, Kalogeropoulou C, Paliogianni F, Sirinian C, et al. Effect of long–term treatment with rituximab on pulmonary function and skin fibrosis in patients with diffuse systemic sclerosis. *Clin Exp Rheumatol* (2012) 30:S17–22.

138. Moazedi–Fuerst FC, Kielhauser SM, Brickmann K, Hermann J, Lutfi A, Meilinger M, et al. Rituximab for systemic sclerosis: arrest of pulmonary disease progression in five cases. results of a lower dosage and shorter interval regimen. *Scand J Rheumatol* (2014) 43:257–8. doi: 10.3109/03009742.2013.869617

139. Smith V, Van Praet JT, Vandooren B, van der Cruyssen B, Naeyaert JM, Decuman S, et al. Rituximab in diffuse cutaneous systemic sclerosis: An open–label clinical and histopathological study. *Ann Rheum Dis* (2010) 69:193–7. doi: 10.1136/ARD.2008.095463

140. Smith V, Piette Y, Van Praet JT, Decuman S, Deschepper E, Elewaut D, et al. Two–year results of an open pilot study of a 2–treatment course with rituximab in patients with early systemic sclerosis with diffuse skin involvement. *J Rheumatol* (2013) 40:52–7. doi: 10.3899/JRHEUM.120778

141. Daoussis D, Liossis SNC, Tsamandas AC, Kalogeropoulou C, Kazantzi A, Sirinian C, et al. Experience with rituximab in scleroderma: results from a 1–year, proof–of–principle study. *Rheumatol (Oxford)* (2010) 49:271–80. doi: 10.1093/RHEUMATOLOGY/KEP093

142. Daoussis D, Melissaropoulos K, Sakellaropoulos G, Antonopoulos I, Markatseli TE, Simopoulou T, et al. A multicenter, open–label, comparative study of b–cell depletion therapy with rituximab for systemic sclerosis–associated interstitial lung disease. *Semin Arthritis Rheum* (2017) 46:625–31. doi: 10.1016/J.SEMARTHRIT.2016.10.003

143. Fraticelli P, Fischetti C, Salaffi F, Carotti M, Mattioli M, Pomponio G, et al. Combination therapy with rituximab and mycophenolate mofetil in systemic sclerosis. a single–centre case series study. *Clin Exp Rheumatol* (2018) 36:S142–5.

144. Sircar G, Goswami RP, Sircar D, Ghosh A, Ghosh P. Intravenous cyclophosphamide vs rituximab for the treatment of early diffuse scleroderma lung disease: open label, randomized, controlled trial. *Rheumatol (Oxford)* (2018) 57:2106–13. doi: 10.1093/RHEUMATOLOGY/KEY213

145. Jordan S, Distler JHW, Maurer B, Huscher D, Van Laar JM, Allanore Y, et al. Effects and safety of rituximab in systemic sclerosis: An analysis from the European scleroderma trial and research (EUSTAR) group. *Ann Rheum Dis* (2015) 74:1188–94. doi: 10.1136/annrheumdis–2013–204522

146. De Lauretis A, Sestini P, Pantelidis P, Hoyles R, Hansell DM, Goh NSL, et al. Serum interleukin 6 is predictive of early functional decline and mortality in interstitial lung disease associated with systemic sclerosis. *J Rheumatol* (2013) 40:435–46. doi: 10.3899/jrheum.120725

147. Ebata S, Yoshizaki A, Fukasawa T, Yoshizaki–Ogawa A, Asano Y, Kashiwabara K, et al. Percentage of residual b cells after 2 weeks of rituximab treatment predicts the improvement of systemic sclerosis–associated interstitial lung disease. *J Dermatol* (2022) 49(1):179–83. doi: 10.1111/1346-8138.16206

148. Fraticelli P, De Vita S, Franzolini N, Svegliati S, Scott CA, Tonnini C, et al. Reduced type I collagen gene expression by skin fibroblasts of patients with systemic sclerosis after one treatment course with rituximab. *Clin Exp Rheumatol* (2015) 33:160–7.

149. Elhai M, Boubaya M, Distler O, Smith V, Matucci–Cerinic M, Alegre Sancho JJ, et al. Outcomes of patients with systemic sclerosis treated with rituximab in contemporary practice: A prospective cohort study. *Ann Rheum Dis* (2019) 78:979–87. doi: 10.1136/annrheumdis–2018–214816

150. Goswami RP, Ray A, Chatterjee M, Mukherjee A, Sircar G, Ghosh P. Rituximab in the treatment of systemic sclerosis–related interstitial lung disease: A systematic review and meta–analysis. *Rheumatol (United Kingdom)* (2021) 60:557–67. doi: 10.1093/rheumatology/keaa550

151. Tang R, Yu J, Shi Y, Zou P, Zeng Z, Tang B, et al. Safety and efficacy of rituximab in systemic sclerosis: A systematic review and meta–analysis. *Int Immunopharmacol* (2020) 83. doi: 10.1016/j.intimp.2020.106389

152. Ebata S, Yoshizaki A, Oba K, Kashiwabara K, Ueda K, Uemura Y, et al. Safety and efficacy of rituximab in systemic sclerosis (DESIRES): a double–blind, investigator–initiated, randomised, placebo–controlled trial. *Lancet Rheumatol* (2021) 3:e489–97. doi: 10.1016/S2665–9913(21)00107–7

153. Saunders P, Tsipouri V, Keir GJ, Ashby D, Flather MD, Parfrey H, et al. Rituximab versus cyclophosphamide for the treatment of connective tissue diseaseassociated interstitial lung disease (RECITAL): Study protocol for a randomised controlled trial. *Trials* (2017) 18(1):275. doi: 10.1186/s13063–017–2016–2

154. Bonroy C, Smith V, Deschepper E, De Keyser F DK. Specific antinuclear antibody level changes after b cell depletion therapy in systemic sclerosis are associated with improvement of skin thickening. *J Rheumatol* (2016) 43:681LP – 681. doi: 10.3899/jrheum.150105.C1

155. Lafyatis R, Kissin E, York M, Farina G, Viger K, Fritzler MJ, et al. B cell depletion with rituximab in patients with diffuse cutaneous systemic sclerosis. *Arthritis Rheum* (2009) 60:578–83. doi: 10.1002/art.24249

156. Sumida H, Asano Y, Tamaki Z, Aozasa N, Taniguchi T, Takahashi T, et al. Successful experience of rituximab therapy for systemic sclerosis–associated interstitial lung disease with concomitant systemic lupus erythematosus. *J Dermatol* (2014) 41:418–20. doi: 10.1111/1346–8138.12461

157. Hofmann K, Clauder AK, Manz RA. Targeting b cells and plasma cells in autoimmune diseases. *Front Immunol* (2018) 9:835/BIBTEX. doi: 10.3389/FIMMU.2018.00835/BIBTEX

158. Streicher K, Sridhar S, Kuziora M, Morehouse CA, Higgs BW, Sebastian Y, et al. Baseline plasma cell gene signature predicts improvement in systemic sclerosis skin scores following treatment with inebilizumab (MEDI–551) and correlates with disease activity in systemic lupus erythematosus and chronic obstructive pulmonary disease. *Arthritis Rheumatol (Hoboken NJ)* (2018) 70:2087–95. doi: 10.1002/ART.40656

159. Schiopu E, Chatterjee S, Hsu V, Flor A, Cimbora D, Patra K, et al. Safety and tolerability of an anti–CD19 monoclonal antibody, MEDI–551, in subjects with systemic sclerosis: A phase I, randomized, placebo–controlled, escalating single–dose study. *Arthritis Res Ther* (2016) 18:1–14. doi: 10.1186/S13075–016–1021–2/TABLES/5

160. Benfaremo D, Gabrielli A. Is there a future for anti–CD38 antibody therapy in systemic autoimmune diseases? *Cells* (2020) 9. doi: 10.3390/CELLS9010077

161. Gordon JK, Martyanov V, Franks JM, Bernstein EJ, Szymonifka J, Magro C, et al. Belimumab for the treatment of early diffuse systemic sclerosis: Results of a randomized, double–blind, placebo–controlled, pilot trial. *Arthritis Rheumatol* (2018) 70:308–16. doi: 10.1002/ART.40358/ABSTRACT

162. Khanna D, Lin CJF, Furst DE, Goldin J, Kim G, Kuwana M, et al. Tocilizumab in systemic sclerosis: a randomised, double–blind, placebo–controlled, phase 3 trial. *Lancet Respir Med* (2020) 8:963–74. doi: 10.1016/S2213–2600(20)30318–0

163. Khanna D, Denton CP, Jahreis A, van Laar JM, Frech TM, Anderson ME, et al. Safety and efficacy of subcutaneous tocilizumab in adults with systemic sclerosis (faSScinate): a phase 2, randomised, controlled trial. *Lancet* (2016) 387:2630–40. doi: 10.1016/S0140–6736(16)00232–4/ATTACHMENT/99F33BB7–93E6–4708–94C8–06E25B85693D/MMC1.PDF

164. Wang J, Wang J, Qi X, Sun Z, Zhang T, Cui Y, et al. The efficacy and safety of pirfenidone combined with immunosuppressant therapy in connective tissue disease-associated interstitial lung disease: A 24-week prospective controlled cohort study. *Front Med (Lausanne)* (2022) 9:871861. doi: 10.3389/fmed.2022.871861

165. Distler O, Highland KB, Gahlemann M, Azuma A, Fischer A, Mayes MD, et al. Nintedanib for systemic sclerosis–associated interstitial lung disease. *N Engl J Med* (2019) 380:2518–28. doi: 10.1056/nejmoa1903076

Frontiers in Immunology

Explores novel approaches and diagnoses to treat immune disorders.

The official journal of the International Union of Immunological Societies (IUIS) and the most cited in its field, leading the way for research across basic, translational and clinical immunology.

Discover the latest Research Topics

See more →

Frontiers

Avenue du Tribunal-Fédéral 34
1005 Lausanne, Switzerland
frontiersin.org

Contact us

+41 (0)21 510 17 00
frontiersin.org/about/contact